

Technical Report Documentation Page

1. Report No. FHWA/TX-08/0-5207-1		2. Government Accession No.	3. Recipient's Catalog No.	
4. Title and Subtitle Effects of Texas Fly Ash on Air-Entrainment in Concrete: Comprehensive Report			5. Report Date February 2008; Revised January 2009	
			6. Performing Organization Code	
7. Author(s) Dr. Kevin Folliard, Dr. Kenneth Hover, Nathan Harris, M. Tyler Ley, and Andy Naranjo			8. Performing Organization Report No. 0-5207-1	
9. Performing Organization Name and Address Center for Transportation Research The University of Texas at Austin 3208 Red River, Suite 200 Austin, TX 78705-2650			10. Work Unit No. (TRAIS)	
			11. Contract or Grant No. 0-5207	
12. Sponsoring Agency Name and Address Texas Department of Transportation Research and Technology Implementation Office P.O. Box 5080 Austin, TX 78763-5080			13. Type of Report and Period Covered Technical Report 9/4/2004 - 8/31/2007	
			14. Sponsoring Agency Code	
15. Supplementary Notes Project performed in cooperation with the Texas Department of Transportation and the Federal Highway Administration.				
16. Abstract This report summarizes a comprehensive joint-research project, funded by The Texas Department of Transportation (TxDOT) and performed by researchers at The University of Texas at Austin and Cornell University. This three-volume report is perhaps the most complete study to date on this topic. It is expected that the key findings from this study will be of benefit to practitioners in Texas and beyond.				
17. Key Words Texas, Flyash, Fly Ash analysis, Air-Entrainment in Concrete, Cementitious Materials, slag, silica, ASTM, LOI			18. Distribution Statement No restrictions. This document is available to the public through the National Technical Information Service, Springfield, Virginia 22161; www.ntis.gov.	
19. Security Classif. (of report) Unclassified	20. Security Classif. (of this page) Unclassified	21. No. of pages 578		22. Price



Effects of Texas Fly Ash on Air-Entrainment in Concrete: Comprehensive Report

Dr. Kevin Folliard
Dr. Kenneth Hover
Nathan Harris
M. Tyler Ley
Andy Naranjo

CTR Technical Report:	0-5207-1
Report Date:	February 2008; Revised January 2009
Project:	0-5207
Project Title:	Effects of Texas Flyash on Air-Entrainment in Concrete
Sponsoring Agency:	Texas Department of Transportation
Performing Agency:	Center for Transportation Research at The University of Texas at Austin

Project performed in cooperation with the Texas Department of Transportation and the Federal Highway Administration.

Center for Transportation Research
The University of Texas at Austin
3208 Red River
Austin, TX 78705

www.utexas.edu/research/ctr

Copyright (c) 2008
Center for Transportation Research
The University of Texas at Austin

All rights reserved
Printed in the United States of America

Disclaimers

Authors' Disclaimer: The contents of this report reflect the views of the authors, who are responsible for the facts and the accuracy of the data presented herein. The contents do not necessarily reflect the official view or policies of the Federal Highway Administration or the Texas Department of Transportation. This report does not constitute a standard, specification, or regulation.

Patent Disclaimer: There was no invention or discovery conceived or first actually reduced to practice in the course of or under this contract, including any art, method, process, machine manufacture, design or composition of matter, or any new useful improvement thereof, or any variety of plant, which is or may be patentable under the patent laws of the United States of America or any foreign country.

Engineering Disclaimer

NOT INTENDED FOR CONSTRUCTION, BIDDING, OR PERMIT PURPOSES.

Project Engineer: David W. Fowler
Professional Engineer License Number: Texas No. 27859
P. E. Designation: Researcher

Acknowledgments

The authors express appreciation to the TxDOT Project Director, Tom Yarbrough, and the members of the Project Monitoring Committee.

Table of Contents

Chapter 1. Introduction and Scope	1
--	----------

Volume I

Chapter 2. Evaluating the Influence of Fly Ash on Air-Entrained Concrete.....	3
--	----------

2.1 Research objectives.....	3
2.2 Problems with air entrained concrete.....	3
2.3 Predicting fly ash influence on AEA dosage	4
2.4 Texas DOT sponsors research into predicting fly ash-AEA interactions	4
2.5 Existing tests for predicting fly ash-AEA interactions	5
2.6 Expansion of research objectives.....	8
2.7 Overall plan and progress of the research.....	9

Chapter 3. Background	19
------------------------------------	-----------

3.1 Introduction.....	19
3.2 Supplementary Cementitious Materials.....	19
3.3 Fly Ash Production	23
3.4 ASTM C618 Specification for Fly Ash	50
3.5 Effects of fly ash on air entrainment: the current state of knowledge	52

Chapter 4. Experimental Methods and the Collected Properties of the Materials	73
--	-----------

4.1 Introduction.....	73
4.2 Ash samples and properties	73

Chapter 5. Assessment of the ASTM C311 Loss on Ignition Test as a Measurement of Carbon Content	99
--	-----------

5.1 Introduction.....	99
5.2 Background.....	100
5.3 Summary comments on the utility of ASTM C311 as an indicator of carbon content in fly ash.....	115
5.4 Towards the development of a modified LOI procedure.....	117
5.5 Experimental trials of the Modified LOI test to evaluate fly ash	120
5.6 Discussion.....	123
5.7 Sources of variability in the test	130
5.8 Implementation of the modified LOI test in industry	134
5.9 Conclusions and future work	134

Chapter 6. Evaluation of the Foam Index Test and Development of a Proposed Standard Test	137
---	------------

6.1 The Use of the Foam Index Test to Predict AEA Dosage in Concrete Containing Fly Ash: Part I-Evaluation of the State of Practice.....	137
6.2 The Use of the Foam Index Test to Predict AEA Dosage in Concrete Containing Fly Ash: Part II-Development of a Standard Test Method: Apparatus and Procedure	157
6.3 The Use of the Foam Index Test to Predict AEA Dosage in Concrete Containing Fly Ash: Part III-Development of a Standard Test Method—Proportions of Materials	176
6.4 Other factors	190

6.5 Conclusions.....	190
6.6 Recommendations for further study	191
Chapter 7. Fly Ash Color Analysis.....	193
7.1 Analysis of Fly Ash by Flatbed Color Scanner: Part I— Development of Test Method and Grayscale Analysis	193
7.2 Analysis of Fly ash by flatbed color scanner: Part II-Change in grayscale as method for identifying organic carbon in fly ash	218
Chapter 8. Synthesis	235
8.1 Main objectives.....	235
8.2 Lessons learned regarding fly ash-AEA interactions	235
8.3 Fundamental factors influencing fly ash-AEA interactions	235
8.4 Industry implementation plan	261
8.5 Contributions of this research to the state of the art	264
Chapter 9. Conclusions and Future Research.....	265
9.1 Conclusions.....	265
9.2 Future research recommendations	270
9.3 Closing items	273

Volume II

Chapter 10. The Effects of Fly Ash on the Ability to Entrain and Stabilize Air in Concrete.....	275
10.1 Introduction.....	275
Chapter 11. Investigation of Air-Entraining Admixture Dosage in Fly Ash Concrete	279
11.1 Introduction.....	279
11.2 Research Significance.....	279
11.3 Experimental.....	280
11.4 Results.....	284
11.5 Conclusions.....	287
Chapter 12. Evaluation and Improvement of the ASTM C 311 Air Entrainment of Mortar with Fly Ash Test.....	291
12.1 Introduction.....	291
12.2 Experimental Methods.....	293
12.3 Results and Discussion	295
12.4 Implementation	303
12.5 Applications of Finding to Other ASTM Mortar Tests	303
12.6 Conclusions.....	303
Chapter 13. Determining the Air-Entraining Admixture Dosage Response from a Single Concrete Mixture.....	305
13.1 Introduction.....	305
13.2 Experimental.....	307
13.3 Results and Discussion	309
13.4 Conclusions.....	317

Chapter 14. Investigation of the Frost Resistance of Concrete through Measurement of Fresh and Hardened Properties and Resistance to Rapid Freezing and Thawing Cycles	319
14.1 Introduction.....	319
14.2 Experimental.....	323
14.3 Results.....	327
14.4 Discussion.....	331
14.5 Conclusions.....	333
Chapter 15. Observations of Air-Bubbles from Fresh Cement Paste.....	335
15.1 Introduction.....	335
15.2 Experimental Methods.....	338
15.3 Results and Discussion	341
15.4 Summary of Key Observations.....	353
Chapter 16. The Physical and Chemical Characteristics of the Shell of Air-Entrained Bubbles in Cement Paste.....	355
16.1 Introduction.....	355
16.2 Experimental Methods.....	356
16.3 Results and Discussion	360
16.4 Discussion of Mechanisms	375
16.5 Conclusions.....	377
Chapter 17. Conclusions.....	379
17.1 Investigation of Air-Entraining Admixture Dosage in Fly Ash Concrete	379
17.2 Evaluation and Improvement of the ASTM C 311 Air-Entrainment of Mortar with Fly Ash Test.....	379
17.3 Determining the Air-Entraining Admixture Dosage Response From a Single Concrete Mixture	379
17.4 Investigation of the Frost Resistance of Concrete through Measurement of Fresh and Hardened Properties, and Resistance to Rapid Freezing and Thawing Cycles	380
17.5 Observations of Air Bubbles from Fresh Cement Paste	380
17.6 The Physical and Chemical Characteristics of the Shell of Air-Entrained Bubbles in Cement Paste	381
17.7 Recommendations.....	382
17.8 Research Needs.....	383

Volume III

Chapter 18. Clustering of Air Voids Around Aggregates in Air-Entrained Concrete.....	385
18.1 Introduction.....	385
18.2 Research Objectives.....	385
18.3 Project Scope	386
Chapter 19. Literature Review	387
19.1 Air-Entrained Concrete.....	387
19.2 Air-Entraining Admixtures	388
19.3 Factors Affecting Air-entrainment.....	388

19.4 Effect of Air-entrainment on Concrete Properties	390
19.5 Issues with Air-entrained Concrete.....	390
19.6 Re-tempering Air-Entrained Concrete.....	391
19.7 Past Research on Air Void Clustering	392
Chapter 20. Materials.....	395
20.1 Cement	395
20.2 Aggregates	395
20.3 Admixtures.....	395
Chapter 21. Research Plan.....	397
21.1 Mixing Procedure	397
21.2 Mix Design	399
21.3 Phase I.....	399
21.4 Phase II	404
21.5 Case Studies.....	405
Chapter 22. Test Results and Analysis.....	407
22.1 Phase I.....	407
22.2 Phase II	420
22.3 Hardened Air Void Analysis.....	434
Chapter 23. Field Case Studies	439
23.1 Case Study #1	439
23.2 Case Study #2	440
23.3 Case Study #3	442
23.4 Case Study #4	445
23.5 Case Study #5	446
23.6 Case Study #6	447
23.7 Case Study #7	448
23.8 Summary.....	449
Chapter 24. Conclusions, Recommendations, and Future Research Needs.....	451
24.1 Fresh Concrete Properties	451
24.2 Strength Properties.....	451
24.3 Clustering of Air Voids.....	451
24.4 Hardened Air Void Characteristics	452
24.5 Field Case Studies.....	452
24.6 Recommendations.....	452
24.7 Future Research Needed	453
Chapter 25. Overall Conclusions and Recommendations for Future Research	455
25.1 Summary.....	455
25.2 VOLUME I – Conclusions and Recommendation for Future Research	455
25.3 VOLUME II – Conclusions and Recommendation for Future Research	458
25.4 VOLUME III – Conclusions and Recommendation for Future Research.....	462
References.....	465
Referenced Standards.....	481
Volume I—Appendix A: Supplementary Information.....	485

Volume II—Appendix A: Hardened Air-Void Analysis Parameters.....	509
Volume II—Appendix B: Sample Preparation for Hardened Air-Void Analysis	517
Volume II—Appendix C: Summary of Test Results for Fly Ash.....	521
Volume III—Appendix A: Fresh Concrete Properties for Phase I Mixtures	523
Volume III—Appendix B: Hardened Concrete Properties for Phase I Mixtures	529
Volume III—Appendix C: Fresh Concrete Properties for Phase II Mixtures.....	539
Volume III—Appendix D: Hardened Concrete Properties for Phase II Mixtures	541
Volume III—Appendix E: Hardened Air Analysis for Phase I and Phase II Mixtures.....	547

List of Figures

Figure 2.1: AEA dosages for fly ash concrete versus fly ash loss on ignition content.....	6
Figure 2.2: Foam index values produced by four variations of the foam index test on four Texas ash samples.....	7
Figure 2.3: Correlation between fly ash colorimetric properties and concrete AEA dosage.	8
Figure 2.4: Fly ash-AEA interactions research approach- Overall plan.....	10
Figure 2.5: Interactions research approach- fly ash test suite. Asterisk (*) indicates tests which require special scientific apparatus and technical expertise not generally common to the industry	12
Figure 2.6: Fly ash-AEA interactions research approach—Development of new or improved test methods.....	15
Figure 2.7: Fly ash AEA interactions research approach—Implementation of findings.....	17
Figure 3.1: Supplementary cementitious materials from left to right, fly ash (Class C), metakaolin (calcined clay), silica fume, fly ash (class F), slag and calcined shale (Kosmatka et al., 2003).....	20
Figure 3.2: Proximate composition (minus ash) of various coal ranks (Averitt, 1981).....	26
Figure 3.3: Calorific value, Btu/lb (Averitt, 1981).	27
Figure 3.4: Model of coal molecular structure by P.H. Given (1960).....	27
Figure 3.5: Division of the basic components of coal (Ward, 1984).....	30
Figure 3.6: Distribution of coal in top coal rich countries (EIA, 2004).....	35
Figure 3.7: U.S. coal distribution.....	36
Figure 3.8: Pulverized coal fired power plant schematic.....	41
Figure 3.9: Coal combustion and fly ash formation.	43
Figure 3.10: Fly ash morphogenesis scheme illustrating probable relationship of opacity to particle composition and relationship of particle shape to exposure in combustion chamber (Fisher et al. 1987).....	47
Figure 3.11: SEM image of fly ash, 500x magnification.....	47
Figure 3.12: Daily variations in properties of fly ash produced b a generating station under continuous operations. From Helmuth (1987).....	49
Figure 3.13: SEM image of air void with ice crystals (a) and after sublimation of ice (b) (bars are 10 μ m). From Corr, 2002.	53
Figure 3.14: Relationship between foam index and LOI for all ash samples (both Class C and F) from Hurt et al. (2001). Foam index units are in mL of 10% concentration of commercial AEA normalized by 2 g ash.....	58
Figure 3.15: Organic coal residuals particle size distribution in Class F ash samples, diameters (d) are in microns. From Kulaots et al. (2004).....	63
Figure 3.16: Organic coal residuals particle size distribution in Class C ash samples, diameters (d) are in microns. From Kulaots et al. 2004.....	64

Figure 3.17: Specific surfactant adsorptivity as a function of conversion during the high-temperature combustion of bituminous and lignite coal, Hachmann et al. (1998).	67
Figure 3.18: Relationship between foam index and BET specific surface area. From Hurt et al. (2001)	68
Figure 3.19: Interactions between surfactant and non-polar carbon surface (left) and oxidized carbon surface (right), (Hurt et al., 2004).	70
Figure 4.1: Calcium ion concentrations in of solution of fly ash.....	76
Figure 4.2: Calcium ion concentrations of ash solutions versus ash percent calcium oxide content.....	77
Figure 4.3: X-ray diffractogram for ash sample FR-2 showing the identification of the presence of mullite ($3\text{Al}_2\text{O}_3\cdot\text{SiO}_2$).	78
Figure 4.4: Particle size distributions of six class F ash samples. Particle sizes are in micrometers.....	80
Figure 4.5: Organic carbon content of the individual particle size fractions of ashes FB-1 and FR-2.....	82
Figure 4.6: Fraction of total organic carbon in sample contributed by each size fraction.....	83
Figure 4.7: Thermogravimetric analysis of sample FR-2 temperature ramp of 10°C per min under air (a) and nitrogen (b).....	84
Figure 4.8: Nitrogen adsorption isotherm for sample FR-1.....	86
Figure 4.9: Foam index values of sieved ash fractions for ash samples FB-1 and FR-2.....	92
Figure 4.10: Example of absorbance versus concentrations of a commercially available AEA.	93
Figure 4.11: Mass remaining versus exposure temperature for four fly ash samples. (Mass remaining based on oven-dried weight.	94
Figure 4.12: Ash average grayscale value versus temperature exposure for seven Class F ash samples.	95
Figure 4.13: Ash average grayscale value versus temperature exposure for three Class C ash samples	95
Figure 4.14: Foam index versus temperature exposure for two ash samples.	96
Figure 4.15: Organic carbon content versus temperature exposure for two fly ash samples.....	97
Figure 5.1: Concrete AEA dosages for 6% target air concrete versus ASTM C311 loss on ignition content for Texas ash samples.....	99
Figure 5.2: Performance of the LOI test by heating sample of fly ash in a muffle furnace.	101
Figure 5.3: Mass of carbon black remaining after exposure to air at various temperatures.	103
Figure 5.4: Specific soot oxidation rate as a function of temperature from Park and Appleton (1973).....	104
Figure 5.5: Mass of charcoal remaining after 30 min exposure to air at various temperatures.....	105
Figure 5.6: Mass of charcoal samples remaining after varying durations of exposure to 500°C air.	106

Figure 5.7: The organic carbon content of two ash samples after exposure to various temperatures in an air atmosphere	109
Figure 5.8: Change in mass with temperature of aluminum, iron and silicon oxides.....	111
Figure 5.9: Thermo gravimetric analysis of sample FR-2 temperature ramp of 10°C per min under air (a) and nitrogen (b).....	113
Figure 5.10: Fly ash sample mass remaining after 60 min of heating.....	114
Figure 5.11: Modified loss on ignition values versus ASTM C 311 loss on ignition values (compared against the line $x = y$).....	121
Figure 5.12: ASTM C 311 loss on ignition values versus organic carbon content of Texas commercial fly ash samples (compared against the line $x = y$).....	122
Figure 5.13: Modified loss on ignition versus total organic carbon content of Texas commercial fly ash samples (compared against the line $x = y$).....	122
Figure 5.14: Mass loss in four separate temperature ranges for seven ash samples.....	125
Figure 5.15: Concrete AEA dosages for 6% air versus modified loss on ignition values of sixteen Texas ash samples.	128
Figure 5.16: AEA dosages for fly ash concrete versus ASTM C311 loss on ignition.	128
Figure 5.17: Comparison of mass changes of the two ash classes in three temperature divisions.....	129
Figure 5.18: Map of the mass losses from fly ash sample located at the center of the unit area.....	133
Figure 6.1: Required dosage of AEA S1 to produce 6% air in a concrete mixture containing fly ash from four sources. Dosage is scaled to mL of AEA per 100 kg of cementitious materials (cement + ash).	142
Figure 6.2: Containers used in the four foam index test variants.	144
Figure 6.3: Sequence of foam accumulation at the liquid-air interface of the foam index test. The test endpoint is reached when the interface is completely covered with foam, as shown in e.....	147
Figure 6.4: The foam index values of fly ash samples L, ML, MH and H as determined by four foam index test variants. Each value represents the mean AEA volume of five tests.	150
Figure 6.5: Correlations of specific foam index values with concrete air data for the four foam index test variants.	151
Figure 6.6: Comparative results of test methods in which each method uses a unique set of ingredients and proportions (a) and comparative results of test methods in which a standard set of ingredients and proportions were applied in all tests (b).	155
Figure 6.7: Foam index test container dimensions.	161
Figure 6.8: Containers used in the foam index variability study on container geometry.	162
Figure 6.9: Specific foam index versus $1/\gamma h$ for fifty-two tests in eight containers. Air/paste ratios computed for t_f equal to 4mm. Error bars show the minimum resolution as plus or minus one drop of AEA solution.....	163
Figure 6.10: Specific foam index versus fill ratio. The value of $1/\gamma h$ was equal to 0.02 mm^{-1} in all tests.....	165

Figure 6.11: Relationships among container diameter, filled height, and minimum resolution, R_{min} .	167
Figure 6.12: The shaded zone identifies the range of acceptable solutions for a container for the foam index test.	168
Figure 6.13: Specific foam index obtained at various shaking frequencies and shaking durations.	170
Figure 6.14: Specific foam index values of four ash samples for two values of R_{min} .	172
Figure 6.15: Percentage of tests within one drop of the mean number of AEA drops to transfer a minimum of 20 microliters of AEA versus pipet standard deviation. Variable v is equal to drop volume in microliters and variable c_{AEA} is equal to AEA concentration.	173
Figure 6.16: Specific foam index values of four fly ash samples produced by three test operators. Each horizontal line in the graph represents a single drop volume ($R_{min} = 8 \text{ mL AEA per } 100 \text{ kg cm}$).	174
Figure 6.17: Specific foam index versus water-to-cement ratios.	179
Figure 6.18: Specific foam index per percent air content versus water-to-cement ratios.	180
Figure 6.19: The foam index values of four commercial fly ash samples for a w/cm of 2.0 and various a/cm ratios between 0.1 and 1.0.	183
Figure 6.20: Effects of water to cementitious materials ratio (y-axis) and ash to cementitious materials ratio (x-axis) on foam index values with other test variables held constant. Foam index values are in units $\text{mL AEA}/100 \text{ kg cm}$.	184
Figure 6.21: Estimated foam index values using regression coefficients versus actual foam index test data. Reference line shown is $x = y$.	185
Figure 6.22: Estimated specific foam index values per percent air using regression coefficients versus actual test data. The reference line shown is $x = y$.	186
Figure 6.23: Specific foam index versus grams cement in test, water volume was equal to 25 mL in all tests.	188
Figure 6.24: Specific foam index per percent air content versus water-to-cement ratios.	189
Figure 7.1: Ash samples arranged in order of descending LOI values from left to right and top to bottom. (Percent LOI values are shown below ash codes.)	195
Figure 7.2: Ash samples arranged in order of descending concrete AEA dosage values from left to right and top to bottom. (AEA dosage in units of $\text{mL AEA}/100 \text{ kg cm}$ for 6% air content are shown below ash codes.)	195
Figure 7.3: AEA dosage of fresh concrete versus grayscale value for 18 ash samples.	196
Figure 7.4: Canon CanoScan LiDE 500F color image flatbed scanner.	197
Figure 7.5: Scanning template.	197
Figure 7.6: Fly ash sample scanning materials: 1) oven-dried fly ash, 2) weighing paper, 3) cuvetts, and 4) putty.	198
Figure 7.7: Cuvet filling and stopping with putty plug.	199
Figure 7.8: Position of cuvet during scanning (left) and blocking ambient light with a cardboard box (right).	200

Figure 7.9: Typical scanned image of ash sample in cuvet held in place by the paper template (left), selection of the region of interest for color analysis (right).	200
Figure 7.10: Comparison of grayscale values between two different scanner models.	203
Figure 7.11: Grayscale band of Kodak IT8.7 calibration target.	204
Figure 7.12: Mean grayscale value versus analysis area.	205
Figure 7.13: Effect of background color on chip scan.	206
Figure 7.14: Ash sample scan with background ambient light (left) and with ambient light blocked (right).	207
Figure 7.15: Average 8-bit grayscale value ash samples versus sample moisture content, points are labeled by ash environment.	208
Figure 7.16: Deviation from the reference color of paint chips scanned through different materials.	211
Figure 7.17: Variability in grayscale of 10 samples. The bars on each data point show the minimum and maximum grayscale values of the three scanned sides of each sample.	212
Figure 7.18: The number of individual 24-bit RGB colors per single 8-bit grayscale value.	213
Figure 7.19: Average grayscale values of the Texas ash set. Dotted lines show the average grayscale values of the Class F and C ashes.	215
Figure 7.20: Ash average grayscale value versus temperature exposure for seven Class F ash samples.	222
Figure 7.21: Ash average grayscale value versus temperature exposure for three Class C ash samples.	223
Figure 7.22: Organic carbon content versus temperature exposure for two fly ash samples.	224
Figure 7.23: Change in grayscale value versus organic carbon content for the non-sieved ash samples.	229
Figure 7.24: Change in grayscale value versus organic carbon content for all samples.	230
Figure 7.25: Concrete AEA dosages required for 6 percent air in concrete versus change in grayscale values between 105 and 750°C.	232
Figure 7.26: Concrete AEA dosages required for 6 percent air in concrete versus change in grayscale values between 300 and 500°C.	233
Figure 8.1: Correlation between concrete AEA dosage and organic carbon content of Texas fly ash samples.	239
Figure 8.2: Relationship between modified LOI and Concrete AEA dosage for 6 percent air.	240
Figure 8.3: Relationship between modified LOI and organic carbon content of Texas ash samples.	241
Figure 8.4: Correlation between concrete AEA dosages and foam index values for all Texas fly ash samples.	242
Figure 8.5: Foam index versus temperature exposure for two ash samples.	243

Figure 8.6: Organic carbon content versus temperature exposure for two fly ash samples.	244
Figure 8.7: Foam index versus organic carbon content for two ash samples.	244
Figure 8.8: Foam index values versus organic carbon content for all Texas fly ash samples.....	245
Figure 8.9: Concrete AEA dosages vs. ash grayscale change for the Texas fly ash samples.....	246
Figure 8.10: Grayscale value versus exposure temperature for two Texas ash samples.	247
Figure 8.11: Relationship between change in grayscale value of Texas ash samples and sieved ash fractions when heated from 300 and 500°C and organic carbon content.	248
Figure 8.12: Grayscale values for size fractions sieved from ash FR-2	249
Figure 8.13: Relationship between concrete AEA dosage and BET specific surface area for selected fly ash samples. This pattern mimics the clearer pattern for AEA dose versus organic carbon.	253
Figure 8.14: Correlation between organic carbon content and BET surface area.	254
Figure 8.15: Organic carbon size distributions in two ash samples.....	257
Figure 8.16: Specific foam index values of sieved ash fractions versus organic carbon content of the size fractions (Row B in Tables 8.4 and 8.5), size labels are shown in micrometers.	258
Figure 8.17: Foam index per mg organic carbon content for sieved fractions of two ash samples.....	259
Figure 8.18: Foam index versus estimated solid carbon external surface area for seven fly ash size fractions from two samples.	260
Figure 11.1: Fly ash compositions: major components	282
Figure 11.2: Fly ash compositions: minor components	282
Figure 11.3: Physical test results for fly ashes and concrete mixtures normalized to the values for fly ash 6.....	285
Figure 11.4: Dosage of AEA required to achieve 6% air in concrete versus the LOI value of the fly ash.....	285
Figure 11.5: Dosage of AEA required to achieve 6 percent air in concrete versus the LOI value of the fly ash.....	286
Figure 11.6: The results from the foam index test versus the dosage of AEA to achieve 6% air in concrete.	289
Figure 12.1: ASTM C 311 results with fly ash 1 and 7	296
Figure 12.2: The change in air content for different cm/sand and different dosages of tall oil AEA with fly ash 1.	297
Figure 12.3: The change in flow for different cm/sand and different dosages of tall oil AEA with fly ash 1.	298
Figure 12.4: Air content of a modified mortar mixture with various dosages of tall oil AEA.	299
Figure 12.5: Flow of a modified mortar mixture with various dosages of tall oil AEA.....	299

Figure 12.6: The air content of a modified ASTM C 311 test with various AEA at a dosage of 0, 128, and 512 mL/100 kg of cm.	301
Figure 12.7: The flow of a modified ASTM C 311 test with various AEA at a dosage of 0, 128, and 512 mL /100 kg of cm.....	301
Figure 12.8: A comparison between the results of the modified ASTM C 311 test and the dosage of wood rosin AEA in concrete to produce 6% air for 15 different fly ashes.....	302
Figure 13.1: Air content versus AEA dosage from single mixture method compared to several individual mixtures with a trend line fit to the single mixture method results.	310
Figure 13.2: AEA demand interpolated from single mixture method for two different fly ashes with different dosages of WR.....	312
Figure 14.1: Comparison of air content from the ASTM C 231 pressure method and the hardened air content.....	329
Figure 15.1: Setup #1 showing orientation of bottle, stereoscope, and point light source.	339
Figure 15.2: Time and temperature for the ambient temperature, a specimen under the point light source, and a specimen in the ambient temperature.....	340
Figure 15.3: A cross section of setup #2 showing the reduced paste level and additional water provided by the tube with the modified lid.	341
Figure 15.4: An air-entrained paste containing a tall oil AEA at 143 mL/100 kg cm in setup #1 whose bubbles are pushed by the paste below.	343
Figure 15.5: A non-air-entrained paste sample in setup #1 whose bubbles are pushed by the paste below.....	345
Figure 15.6: A non-air-entrained paste sample in setup #2.	347
Figure 15.7: Average diameter of bubbles in a non-air-entrained paste specimen as shown in Fig. 15.6 in setup #2.....	348
Figure 15.8: The response of bubbles escaped from a mixture containing 26 mL/100 kg cm of Vinsol resin and 81 mL/100 kg cm of normal WR subjected to a pressure 0.7 bar above atmospheric and then returned back to atmospheric pressure.....	350
Figure 15.9: An air-entrained paste sample with wood rosin AEA at 48 mL/100 kg cm in setup #3.	352
Figure 16.1: The experimental setup for the physical testing showing the orientation of bottle, stereoscope, and point light source.	358
Figure 16.2: An air-entrained void is shown emerging from a cement paste surface due to buoyancy with cement grains attached. The paste was made with 48 mL/100 kg of cm of wood rosin AEA.	361
Figure 16.3: A. Air-entrained void (48 mL/100 kg of cm wood rosin AEA) after 45 minutes of hydration, B. Non air-entrained voids after 45 minutes of hydration.	363
Figure 16.4: The response of a mixture containing 26 mL/100 kg cm of Vinsol resin and 81 mL/100 kg of normal range water reducer subjected to a pressure 0.7 bar above atmospheric and then returned back to atmospheric pressure.	365

Figure 16.5: The response of an air-entrained void in a mixture (47 mL/100 kg of cm of synthetic AEA and 81 mL/100 kg of normal range water reducer) subjected to a pressure 0.7 bar above atmospheric and then returned back to atmospheric pressure.	367
Figure 16.6: A void in bleed water above a cement paste (48 mL/100 kg of cm of a wood rosin AEA) was subjected to a pressure 0.7 bar above atmospheric and then returned back to atmospheric pressure.....	369
Figure 16.7: Change in C ₃ S and CaCO ₃ content with time is shown for the bulk cement paste and the air-void shells created with wood rosin and synthetic AEAs	371
Figure 16.8: SEM image of an air-entrained void from a mixture containing wood rosin AEA at 48 mL/100 kg of cement that was allowed to hydrate for 60 days before examination. An overview of the void is shown in Fig. 16.8A. The surface of the air-void is shown in Fig. 16.8B. Fig. 16.8C and 16.8D show the voids surface under increased magnification.	373
Figure 16.9: A SEM image of the interface between the air-void in Fig. 16.8 and the bulk paste. In Fig.16.9B a closeup is shown of Fig. 16.9A.	374
Figure 21.1: Mixing Procedure	398
Figure 21.2: 3 ft ³ Drum Mixer	400
Figure 21.3: Sample Prepared for Composite Rating Evaluation.....	402
Figure 21.4: Samples prepared for hardened air void analysis. (a) Low air content, (b) high air content	403
Figure 21.5: 9 ft ³ Drum Mixer	404
Figure 22.1: Change in Slump for Phase I Mixtures	408
Figure 22.2: Unit Weight vs. Fresh Air Content.....	409
Figure 22.3: Gravimetric Air Content vs. Air Content (pressure method).....	409
Figure 22.4: Changes in Air Content for Phase I Mixtures	410
Figure 22.5: 28-Day Compressive Strength vs. Air Content (Pressure Method) for Mixtures Containing AEA “A”.....	411
Figure 22.6: 28-Day Compressive Strength vs. Air Content (pressure method) for Mixtures Containing AEA “B”.....	413
Figure 22.7: 28-Day Compressive Strength vs. Air Content (pressure method) for Mixtures Containing AEA “C”.....	414
Figure 22.8: 28-Day Compressive Strength vs. Air Content (pressure method) for Mixtures Re-tempered to a 0.50 w/c and Containing AEA “A”.....	416
Figure 22.9: Changes in Composite Rating after Re-tempering Phase I Mixtures.....	418
Figure 22.10: Composite Rating vs. Air Content (pressure method) for Phase I Mixtures.....	419
Figure 22.11: Composite Rating vs. 28-Day Compressive Strength for Mixtures Re-tempered to a 0.48 w/c for all AEA Types	419
Figure 22.12: Calculated % Strength Loss vs. Composite Cluster Rating	420
Figure 22.13: Change in slump for Phase II Mixtures.....	421
Figure 22.14: Unit Weight vs. Air Content (pressure method) for Phase II Mixtures	422

Figure 22.15: Gravimetric Air Content vs. Air content (pressure method) for Phase II Mixtures	423
Figure 22.16: Changes in Air Content for Phase II Mixtures	424
Figure 22.17: 28-Day Compressive Strength vs. Air Content (pressure method) for Mixtures Containing AEA “A” and Limestone Coarse Aggregate	425
Figure 22.18: 28-Day Compressive Strength vs. Air Content (pressure method) for Mixtures Containing AEA “B” and Limestone Coarse Aggregate	425
Figure 22.19: 28-Day Compressive Strength vs. Air Content (pressure method) for Mixtures Containing AEA “A” and Siliceous Coarse Aggregate	426
Figure 22.20: 28-Day Splitting Tensile Strength vs. Air Content (pressure method) for Mixtures Containing AEA “A” and Limestone Coarse Aggregate	427
Figure 22.21: 28-Day Splitting Tensile Strength vs. Air Content (pressure method) for Mixtures Containing AEA “B” and Limestone Coarse Aggregate	427
Figure 22.22: 28-Day Splitting Tensile Strength vs. Air Content (pressure method) for Mixtures Containing AEA “A” and Siliceous Coarse Aggregate	428
Figure 22.23: 7-Day Flexural Strength vs. Air Content (pressure method) for Mixtures Containing AEA “A” and Limestone Coarse Aggregate.....	429
Figure 22.24: 7-Day Flexural Strength vs. Air Content (pressure method) for Mixtures Containing AEA “B” and Limestone Coarse Aggregate.....	429
Figure 22.25: 7-Day Flexural Strength vs. Air Content (pressure method) for Mixtures Containing AEA “A” and Siliceous Coarse Aggregate.....	430
Figure 22.26: Changes in Composite Cluster Ratings for Phase II Mixtures.....	431
Figure 22.27: Composite Cluster Ratings vs. Air Content (pressure method)	432
Figure 22.28: Composite Cluster Ratings vs. 28 Day Compressive Strength	433
Figure 22.29: Composite Cluster Ratings vs. 28 Day Splitting Tensile Strength.....	433
Figure 22.30: Composite Cluster Ratings vs. 7-Day Flexural Strength	434
Figure 22.31: Fresh Air Content vs. Hardened Air Content.....	435
Figure 22.32: Changes in Spacing Factor	436
Figure 22.33: Changes in Specific Surface.....	437
Figure 22.34: Composite Rating vs. Spacing Factor	438
Figure 23.1: Clustering of the Air Voids Around the Aggregate (Photo courtesy of E. Morgan).....	440
Figure 23.2: (a), (b), and (c) show evidence of re-tempering, (a) and (b) show clustering of the air void around the aggregate, but not within the low w/c paste (Photos courtesy of E. Morgan)	442
Figure 23.3: Evidence of Re-tempered Concrete. (a) Area of low w/c paste in core #1, (b) Area of low w/c paste in core #3 (photos courtesy of E. Morgan).....	443
Figure 23.4: Clustering of Air Voids Around the Coarse Aggregate (a) Core #1, (b) Core #3 (Photo Courtesy of E. Morgan).....	444
Figure 23.5: Clustering of Air Void within the Paste (Photo Courtesy of E. Morgan)	444
Figure 23.6: Air Void Cluster at Aggregate Paste Interface (Photo courtesy of E. Morgan).....	445

Figure 23.7: Excessive Air Voids Around Aggregates (Photo courtesy of E. Morgan).....	447
Figure 23.8: Clustering of the Air Voids Along Aggregate Sockets (Photo courtesy of E. Morgan).....	448
Figure 23.9: Evidence of Re-tempering and Clustering of the Air Voids Around the Aggregate (Photo courtesy of E. Morgan).....	449
Figure A1, Volume 1. RGB and corresponding grayscale values of selected colors.	487
Figure A2, Volume 1. The number of individual 24-bit RGB colors per single 8-bit grayscale value.....	487
Figure A3, Volume 1. The number of individual 24-bit RGB colors per single 8-bit grayscale value for various RGB weights.....	488
Figure A4, Volume 1. Selection of the region of interest for color analysis.	490
Figure A5, Volume 1. Large residual coal particles sieved from fly ash.	494
Figure A6, Volume 1. Scanning electron micrograph of a large carbon particle sieved from fly ash (top).	495
Figure A7, Volume 1. Magnetic ash particles.	496
Figure A8, Volume 1. Elemental analysis of magnetic fly ash. Peak height corresponds with concentration within the analysis region.	496
Figure A9, Volume 1. An enlarged view of 64 pixels (24-bit color) from the analysis region (left) and the average grayscale value (8-bit color) of the pixels (right).	497
Figure A10, Volume 1. Estimated gray values versus measured gray values of the six experimental samples.....	500
Figure A11, Volume 1. Actual grayscale value versus predicted grayscale value.	501
Figure A12, Volume 1. Predicted grayscale change versus measured grayscale change of five ash pairs	503
Figure A13, Volume 1. Measured grayscale value change versus predicted grayscale change between 500-800°C.....	506
Fig. A.1, Volume 2. A raw image and images with reported threshold values.	515
Fig. A.2, Volume 2. Percentage white displayed on the screen as a function of the threshold value chosen for two different locations on the sample surface.	516
Figure B.1, Volume 3. 7-Day Compressive Strength vs. Air Content (pressure method) for Mixtures Containing AEA “A” and Re-tempered to a 0.48 w/c	533
Figure B.2, Volume 3. 7-Day Compressive Strength vs. Air Content (pressure method) for Mixtures Containing AEA “B” and Re-tempered to a 0.48 w/c	533
Figure B.3, Volume 3. 7-Day Compressive Strength vs. Air Content (pressure method) for Mixtures Containing AEA “C” and re-tempered to a 0.48 w/c	534
Figure B.4, Volume 3. 7-Day Compressive Strength vs. Air Content (pressure method) for Mixtures Containing AEA “A” and Re-tempered to a 0.47 w/c	534
Figure B.5, Volume 3. 7-Day Compressive Strength vs. Air Content (pressure method) for Mixtures Containing AEA “A” and Re-tempered to a 0.50 w/c	535

Figure D.1, Volume 3. 7-Day Compressive Strength vs. Air Content (pressure method) for Mixtures Containing AEA “A” and Limestone Coarse Aggregate and Re-tempered to a 0.48 w/c	543
Figure D.2, Volume 3. 7-Day Compressive Strength vs. Air Content (pressure method) for Mixtures Containing AEA “B” and Limestone Coarse Aggregate and Re-tempered to a 0.48 w/c	543
Figure D.3, Volume 3. 7-Day Splitting Tensile Strength vs. Air Content (pressure method) for Mixtures Containing AEA “A” and Limestone Coarse Aggregate and Re-tempered to a 0.48 w/c	544
Figure D.4, Volume 3. 7-Day Splitting Tensile Strength vs. Air Content (pressure method) for Mixtures Containing AEA “B” and Limestone Coarse Aggregate and Re-tempered to a 0.48 w/c	544
Figure D.5, Volume 3. 7-Day Splitting Tensile Strength vs. Air Content (pressure method) for Mixtures Containing AEA “A” and Siliceous Coarse Aggregate and Re-tempered to a 0.48 w/c	545

List of Tables

Table 3.1: Summary of the effects of SCMs on selected properties of fresh concrete (horizontal arrows indicate little to no effects), Thomas and Wilson, 2002.	22
Table 3.2: Summary of the effects of SCMs on selected properties of hardened concrete (horizontal arrows indicate little to no effects), Thomas and Wilson, 2002.	23
Table 3.3: Advantages and disadvantages of surface and underground mining (Ward, 1984)	29
Table 3.4: Silicate and oxide mineral species in coal. From Ishii (2000).	32
Table 3.5: Carbonate, sulfide, sulfate, phosphate and chloride minerals in coal. From Ishii (2000).	33
Table 3.6: States with the largest coal reserves (EIA, 2006).	37
Table 3.7: U.S. Coal Production by State (EIA, 2006).	37
Table 3.8: Characteristics of combustion methods (Miller, 2005).	39
Table 3.9: Coal combustion by-products effects on the environment and human health (Miller, 2005).	44
Table 3.10: Typical compositions of fly ashes, % (Helmuth, 1987).	48
Table 3.11: ASTM C618 Standard specification chemical requirements for fly ash.	51
Table 3.12: Recommended total target air content for concrete, (ACI, 1991).	54
Table 3.13: Effects of supplementary cementitious materials on air content. From Whiting and Nagi (1998).	56
Table 4.1: Fly ash bulk chemistry by X-ray fluorescence (XRF). Testing performed at the Materials Analysis and Research Laboratory at Iowa State University during the Fall of 2006. (Note: sample FL-2 not included).	75
Table 4.2: Major minerals identified by x-ray diffraction of four fly ash samples.	79
Table 4.3: Moisture content, loss on ignition, inorganic carbon, total carbon and organic carbon contents of Texas fly ash samples.	81
Table 4.4: BET surface area and t-plot micropore area for selected fly ash samples.	87
Table 4.5: Grayscale values of oven-dried ash samples and change in grayscale values between 300 to 500°C and 25 to 750°C.	88
Table 4.6: Riedvelt analysis of the type I/II cement.	89
Table 4.7: Components and masses of the materials used in the concrete air tests.	89
Table 4.8: Concrete AEA dosage for 6 percent air, concrete slump and water reducer requirement.	90
Table 4.9: Specific foam index and minimum precision, R_{min} , for the Texas fly ash samples.	91
Table 5.1: Decomposition commencement temperatures in air for carbonates found in coal (Gluskoter et al. 1981, Duval, 1963).	108
Table 5.2: Dehydration temperatures of calcium hydroxide, calcium sulfate hemi-hydrate and gypsum (Duval 1963).	111

Table 5.3: Mass loss (negative value indicates mass gain) in three temperature regimes, soluble calcium contents (units mg Ca ²⁺ /L), organic and inorganic carbon contents (both in units percent mass) for four fly ash samples.....	115
Table 5.4: Comparison of percent mass change to percent organic carbon content change in three temperature regimes for two ash samples.....	118
Table 5.5: Comparison of ash percent mass change between 300 and 500°C due to 60 min exposure and total organic carbon content.....	119
Table 5.6: Sample modified loss on ignition data sheet.	120
Table 5.7: Linear regression statistics of the trend lines in Figure 5.14.	125
Table 5.8: Multi-linear ($y = m_1x_1 + m_2x_2 + \dots + m_nx_n + b$) regression analysis results (from JMP), $y =$ change in mass between 500 and 750°C, parameters are percent inorganic carbon and bulk chemistry oxides.	131
Table 6.1: Summary of several foam index test methods reported in the literature and/or used in industry. (“U” indicates that the value was not specified, * estimated volume for kitchen type blender.).....	139
Table 6.2: Fly ash and AEA sample data.....	141
Table 6.3: Components and masses of the materials used in the concrete air tests.....	141
Table 6.4: Characteristics of four foam index tests evaluated.	143
Table 6.5: Metrics for the comparison of the four foam index test variants.....	143
Table 6.6: The mean number of drops and AEA solution volumes for five repeated tests of each ash. Drop volume and AEA solutions concentrations (shown beneath the heading “Drops”) are not equal in all tests.	148
Table 6.7: The mean, standard deviation and coefficient of variation of drops of AEA for five repeated tests for each ash. Means and standard deviations are presented in units of mL undiluted AEA per 100 kg cementitious materials.	149
Table 6.8: Regression equations, coefficients of determination and standard errors of the foam index test-concrete AEA dosage relationships	151
Table 6.9: The AEA requirement, as predicted by the four foam index test methods, for desired 6% air in concrete containing the indicated fly ash as 20% of total cementitious materials.	152
Table 6.10: Modifications to the four test methods so that each test contained the same proportions of water, ash and cement.	154
Table 6.11: The mean, standard deviation and coefficient of variation of drops of AEA for three repeated tests for each ash.....	154
Table 6.12: Average relative foam index across all four ashes for each method.	155
Table 6.13: Coefficients of determination and standard errors of the foam index test-concrete AEA dosage regressions.....	156
Table 6.14: Material Properties.....	159
Table 6.15: Description of test containers.	161
Table 6.16: Description of an ideal container for the foam index test.....	169
Table 6.17: Material properties.....	177

Table 6.18: AEA dilution and drop size for each a/cm ratio tested.....	182
Table 6.19: Linear regression coefficients of the two variables w/cm and a/cm and y-intercept.....	184
Table 6.20: Linear regression coefficients of the three variables water, cement and ash and y-intercept to produce estimated of specific foam index per percent air.	186
Table 7.1: Twenty-four-bit color conversion weights	201
Table 7.2: RGB and grayscale values of selected Kodak IT8.7 gray patches as determined by author’s scanner.	204
Table 7.3: Compaction method description.....	209
Table 7.4: Grayscale values of ash samples prepared with differing degrees of compaction.....	209
Table 7.5: Relative change in grayscale values compared to method A	209
Table 7.6: Sources of variability in the test procedure and their effects on measured grayscale values.	214
Table 7.7: Twenty-four-bit color conversion weights	219
Table 7.8: Grayscale values, and grayscale difference after exposure to 105 and 750°C, and concrete AEA dosages.	225
Table 7.9: Change in grayscale values between 300 and 500°C and organic carbon content of ash samples.	226
Table 7.10: Fly ash bulk chemistry by X-ray fluorescence (XRF), note sample FL-2 is not included.....	227
Table 7.11: Regression analysis results (from JMP), Y= change in grayscale value, parameters organic carbon and calcium oxide.....	228
Table 8.1: Lessons learned regarding fly ash-AEA interactions and the tests that contributed to the learning.	237
Table 8.2: Fundamental factors that influenced the lessons learned in Table 8.1	238
Table 8.3: Factors influencing ASTM C311 LOI results.	251
Table 8.4: Properties of sieved fractions of Ash FB-1.....	255
Table 8.5: Properties of sieved fractions of Ash FR-2.....	256
Table 11.1: Chemical and physical properties of fly ashes	281
Table 11.2: Standard concrete mixture proportions.....	283
Table 12.1: Mortar mixture design	292
Table 12.2: Composition of the Type I/II cement as determined by RQXRD	293
Table 12.3: Oxide analysis, LOI, and AEA demand in concrete with fly ash.....	294
Table 12.4: Composition of the Type I/II cement as determined by RQXRD	295
Table 12.5: The average percent difference for the percent air content and flow of replicate mixes of 15 different fly ashes with a wood rosin AEA with the modified mixture.	302
Table 13.1: Composition of the Type I/II cement as determined by RQXRD	307
Table 13.2: Oxide analysis and LOI data for three fly ashes.....	308

Table 13.3: Concrete Mixture Design.....	308
Table 13.4: Comparison of measured air content in mixtures with single dosages of AEA and that predicted by a mixture using multiple dosages of AEA.	311
Table 13.5: AEA demand for two fly ashes with different dosages of WR.	312
Table 13.6: A ranking of several fly ashes commercially used in concrete by the AEA demand from the single mixture method	314
Table 13.7: Effects of mixing temperature and fly ash replacement on AEA demand in concrete for three fly ashes.	315
Table 13.8: Effects of AEA type on AEA demand in concrete for three fly ashes.	315
Table 14.1: Composition of the Type I/II cement as obtained through RQRXD.....	323
Table 14.2: Oxide analysis and LOI data for three fly ashes.....	324
Table 14.3: Concrete Mixture Composition	325
Table 14.4: Aggregate correction factor for three aggregate sources with various moisture content.....	326
Table 14.5: Repeatability of five different mixtures each analyzed twice with the AVA.....	327
Table 14.6: Comparison of estimates from the pressure meter, hardened air-void analysis and the air void analyzer.	328
Table 14.7: Comparison of mixture information, fresh air volume, hardened air-void analysis, and rapid freeze-thaw testing.	330
Table 15.1: Summary of previous research completed on air-void stability and the bubble shell.....	337
Table 15.2: Mixtures investigated.....	338
Table 16.1: Summary of the RQXRD analysis for the air-void shells and bulk paste.	357
Table 19.1: Classification and Performance Characteristics of Air-Entraining Admixtures (adapted from Kosmatka et al. 2002).....	388
Table 20.1: Cement Chemical Analysis.....	395
Table 20.2: Aggregate Properties	396
Table 20.3: Aggregate Gradation.....	396
Table 20.4: Air-entraining Admixtures.....	396
Table 21.1: Mix Design Proportions.....	399
Table 21.2: Sample Calculations of Composite Rating	402
Table 22.1: Compressive Strength Loss due to Air Void Clustering for Mixtures 1-7	412
Table 22.2: Compressive Strength Loss due to Air Void Clustering for Mixtures 14-20	415
Table 22.3: Compressive Strength Loss due to Air Void Clustering for Mixtures 8-13	417
Table 23.1: Field Test Results	439
Table 23.2: Core Test Results.....	440
Table 23.3: 28-Day Compressive Strengths and Hardened Air Contents of Core Samples.....	441
Table 23.4: 7-Day Flexural Strengths of Concrete	443
Table 23.5: Compressive Strengths of Concrete Core Samples	443
Table 23.6: Compressive Strengths of Concrete Cylinders	445

Table 23.7: 31-Day Compressive Strengths of Core Samples.....	446
Table 23.8: Compressive Strengths of Concrete.....	447
Table A1, Volume 1. Twenty-four-bit color conversion weights.....	486
Table A2, Volume 1. Minimum, maximum and average RGB values of the 64 pixels in Figure A9.	498
Table A3, Volume 1. Ingredients, compositions and gray values of six samples.	499
Table A4, Volume 1. Regression coefficients.	499
Table A5, Volume 1. Regression coefficients	501
Table A6, Volume 1. Change in percent metal oxides content, percent carbon content and grayscale value between pairs of ashes collected from the same source.	503
Table A7, Volume 1. Regression coefficient and statistics.	505
Table A.1, Volume 2. Results from a hardened air-void analysis with different traverse lengths.	512
Table A.2, Volume 2. Comparison of the threshold value chosen for three different users.....	513
Table A.3, Volume 2. A comparison of hardened air-void results with different threshold values.	514
Table A.1, Volume 3. Fresh Concrete Properties for Re-tempered Mixtures Containing Air-Entraining Admixture “A”	523
Table A.2, Volume 3. Fresh Concrete Properties for Re-tempered Mixtures Containing Air-Entraining Admixture “A”	524
Table A.3, Volume 3. Fresh Concrete Properties for Re-tempered Mixtures Containing Air-Entraining Admixture “B” & “C”	525
Table A.4, Volume 3. Fresh Concrete Properties for Non-Re-tempered Mixtures	526
Table B.1, Volume 3. Compressive Strengths for Re-tempered Mixtures Containing Air- Entraining Admixture “A”	529
Table B.2, Volume 3. Compressive Strengths for Re-tempered Mixtures Containing Air- Entraining Admixture “A”	530
Table B.3, Volume 3. Compressive Strengths for Re-tempered Mixtures Containing Air- Entraining Admixture B & C.....	531
Table B.4, Volume 3. Compressive Strengths for Non-Re-tempered Mixtures.....	532
Table B.5, Volume 3. Composite Clustering Ratings for Re-tempered Mixtures Containing Air-Entraining Admixture “A”	536
Table B.6, Volume 3. Composite Clustering Ratings for Re-tempered Mixtures Containing Air-Entraining Admixtures “B” and “C”	537
Table B.7, Volume 3. Composite Clustering Ratings for Non- Re-tempered Mixtures.....	537
Table C.1, Volume 3. Fresh Concrete Properties for Re-tempered Mixtures Containing Air-Entraining Admixtures “A” and “B”.....	539
Table C.2, Volume 3. Fresh Concrete Properties for Non-Re-tempered Mixtures Containing Air-Entraining Admixtures “A” and “B”.....	540

Table D.1, Volume 3. Hardened Concrete Properties for Re-tempered Mixtures Containing Air-Entraining Admixtures “A” and “B”	541
Table D.2, Volume 3. Hardened Concrete Properties for Non-Re-tempered Mixtures Containing Air-Entraining Admixtures “A” and “B”	542
Table D.3, Volume 3. Composite Clustering Ratings for Re-tempered Mixtures.....	545
Table D.4, Volume 3. Composite Clustering Ratings for Non-Re-tempered Mixtures	546
Table E.1, Volume 3. Hardened Air Void Analysis	547

Chapter 1. Introduction and Scope

In order to produce durable concrete in regions exposed to cycles of freezing and thawing, it is essential that concrete be air entrained. Air entrainment is achieved through the use of air-entraining admixtures (AEAs), which have been used successfully for over 60 years. However, there are some practical difficulties in properly entraining air in concrete as many factors impact the ability to generate the desired air-void system, including issues related to materials, mixture proportions, mixing, placing, consolidating, and climatic conditions. In recent years, concrete producers and contractors in the state of Texas have experienced particular difficulties with air-entrained concrete. Some of these difficulties were attributed to changes in the characteristics of fly ash due to the installation of low-NO_x burners in coal-burning power plants. Other problems, independent of fly ash, were also reported in which significant discrepancies were found between the air content measured in fresh concrete and the air content measured in hardened concrete.

Because of the aforementioned problems, the Texas Department of Transportation (TxDOT) initiated a research project (TxDOT 5207, Effects of Texas Fly Ash on Air-Entrainment in Concrete), with the following main objectives:

- Investigate and recommend test methods for assessing fly ash and effects on air entrainment
- Develop guidelines for managing air content when using fly ash
- Investigate test methods to estimate air-void system using fresh concrete
- Investigate the reported discrepancy between fresh and hardened properties in concrete
- Investigate the occurrence of air-void clustering in air-entrained concrete

These objectives constitute a diverse set of research topics that are not only fundamental to properties encountered in the state of Texas but throughout the world where air-entrained concrete is used. To meet these objectives, a research team led by Dr. Kevin Folliard (UT) and Dr. Kenneth C. Hover (Cornell University) was assembled, with the joint research conducted at both universities.

This final report is comprehensive and describes in detail the major aspects of the research performed at both The University of Texas at Austin and Cornell University. The report is presented in three volumes, as shown:

- **Volume 1 (Chapters 2–9)**—“Evaluating the Influence of Fly Ash on Air-Entrained Concrete,” based on Nathan Harris’s Ph.D. Dissertation at Cornell University (2007).
- **Volume 2 (Chapters 10–17)**—“The Effects of Fly Ash on the Ability to Entrain and Stabilize Air in Concrete,” Tyler Ley’s Ph.D. Dissertation at The University of Texas at Austin (2007).

- **Volume 3 (Chapters 18–24)**—“Clustering of Air Voids around Aggregates in Air-Entrained Concrete,” Andrew Naranjo’s M.S. Thesis at The University of Texas at Austin (2007).

After presenting the three volumes described, a brief concluding chapter is presented that summarizes the key findings and recommendations and identifies future research needs.

VOLUME I

Chapter 2. Evaluating the Influence of Fly Ash on Air-Entrained Concrete

2.1 Research objectives

The main objectives of the research described herein are to:

1. To better understand fundamental behavior and predict performance identify and characterize the properties of fly ash that influence interaction with the industrial surfactants known as air entraining admixtures (AEAs) in concrete.
2. Identify or develop effective methods for measuring the interactions between fly ash and AEAs so that variability in the fly ash can be detected and the AEA dosage of concrete incorporating the ash can be adjusted to compensate.
3. Develop a plan for industry implementation of the test methods.

This research was conducted in response to the problem of the difficulty in predicting the dosage of air entraining admixture required to achieve a specified total air content in concrete that incorporates fly ash as a cementitious material, and must resist the action of freezing and thawing of absorbed water in the service environment. The nature of this problem and a synopsis of the state-of-the-practice and of the challenges involved follows in this introduction. A more detailed background and literature survey can be found in Chapter 3.

2.2 Problems with air entrained concrete

In many regions of the world climatic conditions necessitate the need for air-entrained concrete. Incorporation of the adequate amount of finely dispersed air voids in concrete is crucial to the serviceability of concrete. Generally speaking, if the volume of air voids in the hardened concrete is too low, or if the air voids are too dispersed in the hardened cement paste, the concrete will not resist the damage caused by freezing and thawing, potentially resulting in the concrete failing its intended purpose.¹ Conversely, if the air content is too high, then the strength of the concrete may be compromised also potentially resulting in inadequate performance.

To produce the correct air content in concrete, precise volumes of specialty surfactants called air entraining admixtures (AEAs) are added during batching to stabilize air bubbles in the fresh concrete. However, the required AEA dosage can vary due to a wide variety of factors including intended air content, mixture proportions and ingredients, and specifics of how the concrete is batched, mixed, and transported. When properties of mixed ingredients influence AEA dosage change in a predictable manner, the AEA dosage can be adjusted to compensate. However if changes in those properties occur unnoticed, then the result can be under- or over-dosed air content and unacceptable concrete. Detecting changing characteristics of ingredients is particularly important when pulverized coal fly ash is used as a supplementary cementitious material (SCM) in concrete. This is because of the tendency of constituents in the ash (generally

¹ As discussed in detail in Chapter 2 and the references therein, air voids serve as pressure relief zones to accommodate the expansion associated with the freezing of water absorbed in the pores of the concrete.

supposed to be related to forms of carbon) that can inhibit the ability of the AEA to stabilize air bubbles in fresh concrete.

Fly ash used in concrete is produced as a byproduct of pulverized coal combustion, typically in coal-fired electric power plants. It is formed within combustion chambers and at high temperatures, from mineral inclusions present in coal that are liberated as the combustible portion of the coal is consumed. Fly ash consists mostly of fine, glassy, spherical particles typically less than 60 μm in diameter that are carried by the flue gases from the combustion chamber (or “fly”) and are collected in particulate controls systems. Small but variable amounts and forms of carbon are present with the mineral species in the ash, but as long as certain physical and chemical requirements are met, the ash usually requires no further beneficiation and can be distributed to batch plants for use in concrete. Fly ash is used in addition to or as a partial replacement for portland cement, sometimes in combination with other supplementary cementitious materials (SCMs) as the binder for the aggregates. Fly ash is typically present as 15 to 30 percent (or more) of the total cementitious materials in a concrete system.

Fly ash, by the nature of its formation, can be highly variable. It is a byproduct of the production of electrical power. From the viewpoint of the power companies that produce fly ash, quality of the ash is secondary to economical operation of the power plant. Thus, ash properties can be highly variable depending on the parent coal material, plant operation/combustion conditions, and collection methods. This variability can directly influence AEA dosage.

2.3 Predicting fly ash influence on AEA dosage

The incorporation of fly ash in concrete can provide numerous benefits for concrete properties, economics, and sustainability. However, the risk of jobsite rejection of fresh concrete, or the risk of compromised performance of hardened concrete containing fly ash has in some cases prevented the industry from taking full advantage of the material. From the viewpoint of the practitioner, this problem can be remedied by the application of a test (either standard, modified or new) that reliably predicts AEA interactions in cementitious materials. This type of test could be used by ash producers/distributors, cement producers or concrete producers to identify the influence of a certain material on AEA dosage, and to guide compensating adjustments to the mixture.

2.4 Texas DOT sponsors research into predicting fly ash-AEA interactions

The Texas Department of Transportation (TxDOT), like other agencies, requires air entrained concrete for all bridge decks in the state. Problems with variable air content in concrete containing fly ash, however, have developed in recent years. Problems were typically manifested by the rejection of concrete at the jobsite due to high or low air content, or in some cases, by low strength cylinder tests which, when investigated, were found to possess excessive air contents (some deck cores contained air contents as high as 14 percent, more than double the specified air content). The excessive air contents are suspected to be the result of a) the concrete producer having initially increased AEA dosage to compensate for a change in fly ash properties that increased AEA interaction and b) excessive air content when a subsequent change to a less interactive ash was undetected. This highlights the need for a method of identifying and predicting ash-AEA interactions in concrete.

To address this issue, TxDOT sponsored research performed jointly by The University of Texas (Austin) and Cornell University to assess or develop testing methods that can predict AEA interactions with fly ash.

2.5 Existing tests for predicting fly ash-AEA interactions

A suitable starting point for the investigation is an examination of two tests currently used for assessing fly ash properties related to AEA interactions. The first, loss on ignition, is an industry standard test that is routinely performed on fly ash. Test results are passed from the ash distributor to the concrete producer when ash is delivered. The second, foam index, is not a standard test although several variations of this test have seen limited use.

2.5.1 Loss on ignition: the industry method for predicting fly ash-AEA interactions

The loss on ignition test measures mass lost when ash is heated to 750°C. Many have linked fly ash-AEA interactions with the results of the standard loss on ignition (LOI) test (ASTM C 311). Some researchers have concluded that as fly ash LOI increases, AEA dosage also increases (Whiting and Nagi, 1998; Hurt et al., 2001). Therefore, the specification of fly ash for use in concrete developed by ASTM (ASTM C 618), which has been adopted by many state/local agencies to govern the quality of fly ash for concrete, limits the maximum LOI content of ash to 6 percent to control the impact of fly ash on AEA dosage.

Why use LOI?

The LOI test is the only industry-standard test routinely used to provide information about the likelihood of fly ash-AEA interaction. The LOI test is used for this purpose based on two assumptions:

Assumption 1: Many link the observed problems with AEA interaction to the presence of so called “carbon” in the ash, as inferred by estimates of “carbon” mass (Freeman et al., 1997; Hill et al., 1997). This is based on the well-known tendency of organic compounds, such as the surfactants, which are used as AEA’s to adsorb to the surfaces of carbon particles.

Assumption 2: Many interpret LOI to be a measurement of the mass of so called “carbon” (Whiting and Nagi 1998, Hurt et al. 2001). This is based on the well known fact that some forms of carbon commonly found in fly ash are oxidized to CO₂ and water vapor at temperatures of 750°C or less.

What might be wrong with LOI?

The two assumptions listed above are linked in the LOI test. The LOI test is therefore used as a measurement of the “carbon” content of ash. Test results are used to infer the influence of the ash on AEA dosage in concrete.

LOI test results and ash influence on AEA dosage can be poorly correlated. Figure 2.1 gives an example of the ineffectiveness of the LOI test as a predictor of the dosage of AEA required to entrain 6 percent air in concrete mixes incorporating several Texas commercial fly ashes. Data for concrete AEA dosage were collected by Ley at the University of Texas. Other methods used to determine the values shown are discussed throughout this report. As shown by the figure, contrary to common expectations, there is only an approximate relationship ($R^2 = 0.3$) between AEA dosage and LOI for these ash samples. The loss on ignition test is thus not particularly useful for assessing ash quality with respect to AEA dosage requirement for these ashes.

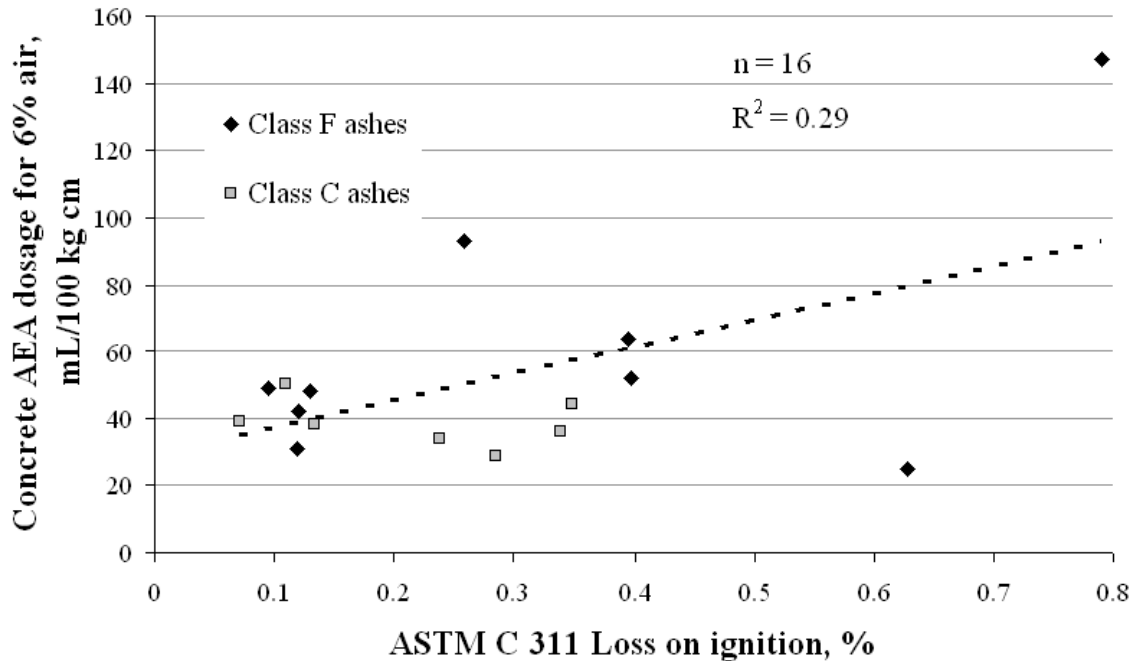


Figure 2.1: AEA dosages for fly ash concrete versus fly ash loss on ignition content.

Based on Figure 2.1, it can be concluded that either the assumption that the primary source of AEA interaction is carbon in the ash, or the assumption that LOI measures carbon in the ash, is incorrect, or the combination of the two assumptions is unreliable. On the basis of this project, it is hypothesized that, while both assumptions are based on fact, both assumptions are far more complex than previously recognized. Therefore in certain specific cases, the combination of the two assumptions may lead to useful predictions, while for others cases the assumptions do not lead to useful conclusions.

2.5.2 The foam index test

The foam index test is much less prominent in industry than LOI and no accepted standard protocol exists. The test was introduced by Dodson (1990) in the 1980s and has seen limited use in industry and received some attention from researchers. The foam index test is a titration test that combines cementitious materials with water in a container whereupon the materials are titrated with AEA or other surfactant until a defined endpoint is reached. Some have concluded that the foam index test may be suitable for estimating AEA dosage in concrete (Gebler and Klieger, 1983; Whiting and Nagi, 1998).

Why use foam index?

Unlike the LOI test described above, the foam index test directly measures the results of interactions between cementitious materials and AEAs. In the foam index test the AEA that is titrated stabilizes foam upon agitation of the materials. The volume of foam produced is dependent on the interactions of the test materials with the AEA. If AEA is adsorbed or “taken-up” by constituents of the ash (or cement or water) in the foam index test, the foam-stabilizing capacity of the AEA will be hindered. If AEA is adsorbed in the test, the volume of AEA

required to stabilize a fixed volume of foam will increase. Because this is also true in the case of AEA dosage in concrete, it seems likely that correlations could be established to predict concrete behavior from foam index tests.

Shortcoming of the foam index test

While the foam index test combines cementitious materials with water and AEA, the mixture is not representative of actual concrete mixtures. Because a highly fluid mixture is required, water-to-cement ratios are typically 5 times or more great in the test than in actual concrete. Furthermore, aggregates and chemical admixtures other than AEA are typically not added to the test although these materials can also interact with AEAs.

An additional shortcoming of the foam index test is that no industry wide standard exists. Because the test is simple to perform and requires no sophisticated apparatus (only a container and titration device), numerous variants of the test have been used (Dodson, 1990; Gebler and Klieger, 1983; Freeman et al., 1997; Hill et al., 1997; Smith et al., 1997; Baltrus and LaCount, 2001; Kulaots et al., 2003). Figure 2.2 shows examples of differences produced by four test variants on four Texas ash samples. These variants differ in container sizes, test materials quantities, material proportions, titrants and in other methods of testing procedure. As shown in Figure 2.2, foam index values (shown in volumes of AEA solution) vary differently from test to test. Also the relative rankings of the ash samples (in volumes of AEA) are not consistent among the test variants. Variations make it difficult (and sometimes impossible) to meaningfully compare results from one technique with the results of another, further confusing an already complicated situation.

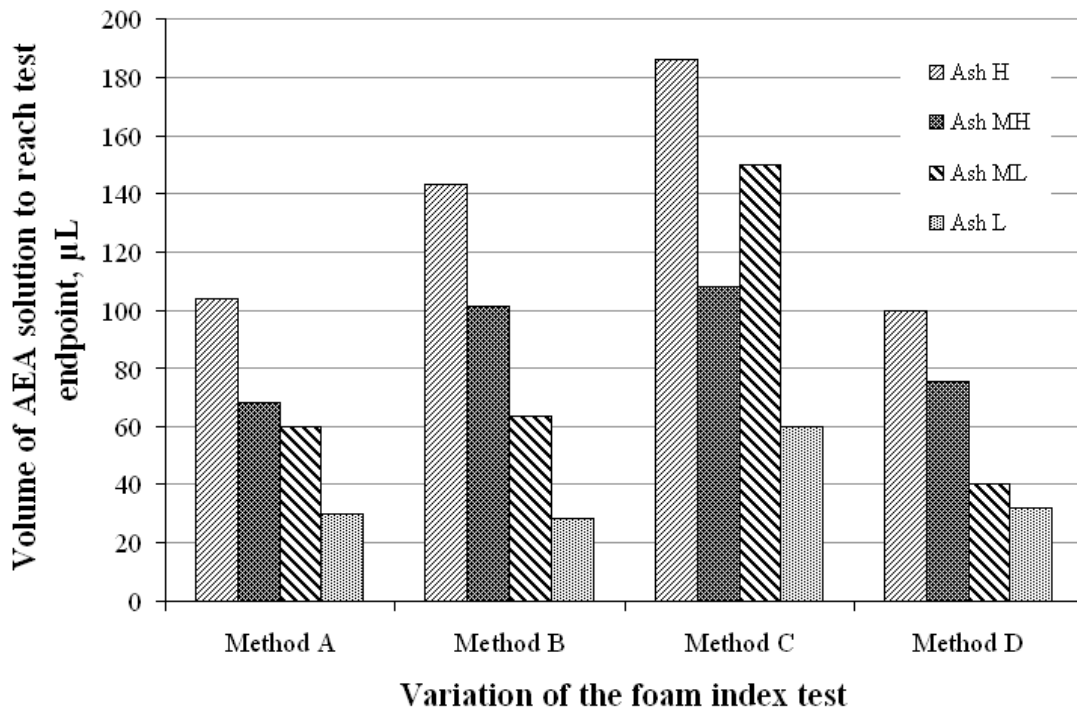


Figure 2.2: Foam index values produced by four variations of the foam index test on four Texas ash samples.

2.5.3 Other tests and procedures that may be of value

In addition to the LOI and foam index tests, other tests not commonly used in the concrete industry were identified as having potential value for measuring properties of fly ash. Such tests include total organic analysis and thermo gravimetric analysis for identifying forms of carbon or other materials in ash that are removed by exposure to oxidizing environments. Also included was x-ray fluorescence and x-ray diffraction for analysis of the chemistry and mineralogy of ash. Other tests were utilized and will be described.

Of particular interest was a colorimetric analysis method that was developed on the basis of an observed link between ash color and performance. Figure 2.3 shows a correlation between colorimetric properties of Texas ash sample (change in grayscale value upon heating at 750°C) and concrete AEA dosage. Development, performance, and application of this test method are described herein.

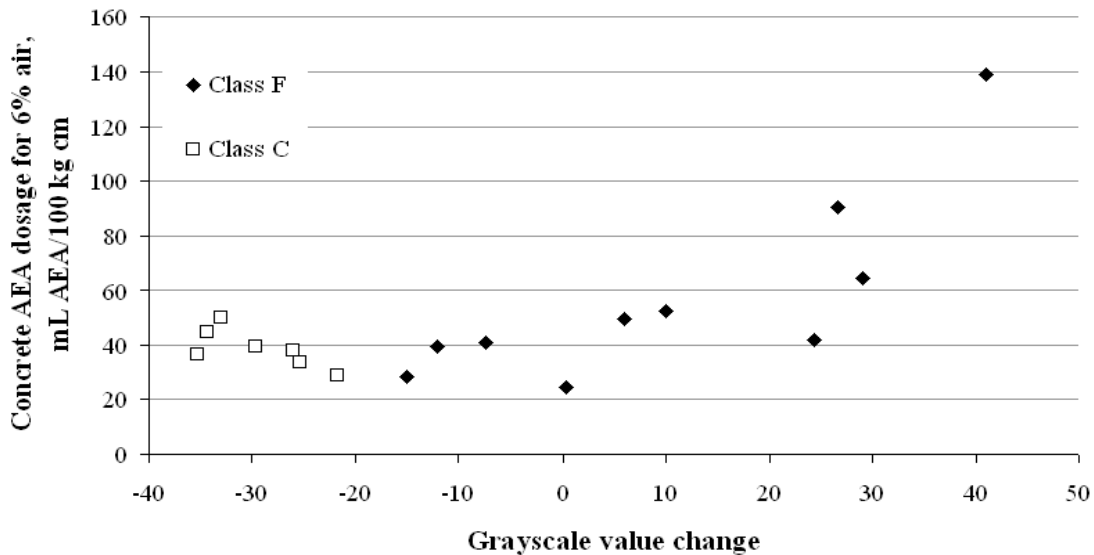


Figure 2.3: Correlation between fly ash colorimetric properties and concrete AEA dosage.

2.5.4 Combinations of tests

Because of the complex nature of fly ash-AEA interactions, it is unlikely that a single test method is suitable for measuring all the properties of fly ash that influence air entrainment. Instead, a suite of tests is likely most useful for characterizing the properties and potential influence of ash on AEA dosage. This research proposes a suite of three tests for use by the ash producer, ash broker and concrete producer for assessing fly ash quality with regards to influence on air entrainment of concrete.

2.6 Expansion of research objectives

Identifying and characterizing ash properties that influence AEA interactions and understanding fundamental behavior were essential to real progress. Because it was often likewise necessary to initiate laboratory work before fully understanding all aspects of ash properties and chemical interactions, there was an iterative nature to much of the work.

Development or modification of test methods was sometimes the result of having come to an understanding of the mechanisms involved, but understanding was often a product of experimentation and testing. Finally, plans and suggestions for implementation have been proposed, but implementation, per se, is beyond the scope of this work. A more detailed look at the research approach follows in the next section.

2.7 Overall plan and progress of the research

Research generally proceeded in accordance with plan shown in Figure 2.4

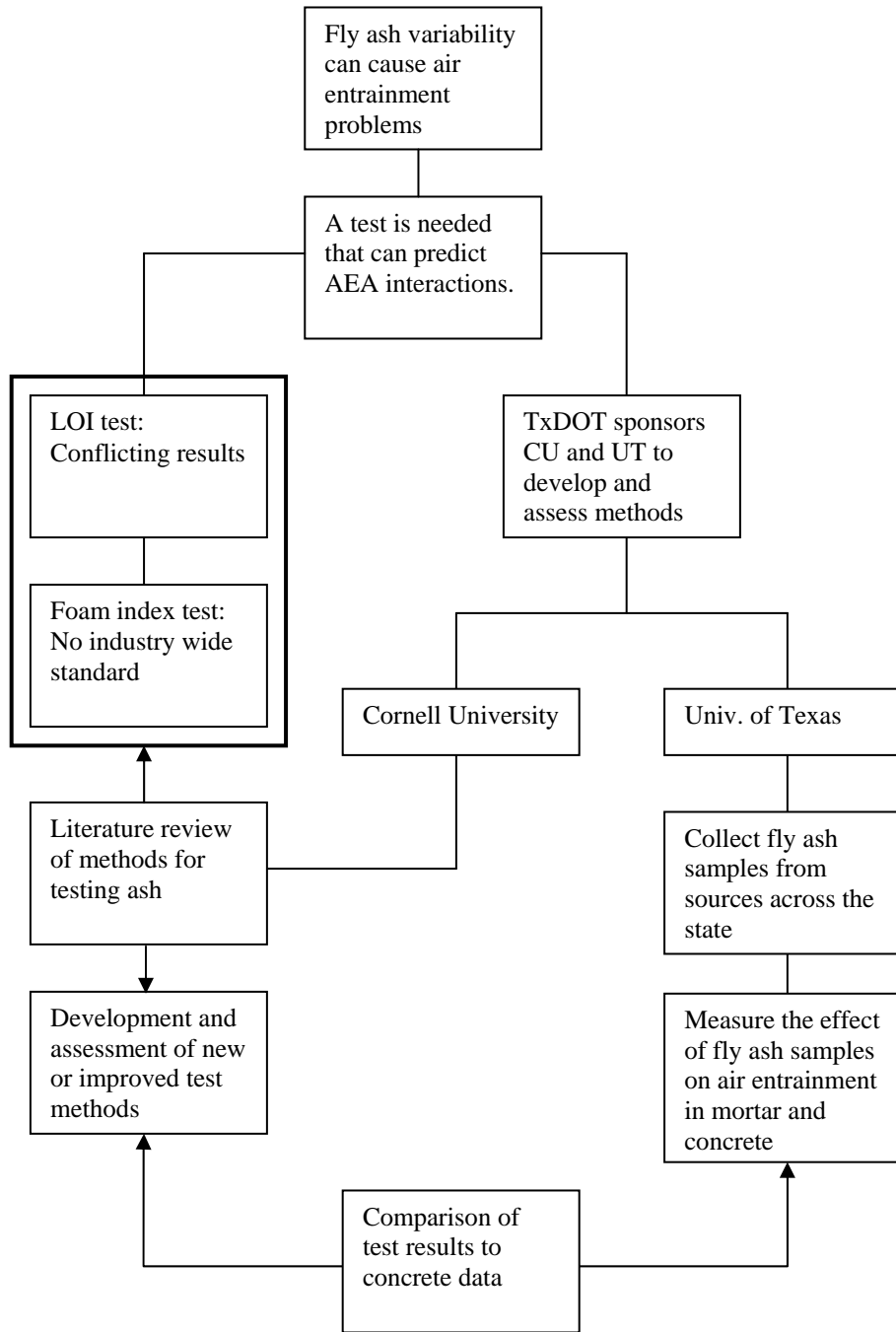


Figure 2.4: Fly ash-AEA interactions research approach- Overall plan.

2.7.2 Research Performed at the University of Texas

The University of Texas at Austin (UT) team communicated with the sponsor and industry, and generated the baseline data set for the influence of fly ash and AEA on concrete and mortar air content. (UT) researchers collected twenty-three ash samples produced at various power plants across the state of Texas.

UT developed a consistent technique for producing mortar and concrete with fly ash to compare the influence of individual ash samples on concrete AEA dosage (Ley, 2007). The resulting data set involves AEA dosage required to produce 6 percent air in concrete for each ash. This data was used as a benchmark for evaluating the various tests identified in this research (such as for the standard LOI test shown in Figure 2.1). UT also has prime administrative responsibility for the project, and will oversee compilation of the final report.

2.7.3 Research performed at Cornell University

Cornell's primary responsibility is the assessment and development of test methods for identifying ash characteristics and predicting AEA interaction. This was accomplished by first reviewing the literature to identify test methods and to gain insight on ash characteristics that could affect AEA performance. Figure 2.5 summarizes testing methods that include LOI and foam index as well as other methods that can be used to measure interactions with AEA, estimate the "carbon" properties, or characterize the mineral fraction of ash. The tests used to characterize the mineral components of ash (except for atomic absorption) are routinely used in industry and are generally not expected to offer information regarding AEA interactions.

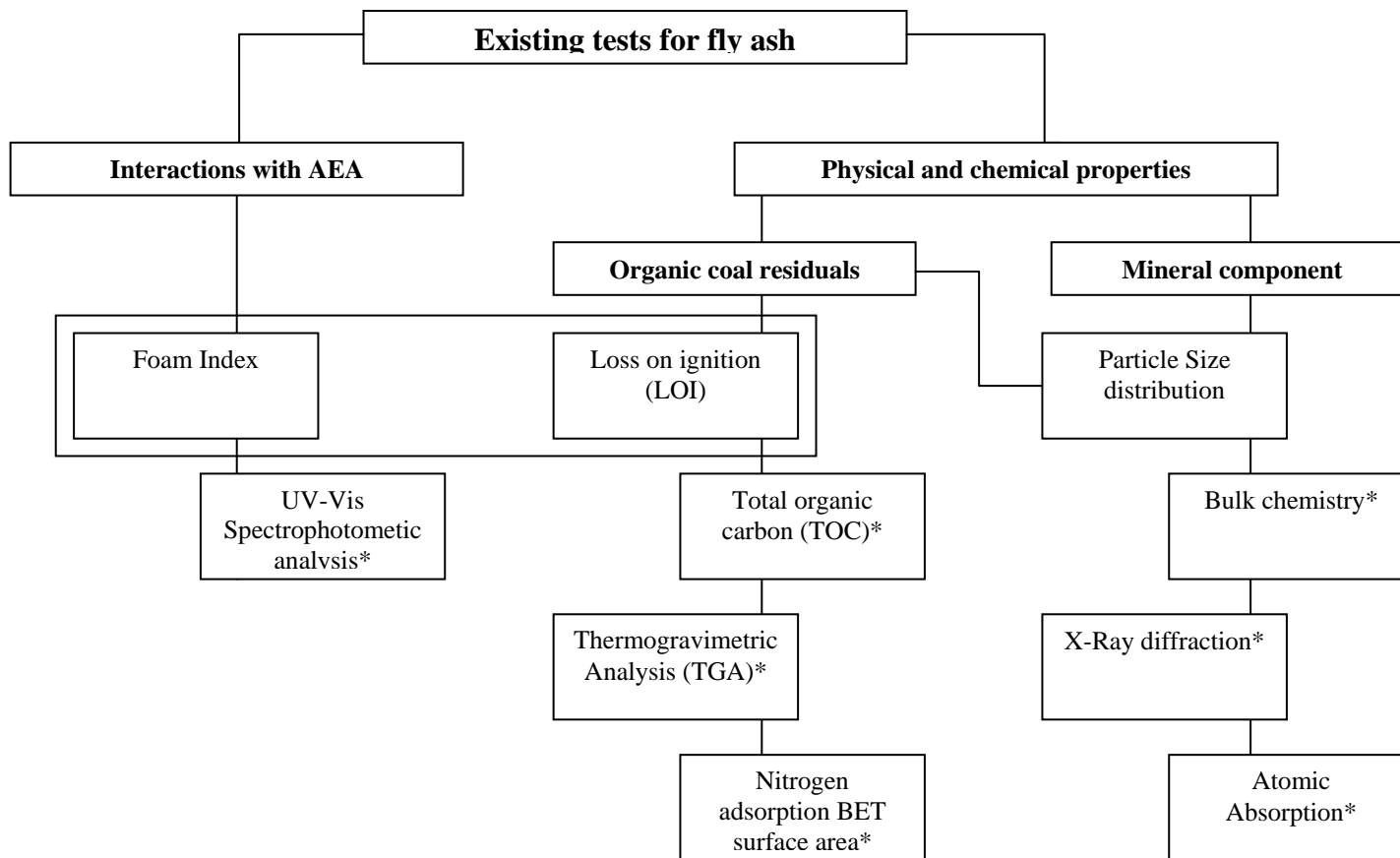


Figure 2.5: Interactions research approach- fly ash test suite. Asterisk (*) indicates tests which require special scientific apparatus and technical expertise not generally common to the industry

All tests shown in Figure 2.5 were applied to the Texas ash set either in whole or to smaller subsets. The tests that are marked with an asterisk (*) are tests which require special scientific apparatus and technical expertise not generally common to the industry.

Of the tests shown in Figure 2.5 the LOI, foam index, thermo gravimetric analysis (TGA), and total organic carbon (TOC) tests were determined to be the most beneficial in measuring the properties of the ash with respect to influence on concrete AEA dosage, or were influential in developing new ash quality assessment techniques. TGA is used to measure the change in mass of a material with change in temperature. TGA is useful in identifying certain materials in a substance based on the temperatures at which they decompose.

The TOC analysis was performed by an instrument used to separate “organic” carbon from “inorganic” carbon. There is no clear consensus on the classification of carbon forms as either “organic” or “inorganic,” and the definition of organic substances has changed over time (Zumdahl, 1993). Nevertheless a working definition for carbon classification for this study is based on the output of the TOC analyzer. The TOC analyzer measures what is referred to as “inorganic” carbon by decomposing a sample with acid to produce carbon dioxide which is then detected and measured by the apparatus. The total carbon content (organic AND inorganic) of a fresh sample is measured by heating a sample to 900°C to oxidize all carbon present. The oxides of carbon are then measured to determine the total carbon content of the sample. The so called “organic” carbon content is simply the difference between total carbon content and the inorganic carbon content. Based on this definition, inorganic carbon is considered to be the carbon that is acid-soluble, such as the carbon in carbonates. Therefore, all other carbon forms which oxidize at temperatures of 900°C and are not acid-soluble are taken as organic carbon. Any form of carbon that is neither decomposed by reaction with acid nor oxidized by heating at 900°C is not detected or measured by the TOC analyzer.

The fact that carbon can exist in more than one form complicates the assumption that “carbon” in fly ash is responsible for the AEA interactions. In practically all references to carbon in fly ash, the terms “carbon,” “unburned carbon,” “char particles” and other terms are referring to organic coal residuals that escape the combustion chamber before being completely consumed. In light of the above discussion, use of the term “carbon content” is imprecise and is rejected here. Throughout this work, the term “organic coal residuals” is used to describe the carbon-rich residue that exists in fly ash due to the incomplete combustion of the organic components of the parent coal material. The organic coal residuals may be present in several structural forms and may have undergone varying degrees of devolatilization and oxidation in the combustion chamber. In addition to organic carbon, organic coal residuals may also contain varying amounts of oxygen, hydrogen, nitrogen, other elements, and minerals matter.

Figure 2.6 shows how studies made using the four primary tests identified above led to improvements to the test methods or the development of new tests for assessing fly ash with respect to AEA interactions. The primary developments are: modified loss on ignition, color analysis, and a proposed “standard” foam index test. These tests are recommended for industrial application on the basis of their correlation with the influence of the ash on AEA dosage in concrete, and through correlation with the results of total organic carbon analysis. The three tests require no special expertise and use apparatus that is either common to the industry (such as a muffle furnace) or are readily acquired.

2.7.4 Assessment of the LOI test

One major outcome of this research is the assessment of LOI as a predictor of AEA interaction. The outcome required investigation of both assumptions described in Section 2.5.1.1, namely, 1) “carbon” is the source of ash-AEA interactions and 2) LOI is a measurement of that carbon. The study of the second assumption was undertaken first to identify what the LOI test actually measures. It was determined that LOI is an inconsistent estimator of the characteristics of ash, including carbon because there is difficulty in defining confidently what the standard LOI test measures.

Based on research described herein, a variation on the LOI test is proposed that does correlate well with measurements of ash total organic carbon (obtained via TOC). There are several important consequences arising from an improved LOI test as follows: 1) when the modified test is used, the property being measured is known., 2) the method may be applicable to other fields in which measurements of TOC are needed for finely divided particulates and 3) even before going back and investigating the validity of the assumption that so called “carbon” causes AEA interaction problems, it was determined that the results of the modified LOI test correlate with other measures of AEA interaction better than the results of the standard LOI test. (And in the process adds support to the notion that carbon mass, at least as defined as TOC, is a key player in the AEA problem.)

Based on the findings of this study, a test similar to the standard LOI is recommended to the industry as an improvement in the estimation of fly ash influence on AEA dosage.

2.7.5 Assessment of the foam index test

The second major outcome in this research was the evaluation of the foam index test as a tool for measuring fly ash-AEA interactions (and more generally cementitious material-AEA interaction). This began with a comparative study of the many variants of the test found in literature and industry. Differences in performance and outcomes of the various tests prompted further studies into the factors that influence test results. During the course of this study the following insights into the foam index test were determined.

- a) A method which makes possible the comparison of test results made using different test containers and test material quantities.
- b) The individual contributions of several factors to the test result including container geometry and fullness, cementitious materials and water proportions, agitation method and others.
- c) Identification of the primary factors influencing test precision and methods for controlling precision.
- d) Sources of variability that if overlooked could cause gross errors in the test results. Based on the finding of this study a reliable standard foam index method is proposed.

In addition to measuring fly ash-AEA interactions in commercial fly ash samples, the foam index test also became a useful tool for identifying the properties of fly ash responsible for the interactions with AEA. The foam index test was used to measure differences in AEA interactions as properties of fly ash, primarily organic carbon content, changed.

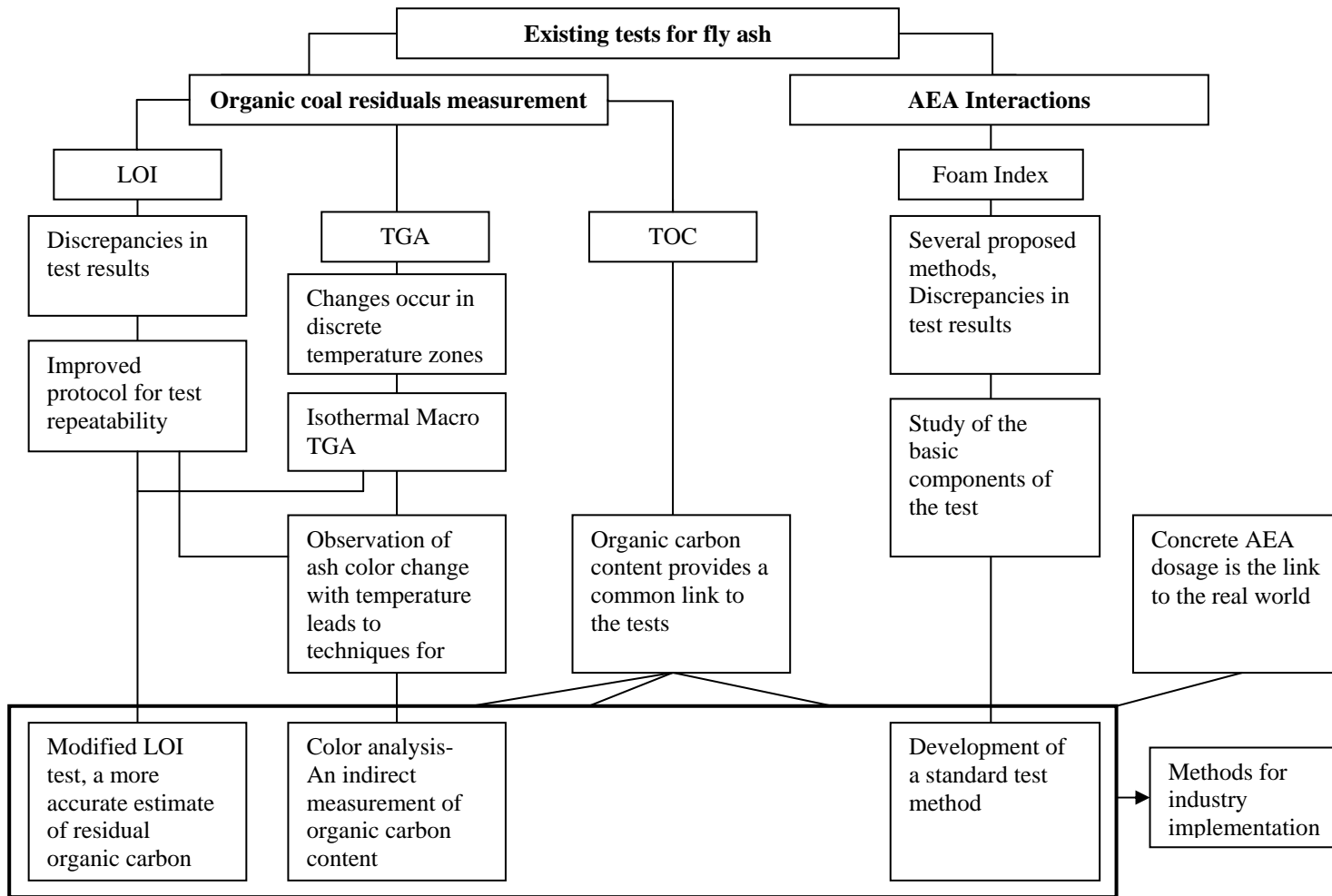


Figure 2.6: Fly ash-AEA interactions research approach—Development of new or improved test methods.

2.7.6 Development of a color analysis test method

During the course of this research, it was observed that ash color was linked to AEA interaction behavior. This observation was particularly apparent when vials containing the samples were ordered according to level of AEA-interaction in concrete or the foam index test. Furthermore, the observation of ash color change due to the removal of organic carbon by the modified LOI test and by thermo-gravimetry tests provided impetus to develop a method for assessing fly ash color and then use the method to study the link between fly ash color and other physical properties, including organic carbon content. The study on fly ash color resulted in several important contributions, including: 1) development of a method for easily capturing and quantifying fly ash color by means of a common desktop color scanner and color analysis software, 2) identification of a link between fly ash color and AEA interactions and 3) determination of a correlation between organic carbon content and change in fly ash color due to heat treatment.

This study resulted in a useful method for assessing fly ash quality with respect to AEA interactions.

2.7.7 Synthesis of test results

The modified LOI, foam index and color analysis tests when coupled with total organic carbon analysis provided information regarding the primary mechanisms influencing fly ash and AEA interactions. The total carbon content of ash also links the three methods to concrete dosage data provided by The University of Texas researchers. Results from other tests in the test suite shown in Figure 2.5 also provide clues concerning the properties of ash and its organic carbon content that affect AEA interactions.

2.7.8 Implementation of findings in the fly ash concrete industry

Figure 2.7 summarizes the recommended implementation of the research finding in the fly ash concrete industry. It is recommended that the test procedures developed for quality control of fly ash be implemented at the three major points of fly ash handling: at the ash producer, the ash broker's materials testing lab and at the concrete producer. Not all tests are of the equal value at each point and are therefore selectively applied. It is noted that the majority of fly ash samples studied in this research were obtained from a limited geographical region of the U.S. Therefore it is possible that the results and general rules for ash influence on AEA dosages determined from this study may not directly apply to regions where fly ash properties, particularly those properties related to organic coal residual type and quantity, differ significantly. In regions where this is the case, the recommended tests can still be utilized when correlated with local data to establish general rules and guidelines for use.

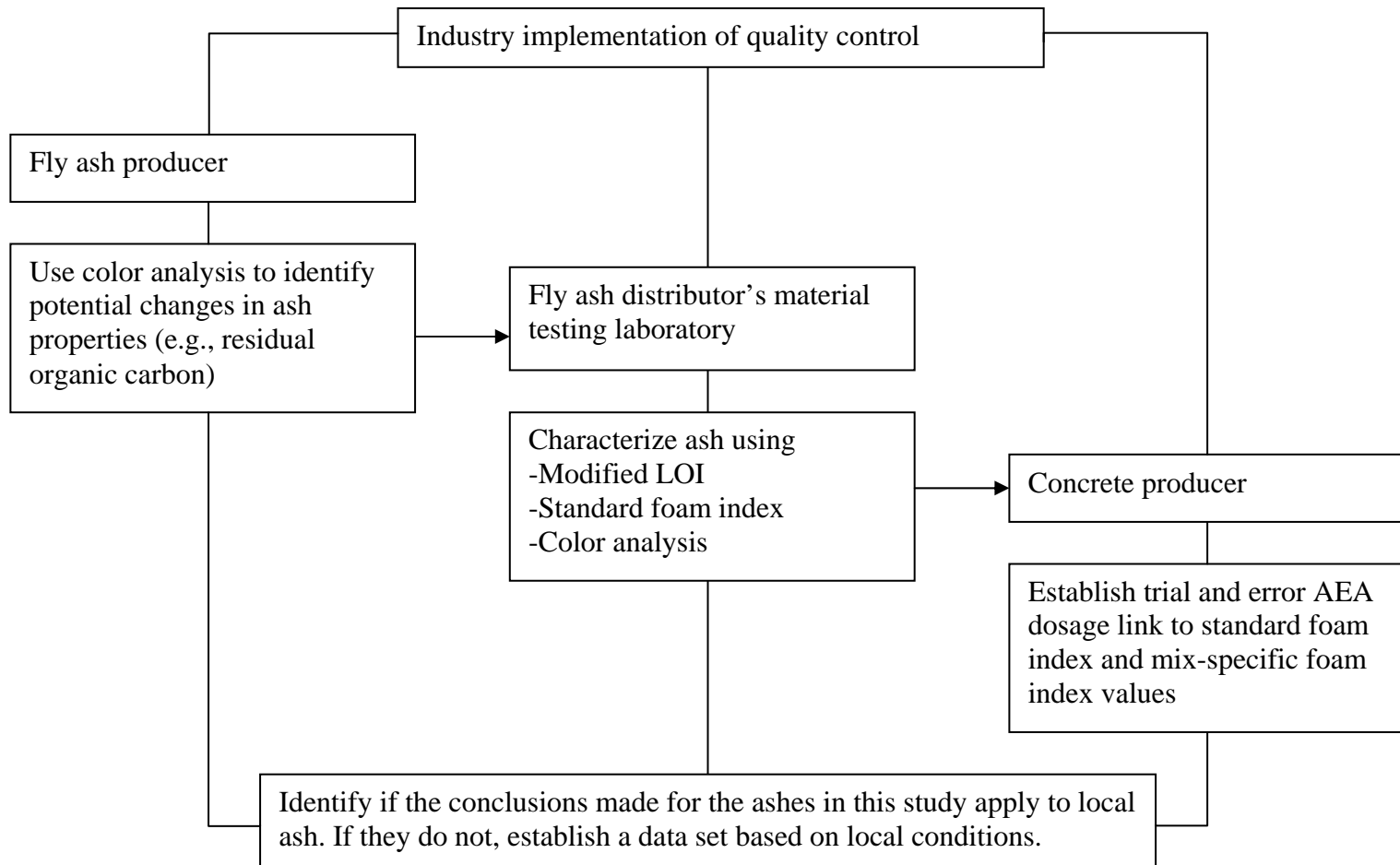


Figure 2.7: Fly ash AEA interactions research approach—Implementation of findings.

Chapter 3. Background

3.1 Introduction

This chapter provides basic information on several seemingly unrelated background topics which converge at the point of the research question. References are provided for further study of these topics. The chapter begins with a description of supplementary cementitious materials with a focus on pulverized coal fly ash. Then the production of fly ash is discussed beginning with coal formation through combustion and the formation of fly ash and its properties and uses. This is followed by discussion of air-entrained concrete. Finally, a review of literature regarding the effects of fly ash on air entrainment and recent developments and insights established before the outset of the project.

3.2 Supplementary Cementitious Materials

Supplementary cementitious materials (SCMs) are receiving increasing attention as important ingredients in the cementitious system of portland cement concrete (Kosmatka et al. 2003). This section defines the characteristics of SCMs, discusses the benefits for using them in portland cement concrete, identifies several SCMs commonly used in the concrete industry, and describes the primary effects that they have on concrete.

3.2.1 What are SCMs?

SCMs are powdered materials that are combined with portland cement in concrete to contribute to the properties of the hardened concrete through hydraulic and/or pozzolanic activity. Hydraulic activity is the ability to self-hydrate, or harden, in the presence of water. Pozzolanic activity is the ability to chemically react with calcium hydroxide (a byproduct of portland cement hydration) in the presence of moisture to form compounds possessing cementing properties (Kosmatka et al., 2003).

SCMs are generally finely-divided, siliceous, or alumino-siliceous materials of primarily glassy structure. Most of the commonly used SCMs are by products of industrial processes and require little processing for use in concrete. Certain pozzolans can be found in nature and used in raw form while others are temperature-treated, naturally occurring materials.

3.2.2 Why use SCMs?

SCMs can be used in addition to or as a replacement for some of the portland cement in concrete (Bradley and Wilson, 2005). SCMs are used to impart certain desirable characteristics to concrete such as water-reduction or workability in the fresh concrete, or decreased heat of hydration, reduced permeability and resistance to sulfate and other forms of chemical attack in the hardened concrete.

The use of SCMs is also beneficial from economic and environmental standpoints. Because many SCMs are industrial waste materials, their incorporation in concrete may allow increased economy (due to the relatively high cost of portland cement and cement shortages during peak demand) and reduction in land-filled materials, energy use and greenhouse gas emissions. (See Marceau et al. 2004.) However, because many SCMs are waste products for other industries, the properties and characteristics of the materials can vary significantly and must be assessed for quality control.

3.2.3 Types of SCMs Available

Several types of SCMs are currently used in industry. The most common forms—fly ash, slag, silica fume and natural pozzolans— are shown in Figure 3.1 and briefly discussed below.



Figure 3.1: Supplementary cementitious materials from left to right, fly ash (Class C), metakaolin (calcined clay), silica fume, fly ash (class F), slag and calcined shale (Kosmatka et al., 2003).

Fly ash

While the term “fly ash” is used to describe any ash that is sufficiently fine to be transported by combustion gases, the pozzolan fly ash is the finely divided mineral residue that is removed from the flue gases of pulverized coal powered electric power plants. The term “fly ash” used in this work always refers to the pulverized coal fly ash unless otherwise noted. Fly ash consists primarily of calcium-alumina-silicate glass in the form of spherical beads generally between 1 and 100 μm in diameters. Fly ashes are typically categorized into classes based primarily on calcium content (either directly or indirectly depending on the specification). Generally, the greater the calcium contents of ashes, the greater the degree of hydraulic activity of the ash. The properties of fly ash will be discussed in detail later. (Kosmatka et al., 2003; Helmuth, 1987; Joshi and Lohtia, 1997; Thomas and Wilson, 2002)

Ground granulated blast furnace slag

Blast furnace slag is a byproduct of the iron production process. Molten slag is tapped from the blast furnace and cooled using various methods to create several types of blast furnace products. Ground granulated blast furnace slag (GGBFS) is produced by quenching molten slag in large quantities of water to form sand-sized grains. The grains are then ground to a fine powder (less than 45 μm in diameter) to form the SCM. GGBFS typically shows the greatest hydraulic activity of all SCMs. ASTM C 989 classifies slag into three grades indicative of its

hydraulic potential. (Moranville-Regourd, 1998; Kosmatka et al., 2003; Thomas and Wilson, 2002)

Silica fume

Silica fume, or microsilica, is the finely divided byproduct of silicon metal smelters. It is the fume that is carried by the exhaust gases from the burning surface of an electric arc furnace and collected in fabric filters. Particles are composed almost entirely of amorphous silica, and such are purely pozzolanic in activity. Silica fume particles are spherical in shape and are typically less than 1 μm and average about 0.1 μm in diameter. (Fidjestøl and Lewis, 1998; Kosmatka et al., 2003; Thomas and Wilson, 2002)

Natural pozzolans

Natural pozzolans consist of both raw pozzolans—such as volcanic ash, diatomaceous earth and opaline cherts and shales—and calcined natural pozzolans including metakaolin, calcined clay and calcined shale. Calcination of the pozzolans is performed by heating the finely ground materials in a kiln to temperatures that change the molecular structure and reactivity of the materials. (Badogiannis et al., 2005; Kosmatka et al., 2003; Thomas and Wilson, 2002)

3.2.4 Effects of SCMs on concrete

The presence of SCMs influences both the plastic and hardened properties of concrete. The effects on the concrete properties may or may not be desirable depending on the intended use of the concrete; therefore, care must be given in selecting the type and proportion of SCMs to be used in a given mix. The general effects of SCMs on concrete properties are shown in Tables 3.1 and 3.2 (Thomas and Wilson, 2002). It should be noted that the individual effects on properties vary among the different SCMs and within a single type of SCM.

Effects of plastic concrete

Fly ash and slag tend to reduce water demand while silica fume and metakaolin tend to increase water demand. Fly ash, slag, and most natural pozzolans tend to increase workability and pumpability while silica fume and metakaolin tend to reduce workability. Most SCMs, particularly silica fume, reduce bleeding in plastic concrete. Most SCMs tend to reduce heat of hydration and increase setting times, though high calcium content fly ash can cause the reverse effects. Many SCMs, particularly low calcium fly ashes, cause increases in the dosage of air-entraining admixtures (specialty surfactants used to stabilize air bubbles in concrete) to produce a given percent air content in concrete. The study of fly ash effects on air-entraining admixture dosages is the purpose of this work. Section 4.3 discusses the current state of knowledge of the industry regarding interactions between fly ash and air-entraining admixtures.

Effects on hardened concrete

Use of low-calcium fly ash, certain slags and calcined shales and clays reduce the early age strength of concrete. Silica fume, metakaolin and some slags increase early age strength. SCMs have been shown to increase long-term strength and reduce permeability. The reduced permeability of the hardened cement matrix reduces chloride ingress and chemical attack. The

use of SCMs has been shown to reduce destructive alkali-silica reaction and increase resistance to sulfate attack (Khatri et al., 1995).

Table 3.1: Summary of the effects of SCMs on selected properties of fresh concrete (horizontal arrows indicate little to no effects), Thomas and Wilson, 2002.

	Fly Ash		Slag	Silica Fume	Natural Pozzolans		
	Class F	Class C			Calcined Shale	Calcined Clay	Metakaolin
Water Demand	↓↓↓	↓↓↓	↓	↑↑↑	↔	↔	↑
Workability	↑	↑	↑	↓↓↓	↑	↑	↓
Bleeding	↓	↓	↔	↓↓↓	↔	↔	↓
Setting Time	↑	↔	↑	↔	↑	↑	↔
Air Entraining Dose	↑↑↑	↑	↔	↑↑↑	↔	↔	↑
Heat of Hydration	↓	↔	↓	↔	↓	↓	↓

Table 3.2: Summary of the effects of SCMs on selected properties of hardened concrete (horizontal arrows indicate little to no effects), Thomas and Wilson, 2002.

	Fly Ash		Slag	Silica Fume	Natural Pozzolans		
	Class F	Class C			Calcined Shale	Calcined Clay	Metakaolin
Early Age Strength Gain	↓	↔	↕	↑↑	↓	↓	↑↑
Long Term Strength Gain	↑	↑	↑	↑↑	↑	↑	↑↑
Permeability	↓	↓	↓	↓↓	↓	↓	↓↓
Chloride Ingress	↓	↓	↓	↓↓	↓	↓	↓↓
ASR	↓↓	↓	↓↓	↓	↓	↓	↓
Sulfate Resistance	↑↑	↑	↑↑	↑	↑	↑	↑
Freezing & Thawing	↔	↔	↔	↔	↔	↔	↔

3.2.5 Conclusion

The use of SCMs is beneficial to portland cement concrete for several reasons. Many SCMs are byproducts of industrial processes and can vary in characteristics and quality. SCMs are mainly composed of siliceous and/or aluminosiliceous materials and can possess hydraulic characteristics, pozzolanic characteristics or both. The effects of SCMs on both plastic and hardened concrete vary among the various types and are selected based on the desired properties which they impart. The use of fly ash, and in particular, its effects on air-entrainment admixtures dosages in fresh concrete are the focus of this work.

3.3 Fly Ash Production

Fly ash used in portland cement concrete is typically produced as a byproduct of the combustion of pulverized coal suspended in air, generally in the boilers of electric power producing facilities. Fly ash is composed chiefly of the mineral components of the coal and is formed as the minerals dispersed through the coal particle are freed as the combustion consumes the carbon and volatile matter constituents of the coal. The fly ash particles exit the combustion chamber with the flue gases and are collected in the particulate control system. The constituents and properties of the ash are dependent on the entire process from coal formation to fly ash recovery. This section provides information on coal formation, composition and combustion as well as fly ash formation, collection and properties.

3.3.1 Coal

Definition of Coal

Coal is a readily combustible, metamorphosed sedimentary rock of organic origins formed by a combination of biological and geological forces over time. Coal is physically and chemically heterogeneous and is composed of both organic and inorganic constituents. Coal is formed as accumulated decaying vegetation (peat) is buried by sedimentation, compacted, and metamorphosed. The biological and geological forces acting on the plant matter bring about both chemical and physical changes. The primary chemical changes are loss of moisture, decrease in volatile constituents (e.g., non-fixed carbon, oxygen, and hydrogen), rearrangement of the molecules of the remaining components, and resulting increases in the proportions of fixed carbon and ash. Physical changes include a darkening of the color, an increase in hardness and compactness, and a change in fracture (Moore, 1940; Tatsch, 1980). The physical and chemical properties of coal vary significantly from the original vegetal matter; however plant remains, such as spores, pollen, resins and woody tissues, and sometimes animal remains can be identified within coal (Neavel, 1981).

Coal is a fossil fuel that is both historically and presently of great importance to world industry and energy production. Coal is the most abundant fossil fuel² in the world with deposits found in every major world region except the Middle East. In the United States, coal composes 95 percent of the fossil fuel resources with over half of the total electricity generated by coal-fired plants (Environmental Literacy Council, 2007). Because of the enormous quantities of coal consumed to meet U.S. energy needs, coal combustion byproducts are a major environmental issue.

Origins of coal

Peat formation has long been recognized as the first step in the conversion of vegetal matter into coal. The conditions for peat formation are: 1) substantial growth of woody, fibrous vegetation, 2) sufficient standing water to prevent the oxidation and bacterial destruction of the accumulating vegetation, and 3) the absence or minimization of inorganic sediment during peat accumulation (Miller, 2005). Two theories explain the accumulation of peat (Moore, 1940). First, and most plausible for the majority of coal deposits found, vegetation in swamp environments dies and submerges *in situ* in stagnant, anaerobic aquatic environments where decomposition and the subsequent release of carbon dioxide is hindered. A second theory suggests that plant matter is carried in streams and rivers and deposited on sea or lake beds where it accumulates.

In either case, successive generations of deposits form thick layers of un-oxidized organic matter. Anaerobic bacteria and fungi break down plant tissues until conditions become too acidic, leaving partially decomposed woody constituents. Observation of modern peat growth reveals that an average rate for the growth of old, compressed peat is approximately 1 foot per century, with about 3 feet of compressed peat required to produce 1 foot of bituminous coal (Moore, 1940). This value is highly dependent on both the climatic and environmental conditions

² At the end of 2002, world recoverable coal reserves totaled approximately 1081 billion short tons, with US reserves approximately 272 billion tons. There is about twice as much recoverable coal in the world as oil and natural gas combined (on an oil-equivalent basis) (EIA, 2004).

of the period. Coal deposits began forming approximately 350 million years during the Upper Carboniferous period and formed in every major geological period since that time (Miller, 2005).

Geologic processes cover the accumulating peat with layers of sedimentation and a future coal seam is formed. This cycle is often repeated over hundreds of thousands of years to form multiple seams inter-bedded in layers of silt, sand and clay (Ward, 1984). Movements of the earth's crusts subject the seams to intense heat and pressure. The magnitude and duration of the high temperatures and pressures directly determines the extent of the "coalification," or degree of conversion from peat to coal.

Coalification

Coalification is the geochemical process that transforms vegetal matter into coal. The general sequence of coalification is:

peat → lignite → sub-bituminous coal → bituminous coal → anthracite

The degree of coalification (or coal rank, with lignite a low rank coal and anthracite a high rank coal) is independent of the vegetal origin, but instead is the result of the temperatures, pressures and length of time to which the deposit is subjected. Figures 3.2 and 3.3 (from Averitt, 1981) compare the constituent proportions and heating value of coals at various levels of coalification. Tatsch described coalification as three geochemical processes: 1) the microbiological degradation of the cellulose (the primary structural material in plant cell walls) of the initial plant material; 2) the conversion of the lignin (another major component of cell walls) of the plants into decayed organic humic substances; and 3) the condensation of these humic substances into the larger chemical structures known as "coal molecules" (Tatsh, 1980). Figure 3.4 shows a model of a typical bituminous vitrinite coal molecule as suggested by P.H. Givens (1960). The organic constituents of coal are represented in the coal molecule, carbon (located at each corner of the benzene rings), hydrogen and oxygen and to a lesser extent, sulfur (not shown) and nitrogen. The inorganic components of coal include water, and a diverse range of minerals.

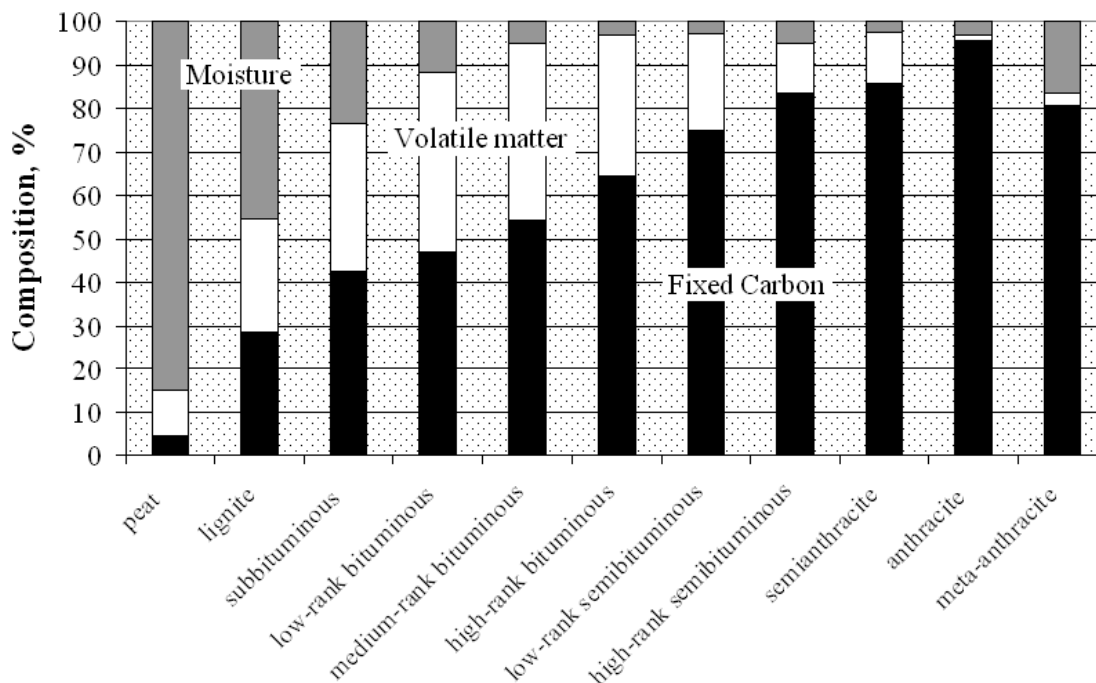


Figure 3.2: Proximate composition (minus ash) of various coal ranks (Averitt, 1981).

Coal structure has been determined to be increasingly ordered as the level of coalification increases (Skinner and Smoot, 1979). Coal structure is composed of lamellae of ordered and amorphous material arranged in randomly oriented layers resulting in relatively large pores in low rank coals. As coalification increases, the structure is compressed, reducing pore size and increasing lamella size and orderliness. Ultimately, coalification leads to graphitization, the ordered arrangement of nearly pure carbon.

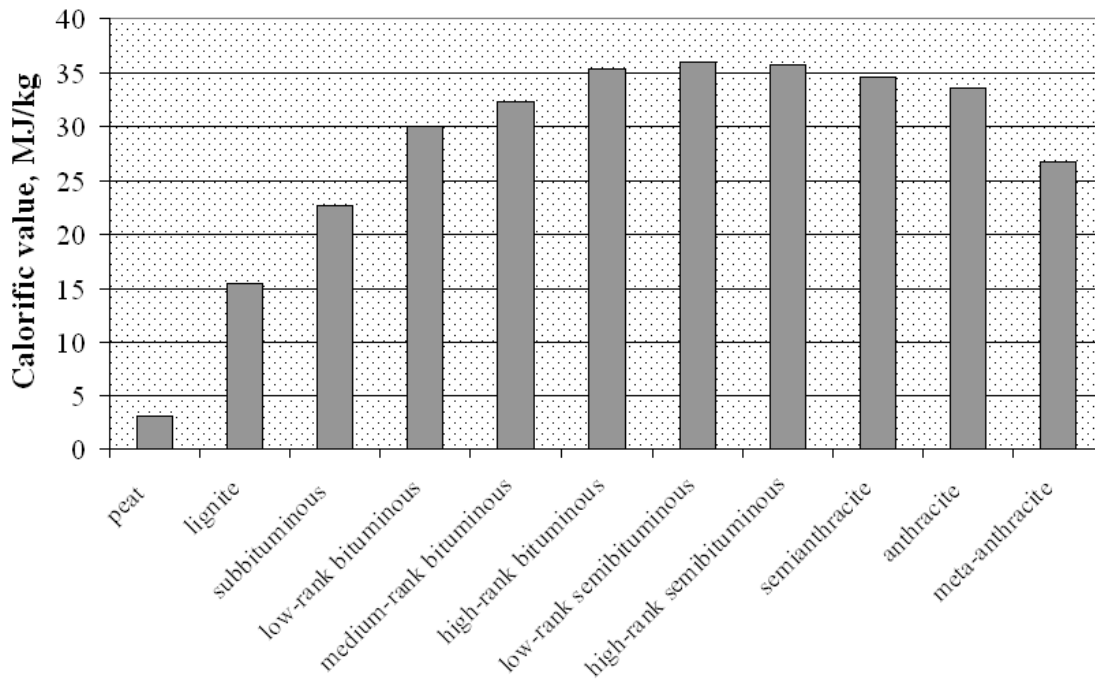


Figure 3.3: Calorific value, Btu/lb (Averitt, 1981).

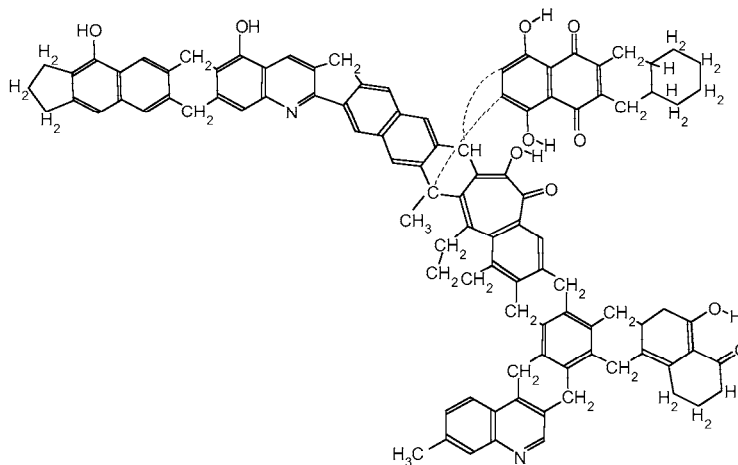


Figure 3.4: Model of coal molecular structure by P.H. Given (1960).

Coal Seams and Extraction

Coal seams range in depth from a fraction of an inch to hundreds of feet³. The seam thickness is dependent on both the continuity of the peat growth environment and the nature of the geologic changes during and after the peat bed was formed. Changes in climate, water availability and deposition of inorganic sediments can terminate peat growth. Erosion forces, fault movement, crust folding, igneous intrusions and other actions can cause irregularities in coal beds.

Coal is extracted using either surface or underground mining techniques. Surface mining is generally employed when the thickness of the material above the coal seam (overburden) is 200 feet or less, and the ratio of overburden thickness to coal seam thickness is equal to or less than 20:1 (Miller, 2005). The advantages and disadvantages of surface and underground mining are compared in Table 3.3.

Surface mining techniques can be divided into three main categories: strip, open-pit and auger mining. Strip mining refers to operations where the overburden is removed to an area immediately adjacent to the working face. Open-pit mining refers to operations where the overburden material is removed to a site at some distance from the working face (Ward, 1984). In auger mining, an auger is drilled into the face of a coal seam exposed on a slope and the coal is removed via conveyor. Approximately 70 percent of the coal mined in the U.S. in 2002 was extracted using surface mining techniques (Miller, 2005).

Underground mining techniques are generally categorized as bord and pillar mining, longwall mining or some combination of the two. Bord and pillar mining is composed of two stages. In the first stage, several intersecting corridors (bords) are cut through the horizontal plane of the seam leaving pillars to support the roof. In the second stage, the pillars are removed and the roof is allowed to collapse into the abandoned area. The longwall mining technique extracts coal from a working face extending 80 to 200 meters in length. Hydraulic roof supports protect the working area and advance with the coal face to allow collapse of the abandoned area.

³ A 266 foot thick brown coal seam in Morwell, Victoria, Australia is the largest known (Moore, 1940).

Table 3.3: Advantages and disadvantages of surface and underground mining (Ward, 1984)

Surface mining	Underground mining
Minimum of development needed prior to coal production	May need to sink shafts or make other unproductive openings in non-coal strata
May need to excavate large volume of overburden to extract coal	Most excavations, apart from the entry and any fault penetrations, etc. are made in saleable coal
Need to provide a suitable location for overburden emplacement	Need to provide timber, steel straps or rock bolts for roof support
Large area of land disturbed by mining	Only area around pit-top is visibly disturbed
More noise and dust pollution to neighboring areas	Subsidence above workings may affect surface installations
Greater safety of mine personnel	Need to provide ventilation and lighting facilities
Fewer and more simple items of machinery required for high coal output	Individual production units may be less costly, but more are required for an equivalent coal output
Difficult working conditions in extreme climates	Underground temperatures rise with depth
Danger of landslides on excavations or spoil piles	Danger of roof falls or gas outbursts
Cost of land regeneration must be considered	Can mine under bodies of water and other sensitive areas
Maximum depth of working limited by cost of overburden removal	Can work coal to greater depths, overburden : coal ratio not critical
Almost all in situ coal recovered	Less than 60% of in situ coal commonly recovered

Coal Preparation

End-use facilities such as power plants require coals with strict requirements pertaining to mineral content, sulfur, volatiles and energy contents. These requirements can be difficult to meet due to variations within coal seams, the depletion of high quality eastern U.S. coals, strict controls on emissions and modern mechanized mining techniques that incorporate significant proportions of the confining rock strata in the output coal (Miller, 2005). As a result of these factors, several techniques are used to improve coal quality.

Before marketing, the coal passes through a preparation plant where it is crushed, screened, cleaned, dewatered and blended. These operations remove unwanted constituents, produce coal particles in various sizes to meet specific market requirements, separate components by density or surface characteristics, remove moisture, and produce a more uniform end product. The mass of rejected or waste material from a preparation plant can represent 20 to 50 percent of the input mass, depending on coal source and processing techniques (Miller 2004).

3.3.2 Coal Constituents

Analysis methods

Two general methods of analysis are typically used to determine the constituents of the coal, proximate and ultimate analysis. Proximate analysis (ASTM D3172) is the most common in industry and is used to determine the relative amounts of moisture, volatile matter, non-volatile mineral matter and “fixed carbon.” Figure 3.5 (Ward, 1984) graphically displays the distribution of these components in a typical coal sample. The proximate analysis constituents are defined in the following sections. Ultimate, or elemental, analysis (ASTM D3176) is used to determine the relative amounts of carbon, hydrogen, nitrogen, sulfur, oxygen and ash in the coal. Ultimate analysis does not separate the elemental constituents according to origin.

total moisture	surface moisture	
	inherent moisture	
mineral matter	non-volatile mineral matter	
	volatile mineral matter	volatile matter
pure coal	volatile organic matter	
	fixed carbon	

Figure 3.5: Division of the basic components of coal (Ward, 1984).

Moisture

Moisture in coal is categorized as either adventitious or inherent (Ward, 1984). Adventitious moisture is held in films on the coal particle surfaces. The origin of this moisture can be through *in situ* seepage or from rain and sprays applied during the mining and preparation plant processing. Inherent moisture describes the water held in the internal capillaries of the coal, incorporated in the coal’s organic compounds, or as part of the crystal structure of clays and other minerals. The adventitious water and much of that within the capillaries can be evaporated at 100°C, while the moisture in the organic compounds and minerals is not liberated of approximately 500°C.

Volatile Matter

The volatile matter refers to the constituents of the coal that are liberated at high temperatures in the absence of air (water excluded), but at temperatures that are below the coal combustion temperature. Volatile matter is found in both the organic and mineral components of the coal. The volatile matter in coal is typically composed of hydrogen, carbon monoxide, methane and other hydrocarbons, tar and carbon dioxide (Speight, 1983) and can range from 2 to 45 percent (depending on coal rank, see Figure 3.2) (Helmuth, 1987).

Non-volatile mineral matter

The non-volatile mineral matter (generally called “ash” in the coal industry but not used here to avoid confusion with “fly ash”) is the incombustible solid material in coal that is typically of inorganic origin. The non-volatile mineral matter of coal varies considerably in both constitution and proportion and can occupy up to 35 percent of the coal by weight. Coals with high proportions of mineral matter are less suitable for utilization in combustion processes than lower mineral content coals because more coal is needed for an equivalent energy output and the amount of waste generated is increased.

Table 3.4: Silicate and oxide mineral species in coal. From Ishii (2000).

Species	Chemical formula	Specific gravity (kg m ⁻³) ^a	Melting point (K)
Silica and silicates-common occurrence			
Quartz	SiO ₂	2650	1983
Kaolinite	Al ₂ O ₃ • 2SiO ₂ • 2H ₂ O		2083
Muscovite	K ₂ O • 3Al ₂ O ₃ • 6SiO ₂ • 2H ₂ O	2900	(Mullite)
Illite	As muscovite with Fe, Ca, and Fe		
Montmorillonite	(1-X)Al ₂ O ₃ • X(MgO, Na ₂ O) • 4SiO ₂ • nH ₂ O		
Chlorite	Al ₂ O ₃ • 5(FeO, MgO) • 3.5SiO ₂ • 7.5H ₂ O		
Orthoclase	K ₂ O • Al ₂ O ₃ • 6SiO ₂	2500	
Plagioclase	Na ₂ O • Al ₂ O ₃ • 6SiO ₂ -Albite CaO • Al ₂ O ₃ • 2SiO ₂ -Anorthite		
Silicates-less common occurrence			
Augite	Al ₂ O ₃ • Ca(Mg, Fe, Al, Ti) • 0.2SiO ₂		
Amphibole	Augite + Na, Fe, P	3100	
Biotite	Al ₂ O ₃ • 6(MgO • FeO) • 6SiO ₂ • 4H ₂ O	3100	
Granite	Al ₂ O ₃ • 3(CaO, MgO, FeO, MnO) • 3SiO ₂		
Epidote	4CaO • 3(Al, Fe)O ₃ • 6SiO ₂ • H ₂ O	3350	
Kyanite	Al ₂ O ₃ • SiO ₂	3350	2083(Mullite)
Sanidite	K ₂ O ₃ • Al ₂ O ₃ • 6SiO ₂	2570	
Strauroilite	Al ₂ O ₃ • FeO • 2SiO ₂ • H ₂ O		
Tourmaline	Na(Fe, Mn) ₃ • 3Al ₂ O ₃ • 6SiO ₂ • 3BO • 2H ₂ O	3100	
Zircon	ZrO ₂ • SiO ₂	4500	2825
Oxides and hydrated oxides			
Rutile	TiO ₂ ^b	4200	2100
Mangetite	Fe ₃ O ₄	5140	1865
Hematite	Fe ₂ O ₃	5200	1840
Limonite	Fe ₂ O ₃ • H ₂ O	4300	675 ^c
Diaspore	Al ₂ O ₃ • H ₂ O	3400	425 ^c

^aThe specific gravity of silicate minerals is in the range of 2500 to 3500 kg m⁻³; it increases with Al₂O₃/SiO₂ ratio and decreases with H₂O content. The silicates containing Na, K, Ca, Mg, and Fe do not have a definite melting point temperature.

^bWith the exception of rutile, the oxide minerals rarely occur in coal.

^cDenotes loss of water.

The mineral matter in coal can be either finely dispersed or in discrete layers. The mineral matter has two origins, either as the inorganic constituents of the original vegetation or as material transported from a distant location. The mineral matter transported to the site of coal formation generally accounts for the majority of the total inorganic minerals and may have entered the coal as dust blown into the ancient swamp, minerals dissolved in water that flowed to the site, deposits left by water percolating through the coal after its formation or any other geologic phenomena that results in the deposition of minerals within the coal layer.

Table 3.5: Carbonate, sulfide, sulfate, phosphate and chloride minerals in coal. From Ishii (2000).

Species	Chemical formula	Specific gravity (kg m ⁻³)	Melting/decomposition temperature (K)
Carbonates			
Calcite	CaCO ₃	2710	1200 ^b
Aragonite	CaCO ₃	2710	1150 ^b
Dolomite	CaCO ₃ • MgCO ₃	2850	1050 ^b
Ankerite	CaCO ₃ • FeCO ₃		1000 ^b
Siderite	FeCO ₃	3830	800 ^b
Sulfides			
Pyrite	FeS ₂	5000	1075 ^b
Marcasite	FeS ₂	4870	1075 ^b
Pyrrhotite	FeS _x	4600	1300
Chalcopyrite	CuFeS	4100	1300
Melnikovite	FeS ₂ +(As,FeS,H ₂ O)	~5000	1075 ^b
Galena	PbS	7500	1370
Mispickel	FeS ₂ • FeAs ₂	~5000	1075 ^b
Sphalerite	ZnS		
Sulfates			
Barytes	BaSO ₄	4500	1855
Gypsum	CaSO ₄ • 2H ₂ O	2320	1725
Kieserite	MgSO ₄ • H ₂ O	2450	1395 ^b
Thenerdite	Na ₂ SO ₄	2680	1157
Mirabilite	Na ₂ SO ₄ • 10H ₂ O	1460	1157
Melanterite	FeSO ₄ • 7H ₂ O	1900	755 ^b
Keramolite	Al ₂ (SO ₄) ₃ • 16H ₂ O	1690	945 ^b
Jarosite	K ₂ SO ₄ • xFe ₂ (SO ₄) ₃	2500	900 ^b
Phosphates			
Apatite	Ca ₅ F(PO ₄) ₃	3100	>1500
Evansite	3Al ₂ O ₃ • P ₂ O ₅ • 18H ₂ O	2560	>1775
Chlorides			
Halite	NaCl	2170	1074
Sylvite	KCl	1980	1043
Bischofite	MgCl ₂ • 6H ₂ O	1570	987

^aCalcite, dolomite, ankerite, siderite, pyrite, barytes, and apatite minerals occur frequently. Gypsum and other sulfates are found mainly in low-rank and weathered coals; other mineral species are rarely found.

^bDenotes the decomposition temperature.

Because of the processes of formation, the amount and type of mineral matter in the coal can vary widely depending on the geologic history of the coal and its geographic location. The major minerals recognized in coal belong to the following mineral groups: silicates, carbonates, oxides, sulfates and sulfides (Ward, 1984, Speight, 1983).

Tables 3.4 and 3.5 from Ishii (2000) present the mineral species names, chemical formulas, specific gravities and melting/decomposition temperatures of coal minerals.

Regional variations in the distribution of minerals are common and many trace elements have been identified in coal mineral matter and ash (Miller, 2005).

Fixed Carbon

The “fixed carbon” is the imprecise term given to the portion of coal that remains after the proportions of moisture, volatiles and ash are accounted for. “Fixed carbon” does not represent the total amount of the element “carbon” in coal, but instead represents the residue of the *organic* constituents of the coal and consists primarily of elemental carbon with small amounts of adsorbed or chemically combined nitrogen, sulfur, hydrogen and oxygen (Ward, 1984).

Carbon in coal

The organically-derived materials in coal are the result of coalification of carbon-based vegetal matter. The vegetal matter and resulting coal also contain other elements in addition to carbon such as oxygen, hydrogen, nitrogen and sulfur. The carbon in the organically-derived material is referred to in this work as “organic carbon” (provided it also meets the definition given in Chapter 2 Section 2.6.3). Organic carbon is present in the solid, organically-derived coal (the percent contribution depends on the degree of coalification) and also in organically-derived volatile matter.

Carbon can also be present in the mineral matter in coal, in particular in carbonate minerals (see Table 3.5). This form of carbon represents “inorganic carbon.” In the context of this work, inorganic carbon is the carbon that is acid soluble.

3.3.3 Distribution

World Distribution

Coal is found on every inhabited continent of the world. The U.S. Energy Information Administration (EIA, 2004) estimated the world recoverable coal reserves to be 1.1 billion short tons. North America contains about a quarter of this total, with nearly 97 percent of that amount within the United States. Eastern Europe and the states of the former Soviet Union contain another quarter of total reserves. Asia contains approximately 20 percent, Australia and Western Europe each with approximately 10 percent, and Africa, Central America and South America containing the remainder (EIA, 2004). Coal is likely located in Antarctica due to its geographic history (Miller, 2005). The world’s major coal producing countries are displayed in Figures 3.6.

United States

The United States contains more coal reserves than any other nation. Figure 3.7 shows the geographical distribution of coal by rank. The coal of the Appalachian and Illinois basins are typically anthracites and bituminous coals deposited during the carboniferous era (300-350 million years ago), while the western coals are typically lignite and sub-bituminous coals of the Upper Jurassic to Tertiary periods (50-150 million years ago). The coal deposits found in the gulf region extending from Texas to Alabama are lignitic in rank and are the lowest rank coals in the U.S. (Miller, 2005).

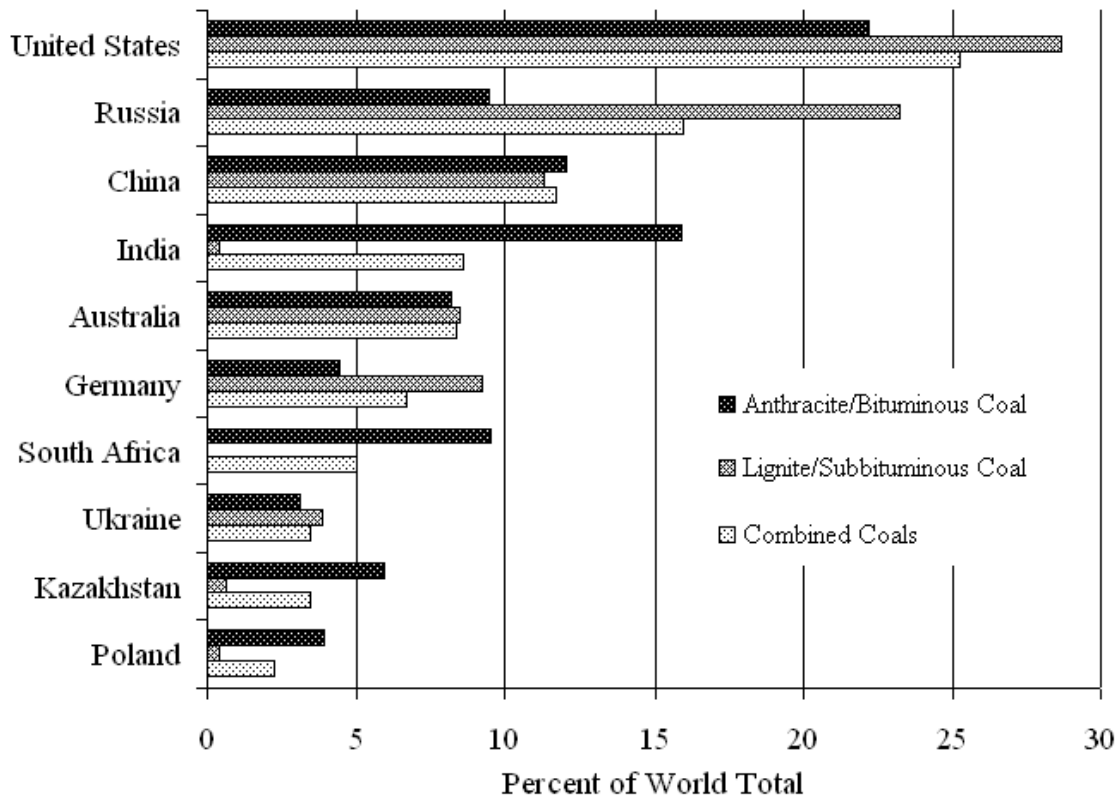


Figure 3.6: Distribution of coal in top coal rich countries (EIA, 2004).

Table 3.6 displays the states with the largest coal reserves. Montana leads the nation, containing approximately 30 percent of the nation's total reserves. In general, the states with the largest reserves also produce the most coal, but not necessarily in the same order as shown in Table 3.7. Wyoming leads the nation in coal production, accounting for approximately 35 percent of U.S. coal production in 2003.

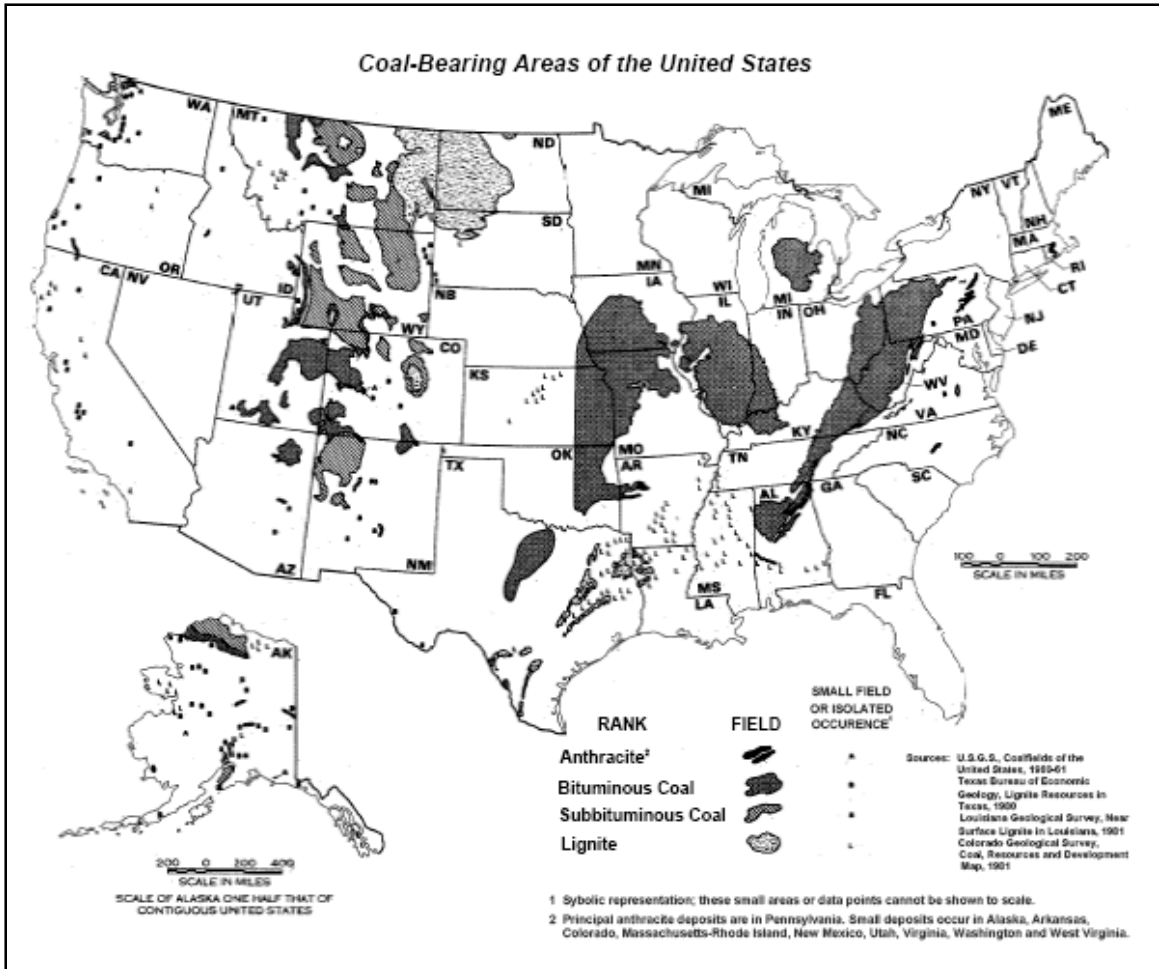


Figure 3.7: U.S. coal distribution
 Source: National Mining Association, September 2005,
http://www.nma.org/pdf/c_bearing_areas.pdf.

Table 3.6: States with the largest coal reserves (EIA, 2006).

<i>State</i>	<i>Reserves (Million Short Tons)</i>
Montana	75,030
Wyoming	42,232
Illinois	38,040
West Virginia	18,246
Kentucky	15,109
Pennsylvania	11,889
Ohio	11,527
Colorado	9,837
Texas	9,622
North Dakota	6,963
<i>Total</i>	238,495
Percentage of U.S. Total	88.9%

Table 3.7: U.S. Coal Production by State (EIA, 2006).

<i>State</i>	<i>Production (Million Short Tons)</i>
Wyoming	375.5
West Virginia	138.4
Kentucky	113.1
Pennsylvania	63.7
Texas	47.5
Montana	37.0
Colorado	35.7
Indiana	35.4
Illinois	31.6
North Dakota	30.8
<i>Total</i>	908.7
Percentage of U.S. Total	85.0%

Texas

Texas is the fifth largest coal producer in the U.S. and leads the nation in coal consumption. In 2003, 96 percent of the coal consumed in Texas, or 102.7 million short tons, went to the generation of electricity. Of this amount, coal produced from Texas mines accounted for 44 percent, with 54 percent from Wyoming, 2 percent from Colorado and a small portion from West Virginia. Out of state coal is imported primarily by railroad.

Moore (1940) classified three major coal fields in Texas, each containing coal of different age and grade. The north-central portion of the state contains a field of Pennsylvanian age coal primarily of bituminous rank, with regions of sub-bituminous coals. The field has three workable thin seams of coal that are high in sulfur and ash.

The small Eagle Pass Field straddles the Rio Grande in the southern portion of the state. This field is composed of sub-bituminous coal beds 5 to 6 feet thick. The major field is the lignite field that extends from the Rio Grande along the gulf to Louisiana and Arkansas (seen in Figure 3.7). The beds are found at comparatively shallow depths and vary from a few inches to 25 feet in thickness.

Wyoming

Wyoming contains the second largest reserves of coal after Montana and produces the most coal annually by a considerable margin. Approximately 54 percent of the state is underlain by coal. Wyoming's ten coal fields are composed of several disconnected regions consisting primarily of sub-bituminous coals. Coal beds in the Wyoming's Powder River Basin region are typically 50 to 100 feet thick.

3.3.4 Coal Use

Up until the mid 1900s, the majority of coal produced was consumed for iron and steel manufacturing, transportation (railroad), household heating and chemical production. From the 1950s to the present, coal consumption has shifted towards electricity production followed by iron and steel manufacturing. The vast majority of coal (approximately 92 percent in 2003) is used for electric power production. Industrial and utility boilers and other industrial uses consume approximately 6 percent of the coal produced while coking consumes about 2 percent. A small portion of coal produced is consumed residentially or commercially, typically for heating (Freeme, 2003).

Four processes are used to produce energy from coal: combustion, carbonization, gasification and liquefaction. Burning coal is the most direct way to release the chemical energy within coal and will be discussed in detail in the following sections. Carbonization (coking) is the driving off of volatiles (water, hydrogen, methane, CO, CO₂, and coal tar) by heating the coal in a low-oxygen environment. The resultant coke burns with very low smoke emissions and is primarily used to fuel blast furnaces and foundries. Gasification is the process of converting solid coal into a gaseous form through carbonization. Coal is gasified to remove impurities, ease transportation, and produce a cleaner-burning fuel. (London, England and several east coast cities of the U.S. were first lighted by coal gas in the early 1800s.) Liquefaction is the conversion of coal to a liquid fuel. Three liquefaction techniques either convert the coal to a gaseous and then liquid form or directly from a solid to a liquid product. The interest in liquefaction of coal in the U.S. rises and falls depending on the cost and availability of petroleum (Miller, 2005).

3.3.5 Combustion Systems

Three combustion systems (fixed-bed, fluidized-bed and suspension-fired) are used in power generation and are selected based on desired output and the type and quality of coal. Table 3.8 compares the characteristics of the three combustion methods. The combustion rate-limiting factor for the three methods is either diffusion-controlled (bulk phase or pore diffusion of reactants or products) or chemically-controlled (adsorption or reactant, reaction, desorption of products) (Skinner and Smoot, 1979).

Table 3.8: Characteristics of combustion methods (Miller, 2005).

Variables	Combustion Method		
	Fixed Bed	Fluidized Bed	Suspension
Particle Size			
Approximate top size	<2 in.	<0.2 in.	180 μm
Average size	0.25 in	0.04 in.	45 μm
System/bed temperature	<1500° F	1500-1800° F	>2200° F
Particle heating rate	$\sim 1^\circ/\text{sec}$	$10^3\text{-}10^4^\circ/\text{sec}$	$10^3\text{-}10^6^\circ/\text{sec}$
Reaction time			
Volatiles	~ 100 sec	10-50 sec	<0.1 sec
Char	~ 1000 sec	100-500 sec	<1 sec
Reactive element description	Diffusion-controlled combustion	Diffusion-controlled combustion	Chemically-controlled combustion

Fixed-bed

In fixed-bed, or stoker, combustion systems, relatively large particles of coal are combusted on a grate through which air enters the fuel bed. Three patterns for fixed-bed systems vary in the method that the coal and combustion air are fed: overfeed, underfeed and cross-feed. In over-feed systems, raw fuel is fed to the top of the bed while combustion air flows through the bottom grate. In underfeed systems the raw coal and combustion air are forced beneath the active fuel bed causing the ash at the top of the bed to spill off. In cross-feed systems, the fuel moves horizontally across the grate while air is introduced from beneath. Coal is continuously added at the front of the bed and ash removed at the opposite end. Fixed-bed combustions systems are generally capable of consuming a wide variety of coals and are ideal when the inflow of fuel is variable (Miller, 2005).

Fluidized-bed

Fluidized-bed combustion (FBC) is the most recent technology for coal combustion. The term “fluidized-bed” refers to the liquid behavior of the solid materials in the combustion chamber due to the suspension of the particles by air forced up through the combustor floor. The fluidized material is composed of coal particles, an inert material (typically sand or coal mineral matter) and limestone. The coal is gradually fed into the bed and the inert material disperses and quickly heats the fuel particles to ignition temperatures through heat transfer.

The advantages of FBC are fuel flexibility, low NO_x emissions, *in situ* control of SO₂ and a potentially lower cost of operation. The turbulence within the combustor allows more uniform heat distribution and more complete coal combustion. The efficiency of the system permits lower combustion temperatures which results in lower NO_x emissions. Further, the furnace heat decomposes the limestone in the fluidized bed to calcium oxide (lime) and carbon dioxide. The CaO then combines with the gaseous sulfur dioxide and oxygen within the system to form calcium sulfate (synthetic gypsum). Depending on the sulfur content of the fuel, the limestone in the fluidized bed can comprise as much as 50 percent of the bed material (Miller, 2005).

Suspension Firing

Suspension firing (shown in Figure 3.8) is the primary combustion method used by the electricity generating industry, primarily because units can be constructed to very large sizes with combustion spaces being as large as 15 meters by 20 meters and 50 meters tall (Turns, 1996). Suspension firing furnaces combust coal pulverized so that less than 2 percent of the particles are larger than 300 μm and 65-70 percent of particles are less than 75 μm for lignites and sub-bituminous coals and 89-85 percent for bituminous and anthracitic coals. After the coal is pulverized it is pneumatically transferred to the primary zone, or lower portion, of the furnace with the primary combustion air (approximately 20 percent of the total combustion air). The primary air is consumed during the combustion of the evolved volatiles. The secondary combustion air (all remaining air) enters the furnace at high velocity to combine with the char and primary combustion products in a manner which promotes stable combustion, control of flame and complete mixing of the fuel and air. The heat generated during combustion is transferred through tubes lining the combustion space to the super-heated steam which drives turbines for electric power generation (Miller, 2005; Ishii, 2000).

Much of the mineral matter present in coal passes through the flame (in an altered form) and is referred to as ash. The ash that is formed can be categorized in two forms. First the fine particles that are small enough to be carried with the flue gases out of the combustion chamber are called fly ash. Fly ash formation is discussed in detail below. Second, the remainder that falls to the floor of the chamber and adheres to the sides of the chamber is called bottom ash.

Two classifications are given to pulverized coal combustors based on the method of bottom ash removal. In “dry-bottom” furnaces, the ash is removed from the combustion chamber in solid form while the ash in “wet-bottom” furnaces flows from the chamber in molten form.

Dry-bottom combustors make up the majority of suspension firing units. The heat release rate of dry-bottom furnaces is slower than wet-bottom furnaces and the exit gas temperature must be maintained lower than the ash fusion temperature. The flame temperature is typically around 1500°C and flue gas exit temperature at about 1000°F. Several burner configurations have been developed for varying combustion temperature and different types of fuel. These configurations vary the location and the number of burners within the furnace. Typically more than 80 percent of the coal ash in dry-bottom furnaces is fly ash that must be removed by particulate control devices.

Wet-bottom furnaces allow easier ash handling and disposal, but have lower efficiency because of slag heat loss. Up to 80 percent of coal ash is retained in the furnace in molten form and is tapped for removal. Wet-bottom furnaces have less fuel flexibility because of the ash fusibility and viscosity constraints, because the ash must melt to cover the walls and then flow easily from the system. Wet-bottom furnaces also have higher flame temperatures which results in higher NO_x emissions.

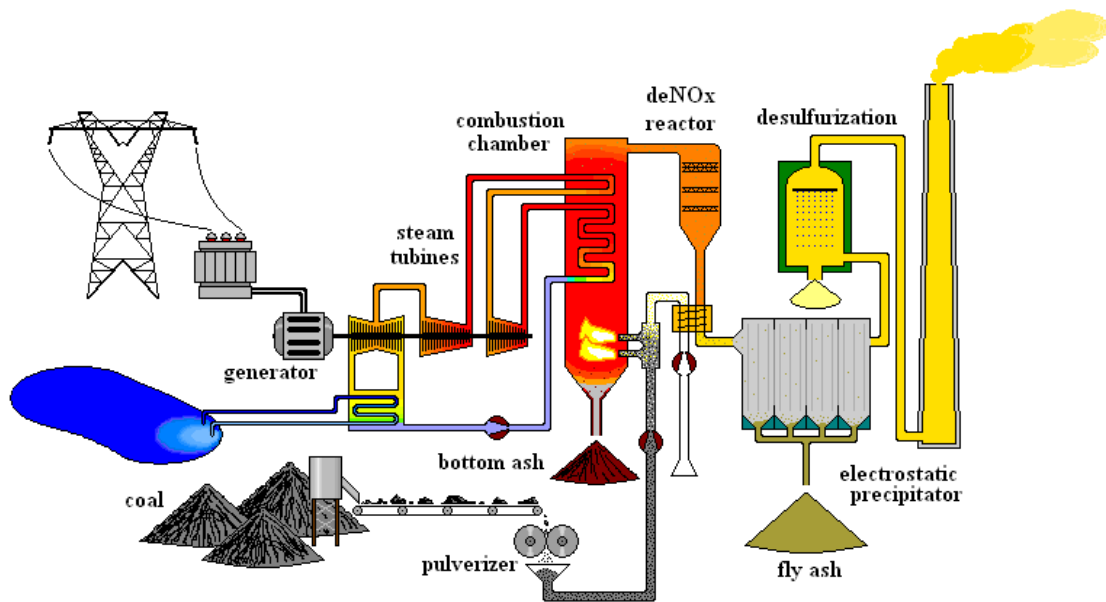


Figure 3.8: Pulverized coal fired power plant schematic.

3.3.6 Combustion Process

The combustion of pulverized coal is a complex process that has been modeled in various ways (Turns, 1996). This section identifies the basic combustion process of pulverized coal and

the primary chemical reactions that take place. The major steps of the pulverized coal combustion and fly ash formation process are: preheating, devolatilization, ignition, char burnout and fly ash formation. Figure 3.9 shows the steps in the coal combustion and fly ash formation processes that are detailed below.

Preheating

Combustion begins when pulverized coal particles, generally less than 50 to 100 microns in diameter, and air are injected into the combustion chamber by the firing unit. The particles are heated first by the preheated air with which it is mixed and then by radiation from the downstream flame as it enters the combustion furnace. At this time the inherent moisture in the coal is driven off. Figure 3.9(1) shows a representation of a typical coal particle containing mineral inclusions and interconnected void system.

Devolatilization

As the temperature of the particle rises above 300-400°C, the volatile materials within the coal are emitted as vapors (Figure 3.9(2)) (Essenhigh, 1981). Initially, the surface area of the coal particle will increase due to expansion. The coal particle may soften and become plastic upon rapid heating. As devolatilization continues, a decrease in surface area occurs as tar within the particle solidifies within the pores or on the surface of the particle (Ishii, 2000). The surface area then rapidly increases as tar evaporates, existing pores are expanded and new pores are opened by the evolving gases, [Figure 3.9(3)]. Devolatilization is completed over a period of a few hundred milliseconds and a carbon-rich char (charcoal) still containing the mineral inclusions remains.

Ignition

Ignition (the initiation of sustained combustion) of the particle can occur in two ways, depending on the properties of the coal particle and the combustion environment. First, when the volatile materials are evolved rapidly, e.g., for small particles or rapid heating, ignition of the released volatiles occurs away from the surface of the coal particle. This type of ignition is called homogenous ignition. (Ishii 2000; Miller 2005) Combustion of the solid char occurs when the volatiles are mostly exhausted.

In the second ignition condition, heterogeneous ignition, the volatiles and char are ignited simultaneously at the surface of the particle. This condition typically occurs in particles larger than 100 microns in diameter where the rate of temperature increase within the particle is relatively slow (Ishii, 2000).

Char burnout

Once the volatiles are removed, the solid, organically-derived, carbon-rich residual of coal, called char, and the inorganic minerals remain. By the time the volatiles have been evolved, combustion is occurring at the char surface. Char combustion occurs at a much slower rate than devolatilization, on the order of several seconds depending on conditions in the combustion chamber (Miller, 2005). The rate of char combustion is controlled by the diffusion of oxygen to the particle surface and is proportional to the square of the particle diameter (Ishii, 2000). Studies have shown that the combustion of char occurs by the chemisorption of oxygen at active sites on the char surfaces. This is followed by the decomposition of the surface carbon oxides to form

carbon monoxide (CO). The CO is then oxidized in the zone around the char particle to form carbon dioxide, CO₂. As the surface carbon oxides decompose new active sites are exposed for oxidation and the process continues until the char is consumed (Miller, 2005).

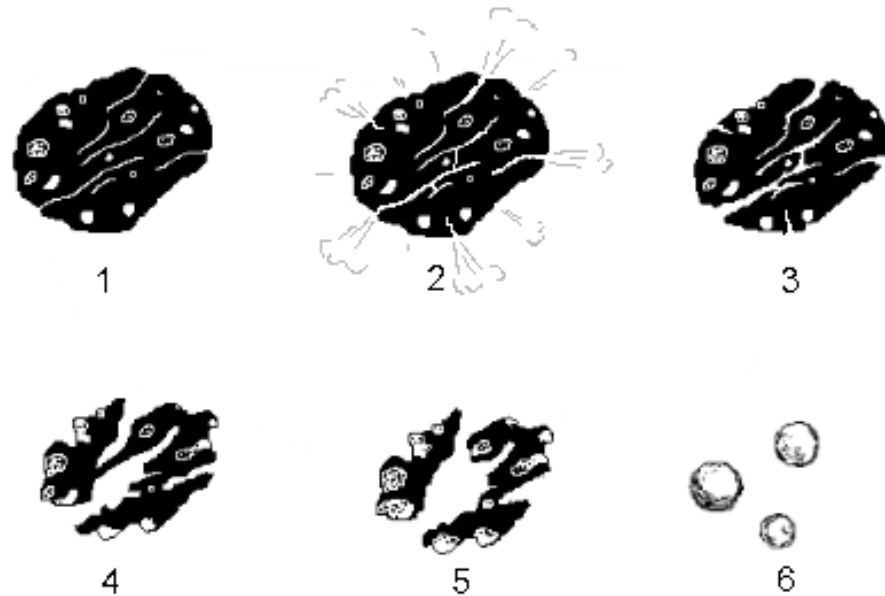


Figure 3.9: Coal combustion and fly ash formation.

Coal Combustion By-products

The combustion of coal produces several types of coal combustion by-products (CCBs). These are divided into two groups, combustion emissions and coal combustion products.

Coal combustion emissions are further divided into particulate matter, sulfur oxides, nitrogen oxides, organic compounds, carbon monoxide, carbon dioxide and trace elements. Table 3.9 lists CCBs and general effects each cause on the environment and human health (Miller, 2005). Trace elements such as cadmium, lead and mercury are present in all coals in small concentrations. During combustion, trace elements are distributed in the bottom ash, fly ash and flue gases. The distribution depends on many factors including volatility.

Coal combustion products (CCP), as labeled by the utility industry and ash marketers, are the materials that can be utilized by several industries. CCPs includes fly ash, bottom ash, boiler slag, flue and gas desulfurization (FGD) materials. Fly ash is the finely divided glassy material that is collected in the particulate control systems of the plant and is discussed in depth in the following sections. Bottom ash is consists of the particles that are too large to be carried out of the combustion chamber and instead fall to the floor. Bottom ash is primarily used in structural fills and road base construction. Boiler slag is the molten ash material that is tapped from the wet-bottom boilers. It is quenched in water to form hard, glassy particles used as blasting grit and roofing granules. FGD materials (primarily synthetic gypsum but also calcium hydroxide and calcium carbonate) are formed by the reaction of calcium-containing reactants with sulfur dioxide in FGD units. Synthetic gypsum is utilized in the production of wallboard as well as for agriculture purposes (Reid, 1981; Goodwin, 1993; Miller, 2005).

3.3.7 Fly Ash Production

Fly ash production is divided into three components, fly ash formation, collection and uses/distribution.

Table 3.9: Coal combustion by-products effects on the environment and human health (Miller, 2005).

CCB	Environment Effects	Health Effects
Particulate Matter	Reduced visibility, soils surfaces	Aggravation of asthma and other respiratory conditions, lung disease
Sulfur oxides	Damage to materials/vegetation, reduced visibility, acid rain	Breathing impairment, respiratory illness
Nitrogen oxides	Damage to materials, reduced visibility, suppresses vegetation growth, smog, acid rain	Breathing impairment in individuals with respiratory illness
Organic compounds	Adverse effects on certain plants	Some known carcinogens
Carbon monoxide	--	Poisonous in high concentrations, low doses dangerous to individuals with cardiovascular disease
Carbon dioxide	Greenhouse gas	Global climate change effects

Fly Ash Formation

Ash is the material that remains after the char matrix that contains the inorganic mineral matter inclusions is consumed by oxidation. Combustion converts the solid carbon of the char into gaseous carbon oxides and the mineral matter is liberated. Fly ash is the finely-divided ash that is suspended in the flue gases exiting the combustion chamber.

The mineral matter while still present in the coal is exposed to temperatures between 1400 and 1700°C for about 50 ms as the pulverized coal passes through the flame front. The mineral matter may experience physically and chemical changes due to the high temperatures. Some of the minerals (for example, pyrites, feldspars and mica) melt whereas others (such as calcite, dolomite and kaolin) are calcined. As char burnout proceeds in the combustion chamber, most of the hot, molten mineral inclusions tend to fuse together, though small portions may vaporize. The agglomeration of molten materials occurs chiefly during the last 25 percent of char combustion. After passing through the flame, interactions between the mineral particles continue for an additional 2 to 5 s as they pass through the furnace and heat transfer sections of the boiler (Reid, 1981).

As the char in a single particle is consumed by combustion, it becomes weak and fractures (as shown in Figure 3.9(5)). The number of resultant char fragments, each containing

mineral matter, determines the number of large fly ash particles formed per original coal particle (Malte and Rees, 1979). The char is consumed by combustion and only the mineral matter, now called ash, remains. As the ash exits the combustion chamber, the material is quenched by cooler temperatures to form primarily spherical glassy beads generally 1 to 100 μm in diameter.

The bulk chemical composition of ash is essentially equal to bulk chemical composition of the mineral matter of the parent coal; however ash mineralogy may be significantly modified due to high temperature exposure. The ash consists primarily of two phases, a crystalline phase and a glassy phase. The ashes can be characterized as crystalline phases in a matrix of aluminosilicate glass (Joshi and Lohitia, 1997). Some alkalis (Na_2O , K_2O) are volatilized in the flame and then condense on cooling particles. Sulfur oxides (mainly SO_3) are partially adsorbed on ash particle surfaces.

Fly ash particles of submicron size appear to be a result of mineral vaporization and subsequent condensation. Mineral vaporization occurs in several forms: (1) above about 1080°C , alkali-metal salts vaporize; (2) at high temperatures, compounds of heavy metals such as As, Cd, Cr, Ni, Pb, Se, Sb, Tl and Zn will boil or sublime; and (3) above 1630°C , silica volatilizes. As the furnace gases cool, the inorganic vapors undergo homogenous nucleation and heterogeneous condensation on particles in the gas stream. Because small particles have greater specific surface areas, they tend to collect larger quantities of the condensed metallic, as well as condensable sulfates (Malte and Reese, 1979).

The term “fly ash” is used to describe all the particulate matter that exits the combustion chamber with the flue gases and is collected by the particulate control systems. This includes the glassy portions, unaltered mineral matter and organic coal residuals that were not completely burned in the combustion chamber. The organic coal residuals are chiefly present as carbon-rich char (though other carbon forms may be present).

Fly Ash Collection

Modern coal-fired power plants typically employ electrostatic precipitators (ESPs) or fabric filters (baghouses) to collect particulate matter. ESPs operate on the principle of attraction between opposite charges. ESPs typically consist of negatively charged electrodes and rows of positively charged collecting plates housed in large hopper-bottomed boxes. A high voltage direct current (up to 100 kV) induces a corona of negatively charged air molecules in the vicinity of the electrodes. As the flue gases enter the ESP, the gas velocity is slowed and the particulate matter suspended in the gas becomes charged due to collisions with the charged air molecules. The charged particulates then flow further into the ESP between the collecting plates. The charge differences cause the particles to migrate out of the flow and collect on the plates. The plates are periodically rapped to remove amassed materials which fall into the hoppers for collection. See also Miller (2005), Bohm (1982) and Slack (1981).

Fabric filters for particulate removal are typically tubular bags arranged in parallel groups within a baghouse. The flue gases and entrained particulates are forced through the porous filter bags where the particles are captured in the filter material or residual dust cake. The filters are cleaned by reversing air flow in offline filters and/or shaking to dislodge the collected ash into hoppers at the bottom of the baghouse (Miller, 2005; Slack, 1981; Englund and Beery, 1975).

Fly Ash Uses/Distribution

In 2005, 71.1 million short tons of fly ash were produced in the U.S. Of this amount, approximately 41 percent was utilized while the remainder was land-filled (American Coal Ash

Association, 2005). The greatest ash utilization was in concrete, concrete products or grout. Other uses for fly ash are as a source of silica and alumina in cement manufacture, structural fills and embankments, flowable fill, soil stabilization, asphalt paving mixtures and others.

Collected ash is either managed by the utility or in most cases by a second party ash distributor that collects the ash, monitors the ash quality and markets the ash to industry. In some cases, the ash is subjected to beneficiation processes to separate or remove certain materials. Methods for reducing the organic coal residuals content in ash are discussed in Section 3.5.2.9

3.3.8 General Properties of Fly Ash

Particle morphology

Fly ash consists of finely divided particles that are primarily spherical in form. Figure 3.10 from Fisher et al. (1987) shows that ash particles can be present in a variety of forms, including solid or hollow spheres, fractured spheres and angular or irregular particles. Particle form is related to both physical composition and exposure conditions in the combustion chamber. Ash particles are typically silt-sized (less than 75 micrometers) with individual particles ranging from less than one to several hundred microns in size. A typical ash particle is approximately 15 to 30 microns in diameter (Figure 3.11). Non-opaque (translucent) solid spheres or hollow, glassy spheres called cenospheres make up over 90 percent of finest particles (less than 20 μm). Large ash particles, particles greater than approximately 0.2 mm in size, are typically angular and irregular in form, though particles of this size generally contribute to less than 5 percent by mass. Plerospheres are considered to be cenospheres which were punctured and filled with smaller materials (Carpenter et al., 1980).

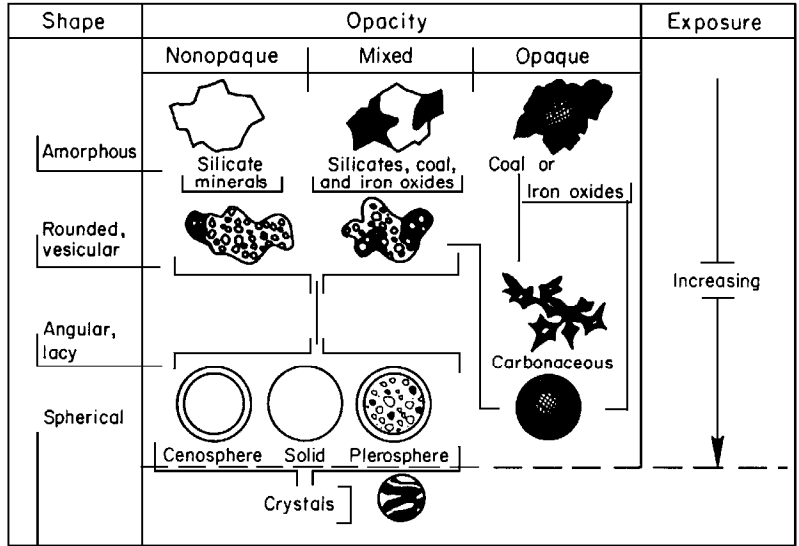


Figure 3.10: Fly ash morphogenesis scheme illustrating probable relationship of opacity to particle composition and relationship of particle shape to exposure in combustion chamber (Fisher et al. 1987).

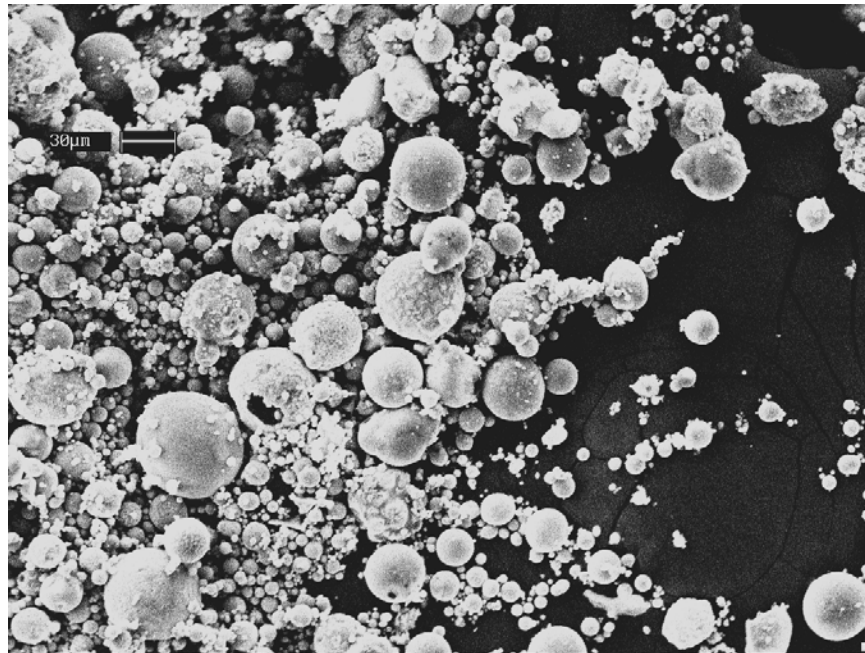


Figure 3.11: SEM image of fly ash, 500x magnification

Fly ash chemistry and mineralogy

Pulverized coal fly ash is a heterogeneous mixture of many different mineral components. Bulk chemical analysis by XRF produces the approximate percentage of the basic metal oxides present in the ash, but does not indicate which mineral groups are present. Table 3.10 includes the prominent minerals present in ash and a general range of percent compositions. Metal oxides detected by the analysis, shown in Table 3.10, are not necessarily present in the

form shown and can be constituents of many different phases. Calcium, for example, may be present as calcium hydroxide, calcium sulfate, calcium carbonate and in a calcium-containing glass.

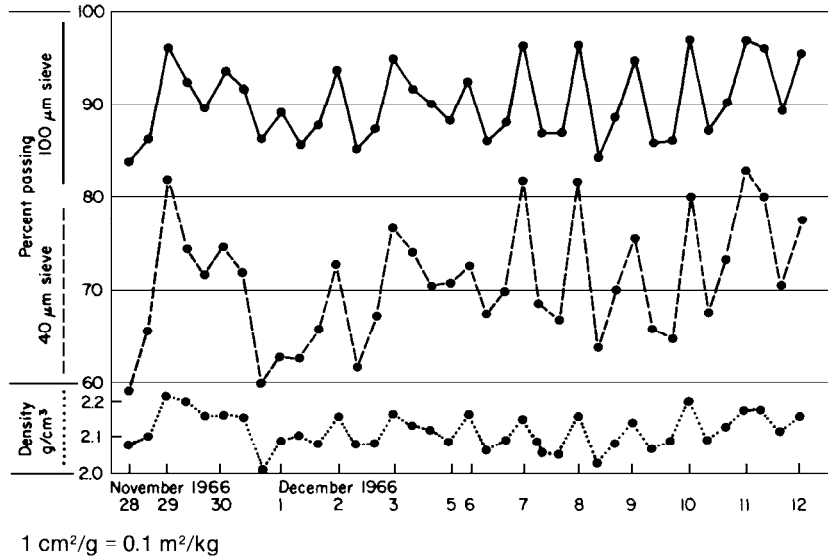
Table 3.10: Typical compositions of fly ashes, % (Helmuth, 1987).

Component	Bituminous coal	Lignite
SiO ₂	47-63	18-50
Al ₂ O ₃	15-35	12-20
Fe ₂ O ₃	4-12	6-8
CaO	1-15	18-50
MgO	1-3	2-6
Na ₂ O	0.2-2	0-5
K ₂ O	1-6	0-5
SO ₃	0-1	1-9

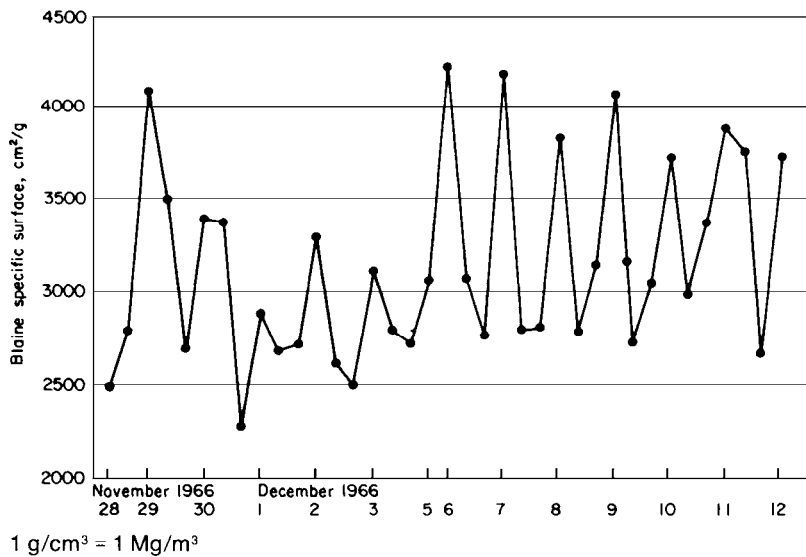
The major inorganic constituents in fly ash are composed of both crystalline and amorphous minerals. The crystalline mineral content can include quartz (SiO₂), mullite (3Al₂O₃·SiO₂), maghemite (Fe₂O₃), periclase (MgO) and other phases. Fly ash amorphous minerals content can consist of various quantities of aluminosilicate, calcium aluminosilicate, calcium aluminate and other glassy phases (Helmuth, 1987; Joshi and Lohitia, 1997). While the crystalline phases present can be determined and quantified using X-ray diffraction, no reliable method for measuring the various amorphous phases exists (though methods are currently in development).

Variability of properties

Because fly ash is a byproduct of the electrical power generation industry, its production and quality is of secondary concern to plant operators for whom the primary concern is economical plant operation. Fly ash is sensitive to many factors throughout its production process, primarily coal source, mineral constituents and combustion chamber environment. Because the conditions within the combustion chamber conditions can vary day by day, even hour by hour, the physical properties can also change as a result. Figure 3.12 gives examples of changes in ash properties (specific gravity and surface area measurements) of fly ash over a period of 2 weeks Helmuth et al. (1987). Other properties of ash beside those shown in Figure 3.12 can also vary. Residual unburned coal content of ash is one property that can vary with time at a single source. Fly ash samples collected by Hill et al. (1998) from a continuously operating power plant over a period of several months showed loss on ignition values (rough measurements of organic coal residuals) varying between 2 and 9 percent.



a. Variations in particle size and density



b. Variations in Blaine surface area.

Figure 3.12: Daily variations in properties of fly ash produced by a generating station under continuous operations. From Helmuth (1987).

3.3.9 Conclusion

Fly ash used in concrete is the by-product of the combustion of coal for electric power generation. Fly ash begins as diverse mineral inclusions in coal which is a complex sedimentary rock of organic origins. Once the coal is extracted, pulverized and combusted, the mineral inclusions are liberated. Drops of molted ash may agglomerate in the combustion chamber and upon exiting are quenched to form primarily glassy particles. The ash is collected by the plant particulate control system and is land-filled or marketed by a distributor for a variety of uses including as a supplementary cementitious material for concrete. Fly ash is a variable material

and its properties must be tested regularly to ensure quality or to be able to make compensatory adjustments.

3.4 ASTM C618 Specification for Fly Ash

Specifiers typically govern the use of fly ash in portland cement concrete by adopting ASTM C618, Standard Specification for Coal Fly Ash and Raw or Calcined Natural Pozzolan for Use as a Mineral Admixture in Concrete. The specification defines the classification of materials, tolerances on the chemical and physical compositions of the materials, and other information regarding testing, storage and packaging. Because fly ash can be created in many types of combustion processes, the standard specification defines fly ash as “the finely divided residue that results from the combustion of ground or powdered coal and that is transported by flue gasses.”

3.4.1 Classification of Pozzolans

ASTM standard C618 classifies pozzolans into three categories: Classes N, F and C. Class N pozzolans are raw or calcined natural pozzolans such as volcanic ash, calcined clays (metakaolin), diatomaceous earth and others that meet the requirements of the class. The designations *Class F* and *Class C* are reserved for describing pulverized coal combustion fly ashes. Class F fly ashes have primarily pozzolanic properties while Class C ashes possess both pozzolanic and hydraulic properties; however, the extents of these properties exist on a continuum and the division made by the standard is to some extent arbitrary.

The standard specification, and many other literary sources on fly ash use in concrete (ASTM C618; Helmuth, 1987; Joshi and Lohit, 1997), state that Class F fly ash is typically produced by the combustion of anthracite or bituminous coals while Class C fly ash is normally produced as a byproduct of the combustion of lignite or sub-bituminous coals. While this rule-of-thumb may be true for parts of the industry, both the Class F and Class C ash samples produced in the state of Texas, which were the focus of the research in this study, were collected from combustion units that were burning nearly equal proportioned mixes of Texas lignite coal and Wyoming sub-bituminous coal.

3.4.2 Chemical Requirements, Class C versus Class F Ash

The classification of an ash as Class C or Class F is not made by a measurement of the cementitious behavior of the ash but by its chemical composition. Normally, fly ash is composed chiefly of the oxides of silicon, aluminum, iron and calcium with lesser quantities of the oxides of sodium, potassium, magnesium, titanium, phosphorus, barium, manganese, strontium and sulfur. Together, these oxides typically compose 99 percent or more of the inorganic fraction of the moisture-free ash. Ash received from a producer or distributor will likely also contain moisture and organic coal residuals. ASTM C618 classifies ash type based on the sum of the percentages of the oxides of silicon, aluminum and iron as a minimum percentage of the total moisture-free, inorganic constituents of the ash. The sums of silica, alumina and iron oxides for Class F and Class C ashes are shown in Table 3.11.

Though not explicit in the specification standard, the sum of silicon, aluminum and iron oxides as a percentage of total oxides is lower for Class C pozzolans than Class F pozzolans because of the typically larger amounts of calcium oxides present in the cementitious Class C ashes.

Table 3.11: ASTM C618 Standard specification chemical requirements for fly ash.

	Class F	Class C
SiO ₂ + Al ₂ O ₃ + Fe ₂ O ₃ , min, %	70.0	50.0
SO ₃ (sulfur trioxide), max, %	5.0	5.0
Moisture content, max, %	3.0	3.0
Loss on Ignition, max, %	6.0 ¹	6.0

¹Class F ash containing up to 12.0% loss on ignition may be used if either acceptable performance records or laboratory test results are made available.

3.4.3 Moisture Content

ASTM C618 limits the moisture content of ash samples for use in portland-cement concrete to 3 percent by mass of the oven-dried sample. Any moisture that may have existed in the parent coal was likely evaporated rapidly in the high temperatures of the combustion chamber. However, fly ash can come into contact with moisture from other sources at several points in the system between production and use in concrete. Wet methods of pollution control, such as spraying a lime solution to scrub the flue gases of sulfur oxides, or ash collection can be employed, depending on the power plant post-combustion system. The ash may also be exposed to precipitation or humidity during storage or transportation. Experience from the use of ash in the laboratory suggests that it is hygroscopic and readily adsorbs moisture from the environment. The ash must be sufficiently dry to be transported by vacuum or pressure lines into storage silos.

The measurement method for the moisture content of ash samples is given by ASTM C 311, Standard Test Method for Sampling and Testing Fly Ash or Natural Pozzolans for Use as a Mineral Admixture in Portland-Cement Concrete. For the test, a weighed sample is dried in an oven at 105 to 110°C until its weight becomes stable. The moisture content, in percent, is calculated as the mass lost during drying divided by the weight of the oven-dried sample all multiplied by one-hundred.

3.4.4 Loss on Ignition

The loss on ignition (LOI) test is used to measure the change in ash mass between oven-drying temperatures and 750 ± 50°C. ASTM C618 limits the losses due to high-temperature treatment to 6 percent for both Class F and C ashes, though 12 percent losses for Class F ash are allowable if either acceptable performance records or laboratory test results are made available. (ASTM C618 does not specify what acceptable performance records or laboratory results are necessary.)

The LOI procedure for fly ash and natural pozzolans is standardized in ASTM C 311, which is a modification of the LOI procedure for hydraulic cement described in ASTM C 114, Standard Test Methods for Chemical Analysis of Hydraulic Cement, such that the peak furnace temperature is 950°C for cement, but only 750°C for fly ash.. The standard states that 1 g of the ash sample used in the determination of the moisture content be placed in an uncovered porcelain crucible and heated in a muffle furnace (an air atmosphere furnace) at 750 ± 50°C until a constant weight is obtained. The test specifies that the test be performed with an initial heating period of 15 min and a minimum of 5 min per interval for subsequent heating intervals. LOI is

calculated as the percent change in mass between 105 and 750°C based on oven-dry mass. Harris (2006) has recently addressed procedural issues to improve precision of the test.

3.5 Effects of fly ash on air entrainment: the current state of knowledge

The incorporation of fly ash as a supplementary cementitious material in concrete can increase the required dosage of air entraining admixtures (AEA) relative to concrete without fly ash. AEAs are added to concrete to improve its resistance to damage caused by repeated freezing and thawing. In this section, the properties of air-entrained concrete are discussed followed by a review of the state of knowledge concerning fly ash and AEA interactions at the outset of this project.

3.5.1 Air-entrained concrete

Freeze-thaw resistance

The hardened cement matrix of portland cement concrete contains an extensive network of interconnected pores that formed as the cement grains hardened (Helmuth, 2006). When hardened concrete is exposed to moisture, water is absorbed into this pore system. If saturated or nearly saturated when the concrete is subsequently frozen, the water within the pores also freezes and induces stress in the hardened cement matrix due to expansion of water and other mechanisms (Neville, 1997). Tensile stresses associated with freezing of absorbed water can result in cracking and localized failure of the matrix. Repeated freezing and thawing of the concrete cause degradation, as the most exposed and/or weakest or most porous layers of the concrete crack and spall.

Micro air bubbles are intentionally entrained in the cement matrix of fresh concrete to improve resistance to damage caused by freezing and thawing of the hardened concrete (Mehta, 2006). The bubbles are suspended in the matrix and upon hardening result in spherical air-filled spaces. The resulting air voids are present in a wide range of sizes varying from 10's μm to the size the coarse aggregate particles (Hover, 2006). These voids intersect the pore system of the matrix, and when the concrete freezes, act as reservoirs to accept the expansion of ice and unfrozen water thus reducing the buildup of pressure and decreasing the likelihood of cracking. Figure 3.13 shows an SEM image of an air void in young concrete paste containing ice crystals (Figure 3.13a) and the same void after sublimation of the ice (Figure 3.13b). The voids remain dry, even when the pore system is saturated or nearly saturated for the reasons described by Hover (2006).

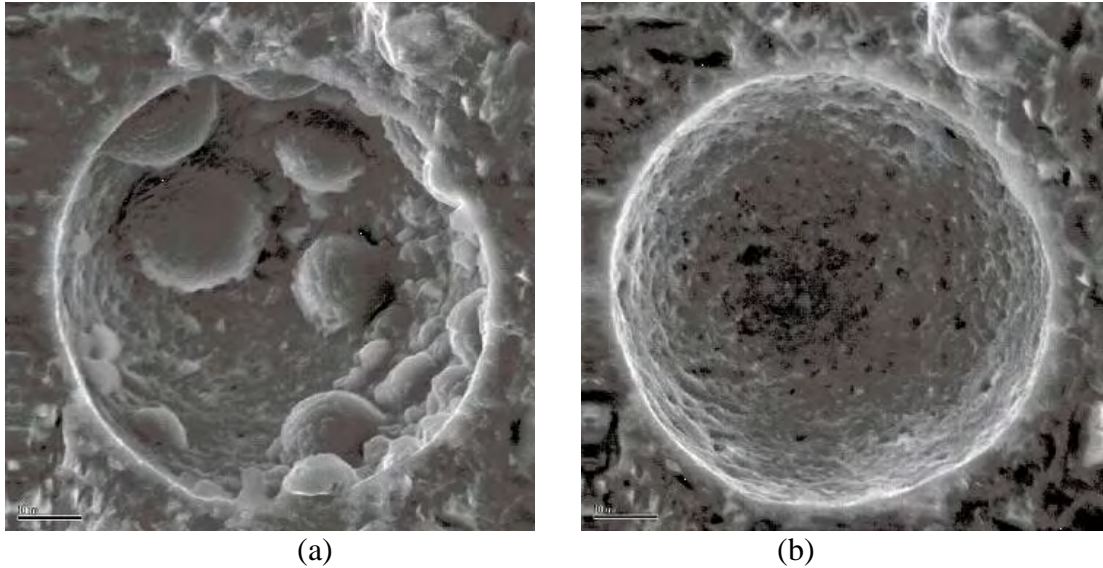


Figure 3.13: SEM image of air void with ice crystals (a) and after sublimation of ice (b) (bars are 10 μm). From Corr, 2002.

Entraining air

Air voids are trapped in fresh paste as the kneading and folding action of concrete mixing forms air bubbles that are stabilized by a surfactant known as an air entraining admixture. Air voids in concrete exist as both intentionally stabilized bubbles and due to air that also trapped in the concrete as a result of placing. Voids that fall into the latter category are typically referred to as “entrapped” air and are distinguished primarily by their non-spherical shape and larger size (generally greater than 1 mm). (The 1 mm threshold is due merely to the fact that for air bubbles in water, the predominance of surface tension forces pulls bubbles that are less than about 1 mm in diameter into a spherical shape. As bubbles grow larger gravity forces predominate and irregular shapes appear (Hover, 2006). It is hypothesized that air voids remain in the paste due to the fine particles which act as a net to keep the bubbles from rising out of the paste and because of static charges that bind the bubbles to the cement particles (Rixom and Mailvaganam, 1986; Dolch 1984).

Table 3.12: Recommended total target air content for concrete, (ACI, 1991).

Nominal maximum aggregate size, in. (mm)	Air content, percent*		
	Severe exposure**	Moderate exposure†	Mild exposure††
< 3/8 (< 9.5)	9	7	5
3/8 (9.5)	7-1/2	6	4-1/2
1/2 (12.5)	7	5-1/2	4
3/4 (19.0)	6	5	3-1/2
1 (25.0)	6	4-1/2	3
1-1/2 (37.5)	5-1/2	4-1/2	2-1/2
2 (50)‡	5	4	2
3 (75)‡	4-1/2	3-1/2	1-1/2

- * Project specifications often allow the air content of the concrete to be within -1 to +2 percentage points of the table target values.
- ** Concrete exposed to wet-freeze-thaw conditions, deicers, or other aggressive agents.
- † Concrete exposed to freezing but not continually moist, and not in contact with deicers or aggressive chemicals.
- †† Concrete not exposed to freezing conditions, deicers, or aggressive agents.
- ‡ These air contents apply to the total mix, as for the preceding aggregate sizes. When testing these concretes, however, aggregate larger than 1-1/2 inch (37.5 mm) is removed by handpicking or sieving and air content is determined on the minus 1-1/2 inch (37.5 mm) fraction of mix. (Tolerance on air content as delivered applies to this value.)

The air content required for a given concrete is dependent on the environmental conditions to which the hardened concrete will be exposed and the amount of paste present in the concrete. The higher the paste content, the more air voids (and hence air volume) necessary for protection. Table 3.12 from ACI 211.1 (also Whiting and Nagi, 1998; Kosmatka et al., 2003) shows the recommended total air content of concrete based on exposure conditions and maximum coarse aggregate size. Coarse aggregate size is used because the ACI 211 mix design method produces higher paste contents for smaller coarse aggregate sizes (Hover, 2006). Air content of fresh concrete is generally measured in the field by means of a pressure meter (ASTM C 231), volume air meter (ASTM C 173) or by unit weight (ASTM C 138).

Air void system

The term “air void system” is used to describe the characteristics of the air voids distributed in the cement matrix. The ability of the overall air void system to adequately protect the concrete from freeze/thaw related damage is dependent on the percent volume and distribution of air in the paste. ASTM C 457 Standard Practice for Microscopical Determination of Air-Void Content and Parameters of the Air-Void System in Hardened Concrete is used to estimate several parameters for an approximate assessment of air content and void distribution. The measured parameters are compared to traditional standards to determine if the measured system is adequate for freeze/thaw protection (Hover, 2006; Whiting and Nagi, 1998).

Air entraining admixtures

Air entraining admixtures (AEAs) are specialty surfactants added to the fresh concrete. In general terms, surfactants are materials which when dissolved at low concentrations influence the interfacial behavior of solutions. A characteristic of all surfactant molecules is they are composed of hydrophobic and hydrophilic groups. The hydrophilic portion of a surfactant molecule is typically ionic (though nonionic surfactants also exist) and interacts with polar water molecules based on electric charges. The hydrophobic portion of a surfactant molecule is always nonionic and frequently is composed of hydrocarbons. Several types of surfactants exist and are described various sources (Rosen, 2004; Tsujii, 1998).

When added to pure water, surfactants congregate at the solution interfaces and reduce surface tension. When agitated the interfaces are folded and sheared and trap pockets of air in the solution to create bubbles. Lower surface tension allows small bubbles to be formed with less energy input. The surfactant molecules are aligned at the air water boundary of the bubbles, with the hydrophobic portions oriented towards the air and the hydrophilic ends oriented toward the water, and impart elasticity and strength and thus stability to the bubble wall. The orientation of the surfactant molecule provides resistance to the coalescing of neighboring bubbles due to the like charges of the hydrophilic interfaces (Shaw, 1985; Myers, 1946).

When AEAs (which are typically anionic surfactants) are added to fresh concrete paste, the interactions that occur between the AEA and solution are more complex than those in pure water due to the presence of solid particles with charged surfaces and the abundance of ions in solution (Powers, 1968; Bruere, 1971). Nevertheless, the net effects are similar, such that bubbles trapped during mixing are subsequently stabilized by the AEA and retained in the fresh concrete.

Most surfactants can be used as an air entraining admixtures in concrete, though the types used to produce AE concrete are typically those that are most economical (Dolch, 1984; Whiting and Nagi, 1998; Edmeades and Hewlett, 1998; Rixom and Mailvananam, 1986). Many air entraining admixtures are readily available in the chemical industry. Most AEA's are proprietary and complex mixtures of blended materials. ASTM C 260, Standard Specification for Air-Entraining Admixtures for Concrete, is used to govern the quality of commercial AEAs.

Air entraining admixture dosing

AEA dosage is typically a function of the amount of cement or cementitious materials in a mix and is often expressed as mL AEA per 100 kg of cement (or cementitious materials). The AEA dosage required varies among AEA types and for desired air content. Several factors regarding the concrete ingredients can influence AEA dosage of a given concrete mix including cement content and fineness, maximum aggregate size, sand grading, mixing water, sequence of materials addition and others (Whiting and Nagi, 1998). The addition of supplementary cementitious materials, particularly fly ash, can increase the required AEA dosage (Table 3.13).

Table 3.13: Effects of supplementary cementitious materials on air content. From Whiting and Nagi (1998).

Material	Effects	Guidance
Fly ash	<p>Air content decreases with increase in LOI (carbon content).</p> <p>Air-void system may be more unstable with some combinations of fly ash/cement air-entraining admixtures.</p>	<p>Changes in LOI or fly ash source require that air-entraining admixtures dosage be adjusted.</p> <p>Perform “foam index” test to estimate dosage.</p> <p>Prepare trial mixes and evaluate air-void system.</p>
Ground granulated blast furnace slag	Decrease in air content with increased fineness of GGBFS.	Use up to 100% more air-entraining admixtures for finely ground slags.
Silica fume	Decrease in air content with increase in silica fume content.	Increase air-entraining admixture dosage up to 100% for fume contents up to 10%.
Metakaolin	No apparent effect.	Adjust air-entraining admixtures dosage if needed.

3.5.2 Fly ash increases AEA dosage in concrete

Studies on AEA and fly ash interaction

As shown in Tables 3.1 and 3.13, incorporation of fly ash in concrete can result in an increase in the AEA dosage. Gebler and Klieger (1983) reported a study in which concretes containing portland cement and fly ash were evaluated to determine the effect of fly ash on air-void stability. The study concluded that all concretes incorporating fly ash required more AEA than concretes that did not incorporate ash. Concretes containing Class C ash required less AEA than concretes containing Class F ash. Air contents of concrete containing Class C fly ash appeared to be more stable (less change in air content over time) than those of concrete containing Class F fly ash. The primary factor influencing AEA dosage and air void stability was identified as the organic materials content of the ashes, which were lower in Class C ash than Class F ash. Overall it was concluded that the higher the organic residuals content of a fly ash, the higher the air-entraining admixture requirement for concrete in which the admixture is used.

Carbonaceous residue in ash

High levels of organic coal residuals in fly ashes can have a negative impact on the use of fly ash in concrete- the main market for fly ash. High levels of organic coal residuals can cause undesirable darkening of the ash (Yu et al., 2000; Hoffman, 2007; Hurt, 2001) and increase LOI contents possibly causing the ash to fail the ASTM C618 specifications for LOI content. Most importantly, increased organic coal residuals in ash can unfavorably influence air-entrainment of concrete as is discussed in the following sections. This is related to the generally proposed hypothesis that higher levels of organic residuals in fly ash are responsible for higher adsorption of the organic-based AEA's (Gebler and Klieger, 1983; Gao et al., 1997; Freeman et al., 1997; Hill et al., 1997; Hill et al., 1998; Yu et al., 2000; Joshi and Lohitia, 1997; Hurt et al., 2001). This presents a problem for concrete manufactures because fly ash variability from source to source and variability within a single can make accurate AEA dosing difficult. Furthermore, concrete mixtures requiring high AEA dosage have been shown to have unreliable performance (Gebler and Klieger, 1983).

It is the current author's opinion that the hypothesis that adsorption of AEA by the organic coal residuals is the primary mechanism influencing fly ash-AEA interactions has not been scientifically proven. While the adsorption hypothesis is a likely explanation, the experiments and studies described below that were used by researchers to support the adsorption hypothesis measure ash-AEA interactions but do not directly measure adsorption. Despite the lack of clear evidence, many researchers (Freeman et al., 1997; Sabanegh et al., 1997; Gao et al., 1997; Hill et al., 1997; Kulaots et al., 2000, 2004; Hurt et al., 2001; Baltrus and LaCount, 2001) refer to the phenomenon of ash-AEA interaction as "AEA adsorption," primarily adsorption on solid carbon which is a form of organic coal residuals. Use of the term "adsorption" in this literature survey is done to reflect the words of the researchers. In many cases "adsorption" could be replaced by the more general "AEA interactions" which reflects the true state of knowledge.

Whiting and Nagi (1998) reported that air content in concretes decrease as LOI (or carbon content) in fly ash increases (Table 3.13). Several researchers have concluded that this is due to the adsorption of AEA from fresh concrete aqueous solutions onto the surfaces of solid organic coal residuals. AEA molecules adsorbed onto organic coal residuals can no longer perform their intended function, thus making less AEA available to stabilize air bubbles, often decreasing air content as a result. To compensate, additional AEA must be added until all adsorption sites on the organic residuals are occupied, then the remaining AEA will perform as intended.

The problem of organic coal residuals in fly ashes has reportedly become more serious since the adoption of the Clean Air Act Amendments (CAAA) in 1990. Implementation of the CAAA requirements resulted in many power generating plants retrofitting their facilities with low-NO_x burners which brought about changes in the fly ash byproducts (Hill et al. 1997, Hower et al. 1999). Hurt et al. (2001) reported that low-NO_x burners involved, in combination with some other changes to the boiler, a reduction in air fed to the primary combustion zone resulting in a reducing (oxygen deficient) environment in certain portions of the boiler. The remaining air was fed downstream in order to complete combustion. This reduced NO_x emissions, but was often accompanied by higher "carbon" content in fly ash and/or changes to the nature of the carbon. According to Hurt et al. (2001) the reasons for the changes in fly ash are not fully understood, but are related to poorer mixing of the air and fuel and possibly reduced residence time for particles under combustion conditions. It was also reported that even when higher levels of carbon were not observed in the post-low NO_x retrofit periods; there was degradation in the

performance of the ashes. Ashes that would meet ASTM and state requirements for pozzolanic additives would have negative impacts on air entrainment. It was concluded that post-retrofit problems included both increased organic coal residuals content as well as changes in the nature of the organic residuals.

Hurt et al. (2001) used the foam index test (described in Section 3.5.2.5) to measure interactions between fly ash and AEAs. They showed, based on a study of ninety ash samples, that foam index correlated with LOI for LOI values up to about 65 percent, as shown in Figure 3.14. They suggested that the interactions between fly ash and AEA as measured by the foam index test were not caused by the mineral portion of ash but by the adsorption of AEA onto organic coal residuals in ash.

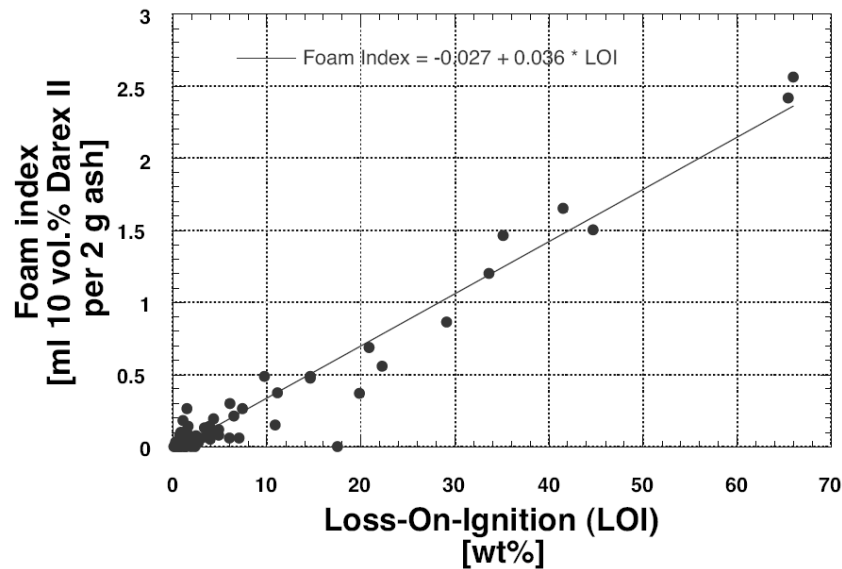


Figure 3.14: Relationship between foam index and LOI for all ash samples (both Class C and F) from Hurt et al. (2001). Foam index units are in mL of 10% concentration of commercial AEA normalized by 2 g ash.

It should be noted that a very broad range in LOI was used in this study by Hurt et al. (2001). When LOI is restricted in value to 6 percent or less to represent ashes used in actual concrete (ASTM C618), the trend shown in Figure 3.14 becomes less clear.

Contrary to the conclusion of Hurt et al. (2001), several studies using smaller ash sets concluded that the LOI test alone may not be suitable for estimating the interaction between fly ash and air entraining admixtures in concrete (Gao et al., 1997; Freeman et al., 1997; Smith et al., 1997). The influence of fly ash on concrete air entrainment is not measured directly; instead the use of the foam index test is used to measure ash-AEA interactions. The following sections describe the use of the LOI test in measuring the content of organic coal residuals, alternatives to the LOI test and the use of the foam index test to measure fly ash-AEA interactions.

Loss on ignition and carbon content

As mentioned previously, the ASTM C311 loss on ignition test is commonly viewed as a measurement of the “carbon” content of fly ash. The test procedure itself does not make such

claims. Conflicting conclusions on the suitability of the LOI as a measurement of organic coal residuals exist in the literature. Schlorholtz (2006) summarized the finding of five studies which showed LOI content correlated strongly with elemental carbon content (linear correlation $LOI = 0.42 + 1.055 * (\text{carbon content})$, $R^2 = 0.99$). However, other researchers have shown that the LOI test frequently over-estimates the organic coal residuals content in ash (Fan and Brown, 2001; Brown and Dykstra, 1995; Paya et al., 2002). One study showed errors as high as a factor of 10 (Fan and Brown, 2001). These studies have suggested that certain minerals or other constituents present in ash can dehydrate, decompose or volatilize at the temperatures used in the standard LOI test, resulting in mass losses which incorrectly attributed to organic coal residuals.

Alternatives to the Loss on Ignition Test

Some researchers have proposed alternatives to the standard loss on ignition test. Brown and Dykstra (1995) and Fan and Brown (2001) used thermo gravimetric analysis to measure organic carbon content in fly ash samples. The method they employed tested approximately 25 mg samples of oven-dried fly ash in a programmable TGA instrument. The samples were heated at a rate of 20°C/min to 750°C under a flowing nitrogen atmosphere. The sample remained under isothermal conditions until the mass stabilized then the gas flow was switched from nitrogen to air. After switching to air, a sudden drop in sample mass was typically observed as the organic carbon in the sample was oxidized. When the mass stabilized, the test was complete. The organic carbon content of the sample was assumed to be equal to the percent change in mass that occurred after the nitrogen was switched to air.

Payá et al. (2002) suggested the use of thermo-gravimetry (using a method similar to the method suggested by Fan and Brown and Brown and Dykstra), high resolution thermo-gravimetry, and differential thermal analysis as alternatives to the standard LOI test for measuring organic coal residuals in fly ash. High resolution thermo-gravimetry (HRTG) differs from thermo-gravimetry in that two heating rates are using during the test. A heating rate of 20°C per min is used when little change in weight (less than 1 microgram per second) is detected. The heating rate decreases to 1°C per min when weight loss occurs. This technique allows improved precision in the measurement of the temperature ranges in which reactions take place, time for completion of the reaction and avoidance of overlapping of reactions that occur at different temperatures. The authors suggested that HRTG could improve measurements of carbon in ash by separating the carbon oxidation reaction from other reactions that occur as fly ash is heated.

Payá et al. (2002) suggested two HRTG methods, the first using an air atmosphere and the second using a nitrogen atmosphere. The carbon content of ash, as determined by the HRTG in air, was measured by analyzing the graph of sample mass remaining versus temperature, and its derivative curve, produced during the test. The carbon content was equal to the change in mass that began at approximately 450°C (as established by a dramatic decrease in the derivative curve) and continued until the rate of change in mass with temperature (derivative) returned to zero. The second method, performed under a nitrogen atmosphere, measures oxidation of carbon by the reduction of iron oxides according to the reaction shown in equation (1).



The reaction shown in Equation (3.1) began at approximately 800°C. The change in mass that occurs due to this reaction is the sum of the masses of carbon and oxygen reacted. The carbon content is then the mass loss multiplied by carbon fraction of the carbon monoxide (0.43).

No data was presented by the authors to indicate how the two HRTG methods compared to other methods available to measure carbon content.

Payá et al. (2002) also suggested the use of differential thermal analysis (DTA) to measure the organic coal residuals content of fly ash. DTA measures the differences in energy released or absorbed by a material as a function of temperature. Oxidation of carbon char (a form of organic coal residuals) in ash is an exothermic reaction and the heat energy produced by the reaction is proportional to the amount of carbon oxidized. DTA was used measure the heat energy produced by the reaction from which the carbon content could then be determined from the measured heat energy through an appropriate calibration. Data presented showed a reasonable correlation between DTA results and carbon content; however, the method used to determine the carbon content of the ashes was not given, so it unclear how this method compares to others.

The foam index test

Table 3.13 showed that the foam index test can be used to estimate the AEA dosage in concrete containing fly ash. The foam index test, developed by Dodson (1990), is a simple laboratory titration procedure used to characterize the degree of interaction between cementitious materials and air entraining admixtures. No standard foam index test exists, and several variations of the test have been used in research and industry (Dodson, 1990; Gebler and Klieger, 1983; Freeman et al., 1997; Hill et al., 1997; Smith et al., 1997; Baltrus and LaCount, 2001; Kulaots et al., 2003). Common to all methods, the cementitious materials and water are combined in a sealable container and titrated with surfactant, typically a commercial AEA. After each titration the mixture is agitated, typically by shaking the container in hand, to mix the materials and create foam. The endpoint of the test is reached when sufficient surfactant has been added to produce a layer of foam that completely covers the top of the paste after agitation. The “foam index” is the total amount of AEA (typically a volume amount since surfactant solutions are used as the titrant) required to reach the endpoint. The amount of surfactant required is dependent on the interactions that occur between the surfactant and test materials. Relatively large doses of surfactant indicate that the nature of the interactions result in the surfactant being less efficient at stabilizing air bubbles. Therefore, large foam index values suggest that potential difficulties may occur if the materials are used in air-entrained concrete.

Gebler and Klieger (1983) concluded that the foam index test was an effective and rapid test to predict relative air-entraining admixture dosage requirements for concrete. No other studies were identified which correlate fly ash foam index test results with concrete air content or the ability of the foam index test to predict the AEA dosage of concrete.

Hurt et al. (2001) suggested that several factors in the test make it difficult to compare results from one version of the foam index test to another. The reasons identified were the concentration and composition of the AEA (titrant), the time that the mix is allowed to sit, the proportions and compositions of the different non-AEA components (e.g. cement) and the age of the AEA. It was concluded that it can be misleading to compare the numerical results obtained in one laboratory with those obtained in another without taking such differences into account.

Kulaots et al. (2003) concluded that though two typical concrete AEAs produced different foam index values (different volumes of AEA were required to reach the endpoint), the foam index values of typical AEAs from different sources can be “reasonably” correlated with each other. Kulaots et al. identified that “aging,” or degradation in the performance, of the

commercial AEA occurred based on the apparent increase foam index values of standard samples if the same solution were used.

In addition, Kulaots et al. (2003) determined via experimentation on the foam-ability of commercial AEAs in solutions of varying chemistry, that both high pH and the presence of finely divided calcium solids favor foaming behavior of AEAs. Based on the results of that study, Kulaots et al. recommended that cement be used in all foam index testing. They proposed the use of a chemically pure reagent grade surfactant, dodecyl-benzenesulfonic acid sodium salt (DBS) as a standard surfactant in the foam index test due to favorable correlations with a commercial AEA. They suggest that the use of DBS as a standard surfactant 1) would limit variability in inter-laboratory testing due to potential variability in commercial AEAs, 2) is not sensitive to ageing effects and 3) is less sensitive to solution chemistry.

Manz (1999) reported that a research task group for ASTM Subcommittee CO9.24 on Mineral Admixtures has called for the development of a refined and standardized foam index test method for laboratory and field use.

Baltrus and LaCount (2001) studied the adsorption of AEA onto fly ash by means of ultra-violet visible light (UV-Vis) spectrophotometry and the foam index test. A spectrophotometer was used to determine the concentration of surfactant (a commercial AEA) in water by measuring the absorbance of light by the solution. A surfactant absorbs a unique combination of wavelengths with certain wavelengths more sensitive to the surfactant than others. The greater the concentration of surfactant in solution, the more light is absorbed by the solution. A spectrophotometer transmits light through a container of the surfactant solution and a detector receives the light after it passes through the sample and measures the intensity over a range of wavelengths. The differences in intensity from a blank sample are calibrated with prepared surfactant solutions. Baltrus and LaCount (2001) and others (Hill et al., 2007; Yu et al., 2000) used UV-Vis spectrophotometry to measure change in surfactant concentration in solutions after the addition of fly ash. Decreases in concentration were considered to be due to the adsorption of surfactant on the fly ash. Based on a study of thirteen ash samples, Baltrus and LaCount found that no clear relationship existed between the adsorption of a commercial surfactant as measured by UV-Vis spectrophotometry and the foam index test. In addition, it was found that the adsorption of AEA by fly ash requires an equilibration time longer than used for the foam index test. It was concluded that the foam index test is a poor tool for measuring interactions between AEA and organic coal residuals. However, it should be noted that Baltrus and LaCount also acknowledged that the precipitation of the commercial AEA with soluble calcium and magnesium ions in solution likely influences the adsorption measurements of surfactant concentration in solution by UV-Vis spectrophotometry.

Forms of organic coal residuals in ash

Several studies have been undertaken to identify and classify forms of organic coal residuals in ash as well as examine the size distribution of the organic residuals. Maroto-Valer et al. (1998, 1999a and 1999b) studied the forms of organic coal residuals present in fly ash samples. Sieving and electrostatic separation methods (electrostatic separation is discussed with other methods of ash beneficiation at the end of this chapter) were used to produce organic coal residual-rich fractions of ash, which were then separated by density by centrifugation (See Maroto-Valer et al. 1999a). The authors microscopically identified three types of solid organic coal residuals present in the ash samples: inertinite (char particles that appear unaltered from the parent coal that were likely entrained in the flue gases from the combustor prior to melting or

combustion), isotropic coke (particles which appeared to have passed through a molten stage and possess a disordered structure) and anisotropic coke (also appeared to have been molten at some point but possessed a developed alignment of crystallites). They concluded that specific surface area differed across the forms of organic coal residuals, with inertinite having the lowest specific surface area (15-25 m²/g), with isotropic (25-35 m²/g) and then anisotropic (35-60 m²/g) char having increasingly greater specific surface areas.

Hill et al. (1997) showed that four Class F fly ash samples showed widely different behavior with respect to the air content in mortar despite similar LOI contents. Nitrogen BET surface area analysis showed that the samples had similar specific surface areas; however liquid and vapor phase adsorption tests showed differences in adsorption capacity. Hill et al. concluded that differences in adsorption capacity were a result of organic coal residual form distribution. Differential thermal analysis of concentrated fly ash carbonaceous material showed a lower temperature exothermic peak was more prominent in ash samples that showed poor air entrainment properties. However, this result was not substantiated in further studies (see Hill et al. 1998). It was suggested that organic coal residuals in the form of isotropic, disordered char (instead of anisotropic char, or inertinite) was responsible for the increased adsorption activity of the ash.

In a follow-up study, Hill et al. (1998) studied the influence of fly ash samples on air entrainment in mortar, and measured the properties of the ash by means of LOI, foam index, differential thermal analysis, BET surface area by nitrogen adsorption and microscopical analysis. The ash samples were collected from a single source over a period of several months with LOI values varying between 2 and 9 percent. It was reported that microscopical analysis of ash samples provided evidence that a significant portion of the organic coal residuals in ash was less than one micron in size. However no link between the microscopical characterization of organic coal residual type in the ash and ash-AEA behavior was established by the study.

Kulaots et al. (2004) examined the LOI, foam index and BET specific surface area by nitrogen adsorption of the sieved fractions of several Class F and C fly ashes. The tests showed that about 80 percent of the carbon of Class F ashes (in the five samples studied) was contained in the fractions less than 100 μm in size (Figure 3.15). It was also noted in the study that a “great many particles” were less than 1 μm in size.

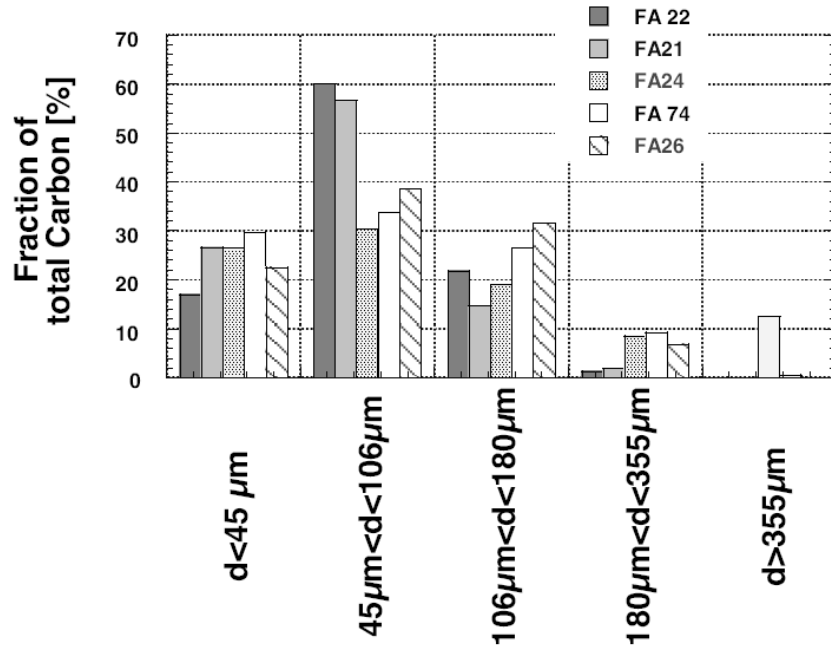


Figure 3.15: Organic coal residuals particle size distribution in Class F ash samples, diameters (d) are in microns. From Kulaots et al. (2004).

Kulaots et al. (2004) also concluded that organic coal residuals in Class C ash (of four samples studied) were generally present in two groups: between about 180 to 500 μm and less 45 μm . Optical microscopy revealed that most of the carbon particles were heavily covered with minerals. Whether this was a result of adhesion or fusion of the minerals on top of the carbon particles remains unclear.

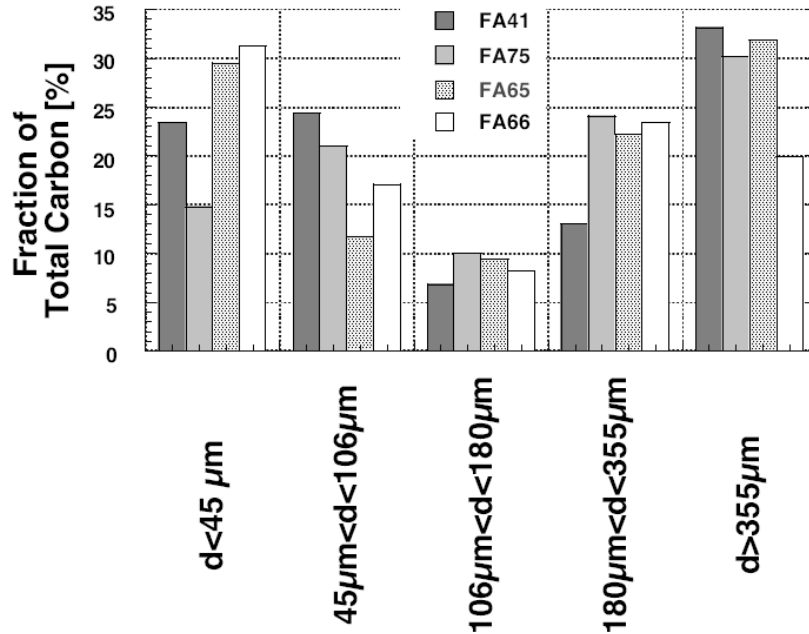


Figure 3.16: Organic coal residuals particle size distribution in Class C ash samples, diameters (d) are in microns. From Kulaots et al. 2004.

Organic coal residuals surface area and surface accessibility

Several studies have been performed to identify the properties of ash and organic coal residuals content. Because most researchers have hypothesized that the primary factor influencing fly ash-AEA interaction is the adsorption of AEA on the surfaces of organic coal residuals, studies of ash surface area and surface area accessibility to AEA have been undertaken. The studies use nitrogen adsorption and BET theory (Adamson, 1982) to measure the specific surface areas of the ash samples. The contribution to specific surface area of the inorganic portion of the ash is separated from the contribution from organic coal residuals content by first measuring the specific surface area of as-received ash, and then measuring again after removal of the organic coal residuals. The difference between the two measured surface areas is then attributed to the organic coal residuals. Removal of the organic coal residuals is achieved by exposing the ash to high temperatures (typically greater than 700°C) in an oxidizing environment to oxidize the organic material. The studies of fly ash specific surface area found in literature are summarized below.

Freeman et al. (1997) used LOI, BET surface area and the foam index test to measure the properties of four fly ash samples in addition to samples of coal, activated charcoal and pelletized carbon black. Based on the observation that removal of organic coal residuals by ash oxidation decreases foam index values of ash, Freeman et al. concluded that solid carbonaceous material in fly ash adsorbs AEAs from aqueous solutions in concrete mixtures rendering them incapable of stabilizing air bubbles. Freeman et al. (1997) showed that foam index values correlate “crudely” with ash LOI and somewhat better with nitrogen BET specific surface area of ash. It was also shown that different carbon-containing materials, such as fly ashes, activated carbon, pelletized carbon blacks and coal samples, showed widely different degrees of AEA

interactions and that degree of interaction appeared to be well correlated with specific surface area.

Gao et al. (1997) determined that carbon blacks interact with commercial AEAs in a manner similar to fly ash. It was observed that the degree of interaction between AEA and carbon black correlated well with reciprocal of the primary particle size and with nitrogen BET surface area. It was shown that as the primary particle size decreases, the specific surface area increases and interactions with AEA (as measured by the foam index test) also increase. This suggested that external surface area of the carbon blacks played an important role in the AEA adsorption process. In addition, it was shown that foam index values (mL of AEA solution) normalized by LOI content were higher for carbon black compared to fly ash. The presence of soot, which is similar in properties to carbon black, was identified in at least trace amounts in fly ash. It was concluded that the presence of soot in fly ash may cause problems with air entrainment; however, the authors suggested that soot concentrations are likely too low in typical fly ash samples to have a significant influence.

Hill et al. (1998) studied the influence of fly ash samples on air entrainment in mortar, and measured the properties of the ash by means of LOI, foam index; differential thermal analysis and BET surface area by nitrogen adsorption. The ash samples were collected from a single source over a period of several months with LOI values varying between 2 and 9 percent. It was concluded from the study that “the majority” of the surface area of the ash exists on the organic coal residuals present in the ash. It was also found that organic coal residuals surface area correlates well with both mortar air entrainment and foam index test results, with increased surface area corresponding to lower mortar air content and higher foam index values.

Kulaots et al. (2004) reported that the finest ash fractions (less than 100 μm) “adsorb” the greatest percentages of total AEA because 1) the mass of the finest organic residual particles is greater than the mass of larger coal particles and 2) because the finer particles offer greater accessibility to their adsorptive surfaces, i.e., greater surface area per unit mass of carbon. The adsorptive surfaces are hypothesized to be the surfaces which compose the geometrical boundary of the particles that are most accessible on short time scales.

Recognizing that most studies focused on a limited number of fly ash samples, Smith et al. (1997) studied forty Class F and Class C samples. The results of this study suggested a fair correlation between foam index and LOI, in apparent disagreement with other studies. However, the study also showed that BET specific surface did not correlate well with the fly ash performance in the foam index test.

Hachmann et al. (1998) examined what they termed the AEA “adsorption” capacity and BET specific surface area of coal at varying degrees of combustion. The samples were generated with a model combustion process under controlled conditions. “Adsorption” was the term used for AEA-ash interaction as measured by the foam index test. This term is based on the presumption that the interaction between fly ash and AEA is due to the adsorption of AEA molecules onto the organic coal residuals surfaces. A representative high rank bituminous coal that produced class F fly ash and representative lignite that generally produced class C fly ash were used in the study. The experimental setup simulated high temperature pulverized coal combustor conditions. Runs were carried out on the two coals in a high-temperature flow reactor from which samples were taken at different residence times and rapidly quenched.

The results of the study by Hachmann et al. (1998) are shown in Figure 3.17 in which the x-axis, conversion (coal basis) is the degree of conversion (in percent) of coal to heat energy. Pyrolysis, or devolatilization, of the coal occurs at conversion values between zero and 50 to 60

percent. Following pyrolysis, char combustion constitutes the remainder of the coal conversion. The results showed that the “specific surfactant (AEA) adsorption” (the volume of AEA required to reach foam index normalized by the organic coal residual content) of the parent coal and partially devolatilized chars (coal conversion between 0 and 30 percent) was very low, but rose sharply near the end of devolatilization (conversion between 30 and 60 percent). As the char combustion preceded, AEA “adsorptivity” decreased. The BET surface area of the parent coals was initially small but increased as the devolatilization occurred, reaching a maximum value (of around 150-200 m²/g of carbon) before the combustion of the char began. As char combustion proceeded, the specific surface decreased. The authors noted that when the specific surface of the coal during combustion was at maximum value, the specific AEA “adsorptivity” was still at or near minimum. The authors hypothesized that the surfaces being identified in nitrogen adsorption for BET surface area were unavailable for AEA adsorption. One possible explanation was the difference in time scales between the nitrogen adsorption, which involves a long equilibration time, and AEA adsorption during the foam index tests, which is complete in less than ten minutes. It was postulated that the larger size of the surfactant molecules and liquid phase diffusion transport limitations are reasons why the two adsorptives might also give different behaviors. In particular, it was hypothesized that micropores (pores smaller than 20 Å) were accessible to nitrogen molecules, but not to the surfactant molecules.

An extensive study on interactions between fly ash and air entraining admixtures by Hurt et al. (2001) measured LOI, foam index, surface area and porosity of ninety fly ashes from around the U.S. The majority of the samples were Class F ashes with LOI values between near zero to 66 percent. Several Class C ash samples were also included in the set. The samples with highest LOI values had been subjected to separation processes. Based on the study it was concluded that ash “absorptivity” (the same presumption mentioned above but in reality is fly ash-AEA interaction as measured by the foam index test) correlates with residual carbon content (Figure 3.14). It was also concluded that in addition to mass, the specific surface and surface polarity of the carbonaceous material in ash also plays a significant role in determining suitability for air entrained concrete. Foam index values of the ash samples against specific surface area are shown in Figure 3.18. Foam index values are given in mL of 10 percent concentration of commercial AEA normalized by 2 grams (the mass of ash used in the test).

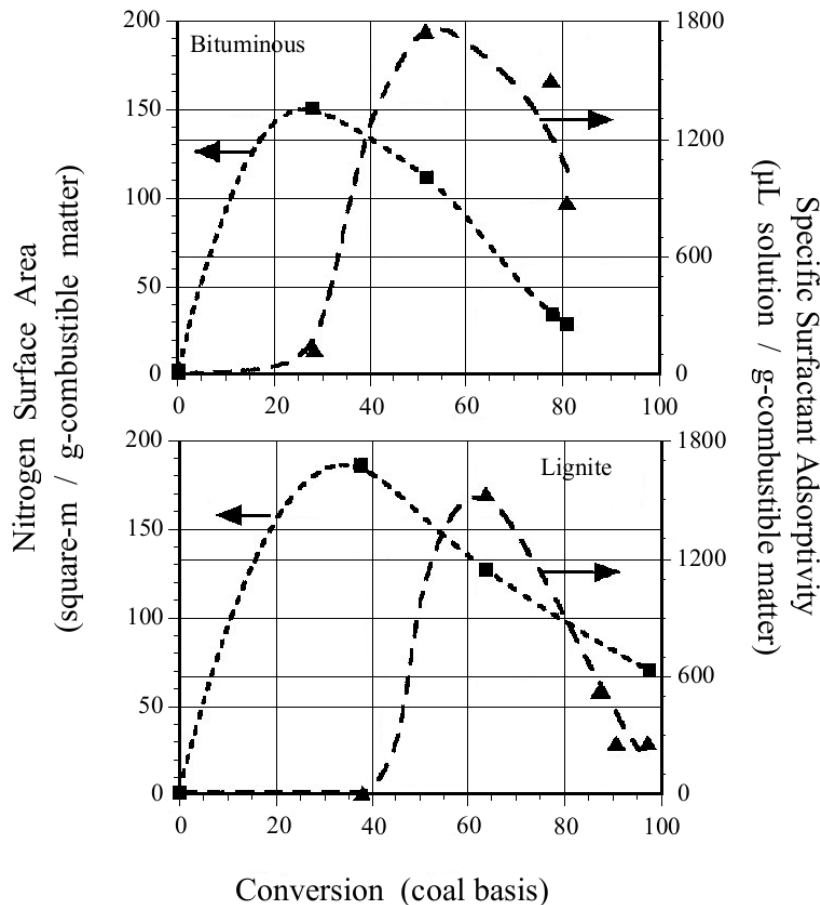


Figure 3.17: Specific surfactant adsorptivity as a function of conversion during the high-temperature combustion of bituminous and lignite coal, Hachmann et al. (1998).

Hurt et al. (2001) concluded that Class C ashes had higher specific surface areas per unit mass of carbon (typically 200–400 m²/g-carbon) than did class F ashes (typically 20-80 m²/g carbon). Porosity analysis of the particles of organic coal residuals was performed by Dubinin-Radushkevitch theory (Gregg and Sing, 1982). Based on the analysis it was determined that much of the surface area in the two classes was available in organic coal residual particle micropores (pores less than 20 Å in diameter). Class C ashes had higher micropore and mesopore (pores between 20 and 200 Å) volumes relative to class F ashes; however, Class C ashes did not show greater ash-AEA interactions. Hurt et al. (2001) concluded that ash carbon microporosity is not a major factor in AEA interactions. Most of the microporous carbon surface is not accessible to the relatively large AEA molecules. Nevertheless, porosity analysis alone proved unable to explain the different trends observed in the sample bank.

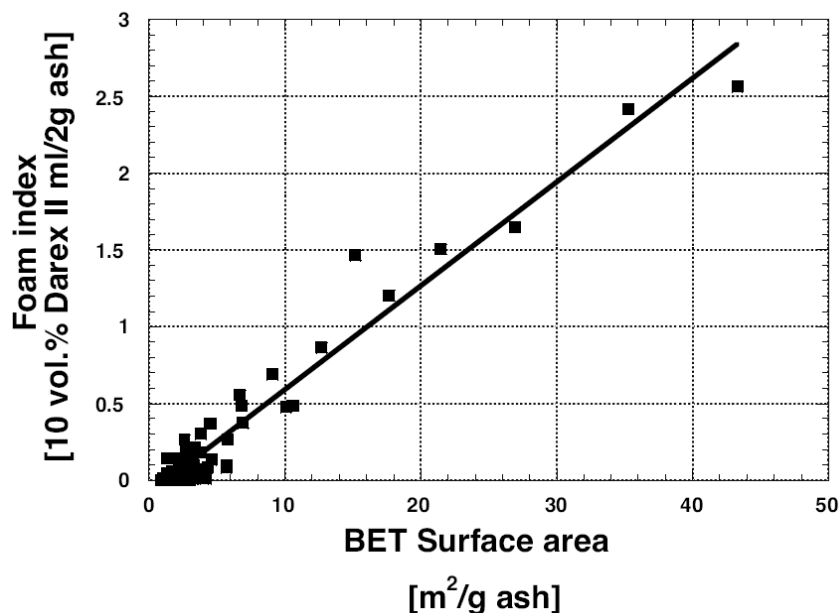


Figure 3.18: Relationship between foam index and BET specific surface area. From Hurt et al. (2001)

As mentioned previously, Baltrus and LaCount (2001) concluded that the so-called “adsorption” of AEA (measured by changes in AEA concentration in water ascribed to the adsorption of the AEA onto fly ash) is a time-dependent process. A study on “adsorption time” of surfactant on fly ash by Hill et al. (1997) also using UV-Vis spectrophotometry showed that for some fly ashes, AEA saturation was reached in approximately 500 seconds, while for some separated high carbon fly ash samples the saturation levels were reached only after 1500 seconds of adsorption.

Hurt et al. (2001) examined the influence of time and particle size on the results of the foam index test. The study used a spectrophotometric method to measure the change in AEA concentration in aqueous mixtures containing fly ash samples. The study showed that adsorption was time dependent with approximately 1 hour required to “saturate” a high organic coal residual content fly ash sample with AEA. This time frame was also reported by Yu et al. (2000). Hurt et al. reported that a foam index test on the same ash sample was completed in just 10 min and suggested that at the endpoint of the foam index test, the ash was still in the process of “adsorbing” AEA from the solution. Hurt et al. (2001) reported that most of the AEA uptake on the ash initially occurred rapidly and then at a slower rate as time progressed. It was postulated that the initial adsorption occurs almost instantly on the easily accessible regions of the surfaces of organic coal residuals and decreases as the accessible sites are filled.

Organic coal residuals surface polarity

In addition to physically accessible surface area, the nature of the carbon surface and its ability to form bonds with AEA molecules are likely important factors in fly ash-AEA interactions. Some studies into the polarity of the surfaces of organic coal residuals and possible mechanisms for AEA adsorption are discussed below.

Hill et al. (1997) reported that chemical analysis showed greater oxygen content in the organic residuals of ashes that showed higher ash-AEA interactions. It was hypothesized that the higher oxygen content was related to a higher concentration of oxygen-containing molecules bonded to the carbon surface. Carbons with higher oxygen group contents on their surfaces were believed to be more polar compared to samples with relatively low oxygen content. It was hypothesized by Hill et al. the mechanism of AEA adsorption is that polar sites on carbon surfaces bond with the polar ends of surfactant molecules, thus removing them from solution.

Sabanegh et al. (1997) studied the effects of air oxidation of commercial ash on AEA interaction by means of the foam index test. In the study, samples of the ash were heated in an air-atmosphere furnace at different temperatures between 100 and 700°C. After heat treatment, the samples were characterized by LOI and foam index testing. The authors reported that foam index results decreased gradually for specimens that had been heated to between 200 and 450°C even though LOI values remained unchanged. The authors hypothesized that the increase in foam index was the result of changes in the properties of the organic carbon surface due to heat treatment. It was postulated that heat-treatment introduced polar functionalities onto the residual carbon surfaces resulting in the initially non-polar, hydrophobic surfaces becoming polar and hydrophilic, thus diminishing the ability of the hydrophobic portions of the AEA molecules to adsorb on the carbon. Therefore, contrary to the suggestions of Hill et al. (1997), the authors suspected that non-polar carbon surfaces were primarily responsible for the adsorption of AEA from solution. This hypothesis was also made by Hachmann et al. (1998) and Gao et al. (1997). Smith et al. (1997) postulated that the polarity of the organic coal residuals surface made a difference in the ability of the coal to adsorb AEAs and hypothesized that low NO_x burner retrofits may modify the polar character of the organic coal residuals surface.

Hurt et al. (2001) studied the effect of surface oxidation of fly ash on AEA interactions. The oxidation of carbon surfaces was done by exposing ash to ozone, O₃. Depending on the ozone input concentration, ash amount and contact time, AEA interactions decreased by a factor of two or more with only 0-3 g O₃/kg-ash ozone introduced into the ozonation system. Class C ashes required about 5-8 times by mass more ozone for surface passivation relative to class F ashes. This appeared directly related to the higher surface areas in class C ashes, which was higher by the same factor of about 5-8, relative to class F ashes. The ozonation process is described further in the following section on ash beneficiation.

Based on the study, Hurt et al. postulated that the mineral portion of fly ash is mostly polar, whereas the organic coal residuals can be either polar or non-polar depending on the concentration of oxygen functional complexes covering the surface. They suggested that the non-polar portion of the carbon is the primary site for adsorption of the non-polar portion of the AEA molecules. The higher the non-polar carbon surface area in the ash, the higher the AEA uptake. The polarity of the ashes was directly related to the extent of oxidation of the carbon surface. The greater the degree of oxidation, the more polar the surface.

Hurt et al. (2001) described the organic coal residuals-surfactant interactions and the effect of ozonation on organic coal residuals as follows. In an aqueous solution containing organic coal residuals and surfactant, the non-polar (hydrophobic) portions of the surfactant molecules adsorb onto the non-polar carbon surface by means of Van Der Waals dispersion forces, while the anionic (hydrophilic) portion of the surfactant remains in the solution (Figure 3.19, left). The effect of ozonation on organic coal residuals is the formation of oxide functionalities on the carbon surfaces that polarize the surface. In the presence of surfactant, Van Der Waals forces are too weak for the surfactant to displace the interacting water molecules,

which form hydrogen bonds with the surface oxides (Figure 3.19, right). In freshly mixed concrete containing ozone-treated ash and air entraining admixtures, the AEAs are not adsorbed onto the surface of organic coal residuals and hence AEA dosage can be reduced. Other effects of ozone-treated ash on the properties of concrete, such as influence on water demand, were not reported in the study.

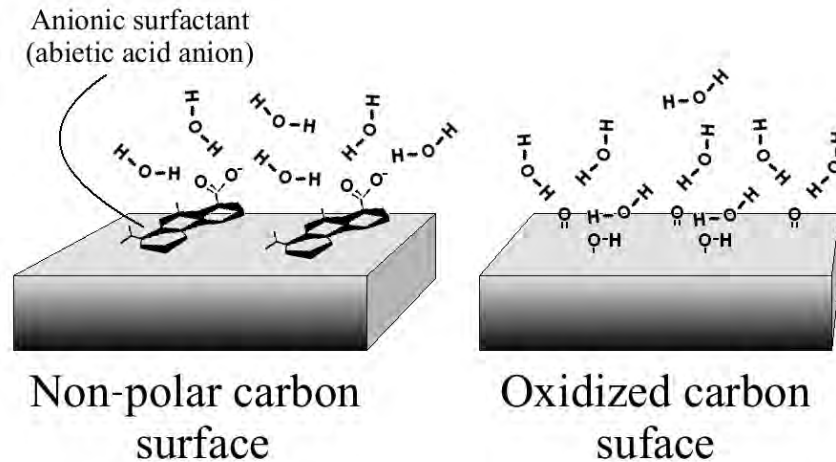


Figure 3.19: Interactions between surfactant and non-polar carbon surface (left) and oxidized carbon surface (right), (Hurt et al., 2004).

Fly Ash Beneficiation

Several methods exist for the reducing the organic coal residuals content of ash so that the ash can be sold to the concrete industry. This is called beneficiation. The most popular methods are carbon burnout, froth floatation, electrostatic separation and chemical treatment.

Carbon burnout is the removal of organic coal residuals by re-heating post-combustion ash to oxidation temperatures (Okoh et al., 1997; Boyd and Cochran, 1994; Zacarias, 2002). In most cases burn-out is achieved with the aid of a fluidized bed combustor in a stand-alone system separate from the primary electric power plant. Maximum exposure temperatures in the burnout process are much lower than temperatures within the utility combustion chamber (generally 700 to 1000°C); however residence time in the combustor is significantly longer (several minutes).

Froth floatation is the physical separation of particles suspended in water in which the organic coal residuals in the form of organic carbon particles adhere to bubbles and can be removed with the froth. For separation, a specially selected floatation reagent (e.g., fuel oil, Walker and Wheeler, 2006) is added to a slurry of ash to cause the carbon particle surfaces to become hydrophobic (Hwang, 1991). The slurry is then aerated to form bubbles to which the carbon particles become attached and float to the top of the slurry for collection. The process reduces the organic coal residuals in the fly ash slurry and the remaining fly ash is removed and dried for use in concrete (Hwang, 1991; Walker and Wheelock, 2005).

Electrostatic separation uses opposing charges to separate the mineral components from the organic components of ash. In triboelectrostatic (production of electrical charge due to friction) beneficiation techniques described in literature (Soong et al., 1999; Stencel et al., 1999; Li et al., 1999), contact with metal (copper), causes the organic particles to become positively

charged, and the inorganic mineral particles become negatively charged. The charged particles are then passed through an electrostatic separator consisting of two conducting electrodes, across which a high voltage is applied. Organic particles (unburned coal) are attracted to the negative plate, and non-carbon minerals are attracted to the positive plate. The separated material streams are individually collected—high and low organic coal residuals content. The low coal ash is used in concrete and the high coal ash is returned as a feedstock for combustion (depending on the final properties of both).

Two methods of chemical treatment have been identified for the beneficiation of fly ash with regard to interactions between air entraining admixtures. Unlike those described above, these methods do not separate or destroy organic coal residuals in ash but change the nature of their interactions with AEAs. The first method is the use of a “sacrificial agent” either added to freshly mixed concrete or applied directly to the ash to neutralize the interactions between organic coal residuals and air entraining admixtures (Hill et al., 2004). Such a sacrificial agent is not necessarily an air entraining agent but is preferentially adsorbed onto the surfaces of organic coal residuals so that the interactions between the organic residuals and AEAs are reduced. The developers of the sacrificial agent claim that the agent has little or no influence on the air entrainment process provided by typical air entrainment agents and having no negative effects on the properties of the fresh and hardened concrete.

The second method of chemical treatment of ash is the use of ozonation to change the surface properties of the organic coal residuals (Hurt et al., 2001; Gao et al., 2001; Chen et al., 2003). The method utilizes a special apparatus which forces air containing ozone, O₃, in concentrations of 550 ppm to 2-vol%, through a column of dry ash in a glass reaction tube for 1 min to several hours. Results of the experiments on fly ash samples obtained from several sources showed that foam index decreased with increasing exposure (time/concentration) to ozone. The researchers concluded that ozonation does not decrease the organic carbon residuals content in ash but reduces the ash-AEA interactions (suspected by Hurt et al. (2004) to be due to the organic coal residuals surface characteristics).

Conclusions regarding fly ash-AEA interactions

The following general conclusions regarding interactions between fly ash and AEA are made based on a review of the current literature.

1. There is general agreement among several studies that organic coal residuals present in fly ash are responsible for increased AEA dosages of concrete. Researchers postulate that air entraining admixture (surfactant) is adsorbed from solution onto the organic coal residuals surface, thus rendering it unable to stabilize air bubbles in fresh concrete pastes.
2. Researchers have suggested that organic coal residuals mass, form, surface area, pore size and surface polarity play roles in AEA adsorption. Disagreements regarding the significance of the individual contributions of each exist. Many researchers have provided evidence that no relationships between LOI (often interpreted as “carbon content”) and AEA can be established. However, other researchers have shown that trends exist when large enough ranges in LOI are examined. In any case, no consistently reliable relationship between organic coal residuals and AEA behavior in ash suitable for use in concrete has been identified.
3. Organic coal residuals in the form of char are present in ash in three main forms: inertinite, isotropic and anisotropic coke. Isotropic coke may have the potential to be the

most active in adsorbing AEA; however, a relationship between coke type and content with AEA adsorption behavior has not been established.

4. Organic coal residuals have high specific surface relative to the inorganic portion of the ash (by factors of 10 to 200 times reported by Freeman et al., 1997). The surface area exists on the geometrical boundaries of the particles and on extensive system of pores in the char particles though the contribution of each has not been measured.
5. It is hypothesized that the accessibility and polarity of the residual carbon surface influences ash interactions with AEA.
6. It is hypothesized that the adsorption of AEA on fly ash occurs rapidly initially (less than 10 min) but slows as adsorption sites are filled and less accessible surfaces participate in adsorption. Time to complete adsorption has been suggested as 20 min to 2 hours.
7. It is hypothesized that micropores (pores smaller than 20 Å) that are accessible to nitrogen molecules (in nitrogen BET surface area measurements) may not be accessible to AEA molecules, particularly at short time scales (less than 10 min).
8. The smallest size fractions of ash (less than 100 μm) have the greatest influence on ash-AEA interactions, suspected to be due to high geometric external surface area per unit mass.
9. Researchers have postulated that residual carbon surface polarity influences may influence interactions between ash and surfactants. Some researchers postulate that non-polar carbon surfaces adsorb the non-polar portions of surfactant molecules, while the polar portion remains in solution. Other researchers suggest that polar surfaces are responsible for AEA adsorption by interacting with the polar portion of surfactants.
10. Oxidizing organic coal residuals surfaces appears to decrease ash-AEA interactions, favoring the former theory of AEA adsorption in conclusion 9.
11. The organic coal residuals in Class C ash can have greater specific surface (5 to 10 times greater) and higher micropore and mesopore (20 to 500 Å) volumes than Class F ash char. Based on the samples studied, Class C ash typically has less (by mass) organic coal residuals than F ash.

Chapter 4. Experimental Methods and the Collected Properties of the Materials

4.1 Introduction

This chapter summarizes the properties of the twenty-two fly ash samples studied during the course of this research. The test methods shown in Figures 2.5 and 2.6 are described and the results of those tests on the fly ash samples are given.

4.2 Ash samples and properties

4.2.1 Ash samples

Twenty-two ash samples were obtained from ash suppliers in the state of Texas. The ashes are typically named after the power plant in which they were produced. In this work, the samples are identified by a two letters followed by a single digit. The first letter is either a “C” or “F” denoting the classification of the ash by ASTM C 618, the standard specification for coal fly ash and raw or calcined natural pozzolan for use as a mineral admixture in concrete. The second letter in the name identifies the ash source and the digit identifies the sample number from the source.

The left column of Table 4.1 identifies the fifteen class F samples and seven class C samples used in this study. Several of the ashes were produced from the same power plant; in all, eleven different ash sources are represented. For several of the ash samples from a common source (FB-1 and -2, FM-1 and -2, FR-1 and -2, and CG-1 and -2) the ashes represent samples taken before (samples ending with -1) and after (samples ending with -2) the plant switched from using conventional burners to low-NO_x burners. However, no data are available concerning other changes made along with the installation of low NO_x burners, or changes to operating parameters before, during, or after combustion, or changes to ash collection or handling methods, or changes to the raw input coal. The ashes marked with an asterisk have been subjected to a beneficiation process where they were treated with a “sacrificial” agent in an attempt to neutralize the adsorption-related interactions of the ash with AEA (See *Fly Ash Beneficiation* in Chapter 3; Hill et al., 2004). The agent was applied to the ash by the ash distributor, Boral MTI⁴, and the composition of the material is proprietary. These so called “chemically treated” samples were only examined selectively in this work due to the fact that properties of the chemical treatment, the amount applied, and its potential effects on ash were unknown.

4.2.2 Properties of the ash mineral portion

Bulk chemistry by x-ray fluorescence

The elemental composition of the fly ash samples was determined by x-ray fluorescence spectroscopy at the Materials Analysis and Research Laboratory at Iowa State University, using a Philips PW2404 XRF spectrometer. X-ray fluorescence refers to the secondary x-rays given off by an element when it is bombarded by high-energy x-rays. Each element produces a unique x-

⁴ Boral Materials Technology Inc., San Antonio, TX.

ray fluorescence signature. Analyzing the x-ray fluorescence (XRF) emitted from a sample can be used to identify the presence and quantity of elements present. For further information see Jenkins (1999).

The fly ash samples were prepared by grinding the samples to a fine powder using a shatterbox (a ring mill). The samples were then heated to about 1100°C and fused into a glass disk using a lithium borate flux. The samples were then analyzed by the XRF spectrometer. The results of the XRF analysis are summarized in Table 4.1. The classification of the samples by ASTM C 618, the standard specification for fly ash used in concrete, as either Class F or C is shown by the fifth column from the left. According to ASTM C618, ash samples in which the sum of silica (SiO_2), alumina (Al_2O_3) and iron oxide (Fe_2O_3) contents is at least 70 percent are designated as “Class F” ashes and those in which the sum is at least 50 percent but less than 70 percent are designated as “Class C” ashes. Though not explicitly stated in the specification, the difference in the sums of the three oxides between the two classes is commonly due to greater calcium oxide (CaO) contents in Class C ashes than Class F ashes. This trend holds for the Class C ash samples in Figure 4.1, with calcium oxide contents ranging between 23.8 percent and 28.7 percent for the class C ashes and between 8.6 percent and 15.6 percent for the class F samples. As can be seen from the sums of the three oxides, ash composition exists on a continuum and the division between the two classes by ASTM C 618 is somewhat arbitrary. All of the ashes in the data set meet the ASTM C 618 limit on sulfur trioxide (SO_3) content of 5 percent maximum.

It should be noted that bulk chemical analysis by XRF produces the approximate percentage of the basic metal oxides present in the ash, but does not indicate which specific mineral groups are present. As noted earlier, the major inorganic components in fly ash are composed of both crystalline and amorphous minerals. The crystalline mineral content can include quartz (SiO_2), mullite ($3\text{Al}_2\text{O}_3 \cdot \text{SiO}_2$), maghemite (Fe_2O_3), periclase (MgO) and other phases. Fly ash amorphous mineral content can consist of various quantities of aluminosilicate, calcium aluminosilicate, calcium aluminate and other glassy phases (Helmuth, 1987; Joshi and Lohtia, 1997). Metal elements detected XRF analysis can be constituents of many different phases. Calcium, for example, may be present as calcium hydroxide, calcium sulfate, tricalcium aluminate, calcium carbonate or in a calcium-containing glass. While the crystalline phases present can be determined and quantified using x-ray diffraction, no reliable method for measuring the various amorphous phases exists (though methods are currently in development).

Soluble calcium (Atomic absorption spectroscopy)

As mentioned above, calcium in fly ash can be present in a variety of possible forms. Because of the propensity of anionic surfactants to combine with calcium or magnesium cations dissolved in solution, it was hypothesized that the presence of soluble calcium in fly ash could be a contributor to AEA interactions. Atomic absorption spectroscopy (AAS) was used to determine the amount of soluble calcium present in solutions of fly ash.

Table 4.1: Fly ash bulk chemistry by X-ray fluorescence (XRF). Testing performed at the Materials Analysis and Research Laboratory at Iowa State University during the Fall of 2006. (Note: sample FL-2 not included).

Sample name	SiO ₂ (%)	Al ₂ O ₃ (%)	Fe ₂ O ₃ (%)	SiO ₂ + Al ₂ O ₃ +Fe ₂ O ₃ (%)	CaO (%)	MgO (%)	SO ₃ (%)	Na ₂ O (%)	K ₂ O (%)	TiO ₂ (%)	P ₂ O ₅ (%)	SrO (%)	Mn ₂ O ₃ (%)	BaO (%)	Oxide SUM
FB-1	52.2	19.4	4.7	76.4	14.0	3.2	0.9	0.7	1.1	1.1	0.2	0.3	0.2	0.2	98.2
FB-2	50.8	18.6	7.9	77.3	14.0	2.9	0.9	0.5	0.9	1.2	0.2	0.3	0.2	0.2	98.7
FB-3*	49.1	19.6	7.9	76.6	14.7	3.0	1.1	0.6	0.9	1.3	0.2	0.3	0.2	0.3	99.1
FC-1	47.2	22.5	4.7	74.4	14.3	3.6	0.6	1.6	0.8	1.1	1.5	0.3	0.0	0.8	99.1
FC-2*	49.9	21.4	5.1	76.3	12.8	3.5	0.4	1.4	1.0	1.1	1.4	0.3	0.0	0.7	98.9
FL-1	55.0	19.2	7.2	81.4	11.1	2.7	0.6	0.5	0.9	1.3	0.2	0.2	0.1	0.2	99.2
FM-1	50.9	20.1	8.1	79.2	11.7	3.0	0.7	0.7	1.1	1.2	0.1	0.4	0.1	0.3	98.4
FM-2	54.4	20.6	8.4	83.4	8.6	2.7	0.5	0.5	1.2	1.2	0.1	0.2	0.1	0.2	98.7
FM-3*	54.6	19.8	8.7	83.1	9.0	2.5	0.4	0.6	1.1	1.1	0.1	0.2	0.1	0.3	98.6
FR-1	48.3	24.5	3.4	76.2	15.6	2.5	0.7	0.2	0.7	1.6	0.2	0.2	0.1	0.1	98.2
FR-2	51.9	23.3	4.5	79.7	12.4	2.1	0.8	0.3	0.8	1.5	0.2	0.1	0.1	0.2	98.0
FR-3*	52.0	23.3	4.5	79.7	11.8	2.0	0.7	0.2	0.8	1.5	0.2	0.1	0.1	0.2	97.3
FR-4*	53.1	23.3	3.9	80.2	11.4	2.1	0.7	0.4	0.7	1.5	0.1	0.1	0.1	0.1	97.5
FT-1	63.2	17.9	4.0	85.2	7.7	2.0	0.2	0.4	1.1	1.2	0.2	0.1	0.1	0.2	98.3
CD-2	34.8	19.9	5.7	60.4	26.3	4.8	1.7	1.7	0.4	1.7	1.3	0.5	0.0	0.8	99.6
CF-1	33.7	18.4	6.8	58.9	27.2	5.9	1.9	1.9	0.4	1.4	1.1	0.5	0.0	0.8	100.1
CG-1	38.2	20.5	5.6	64.3	23.8	4.5	1.1	1.6	0.5	1.6	1.3	0.5	0.0	0.8	100.0
CG-2	37.4	20.2	6.2	63.7	24.6	4.3	1.2	1.6	0.4	1.7	1.0	0.5	0.1	0.7	99.8
CP-1	33.4	17.8	6.8	57.9	27.4	5.5	2.8	1.8	0.3	1.4	1.1	0.5	0.0	0.9	99.7
CP-2	35.7	19.2	6.6	61.4	24.4	4.6	2.6	1.7	0.5	1.5	1.3	0.4	0.0	0.8	99.3
CP-2 repeat	35.8	19.2	6.5	61.5	24.3	4.6	2.6	1.7	0.5	1.5	1.3	0.4	0.0	0.8	99.2
CW-1	30.9	17.5	6.1	54.4	28.7	6.6	3.7	2.1	0.3	1.4	0.8	0.5	0.0	0.8	99.5

AAS is used to determine concentrations of metals dissolved in liquid samples. In elemental form, metals absorb ultraviolet light when excited by heat. Each metal element has a characteristic wavelength that is absorbed. The AAS instrument is used to detect a specific element in a flame by directing a beam of ultraviolet light of the characteristic wavelength through the flame and onto a detector. A liquid sample containing the metal is aspirated into the flame and the metal absorbs a portion of the UV light thus decreasing its intensity. The detector measures the change in intensity and the instrument's software converts the change to absorbance. The higher the concentration of metal in solution, the greater is the absorbance. An absorbance versus concentration calibration curve is established using prepared samples of known concentration.

For the analysis of soluble calcium ion content in the ash samples, solutions of calcium hydroxide, $\text{Ca}(\text{OH})_2$, ranging between 0 and 100 mg Ca^{2+} per liter were used to calibrate the instrument. Samples were prepared by placing 5g of ash into 100 mL of distilled water. The sample was shaken for 60 s with a frequency of 2 to 3 shakes per second and maximum displacement of 0.2 to 0.25 m. The samples were left undisturbed for 2 min to allow the largest particles to settle out. Ten mL of the solution was extracted with a pipet from the liquid below the surface and above the layer of settled ash. The extracted liquid was placed in a centrifuge tube and centrifuged at 4500 rpm for 4 min. The liquid was then diluted with distilled water to 20% concentration and measured by a Perkin Elmer AAnalyst 100. The results of the measurements are shown in Figure 4.1.

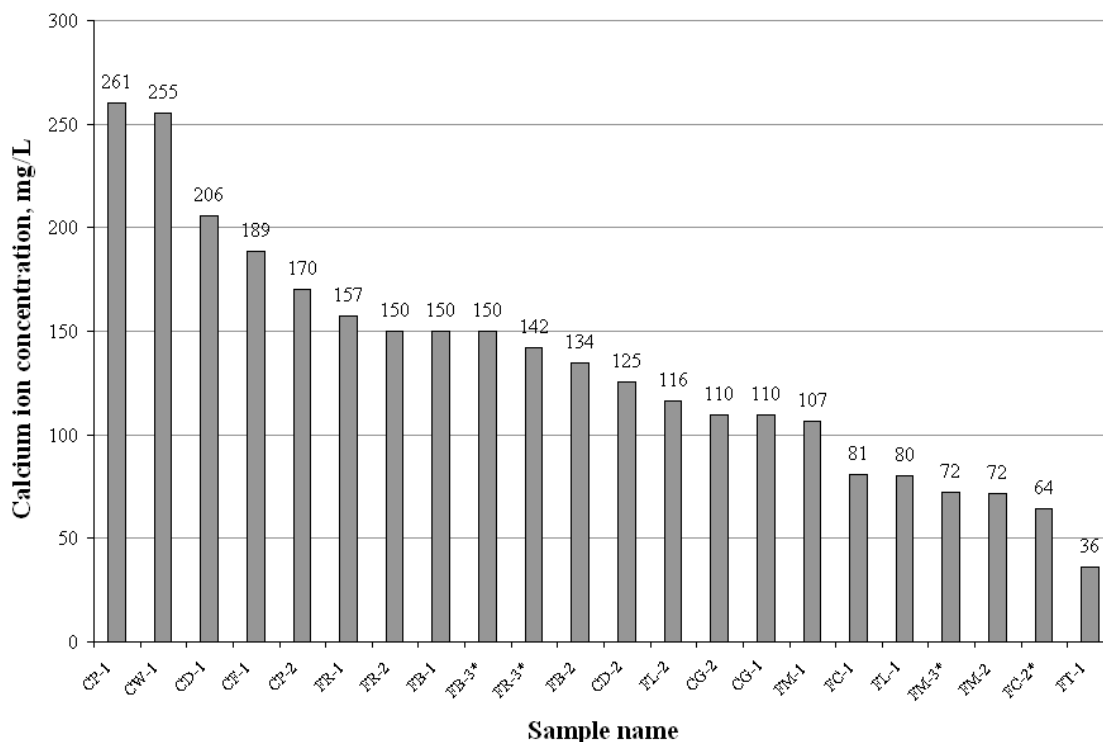


Figure 4.1: Calcium ion concentrations in of solution of fly ash.

The calcium ion concentrations of ash solution shown in Figure 4.2 show a wide range of soluble calcium among the various fly ash samples. For the most part, ashes classified as class C produced the highest calcium ion concentrations; however, there were several exceptions. Calcium ion concentration is plotted against calcium oxide content as determined by XRF in Figure 4.6. The figure confirms the general trend of increasing calcium ion concentration with increasing calcium oxide content. The separation of the two data clusters indicates the split between F and C classes.

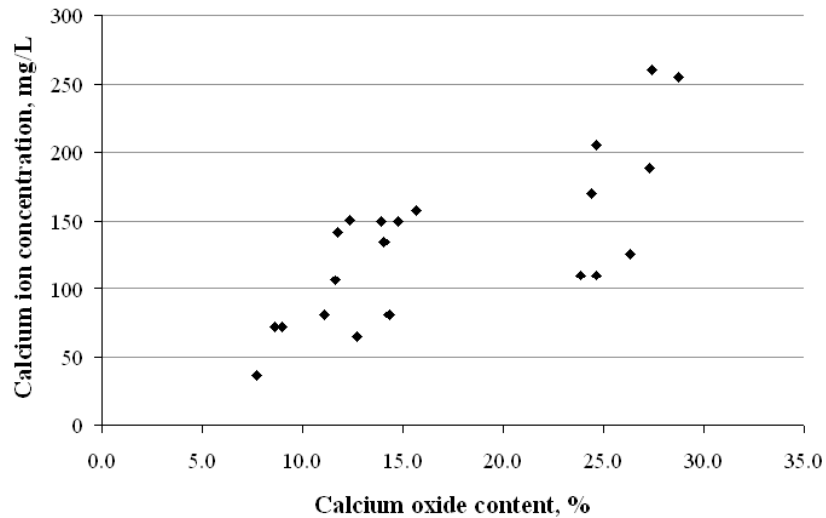


Figure 4.2: Calcium ion concentrations of ash solutions versus ash percent calcium oxide content.

X-ray diffraction

X-ray diffraction (XRD) is the diffraction or scattering of x-rays by the regularly spaced atoms of a crystal. The refraction angles can be used to determine the crystal structure or identify crystals in a material (Nuffield 1966). A Scintag, Inc. Theta-Theta Diffractometer at the Cornell Center for Materials Research was used to characterize four of the Texas ash samples.

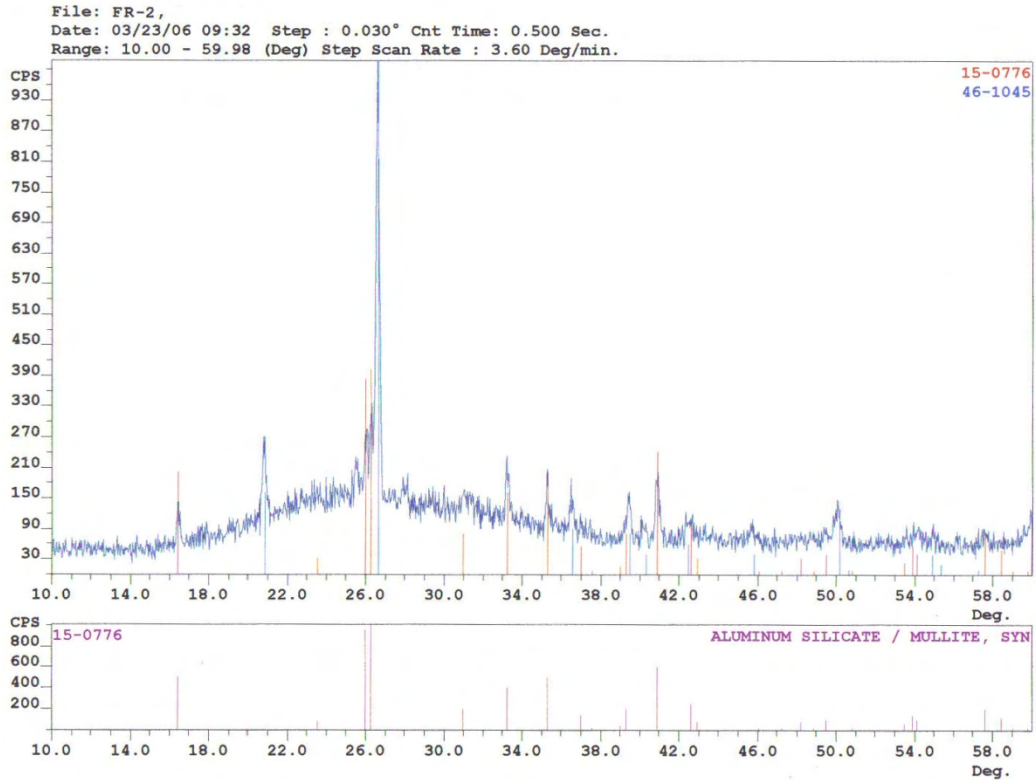


Figure 4.3: X-ray diffractogram for ash sample FR-2 showing the identification of the presence of mullite ($3\text{Al}_2\text{O}_3 \cdot \text{SiO}_2$).

A typical output graph from the analysis is shown in Figure 4.3. The figure shows a series of peaks which correspond to measured angles of x-ray diffraction. The locations of the peaks are matched against a database of materials to identify the main constituents. For example, in the lower part of Figure 4.3 the peak locations for the mineral mullite ($3\text{Al}_2\text{O}_3 \cdot \text{SiO}_2$) are shown. The large peak on the graph corresponds to the presence of quartz in the ash. The undulating data between the clearly defined peaks is due to the presence of amorphous mineral material which makes up the majority of the sample.

Table 4.2: Major minerals identified by x-ray diffraction of four fly ash samples.

Sample name	Minerals present, beginning with the most prominent minerals
FR-1	Quartz, mullite, calcium sulfate anhydrite
FR-2	Quartz, mullite, calcium sulfate anhydrite
CD-2	Quartz, tricalcium aluminate, calcium sulfate anhydrite
CP-2	Quartz, tricalcium aluminate, calcium sulfate anhydrite

The x-ray diffraction techniques used in this study identified the species present, but were not capable of determining the quantity of the specific minerals present in the ash. However, qualitative comparisons of the minerals present can be made based on the relative heights of the minerals' corresponding peaks. Because of the "noise" in the data caused by the relatively large amount of glassy material present in the samples, identification of the presence of certain minerals (carbonates in particular) present only in small amounts was difficult or impossible. This limited the usefulness of the test since many of the materials suspected to influence certain fly ash test results (such as the standard loss on ignition test) are likely to be present only in small fractions. Table 4.2 presents the major crystalline minerals identified in four fly ash samples.

Particle size distribution

The particle size distributions of six of the class F samples were analyzed by dry sieving. U.S. standard sieves numbers 120, 140, 170, 200, 230 and 325 were used. For the analyses, 250 to 300 g of oven-dried fly ash (105°C for 24 h) was sieved for 15 min. Unaccounted mass losses (determined by summing the sieved fractions) ranged from 0.5 percent for sample FR-1 to 2.4 percent for sample FB-2. The results of the analyses are shown in Figure 4.4. The results show that for all five samples, 73-83 percent of the ash particles are less than 63 μm in size.

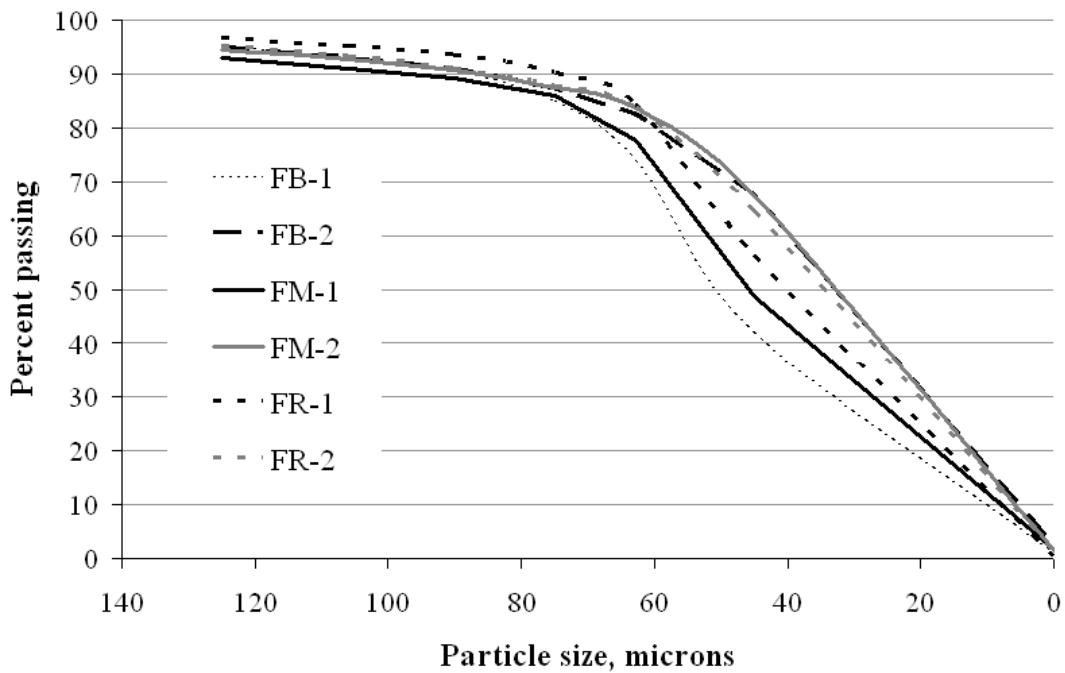


Figure 4.4: Particle size distributions of six class F ash samples. Particle sizes are in micrometers.

4.2.3 Properties of the ash residual coal

Loss on ignition, modified loss on ignition

The loss on ignition values for the fly ash samples are shown in Table 4.3. The tests were performed in accordance with ASTM C 311, with the additional steps to control variability. Modified loss on ignition values, change in sample mass between 300 and 500°C, were also determined according to the method described and are presented in Table 4.3.

Table 4.3: Moisture content, loss on ignition, inorganic carbon, total carbon and organic carbon contents of Texas fly ash samples.

	Moisture	LOI	Mod LOI	Total carbon	Inorganic carbon	Organic carbon
Sample	%	%	%	%	%	%
FB-1	0.13	0.39	0.32	0.38	0.00	0.38
FB-2	0.18	0.26	0.35	0.40	0.01	0.38
FB-3*	0.19	0.41	-	-	-	-
FC-1	0.07	0.40	0.26	0.32	0.00	0.32
FC-2*	0.16	0.78	-	-	-	-
FL-1	0.01	0.12	0.05	0.09	0.00	0.09
FL-2	0.05	0.18		0.13	0.06	0.07
FM-1	0.07	0.13	0.14	0.17	0.00	0.17
FM-2	0.06	0.10	0.14	0.11	0.00	0.11
FM-3*	0.10	0.56	-	-	-	-
FR-1	0.08	0.63	0.04	0.23	0.21	0.02
FR-2	0.11	0.79	0.70	0.72	0.00	0.72
FR-3*	0.11	0.92	-	-	-	-
FR-4*	0.00	0.00	-	-	-	-
FT-1	0.16	0.12	0.18	0.28	0.00	0.28
CD-2	0.10	0.11	0.04	0.07	0.02	0.05
CF-1	0.04	0.24	0.04	0.11	0.05	0.06
CG-1	0.05	0.13	0.03	0.15	0.01	0.14
CG-2	0.02	0.07	0.01	0.13	0.00	0.13
CP-1	0.12	0.34	0.07	0.19	0.07	0.12
CP-2	0.08	0.28	0.14	0.07	0.03	0.04
CW-1	0.08	0.35	0.12	0.24	0.13	0.12

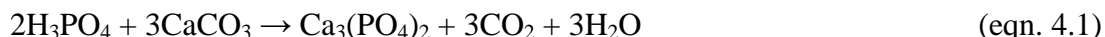
Organic/inorganic carbon content

The organic carbon content was measured using a two step process with a Shimadzu TOC-VCPN with solid sample combustion unit (SSM-5000A). The two steps were, first, determination of the total carbon content, and second, the determination of the inorganic carbon content. The organic carbon content was then determined by subtracting the inorganic carbon content from the total carbon content.

The total carbon content is measured by heating the samples to 900°C in the TOC solid sample module furnace. Inside the furnace (which has an air atmosphere) organic carbon is oxidized and inorganic carbon is decomposed, both producing CO₂ in the process. The gaseous carbon, in the form of carbon dioxide then passes through a carbon measurement device that consists of an infrared light source, flow cell and infrared sensor (NDIR method). As a carrier gas (100 percent pure oxygen) flows through the flow cell, the gaseous carbon driven off the sample is carried between the infrared source and sensor. The sensor detects a change in the intensity of the light due to the absorption of the light by the carbon in the flow cell. The sensor unit then converts the change in light detected into an output voltage. The change in voltage over time is used to produce an area (of voltage multiplied by time) proportional to the amount of

carbon measured. The amount of carbon detected can be determined by calibrating the instrument with a material with established carbon content. Pure solid glucose was used to establish the calibration for coal fly ash residual carbon.

The inorganic carbon content of the ash is determined by immersing the sample in 33 percent phosphoric acid and heating the sample to 200°C in the furnace of the TOC solid sample module. The acid causes the decarbonation of the carbonates present in the sample, as shown by the example of calcium carbonate in equation (4.1). The carbon dioxide released in the reaction passes through the flow cell of the detector and the absorption of the infrared light by the carbon is quantified as discussed above. Reagent grade solid calcium carbonate was used to calibrate the inorganic carbon measurements. The results of the analyses on the ash samples are given in Table 4.3.



The organic carbon contents of the sieved ash fractions of samples FB-1 and FR-2 shown in Figure 4.4 were measured according to the procedure described above. The results of the analysis are shown in Figure 4.5. The contributions of each size fraction to total organic carbon content obtained from the data in Figures 4.4 and 4.5 are shown in Figure 4.6.

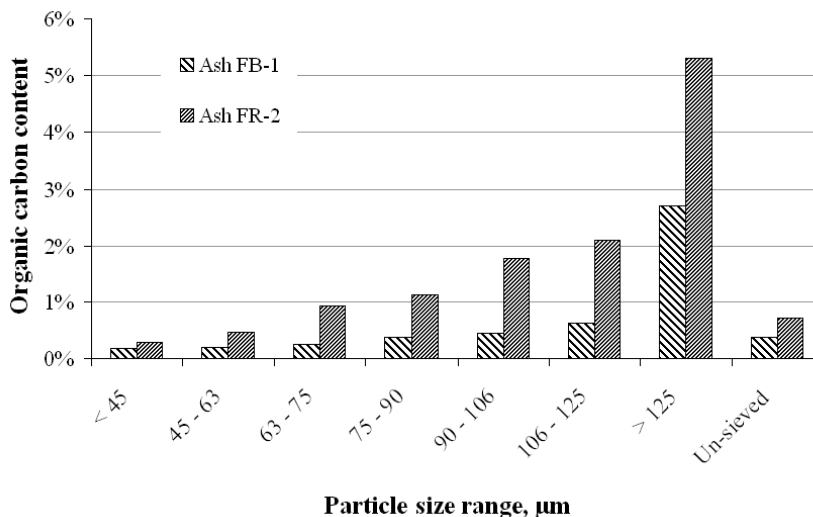


Figure 4.5: Organic carbon content of the individual particle size fractions of ashes FB-1 and FR-2.

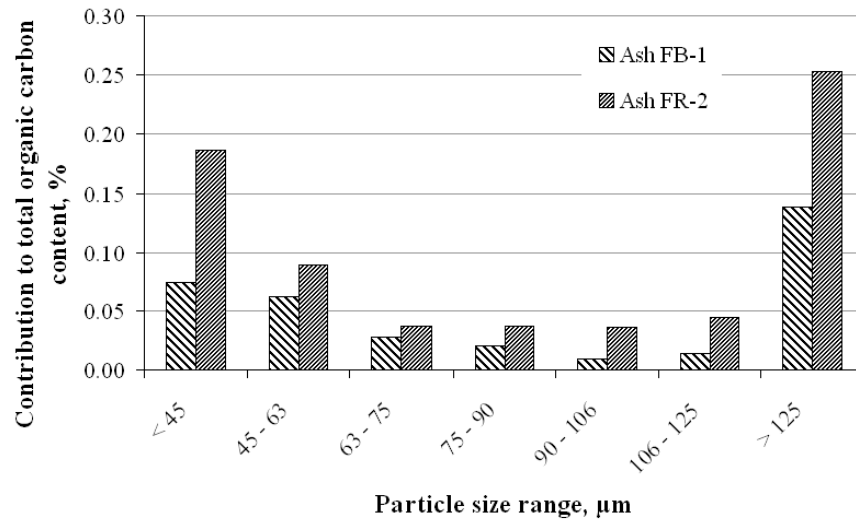


Figure 4.6: Fraction of total organic carbon in sample contributed by each size fraction.

Thermogravimetric analysis, macro-TGA

Thermogravimetric analysis (TGA) is the study of changes in weight due to changes in temperature. Automated TGA instruments consist of a high-precision balance with a pan used to hold the sample. The pan and sample are placed in an electrically heated furnace with thermocouple to accurately measure the temperature. The atmosphere and flow conditions within the furnace are controlled depending on the desired reactions. A computer is used to control the instrument the temperature and atmosphere and gather weight and temperature change data.

As mentioned in chapter 3, some researchers (Fan and Brown 2001, Paya et al.2002) have suggested the use of TGA to measure the quantities of certain materials in fly ash by a combination of controlling the atmosphere (either inert or oxidizing) and temperatures to isolate individual reactions, such as the thermal decomposition of mineral or the oxidation of organic carbon.

A TA Instruments Q500 Thermogravimetric Analyzer was used to characterize certain ash samples. Figure 4.7 shows weight versus temperature of sample FR-2 heated at 10°C per min from room temperature to 900°C. Figure 4.7(a) shows the results of the test performed under a flowing air atmosphere and Figure 4.7(b) under nitrogen.

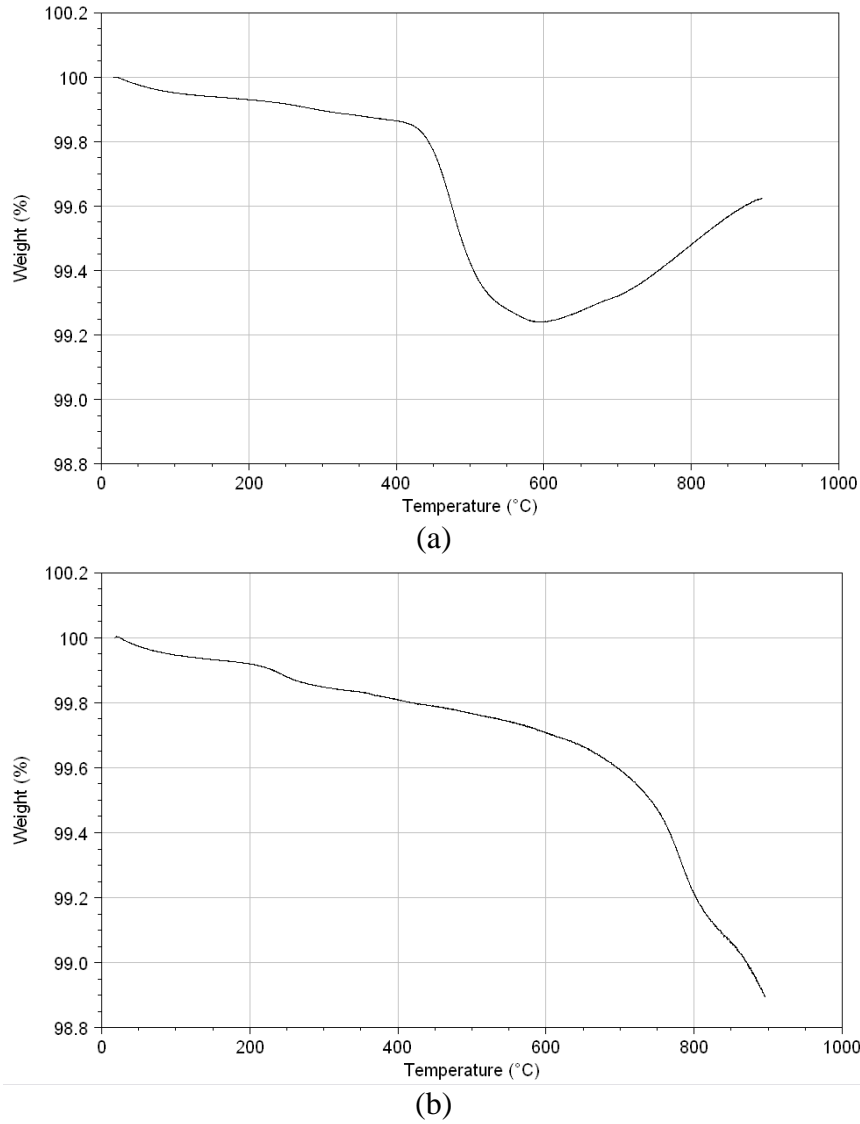


Figure 4.7: Thermogravimetric analysis of sample FR-2 temperature ramp of 10°C per min under air (a) and nitrogen (b).

Additional thermo gravimetric analysis was performed on much larger samples (1 to 2 grams instead of the 50 to 75 milligrams used in TGA) and much larger time-steps between measurements (30 min or more instead of 10 s used in TGA) using an air-atmosphere furnace (called “Macro-TGA” hereafter). For these tests, samples were placed into a preheated furnace and allowed to remain in isothermal conditions for a certain time period. Then, the samples were removed from the furnace, cooled in a desiccator to within about 10°C, and weighed on a desktop scale. After weighing the samples could be returned to the furnace for additional exposure at the same temperature or exposure to a different temperature and the process repeated. Thus changes in sample mass with time or temperature could be tested. The classical ASTM C 311 Loss on Ignition Test is thus a form of what is called here, “Macro-TGA.”

Macro-TGA proved to be a valuable tool for identifying the major factors influencing ash-AEA interactions. Macro-TGA proved to be very versatile, in addition to mass change,

changes in other properties of the sample such as color, foam index value, and organic carbon content could be measured with respect to temperature. Such measurements are shown in figures 4.11-4.15.

Surface area and porosimetry measurements

Surface area and porosimetry measurements were made on a select group of ashes using a Micromeritics ASAP 2020, surface area and porosimetry system. The system uses nitrogen gas adsorption to measure the specific surface area and pore size distribution of powdered or solid materials. To make the measurement, a dry sample is evacuated of all gas and cooled to a temperature of 77K (the temperature of liquid nitrogen). At this temperature nitrogen gas physically adsorbs on the surface of the sample. This adsorption of nitrogen onto the sample surfaces is considered to be a reversible condensation of molecule layers.

The device then adds measured volumes of nitrogen gas onto the sample and an adsorption isotherm (Figure 4.8) is recorded as volume of gas adsorbed versus relative pressure (i.e., sample pressure / saturation vapor pressure) which is unique to the sample. The use of relative pressure is convenient and is scaled from 0 to 1. A relative pressure of 1 represents a completely saturated sample, i.e., all of the available surface structure is filled with liquid-like gas. Once the adsorption isotherm is constructed, various proposed models, such as the BET (after Brunauer, Emmett and Teller) equation, is used to give estimates specific surface area and porosimetry characteristics.

The results of the tests on a sub-group of ashes are shown in Table 4.4. Determination of BET surface area and t-plot micropore surface area is described by Adamson, (1982). The sample labeled “FR-2 ox” is the sample FR-2 except that it was heated in an air atmosphere furnace at 750°C for 2 h to oxidize residual coal. Therefore it is approximately represents the surface area of only the mineral fraction of the ash, provided that changes to the mineral component of the ash due to heating had little or no influence on specific surface area. The change in surface area due to heating is 3.4 m²/g, about 84 percent decrease from the value before oxidation.

FR-1 Isotherm

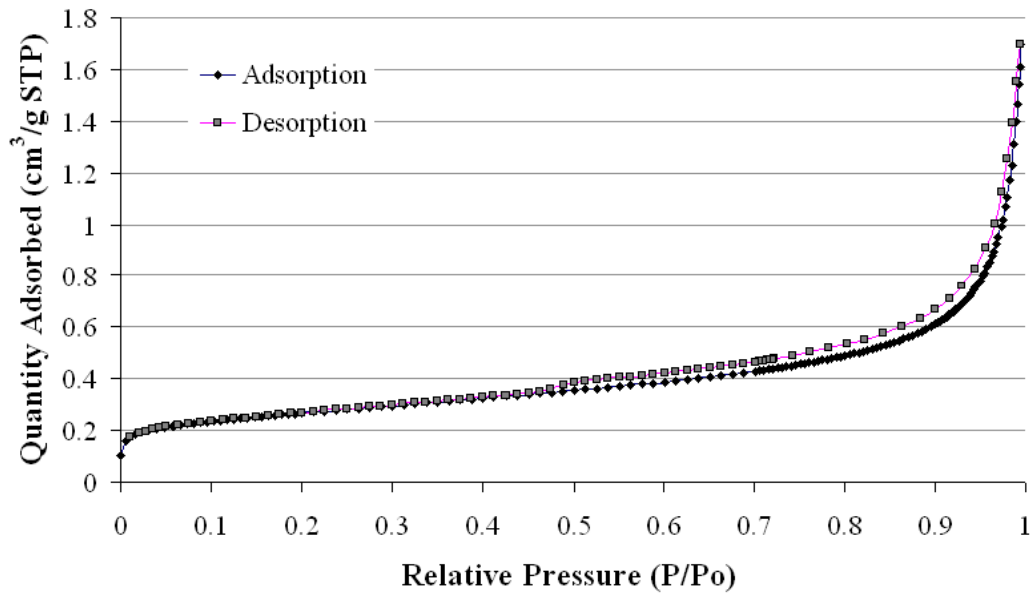


Figure 4.8: Nitrogen adsorption isotherm for sample FR-1.

Table 4.4: BET surface area and t-plot micropore area for selected fly ash samples.

Sample	BET surface area micropore area	
	m ² /g	m ² /g
FB-1	1.7	0.7
FB-2	1.6	0.8
FL-1	1.0	0.2
FM-2	0.8	0.2
FR-1	1.0	0.2
FR-2	4.0	1.6
FR-3	3.9	1.4
CD-1	1.3	0.2
CG-1	0.8	0.1
CP-2	1.0	0.2
CW-1	0.9	0.6
FR-2 ox	0.7	0.1

Color analysis

Color analysis of the ash samples was performed using the method described in Chapter 7. The basic procedure is performed by first, create a digital image of a prepared ash sample (oven-dried at 105°C for 24 h, placed into a standard sample holder and consolidated in accordance with the described procedure) and then, using image analysis software, convert a representative portion of the sample image color to a grayscale numerical value. The oven-dried grayscale values and change in grayscale values between 300 to 500°C and 105 to 750°C are shown in Table 4.5. Change in grayscale analyses was performed by heating two similar samples (3 g each, heat for 1 h in an air atmosphere furnace) at the two indicated temperatures and then determining the grayscale value of each. The change in grayscale value is equal to the grayscale value determined for the higher temperature minus the value of the lower temperature.

Table 4.5: Grayscale values of oven-dried ash samples and change in grayscale values between 300 to 500°C and 25 to 750°C.

	oven dry	300-500 °C change	105-750 °C change
FB-1	109.3	27.0	29.0
FB-2	91.3	33.5	26.7
FC-1	129.0	26.0	10.0
FL-1	132.7	5.0	-15.0
FL-2	130.7	3.0	-12.0
FM-1	137.3	12.5	-7.3
FM-2	124.7	5.0	6.0
FR-1	172.4	7.0	0.3
FR-2	110.0	36.0	41.0
FT-1	108.7	30.8	24.3
CD-2	165.7	0.2	-33.0
CF-1	144.0	-1.7	-25.3
CG-1	152.0	2.8	-29.7
CG-2	158.7	2.6	-26.0
CP-1	145.3	-2.0	-35.3
CP-2	149.0	-0.9	-21.7
CW-1	144.3	-3.8	-34.3

4.2.4 Properties of ash interactions with AEA

Concrete AEA dosage

Fresh concrete air tests were performed at The University of Texas, Austin to determine the influence of the fly ash samples on AEA demand for 6 percent air content. A detailed description of the test method is found in Ley (2007). The tests were performed by mixing 64-L batches of concrete in an 85-L mixer. All materials used in the mixtures were stored in the mixing room for at least 24 hours at 23°C prior to mixing to keep the mixing temperature constant. All mixtures had water to cementitious material ratios of 0.45 and contained 335 kg/m³ (equivalent to 6 sacks of cement/CY), of total cementitious materials composed of 80 percent cement and 20 percent fly ash (by mass). The cement used in all mixtures met the requirements of ASTM C 150 as a Type I and II with alkali content (Na₂O_{eq}) of 0.53 and a Blaine of 3630 cm²/g. The phases of the cement are reported in Table 4.6 as determined by a Rietveld quantitative x-ray diffraction (RQXRD) (Rietveld, 1969). Texas river gravel and sand were used and the mixtures were proportioned as shown in Table 4.7. The fresh concrete was brought to a constant slump (ASTM C 143) of 76 mm +/- 25 mm using an ASTM C 494 Type D normal range water reducer.

Table 4.6: Riedvelt analysis of the type I/II cement.

Phase	Percent composition
C ₃ S	68.0
C ₂ S	15.7
C ₃ A	2.7
C ₄ AF	8.7
Gypsum	1.3
CaCO ₃	2.6

Table 4.7: Components and masses of the materials used in the concrete air tests.

Component	Mass (kg/m ³)
Cement	268
Fly Ash	67
Coarse Aggregate	1098
Fine Aggregate	742
Water	151
AEA (wood rosin based)	Varied
NRWR	Varied

After the desired slump was obtained, unit weight (ASTM C 138) and pressure meter (ASTM C 231) measurements were made. The concrete used in the slump test was returned to the mixer and approximately 57 L of concrete remained. Next, a wood rosin-based commercial AEA was added to the mixture and mixed for three minutes. Slump and unit weight measurements were taken after each dosage-and-mixing cycle and returned to the mixer to receive additional AEA doses. After sufficient AEA was added to change the unit weight to that corresponding to $6 \pm \frac{1}{2}\%$ air content, the dosing was stopped and final slump and unit weight readings were taken and the air content verified by pressure meter. The dose of AEA required for exactly 6 percent air was interpolated from linear curve-fits of the dosage-air content data. The test results are shown in Table 4.8.

Table 4.8: Concrete AEA dosage for 6 percent air, concrete slump and water reducer requirement.

Sample	AEA demand (mL/100 kg cm)	slump (mm)	Water reducer (mL/100 kg cm)
FB-1	64	89	48
FB-2	93	83	50
FB-3*	44	57	132
FC-1	52	76	72
FC-2*	49	95	68
FL-1	31	100	83
FM-1	48	64	58
FM-2	49	70	46
FM-3*	83	83	47
FR-2	147	83	71
FR-3*	138	57	111
FT-1	42	89	64
CD-1	32	95	45
CD-2	50	64	46
CF-1	34	95	66
CG-1	38	64	45
CG-2	39	95	46
CP-1	36	70	81
CW-1	44	76	51

Foam index

Foam index test results were obtained using the recommendations for a standard test reported in Chapter 6. The tests were performed in a 58 mL container with 26 mm inner diameter. The filled height was equal to 50 mm. Each test combined 9.1g of cement and 2.3g of ash (ash/cm equal to 0.2). The test incorporated 22.7 mL of water (w/cm equal to 2.0). The same cement and commercial AEA (wood rosin-based) was used in the test. AEA concentration and drop size were varied to achieve the R_{min} values shown in Table 4.9.

Foam index tests were also performed on the sieved ash fractions from ash samples FB-1 and FB-2 shown in Figure 4.4. The foam index tests were performed using a 132 mL container with an inner diameter of 45 mm. The filled height was equal to 18 mm. Each test combined 5 g cement and 5 g of ash with 25 mL of water. Test precision R_{min} was equal to 20 mL AEA/100 kg cm. The results of the test (values given are the averages of two tests) are shown in Figure 4.9. The standard foam index test developed in Chapter 6 was not used for this test since the test was completed before the development of the recommended standard. Therefore the test values cannot be directly compared to those in Table 4.9. However, the general trends in behavior and relative values can be compared between test methods.

Table 4.9: Specific foam index and minimum precision, R_{min} , for the Texas fly ash samples.

Ash sample	Foam index mL AEA/ 100 kg cm	Rmin mL AEA/ 100 kg cm
CD-2	13.2	4.4
CF-1	17.6	2.2
CG-1	17.6	2.2
CG-2	15.4	2.2
CP-1	13.2	2.2
CP-2	15.4	2.2
CW-1	13.2	2.2
FB-1	48.5	4.4
FB-2	66.1	4.4
FB-2*	22.0	2.2
FC-1	44.1	4.4
FC-2*	17.6	4.4
FL-1	13.2	2.2
FL-2	13.2	2.2
FM-1	26.4	4.4
FM-2	35.2	4.4
FM-3*	39.6	4.4
FR-1	15.4	2.2
FR-2	92.5	4.4
FR-4*	22.0	4.4
FT-1	37.4	2.2

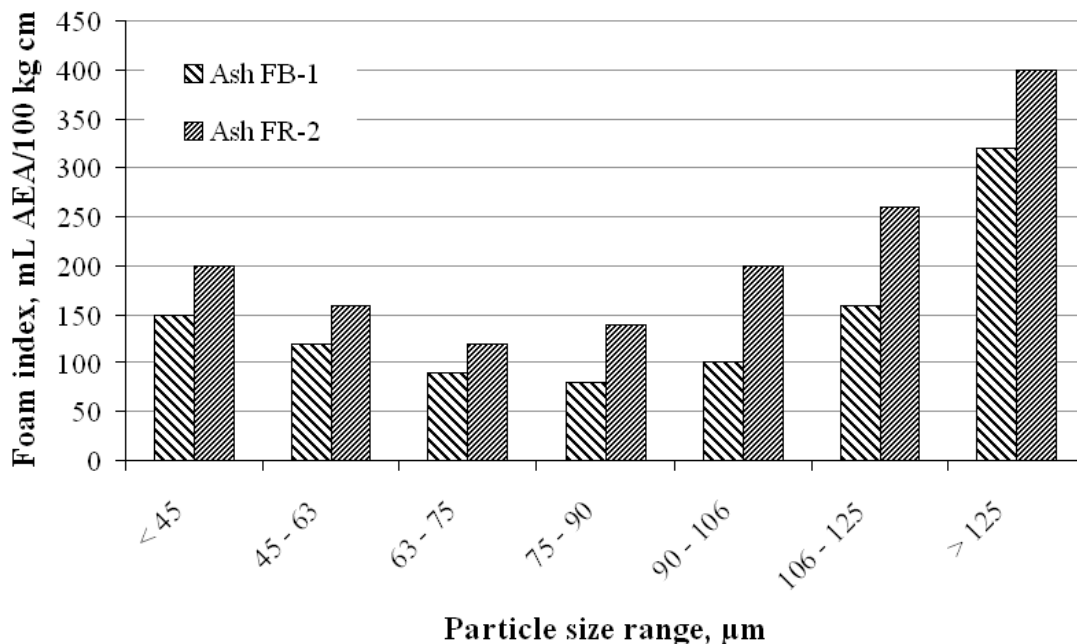


Figure 4.9: Foam index values of sieved ash fractions for ash samples FB-1 and FR-2.

UV-Vis spectrophotometry

A spectrophotometer was used to determine the concentration of surfactants (such as commercial AEA) in water by measuring the absorbance of light by the solution. A surfactant absorbs a unique combination of wavelengths with certain wavelengths more sensitive to the surfactant than others. The greater the concentration of surfactant in solution, the more light is absorbed by the solution. A spectrophotometer transmits light through a container of holding the surfactant solution and a detector receives the light after it passes through the sample and measures the intensity and converts the intensity to absorbance over a range of wavelengths. The differences in intensity from a blank sample are calibrated with prepared surfactant solutions. An example calibration over a range of wavelengths is shown in Figure 4.10.

UV-Vis spectrophotometry was shown to be capable of measuring concentrations of AEA in solutions of distilled water. Considerable effort was made to identify a technique for measuring the influence of fly ash on surfactant concentrations in water. Typical experimental test methods combined varying amounts of fly ash (generally 0.1 to 1 g ash in 200 mL water) to which a measured amount of surfactant was added. After allowing time for interactions between fly ash and AEA to occur (time ranges varied between 10 seconds to 1 h), ash particles were separated from the water by filtration or centrifugation. The absorbance of the solution was then measured and compared to calibrated standards based on one or more wavelengths.

Despite the use of a variety of experimental techniques, the method repeated proved incapable of identifying differences between several ash samples. Based on the inability to produce meaningful results, further use of the test was abandoned. It was speculated that the formation of insoluble products by the precipitation of anionic surfactants with divalent ions in solution may be a principle factor in the failure of the application of the test. This limitation of

the test was previously identified by Baltrus and LaCount (2001) as a problematic factor. Potential techniques for overcoming the problems with the test are given in Chapter 9.

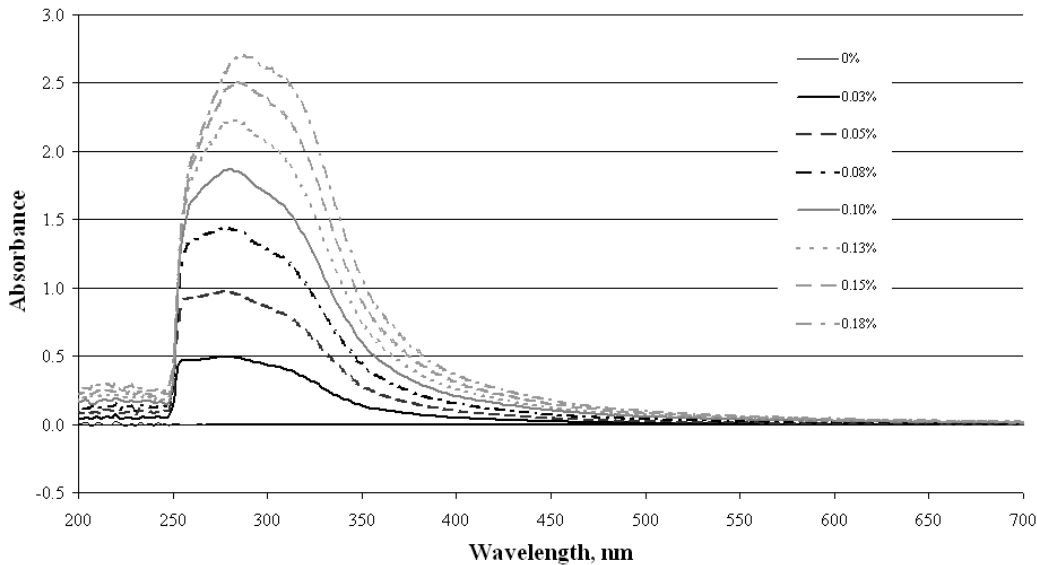


Figure 4.10: Example of absorbance versus concentrations of a commercially available AEA.

4.2.5 Changes in ash properties due to temperature exposure

As mention above, macro-TGA was determined to be a valuable tool in this research due to the application of the method to ash other properties besides mass. The variations on this test method are described below. Common to all tests is that samples of ash, generally between 1 and 5 g each, (or other materials as discussed in Chapter 5) are placed into porcelain crucibles or bowls and placed in a preheated furnace for a given amount of time, typically 30 m to 2 h, depending primarily on sample size (large samples were found to generally require more time equilibrate in mass or organic carbon content). After the heating duration is complete, the samples are removed to a desiccator to cool. After cooling the property of the ash in question is assessed.

For mass measurements the same samples can then be returned to the furnace for heating to an incrementally higher temperature and the process is repeated until the mass has been measured over the desired range of temperatures. For tests that result in alteration of the sample, such as color analysis, foam index or total carbon analysis. Fresh samples are placed into the furnace at the subsequent incremental temperature increase and the process is repeated over the desired range of temperatures.

Macro-TGA

Change in ash mass with temperature was performed according to the method described above. For each ash sample, 1 g of ash was used and heating durations of 30 min were used at each temperature interval. The results of the analysis are shown in Figure 4.11.

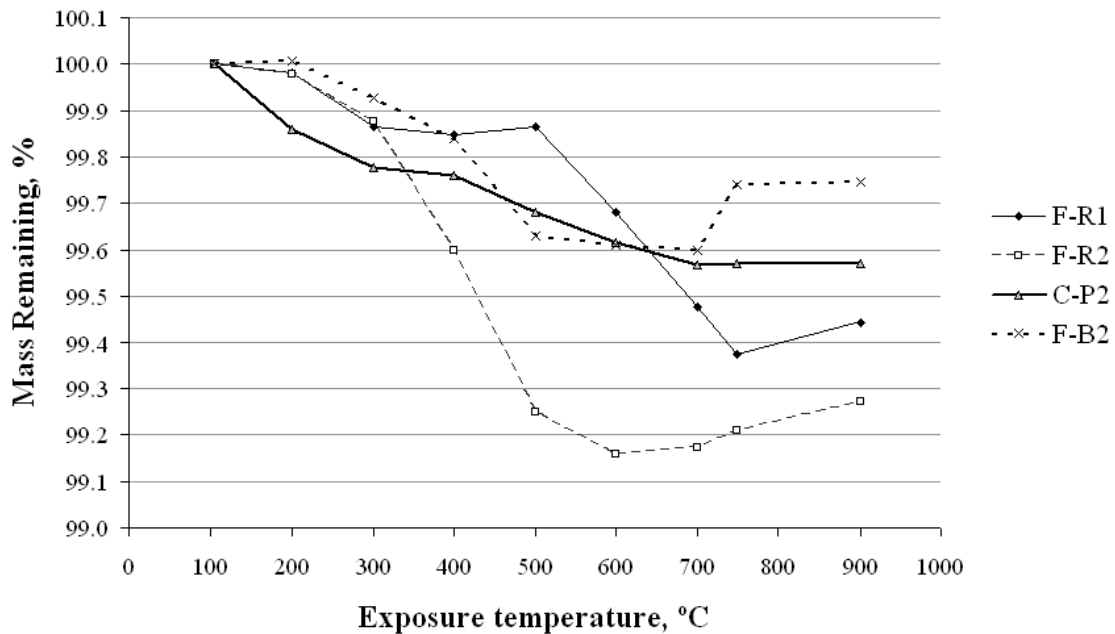


Figure 4.11: Mass remaining versus exposure temperature for four fly ash samples. (Mass remaining based on oven-dried weight.)

Change in ash grayscale value with temperature

Analyses of the changes in ash grayscale value with temperature were performed on seven Class F and three Class C samples. For each temperature and ash sample, 3 g of ash was heated in a porcelain bowl. The heating process was done as described above with exposure duration of 1 h for each temperature interval. After cooling, the sample was immediately placed in a standard sample holder and the grayscale value analyzed according to the method described in Chapter 7. The results of the analyses are shown in Figures 4.12 and 4.13.

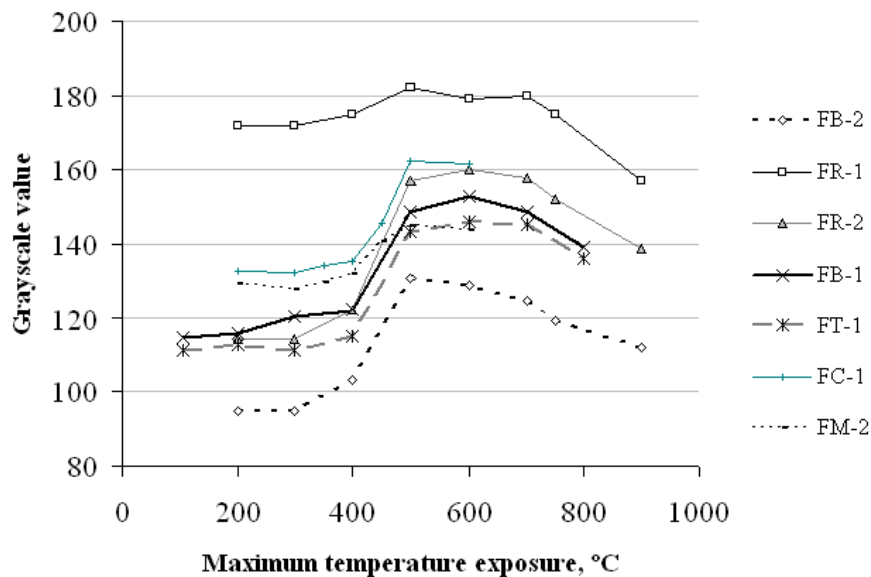


Figure 4.12: Ash average grayscale value versus temperature exposure for seven Class F ash samples.

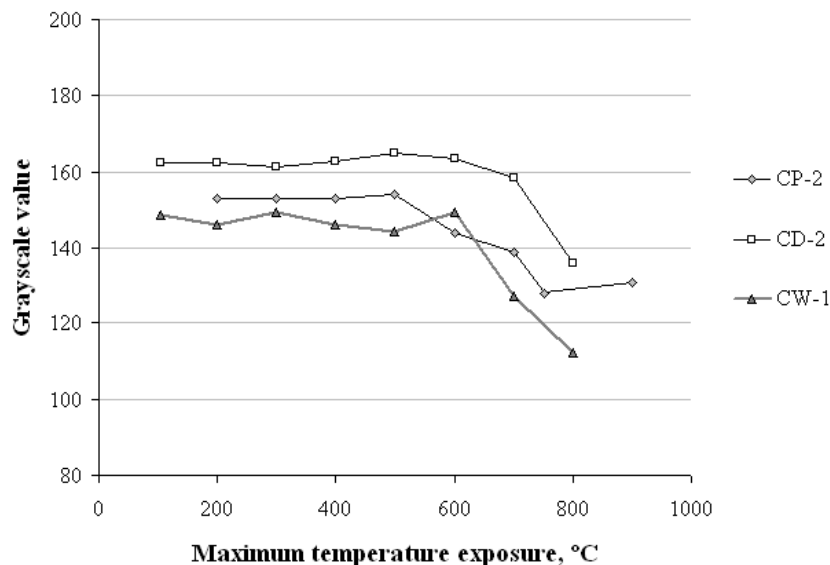


Figure 4.13: Ash average grayscale value versus temperature exposure for three Class C ash samples

Change in foam index value with temperature

Foam index tests were performed on temperature-treated samples of ashes FB-1 and FB-2. Temperature treatment was performed as described above using 5 g samples in porcelain bowls. Exposure duration was 2 h at each temperature. After heat treatment the samples were assessed by means of the foam index test. The foam index tests were performed using a 132 mL

container with an inner diameter of 45 mm. The filled height was equal to 22 mm. Each test combined 5 g cement and 10 g of ash with 30 mL of water. Test precision R_{min} was equal to 20 mL AEA/100 kg cm. The results of the test are shown in Figure 4.14.

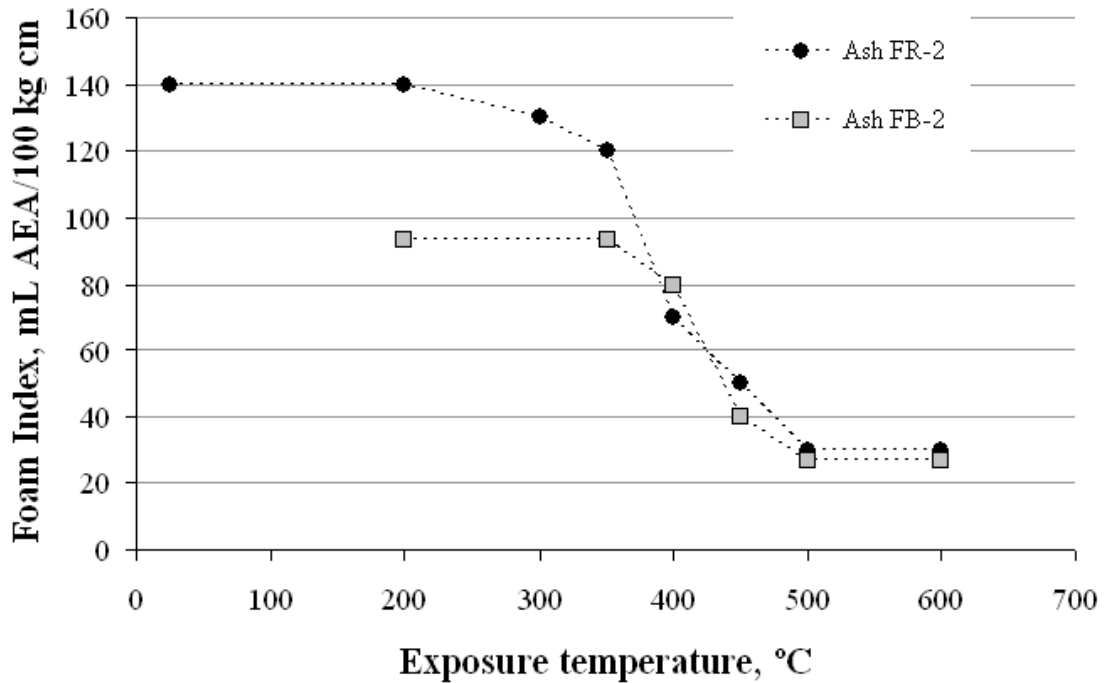


Figure 4.14: Foam index versus temperature exposure for two ash samples.

Change in organic carbon content with temperature

Analyses of the changes in ash organic carbon content with temperature were performed on ashes FB-1 and FR-2. For each temperature and ash sample, 1 g of ash was heated in a porcelain crucible. The heating process was done as described above with exposure duration of 30 min for each temperature interval. After cooling, the sample was analyzed for organic carbon content as described above. The results of the analyses are shown in Figures 4.15. Each point in the figure is the average of two organic carbon measurements.

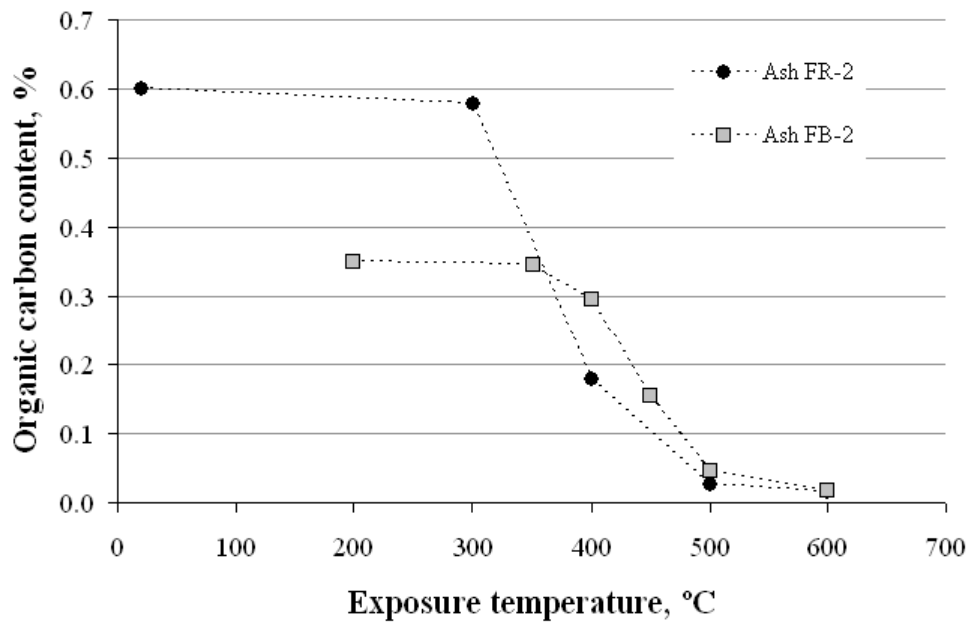


Figure 4.15: Organic carbon content versus temperature exposure for two fly ash samples.

Chapter 5. Assessment of the ASTM C311 Loss on Ignition Test as a Measurement of Carbon Content

5.1 Introduction

The results of ASTM C311, loss on ignition, are frequently interpreted as an indication of the likelihood of interaction between a given fly ash and the surfactants known as air entraining admixtures (AEA's). As introduced in Chapter 2, this has been justified because of the general assumption that AEA molecules adsorb or otherwise interact with the so called "carbon" in the ash, coupled with the assumption that the ASTM C311 loss on ignition procedure indicates "carbon" by measuring mass lost from the ash after exposure to furnace temperature of 750°C. Both of these assumptions are reasonable; carbon-surfactant interaction is well known and documented in many applications from shampoos to dishwashing detergents (Jankowska et al, 1991; Cheremisinoff and Morresi, 1980), and LOI has traditionally been used as an indicator of organic coal residuals (Fan and Brown, 2001). In contrast to this state of the practice, Figure 5.1 shows that for the samples evaluated in this study there is not a general correlation between LOI and the dosage of AEA required to stabilize 6% air in fresh concrete. (An improved correlation may exist for a fixed set of materials.)

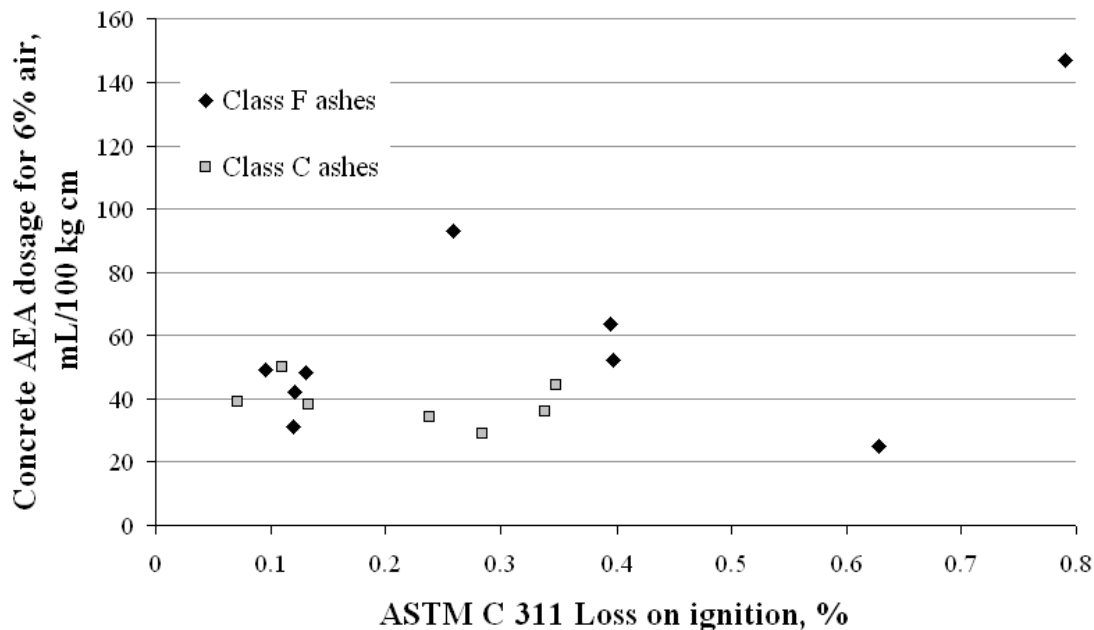


Figure 5.1: Concrete AEA dosages for 6% target air concrete versus ASTM C311 loss on ignition content for Texas ash samples.

This chapter reports work performed to explore the reasons for the scatter in Figure 5.1, and to develop a modified LOI procedure to serve as a more reliable indicator of ash-AEA interaction. Whereas the research project as a whole embraces the question of whether "carbon" (in some form or forms) is in fact the primary cause of ash-AEA interaction, the focus of the work reported in this chapter is the degree to which the ASTM C311 LOI test is in fact a reliable

measure of “carbon” (in some form or forms) in the fly ash. The chapter begins with a background discussion of the various forms of carbon that can be present in fly ash and reports on their differencing behavior under conditions similar to those in the C311 test. The targeted literature review includes a discussion of mass changes under LOI conditions that are related to “inorganic carbon” (e.g., carbonates) and to non-carbon species. This background review will be augmented with the results of recent experiments conducted by the author to further point out that in the conduct of the LOI test: 1) not all “carbon” is removed from fly ash, 2) some carbon is removed but may not be measured, 3) not all losses are due to carbon, and 4) the LOI value reported is the net result of mass-losses and mass-gains, in which the gains partially mask the losses.

In the process of examining the LOI test and correlating LOI results with the results of Thermogravimetric Analysis (TGA) and Total Carbon Analysis (TOC), the author discovered that by taking intermediate mass loss readings at 300°C and 500°C the standard C311 LOI test can be used as reliable indicator of the “organic carbon” content of fly ash. Furthermore, and somewhat serendipitously, it is demonstrated that “organic carbon” as estimated by the proposed modification to ASTM is a useful indicator of the likelihood of ash-AEA interaction for the materials evaluated here.

5.2 Background

5.2.1 The ASTM C311 LOI test

The ASTM C311 LOI test is described in Chapter 3 Section 3.4.4. Figure 5.2 shows samples of fly ash in porcelain crucibles heated in an air-atmosphere muffle furnace during performance of the test.

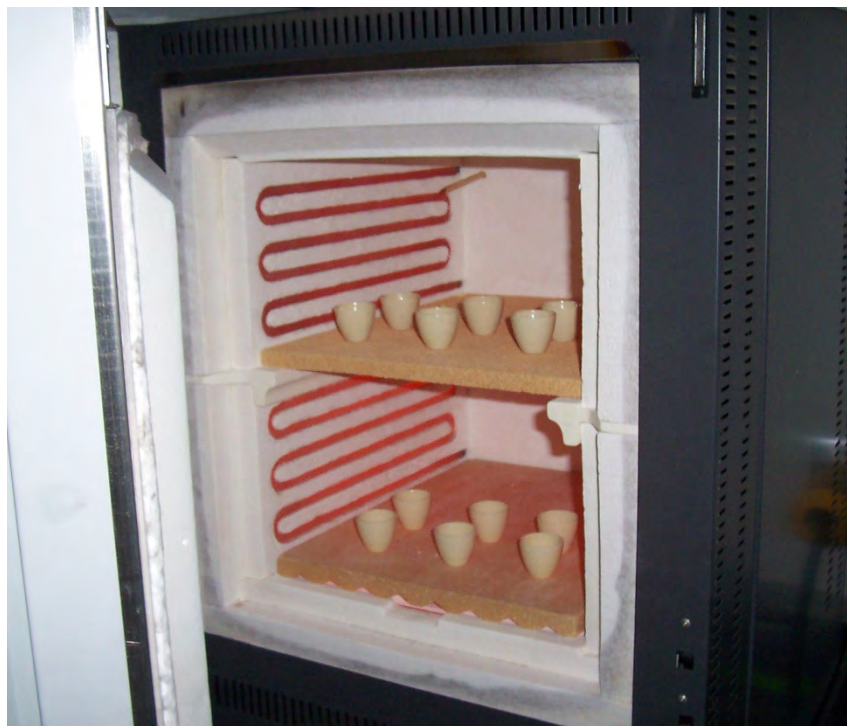


Figure 5.2: Performance of the LOI test by heating sample of fly ash in a muffle furnace.

Harris et al. (2006) determined that the standard LOI test is sensitive to several factors in the test method that are not specifically controlled by the ASTM C311 test procedure. These factors include exposure time at elevated temperature, ash cooling environment, and cooling time after removal from the furnace. Other factors that have been identified during this study, such as furnace spatial variability and mass measurement errors are discussed later in this chapter. Control of these factors is necessary to avoid significant errors in LOI measurements.

It is critical to note that the LOI test does not purport to be anything other than what its procedure implies: a measure of the net change in mass after exposure to 750°C, corrected for moisture loss up to 105°C. The test method is not intended as a carbon content measurement, even though LOI results are often interpreted as such (Schlorholtz, 2006).

5.2.2 General comments on carbon in fly

The standard LOI test is often referred to as a test to measure the carbon content of ash (Freeman et al., 1997; Hurt et al., 2001). As described in Chapter 2, use of the term “carbon” is imprecise since carbon can exist in several different forms. For the purposes of this work, classification of carbon forms as “inorganic” and “organic” are used according to the definitions provided in Section 2.6.2. In this chapter, the forms of carbon that can exist in ash are described as well as the behavior of the forms in the LOI test.

The forms of carbon in fly ash behave differently when exposed to elevated temperatures. Hill et al. (1997) concluded, based on the study of ash samples by DTA, (differential thermo gravimetric analysis) that forms of carbon (individual forms other than carbonates were not identified) are oxidized at different temperatures. Exothermic peaks that were shown to not be the result of calcination of carbonates occurred at various temperatures between 540 and 600°C. Interpretation of TGA mass loss versus temperature data by Paya et al. (2002) suggested that

carbon (again, individual forms were not identified) was oxidized in air at temperatures between 450 and 750°C. This temperature range was also reported by Sabanegh et al. (1997). Fan and Brown (2001) suggested that volatile organic compounds (VOCs) present in fly ash are vaporized when ash is heated to 750°C in an inert atmosphere. A specific temperature range for which VOCs are devolatilized from ash has not been identified; however devolatilization of pulverized coal begins at coal temperatures of 350 to 400°C (Ishii, 2000). Further, despite the general interpretation that the LOI test measures carbon in ash by removing it at 750°C, some forms of carbon may not be removed or only partially removed during the LOI test.

5.2.3 Forms of carbon in fly ash

Several differing forms of carbon have been identified in fly ash. These forms are volatile organic compounds, soot, coal char and carbonates.

Volatile organic compounds

Fan and Brown (2001) determined that volatile organic compounds (VOCs) may be present in certain fly ash samples and contribute an estimated 0 to 97 percent of the LOI measurement (based on tests of seventy ash samples). The researchers observed that the presence of VOCs darkened the appearance of ash and caused ash to have oily consistencies. The presence of VOCs was determined only qualitatively by placing ash samples in benzene to dissolve the compounds, and comparing the change in the color of the filtered benzene to pure benzene.

Fan and Brown postulated that the VOCs found in ash samples had been driven off the pulverized coal particles as the coal entered the combustion chamber and experienced rapid heating (See Chapter 3 Section 3.3.6.2). Some portion of the volatiles were combusted while, depending on the combustion conditions, some portion may have exited the combustion chamber and condensed on the surfaces of the fine ash and solid organic coal residuals upon cooling (Helmuth, 1987).

Fan and Brown (2001) suggested that the VOCs present in ash are produced by the volatilization of tar. Tar composes about 40 to 80 percent of the total volatiles in coal and is defined as all the volatilized matter, except water, that is liquid at room temperature. Tar is a dark brown to black liquid and is composed of a variety of aromatic hydrocarbons such as benzene, toluene, xylene and many other species (Howard, 1981).

Soot

The presence of soot in fly ash was identified by Gao et al. (1997). Soot forms as a byproduct of incomplete combustion of coal (or other hydrocarbons) due to insufficient oxygen. Soot particles are generally an order of magnitude smaller than the smallest fly ash mineral particles; individual soot particles identified by Gao et al. averaged approximately 40 nm in size. A large portion of the elemental carbon present in soot is embedded in tiny graphite-like crystallites, each of which is composed of randomly arranged lamellae (Skinner and Smoot, 1979; Hess and Herd, 1993).

The author gained further insight on the behavior of soot by performing LOI tests on samples of the powdered material known as “carbon black,” a generic term for a form of soot manufactured by the controlled partial combustion of hydrocarbons in a low-oxygen environment. The average particle diameters of carbon blacks range from 0.01 to 0.4 microns (μm), and typically flocculate in clusters with average diameters ranging from 0.1 to 0.8 μm .

Generally, carbon blacks contain over 97 to 99 percent elemental carbon with the remainder consisting primarily of chemically bound hydrogen, oxygen, nitrogen and sulfur (Donnet et al., 1993). The anisotropic structure of the carbon in carbon black (and soot) is thought to play a role in resisting oxidation (Skinner and Smoot, 1979).

The author performed the C311 LOI test on 1 g samples of carbon black, periodically measuring mass after stepwise exposure to furnace temperatures of 20, 300, 500, 750, and 1000°C (furnace limit). The results of the experiment are shown in Figure 5.3.

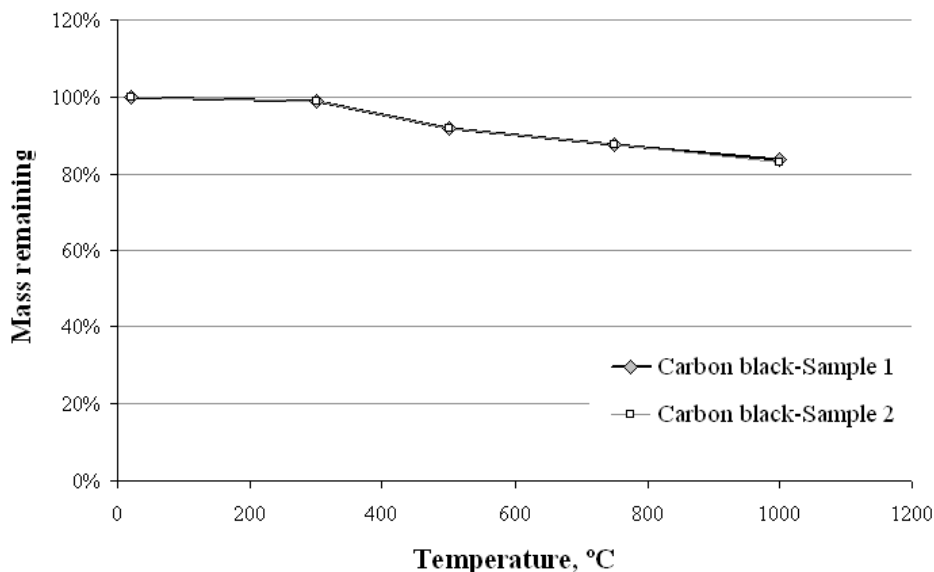


Figure 5.3: Mass of carbon black remaining after exposure to air at various temperatures.

As shown in Figure 5.3, only a small fraction of the mass of carbon black was lost over this testing regime up to 1000°C. Continued exposure at 1000°C for 24 hours resulted in less than 1 percent additional mass loss.

These experimental results are in agreement with Park and Appleton's more in-depth analysis as shown in Figure 5.4 (Park and Appleton 1973), which shows the specific oxidation rate of soot, where P_o is the partial pressure of oxygen. For temperature, $T = 1000$ °C (1273 °C), the reciprocal temperature represented by the x-axis is about 8. The corresponding specific soot oxidation rate is quite low, and, as such, it appears that the oxidation of soot occurs at a slow rate at the temperatures and pressures of the C311 LOI test. Thus one would expect that the LOI test will not indicate carbon in the form of soot in fly ash.

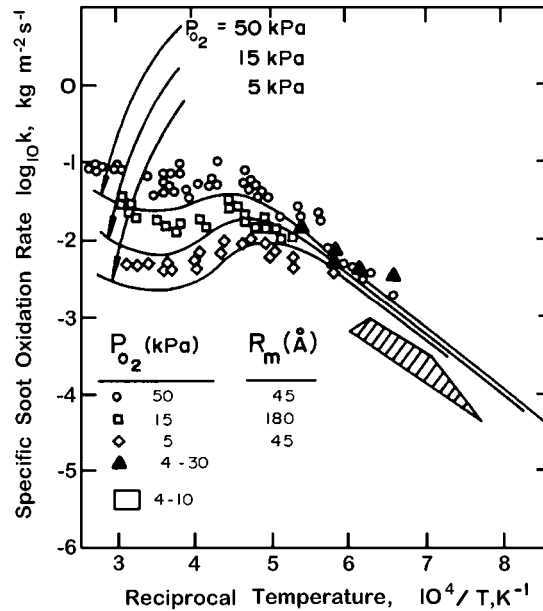


Figure 5.4: Specific soot oxidation rate as a function of temperature from Park and Appleton (1973).

Charcoal or “Carbon Char”

In contrast with the difficulty in detecting soot via the LOI procedure, charcoal, another form of carbon that is likely to be present in fly ash, is readily detectable. Charcoal is the carbon char that remains after the pyrolysis (heating in a low-oxygen environment) of any hydrocarbon-based material such as coal. As the coal is heated in the combustion chamber of a boiler, volatile components within the material are evolved and moisture is driven off. This is followed by the evolution of hydrogen-rich compounds until no further materials can be evolved. Since lack of oxygen prevents complete combustion, what remains is the carbon-rich “char” phase and mineral ash.

Residual carbon char is often regarded as the main carbon form of interest with regard to AEA interactions in concrete (Freeman et al. 1997; Hurt et al. 2001). For some ash samples in general, carbon char may be the primary source of ignition losses with only minor contributions from other sources (Brown and Dykstra 1995, Fan and Brown, 2001). In other ash samples, such as the Texas commercial ash samples studied in this work, LOI contents are relatively small (typically less than 1 percent for the samples studied) and contributions to the measurement from other sources are relatively large.

Given that something on the order of 3 to 97 percent (Fan and Brown, 2001) of the carbon present in fly ash could be composed of charcoal (more formally known as “carbon char”), the author found it instructive to perform the C311 LOI test on pulverized charcoal, manufactured by Norit⁵, with more than 90 percent of the particles smaller than 45 microns. This form of carbon char could differ from that found in fly ash since it was intentionally heated in a low oxygen environment with a slow heating rate over a longer period of time towards the goal of inhibiting combustion. In the power plant the pulverized coal experiences a rapid heating rate

⁵ Norit NV, Borne, The Netherlands.

over a short period with forced air towards the goal of maximizing combustion. Nevertheless, 1.7 g samples of manufactured, pulverized charcoal were heated using the LOI procedure but at various temperatures, with the results shown in Figure 5.5. A second analysis was performed on 1 g samples of charcoal in which the samples were heated at 500°C and mass change was measured as a function of duration of exposure. The test was performed by first heating the samples at 400°C for 30 min. The samples were then removed from the furnace and placed in a desiccator to cool for 30 min, and then weighed. As the samples cooled, the temperature of the furnace was increased to 500°C. The following steps were then repeated until the samples reached a constant mass: the samples were placed in the preheated furnace for approximately 30 min, removed and cooled in a desiccator for 30 min and then weighed. Then two of the samples were stirred with a glass stirring rod and reweighed. Reweighing was done to measure any loss of mass that occurred during stirring, since it was observed that a small portion of the sample sometimes adhered to the glass stirring rod. Stirring of the samples was performed to remove the ash buildup and increase the amount of charcoal at the top surface of the sample. After weighing, all samples were then returned to the furnace. Figure 5.6 shows the behavior of the sample masses versus exposure time after corrections for any loss of mass during stirring.

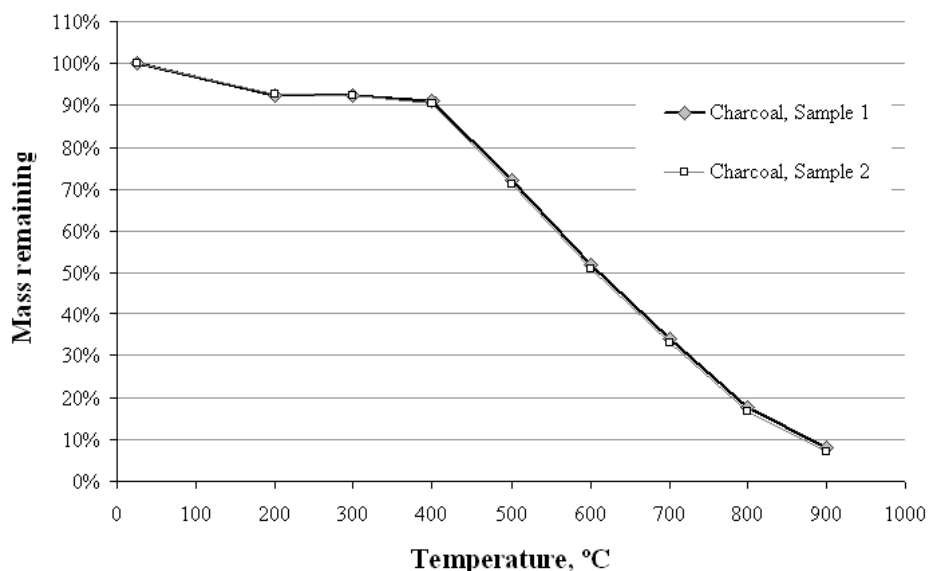


Figure 5.5: Mass of charcoal remaining after 30 min exposure to air at various temperatures.

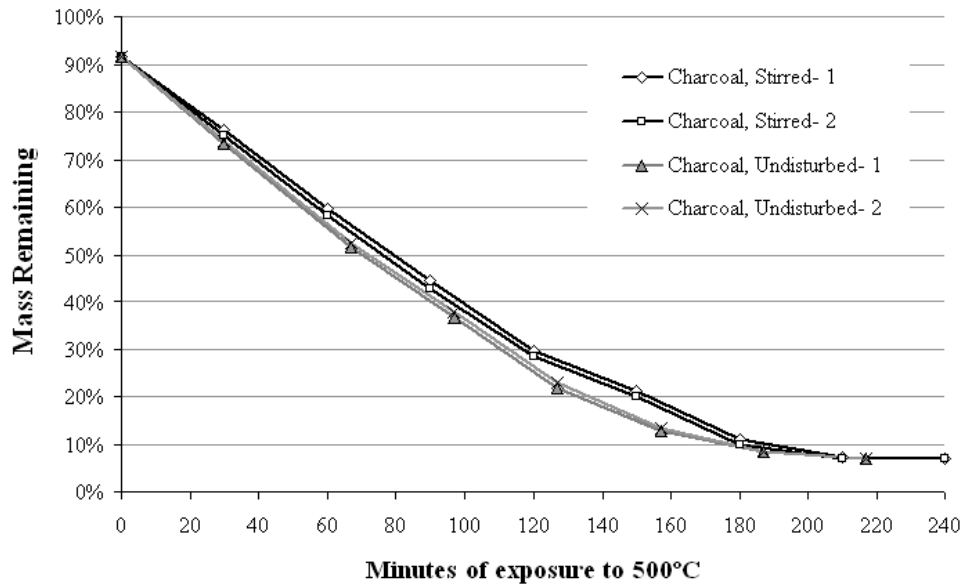


Figure 5.6: Mass of charcoal samples remaining after varying durations of exposure to 500°C air.

As seen in Figure 5.5, the pulverized charcoal lost less than 10 percent mass between room temperature and 200°C. This was followed by near constant mass until demonstrating a near constant rate of mass loss of about 20 percent per 100°C from 400 to 800°C, with a slight reduction in rate from 800 to 900°C. After exposure to temperatures greater than 400°C, a light-brown-colored layer of ash appeared at the top of the black charcoal sample. As the charcoal was consumed, the thickness of the ash layer increased. This continued until the black char was consumed and only ash was visible in the crucible. After cooling the remaining material was examined, consisting primarily of light-colored ash. When the ash was stirred, a thin layer of black un-oxidized charcoal was observed beneath the upper ash layer. It appeared that the ash residue that remained at the surface of the charcoal may have inhibited oxygen diffusion to the charcoal. However, as evident in Figure 5.6, intermittent stirring of the samples did not increase the reaction rate. In fact, the stirred samples showed a slightly slower reaction rate for the majority of the test. However, after approximately 200 min of exposure, there is negligible difference between the stirred and unstirred samples heated at 500°C. (Stirring samples can alter sample mass when some of the material adheres to the stirring device. An average of 0.00018 g of charcoal was lost during stirring as based on twelve measurements, with more material adhering to the stirring rod earlier in the test. Less than 0.0001 g was lost for the final round of stirring.)

Analysis of charcoal mass change under constant temperature (Figure 5.6) showed that the same percentage of mass-loss achieved by heating the sample to 900°C in Figure 5.5 could be achieved by heating the samples to 500°C for 210 min. Total carbon analysis of the residual material in the crucibles after heating to 500°C for 240 min showed less than 0.01 percent carbon remaining. It is thus concluded that the ASTM C311 procedure is not only a highly effective way to remove charcoal-like carbon from fly ash, but that this can also be reliably accomplished by heating to only 500°C for a minimum exposure time of 240 min.

Carbonates

It is well known that fly ash contains carbonates, where carbon is 20 percent of the mass of the carbonate group (CO₃)²⁻. Although calcium carbonate CaCO₃ is a common constituent of coal and thus fly ash, approximately 60 carbonate minerals are known, but many are comparatively rare (Brown and Dykstra 1995, Deer et al., 1966). Table 5.1 lists five commonly occurring carbonates found in coal (Gluskoter et al. 1981). The source of calcium carbonate in fly ash can be the natural coal minerals fraction, or the finely divided limestone added to control sulfur emissions. Although this form of carbon does not further oxidize or otherwise “combust” or “ignite” in the LOI procedure, at sufficiently high temperatures, carbonate decomposes by releasing gaseous carbon dioxide as is shown by equation (5.1) for calcite.



The temperatures at which various carbonates decompose are shown in Table 5.1. The results of thermo gravimetric analyses of carbonates, primarily calcite, performed by several researchers are summarized by Duval (1963). In general, decomposition commencement temperature range was found to be dependent on sample mass (larger samples requiring higher temperatures to completely decompose) and atmosphere chemistry and flow rate.

Carbonates also decompose to CO₂ by reacting with acids at low temperature, forming a basis for distinguishing between so called “organic” and “inorganic” carbon (as described in Section 5.6.2). Even though carbon in the carbonate fraction contributes to the “total carbon” content of ash, it is not likely that this form of carbon that interacts with AEAs. Thus any influence of carbon from carbonates in the LOI procedure will impede interpretation of the results as a measure of AEA interaction, but fortunately, using alternate methods it is possible to identify the inorganic carbon and thus delete it from consideration as will be described.

The amount of carbonates which must be present in ash to influence the LOI test result is dependent on the required precision of the test. Calcination of calcium carbonate results in a 44 percent reduction of CaCO₃ mass. For ash samples with total LOI contents at or less than 1 percent, (such as the Texas ashes studied) ash CaCO₃ contents of 0.2 percent could contribute 10 percent or more to the LOI measurement. Brown and Dykstra (1995) estimated mass changes due to calcination of carbonates between zero and 2 percent (which contributed up to 90 percent of LOI content) based on thermo gravimetric analyses. Paya et al. (2002) showed carbonate decomposition contributing about 1 percent (roughly 50 percent of LOI) to mass losses in two ash samples.

Table 5.1: Decomposition commencement temperatures in air for carbonates found in coal (Gluskoter et al. 1981, Duval, 1963).

Name	Formula	Decomposition commencement temperature, °C
Calcite	CaCO ₃	600-675
Siderite	FeCO ₃	425
Dolomite	(Ca, Mg)CO ₃	450-600
Witherite	BaCO ₃	1085
Ankerite	(Ca, Fe, Mg)CO ₃	650

Organic carbon content versus temperature for fly ash samples

An experiment measuring the change in ash organic carbon content with temperature was described in Section 4.2.5.4. Experimental results are shown in Figure 5.7.

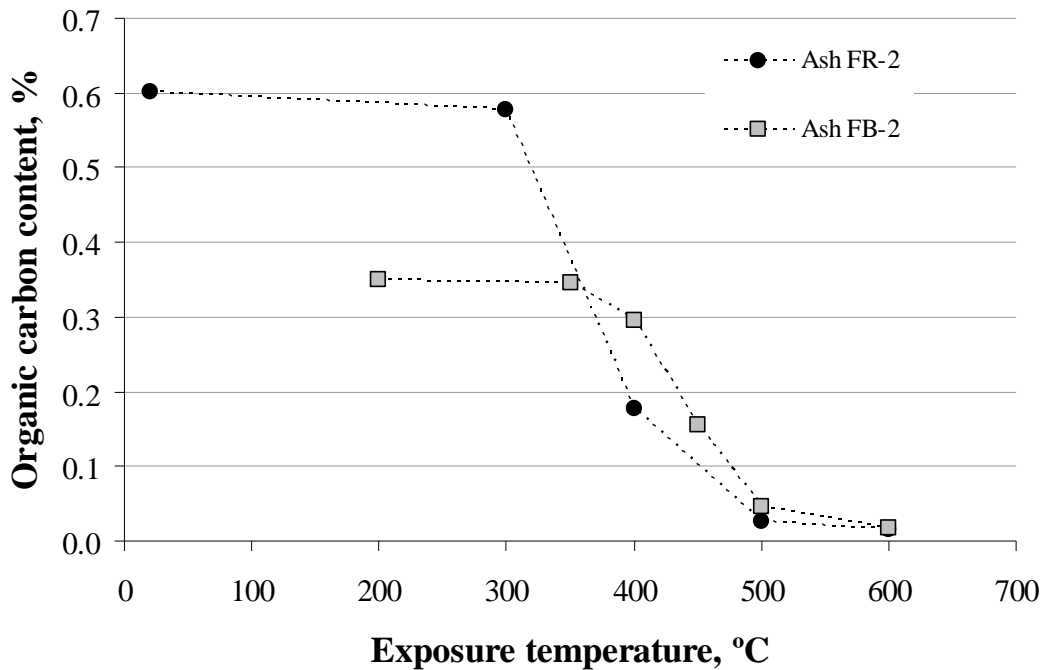


Figure 5.7: The organic carbon content of two ash samples after exposure to various temperatures in an air atmosphere

The results of the analysis of the change in organic carbon content of ash with temperature (Figure 5.7) shows that 86 percent (Ash FB-2) and 92 percent (Ash FR-2) of ash organic carbon content of the two ash samples is removed between 300 and 500°C. The organic carbon content of Ash FB-2 was reduced to 0.05 percent (approximately 13 percent of the organic carbon present at the beginning of the test) after exposure to 500°C. After exposure to 600°C, 0.02 percent carbon remains. For Ash FR-2, after exposure to 500°C, 0.03 percent carbon (approximately 4 percent of the organic carbon present in the as-received ash) remains. By 600°C, the remaining organic carbon is reduced to 0.02 percent.

Inorganic carbon measurements of the as-received ash showed less than 0.01 percent of carbon. Therefore, the organic carbon for the two fly ash samples studied was essentially equal to the total carbon content of the samples.

5.2.4 Non-carbon mass changes during the LOI test

In addition to the complication of multiple forms of carbon present in ash, other factors have been identified which influence LOI results. These other factors are the removal of non-carbon materials from ash and mass gains in ash during LOI testing.

Mineral dehydration

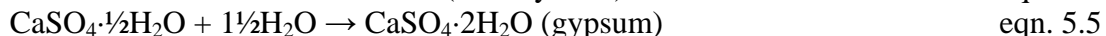
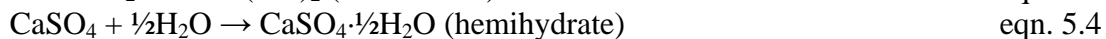
The dehydration (removal of chemically bound water that remains after oven-drying at temperatures near 100°C) of minerals, such as calcium hydroxide or gypsum, present in fly ash can occur at the temperatures of the LOI test and results in decreases in ash mass.

Calcium hydroxide or “slaked lime,” $\text{Ca}(\text{OH})_2$, and gypsum, $\text{CaSO}_4 \cdot 2\text{H}_2\text{O}$, can exist in the ash as a result of coal chemistry or as a result of emissions-control steps during combustion or downstream of the combustion chamber (Brown and Dykstra, 1995; Miller, 2005). In fluidized bed combustors (FBC) or limestone-injection, multi-burner (LIMB) systems, finely divided limestone (chiefly composed of calcite, though some dolomite (Ca , Mg) CO_3 may also be present) is added to the combustor. The limestone is calcined by the high temperatures resulting in the removal of gaseous carbon dioxide according to equation 5.1. The solid calcium oxide that remains after the initial reaction can combine with oxygen and sulfur dioxide (a pollutant formed as a byproduct of coal combustion) to form calcium sulfate anhydrite as described in equation (2).



Calcite, calcium oxide and calcium sulfate anhydrite particles can exit the combustion chamber and be collected with the fly ash in the particulate-controls systems of the power plant. In pulverized coal combustion units, an aqueous lime solution may be sprayed into the flue exit gases at some point downstream of the combustion chamber to control sulfur dioxide emissions (Miller, 2005). In this case only the reaction shown by equation 5.2 occurs.

Calcium oxide and calcium sulfate are hygroscopic materials and readily combine with water to form hydrated minerals. Calcium oxide combines with water, shown in equation 5.3, either from the atmosphere or in direct physical contact to produce calcium hydroxide, $\text{Ca}(\text{OH})_2$. Calcium sulfate anhydrite combines with water to first form calcium sulfate hemi-hydrate (or plaster of Paris) and then with more water to form gypsum as shown in equations 5.4 and 5.5. The reactions shown in equations (5.3) to (5.5) are exothermic.



When slaked lime, hemi-hydrate or gypsum is exposed to sufficiently high temperatures, the reverse reactions of equations (5.3 to 5.5) occur. The temperatures at which dehydration of these minerals commences are shown in Table 5.2. When the minerals are present in ash, dehydration occurs during the LOI test resulting in mass losses that are measured by the test.

Brown and Dykstra (1995) estimated mineral dehydration in seven ash samples contributed between 3 and 40 percent of the LOI measurement. Calcium hydroxide contents as low as 0.4 percent and gypsum contents as low as 0.5 percent could contribute to 10 percent or more of the LOI measurements of Texas fly ash samples.

Table 5.2: Dehydration temperatures of calcium hydroxide, calcium sulfate hemi-hydrate and gypsum (Duval 1963).

Mineral name	Formula	Dehydration temperature, °C
Slaked lime	Ca(OH) ₂	395-425
Hemi-hydrate	CaSO ₄ ·½H ₂ O	150-190
Gypsum	CaSO ₄ ·2H ₂ O	110-150

Other non-carbon losses

To explore mass changes with non-carbon compounds in ash, the author conducted a series of experiments in which samples were heated at discrete temperature intervals, measuring the change in mass after each interval. The typical procedure was to fill two weighed 10 mL porcelain crucibles with 2 g samples of laboratory grade alumina (Al₂O₃), laboratory grade iron oxide (Fe₂O₃) and silica flour (SiO₂). (Analysis of the silica flour by x-ray diffraction showed no minerals present other than quartz) Then the crucibles were transferred to a preheated furnace between 200 and 900°C and heated for 30 min. The crucibles were then removed from the furnace and placed in a desiccator to cool to near room temperature (typically 15 to 20 min). After cooling the samples were weighed and returned to the furnace which had been preheated to the subsequent temperature interval. Results are shown in Figure 5.8.

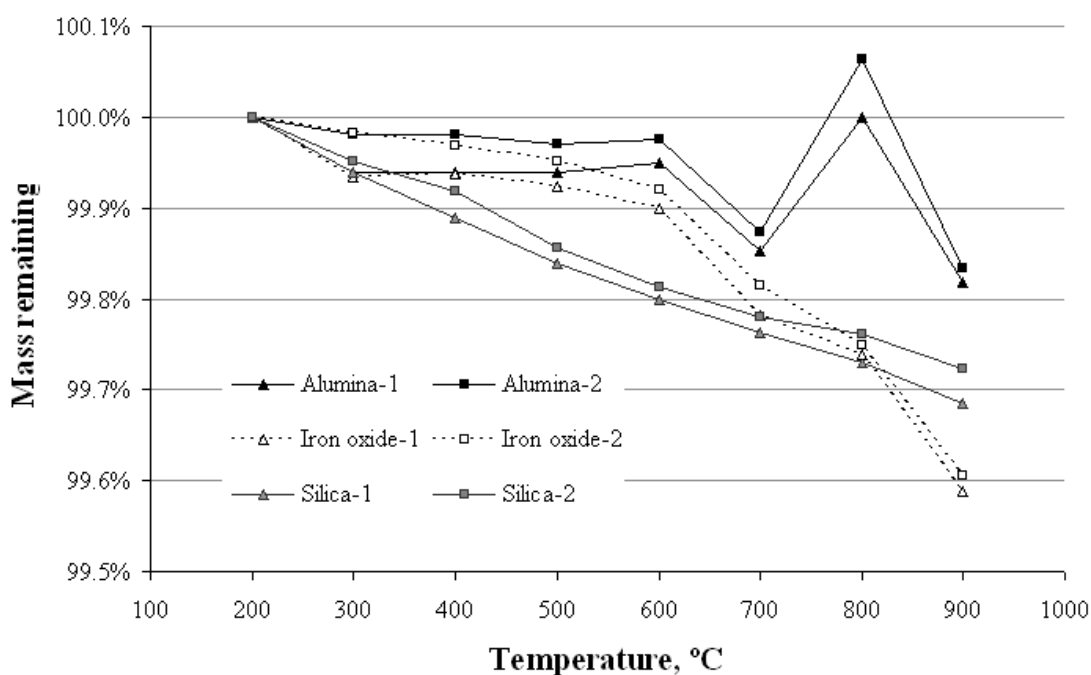


Figure 5.8: Change in mass with temperature of aluminum, iron and silicon oxides.

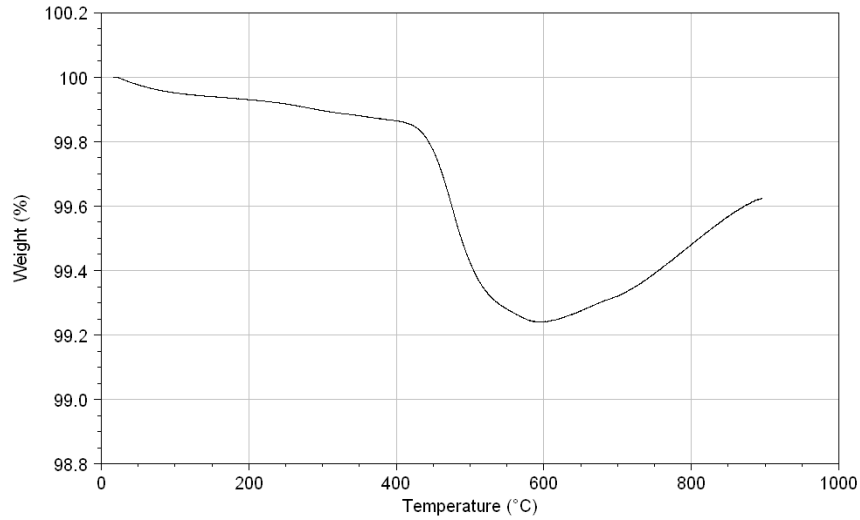
Mass changes in Figure 5.8 are calculated based on the mass at 200°C. At temperatures above 200°C, silica maintains a nearly constant mass loss rate, losing approximately 0.3 percent by 900°C. The aluminum and iron oxides are less uniform in behavior. The mass of alumina remains nearly constant between 300 and 600°C, with the interesting yet repeatable behavior shown between 600 and 900°C. Iron oxide experiences a slow decrease in mass between 200 and 500°C, and then transitions to a relatively high rate of mass loss between 600 C and 900°C.

The results of these experiments suggest that multiple common constituents of fly ash experience changes in mass over the temperature range of the standard LOI test. The significance of these mass changes will depend on the composition of the ash, and on the relative proportions of these constituents compared to various forms of carbon present. Though the losses in mass seen in the above experiment are relatively small (less than 0.5 percent mass lost by 900°C), such changes are of the same order of magnitude of the inferred carbon content of samples similar to the Texas ashes studied here.

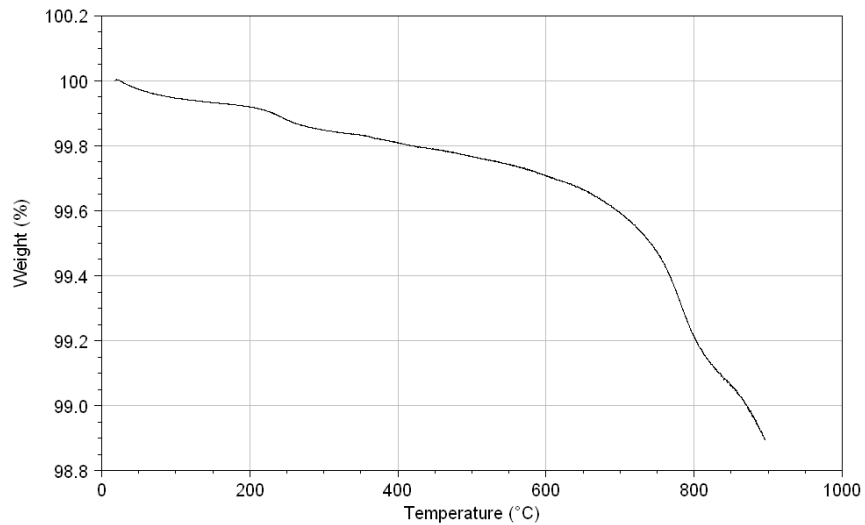
Observed mass gain during the LOI test

Texas fly ash sample FR-2 was subjected to Thermo Gravimetric Analysis (TGA) as described in Chapter 4 Section 4.2.3.3. The results of the analyses are shown in Figure 5.9. It is observed that at temperatures greater than 600°C, the ash sample gained mass in an air atmosphere. This behavior was again observed in Macro TGA tests (described in Section 4.2.5.1) of four fly ash samples shown in Figure 5.10. Additional testing showed that when the same ash sample was heated over the same temperature range in an inert (nitrogen) atmosphere, the sample did not gain mass (See Figure 5.9b).

Any mass increase that takes place during the LOI test will offset or mask the losses that the test is intended to identify. The apparent gain in mass in air and absence of this gain in nitrogen suggests that the mass gain shown here is related to oxidation of certain minerals in the ash (Hurt et al. 2001). The magnitude of mass gain is unique to each sample and is likely dependent on specific minerals present. No further study was made to identify the specific reactions that produce mass gains in ash, though some attention was given to a corresponding darkening of ash samples at temperatures greater than 700°C, as described in Chapter 7 on fly ash color analysis.



(a)



(b)

Figure 5.9: Thermo gravimetric analysis of sample FR-2 temperature ramp of 10°C per min under air (a) and nitrogen (b).

Mass losses and gains are not differentiated by the LOI test

Based on the above discussions, it is clear that multiple reactions can occur in ash during the LOI test, each occurring at different temperatures and at different reaction rates, independently resulting in either decreases or increases in sample mass. This is illustrated by the Macro TGA test results of four fly ash samples in Figure 5.10. The differences in mass changes between the samples reflect differing chemical and mineralogical compositions and certain ingredients that cause changes to the ash mass may be present in varying amounts or not present at all from sample to sample.

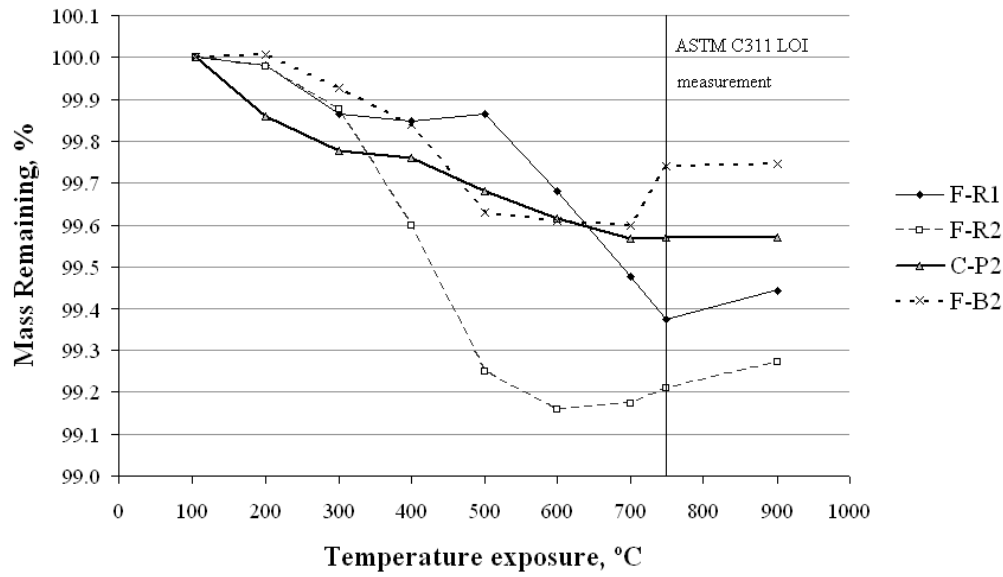


Figure 5.10: Fly ash sample mass remaining after 60 min of heating.

Identification of the sources of the changes in ash mass in Figure 5.10 is challenging based on the limited tools available for assessing ash composition; however, correlations between mass change in discrete temperature regimes and certain material properties were identified as shown in Table 5.3. Mass change between 105 and 300°C appears to correlate with Ca^{2+} concentration in solution (the test procedure is described in Section 4.2.2.2). A possible explanation for this correlation is that gypsum and/or calcium sulfate hemi-hydrate present in ash are 1) both dehydrated in the temperature range of 105 to 300°C and 2) are major contributors to the calcium ion concentration in aqueous ash solutions. Mass change between 300 to 500°C correlates with organic carbon measurements. The 300 to 500°C temperature range was shown in Figure 5.7 to be the range in which organic carbon removal was most prominent. This potential relationship is discussed further later. Mass change between 500 and 750°C correlates with the inorganic carbon measurements. This correlation suggests that a portion of the losses above 500°C may be due to carbonate calcination which occurs in the temperature range (Table 5.1).

Table 5.3: Mass loss (negative value indicates mass gain) in three temperature regimes, soluble calcium contents (units mg Ca²⁺/L), organic and inorganic carbon contents (both in units percent mass) for four fly ash samples.

Sample name	F-B2	F-R1	F-R2	C-P2
Temp range (°C)	Mass change, %			
105-300	0.07	0.13	0.12	0.22
300-500	0.30	0.00	0.63	0.10
500-750	-0.11	0.49	0.04	0.11
Soluble Ca (Ca ²⁺ mg/L)	134	157	150	170
Organic C (%)	0.38	0.02	0.72	0.04
Inorganic C (%)	0.01	0.21	0.00	0.03

It is possible that the correlations discussed above are coincidental and that other reaction besides or in addition to those shown are responsible for the behavior observed in Figure 5.10. Nevertheless, the example demonstrates that mass changes which occur due to individual reactions are not differentiated by the current LOI test protocol; instead the test only measures the net change in sample mass between oven drying (105°C) and 750 ± 50°C.

5.3 Summary comments on the utility of ASTM C311 as an indicator of carbon content in fly ash

While the ASTM C311 LOI standard does not claim to be a measurement of ash carbon content, the measurement made by the test is generally referred to in industry as the carbon content. Assessment of what is truly included in the test measurement has shown the test to be influenced by forms of organic carbon, inorganic carbon, non-carbon materials, and other issues.

5.3.1 Issues related to organic carbon

Among the changes in mass detected in the LOI is the associated with the devolatilization or oxidation of organic carbon constituents. Organic carbon can be present in ash in several forms including volatile organic compounds, soot and carbon char.

Volatile organic compounds

Volatile organic compounds are hypothesized to be present in fly ash due to the condensation of non-combusted volatile matter on the fly ash particles after passing from the combustion chamber. It has been shown that VOCs can be removed from fly ash during the LOI test, and the resulting change in ash mass is measured in the test. VOCs have been shown to contribute anywhere from zero to 97 percent of total LOI mass change (Fan and Brown, 2001).

Soot

Soot can be present in ash due to the incomplete combustion of carbonaceous materials in the combustion chamber. Based on the relatively slow rate of oxidation (relative to other forms of organic carbon such as carbon char) under LOI conditions, it is likely the LOI test does not accurately indicate carbon content in the form of soot.

Carbon char

Carbon char can be present in ash due to incomplete combustion of the parent coal. It has been hypothesized by some researchers that carbon char is the primary carbon form in ash influencing interactions between fly ash and AEAs. It is estimated that carbon char may compose between 3 and 97 percent (Fan and Brown, 2001) of the carbon in ash. Oxidation of carbon char was shown to occur at 500°C and is therefore likely removed from ash by the standard LOI test.

5.3.2 Issues related to inorganic carbon

Inorganic carbon in the form of carbonates can be present in fly ash. Some carbonate forms are calcined at the temperature of the standard LOI test and the resulting mass loss is measured with the other mass altering reactions of the test.

5.3.3 Issues related to non-carbon constituents in fly ash

The non carbon materials calcium hydroxide, calcium sulfate hemi-hydrate and gypsum which can be present in ash, may dehydrate under LOI test conditions. The loss of water may contribute to the LOI measurement. Oxides of silicon, aluminum and iron (common components in ash, See Chapter 4 Section 4.2.2.1) showed mass losses of between 0.1 and 0.3 percent when exposed to LOI test conditions. Though small, the mass changes are of the same order of magnitude as Texas ash LOI losses. Mass gains were shown to occur in ash samples FB-2 and FR-2 (Figure 5.10) at temperatures above 600°C. Mass gains could mask some of the mass losses that the test is intended to identify.

5.3.4 Utility of the LOI test as a measurement of carbon

The standard LOI test can measure the contributions of several reactions to mass change. The reactions include various forms of carbon removal as well as mass losses and gains due to reactions in non-carbon materials. The contributions of the various reactions to change in mass cannot be individually distinguished by the test. Therefore, interpreting LOI measurements as carbon content may not be accurate for all ashes and applications.

5.3.5 The need for improvement

It is clear then that there is room for improvement. Based on the discussion and experimental results presented thus far in this chapter, a modification of the C311 LOI test is proposed as presented in the following sections.

5.4 Towards the development of a modified LOI procedure

5.4.1 General

With the modifications already proposed by Harris (2006) coupled with the suggestions included at the end of this chapter, the LOI procedure itself can be made repeatable and sufficiently precise for the required measurements. Since the method is in general use and has been for many years, and is a standard feature of quality control programs for cementitious materials in general, it is desirable to modify the current test rather than to create a new method, if such can be done effectively. The challenge, then, is to modify the test so that the results more reliably indicate the presence of carbon in whatever form, or the presence of whatever constituent in fly ash that interferes the ability of an AEA to stabilize air bubbles in fresh concrete. In reviewing the background literature and experiments presented thus far in this chapter, it appears that modifying the test so that it specifically estimates organic carbon content may be a productive starting point. Further, the experimental results shown in Figure 5.10 suggest that the key to estimating organic carbon may be modifying the furnace temperatures at which mass loss is recorded. In particular, it is proposed that the ASTM C311 test be modified so that mass loss is recorded after 60 minutes exposure to temperatures of 300°C, 500°C, and 750°C, as will be explained in detail

5.4.2 Rationale for the modified test temperature range

The use of the 300 to 500°C range in the modified LOI test is based on studies of charcoal oxidation and fly ash total organic carbon content reported in Sections 5.2.3.3 and 5.2.3.5. It was determined that the non-mineral fraction of charcoal, including all organic carbon, could be removed by exposing charcoal to 500°C in air. Similarly, total organic carbon content of heat-treated fly ash was shown to be at least 85 percent removed by exposure to temperatures between 300 and 500°C for 30 min at each temperature interval (300, 400 and 500°C).

The experimental results shown in Figure 5.5 may lead to the incorrect conclusion that temperatures higher than 500°C and up to 900°C are required for complete removal of the non-mineral fraction in charcoal; however, the results of the experiment shown in Figure 5.6 suggest that temperatures greater than 500°C are unnecessary for the complete removal of organic carbon. The reason why the material was not completely removed at 500°C (after 30 min) in the former experiment is that insufficient time was available for the reactions to occur completely. Figure 5.6 shows that about 220 min were required for complete removal of the organic carbon.

Based on the results of the experiments performed on the oxidation of pulverized charcoal, it can be concluded that complete removal of the organic carbon fraction of 1 g of charcoal can occur at 500°C in 220 min for the test conditions used.

Removal of organic carbon in fly ash was shown to be sensitive to exposure temperature (test results shown in Figure 5.7). In general terms, for both ash samples FR-2 and FB-2, rapid organic carbon loss did not occur until a minimum temperature threshold was reached. For Ash FR-2, organic carbon content changed from 0.60 percent to 0.58 percent between room temperature and 300°C. After exposure to 400°C and then 500°C, the organic carbon content decreased relatively rapidly to 0.03 percent. For Ash FB-2, organic carbon content remained constant until 350°C, and then decreased relatively rapidly up to 500°C. At 600°C, further losses of 0.01 to 0.03 percent were observed in the samples. The change in organic carbon content between 300 and 500°C represents 86 percent of the total organic carbon content of Ash FB-2 and 92 percent of the organic carbon content of Ash FR-2 before heating.

The proposed modification to the LOI test postulates that the mass loss that occurs in the ash between 300 and 500°C is an estimate of the organic carbon content of the ash. Table 5.4 shows that mass losses in temperature range of 300-500°C are similar to the organic carbon contents in the same range. Table 5.4 also shows that mass losses between 105-300°C and 500-600°C generally differ from the organic carbon content losses. A possible reason for the differences between mass loss and organic carbon loss in the 105-300°C range is the presence of minerals that dehydrate at the same temperature interval. As shown previously, dehydration produces mass losses that are not related to organic carbon. The presence of inorganic carbon is not a possible explanation for the differences between mass loss and organic carbon loss in the 500-600°C for ash FR-2 since the inorganic carbon content of the ash was shown to be less than 0.01 percent. However a possible explanation for the difference could be mineral oxide decomposition suggested by Figure 5.8.

Based on Table 5.4, mass change that occurs in the range of 300 to 500°C appears to be primarily due to the change in organic carbon content. Changes in mass that occur outside of 300 to 500°C range may be influenced by reactions that are not the result of organic carbon removal. For this reason, use of the mass change in ash between 300 to 500°C was studied as a proposed estimate of the organic carbon content in ash.

It was concluded based on the experiment in which charcoal was heated to 500°C, that time of exposure was crucial to removing the organic carbon content. This conclusion was applied to the ash samples by increasing exposure time in the furnace. The differences in mass change and organic carbon content were shown to decrease when exposure time for the ash samples in the furnace was increased from 30 min to 60 min as shown in Table 5.5. Exposure beyond 60 min did not cause further mass change in the two samples.

Table 5.4: Comparison of percent mass change to percent organic carbon content change in three temperature regimes for two ash samples.

Temperature range, °C	Ash FB-2		Ash FR-2	
	Mass loss, %	Organic carbon content loss, %	Mass loss, %	Organic carbon content loss, %
105-300	0.07	0.00	0.12	0.02
300-500	0.30	0.30	0.63	0.55
500-600	0.02	0.03	0.09	0.01

Table 5.5: Comparison of ash percent mass change between 300 and 500°C due to 60 min exposure and total organic carbon content.

Mass change between 300 and 500°C, %					
Ash Sample	Total organic carbon content ¹ , %	30 min exposure		60 min exposure	
		Mass Loss	% Organic Carbon Removed	Mass Loss	% Organic Carbon Removed
FB-2	0.38	0.30	79%	0.35	92%
FR-2	0.72	0.63	88%	0.70	97%

1. As measured by Total Carbon Analyzer

Based on this information, the proposed modification to the LOI test is that the organic carbon content of ash could be estimated by measuring the mass loss in which occurs between heating the ash to 300°C for 60 min and the heating the ash to 500°C for 60 min. The proposed modification thus balances the uncertainty in total carbon removal against the uncertainty of non-carbon mass losses. The details of the modified test are given below.

5.4.3 The modified LOI test

The modified LOI test focuses on the narrow temperature range in which greater than 92 percent of organic carbon oxidation occurs by recording mass lost between the temperatures of 300 and 500°C, and reporting the resulting percentage of the oven-dried mass as “estimated organic carbon.” Mass is also recorded at 750°C and the resulting percentage of the oven-dried mass reported conventionally as “Loss on Ignition.” Thus the only difference in the modified test is that the operator stops the test at 300°C, takes a measurement, and then continues to 500°C, takes a second measurement and then continues on to 750°C. It is therefore not an alternative test, but is a way to get additional and often very useful data from the current test.

5.4.4 Proposed Procedure

The following test procedure is a modification of the ASTM C311 loss on ignition test standard. Additional advice and procedural details are found in Section 5.7.

Test Apparatus

- 10 mL Porcelain crucibles
- Scale, accuracy to 0.0001 g
- Air atmosphere furnace
- Weighing paper
- Spatula
- Metal tongs

Test Procedure

1. Clean crucibles with detergent and water. Rinse with distilled water and dry.
2. Prepare a data sheet similar to the example shown in Table 5.6.
3. Preheat oven to 105°C.
4. Using metal tongs, place crucibles on clean or covered countertop.
5. Weigh each crucible on a scale accurate to 0.0001 g. Record crucible mass, M_c .
6. For each ash sample, transfer approximately 0.9-1.1 g ash with a spatula onto a piece of weighing paper and pour ash from weighing paper into empty crucible. When switching to a new ash sample, wipe spatula clean to avoid sample contamination.
7. Weigh crucible and ash and record value, M_{c+a} .
8. Place crucibles in 105° C oven and dry sample for at least 12 hours.
9. Remove crucibles from oven and place in desiccator. Cool to room temperature (approximately 15-20 min depending on number of crucibles).
10. Place uncovered crucibles in preheated 300°C furnace and heat for 60 min.
11. Remove crucibles from furnace and place in desiccator. Cool to room temperature (approximately 15-20 min) and weigh, M_{300} .
12. Repeat steps 10 through 12 for furnace temperature of 500°C and record M_{500} .
13. Repeat steps 10 through 12 for furnace temperature of 750°C and record M_{750} .
14. Calculate moisture content:
15. Calculate modified loss on ignition:
16. Calculate standard loss on ignition: 105 to 750.
17. Dispose of ash and clean crucibles.

Table 5.6: Sample modified loss on ignition data sheet.

	Ash name	Cruc ID #	M_c (grams)	M_{c+a} (grams)	M_{105} (grams)	M_{300} (grams)	M_{500} (grams)	M_{750} (grams)	Moisture Content %	LOI _{mod} %
1										
2										

5.5 Experimental trials of the Modified LOI test to evaluate fly ash

Comparisons of the results of the standard LOI tests, modified LOI tests and total organic carbon analyses on the set of Texas fly ashes are presented in Figures 5.11 through 5.13 (the values for each ash are given in Chapter 4 Section 4.2.3.1). Figure 5.11 shows the standard LOI results of nine Class F and seven Class C Texas ashes compared to the corresponding modified LOI values. For all but four of the ash samples (Ashes FB-2, FM-1, FM-2, and FT-1) the standard LOI contents are greater than the modified LOI contents.

Figure 5.12 shows the standard LOI results of the ashes in comparison to the corresponding organic carbon contents. Similar to the comparison shown in Figure 5.11, the results of the standard LOI tests are greater than the organic carbon contents for all ashes except FB-2, FM-1, FT-1, CG-2 (CG-1 and FM-2 show about 0.1 percent difference which is within one standard deviation of test variability described below).

Figure 5.13 compares the modified LOI content of the ashes to the corresponding organic carbon contents. For all but three of the samples (Ashes FM-2, FR-1, CP-2), the modified LOI values are less than the organic carbon values. Linear regression analysis consisting only of the Class F ash samples in which the modified loss on ignition is the dependent y-variable and organic carbon content is the independent x-variable produces a correlation having an R^2 value of 0.97, adjusted R^2 value of 0.96 and standard error of the estimate equal to 0.04 percent. When the Class C ash samples are included in the regression, R^2 reduces to 0.90, adjusted R^2 becomes 0.89 and the standard error of the estimate increases to 0.06 percent. This observation suggests that some characteristic common to the Class C samples may be influencing one or both of the measurements.

Each modified LOI test value plotted in Figures 5.11 and 5.13 is the average of two tests. The difference in test values is a measure of the repeatability of the test. For the sixteen samples tested the mean difference between the sample pair modified LOI values were 0.0 percent, the maximum and minimum differences were 0.3 and -0.2 percent, and the standard deviation was 0.014 percent. This level of repeatability was common for the furnace, ash samples and test protocol used in this study. Potential sources of variability in the test are discussed in Section 5.7.

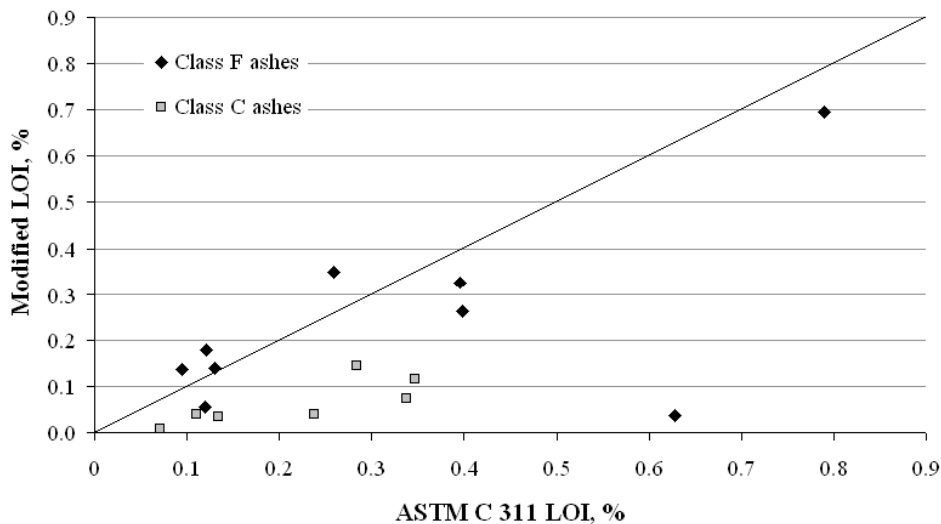


Figure 5.11: Modified loss on ignition values versus ASTM C 311 loss on ignition values (compared against the line $x = y$).

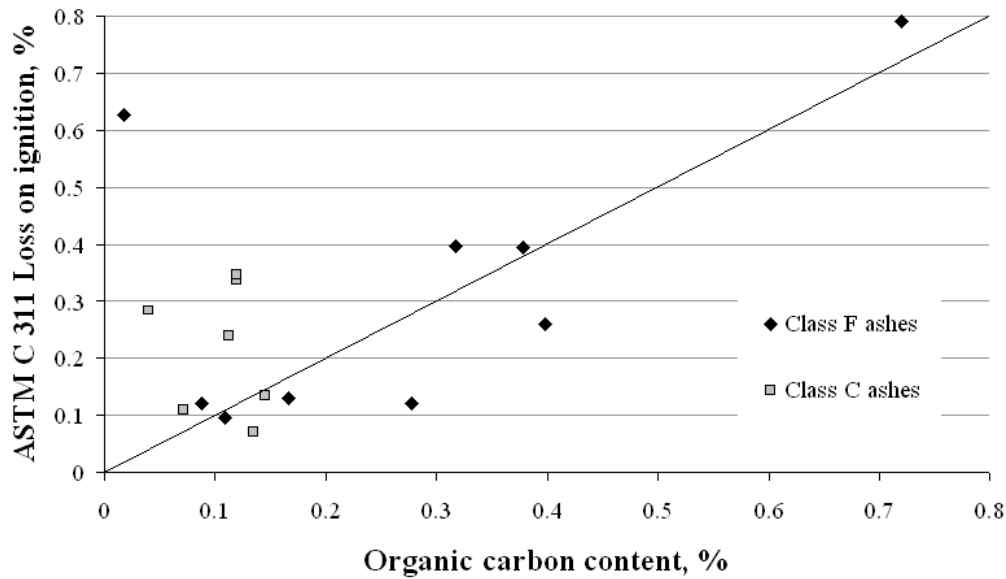


Figure 5.12: ASTM C 311 loss on ignition values versus organic carbon content of Texas commercial fly ash samples (compared against the line $x = y$).

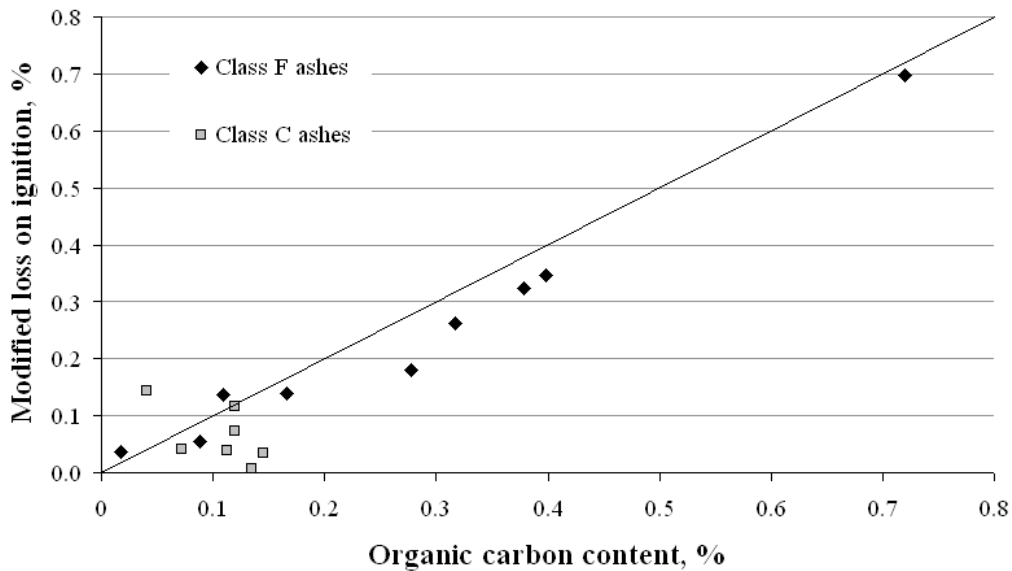


Figure 5.13: Modified loss on ignition versus total organic carbon content of Texas commercial fly ash samples (compared against the line $x = y$).

5.5.2 Regression analysis of standard LOI values and chemical properties

Multi-linear regression was used to identify relationships between standard LOI values and the following chemical properties: organic carbon content, inorganic carbon content, soluble calcium ion concentration, calcium oxide content and sulfate content. Calcium ion concentration (Chapter 4 Section 4.2.2.2) and calcium oxide content (Chapter 4 Section 4.2.2.1) were included

because of the possibility that gypsum, calcium sulfate hemi-hydrate or calcium hydroxide could play a part in mass loss due to dehydration. Sulfate content (Chapter 4 Section 4.2.2.1) was also included as a possible link to the forms of calcium sulfate.

The regression produced R^2 and adjusted R^2 values of 0.83 and 0.75 respectively. The analysis showed that of the chemical properties analyzed, only the contributions from inorganic carbon and organic carbon contents were statistically significant. These results do not necessarily imply that gypsum, calcium sulfate hemi-hydrate or calcium hydroxide do not influence LOI measurements; instead, it is possible that soluble calcium ion concentration, calcium oxide content and sulfate content are not accurate predictors of the gypsum, calcium sulfate hemi-hydrate or calcium hydroxide contents in ash. The analysis suggests that inorganic carbon content can make a major contribution to the LOI measurement of the ash.

5.5.3 Regression analysis of modified LOI values and chemical properties

Multi-linear regression was used to identify relationships between modified LOI values and the following chemical properties used in the previously described regression analysis: organic carbon content, inorganic carbon content, soluble calcium ion concentration, calcium oxide content and sulfate content. Regression analysis showed no statistically significant relationship between modified LOI values and inorganic carbon content or soluble calcium ion concentration; however, regression analysis did suggest contributions from calcium oxide and sulfate contents (R^2 equal to 0.94, adjusted R^2 equal to 0.92 and standard error equal to 0.05 percent). This result suggests that materials other than organic carbon present in ash such as calcium contain minerals and/or sulfate containing minerals (gypsum and calcium sulfate hemi-hydrate contain both) may be influencing the modified LOI results.

5.6 Discussion

5.6.1 Mass loss in standard LOI is greater than modified LOI and organic carbon content

Figure 5.11 shows that the mass losses which occur in the standard LOI test are typically greater than the losses measured by the modified LOI test (though four samples show comparatively lower LOI losses). This result is expected since the wider temperature range used in the standard LOI test includes the mass losses that may occur at temperatures between 105 and 300°C and between 500 and 750°C that are not included in the modified LOI test.

Based on Figure 5.12, it was observed that the standard LOI test tended to overestimate the organic carbon content of the ash samples. This result is also expected since the standard LOI test may also measure the losses due to sources other than organic carbon which were discussed in Section 5.2. For example, all of the class C ashes and some of the Class F ashes contained measurable amounts of inorganic carbon ranging from 0.03 percent to 0.2 percent. The regression analysis on ash standard LOI and chemical properties discussed in Section 5.5.1 indicated that inorganic carbon in the ash samples was a statistically significant contributor to the LOI measurement. The regression analysis, however, suggests that organic and inorganic carbon did not account for all of the LOI measurement; therefore, other materials are also contributing. While calcium- and sulfate-containing minerals could not be linked to the LOI measurement based on the regression analysis, other sources of mass loss such as mineral oxide decomposition (Section 5.2.4.3) may play a role.

As shown in Figures 5.9 and 5.10, and discussed in Section 5.2.4.3, mass gains can occur in fly ash samples at temperatures above approximately 600°C. Such gains in mass may be responsible for the samples which showed LOI losses lower than the corresponding modified LOI losses. This situation would occur when a portion of mass losses which occur in the 300 to 500°C temperature range are replaced by mass gains in the 700 to 800°C temperature range of the standard test. The result would be a net lower mass loss in the standard test. Regression analysis performed to identify common chemical properties in the samples which had higher modified LOI contents than standard LOI contents were inconclusive. The limited number of samples (only four qualified) possibly contributed to the difficulty in identifying statistically significant relationships.

5.6.2 Mass loss by modified LOI typically less than total organic carbon content

As shown in Figure 5.13, the modified LOI test typically underestimates the organic carbon content of both the Class C and Class F ash samples by about 0.03 percent. This may be due to 1) unrecorded loss of organic carbon at less than 300°C, 2) residual organic carbon that had not been removed at 500°C (but was removed at 900°C by the TOC analyzer) or 3) an overestimated organic carbon content by the TOC analyzer. With regard to the first two possibilities, it could be argued that the temperature range of the modified LOI test could be expanded to less than 300°C and/or greater than 500°C to include a greater contribution of organic carbon. This argument was explored with the following experiment.

Due to the possibility that some organic carbon could be removed at temperatures below 300°C, the modified LOI test was performed using seven ash samples (Ashes FB-1, FB-2, FC-1, FL-1, FM-1, FR-1 and FR-2) and mass change was measured at 250, 300, 350, 400 and 500°C. The change in mass of the seven samples which occurred in the temperature range beginning with one of each of the four temperatures between 250 and 400°C and ending at 500°C was compared to the organic carbon contents of the ashes. Test results are shown in Figure 5.14 and linear regression statistics of the four test ranges are shown in Table 5.7.

Figure 5.14 generally shows that increasing the temperature range of the test increases the measured mass loss in that range. When the starting temperature is moved from 300 to 250°C, the mass changes increase; however, the regression statistics show a less favorable correlation with organic carbon content (based on a decreasing R^2 and increasing standard error). This result suggests that increasing the temperature range of the modified LOI test runs the risk of measuring the contributions of material other than organic carbon which and may explain the worsening of the correlation for mass loss between 250 and 500°C in comparison to mass loss between 300 and 500°C. Because the properties of the ash samples vary, it is possible that the optimal temperature ranges for measuring organic carbon content may also vary from ash to ash. Nevertheless, based on the results of the experiment, an initial temperature of 300°C appears to produce the most accurate results (though there is a possibility that some temperature in the range of 250 to 350 other than 300°C may prove to be an optimum temperature for the ash samples studied).

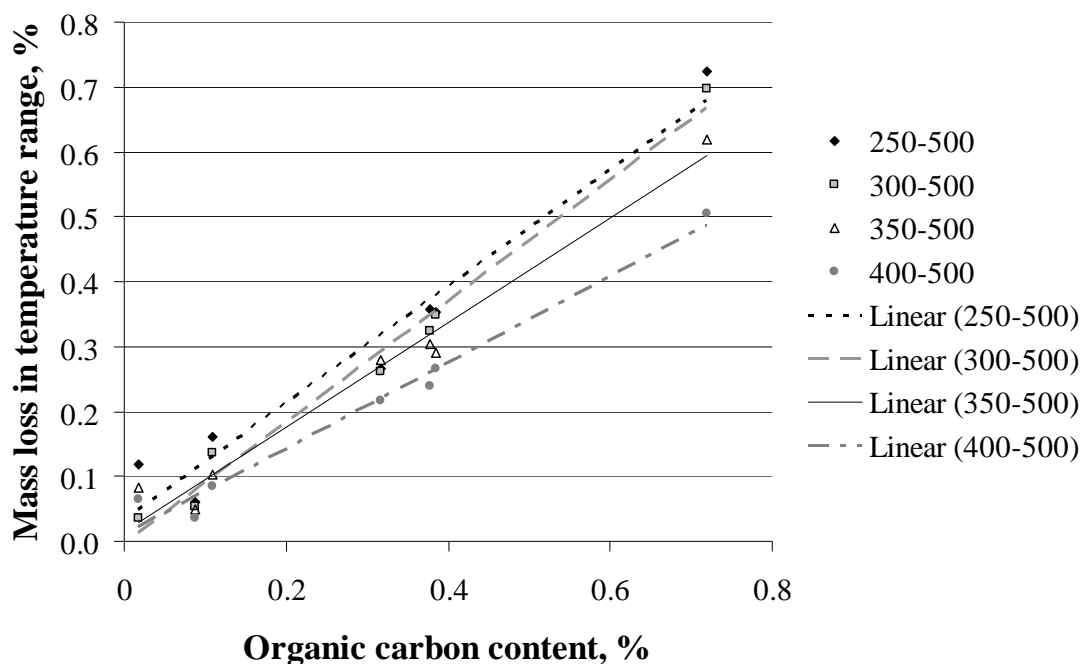


Figure 5.14: Mass loss in four separate temperature ranges for seven ash samples.

Table 5.7: Linear regression statistics of the trend lines in Figure 5.14.

Temperature range, °C	R ²	slope	y-intercept	Standard error, %
250-500	0.95	0.90	0.03	0.05
300-500	0.98	0.93	0.00	0.03
350-500	0.97	0.80	0.02	0.04
400-500	0.98	0.66	0.01	0.03

The seven samples used in the test reported in Figure 5.14 were measured for organic carbon content after 60 min of exposure to 500°C. The average organic carbon content of the seven samples was 0.01 percent with no sample having greater than 0.02 percent. Based on these results, it is most probable that the underestimate of the organic carbon content by the modified LOI is not due to incomplete removal of organic carbon by 500°C.

Inorganic carbon measurement using the solid sample module of the TOC may underestimate the amount of inorganic carbon in fly ash samples. This is due to the method in which the inorganic carbon is measured. As discussed in Chapter 3 Section 3.2.3.2, inorganic carbon content of ash is measured by immersing the sample in phosphoric acid to decompose the carbonates. The carbon dioxide produced as a byproduct of the reaction is then measured by the TOC. Though the phosphoric acid is diluted to 33 percent, the solution is still relatively viscous

and complete submergence and wetting of the sample in the acid can be difficult. The amount of acid that can be placed in the sample is limited by the testing apparatus. Decreasing the ash sample size is possible; however, because the inorganic carbon content of the samples is very low, less than 0.05 percent, decreasing the sample size less than 0.5g causes the measurement of the inorganic carbon to become lost in the background noise of the device. The result is that if the inorganic carbon content measurement of an ash is lower than the true value, then organic carbon content will then be over-estimated.

5.6.3 Modified LOI a more reliable measurement of organic carbon content than standard LOI

As shown by Figures 5.12 and 5.13, the modified LOI test provided a more statistically reliable measurement of the organic carbon content of fly ash than did the ASTM C 311 LOI test for the ash samples studied. Linear regression of the modified LOI and organic carbon data on all ash samples irrespective of class shown in Figure 5.13 produces R^2 and adjusted R^2 values of 0.90 and 0.89 respectively and a standard error of 0.06 percent.

Regression on the standard ASTM and organic carbon data Figure 5.12 produces an R^2 value of only 0.29. The results of Figure 5.13 suggest that the modified test is a useful a measure of organic carbon for all of the Texas ashes studied.

Reactions that can occur in the 300 to 500°C temperature range other than carbon oxidation do not appear to play significant roles. One reaction in particular, the dehydration of calcium hydroxide, begins between 300 and 400°C as shown in Table 5.2. It is possible that calcium hydroxide was a factor in the three ash samples shown plotted above the diagonal line in Figure 5.13, since a reaction such as calcium hydroxide dehydration would increase the modified LOI content. Mass losses, other than carbon oxidation, that occur in the 300 to 500°C range could be assessed by heating the samples in an inert atmosphere. It is noted however, that volatile organics may be lost at temperatures lower than 300C, and soot may not yet be removed at 500C, so ashes with significant VOC or soot contents may not be good candidates for evaluation by modified LOI.

5.6.4 Modified LOI a better predictor of organic carbon in Class F ashes than C ashes

As shown in Figure 5.13, the relationship between modified LOI results and organic carbon content is clearer for Class F ash samples than Class C ash samples. Linear regression of the test values from Figure 5.13 for the Class F ash samples produces R^2 and adjusted R^2 values of 0.97 and 0.96 respectively and a standard error of 0.04 percent. A similarly strong correlation could not be established for the Class C ashes. The difference may be due in part to the lack of sufficient samples with varying organic carbon content. One possible explanation for the greater errors is the difficulty in measuring inorganic carbon in fly ash which was discussed in Section 5.6.2. It was found that the Class C ashes typically had greater inorganic carbon contents than the Class F ashes used in this study. More accurate measurement of the inorganic carbon in the ash would aid in identifying the source of the errors.

5.6.5 Properties of ash measured by total organic carbon analysis

Total organic carbon measurement of fly ash may potentially include various forms of organic coal residuals such as coal char, VOCs, soot that is oxidized at 900°C and any other source of organic carbon not identified in this work. The Texas fly ash samples tested are not

considered to have significant VOC contents since the properties associated with the presence of VOCs in ash described by Fan and Brown (2001) were not observed on the ash samples. This conclusion was supported by a simple qualitative test for identifying the presence of VOCs in ash proposed by Fan and Brown (2001). The test was performed by placing 1 g samples of ash in 15 mL of organic solvent (benzene was used by Fan and Brown, toluene was used here). The samples were heated at 60°C for 10 min, then cooled for 30 min. The fly ash was separated from the solvent by filtration. The presence of organic residue darkens the solvent to varying shades of black depending on the amount of VOCs present. None of the ash samples studied produced discernible darkening of the solvent.

Gao et al. (1997) suggested that soot is typically only found in trace amount in fly ash and is not likely to significantly influence carbon content or fly ash-AEA interactions. The presence of soot in the Texas fly ash samples could not be determined based on the analysis used in this study.

5.6.6 Benefits of the modified test

The development of the modified LOI test has provided the following benefits:

- The modified LOI test provides a clearer definition of the properties of ash being measured than the standard LOI test. Because the standard LOI test incorporates contributions from several potential reactions that cannot be resolved by the test, the comparison of LOI values between differing ashes has little value. The modified LOI test is a more refined estimation of organic carbon content.
- The modified LOI test may be applicable to other fields where the organic carbon content of finely divided solids is desired.

The results of the modified LOI test correlate with other measures of fly ash-AEA interaction better than the results of the standard LOI test. The difference in correlations can be observed by comparing Figure 5.15 (concrete AEA dosage data versus the modified LOI values) and Figure 5.16 (correlation between concrete dosage and standard LOI). This observation provides strong support to the notion that carbon mass, defined as total organic carbon, is a major factor in the fly ash-AEA problem.

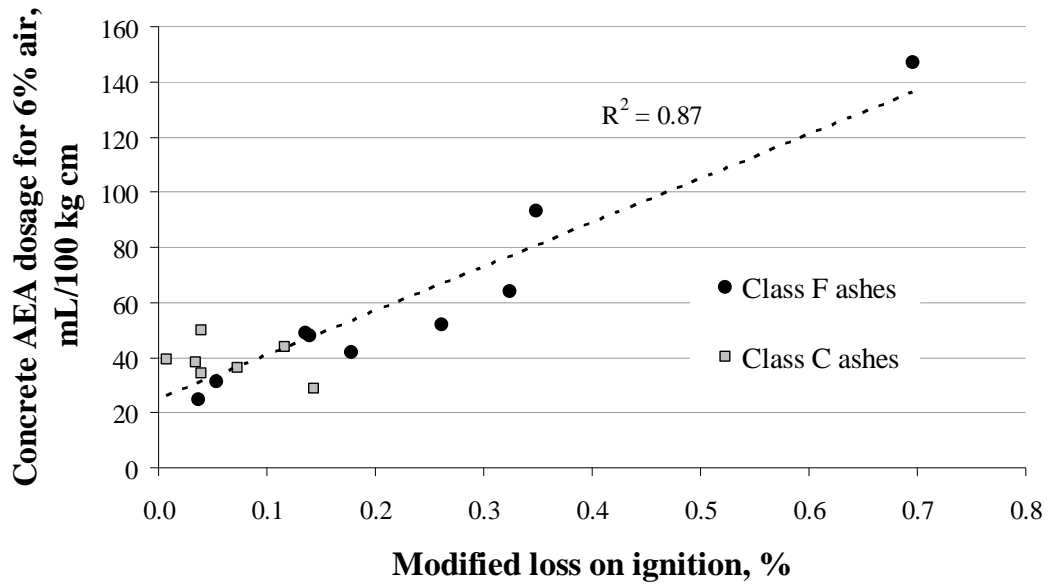


Figure 5.15: Concrete AEA dosages for 6% air versus modified loss on ignition values of sixteen Texas ash samples.

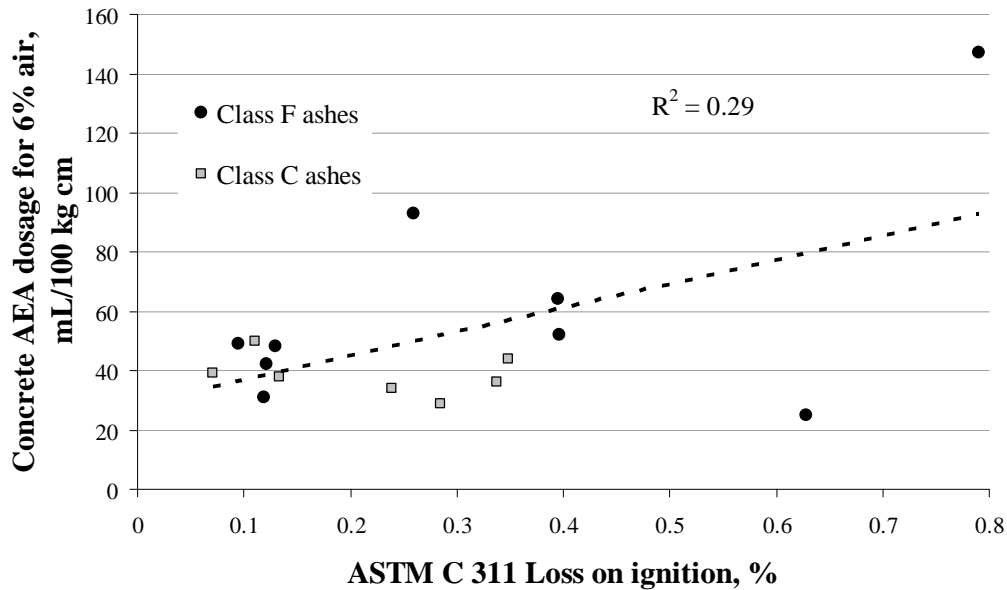


Figure 5.16: AEA dosages for fly ash concrete versus ASTM C311 loss on ignition.

5.6.7 Difference between standard LOI and modified LOI

The difference between standard LOI and modified LOI values is an approximation of the net mass changes that occur due to reactions other than organic carbon oxidation. It can be helpful to consider the modified LOI test as one of three specific regions of interest within the 105 to 750°C temperature range of standard LOI test, i.e., 105-300, 300-500 and 500-750°C.

Mass losses in the 300 to 500°C division were shown to correlate with organic carbon content. The losses in the remaining temperature divisions were studied to identify if correlations with other ash properties could be established.

Figure 5.17 compares the general differences in mass loss between Class F and C ashes in the three temperature divisions (negative mass loss indicates mass gain). For all three temperature divisions, the Class F samples show greater variability in mass change (relative to the Class C ashes) as indicated by the spread in the data points. Class C samples show comparatively little variability in the three temperature divisions, with mass loss in each temperature division between approximately 0 and 0.15 percent. In the 105 to 300°C division, mass changes are similar between the two ash classes. In the 300 to 500°C division, mass changes in the Class F ashes reflect the greater variety in organic carbon content relative to Class C ashes. In the 500-750°C division, again greater variation is observed in the Class F ash samples with five samples showing net mass gains and four samples showing net mass losses. Virtually none of the Class C ash samples show net mass gain in the 500 to 750°C division. One must refrain from generalizing relative to ash type, however, as the specific collection of Type C ashes available for this study may be unusually uniform.

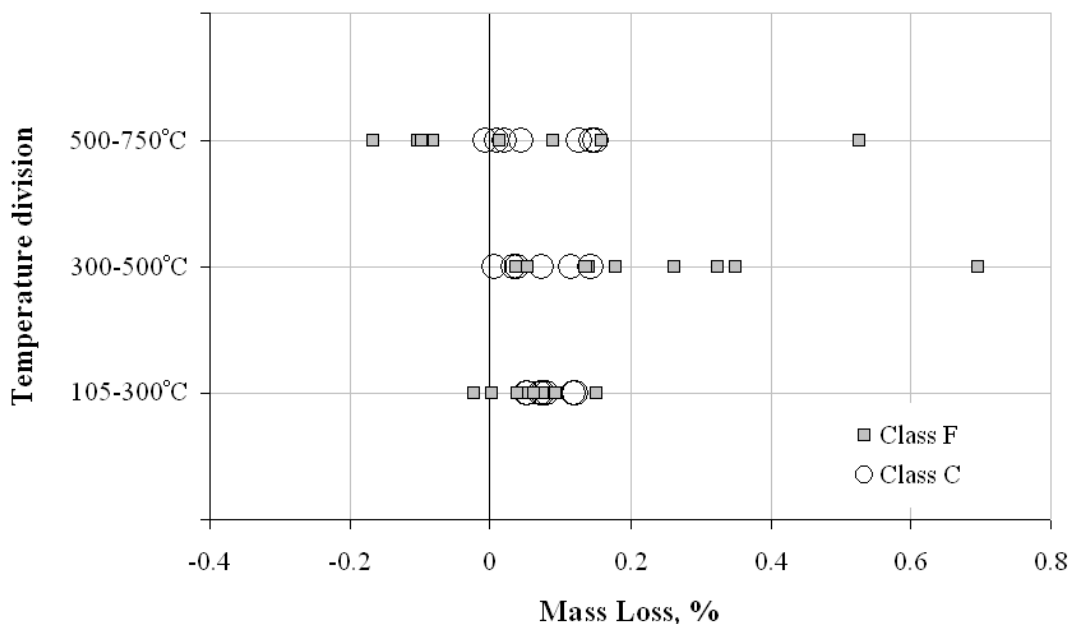


Figure 5.17: Comparison of mass changes of the two ash classes in three temperature divisions.

Further analysis was done using multi-linear regression to identify correlations between the temperature divisions and the ash material properties like bulk chemistry oxides content, soluble calcium and inorganic carbon content. No statistically significant correlations were established for the 105-300°C division. No contributions from factors other than organic carbon to mass changes in the 300 to 500°C division were identified. The 500-750°C division correlated (R^2 and adjusted R^2 equal to 0.92 and 0.88) with inorganic carbon and the presence of the oxides of iron, calcium, silicon and potassium. The regression analysis results are shown in Table 5.8. The parameter estimate for inorganic carbon is a positive value suggesting that inorganic carbon

plays a role in mass loss (mass losses are indicated by positive values, and mass gains are indicated by negative values consistent with standard LOI value reporting). This result is expected since carbonate decomposition can occur in the 500 to 750°C temperature range (Table 5.1) resulting in mass loss. The parameter estimates for oxides of iron, calcium, silica and potassium have negative values suggesting that the oxides may contribute to mass gains. The validity of this correlation should be tested using a larger ash sample set than was used in this study (n = 16).

Studies of correlations between mass changes in the 105-300 and 500-750°C divisions and differences between standard LOI values and modified LOI values with ash performance in concrete did not produce any notable relationships. Nevertheless, other correlations may be found to be useful and the author recommends that further study be performed to identify the contributions of ash constituents to mass changes in the different temperature divisions.

5.7 Sources of variability in the test

Similar to the standard LOI test, several potential sources of variability exist in the modified loss on ignition test. Some of these sources were discussed by Harris et al. (2006). The main sources of variability identified during this study were due to mass measurements, furnace variability and ash oxidation rates. These sources are discussed in detail in the following sections.

Table 5.8: Multi-linear ($y = m_1x_1 + m_2x_2 + \dots + m_nx_n + b$) regression analysis results (from JMP⁶), $y =$ change in mass between 500 and 750°C, parameters are percent inorganic carbon and bulk chemistry oxides.

Summary of fit					
RSquare			0.92		
RSquare Adj			0.88		
Root Mean Square Error			0.06		
Mean of Response			0.05		
Observations (or Sum Wgts)			16		

Analysis of variance					
Source	DF	sum of squares	mean square	F Ratio	
Model	5	0.37	0.07	24.0	
Error	10	0.03	0.00	Prob > F	<0.0001
C. Total	15	0.40			

Parameter estimates				
Term	estimate	std error	t Ratio	Prob> t
Intercept	2.393	0.642	3.7	3.9E-03
Inorganic carbon, %	1.606	0.291	5.5	2.6E-04
Fe ₂ O ₃ , %	-0.037	0.012	-3.0	1.4E-02
CaO, %	-0.046	0.012	-3.8	3.5E-03
SiO ₂ , %	-0.021	0.009	-2.4	4.1E-02
K ₂ O, %	-0.547	0.184	-3.0	1.4E-02

Effects test					
Source	Nparm	DF	sum of squares	F Ratio	Prob > F
Inorg carbon	1	1	0.09	30	2.6E-04
Fe ₂ O ₃	1	1	0.03	9	1.4E-02
CaO	1	1	0.04	14	3.5E-03
SiO ₂	1	1	0.02	6	4.1E-02
K ₂ O	1	1	0.03	9	1.4E-02

5.7.2 Small mass loss in Texas ashes

The Texas fly ashes studied in this work have modified LOI values that range from less than 0.1 percent to approximately 0.7 percent. In order to distinguish differences in the samples, a resolution of no greater than 0.1 percent is recommended, and 0.01 percent is preferred. When 1 g samples are tested, mass losses of 0.1 percent are equivalent to changes of 1 mg. The calibrated scales used and recommended in this study have a resolution of 0.1 mg (0.0001 g) which is adequate for such measurements. However, it was observed that measurements of this magnitude were sensitive to many factors including air currents over the scale, moisture

⁶ SAS Institute Inc., 2006.

adsorption, static electric charges, fingerprints/handling, and sample temperature. These factors could produce errors in mass measurements on the order of tenths of a milligram to several milligrams. Such measurement errors must be minimized by a tightly controlled experimental procedure which includes careful handling of the test specimens.

Four methods for controlling errors in mass measurements are discussed below. These methods are: use of a desiccator for storing ash samples before mass measurements, avoiding touching the sample with ungloved hands, avoiding the buildup of static charges on the sample, and allowing a sample to cool sufficiently before weighing.

Use of a desiccator

The use of a desiccator to store samples between removal from the furnace and weighing is recommended since fly ash is a hygroscopic material and can adsorb moisture from the air which increases mass. A desiccator is a closed container that contains a desiccating agent that absorbs moisture from the container air. The desiccant in the container must be periodically changed or regenerated for effective use.

Sample Handling

In addition to moisture, other materials picked up by the crucibles can cause errors in mass measurements. These other materials can be oils in fingerprints, debris on a countertop or other sources. To avoid the transfer of oils from the skin, wear gloves or use tongs to handle crucibles. The latter is recommended to avoid the buildup of static electric charges on samples as discussed in the following section. Countertops on which crucibles will be kept should be clean or covered with a lint-free towel.

The samples are likewise sensitive to losses of material due to tipping of the crucibles or loss of fine particulate matter due to rapid air flow. Care should be taken when transferring crucibles, particularly into or out of the desiccator, to avoid striking the crucibles and disturbing the contents.

Static electric charges

During the course of this study, it was observed that static electric charges which can build up on crucibles can cause errors in mass measurements. A sufficiently strong static electric charge induced on a crucible or other object caused scales to measure a weight greater than the weight of the object before the charge was induced. Then, perhaps due to the slow dissipation of the charge, the displayed mass would gradually decrease towards the actual, charge-free mass of the sample. This observation was made on two separate calibrated laboratory scales.

While the mechanisms of charge transfer and effects on weighing were not studied in detail, it was observed that avoiding the use of polymer gloves and, instead, using metal tongs to handle crucibles generally resulting in no build up of significant charges. Charges on crucible and scale pans can be neutralized by contact with grounded objects.

Sample temperature upon weighing

Temperature differences between a weighed object and the ambient scale temperature can affect mass measurements. A study of the factors that introduce variability into the LOI test by Harris et al. (2006) concluded that differences in temperature between 10 mL porcelain crucibles (the same type of crucibles used in this study) and the ambient laboratory temperature greater

than 10°C created errors in mass measurement greater than 1 mg (0.1 percent of the sample mass). The error increases as the temperature difference increases. Such errors are significant when assessing 1 g ash samples in the modified LOI test.

Errors in mass measurement due to temperature differences can be controlled by allowing test samples removed from the furnace to cool to ambient temperatures after removal from the furnace. The length of cooling time depends on the initial and final temperatures, cooling location and number of samples cooled together (when cooled in a single desiccator). Generally 25 to 30 min of cooling time was sufficient to cool 500°C crucibles in 20°C air.

5.7.3 Furnace variability

Variability in testing furnaces can exist among commercial models and within a single furnace. Spatial variability within a furnace can influence performance of the modified LOI test. The modified LOI test is sensitive to furnace variability since the test focuses on a narrow temperature range designed to exclude contribution to mass change from non-organic-carbon sources. Variability within a furnace can cause the temperature range to expand, contract or shift, resulting in the incomplete measurement of the carbon or unintentional measurement of other reactions.

Heiri et al. (2001) observed that furnace spatial variability resulted in variation in LOI values of mixed lake sediments heated to 550°C to remove organic carbon. Heiri observed generally that samples at the center of the furnace lost more weight relative to marginal samples.

The influence of specimen furnace location on mass loss was assessed with the following experiment. The two shelves in the furnace were each divided into sixteen equal areas as shown in Figure 5.18. Pre-weighed crucibles, thirty-two in all, containing one gram of ash apiece were placed in the center of each unit area. The ash used in the experiment was taken from a single sample and was assumed homogenous based on a history of consistent test results. The furnace was heated to 300°C. Upon reaching 300°C, the samples were exposed for an additional 30 minutes then removed from the furnace, cooled and weighed. The results of the test are shown graphically in Figure 5.18.

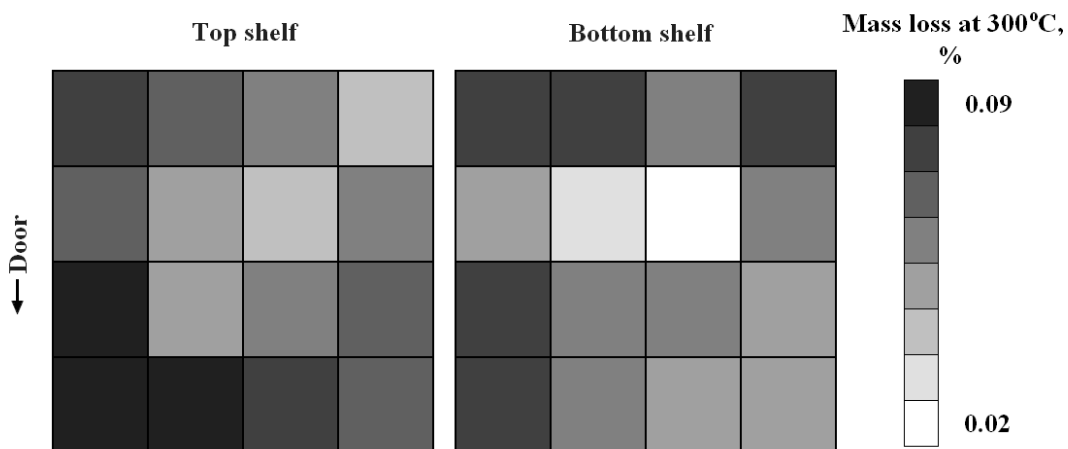


Figure 5.18: Map of the mass losses from fly ash sample located at the center of the unit area.

Each gray square in Figure 5.18 represents one unit area. The color of the square indicates the loss in mass measured in the crucible that was positioned at the center of the square during testing. Figure 5.18 shows mass losses in the samples varying between 0.02 and 0.09 percent. In separate testing, the same ash sample used in the experiment produced losses of about 0.12 percent after exposure to 300°C for 60 min or greater.

The results of this experiment suggest that spatial variability within a testing furnace should be considered. Evaluation of furnaces by the method used by Heiri et al. or the experiment discussed above should be performed to identify regions of the furnace that may produce inconsistent results. Based on the results of the experiment discussed above, it was concluded that the area of the furnace represented by the central four squares of the top shelf be used for all testing to ensure consistent heating. The left and right sides of both shelves and the central portion of the bottom shelf was avoided due to potentially large variability.

5.7.4 Temperature range/exposure time may vary for different ash types

The temperatures and exposure times suggested for the modified LOI test were found to be most suitable for the Texas commercial ash samples studied in this work. It is possible that ashes produced from other sources that may have greater organic carbon content or different parent coals may require longer high temperature exposure times or different temperature range to allow complete combustion of the organic coal residuals present.

Additional modified LOI and supplementary carbon content testing is recommended for fly ashes produced from a variety of sources to determine whether the 300 to 500°C temperature range is suitable for ashes that differ widely from the Texas commercial ashes studied.

5.8 Implementation of the modified LOI test in industry

The modified LOI test can be used in conjunction with the standard LOI test to provide valuable information regarding potential fly ash-AEA interactions. The modified LOI test can be performed in any testing laboratory that currently performs the standard LOI test since no additional testing apparatus is necessary.

It is recommended that fly ash distributors assess both the modified LOI and standard LOI contents of ash regularly to identify changes in ash properties that might influence behavior in concrete. The test results should be reported to the concrete producer upon delivery of the ash. The concrete producer would benefit from this information by keeping a log that includes fly ash LOI and modified LOI, percent fly ash used in concrete mixes and AEA dosage requirements for concrete to produce a given air content. As information is collected, trends between modified LOI content and concrete AEA dosages should become apparent.

Based on the fly ash samples studied in this test, a 0.1 percent increase in modified LOI value caused an increase in AEA dosage in concrete of 20 mL AEA/100 kg cementitious materials (see Figure 5.15). It should be noted that other factors in addition to fly ash can also influence AEA dosage and should be taken into account.

5.9 Conclusions and future work

1. The ASTM C311 LOI test measurement for fly ash is routinely interpreted as a measure of carbon content. This may not always be an accurate interpretation.
2. Several forms of carbon are present in ash including: carbon char, volatile organic compounds, soot and carbonates. The various forms of carbon behave differently under

LOI test conditions. The temperatures at which carbon containing materials are oxidized or decompose vary.

3. Carbon in the form of soot may not be measured by the LOI test. Carbon black, a form of manufactured soot, did not readily oxidize under the conditions of the LOI test.
4. Certain non-carbon materials can be removed from ash under LOI test conditions. Calcium hydroxide, calcium sulfate hemi-hydrate and gypsum, which may be present in ash, were shown to dehydrate under LOI conditions. Oxides of silicon, iron and aluminum were also shown to lose mass (between 0.1-0.3 percent measured at 750°C) when exposed to LOI test conditions.
5. Some fly ash samples were shown to gain mass under LOI test conditions. The mass gains typically occurred at temperatures greater than 600°C. Thermo gravimetric analysis of Ash FR-2 showed that mass gain does not occur in an inert (nitrogen) environment suggesting that mass gain may be due to oxidation of ash materials.
6. The individual contributions of different materials in ash to mass change are not differentiated by the LOI test; instead the LOI value is the sum of mass losses and gains that occur during the test.
7. Manufactured charcoal, which is similar in nature to coal char found in ash, can completely oxidize in air at 500°C provided sufficient time is allowed for the reaction to complete (220 minutes for 1.7 g samples in a muffle furnace).
8. The organic carbon content of two fly ash samples was shown to be at least 85 percent removed at temperatures between 300 and 500°C in air (1 g samples and 30 min exposure at each temperature interval).
9. A modified LOI test was proposed which measures the change in ash mass between 300 and 500°C.
10. The modified LOI test which measures mass loss of 1 g samples in the temperature range of 300 to 500°C (60 min exposure at each temperature) correlates more reliably with ash organic carbon content than the standard LOI test.
11. The modified LOI test correlates more reliably with concrete AEA dosage data than the standard LOI test.
12. The modified LOI may not indicate the presence of either VOC's or soot.
13. The modified LOI test is sensitive to several sources of variability including, handling effects on mass measurements, furnace variability and ash source.
14. The modified LOI test is recommended for implementation in industry. The modified LOI procedure can be combined with the standard LOI procedure currently in regular use. Fly ash distributors should regularly assess ash quality by use of both the standard LOI and modified LOI to detect potential changes in properties. Modified LOI measurements could be used to estimate potential influence of fly ash on concrete AEA dosages.

It is recommended that methods of assessing the forms of organic carbon measured by the LOI test be identified and used to study the contributions of the individual forms. One possible method for identifying the contribution of VOCs to organic carbon is to perform furnace thermo gravimetric analysis of ash in an inert atmosphere and measure the change in organic carbon with temperature. This could shed light on the presence of VOCs that may be driven off in the modified LOI temperature range. In addition, a study of the effects of VOCs on AEAs is necessary to determine the implications of the presence of VOCs in ash.

Evaluation of the proposed modified LOI procedure on a group of ash samples possessing a larger range of organic carbon content than the Texas ashes is necessary to identify the ability of the test to measure organic carbon in ashes produced at other sources. It is possible that ashes with larger organic carbon content may require greater exposure time to complete the test.

The ability of the modified LOI test to predict fly ash-AEA interactions in concrete should be studied for a variety of ashes from different coal sources to identify whether the relationship observed in this study is directly applicable to other ash types.

Chapter 6. Evaluation of the Foam Index Test and Development of a Proposed Standard Test

The foam index test has received limited use in industry as a method for assessing the interactions between cementitious materials and air entraining admixtures. The foam index test is a titration test that combines cementitious materials with water in a container whereupon the materials are titrated with AEA or other surfactant until a defined endpoint is reached.

Two limitations of the foam index test are 1) the test ingredient proportions differ considerably from actual concrete therefore the interactions with AEAs that occur in the test may not be representative of the interactions which occur in concrete and 2) no industry-wide standard protocol exists for the test. This chapter addresses the second limitation. The first limitation will be examined in Chapter 9.

6.1 The Use of the Foam Index Test to Predict AEA Dosage in Concrete Containing Fly Ash: Part I-Evaluation of the State of Practice

Foam index tests are performed to predict the influence of concrete mixture ingredients on the dosage of air entraining admixture (AEA) required to achieve a given air content in fresh concrete. Ingredients that could affect AEA dosage include AEA type, other admixtures, water source, aggregate impurities, cement and cementitious materials, and the nature of the mixing action. This particular study focused on coal fly ash and AEA interaction. Certain fly ashes, when used in portland cement concrete have been shown to increase the dosage of air entraining admixture required to obtain a target air content (Gebler & Klieger 1983, Helmuth 1987, Hill et al. 1997, Joshi & Lohtia 1997, Kulaots et al. 2004, Gao et al. 1997). As an example of the need for a predictive test, Figure 6.1 shows dosage of one specific AEA required to achieve an air content of 6 percent in fresh concrete incorporating fly ash from multiple sources.

6.1.1 Background

Several variations on foam index tests have been proposed (Dodson 1990, Gebler and Klieger 1983, Freeman 1997, Baltrus and LaCount 2001, Kulaots et al. 2003). Variations have evolved quickly because the test is simple to perform and no sophisticated equipment or special training is required.

In general all foam index tests combine water and cementitious materials in a sealable container. The container is capped and agitated for a prescribed period of time to wet the solid materials. Next, measured drops of AEA at variable concentrations are added (or “titrated”) to the test container by means of a pipette or similar device. The container is then recapped and vigorously agitated to mix the contents and to create and stabilize foam. After agitation the container is immediately uncapped and a rest period is observed. At the end of the rest period the foam that remains at the liquid surface is observed. If the foam completely covers the surface so that the underlying water is not visible, then the endpoint is reached. If there is no foam or incomplete foam coverage of the liquid surface, then another drop of AEA is added and the mixture is re-agitated. Additional increments of AEA are added and the container agitated until the foam-coverage endpoint is reached. During the test, the number of drops added to the container is recorded. The cumulative volume of surfactant required to create the endpoint conditions is the foam index, and varies depending on the degree of interaction between the

cementitious materials and the surfactant, and on the geometry, proportions, and mixing action unique to the particular apparatus used.

Several foam index test procedures reported in the literature or used in industry are summarized in Table 6.1. Columns 1 to 10 show the variable characteristics of the test including the container volume, quantities of test materials, agitation durations, etc. In most instances the surfactant used as the titrant was not specified or was referred to as “a commercial AEA.”

Columns 11 to 14 of Table 6.1 show the metrics for comparison of the various tests. Note that in column 12, ash to cementitious ratio, ash/cm is equal to 1.0 when no cement is present. The test-materials volume to container-volume ratio, column 13, is a measure of the fraction of the test container occupied by water, cement and ash. The remainder of the volume is the air filled space (or “head space”) above the liquid. The μL of AEA per drop, column 14, is the volume of undiluted AEA added to the test solution in each incremental dose. It is calculated as the drop size (column 7) multiplied by the concentration (column 6). Concentration is the volume fraction of liquid AEA (as received by the manufacturer) in the AEA-water solution (dilution and drop size are discussed in detail in section 8). The μL of AEA per drop can be calculated only when both drop size and AEA concentration are known.

The tests summarized in Table 6.1 share some common aspects. For example, the general procedure of each test is similar and the water/cm ratios were uniform at 2.5 (except for industry method 1). There are major differences in the various test methods, however. The ash/cm ratio is either 20 percent ash and 80 percent cement or 100 percent ash. Most were agitated by shaking the test containers by hand while other methods used a kitchen-type blender to mix the materials and create foam. The tests performed in blenders used larger quantities of water and ash than the tests performed in containers that were shaken by hand. The volume fraction of the container occupied by the water, cement and ash varies from 8 percent to 40 percent.

In light of the multiple variations on foam index tests, ASTM Subcommittee CO9.24 on Mineral Admixtures has identified a need to develop a foam index test method for laboratory and field use (Manz, 1999). A standard test would allow comparison of results among laboratories and would benefit the concrete industry by evaluating the impact of cementitious materials on AEA dosage.

6.1.2 Objective

The aim of this research was to determine how differing foam index methods compare in predicting AEA dosage of fresh concrete containing fly ash. In this study, three foam index test methods, chosen to be representative of the methods found in Table 6.1, plus an additional hybrid method were compared by means of the ability of each to predict AEA dosages in fresh concrete.

Table 6.1: Summary of several foam index test methods reported in the literature and/or used in industry. (“U” indicates that the value was not specified, * estimated volume for kitchen type blender.)

Method	1	2	3	4	5	6	7	8	9	10	11	12	13	14
	Container type	Container volume, mL	Water, mL	Ash, g, s.g. = 2.5	Cement, g, s.g. = 3.15	AEA concentration, % ⁷	Drop size, μ L	Initial mix, sec	Shake / blend, sec	Rest period, sec	Water / cementitious ⁸	Ash / cementitious	Test materials volume / container volume	μ L undiluted AEA/ drop
Dodson, 1990	Bottle	475	50	4	16	4.8	200	60	15	15	2.5	0.2	0.12	9.6
Meininger, 1983	Bottle	475	50	4	16	U	U	15	15	45	2.5	0.2	0.12	U
Freeman, 1997	Bottle	350	25	2	8	10	U	60	15	45	2.5	0.2	0.08	U
Külaots, 2003	Bottle	70	25	2	8	10	20	60	15	45	2.5	0.2	0.40	2
Baltrus, 2001	Bottle	15	5	2	-	2.4	50	60	15	15	2.5	1.0	0.39	1.2
Industry-1	Blender	1300*	250	30	-	U	100	10	10	30	8.3	1.0	0.20	U
Industry-2	Blender	1300*	200	80	-	100	U	10	10	0	2.5	1.0	0.18	U

⁷ AEA concentration is the volume percentage of undiluted AEA in aqueous solution. For example, in the Külaots 2003 method, 10% AEA concentration was prepared by combining 1 part commercial AEA as received from the manufacturer with 9 parts water (by volume).

⁸ w/cm is the mass of water divided by total mass of cementitious materials

6.1.3 Terms

The following terms are used throughout this chapter to refer to characteristics of the foam index test.

Air entraining admixture (AEA): Natural organic- or synthetic-based surfactants, usually in solution form, which stabilize air bubbles in fresh concrete generated by mixing action

Foam index test method: Any test method used to measure the ability of an air-entraining admixture to stabilize foam in a mixture of water, cement and/or cementitious materials by titrating with AEA and agitating the materials until a predetermined amount of foam is stabilized.

Foam index: The total volume of air entraining admixture added drop-wise to the test liquid to reach the test endpoint (described below). This index, as typically reported, is unique to the specific test method used.

Specific Foam Index: The normalization of foam index to express the results as the volume of undiluted AEA per unit mass of cement, ash or the combined mass of cementitious materials.

Endpoint: The condition of the foam in the testing container that indicates foam index is reached. In this study, the endpoint is taken as the initial existence of an unbroken blanket of foam at the air-water interface within the testing container at a given time interval (or rest period) after agitation of the testing materials. Note that the thickness or volume of the foam is not normally measured, but is approximately constant for a given test method and set of materials.

6.1.4 Scope

The first step in this study was to develop a data set of the amount of AEA required to stabilize 6 percent air in fresh concrete as affected by fly ash from four different sources (Figure 6.1). Next, four foam index test variants were used to evaluate the four ashes used in the fresh concrete tests. Data from the fresh concrete and foam index tests were compared to evaluate the ability to predict concrete behavior on the basis of foam index tests.

6.1.5 Fly Ash/Cement Samples

The four fly ash samples were chosen from those commonly used in concrete in Texas. Properties of the ash samples are shown in Table 6.2. The samples were selected because of each sample's unique influence on AEA dose in fresh concrete (quantified as AEA dosage for concrete air content of 6 percent in Table 6.2) as described in the following section. The cement used for this study met the ASTM C150 specifications for Type I or Type II with Blaine fineness of 3760 cm²/g and 0.55 percent Na₂O equivalent.

Table 6.2: Fly ash and AEA sample data.

Ash	Type per ASTM C 618	LOI	AEA dosage for concrete air content of 6%	
			mL/100kg cm	Fl oz/100 lb cm
H	F	0.8%	139	2.1
MH	F	0.4%	64	1.0
ML	F	0.1%	49	0.8
L	F	0.6%	24	0.4
Surfactant	Generic Type		Solids content before lab dilution	
Commercial AEA	Wood rosin		7.1%	

6.1.6 Fresh Concrete AEA Dosage

Fresh concrete air tests were performed to determine the influence of the four fly ash samples on AEA demand for 6 percent air content. The tests were performed by mixing 64-L batches of concrete in an 85-L mixer. All materials used in the mixtures were stored in the mixing room for at least 24 hours at 23°C prior to mixing to keep the mixing temperature constant. All mixtures had water to cementitious material ratios of 0.45. All mixtures contained 335 kg/m³ (equivalent to 6 sacks of cement/CY), of total cementitious materials composed of 80 percent cement and 20 percent fly ash (by mass). Texas river gravel and sand were used. Mixture proportions are shown in Table 6.3. The fresh concrete was brought to a constant slump (ASTM C 143) of 76 mm +/- 25 mm using an ASTM C 494 Type D normal range water reducer.

Table 6.3: Components and masses of the materials used in the concrete air tests.

Component	Mass (kg/m ³)
Cement	268
Fly Ash	67
Coarse Aggregate	1098
Fine Aggregate	742
Water	151
AEA (wood rosin based)	Varied
NRWR	Varied

After the desired slump was obtained, unit weight (ASTM C 138) and pressure meter (ASTM C 231) measurements were made. The concrete used in the slump test was returned to the mixer and approximately 57 L of concrete remained. Next, a wood rosin-based commercial

AEA was added to the mixture and mixed for 3 minutes. Slump and unit weight measurements were taken after each dosage-and-mixing cycle and returned to the mixer to receive additional AEA doses. After sufficient AEA was added to change the unit weight to that corresponding to $6 \pm \frac{1}{2} \%$ air content, the dosing was stopped and final slump, and unit weight readings were taken and the air content verified by pressure meter. The dose of AEA required for exactly 6 percent air was interpolated from linear curve-fits of the dosage-air content data.

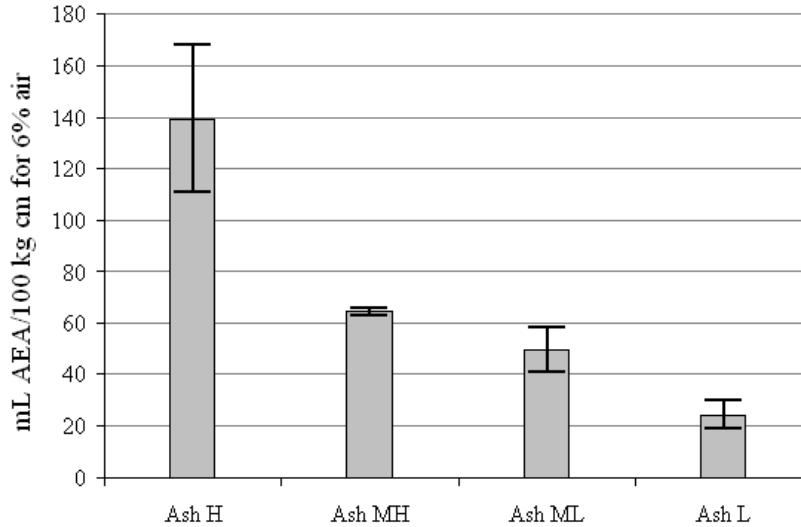


Figure 6.1: Required dosage of AEA S1 to produce 6% air in a concrete mixture containing fly ash from four sources. Dosage is scaled to mL of AEA per 100 kg of cementitious materials (cement + ash).

6.1.7 Foam Index Tests

Four foam index test variants were used in this study. The first variant (water, ash and cement shaken in a jar) was similar to the methods used by Freeman et al. (1997) and Külaots et al. (2004) with container “B” in Figure 6.2 used as the mixing container. The second variant of the test (water and ash shaken in a 20 mL vial, container “A” in Figure 6.2) was similar to that used by Baltrus and LaCount (2001). The third variant (water and ash mixed in a blender, container “D” in Figure 6.2) was similar to the Industry-1 test method. In a fourth variant, ash and cement were combined in a test tube, container “C” in Figure 6.2, with $w/cm = 25$. In this fourth method the container is shaken by hand to mix the materials and create foam.

Table 6.4: Characteristics of four foam index tests evaluated.

	Container type (Figure 2)	Container volume, mL	Container Inner diameter, mm	Water, mL	Ash, g	Cement, g	AEA concentration, %	Drop size, μ L	Initial mix, sec	Shake/ blend, sec	Rest period, sec
Method 1	Bottle- B	132	45	25	2	8	10	10	60	15	45
Method 2	Vial- A	20	23	5	2	--	10	10	60	10	20
Method 3	Blender- D	1300	100	250	30	--	100	30	10	10	45
Method 4	Test Tube- C	53	21	25	1	--	10	10	30	10	15

Table 6.5: Metrics for the comparison of the four foam index test variants.

	Water / cementitious	Ash / cementitious	Test materials volume / container volume	μ L undiluted AEA/ drop	mL AEA/100 kg cm per drop
Method 1	2.5	0.2	0.21	1	10
Method 2	2.5	1.0	0.29	1	50
Method 3	8.3	1.0	0.20	30	100
Method 4	25	1.0	0.48	1	100

The four test variants evaluated are compared in Tables 6.4 and 6.5. While being generally similar in procedure, the four foam index tests differ in several major ways. For methods 1, 2 and 4, the materials are mixed in glass containers and shaken by hand. In the remaining variant, method 3, the materials are mixed in a blender. Combined cement and ash are tested in method 1, while ash is the only solid material tested in the remaining test variants. The water to cementitious materials ratio as well as testing container dimensions differs as well.

Note that none of the test pastes attempt to match the paste used in the concrete mixture. All of the tests pastes have larger water/cm ratios (2.5 to 25) than the concrete (0.45). Method 1 (Bottle Shake method) has an ash/cm ratio equal to that of the concrete; however, the remaining three methods contain no cement. None of the methods incorporate water reducer in the paste.

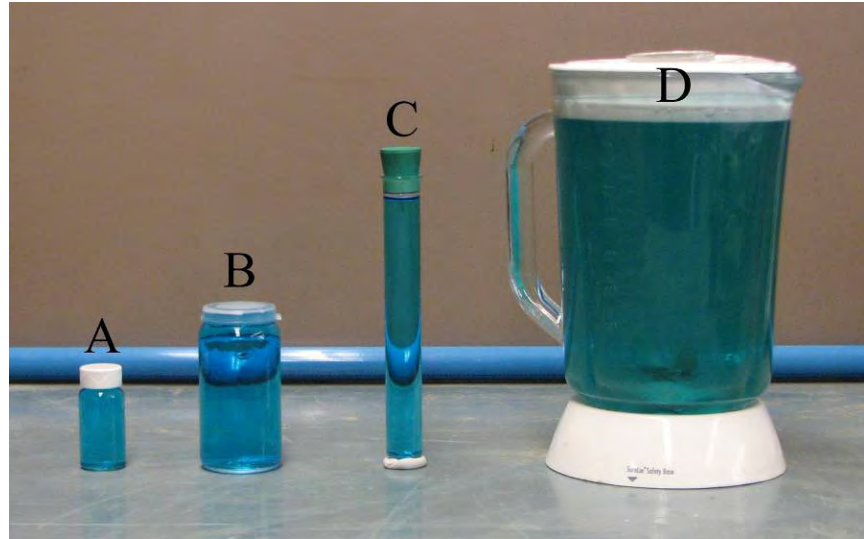


Figure 6.2: Containers used in the four foam index test variants.

Test Procedure- All methods

The four fly ash samples in Table 6.2 were tested with the four variants. The same portland cement and commercial AEA used in the fresh concrete tests were also used in the foam index tests. Each foam index test was repeated five times for each ash. All foam index testing was performed using the following basic method

1. Place distilled water, ash and cement into the test container.
2. Agitate (either by shaking or blending) the container for the initial mix time duration indicated in Table 6.4. For all but method 3, the blender method, shake the container as described below but with a shaking frequency of approximately 2 shakes per second to break up agglomerates and wet the materials. For method 3, blend at the highest setting.
3. Add a single drop of AEA solution (drop size and dilution from Table 6.4), cap bottle and either shake container at 4 shakes per second with a vertical displacement of 0.2 to 0.25 m or blend at the highest setting for the shake/blend duration indicated in Table 6.4.
4. Remove cap immediately and allow the sample to remain undisturbed for the duration of the rest period to allow the foam to reach a “stable” state.
5. At the conclusion of the rest period, observe the foam at the air-water interface for comparison with the predefined endpoint.
6. Steps 3 to 5 are repeated until the endpoint is reached. The cumulative volume of AEA determined using equation (1) required to reach the endpoint is reported as the Foam Index.

6.1.8 AEA concentration, drop size, units and precision

The commercial AEA used in this study is sold in liquid form. Usage guidelines from the manufacturer state that the product does not require dilution for use in concrete. However, dilution of the AEA with water was necessary for all foam index test variants except Method 3- the Blender test. Dilution was needed because only very small volumes of AEA were required to produce the endpoint conditions (cumulative dose of AEA as low as 3 μL or 0.003 mL AEA for Ash L in Method 1- the Bottle Shake test); furthermore, the total volume of AEA added was divided into incremental drops. The minimum drop size in this study was 10 μL , limited by the

pipette used to transfer the AEA. The volume of AEA added with each drop must be small enough to allow differentiation among test samples, but must be large enough to permit reaching the endpoint in a reasonable number of steps. Trial tests were done to find a drop volume and AEA dilution suitable for each test procedure studied. As shown in Table 6.4, a 10 percent concentration of AEA by volume was used with 10 μL drop size, so that 1 μL of AEA (as received from the manufacturer) was present in each 10 μL drop of diluted AEA. For increased control over possible variation in AEA as received from the producer, the solids content was determined by heating samples at 105°C until constant mass was obtained. The solids content is recorded as a percent of liquid AEA mass in Table 6.2.

The test protocols from the foam index methods of Table 6.1 generally report foam index values as volumes of AEA, but because the test procedures use differing quantities of ingredients and AEA concentrations such results cannot be compared directly. One way to avoid this difficulty is to convert cumulative volume of drops of dilute AEA solution to the corresponding volume of undiluted AEA using equation (6.1). The result can be normalized by the mass of cementitious materials used in the test to produce a specific foam index value having units of volume AEA per unit mass of cm, equation (6.2).

$$FI = Dv \frac{c_{AEA}}{100} \quad \text{eqn. 6.1}$$

$$SFI = \frac{FI}{cm} \quad \text{eqn. 6.2}$$

FI is the foam index, in this study reported in units of μL undiluted AEA. *D* is the number of drops of dilute AEA solution added to reach the endpoint. The value of *v* is the volume of a single drop of AEA solution (μL). The variable c_{AEA} is the AEA concentration in percent. *SFI*, or specific foam index, is in units of μL AEA per g of cementitious materials. The variable *cm* is the sum of fly ash and cement used in the test in grams. (Lowercase “cm” is commonly used to represent cementitious materials and should not be confused with “centimeters” when used in conjunction with mass units of g or kg.)

Given that the purpose of the test is to determine how the test materials will affect AEA dosage in fresh concrete, it is reasonable to convert the specific foam index value to the commonly used industry units for admixture dosage of mL AEA per 100 kg cm. *SFI* in units of μL AEA per g cm is numerically equivalent to units of mL AEA per kg cm. Multiplying equation (6.2) by 100 produces the units mL AEA per 100 kg cm. Specific foam index values in this chapter are reported using these units.

It is therefore recommended that units of mL AEA per 100 kg cm be used to describe the incremental dosage in any variant of the foam index test since units of drops or microliters of AEA are not meaningful when comparing tests where varying drop size, AEA dilution, or differing amounts of cementitious materials are tested. (Further, mL AEA per 100 kg cm is a common unit in concrete mixture proportioning.) In Table 6.5, the AEA per drop is given in units of mL AEA per 100 kg cm for each of the four test methods. The values are calculated using $D = 1$ drop in equations (6.1) and (6.2) and then multiplying the specific foam index value by 100.

As typically performed, a precise end-point of the test would actually be reached between two discrete drops. (Most of the time the real end point is reached at something less than the

“nth” drop recorded as the foam index, but something more than (n-1) drops.) Decreasing the amount of AEA present in the incremental drops therefore improves the precision of the test by decreasing the difference in AEA concentration between two discrete drops. However, the minimum amount of AEA in a single drop is limited by the issues described above.

Shaking

The nature of the agitation affects the amount of stable foam produced. None of the test methods reported in the literature includes a detailed description of “shaking by hand,” other than to describe the motion as “vigorous.” For this study, the shaking was controlled to reduce variability by counting the total number of shaking cycles during the shaking interval. A full “shake-cycle” begins with the container held in raised hand then rapidly lowered by 0.2 to 0.25 m and returned to the starting position. The shaking frequency is kept between 40 and 50 shakes in 10s.

Endpoint

The foam index endpoints were judged using the same criteria for each test variant. Depending on the mixture composition, foam begins to appear on the liquid surface after some volume of AEA has been added to the test mixture and the container has been agitated. The amount of foam on the surface increased with each additional drop of AEA added. The rate of increase of foam formation was dependent on the ash and the characteristics of the test procedure, such as the amount of undiluted AEA present per drop.

The sequence of images in Figure 6.3 shows the gradual accumulation of foam in test Method 1- the Bottle Shake test. The images are representative of all the test methods except Method 3- the Blender test. After the addition of one drop and subsequent agitation, only a few bubbles exist around the periphery of the liquid surface (located by the arrows in Figure 6.3a). The liquid appears dark in contrast to the lighter-toned bubbles. After additional drops are added (Figure 6.3b), the amount of foam increases at the surface periphery and spreads slightly towards the center. With increasing dosage of AEA, the center of the liquid surface begins to fill with the foam cover and only a few small regions of the surface remain uncovered (shown by the arrows in Figure 6.3c). Near the end of the test only a few small gaps remain in the foam cover (shown by the arrows in Figure 6.3d). The endpoint is reached when an unbroken foam cover exists on the surface (Figure 6.3e). For Method 3- the Blender test, the foam accumulation typically proceeded from the center of the liquid surface to the outer edge as the AEA dosage increased.

During the rest period, the test container was placed on a surface free from disturbances since movement can cause the foam to redistribute on the surface. For this reason the container cap was removed immediately after agitation. Immediate removal of the cap also allowed any liquid present in the region of contact between the cap and container to flow back into the mixture before the foam was stabilized.

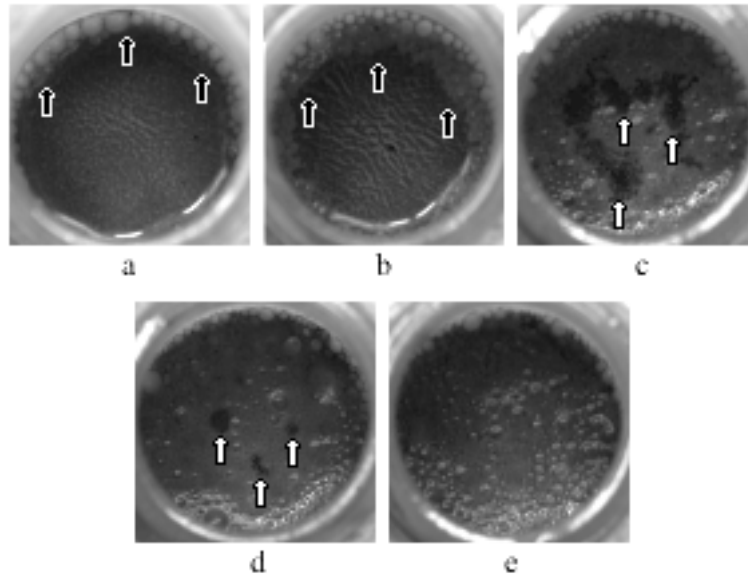


Figure 6.3: Sequence of foam accumulation at the liquid-air interface of the foam index test. The test endpoint is reached when the interface is completely covered with foam, as shown in e.

6.1.9 Test Results

The ability of the foam index tests to predict the AEA requirement of concrete containing fly ash was evaluated by ranking the ashes on the basis of AEA dosage, the correlation between foam index results and fresh concrete AEA dosage data, and the differences between predicted dosages and actual dosages. Other factors of interest are repeatability of the various methods and ease of testing.

Raw Data and Repeatability

Tables 6.6 and 6.7 show the mean foam index values of five tests for each ash sample-test method combination. The foam index values in Table 6.6 are given in values of both “drops” and μL AEA solution as is commonly reported for the tests. The drop volumes and AEA solution concentrations are not equal across all tests; furthermore, differing amounts of materials and different container sizes prevents direct comparison of the values on the basis of number of drops or volume of AEA solution.

In Table 6.7, the mean specific foam index values and standard deviations are given in units of mL AEA per 100 kg cm. The drop increment size is shown in the same units beneath the method description at the top of the table. The coefficients of variation are shown in percent units. For several combinations of ashes and test methods (e.g. Ash ML in the Bottle Shake and Blender tests), all five replicates of any one test method produced identical foam index values, thus the standard deviations and COVs are reported as zero. For all tests, the standard deviation was approximately one discrete dosage increment or less. Changing the AEA increment size can change the variability in the test procedure as discussed in detail in Section 6.2.

Table 6.6: The mean number of drops and AEA solution volumes for five repeated tests of each ash. Drop volume and AEA solutions concentrations (shown beneath the heading “Drops”) are not equal in all tests.

v c_{AEA}	Method 1		Method 2		Method 3		Method 4	
	Bottle Shake Test		Vial Shake Test		Blender Test		Test Tube Shake Test	
	Drops, 20 μ L 5%	AEA solution, μ L	Drops, 20 μ L 5%	AEA solution, μ L	Drops, 30 μ L 100%	AEA solution, μ L	Drops, 20 μ L 5%	AEA solution , μ L
Ash H	10.4	104	14.3	143	6.2	186	10	100
Ash MH	6.8	68	10.2	102	3.6	108	7.6	76
Ash ML	6.0	60	6.3	63	5.0	150	4.0	40
Ash L	3.0	30	2.8	28	2.0	60	3.2	32

Table 6.7: The mean, standard deviation and coefficient of variation of drops of AEA for five repeated tests for each ash. Means and standard deviations are presented in units of mL undiluted AEA per 100 kg cementitious materials.

	Method 1			Method 2			Method 3			Method 4		
	Bottle Shake test, 10 mL AEA / 100 kg cm per drop			Vial Shake test, 50 mL AEA / 100 kg cm per drop			Blender Test, 100 mL AEA / 100 kg cm per drop			Test Tube Shake test, 100 mL AEA / 100 kg cm per drop		
	Mean	σ	COV	Mean	σ	COV	Mean	σ	COV	Mean	σ	COV
Ash H	104	5	5.3	717	61	8.4	620	45	7.2	1000	71	7.1
Ash MH	68	4	6.6	508	38	7.4	360	55	15.2	760	55	7.2
Ash ML	60	0	0.0	317	26	8.2	500	0	0.0	400	71	17.7
Ash L	30	0	0.0	142	20	14.4	200	0	0.0	320	45	14.0

General Observations

Figure 6.4 is arranged with the four ash sources in order of increasing AEA requirement to stabilize 6 percent air in fresh concrete. All foam index test variants rank the ashes in this same order except the blender test, which reverses the order of ML and MH in the sequence. This seeming anomaly was retested and the same results were obtained, and possible reasons are discussed later in this chapter. Also evident in Figure 6.4 is the difference in relative AEA dosages. For example, for the fresh concrete dosage data, the AEA required for Ash H is more than double that of ash MH. None of the foam index test methods reported similar relative results for these two ashes. The test-specific nature of the foam index variants is also evident in foam index results that varied from approximately the same to 10 times greater than required to stabilize 6 percent air in fresh concrete. For example, the specific foam index values for the Bottle Shake test are generally within 25 percent of the dose of AEA required in the concrete tests. The ability to reliably predict AEA dose in concrete on the basis of foam index tests is explored in the next section.

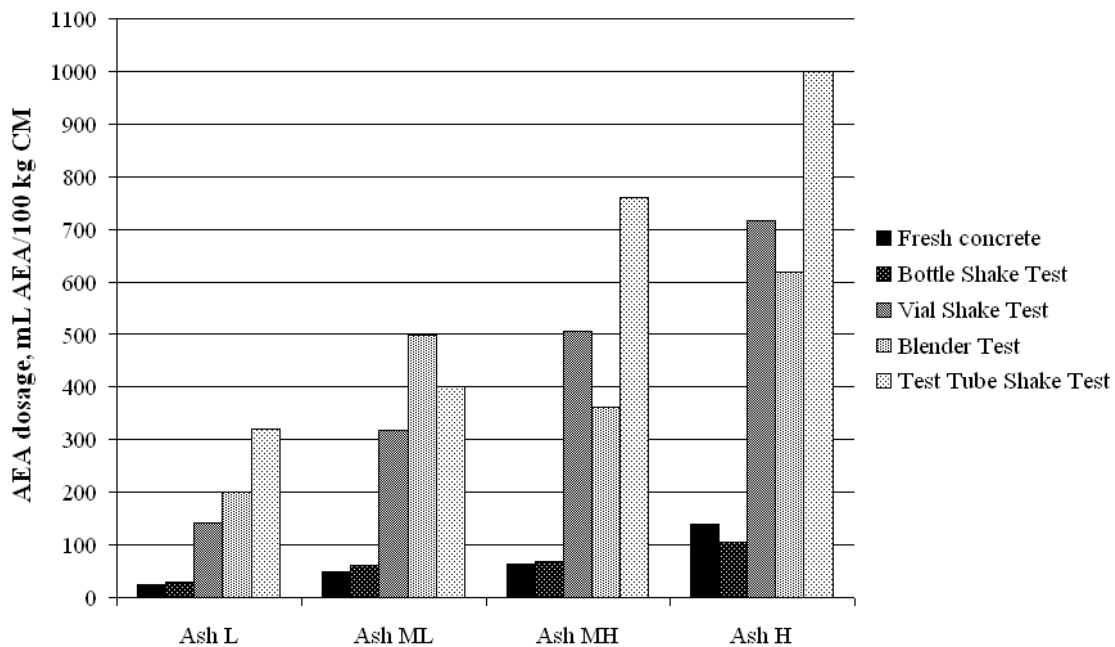


Figure 6.4: The foam index values of fly ash samples L, ML, MH and H as determined by four foam index test variants. Each value represents the mean AEA volume of five tests.

Ability to Predict AEA Dose in Concrete from Foam Index

A comparison of specific foam index values and the dose of AEA required to stabilize 6 percent air in fresh concrete (both in units of mL AEA / 100 kg cm) is shown in Figure 6.5. The coefficients of determination and standard errors of the estimates are shown in Table 6.8. In general, the reasonable R^2 values suggest meaningful correlations, supporting the use of foam index to predict dose of AEA in concrete in the field.

As a predictive tool the Bottle Shake test produced the highest R^2 and lowest standard error of the four test correlations. The Vial Shake test and Test Tube Shake test performed

similarly to the Bottle Shake test (all three have R^2 values ≈ 0.9) but with larger errors. The Blender test showed the weakest correlation with the fresh concrete data. Note, however, that the correlation between foam index and air fresh concrete appears to depend not only on the specific foam index variant, but also on the specific materials being evaluated.

As seen in Figure 6.5, in the Vial Shake test, Ash MH appears to be the single nonconforming sample by overestimating the AEA dose of fresh concrete while in the Blender test, Ash ML appears to do the same. Also evident in Figure 6.5 is the variation in specific foam index values as obtained by different test variants on the same ash samples. For example, with the three tests where no cement was present (all tests except the Bottle Shake test) the specific foam index of Ash H varied between 290 (Vial Shake test) and 1000 (Test Tube Shake test) mL AEA/100 kg cm.

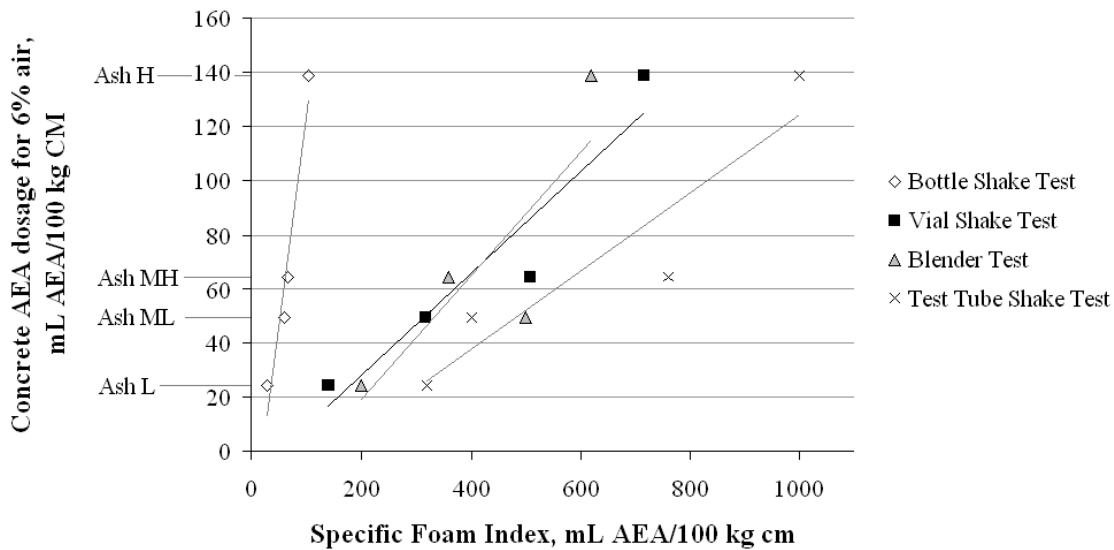


Figure 6.5: Correlations of specific foam index values with concrete air data for the four foam index test variants.

Table 6.8: Regression equations, coefficients of determination and standard errors of the foam index test-concrete AEA dosage relationships

Test Method	X-intercept	Slope	R^2	Standard Error, mL AEA/100 kg cm for 6% air
Bottle Shake	-33.9	1.6	0.94	10
Vial Shake	-10.4	0.19	0.90	13
Blender	-26.8	0.23	0.71	23
Test Tube	-20.4	0.14	0.87	16

Table 6.9 explores the possible results of using these predictive relationships to establish AEA dose in batching concrete for a desired air content of 6 percent. The “actual AEA dose” in Table 6.9 is the dose determined from tests on fresh concrete as reported in section 6.5. The “predicted AEA dose” is the AEA dosage value predicted by the regression analyses on foam index test and fresh concrete data from Table 6.8. When this value is inserted into the relationships established in the laboratory for air content in fresh concrete as a function of AEA dosage, the result is the “expected air for predicted dose” reported in the rightmost column in Table 6.9.

Testing Convenience

Although the convenience of the test is an important consideration, comparison of the effort required to perform the tests is subjective and reflects the opinions and experience of the authors. Convenience considers preparation of the test materials, carrying out the test procedure, recognizing the endpoint, and finally, cleaning the testing apparatus.

Table 6.9: The AEA requirement, as predicted by the four foam index test methods, for desired 6% air in concrete containing the indicated fly ash as 20% of total cementitious materials.

Ash Sample	Actual AEA dose for 6% air, mL/100 kg cm	Predicted AEA dose for 6% air, mL/100 kg cm	Expected air for predicted dose, %
Method 1- Bottle Shake Test			
Ash H	139	130	5.7 ± 1.3
Ash MH	64	73	6.6 ± 0.1
Ash ML	49	61	6.9 ± 1.0
Ash L	24	13	4.5 ± 0.9
Method 2- Vial Shake Test			
Ash H	139	125	5.6 ± 1.3
Ash MH	64	86	7.4 ± 0.1
Ash ML	49	50	6.1 ± 0.9
Ash L	24	16	4.9 ± 1.0
Method 3- Blender Test			
Ash H	139	115	5.2 ± 1.2
Ash MH	64	56	5.4 ± 0.1
Ash ML	49	88	8.9 ± 1.2
Ash L	24	19	5.3 ± 1.0
Method 4- Test Tube Shake Test			
Ash H	139	124	5.5 ± 1.3
Ash MH	64	90	7.7 ± 0.1
Ash ML	49	37	5.1 ± 0.8
Ash L	24	26	6.2 ± 1.2

Preparation for all tests was similar and consisted of weighing the solid samples, and measuring the water volumes. For the Bottle Shake, Vial Shake and Test Tube Shake methods, dilution of AEA was required. Frequent preparation of dilutions may be required due to the effects of possible “ageing” of the AEA dilution as described by Külaots et al. 2003.

Ease of test performance varies widely between the tests in which the material is shaken by hand and the blender test. For the shaking tests where several increments of AEA and

subsequent agitation are required (e.g., tests performed on Ash H), the test can become tedious and tiring, and a potential source of operator variability. In comparison, the electrically powered mixing of the blender test is easy to perform even when many incremental doses of AEA are required, and a constant mixing energy is applied as long as the same blender, setting, and blade are used.

A clear foam index endpoint is critical for the successful use of the test. The endpoints were typically easily identified for the AEA dilutions and drop volumes used in this study. This is supported by the data in Table 6.7 which, for many samples, shows little variation in the number of AEA doses in five replicate tests. The small surface area of the vial and test tube can cause the identification of the endpoint to be more difficult than in the other test variants.

Subsequent study demonstrated that running a foam index test in a container that has not been properly cleaned from the last test can significantly affect the results. Adequately cleaning the glass bottles and test tubes was quickly and easily done using detergent and bottle brushes. Clean-up of the blender was more tedious. Simply rinsing the blender by blending clean water was not sufficient to remove the solid particles that lodged in the contact areas of the gasket and blade assembly at the bottom of the blender jar. Complete disassembly of the blender jar and scrubbing with a bottle brush was necessary to remove the ash particles. Considerable wear of the blender blade and gasket were noted as well, due to the abrasive nature of the cement and ash, making frequent maintenance or replacement necessary for consistent testing.

6.1.10 Discussion

Test Performance

Of the four foam index test variants studied, the most reliable correlation between foam index and concrete results was obtained with the Bottle Shake test. This was also the most repeatable and easiest to perform. On the other hand, the use of a blender to agitate the mixture is desirable to ensure uniform agitation and prevent fatigue (both potential problems when shaking the bottle in hand). In addition, the large surface area of air/mixture interface in the blender jar was ideal for identification of the foam index endpoint. However, the generally poorer correlation with fresh concrete test results suggests that more study is needed to take advantage of the potential benefits of the blender.

The errors in the dosage predictions shown in Table 6.9 were not consistent across ash samples or across test methods from ash to ash, however. For example, correlations obtained for the Vial Shake and Test Tube Shake tests both overestimated the AEA dosage of fresh concrete for 6 percent air for Ash MH but correctly estimated or underestimated the dosage for ash ML while the Blender test results were opposite. This means that the foam index variants did not consistently correlate to each other, and one of the reasons for this is that only the bottle test (in this test series) included both cement and ash as solids. The vial, test tube, and blender tests used fly ash as the only solid. As will be described in greater detail in Section 6.3, portland cement has a generally stabilizing influence on foam while ashes can vary from stabilizing to destabilizing foam. Thus it is important that if multiple foam index tests are to be compared, the same cementitious materials and proportions should be used.

As an example of this principle, a separate test series was conducted in which all four foam index tests used a $w/cm = 2.5$ and an $ash/cm = 0.50$, for each of the four ashes as shown in Table 6.10. (Proportions were selected based on drop size, concentration, and mass of paste to maximize precision of the test as described in Section 6.2. Proportions were not intended to

match the concrete air content tests.) The results, displayed in Table 6.11 and Figure 6.6b, shows the modified foam index test values compared with the fresh concrete AEA dosage. Results of least-squares regressions of fresh concrete AEA dosage as the dependent variable and foam index values as the independent variables were performed and are reported in Table 6.13.

Table 6.10: Modifications to the four test methods so that each test contained the same proportions of water, ash and cement.

Test Method	Water, mL	Ash, g	Cement, g	mL AEA/100 kg cm per drop
1- Bottle Shake test	25	5	5	10
2- Vial Shake test	15	3	3	17
3- Blender test	250	50	50	20
4- Test Tube Shake test	5	1	1	50

Table 6.11: The mean, standard deviation and coefficient of variation of drops of AEA for three repeated tests for each ash.

	Method 1 Bottle Shake test, 10 mL AEA / 100 kg cm per drop			Method 2 Vial Shake test, 8.3 mL AEA / 100 kg cm per drop			Method 3 Blender Test, 10 mL AEA / 100 kg cm per drop			Method 4 Test Tube Shake test, 12.5 mL AEA / 100 kg cm per drop		
	Mean	σ	COV	Mean	σ	COV	Mean	σ	COV	Mean	σ	COV
Ash H	280	10	4	233	0	0	130	10	8	175	5	3
Ash MH	145	5	3	133	10	8	80	0	0	100	0	0
Ash ML	115	5	4	83	0	0	50	10	20	100	0	0
Ash L	50	0	0	33	0	0	20	0	0	50	0	0

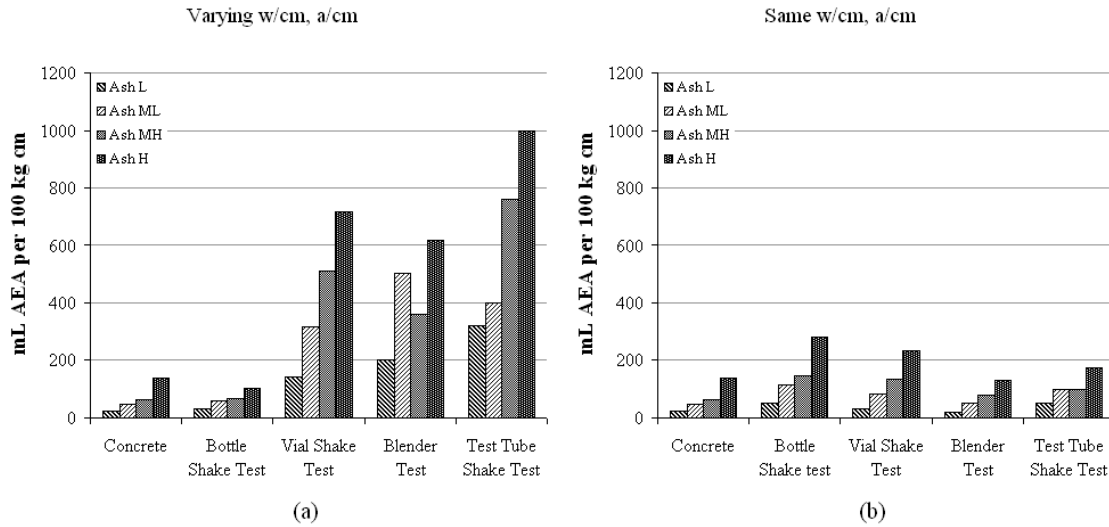


Figure 6.6: Comparative results of test methods in which each method uses a unique set of ingredients and proportions (a) and comparative results of test methods in which a standard set of ingredients and proportions were applied in all tests (b).

When observing Figures 6.6a and 6.6b above, one may first notice that the addition of cement in test methods 2-4 (test 1 already incorporated both cement and ash) dramatically lowers the amount of AEA required to reach the foam index endpoint. While this phenomenon is explored in detail in Section 6.3, it is clear that the inclusion of cement is a key consideration in designing and interpreting foam index tests. It is also obvious that uniform ingredients and proportions reduced the absolute difference in foam index among test methods for any given ash. Further, as shown in Table 6.12, the relative foam index of a given ash was seen to have varied among tests by as much as a factor of about 10 for non-uniform ingredients and proportions, but this was reduced to a maximum factor of about 1 with uniform ingredients and proportions.

Table 6.12: Average relative foam index across all four ashes for each method.

	Bottle Shake	Vial Shake	Blender	Test Tube Shake
Non-standard ingredients	1	6.1	6.6	9.6
Standard Ingredients and proportions	1	0.8	0.5	0.8

Within any given test method uniform ingredients and proportions did not significantly or consistently change ash ranking for a given test, although the ranking of ashes is affected by ingredients and proportions in both the blender and test tube tests. Some of the differences may be related to the fact that changing the ingredients and proportions changes volumes, fill height, and foam/paste volume ratios with corresponding impact on test results as discussed in detail in Section 6.2.

Given the interest in predicting concrete behavior from the results of foam index tests, results obtained using the same paste ingredients show somewhat improved correlations with

concrete dosage data (Table 6.13). The results from the modified tests suggest that each of the methods could be optimized for the ash samples studied. As one component of the optimization, the usage of some amount of portland cement in the test appears to decrease dosage prediction errors and specific foam index values. Further study of the effects of other test variables including matching of the materials proportions of the test with those of a specific concrete mix would aid in the development of a suitable standard test.

Table 6.13: Coefficients of determination and standard errors of the foam index test-concrete AEA dosage regressions.

Test Method	R ²	Standard Error, mL AEA/100 kg cm for 6% air
1- Bottle Shake Test	0.99	4
2- Vial Shake Test	0.97	7
3- Blender Test	0.95	9
4- Test Tube Shake Test	0.96	9

Additional Study

Before the industry can reliably choose or modify a standard foam index test procedure, additional evaluation is required. Variations in specific foam index values of any given ash among the various test procedures suggest that many factors influence the AEA dosage required to produce the foam index endpoint. These other factors include the bottle geometry, water to cementitious materials ratio, ash to cementitious materials ratio, agitation method, volume of the incremental AEA dose and others. These factors should be isolated and studied in greater detail to determine the influence on test results so that the proper boundaries and tolerances can be established for a standardized test. Section 6.2 and Section 6.3 of this study examine the influence of these test variables. Guidelines for a standard method are then recommended.

6.1.11 Conclusions

The following conclusions are based on the materials and tests methods used in this study:

1. Foam index test results are sensitive to the method used, i.e., variations in foam index test methods lead to materials- and test-specific variations in results. Do not expect the same or necessarily comparable results from different foam index test methods even though they may be conceptually similar in general procedure and apparatus.
2. A predictive correlation between foam index test result and the dose of AEA required to stabilize 6 percent air in fresh concrete could be established for any of the four foam index methods studied. The reliability of that correlation varied among test methods and materials, however.
3. Foam index values should be reported in consistent units that normalize cumulative amount and concentration of AEA and the mass of cementitious materials present. Units

of mL of AEA per 100 kg cementitious materials (or US Customary equivalent), as commonly used in the industry for AEA dosages in fresh concrete, are recommended.

4. Test variations can rank ash interaction with AEA differently and can lead to different decisions concerning influence of fly ash or other mix constituents on air content.
5. For the fly ash samples tested in this study, the Bottle Shake test resulted in the strongest correlation with concrete air data followed by the Vial Shake test, Test Tube Shake and finally the Blender test.
6. Of the four foam index test variants studied, the most reliable correlation between foam index and concrete results was obtained with the Bottle Shake test. This was also the most repeatable and easiest to perform
7. A systematic study of the effects of variation in the foam index parameters on test results is necessary before an acceptable standard test method be recommended to the industry.

6.2 The Use of the Foam Index Test to Predict AEA Dosage in Concrete Containing Fly Ash: Part II-Development of a Standard Test Method: Apparatus and Procedure

6.2.1 Background

The foam index test can be a useful tool for predicting the air-entraining admixture (AEA) dosage for concrete containing fly ash or other supplementary cementitious materials. No standard foam index test protocol exists, but the development of a standard would benefit the concrete industry. Section 6.1 of this chapter focused on three foam index tests selected to represent the range of variants found in industry and literature. The three tests were evaluated by correlating test results of commercially available fly ash samples with the AEA dosage required to achieve 6 percent air content in fresh concrete. The results of the study showed that while variants of the test can be used to predict the AEA requirement of concrete mixes, correlations are unique to a given test method and combination of materials. The performance of multiple fly ashes was shown to vary depending on the specific foam index test used.

6.2.2 Introduction

ASTM Subcommittee CO9.24 on Mineral Admixtures has recommended the development of a standard foam index test method (Manz 1999). Before a reliable test can be selected, the factors to which the tests are most sensitive must be identified so that details and tolerances can be established. This study identified the influence of the following factors on the results of foam index tests: container dimensions, container fullness, test materials quantities and proportions, mixing procedure, AEA addition rate, and time between agitation and observation of the foam. Fly ash was the only supplementary cementitious material evaluated in this work, but many of the results are applicable to other SCMs as well.

One of the primary differences among the test variants used in Section 6.1 of this study (Harris et al. 2007) was the agitation method used to mix the ingredients and produce foam. Two of the tests used shaking by hand to mix the materials, and the third method used mechanical mixing via a kitchen-type blender. A clear advantage of mechanical agitation is the uniformity and repeatability of the mixing process (although the authors have also identified test variability in the blender method due to container and mixing blade configuration). Thus further work on a foam index test which uses some standardized mechanical mixing is needed, especially for

laboratory use. Nevertheless, the study reported here concentrated on manual agitation due to the benefits of simpler apparatus and ease of use at the source for cementitious materials or admixtures, or at the concrete batch plant. Thus it became important to develop a protocol that minimized variability associated with manual agitation, while controlling other factors that would apply equally to a mechanically agitated test.

6.2.3 Use of the foam index test

There are at least two basic applications of the foam index test. First, the test could be used to evaluate the influence of a single mixture ingredient on required dosage of AEA, with all other ingredients and proportions standardized (application 1). Alternatively, the test could be used as a mixture-specific evaluation of the combination of ingredients in the paste-phase of a particular concrete (application 2). (Aggregates are not present in a foam index test.) In this second case, all ingredients, consisting of cement, supplementary cementitious materials, water, and chemical admixtures, and proportions (other than water to cementitious materials ratio) would be identical to those used in a proposed mixture. Foam index test values would then be compared with those obtained by testing an established reference mixture. The results of this study apply to both applications of the method.

6.2.4 Scope

The basic foam index test procedure described by Freeman et al. (1997) and Külaots et al. (2003) was selected as the starting point for this investigation, in which 25 mL distilled water, 2.0 g ash and 8.0 g cement ($w/cm = 2.5$) are combined into a container with a tight-fitting cap. In the variant used by the present authors, the container is then shaken by hand for 30 s at approximately 2 shakes per second to break up agglomerates and wet the materials, and the following steps are then repeated until the endpoint is reached:

1. A calibrated pipette is used to add one 20 μ L drop of 5 percent concentration AEA solution to the container.
2. The container is capped and shaken 40 to 50 times over 10 s with a vertical displacement of 0.2 to 0.25 m.
3. The cap is immediately removed and the sample left undisturbed for 15 s to allow the foam to reach a “stable” state.
4. At the conclusion of the rest period, the foam at the air-water interface is observed for determination of the endpoint. (Recall that the endpoint is defined as a continuous foam cover at the air/liquid interface). When endpoint is reached the cumulative volume of AEA solution is recorded.

Variations on this basic test procedure studied included 1) container dimensions and fullness, 3) mixing procedure, 4) time permitted for AEA-cm-water interaction, and 5) time permitted for drainage of unstable foam. Isolation of variables was not always possible.

6.2.5 Reporting foam index values

Heretofore the result of a typical foam index test has been the cumulative volume of diluted AEA required to reach the test endpoint, expressed in number of drops or mL. The authors have subsequently converted the number of drops to a volume measurement of undiluted AEA by multiplying the number of drops by the drop volume and percent concentration. In a standard test where container geometry, mass of cementitious materials, water content, drop

volume and concentration of AEA were fixed, a volume measurement expressed in numbers of drops would be suitable for comparison of results. However, in this study using a range of material proportions and drop volumes, results were normalized by reporting cumulative volume of undiluted AEA divided by mass of cementitious materials, giving units of $\mu\text{L AEA/g cm}$ (μL is microliters and cm is the total mass of cementitious materials). This is numerically equivalent to the unit mL AEA/ kg cm . When multiplied by 100 the result is the unit commonly used in industry for admixture dosage: $\text{mL AEA}/100 \text{ kg cm}$. This value is called the “specific foam index” in this chapter, and is computed with the following equation.

$$SFI = \frac{100 \left(Dv \frac{c_{AEA}}{100} \right)}{cm} \quad \text{eqn. 6.3}$$

where SFI is the specific foam index, D is the number of incremental doses (drops) of AEA solution added to reach the endpoint, v is the volume per drop (μL or mL), c_{AEA} is the percent AEA concentration (e.g. a 10 percent concentration is equal to 10 volume units of AEA as received from the manufacturer mixed with 90 volume units of water) and cm is in units of grams (if drop volume in μL), or kilograms (if drop volume is in mL).

6.2.6 Fly Ash/Cement Samples

The cement and four fly ash samples used in Section 6.1 are also used throughout the work reported in this chapter. Key material properties are shown in Table 6.14.

Table 6.14: Material Properties

Ash	Type per ASTM C 618	LOI	AEA dosage for concrete air content of 6% ¹	
			mL/100kg cm	Fl oz/100 lb cm
H	F	0.8%	139	2.1
MH	F	0.4%	64	1.0
ML	F	0.1%	49	0.8
L	F	0.6%	24	0.4

1. AEA wood rosin based unless noted otherwise

2. Cement met ASTM C150 Type I or Type II, Blaine fineness $376 \text{ m}^2/\text{kg}$, 0.55% Na_2O equivalent

6.2.7 Container geometry

Whether developing a standard test for a single mix component, or a mixture-specific test for a system of ingredients, the starting point is a specimen container. Because this container need only fit in the hand, many different sizes and shapes might be selected, and each of those could be filled to various fractions of their capacity. The influence of container geometry and fullness on foam index was therefore investigated. Although the authors developed the following model for container-effects after a great deal of trial-and-error experimentation, the model is presented first to aid in understanding test results.

Observations of foam index tests using a variety of containers suggest that the thickness of the foam layer that exists on the liquid surface at the test endpoint is nearly constant (approximately 4-5 mm for the AEA and test materials used in this study), regardless of the surface area of the liquid-air interface in the container or amount of paste present. (Figure 6.7 is a representation of the test at the endpoint conditions.) The volume of foam produced is therefore equal to the foam thickness, t_f , multiplied by the surface area of the container at the liquid surface, A_c . The volume of paste present in the container is equal to A_c multiplied by γh where h is the inside height of the capped container and γ is the ratio of the volume of paste to the total volume of the container. The value of γ can range from 0 to 1 and hereafter will be referred to as the fill ratio.

Achieving the endpoint is therefore equivalent to achieving an air/paste volume ratio that can be computed from the thickness of the foam layer, and the filled-height of the paste. Further, this test-specific air/paste ratio associated with endpoint and the dose of AEA required to reach endpoint are related via the principle that in air entrained pastes and concretes the volume of foam stabilized by an AEA relative to the volume of paste is approximately proportional to the volume of AEA per unit mass cm. (This is the rationale behind specifying dosage of AEA in air entrained concrete on the basis of volume of AEA per unit mass cm (Dodson 1990, Rixom and Mailvaganam 1986, Ramachandran 1984, Whiting and Nagi 1998). Thus, at the foam index endpoint, the volume of foam present can be defined as a fraction of the paste volume as shown in equation 6.4. (Note that any air trapped in the paste is ignored in this model, since at the high water contents used in this test the air bubbles escape to the surface.)

$$\frac{A}{p} = \frac{A_c t_f}{A_c \gamma h} = \frac{t_f}{\gamma h} \quad \text{eqn. 6.4}$$

Where A/p is the air/paste ratio, A is the volume of foam (air content) at the surface of the paste at endpoint, p is the volume of paste in the container, A_c is the surface area of the container at the air-paste interface, t_f is the thickness of the foam, γ is the fill ratio and h is the container height. These variables are illustrated in Figure 6.7.

This means that for a given container and thickness of foam layer at endpoint, the greater the fill ratio, γ , the lower the specific AEA dosage (volume AEA per mass cm) that will be reported in the foam index test, since the foam layer will represent a smaller proportion of the paste volume. Likewise, for a constant fill ratio, the same decrease in specific foam index will be observed the taller the container (increasing h). Note also that for containers with constant cross section versus height the results are independent of the surface area of the air-water interface, and thus independent of container width or diameter. The specific foam index should therefore be proportional to the inverse of the fill ratio multiplied by the container height ($1/\gamma h$). The following experiment was performed to evaluate this hypothesis.

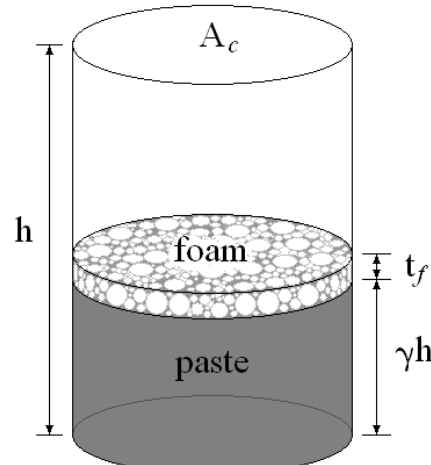


Figure 6.7: Foam index test container dimensions.

Experiment

Fifty-two foam index tests were performed in eight containers of differing dimensions. The containers are pictured in Figure 6.8 with descriptions given in Table 6.15. The same paste composition was used in each test and consisted of 1 part cement, 1 part Ash H and 5 parts water by mass. The tests were performed with fill ratios varying from 8 percent to 86 percent. AEA increments were added in 20 microliter drops of 5 percent concentration.

Table 6.15: Description of test containers.

Container no.	Volume, mL	Ave. interior height, mm	Surface area, mm ²
1	33	41	814
2	66	48	1372
3	132	83	1590
4	25	59	426
5	35	86	405
6	58	109	603
7	24	152	158
8	53	174	305



Figure 6.8: Containers used in the foam index variability study on container geometry.

Results

Specific foam index values (mL AEA/100 kg cm) versus $1/\gamma h$ for all eight containers are shown in Figure 6.9. Though the same AEA and paste composition was used in all tests, specific foam index values varied between approximately 80 and 800 mL AEA/100 kg cm—a ten-fold variation in foam index values due only to changes in container and fill-height. As predicted, the general trend of increasing specific foam index with increasing $1/\gamma h$ appears to be independent of the container type. The upper horizontal axis indicates air/paste volume ratio at endpoint, computed using equation 6.2 with k equal to 4 mm, and the same generally linear trend is evident. The error bars indicate the minimum resolution to plus or minus one incremental AEA dose as discussed later.

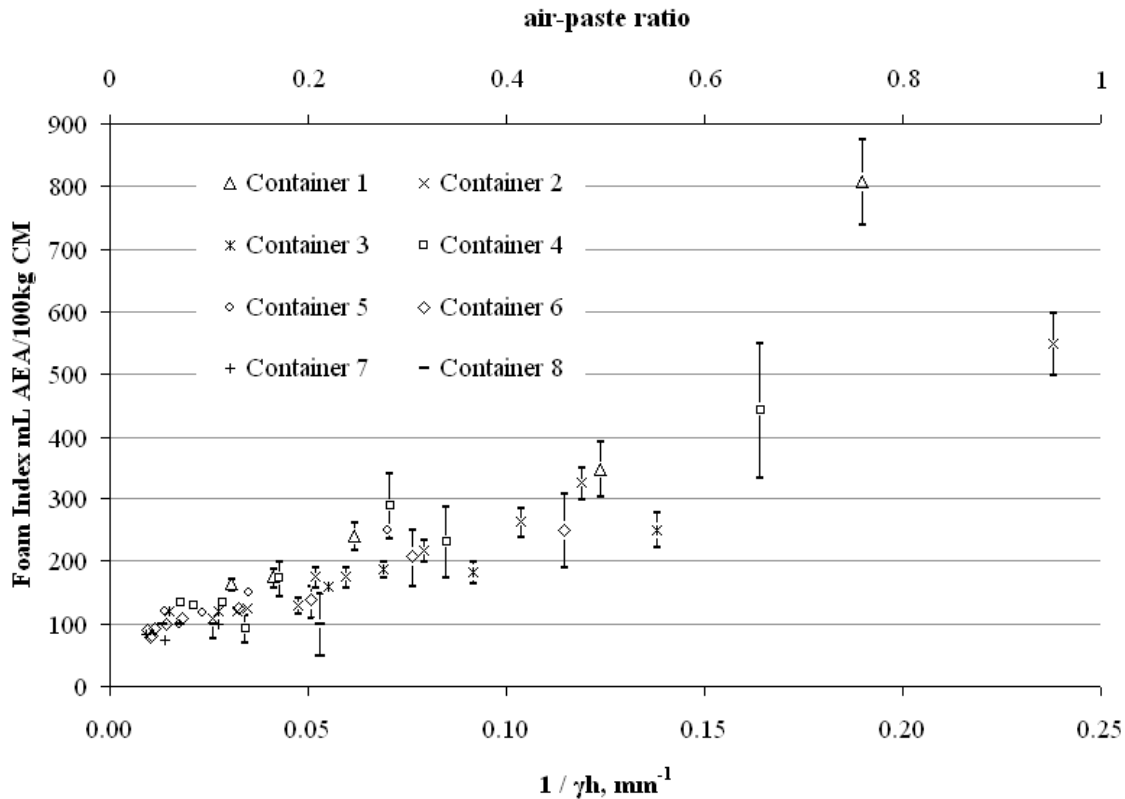


Figure 6.9: Specific foam index versus $1/\gamma h$ for fifty-two tests in eight containers. Air/paste ratios computed for t_f equal to 4mm. Error bars show the minimum resolution as plus or minus one drop of AEA solution.

Discussion

Corroboration of hypothesis

For values of $1/\gamma h$ in the range of 0.01 to 0.17, the specific foam index increases proportionally with $1/\gamma h$ as predicted, confirming that filled height is the key test parameter and not container height, diameter, or even paste volume per se. It is also clear that specific foam index values can only be compared directly among tests with equal filled height. (Corrections from one container to another can be made, and as will be discussed, and container diameter does influence minimum resolution).

Spread in the data may be due to the fact that the containers shown in Figure 6.8 are not uniformly cylindrical with height (with greatest impact at fill ratios near the extremes of zero or one), the ability to accurately measure t_f in all tests, and the effects of very high or low fill ratios (to be discussed.)

Recommendations for a standard test

Limits on container geometry and paste quantity used in the test can be recommended on the basis of the previous discussion and experimental results. Limits on container geometries

were determined based on the air/paste ratio, physical limits on the fill ratio, effects of paste quantity on resolution, and testing convenience.

Air/paste ratio

The foam index test should stabilize an air/paste ratio similar to that of typical air-entrained concrete (even though the water to cementitious ratio is much higher in the test paste, limiting direct comparison). Boundaries of 10 to 20 percent for A/p are reasonable. For t_f values between 4 and 5 mm in equation 6.4, the recommended maximum γh (the height of the paste in the container in mm) based on 10 percent air/paste is 50 mm. For filled heights greater than 50 mm, the air/paste ratio becomes much less than in typical air entrained concrete. A recommended minimum γh of 20 mm is based on 20 percent air/paste.

Fill ratio

As the value of the fill ratio, γ , nears 1, the headspace (the air-filled space above the paste) decreases until insufficient space remains for air, mixing of materials, and accumulation of foam. Thus, for a container of a given height, as γ approaches 1 the specific foam index must also increase due to the inefficiency of mixing and foam formation, as demonstrated by the following experiment.

Two groups of containers were used to perform the test: group 1 consisted of 5 containers with equal inner diameters but different heights, group 2 consisted of 4 containers with equal inner diameters but different heights. The containers were filled with paste of the composition used in the previous experiment. Fill ratios ranged from 0.52 to 0.95 in group 1 and 0.54 to 0.95 in group 2 and were selected so that the filled height of paste (γh) was 50 mm in all tests (i.e., $1/\gamma h = 0.02 \text{ mm}^{-1}$). Test results shown in Figure 6.9 show that for a constant filled height, the specific foam index is independent of fill ratio at values lower than about 0.85. At higher fill ratios the AEA requirement begins to increase rapidly. Given the difference in foam index values between container groups; however, it is suggested that the fill ratio be limited to less than about 75 percent.

Alternatively, as the fill ratio approaches zero, there will be a limit where there are insufficient materials present, both solid and liquid, to adequately form and stabilize the foam. When the limit is reached, specific foam index would again be expected to increase. The limit is likely dependent on container height, since for a constant fill ratio, relatively tall containers will have greater filled heights than relatively short containers. This may be observed in the test results shown in Figure 5.9, for containers 1 and 6. At a fill ratio of 0.13 for container 1 (this corresponds to $1/\gamma h$ equal to 0.19), the specific foam index value deviates with a larger than predicted specific foam index. However, at a fill ratio of 0.08 for container 6 (this corresponds to $1/\gamma h$ equal to 0.11), the specific foam index value behaves as predicted. For all the containers used, fill ratio values of 0.2 or greater produced the predicted linear behavior. Therefore, a minimum fill ratio applicable to the containers used in this study is established at 0.2.

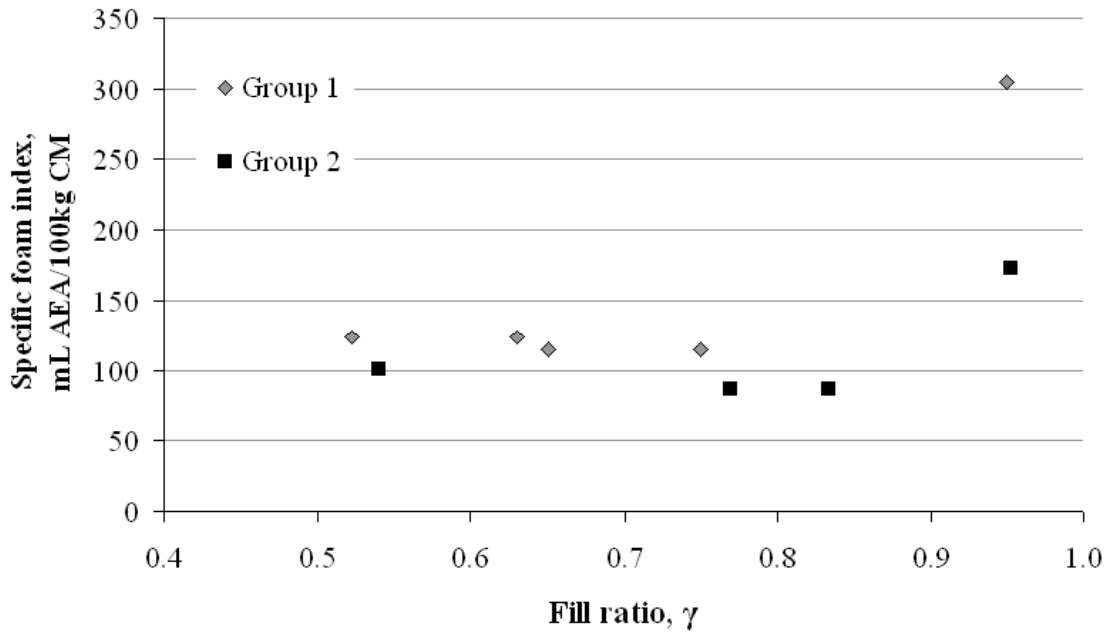


Figure 6.10: Specific foam index versus fill ratio. The value of $1/\gamma h$ was equal to 0.02 mm^{-1} in all tests.

Minimum resolution

The SFI reported is the cumulative result of a number of discrete increments, with \pm the amount of undiluted AEA in one drop defining the minimum resolution of the test, R_{\min} . This is seen in equation 6.5, which is derived from equation 6.3 by inserting a value of 1 for D (a single drop). Minimum resolution is reduced by increasing the mass of cementitious materials, or by reducing drop volume or AEA concentration.

$$R_{\min} = \frac{100 \left(v \frac{c_{AEA}}{100} \right)}{cm} \quad \text{eqn. 6.5}$$

Since the same AEA drop volume and concentration were used in all tests reported in Figure 6.3, the error bars, $\pm R_{\min}$, vary only with mass of cementitious materials. As can be seen in equation 6.5, for a given container the mass of cementitious materials increases with filled-height, decreasing R_{\min} . For example, for Container 4 at with filled height = 6 mm (paste volume = 2.6 mL), $R_{\min} = 111$ mL AEA per 100 kg cm. For the same container filled to 56 mm (paste volume = 23.8 mL), $R_{\min} = 12$ mL AEA per 100 kg cm. Maximizing mass of cementitious materials is therefore recommended to reduce minimum resolution.

The recommended minimum paste volume can be established on the basis of selected R_{\min} and practical limitations on minimum drop volume and concentration. An appropriate value for R_{\min} would be in the range of 10 percent or less of the reported specific foam index, requiring adjustment of test parameters after an approximate SFI has been determined. Otherwise a value no larger than 10 mL/100 kg cm is recommended for R_{\min} on the basis of the materials evaluated

here, corresponding to a 5 to 10 percent minimum uncertainty in specific foam index values between 100 and 200. Further, values of R_{min} greater than 10 mL/100 kg cm could make it difficult to differentiate among the foam-forming or foam-inhibiting potential of some mixture ingredients based on foam index.

For the various pipettes used in this study, drop volumes less than 20 microliters had unacceptable variability (pipette precision is discussed in more detail later). While a wide range of AEA concentrations can be accurately prepared, 5 percent concentration was used in this study. When a drop volume of 20 μ l and a 5 percent concentration are inserted into equation 6.5, one may compute that at least 10g of cementitious materials are required for an R_{min} of 10 mL/100 kg cm. This corresponds to a minimum paste volume of approximately 30 mL, assuming water to cementitious ratio (discussed later in this chapter) between 2 and 2.5 and specific gravities for cement and fly ash of 3.1 to 3.3, and 2 to 3, respectively. If drop volume cannot be reliably reduced further, R_{min} can be halved by doubling the mass of cementitious materials, or diluting the AEA to a 2.5 percent concentration. Whenever the test is performed, however, regardless of the selected parameters, R_{min} should be reported with test results.

Relationships between test values

Based on the results presented in this section, it has been shown that for two cylindrical containers of differing geometries and filled heights, the volume of undiluted AEA required to reach the endpoints in both containers is proportional to containers' cross sections as shown in eqn. 6.6, provided the same paste is used in both tests.

$$\frac{V_{AEA1}}{d_1^2} = \frac{V_{AEA2}}{d_2^2} \quad \text{eqn. 6.6}$$

Where V_{AEA_i} is the volume of undiluted AEA required to reach the endpoint and d_i is the container diameter. For the specific case in which the tests are performed in containers having the same interior diameter ($d_1 = d_2$) the volumes of undiluted AEA required to reach the tests endpoints are constant independent of the amount of paste present even though the dosage of undiluted AEA per unit mass of cementitious materials will depend on test parameters. This means that increases or decreases in paste volume are exactly compensated by a corresponding proportional decreases or increases in air-paste ratios of the endpoints.

One of the implications of this relationship on the test is that if standard container and paste proportions were used for the test, results reported in units of volume of undiluted AEA would be constant regardless of the volume of paste (and corresponding filled height) used. However, because AEA is added in stepped increments, instead of a continuous manner, R_{min} becomes a crucial parameter in the precision of the test. In tests performed with relatively low volume of paste (and therefore low cm) the minimum resolution of the test is greater (lower precision) than a test performed with greater paste volume.

Container diameter, caps, and cleanliness

While choice of container diameter does not influence the specific foam index obtained, diameter does affect mass of paste for any given filled-height, and thus influences the minimum resolution, R_{min} . The relationships expressed in equation 6.5, coupled with the influence of filled height and diameter on paste are summarized in Figure 6.11. The figure also includes a

recommended minimum diameter based on the ability to clearly discern the end point as an unbroken blanket of foam, and a maximum diameter of 60 mm based on the ability to comfortably hold and shake the container.

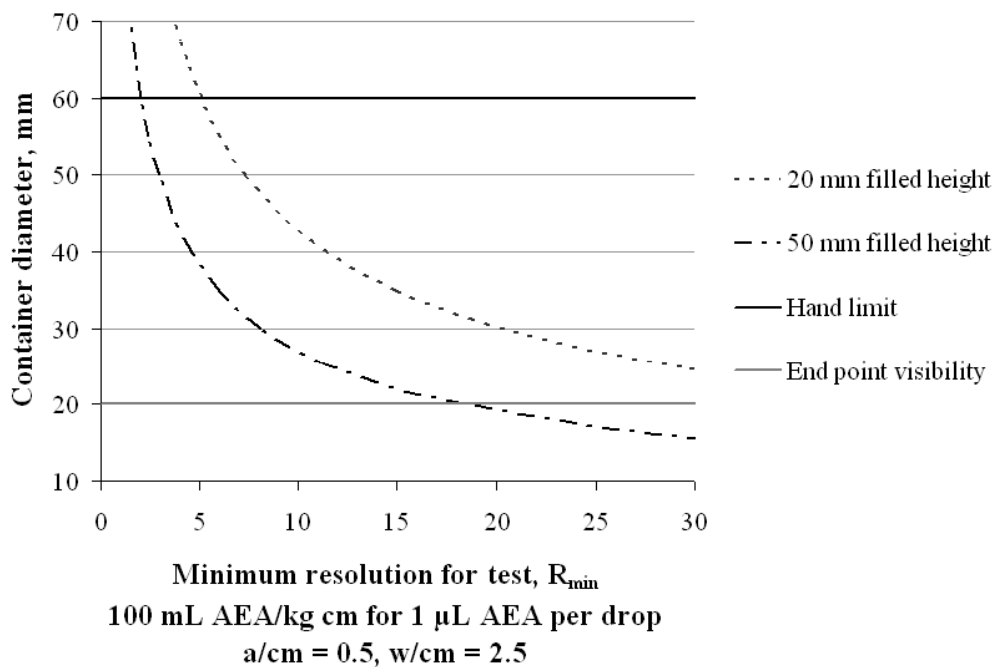


Figure 6.11: Relationships among container diameter, filled height, and minimum resolution, R_{min} .

Test containers must have tightly sealing lids that can be placed on and removed easily to avoid disrupting the foam. Containers with horizontal bases (containers 1 through 5) can be placed on the countertop during the rest period. Containers without horizontal bases (containers 6, 7 and 8) require use of a holder to keep the test materials stable during the rest period.

The containers used in this study were typically cleaned with detergent and brush and reused. Over time, clouding of the container walls was observed in all tests that incorporated cement. It was also observed that while the use of clouded containers considerably increased the amount of AEA required to stabilize foam in distilled water, no measurable effect was observed for foam index tests that included cementitious materials. It is further recommended that container lids with paperboard seals be avoided since solid material can accumulate between the lid and seal, and the seals can absorb the test fluids.

Summary of container geometry

The recommendations for fill ratio, filled height, minimum resolution, and diameter are summarized in Figure 6.12. Since choice of diameter and R_{min} , are coupled as shown previously in Figure 6.11, it may be necessary to adjust drop volume or AEA concentration to find an acceptable solution compatible with available containers.

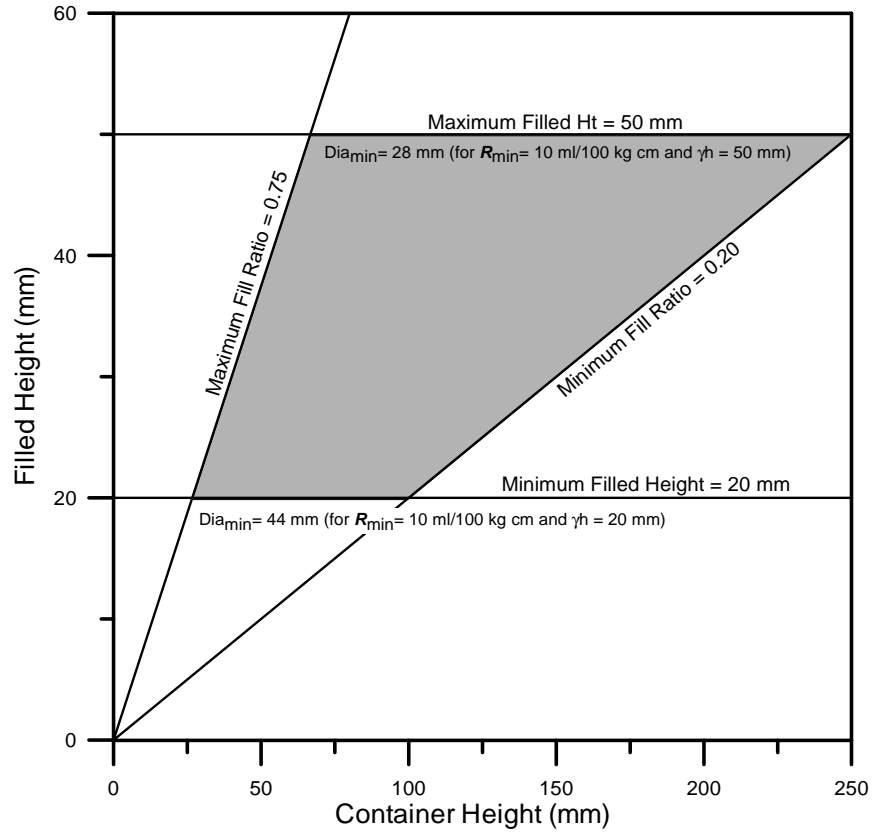


Figure 6.12: The shaded zone identifies the range of acceptable solutions for a container for the foam index test.

On the basis of conducting hundreds of foam index tests in the past two years the authors recommend the following:

Table 6.16: Description of an ideal container for the foam index test

Container	Plastic, wide-mouth, screw on lid, cylindrical shape
Volume	200 mL
Fill ratio	40%
Filled height	40 mm
Diameter	50 mm
Volume of paste	100 mL
Approximate air/paste vol. ratio at endpoint	10%
Volume per drop, v	20 μ L
AEA concentration, c_{AEA}	5%
Undiluted AEA volume per drop	1 μ L per drop
Minimum resolution, R_{min}	5 mL AEA/100 kg cm
Typical range of specific foam index obtained	30 to 200 mL AEA/100 kg cm
Typical range of R_{min} / SFI	3-16%

6.2.8 Container agitation

It was recognized early in the experimental program that variations in agitating the test container affected test results. For that reason a standard protocol was used for the all tests reported in Section 6.1 and for those tests reported above. A full “shake cycle” began with the container held in raised hand then rapidly lowered by 0.2 to 0.25 m and returned to the starting position, with a frequency and duration of approximately 40 shakes in 10 s. The influence of shaking was investigated by performing fourteen tests in which frequency was varied between 1 and 5 shakes per second and the shaking duration was varied between 5 and 15 sec. During a single test the same shaking frequency and duration was used from the first AEA addition until the endpoint was reached. Each test was performed in container no. 3, 2 grams of ash MH, 8 grams of cement and 25 mL of water, with a wood rosin AEA and R_{min} equal to 10 mL/100 kg cm.

Frequency was measured by dividing the number of shaking cycles over the shaking duration to get number of shakes per second. For 1 shake/sec, the shaking was done in-sync with the seconds of a digital timer with little variation in frequency. For shaking frequencies greater than 1 shake/sec, variability was within approximately ± 10 percent of the target frequency, i.e., 2.5 ± 0.2 shakes/sec and 4 ± 0.4 shakes/sec.

As shown in Figure 6.13, foam index values for ash sample MH were primarily sensitive to the number of shakes in the agitation phase, and secondarily sensitive to frequency. For any given number of shakes, higher frequency (more energetic) shaking generally results in a lower

specific foam index, meaning that a lower dose of AEA is required to stabilize enough foam to reach endpoint when the container is shaken more vigorously. It also appears that foam index begins to stabilize after about 40 shakes, and at about this number of shakes approximately the same specific foam index value is obtained for frequencies of 3 to 5 shakes per second. It is obvious, therefore that if manual agitation is to be used it must be standardized, and on the basis of this experiment a frequency of 4 ± 0.5 shakes/sec and duration of 10 s are recommended to minimize the effect of minor variations in technique. This recommendation is also based on the physical difficulty of manually shaking the container at 5 or more shakes per second, or for more than about 15s, particularly when many AEA drop increments are required to reach the endpoint. It is likely that other agitation schemes would be more effective for other containers, masses of materials, paste viscosity, and choice of AEA. This is particularly true when mechanical mixing is considered. As a final note, maximum mixing and foam generation is likely to result from agitation parameters that match the resonant or “sieching” frequency of standing waves in the container. For the small containers typically used in the foam index test such frequencies may be higher than can be achieved by hand shaking (Dean and Daylrimple, 1991).

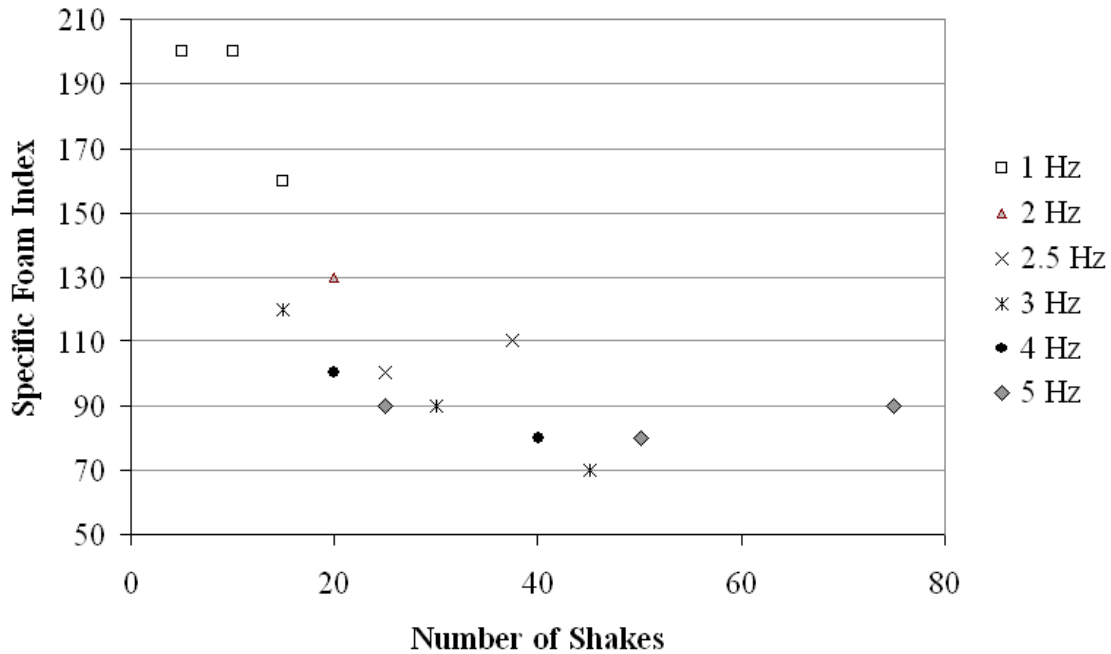


Figure 6.13: Specific foam index obtained at various shaking frequencies and shaking durations.

6.2.9 Rest period duration

The rest period between the end of agitation and the time of observation for determination of endpoint allows unstable bubbles to collapse until a quasi-stable state is reached. Definition of the endpoint therefore includes the time period after agitation at which this quasi-stable foam is observed. To explore foam stability with time and its effect on foam index test results the four fly ash samples were individually tested, using 2g ash, 8g cement, and 25 mL water. After each shaking step, existence of endpoint condition was assessed at 15, 30 and 45

seconds after agitation. In all cases stable endpoints that existed at 15 sec were also stable after 45 sec. It was concluded that for the cementitious materials and AEA used a 15 sec wait period was always sufficient. However, for tests in which endpoint conditions were “just” reached with the addition of the final AEA dose, the foam cover would occasionally break as bubbles collapsed if containers were left undisturbed for several minutes after endpoint was reached. For tests in which the final AEA increment was more than enough additional AEA to reach endpoint the foam could remain stable until the cement on the bubble coatings hardened. A standard rest period of 20 s is therefore recommended so that the combined shaking/rest period duration is an even 30 s. This also allows ample time to tally the number of drops of AEA added and prepare another drop for the following shaking sequence. (A longer rest period is not required as long as the usual ± 1 -drop uncertainty is acceptable.)

6.2.10 Influence of AEA concentration and drop volume on precision

As discussed earlier, the minimum resolution of the test depends on a number of factors including AEA and drop volume. Since these factors also define the size of the foam index increment from one iteration of the test to the next, these factors in combination with the nature of the materials being evaluated define the number of iterations to reach endpoint. Since a single iteration requires addition of an incremental drop followed by 10 seconds of agitation and then a 20 second rest period, many such cycles become tedious and physically tiring (and make the case for automation and mechanical agitation). Based on the experience gained during this study, an upper limit of about twenty shaking sequences is recommended per test, and to reach endpoint in 20 iterations or less it may be necessary to adjust the step-size of the incremental doses by increasing or decreasing drop volume or AEA concentration.

However, since it has been reported that time is required for a given dose of AEA to fully interact with air, water, and cementitious materials, (Külaots et al. 2003, Baltrus and LaCount, 2001) it is possible that agitation and rest period duration may have to be adjusted along with changes in AEA concentration and drop volume (Hill et al. 1997, Yu et al. 2000, Baltrus and LaCount 2001). To evaluate this issue foam index tests were performed on each of the four fly ash samples using undiluted AEA volumes/drop (i.e., R_{\min}) of 6.7 and 13.3 mL AEA/100kg cm/drop, achieved via 20 microliter drops with AEA concentrations of 5 and 10 percent, with 15 g cm (5 g ash and 10 g cement). Container no. 6 was used with 30 mL water.

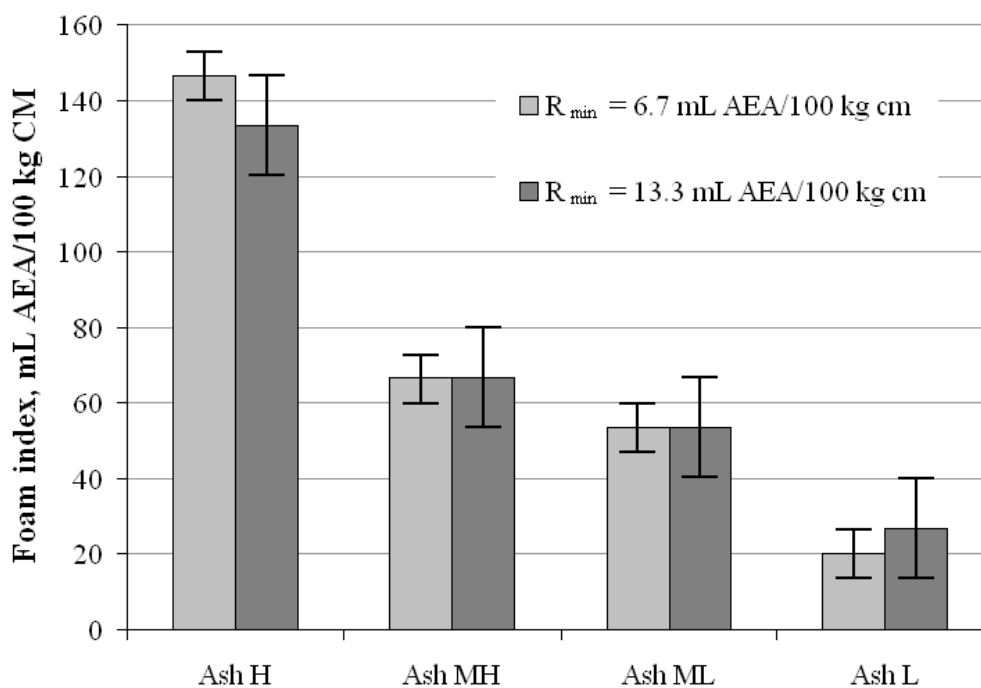


Figure 6.14: Specific foam index values of four ash samples for two values of R_{min} .

The results of the tests are shown in Figure 6.14, where error bars represent plus or minus a single incremental AEA dose (R_{min}). While the differences due to AEA per increment and corresponding number of increments to complete the test are smaller than R_{min} , the increased precision achieved by a smaller R_{min} is clearly shown. It is therefore recommended that dosage be adjusted to adequately identify AEA interactions but not so small that more than about 20 incremental doses are required so as to control the overall duration of the test procedure.

6.2.11 Pipette accuracy/precision

Due to their impact on foam index test results, precision and accuracy of the pipets used in this study were evaluated by determining the mean, standard deviation and distribution of drop volumes, determined by individually weighing 30 drops of distilled water, then calculating water volume based on temperature-adjusted density. Results were normally distributed with a mean of 20.4 μ L and standard deviation of 0.26 μ L.

On the basis of these data, pipette suitability was explored by Monte Carlo simulations, in which normally distributed drop volumes were generated randomly for a given mean and standard deviation. The AEA contents of the simulated drops were calculated by multiplying drop volumes by a given concentration, and the minimum discrete number of drops required were tallied to accumulate a total dose of 20 microliters undiluted AEA (value taken from actual test results reported earlier). Figure 6.15 shows the percentage of simulations (out of 1,000 simulations for each data point) in which the results were within plus or minus one drop of the mean number of drops required to reach the target total AEA volume. Mean drop volume and concentrations were selected so that a single drop consisted of approximately 1 microliter of

undiluted AEA. For each data set, a variety of standard deviations were evaluated to determine the effects on test precision.

Based on these results, for 90 percent of tests to be within 1 drop of the mean of 1,000 tests, a drop-size standard deviation approximately 10 to 12 percent of the mean drop volume is required. Less precise pipettes will result in a minimum uncertainty in test results that exceeds \pm the undiluted AEA dose in a single drop. These results apply to tests in which 20 drops or less is required to reach the endpoint. When greater than 20 drops are required, standard deviation must be decreased still further to maintain 90 percent confidence. For accurate measurements, the value of drop volume, v , in equations 6.3 and 6.5 should be equal to the mean drop volume produced by the pipet.

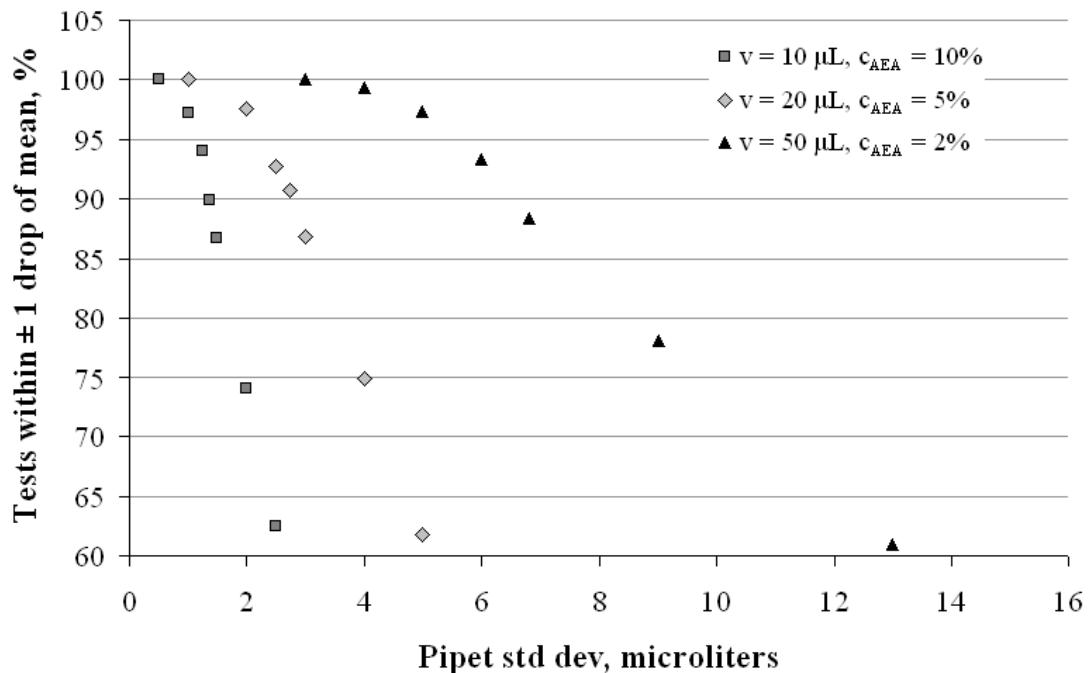


Figure 6.15: Percentage of tests within one drop of the mean number of AEA drops to transfer a minimum of 20 microliters of AEA versus pipet standard deviation. Variable v is equal to drop volume in microliters and variable c_{AEA} is equal to AEA concentration.

6.2.12 AEA degradation with time

Kulaots et al. (2003) as well as the authors have observed an apparent loss of effectiveness or “aging” of commercial AEA solutions over less than a few weeks of laboratory storage, although behavior was inconsistent among various AEA types and concentrations. AEA solutions stored at constant lab temperatures (21-23 C) and opened only during performance of the foam index tests began to degrade after about three weeks. Rate of degradation was more rapid for lower concentrations, or increased headspace above the liquid inside the closed containers, or with exposure to sunlight (or perhaps moonlight). In contrast, leaving containers open to the atmosphere increased AEA effectiveness, perhaps due to increased AEA

concentration as water evaporated. Aging effects alone had a variable influence on foam index results, ranging from no discernable effect to increasing specific foam index by as much as 60%.

Because any change in AEA potency, either increasing or decreasing, will result in inconsistent testing, it is recommended that solutions be replaced after 2 weeks. Test solutions should be stored away from direct sunlight in tightly sealed containers. It is therefore recommended that AEA be stored in full containers, in a dark cabinet, and discarded after two weeks. A foam index test should be performed with known materials for each new supply of AEA to check batch-to-batch variation. (AEA aging effects in the field may be an important topic of study.)

6.2.13 Test Repeatability

The repeatability of the test method based on the guidelines recommended in this chapter were assessed by using container number 6 with filled height of 50 mm and fill ratio of 0.46. The mass of cementitious materials was equal to 12.5 g, with w/cm equal to 2.0, and ash/cm equal to 0.33. Shaking was done at 4 ± 0.5 shakes per second for ten seconds followed by a 20 sec wait period. Drop volume was 20 microliters at a 5 percent AEA concentration. Tests on the four ash samples of Table 1 were performed by three operators in a single lab. The same containers, AEA solution, and pipette (standard deviation of 0.6 μL for 20 μL drops) were used in all tests.

The results of the test are shown in Figure 6.16. The horizontal lines in the figure represent single AEA dose increments ($R_{\min} = 8 \text{ mL AEA}/100 \text{ kg}$). For all ash samples the variability in the test was less than or equal to plus or minus R_{\min} . For Ash H, variation from the mean ranged from 1.5 to -3.1 percent. For ashes MH and ML in which fewer total increments were required, the error of a single incremental dose results in variations of up to 10 percent of the mean value. For Ash L all tests reported the same specific foam index value. These results generally confirm the precision of the test is within plus or minus one incremental dose ($\pm R_{\min}$, per equation 6.5).

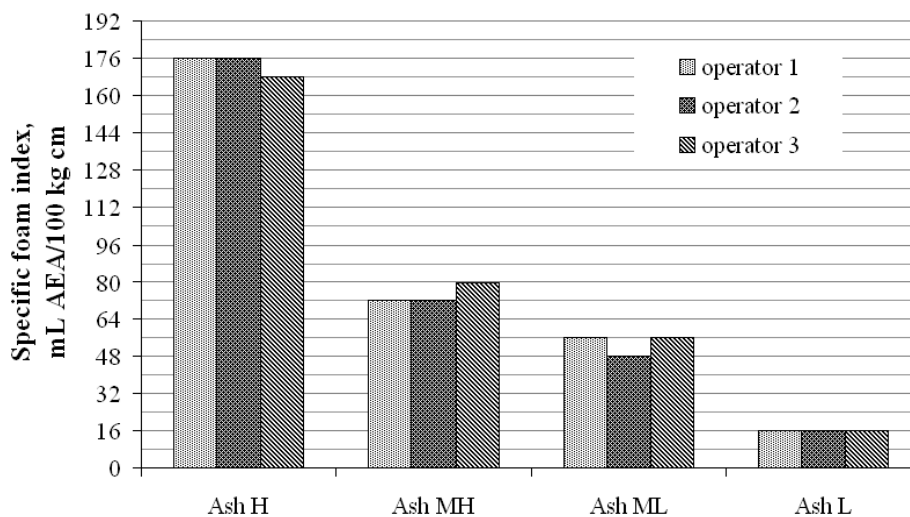


Figure 6.16: Specific foam index values of four fly ash samples produced by three test operators. Each horizontal line in the graph represents a single drop volume ($R_{\min} = 8 \text{ mL AEA per } 100 \text{ kg cm}$).

6.2.14 Comments on material proportions

As discussed in detail later in this chapter, the ratios of water to cement (w/cm), and ash to cementitious materials (a/cm) have a significant influence on foam index test results. In essence, results of foam index tests can only be compared directly when the apparatus and procedure are fixed as described here, and when the w/cm and a/cm values are fixed as well. When performing a foam index test to explore a given concrete mixture, the a/cm for that mixture should be replicated in the foam index test (as well as replicating the cement and ash used in the concrete.) The water to cementitious materials ratio required in the foam index test must be considerably higher than in typical concrete, however, to achieve the fluidity necessary to mix the materials, form a stable foam endpoint, and allow bubbles to rise to the liquid surface after agitation. While w/cm equal to 2.5 is commonly used in foam index tests, and other researchers have used w/cm as high as reported 8.3, the current study used w/cm ranging from 2.5 to 25. It was determined in this study that w/cm of 1.5 is an absolute minimum for foam index testing, and as will be shown, values from 2.0 to 2.5 are recommended. While such values are obviously high relative to typical concrete, it is useful to point out other common tests, such as the volume air meter (ASTM C 173) and the Chace air indicator (AASHTO T-199) increase the w/cm ratio to approximately 3 and 8, respectively, to aid separation of air from paste.

6.2.15 Conclusions

As described in section 6.1, several variations of the foam index test have been used successfully to predict the required dose of AEA in air entrained concrete, but such predictive correlations depend on the specific combination of materials and the specific foam index test method. This is true whether one is using the foam index to evaluate a single component with all other ingredients standardized, or to evaluate a specific combination of materials unique to a particular concrete mixture. If the foam index is to have broader application, allowing comparison of results among multiple users, standardization of the following aspects of the test method is recommended.

1. Test results should be reported in units of mL AEA /100 kg cm (or is US customary equivalent) to account for drop volume, AEA concentration, and mass of cementitious materials, yielding a unit that is numerically compatible with that commonly in use for AEA proportions in concrete mixtures.
2. Results are specific to the container used. Foam index values, in units of mL AEAE/100 kg cm, can only be compared when the filled height of paste in the test containers are equal.
3. For a simple hand-test, as can be performed in any lab or plant site, the geometry of prismatic, sealable containers is defined by limits on interior height, maximum and minimum fill ratio, volume of paste at filled-height, minimum resolution, and convenience, as described in Figures 6.12 and 6.13. An ideal container is described in Table 6.16.
4. While agitation by hand has been shown to be practical and reproducible, foam index test results are sensitive to the number and frequency of shaking cycles. A shaking duration of 10s and shaking frequency of 4 ± 0.5 shakes/sec is recommended.
5. For the AEA and cementitious materials used in this study the duration of the rest period was not a significant factor when kept between 15 and 45 seconds. A 20-second rest period is recommended.

6. AEA effectiveness can degrade with storage time. AEA solutions should be tightly capped in filled containers, stored in the dark, and discarded after 2 weeks.
7. The mean and standard deviation of the drop volume as dispensed by the pipette affects precision of the foam index test. Pipette standard deviation should be no more than about 10 percent of the mean drop volume.
8. The minimum resolution of the test can be adjusted based on drop volume, AEA concentration, and mass of cementitious materials. R_{min} should be computed and reported with test results.
9. Drop volumes of 20 microliters (dispensed with a pipet) and AEA concentrations of 5 percent were determined to be suitable in the tests performed in this chapter. Repeatability of the test among three independent operators in the same lab is within the minimum resolution.

6.2.16 Recommendations for further study

Recommendations for additional improvement to the development of a standard method include: study of the combined effects of agitation frequency and duration with a variety of containers and fill ratios, inter-laboratory comparison of tests for the measurement of test variability, and development of a mechanically agitated foam index test to reduce the variability and labor-intensiveness of agitation by hand.

6.3 The Use of the Foam Index Test to Predict AEA Dosage in Concrete Containing Fly Ash: Part III-Development of a Standard Test Method—Proportions of Materials

The foam index test can be a useful tool for predicting the air-entraining admixture (AEA) dosage for concrete containing fly ash or other supplementary cementitious materials. No standard foam index test protocol exists, but the development of a standard would benefit the concrete industry. This is the third of three parts reporting a study of the comparison of variations on the foam index test and examining the procedural factors that influence results with the goal of developing a standard test. Section 6.1 of this chapter focused on three foam index tests selected to represent the range of variants found in industry and literature. The three tests were evaluated by correlating test results of commercially available fly ash samples with the AEA dosage required to achieve 6 percent air content in fresh concrete. The results of the study showed that while variants of the test can be used to predict the AEA requirement of concrete mixes, correlations are unique to a given test method and combination of materials. The performance of multiple fly ashes was shown to vary depending on the specific foam index test used.

Section 6.2 of this study examined the influence of the following factors on foam index test results: container geometry, container fullness, container agitation, rest period duration, drop volume/AEA concentration, pipette precision and AEA degradation. Based on the findings, recommendations for standard practice were given for each factor.

6.3.1 Introduction

ASTM Subcommittee CO9.24 on Mineral Admixtures has recommended the development of a standard foam index test method (Manz 1999). Before a reliable test can be selected, the factors to which the tests are most sensitive must be identified so that details and

tolerances can be established. This study focuses on the influence of materials proportions on foam index test values. Specifically, the influences of ash/cm and water/cm ratios were examined as well as the effects of the individual ingredients on foam index value. Recommendations for standard practice regarding the proportioning of materials are given.

6.3.2 Scope

The basic test procedure described in the scope of Section 6.2 was used throughout the study. This section discusses several experiments that were performed in which the test procedure was held constant but the material proportions were varied. Variations from the standard test described in Section 6.2 are described when the study is introduced.

6.3.3 Use of the foam index test

Two basic applications of the foam index test were described in Section 6.2 and are mentioned briefly here. First, the test could be used to evaluate the influence of a single mixture ingredient on required dosage of AEA, with all other ingredients and proportions standardized (application 1). Alternatively, the test could be used as a mixture-specific evaluation of the combination of ingredients in the paste-phase of a particular concrete (application 2). The results of this study can be applied to both applications.

6.3.4 Fly Ash/Cement Samples

The cement and four fly ash samples used in Section 6.1 and 6.2 are also used throughout the work reported in this section. Key material properties are shown in Table 6.17.

Table 6.17: Material properties

Ash	Type per ASTM C 618	LOI	AEA dosage for concrete air content of 6% ¹	
			mL/100kg cm	Fl oz/100 lb cm
H	F	0.8%	139	2.1
MH	F	0.4%	64	1.0
ML	F	0.1%	49	0.8
L	F	0.6%	24	0.4

1. AEA wood rosin based unless noted otherwise
2. Cement met ASTM C150 Type I or Type II, Blaine fineness 376 m²/kg, 0.55% Na₂O equivalent

6.3.5 Water, cement and ash proportions

The volume of AEA required to reach the test endpoint as influenced by both water to cementitious materials ratio (w/cm) and ash to cementitious materials ratio (a/cm), individually and in combination, are considered in the following discussion.

6.3.6 Water to cementitious ratio

The water to cementitious materials ratio required in the foam index test must be considerably higher than in typical concrete to achieve the fluidity necessary to mix the materials, form a stable foam endpoint, and allow bubbles to rise to the liquid surface after

agitation. While w/cm equal to 2.5 is commonly used in foam index tests (Dodson, 1990; Baltrus and LaCount, 2001; Kulaots et al. 2003), values as high as 8.3 (Section 6.1) have been used and the authors have used w/cm ranging from 2.5 to 25. It was determined in this study that w/cm of 1.5 is an absolute minimum for foam index testing, and as will be shown, values from 2.0 to 2.5 are recommended. While such values are obviously high relative to typical concrete, it is useful to point out other common tests, such as the volume air meter (ASTM C 173) and the Chase air indicator (AASHTO T-199) increase the w/cm ratio to approximately 3 and 8, respectively, to aid separation of air from paste.

Experiments

Constant paste volume. Six foam index tests were performed using only cement and water for w/cm between 0.8 and 25. Container no. 3 was used for all tests (132 mL, interior height 83 mm, inner diameter 45 mm as described in Harris et al. 2007b). A fill ratio of 0.2 and filled height of 20 mm (paste volume of 28.5 mL) was used in each test to achieve an approximately constant air/paste ratio at endpoint. Cement mass varied between 1.1 and 25.9 g, while water volume varied between 28.1 and 20.2 mL.

Constant cement mass. Five foam index tests were performed using a constant cement mass of 5 g. Water volume was varied between 10.0 and 44.8 mL, and w/cm ratios were varied between 2 and 9. The tests were performed using container no. 6 (58 mL, average interior height 109 mm, inner diameter 28 mm as described in Harris et al. 2007b). Because paste volume differed between the constant-volume and constant-mass series, and differed for each constant-mass experiment, the specific foam index values of both experiments were adjusted to account for the air/paste ratio differences by normalizing specific foam index values by the air/paste ratio using equation 6.7.

$$SFI_{\%air} = \frac{SFI}{\frac{100t_f}{\gamma h}} \quad \text{eqn. 6.7}$$

The denominator of the equation for corrected foam index, $100t_f/\gamma h$, is equal to the air/paste ratio as described in equation 6.2 of Section 6.2 of this study in units of percent with t_f equal to 4 mm. The units of $SFI_{\%air}$ are mL AEA per 100 kg cm per percent air, i.e., the volume of undiluted AEA required per percent air. The results of the experiments are shown in Figures 6.17 and 6.18.

Results

Figure 6.17 presents specific foam index from the constant-volume and constant-mass series versus the water-to-cement ratios. Figure 6.18 presents specific foam index normalized by percent air from the two series versus the water-to-cement ratios. The test endpoint could not be discerned with w/cm equal to 0.8 from the constant volume series due to lack of contrast between the color of the surface foam and the background paste. Also for this case the thickness of the paste prevented rapid rise of air bubbles to the surface. The endpoint of the constant-volume test with w/cm equal to 1.6 was discernible, though w/c ratios of 2 or greater permitted easier identification.

Discussion

The results from the two test series appear to differ in Figure 6.17. However, the SFI values cannot be directly compared between the two series because the tests were performed using different filled heights (each test in the constant cement mass series had a unique filled height) and thus the SFI values must be normalized using equation 6.7, as shown in Figure 6.18.

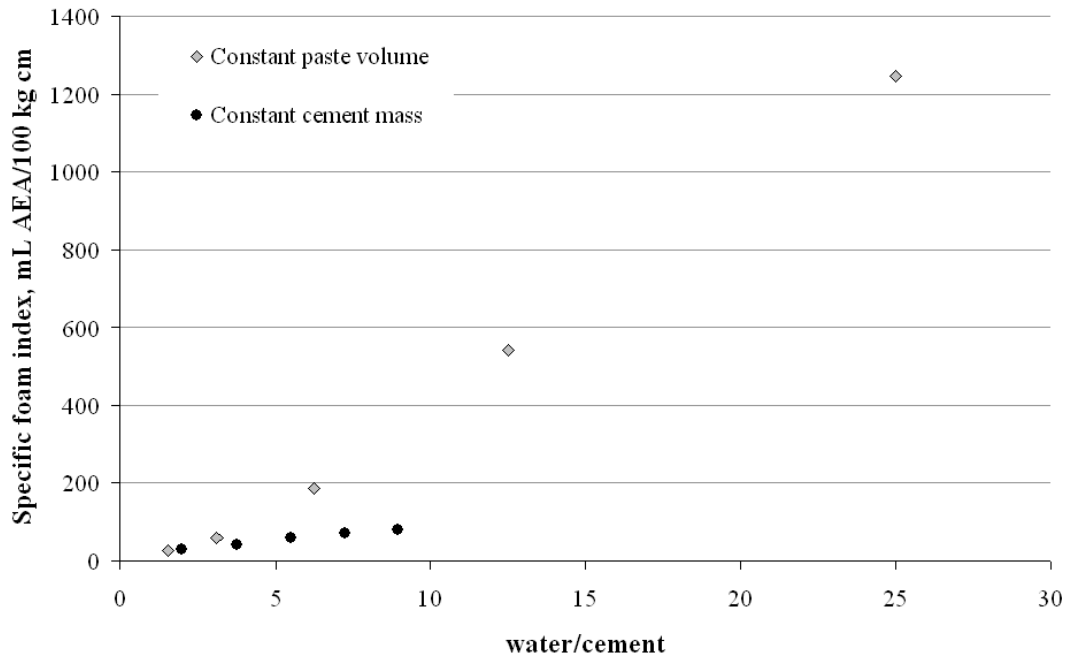


Figure 6.17: Specific foam index versus water-to-cement ratios.

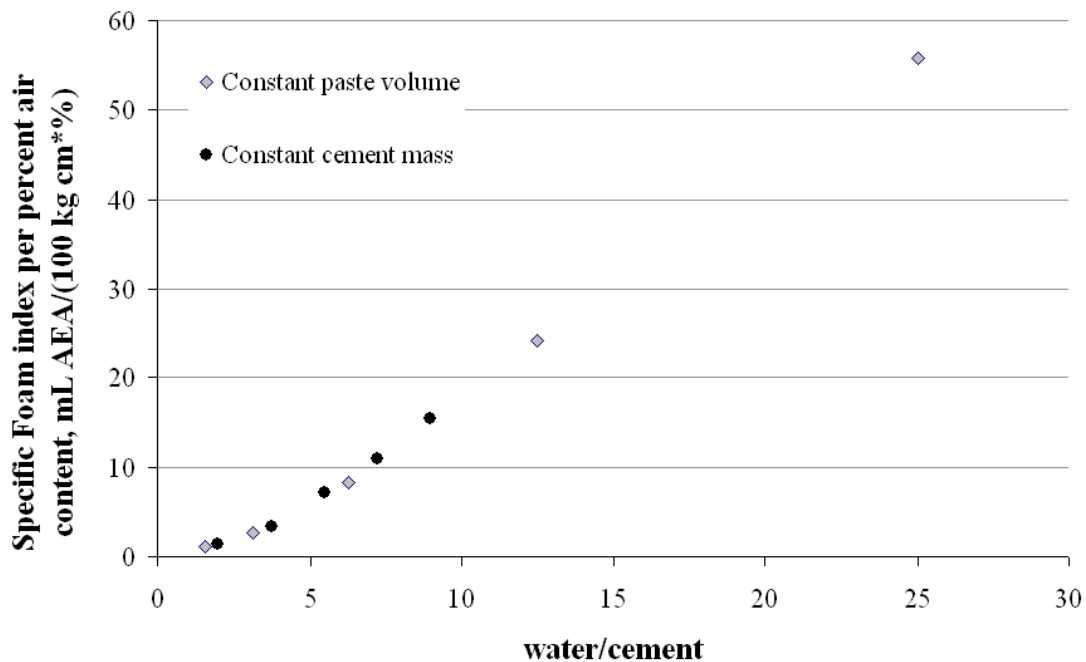


Figure 6.18: Specific foam index per percent air content versus water-to-cement ratios.

Two major issues are apparent from the results in Figures 6.18; first, AEA dosage per percent air content is dependent on water-to-cement ratios, for both constant cement mass and constant paste volume experiments. The increase in specific foam index per percent air with increasing water-to-cement ratios is independent of the amount of cement used in the test since the same results were produced when cement mass decreased (constant volume) and when the cement mass remained constant.

The second major issue is that normalization of specific foam index by percent air content allows comparison of tests made with differing paste compositions, bottle sizes and filled heights. Variation in the value of t_f changes only the scale of the SFI values but not the behavior of the two tests. However, the closely matching data from the two tests suggests that t_f is nearly the same for all tests performed and that the 4 mm assumption is reasonable for both containers.

Based on these observations, the choice of w/cm is critical for the development of a standard foam index test. Values of w/cm less than approximately 1.5 are not suitable, and establishment of an upper limit will be discussed in a later section.

6.3.7 Ash to cementitious ratio

The ash/cm ratio to be used in a foam index test will depend on the objective of the test, and the impact of this ratio is highly sensitive to the specific ash and cement. For a mix-specific test the ash/cm ratio and the specific cement and ash proposed for the concrete mix in question should be used. For a test performed to study the effect of a single ingredient on AEA requirement, a value of ash/cm that clearly highlights the interactions should be chosen, and thought should be given to selection of the particular ash and cement combination. Typical a/cm

ratios for concrete are in the range of 15 to 40 percent (or higher). The following experiment was performed to study how ash/cm affects foam index values.

Experiment

Four different fly ash samples were tested with w/cm equal to 2.0 and a/cm at 0.10, 0.20, 0.33, 0.43, 0.57, 0.80 and 1.0. The total volume of water, ash and cement was kept constant at 28.5 mL, meaning that a constant air/paste ratio (at about 14 percent) was always obtained.

As the a/cm increased from 0.10 to 1.00, AEA requirements increased significantly, making it necessary to increase the volume of undiluted AEA per drop. This was done by changing the AEA concentration (from 5 to 10 percent), drop size (from 10 to 60 μL) or both (Table 6.18). For example, in the extreme case the specific foam index of the test for Ash H with a/cm = 1.00 required 570 μL AEA/ 100 kg cm while the foam index of the test with a/cm = 0.10 with Ash L required 25 μL AEA/100 kg cm. In the latter test, six drops of dilute AEA were required to reach the foam index endpoint. If the same drop size and AEA concentration had been used for the former test, approximately 140 drops would have been required (assuming final dosage were not affected by other factors).

Table 6.18: AEA dilution and drop size for each a/cm ratio tested.

a/cm	AEA dilution, %	Drop size, μL	AEA volume/drop, μL	R_{\min} , (eqn. 3 Part II) mL AEA /100 kg cm /drop
0.10	5	10	0.5	4.1
0.20	5	10	0.5	4.1
0.33	5	20	1.0	8.3
0.43	5	30	1.5	12.5
0.57	10	20	2.0	16.7
0.80	10	40	4.0	33.9
1.00	10	60	6.0	51.3

Results

The specific foam index values are presented in Figure 6.19 for each a/cm. For all of the ash samples, as a/cm increases the AEA requirement per unit mass of cementitious materials also increases in a consistent manner. At each a/cm ratio, the ash samples are clearly differentiated, with the ash samples maintaining the same ranking in specific foam index with ash H requiring the highest AEA dosage followed by ashes MH, ML and L.

Discussion

Behavior of specific foam index values over the range of a/cm tested is highly consistent. Each of the four ash samples show varying degrees of interaction with AEA which increases as the proportion of ash in the paste increases. The data can be closely approximated by exponential or linear curves for each ash sample. The test appears to be able to differentiate ash types at all a/cm ratios.

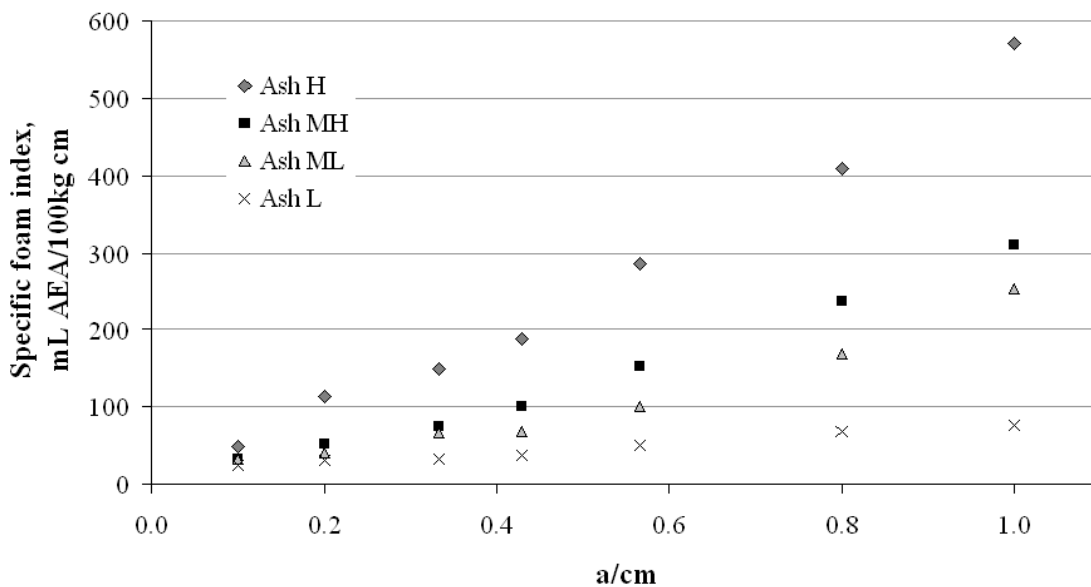


Figure 6.19: The foam index values of four commercial fly ash samples for a w/cm of 2.0 and various a/cm ratios between 0.1 and 1.0.

Combined effects on foam index

The following experiment was designed to examine the combined effects of w/cm and a/cm on foam index test values.

Experimental procedure

Forty-five tests using various water to cementitious (w/cm) and ash to cementitious (a/cm) ratios were conducted to map foam index with the two parameters. Values of w/cm ranged from 1.5 to 25.0, and the values of a/cm ranged from 0 to 1 (using Ash H). The tests were performed using container no. 3 and, as in the previous experiments, a constant volume of paste (28.5 mL) was used in all tests.

Results

The results of the experiment are shown in Figure 6.20. The points in Figure 6.20 represent the w/cm and a/cm values of the individual tests; the contour lines represent the specific foam index values (mL AEA per 100 kg cm). The horizontal line at w/cm equal to 1.5 represents the minimum recommended value of w/cm for the test. The specific foam index values are greatest at maximum w/cm and a/cm values and decrease as both w/cm and a/cm values decrease. The contours are smooth and approximately parallel for values from 0 to 600 mL AEA per 100 kg cm. More scatter and/or non-linear behavior appear at values between 800 and 1000 mL AEA per 100 kg cm. Note, however, that as seen in Table 6.19 the values of R_{\min} increased dramatically at higher a/cm, markedly increasing the uncertainty of the results.

The nearly parallel contours in the lower half of Figure 6.20 suggest a planar relationship that could be modeled with multivariable linear regression. The entire dataset was so analyzed, however, with the surprisingly favorable results shown in Table 6.19. The R^2 and adjusted R^2 values of the regression are both equal to 0.96 and standard error of the estimate is 95 mL AEA/100 kg cm. The predictive value of this regression equation for this dataset is graphically demonstrated in Figure 6.21. The y-intercept value indicates the limits of the regression. For low w/cm (cannot be less than 1.5) and low a/cm (less than 0.2), the regression may predict a negative specific foam index value which is not physically possible; however for w/cm equal to or greater than 2 coupled with a/cm values greater than 0.1, the regression closely matches reality (though the error in the test increases with increasing w/cm above 10). The interaction between w/cm and a/cm deserves further consideration beyond the scope of this study.

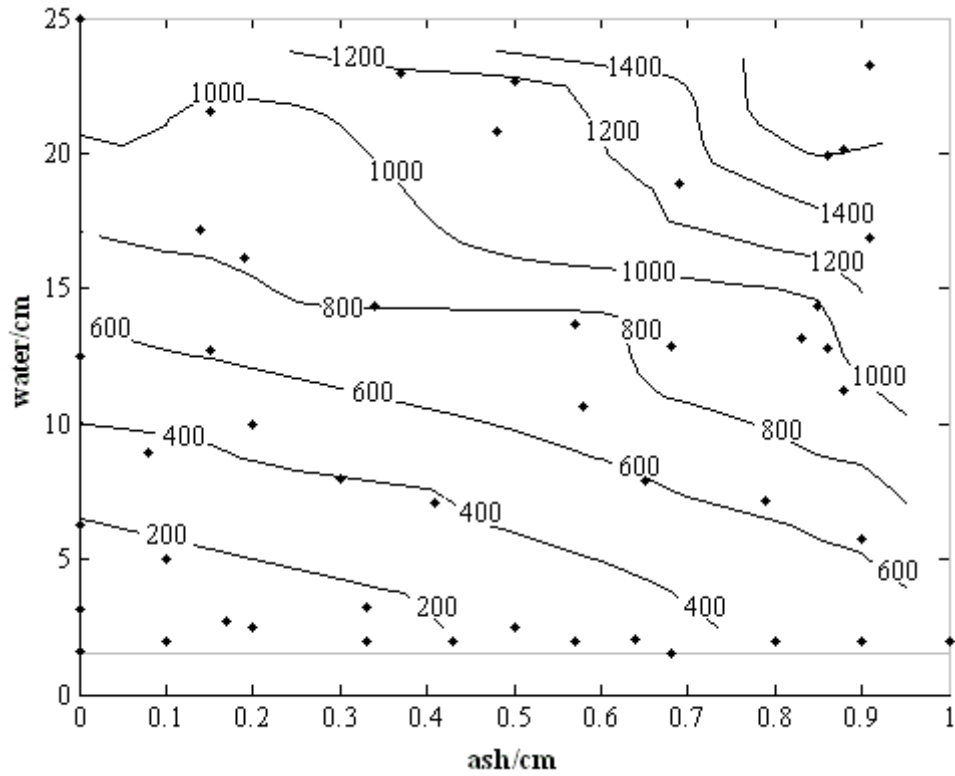


Figure 6.20: Effects of water to cementitious materials ratio (y-axis) and ash to cementitious materials ratio (x-axis) on foam index values with other test variables held constant. Foam index values are in units mL AEA/100 kg cm.

Table 6.19: Linear regression coefficients of the two variables w/cm and a/cm and y-intercept.

Variable	Coefficient
w/cm {1.5-25}	50
a/cm {0-1}	590
y-intercept	-170

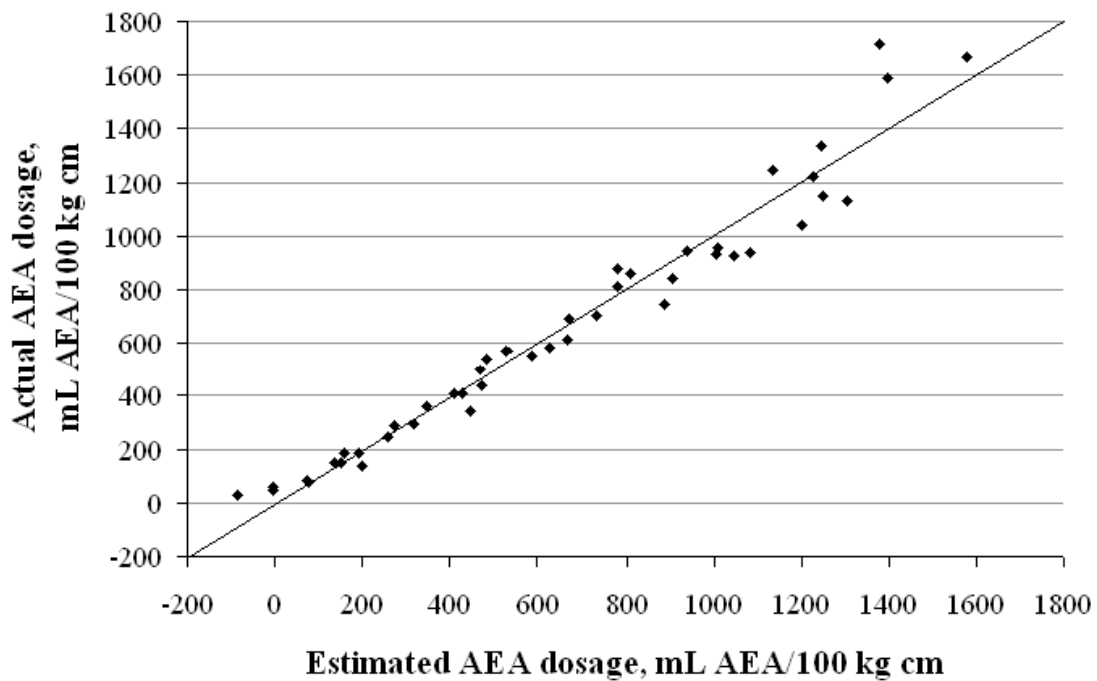


Figure 6.21: Estimated foam index values using regression coefficients versus actual foam index test data. Reference line shown is $x = y$.

Discussion

Two major observations can be made from the test data in Figure 6.20. First, for any given w/cm , increasing a/cm increases specific foam index value. Ash H was used in the test because of its propensity to increase the AEA dosage required to achieve 6 percent air in fresh concrete (Harris et al. 2007a). (This effect may be due to adsorption of AEA on the residual coal in the ash (Gebler and Klieger 1983, Sabanegh 1997, Gao et al. 1997, Freeman et al. 1997, Yu et al. 2000, Harris, 2007c) and/or other mechanisms.) As shown in Figure 6.21, different ash samples would be expected to change the specific foam index values for any given ash/cm. The second major observation is that regardless of a/cm , increasing w/cm increases the AEA requirement. This same behavior was observed in experiments on w/cm discussed above without the presence of ash. The implication of this is that specific foam index in units of mL AEA/100 kg cm (eqn. 6.7, Section 6.3.6.1) normalizes foam index values by mass of cementitious materials only; therefore, direct comparison of specific foam index results cannot be made if differing w/cm ratios are used.

Influence of individual paste ingredients on foam index

Identification of the contributions of individual paste ingredients to specific foam index values would be useful for characterizing the materials in a standard test. The contributions of individual ingredients cannot be determined by regression analysis of the data from the study on combined a/cm and w/cm described above because use of a constant volume in all tests resulted in the quantity of one of the three paste ingredients being dependent on the quantities of the other

two. Instead, the following study was done to identify the influence of water, ash and cement to foam index test values.

Experiment

Twenty-five foam index tests were performed using container no. 6, type I/II cement and Ash H. All test proportions were determined by generating uniformly distributed random values for water content, w/cm and a/cm. The water content was limited to values between 15 and 40 mL, w/cm ratios were limited to values between 2 and 5 and a/cm was limited to values between 0.1 and 0.5. For all tests, 20 microliter drops of 5 percent AEA dilution were used.

After the tests were performed, regression analysis of the specific foam index values was performed to determine the individual contributions of the water, cement and ash contents. Because the paste-filled-height was different in each test, specific foam index values were normalized by percent air content using equation 6.7.

Results

The regression analysis produced R^2 and adjusted R^2 values of 0.97 and 0.96 and standard error of 2.1 mL AEA/100 kg cm³%air. The regression coefficients are shown in Table 6.20. The estimated SFI per percent air versus the actual values of the twenty-five tests are shown in Figure 6.22.

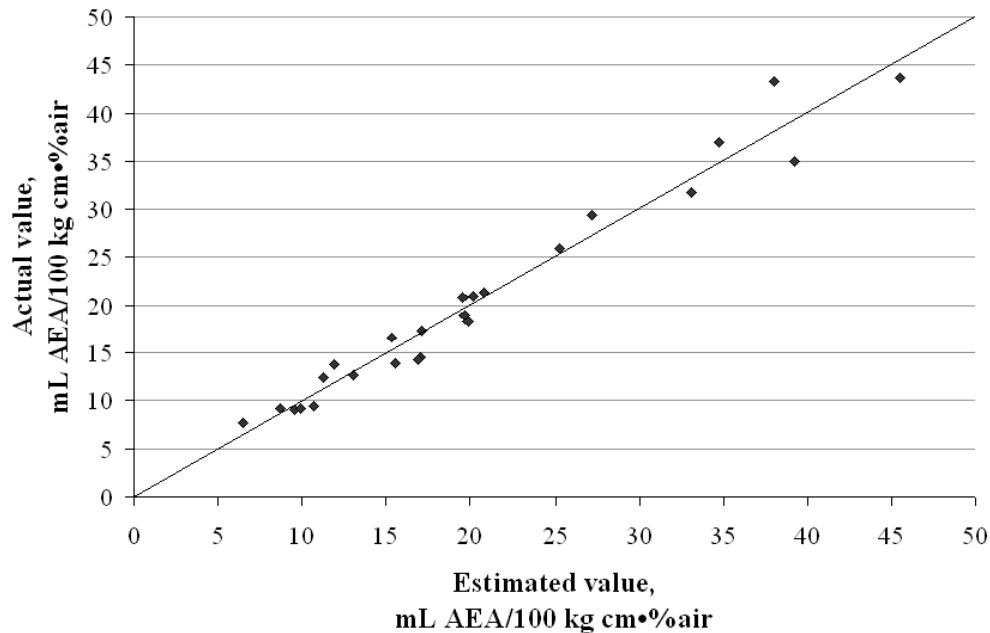


Figure 6.22: Estimated specific foam index values per percent air using regression coefficients versus actual test data. The reference line shown is $x = y$.

Table 6.20: Linear regression coefficients of the three variables water, cement and ash and y-intercept to produce estimated of specific foam index per percent air.

Variable	Coefficient
Water, mL	0.7
Cement, g	-4.1
Ash, g	6.3
y-intercept	9.6

Discussion

The linear regression model is a reasonable fit for the data shown in Figure 6.22. As suspected due to the results of the experiments on w/cm, the increase of water in the test tends to increase specific foam index, as seen in the regression coefficients in Table 6.20. Increasing the cement content in the test actually decreases the AEA requirement. The presence of cement enhances the ability of AEA to stabilize foam in the test, as described further in the following section. On the other hand, ash tends to increase the AEA requirement. The regression coefficients are specific to the materials used in the test, and it is expected that the coefficients would change with the use of other materials particularly for the ash, but such may in fact be a way to characterize various cementitious materials.

The influence of solids on foam index

Solid materials, particularly cement, appear to play a role in stabilizing foam in the test. This hypothesis is based on the literature, the tests reported here and observations made during numerous foam index tests performed in this study. Kulaots et al. (2003) observed that finely divided calcium solids, such as cement and calcium carbonate, are important for stabilizing foam in aqueous solutions containing commercial AEAs. Figures 6.17 and 6.20 show that increasing the cementitious materials (decreasing w/c in the “constant paste” series of Figure 6.18, and w/cm in Figure 6.20) decreases the AEA volume required to form stable foam. However, because paste volume was constant in these tests (increasing solids content corresponds with decreasing water content), the influence of solids on the test was not isolated. To separate the influence of solids content on test values, a series of tests was performed in which the water volume remained constant (25 mL) and the cement mass varied from 1 to 16 g (w/c =1.6 to 25). Container no. 6 was used for all tests (58 mL, average interior height 109 mm, inner diameter 28 mm as described in Harris et al. 2007b). The results are shown in Figures 6.23 and 6.24.

Figure 6.23 shows that as the mass of cement in the constant-water-volume test series increases from 1 to 10 g, the specific foam index decreases from 500 ($R_{min} = 50$) to 10 ($R_{min} = 2.5$) mL AEA/100 kg cm. Specific foam index decreases to 3.1 ($R_{min} = 1.6$) mL AEA/100 kg cm for 16 g of cement. Beyond 16 g cement, the w/c is too small to clearly distinguish the test endpoint. In Figure 6.20, specific foam index per percent air content (given by eqn. 1) versus w/c for the constant-water-volume series is plotted with the “constant paste” and “constant cement” series from Figure 6.20. Figure 6.24 shows that increasing the proportion of cement (decreasing w/c), decreased the AEA requirement in all the series, even though the paste proportions and volumes differed in the three tests. It is also noted that when the data are normalized in this fashion, AEA demand increases in proportion to w/c multiplied by 2.5 for w/c greater than 2.0

($R^2 = 1.00$), regardless of whether cement mass, water mass, or paste volume are held constant. Similarly, Figure 6.24 demonstrates that normalization of specific foam index values by the air/paste ratio shown in eqn. 6.8 can be used to reconcile test values obtained from different containers and with differing volumes of paste. Finally, recall that the stabilizing influence of cement on the foam index test is also supported by the regression coefficient value for cement in Table 6.20. The negative value of the coefficient suggests that cement decreases the AEA volume necessary to stabilize foam.

The mechanism of foam stabilization by cement was not pursued further in this study. However, it was observed in numerous tests that individual bubbles in the surface foam were generally more stable when covered in a layer of solids. The layer of solid materials caused bubbles to be opaque. Any bubbles that possessed no or only a partial coating of solids would typically burst within 20 s after agitation. A “stable” coated bubble could be made to be unstable by washing off the solids from its surface with a gently applied drop of water. Bubbles completely coated with solids were still observed to collapse before the endpoint was reached; therefore the presence of solids is only one of multiple factors influencing foam stability. Whether the observation that coatings of solid materials on bubbles is directly related to the stabilizing influence of increased cement content in the test is unknown and should be studied further.

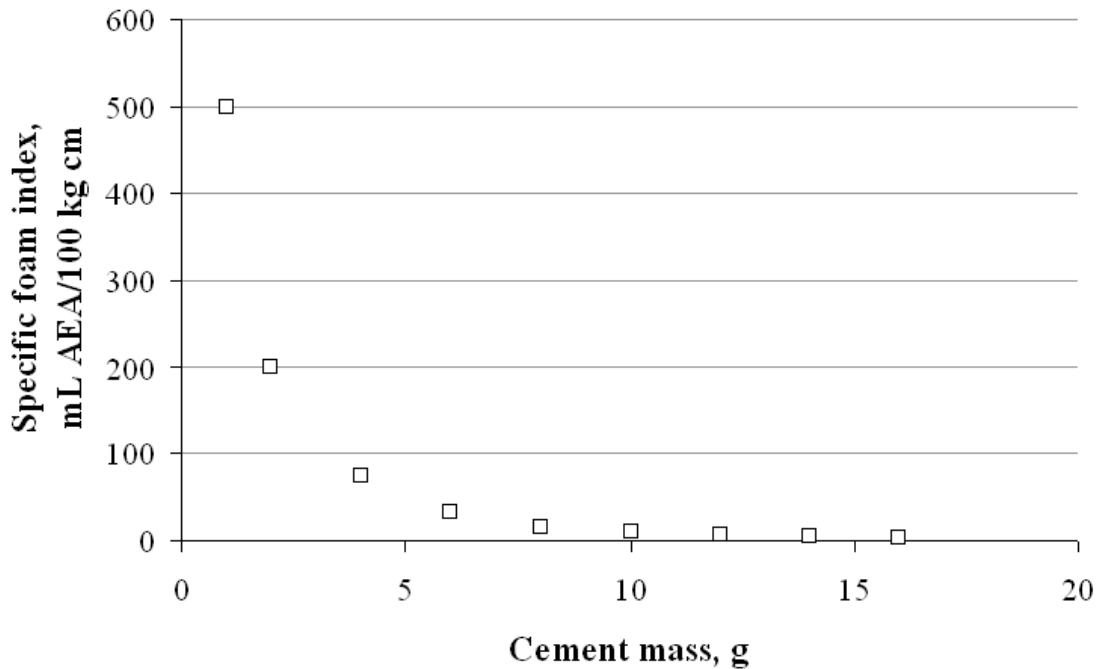


Figure 6.23: Specific foam index versus grams cement in test, water volume was equal to 25 mL in all tests.

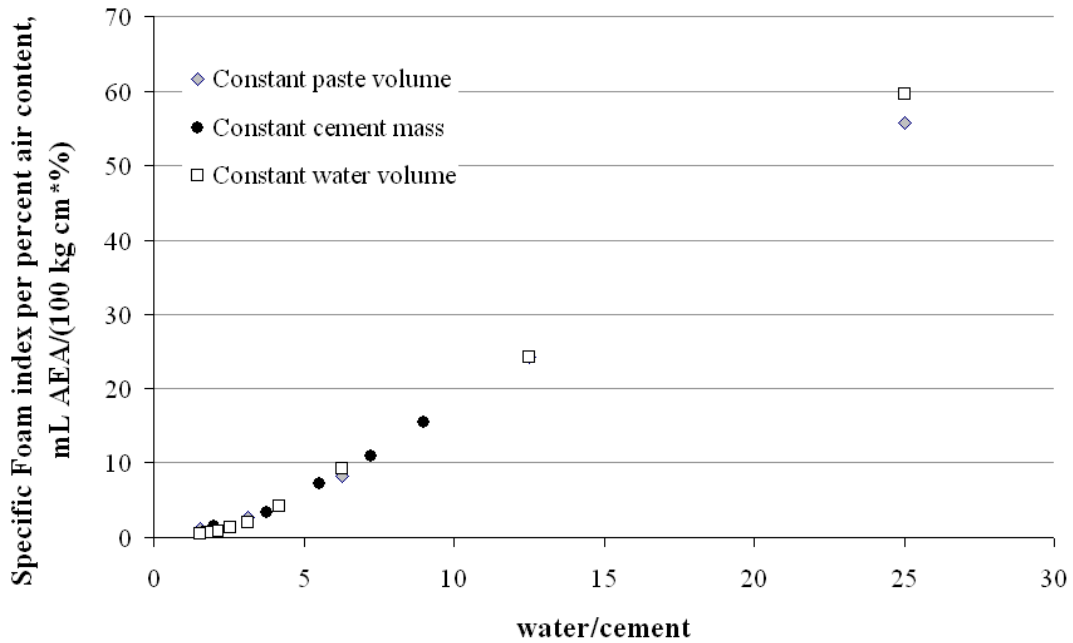


Figure 6.24: Specific foam index per percent air content versus water-to-cement ratios.

6.3.8 Limits on w/cm and a/cm

Establishing a meaningful maximum w/cm based on the test results shown in Figure 6.20 is difficult. One possible method is to limit the w/cm to the region shown in Figure 6.20 where the foam index behavior is linear (as represented by the smooth, parallel contours). Thus a limit in the range of 5 to 10 would likely be suitable. However, test precision is enhanced by minimizing the value of w/cm, as shown by equation 6.5 in Section 6.2, because the minimum resolution R_{\min} , decreases with increasing mass of cementitious materials. After having established a desired filled-height in a foam index test series, reducing w/cm will increase the amount of cementitious materials present and reduce R_{\min} . As discussed earlier, a minimum limit on w/cm exists at approximately 1.5; however, values of at least 2 facilitate identification of the endpoint. It is therefore recommended that w/cm equal to 2 be used for the test.

If supplementary cementitious materials are being tested, a minimum limit of 0.1 for a/cm should be established since test behavior at a/cm values less than 0.1 deviate from the trends shown at higher a/cm values. A maximum limit, based on the experimental results of this study is more difficult to establish. Kulaots et al. (2003) recommended that sufficient cement be present in the test to maintain a high pH in the test liquid because of sensitivity of certain AEAs to pH (but this may be one of the realistic factors that one wants to capture by performing the test in the first place). The influence of a/cm on foam index, as further affected by different AEA's, was beyond the scope of this study, but such should be investigated. In summary, however, since typical values for a/cm of 0.2 to 0.5 are used in industry, a mid-range value 0.33 is recommended for a default standard test application. For mix-specific applications of this test, values that match actual paste proportions should be used.

6.4 Other factors

Other factors can affect the performance of foam index tests and should be given attention. These other factors are the inclusion of other supplementary cementitious materials and chemical admixtures in the test and AEA/surfactant type.

6.4.1 Other SCMs, chemical admixtures

Additional factors in the foam index test may also influence test results. These factors are primarily related to mix-specific testing (test application 2). Factors such as water source and temperature, the use of chemical admixtures other than AEA's, the inclusion of supplementary cementitious materials other than fly ash and using different surfactants will likely affect test results. Limited testing demonstrated that the inclusion of water-reducing admixtures can greatly influence test results. Further study is recommended, as is the study of supplementary cementitious materials (SCMs) other than fly ash. It is likely that different compositions, impurities or trace ingredients, surface characteristics and size distributions of both the SCMs and cement can influence test results.

6.4.2 AEA/Surfactant type

The volume of AEA required to reach foam index in a given test will vary depending on the surfactant used. For mix-specific applications of the test, the specific AEA that is anticipated on the project in question should be used. In other cases, however, it may be useful to use a standard generic surfactant to evaluate the impact of other mixture characteristics. Kulaots et al. (2003) have proposed the use of dodecyl benzenesulfonic acid sodium salt (DBS) for this purpose. While DBS is not a typical concrete admixture, its advantages are generic availability, purity, and a greater stability in storage.

Based on the author's experience, foam index tests performed using various commercial AEA's produced foam and foam index endpoints that were similar in nature. The volumes of AEA used to reach foam index for given ash and testing parameters differed among the various AEA but bubble size and foam thickness at the endpoint was generally uniform. However, the foam stabilized by DBS was different in appearance and behavior than the foam stabilized using the other commercial AEA's. The bubbles stabilized with DBS were much smaller in size and required more time to rise to the surface of the test liquid. The thickness of the resulting foam layer at the liquid surface was thinner with DBS than with the commercial AEA's. It is the opinion of the authors that while the use of a standard surfactant has merit, DBS is not a suitable candidate because the characteristics of foam stabilized by DBS are not consistent with foam stabilized by commercial AEA's.

6.5 Conclusions

Several variations of the foam index test have been used successfully to predict the required dose of AEA in air entrained concrete, but such predictive correlations depend on the specific combination of materials and the specific foam index test method. This is true whether one is using the foam index to evaluate a single component with all other ingredients standardized, or to evaluate a specific combination of materials unique to a particular concrete mixture. If the foam index is to have broader application, allowing comparison of results among multiple users, standardization of the test method is necessary.

Because the specific foam index of a fixed combination of cementitious materials increases with water to cementitious materials ratio, w/cm must be fixed in a standard test. Required values of w/cm are considerably higher than those in ordinary portland cement concrete to achieve adequate mixing and to form a stable, discernable endpoint. A value of 1.5 is an absolute lower bound for a hand-agitated test, and a value of 2.0 is recommended.

Values of ash to cementitious materials will vary depending on the test application. In regards to a standard test (application 1), ash/cm equal to 0.33 is recommended. With regard to mix-specific testing, ash/cm in the typical range used in industry, of approximately 0.2 and greater, can be used in the foam index test.

Normalization of specific foam index values by the air/paste ratio (air is equal to the volume of foam at the paste surface) at the test endpoint, as shown by eqn. 6.7, is necessary for comparison of tests performed with differing volumes of paste or differing containers. When the same container and paste volume (and thus same filled height) is used, specific foam index values can be compared directly.

6.6 Recommendations for further study

This study provides recommendations for a standard foam index based on examination of the individual factors that influence the test. Some of the next major steps that must be taken before the test can be reliably used in industry are 1) to compare foam index results with actual concrete AEA dosages to identify correlations that would allow the test to predict AEA dosages in real concrete, 2) examine the influence of chemical admixtures in addition to AEA on the test and compare the results to real concrete data, and 3) inter-laboratory testing to identify the repeatability of the test performed by multiple users.

Chapter 7. Fly Ash Color Analysis

A method for quantification of ash color was developed during the course of this study. Development of the method was stimulated by the observation that ash color as perceived by the human eye appeared to correlate reasonably well with the dose of air entraining admixture required to produce 6 percent air in fresh concrete. The research investigated the ability to a.) reliably and repeatedly characterize the color of fly ash using a desktop flatbed color scanner, b.) correlate ash color to ash performance, particularly in regard to impact on air entrainment, and c.) correlate ash color to ash composition, first in regard to dark-colored ingredients of carbon and iron compounds, and secondly to ash composition in general.

A method for color analysis which entails making a digital image of an ash sample with a common flatbed scanner and then analyzing the ash image color with image analysis software is described. The color analysis method was utilized to identify correlations between ash color and ash properties, in particular those properties that influence ash-AEA interactions. A test method was developed which measures changes in ash grayscale values when exposed to elevated temperatures in an air atmosphere. The results of the test were found to correlate with ash organic carbon content.

7.1 Analysis of Fly Ash by Flatbed Color Scanner: Part I— Development of Test Method and Grayscale Analysis

Section 7.1 concentrates on the development of the color analysis method, conversion of color data to grayscale, and correlations between ash grayscale value and ash AEA interactions. Section 7.2 applies the color analysis method to a procedure which measures change in ash grayscale value versus temperature exposure. Section 7.2 also presents correlations between ash grayscale value and ash organic carbon content. Additional information regarding detailed aspects of the color analysis procedure and studies performed to identify the chemical properties of ash that contribute to ash grayscale value are located in the Appendix.

7.1.1 Introduction

Of the many physical and chemical properties of fly ash, the color of the bulk material is the most conspicuous. While typically 90 percent or more of the mass of fly ash is composed of oxide compounds that are light tan to white in color, carbon in various forms, and oxides of iron, act as “pigments” such that fly ash meeting the chemical and physical requirements of ASTM C618 can range in color from nearly white to dark gray or black (Yu et al., 2000; FHWA, 2007). The research reported here investigated the ability to a.) reliably and repeatedly characterize the color of fly ash using a desktop flatbed color scanner, b.) correlate ash color to ash performance, particularly in regard to impact on air entrainment, and c.) correlate ash color to ash composition, first in regard to dark-colored ingredients of carbon and iron compounds, and secondly to ash composition in general. The results suggest that the technique may be a useful tool for rapid detection of fly ash characteristics, and might also find application in the evaluation of portland cement and other cementitious materials. Section 7.1 of this chapter concentrates on the development of the color analysis method and conversion of color data to grayscale, and Section 7.2 presents correlations between ash color and ash composition relative to ash behavior in concrete.

7.1.2 Research Significance

Rapidly quantifying the color of fly ash can have important implications for evaluating its uniformity or consistency (between loads or between sources). Architectural concrete or other colored concrete applications might benefit, for example, from a means to evaluate ash color to enable a correlation between ash color and concrete color. Further, analysis of ash color could lead to a means of evaluating ash composition, particularly in regard to the darker ingredients such as iron compounds and various forms of carbon. This can lead to color-based predictions of ash/concrete interaction, such as the interaction between ash content and the required dose of air entraining admixtures.

7.1.3 Background

The work reported here was conducted as part of a joint University of Texas (Austin)-Cornell University program sponsored by the Texas Department of Transportation. The goal of the program was to investigate the influence of fly ash on the dose of air entraining admixture required to achieve specified air contents. The population studied in this program consisted of eighteen fly ash samples obtained from coal-fired power plants located across the state of Texas, each producing an ash acceptable for use in concrete under Texas Department of Transportation Specification DMS-4610 (See references Harris, 2007; Ley, 2007 for more details on this research project.) For the ashes studied in this research, those ashes classified as Type F per ASTM C618 F fly ashes were generally gray in color with the darkness or lightness of the ash varying widely from near white to dark gray. Those ashes classified as Type C per ASTM C618 were generally colored in light shades of tan. These general trends have been observed by others (Yu et al., 2000; FHWA, 2007; TFHRC, 2007, Hoffman, 2007).

Research performed by Yu et al. (2000) showed that the color of fly ash samples obtained from a plant burning a combination of coal and petroleum coke generally darkened with increasing ignition losses (LOI) as measured by ASTM C311. This suggests a correlation between ash color and carbon content, given the general association between carbon content and LOI. While this was demonstrated for ashes varying from light gray for an ash with LOI less than 1 percent, to black for an ash with LOI greater than 65 percent, the trend did not apply to all ashes in the collection. Some ashes that were similar in appearance exhibited markedly different values of LOI, suggesting either that carbon did not always affect color in the same manner, or that LOI does not always indicate carbon alone (Fan, 2001; Brown, 1995; Paya, 2002).

When the eighteen Texas ashes used in the current study are arranged in order of increasing LOI as shown in Figure 7.1, no discernable trend in ash color is apparent. However, when the same ashes are ordered according to required dose of AEA for 6 percent air content (Ley, 2007), as shown in Figure 7.2 a trend in ash color becomes perceptible. Ashes with lower required dose of air entraining admixture are lighter in appearance than those associated with higher required dose of AEA. These qualitative observations stimulated the work reported here, leading to the quantitative relationships described in Figure 7.3. Data for AEA dosage was obtained as part of the Texas-Cornell project, as reported in (Harris, 2007; Ley, 2007). The grayscale data shown in Figure 7.1 were obtained using the methods described in the balance of this section, and the figure is discussed more fully at the conclusion. The method for capturing color digital images of ash samples is first described, supported in turn by analysis of the variability associated with key steps in the procedure.

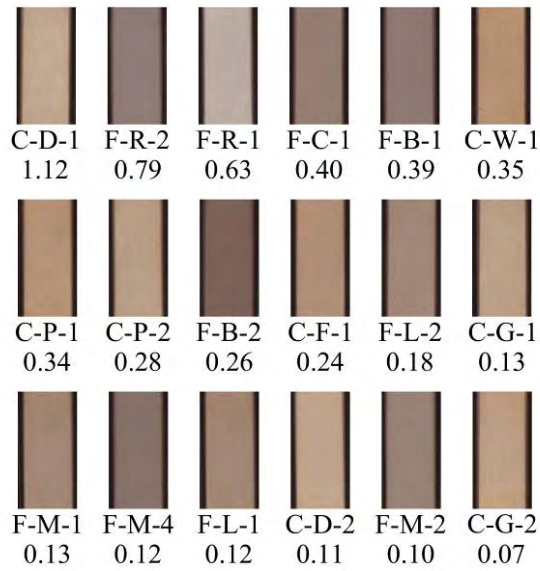


Figure 7.1: Ash samples arranged in order of descending LOI values from left to right and top to bottom. (Percent LOI values are shown below ash codes.)

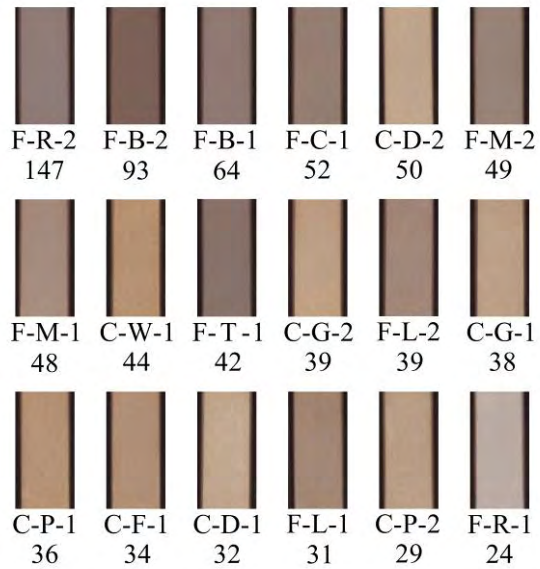


Figure 7.2: Ash samples arranged in order of descending concrete AEA dosage values from left to right and top to bottom. (AEA dosage in units of mL AEA/100 kg cm for 6% air content are shown below ash codes.)

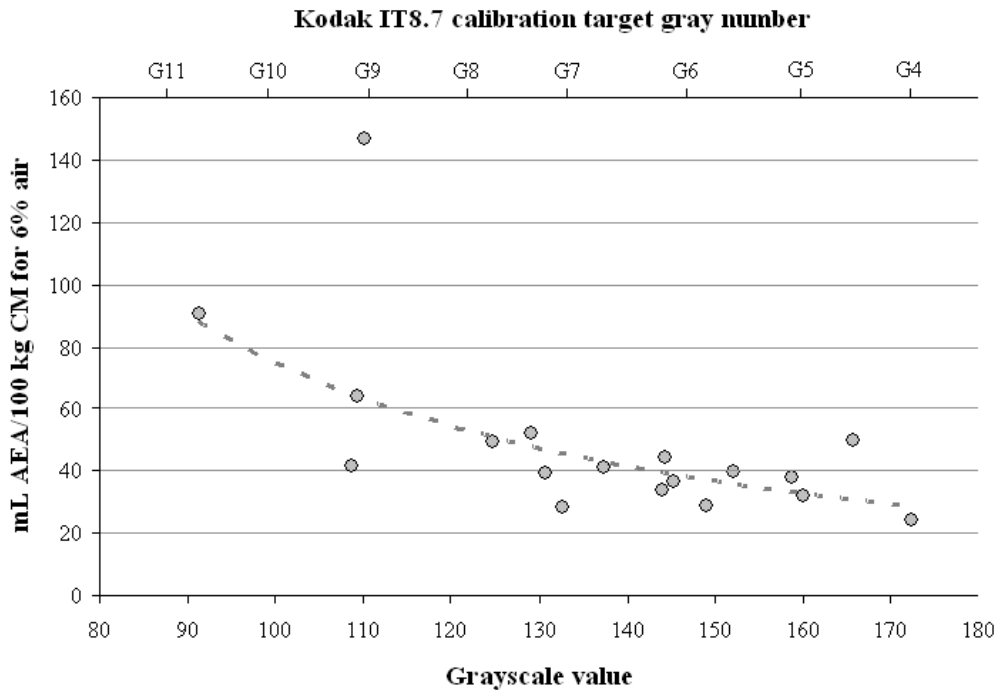


Figure 7.3: AEA dosage of fresh concrete versus grayscale value for 18 ash samples.

7.1.4 Procedure for quantifying ash color

After initial attempts to quantify ash color by means of digital photography proved unsatisfactory (due to variable lighting conditions and white balance), all image capture was performed on a desktop flatbed scanner. The experimental procedure is described in the following sections.

Scanner⁹ Setup

Scanner type

The flatbed color scanner shown in Figure 7.4 was used for all tests done in this study. The scanner employs an LED light source and contact image sensor element to capture image data. This unit has an image area of 219 x 300 mm, and minimum default scanning area of 55 x 110 mm, with selectable optical scanning rate (called “resolution” here) of 75, 100, 150, 200, 300, 400, 600, 800 and 1200 ppi (pixels per inch). A resolution of 400 ppi was sufficient for the work reported here. Though the scanner is capable of exporting 48-bit-depth color images, only 24-bit-depth images were used due to limitations of the color analysis software used.

Scanner template

A template made from black construction paper covered the entire scanner glass with a cut-out “window” exactly the size of the sample to be scanned (Figure 7.5). The template

⁹ A Canon CanoScan LiDE 500F color scanner, shown in Figure 7.4, was used for all scanning tests done in this study.

ensured that samples were positioned in the identical location on the scanning bed for each analysis. This location or “window” was selected to be within the boundaries of the smallest default scanning area option¹⁰ (the “Business Card” option) and 35 mm away from the (lid hinge-side) edge of the glass, since scanning quality is reduced at the perimeter of the glass. The template was secured to the scanner with tape.

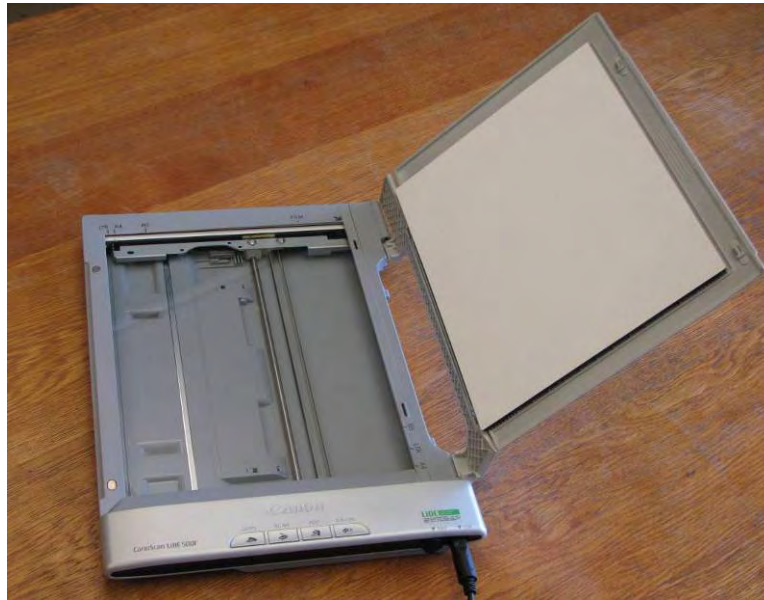


Figure 7.4: Canon CanoScan LiDE 500F color image flatbed scanner.

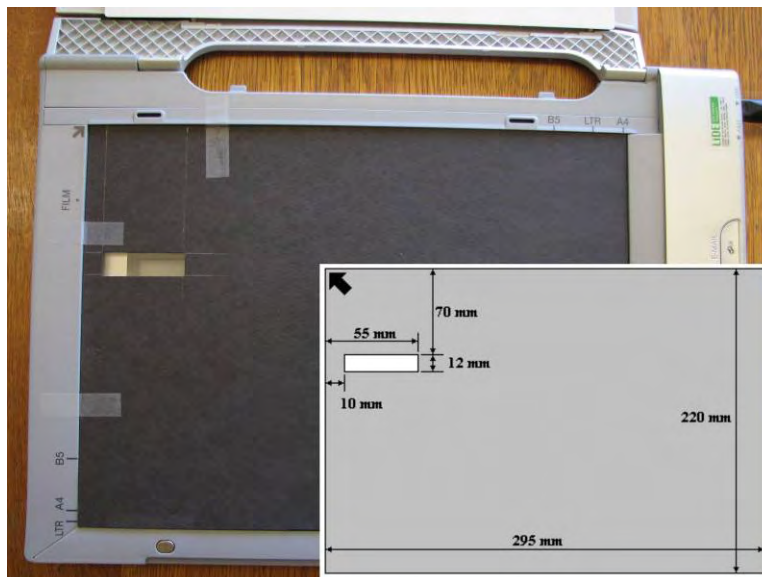


Figure 7.5: Scanning template.

¹⁰ This reduces the time required for each scan and minimizes image file size.

Specimen Preparation

Oven drying

Before scanning, fly ash was first dried for 20 to 24 hours at 105°C in a standard laboratory drying oven. About 5 to 10 grams of ash were dried at a time in 200 ml porcelain bowls. After the ash samples were removed from the oven, they were placed in desiccators to keep moisture from condensing on the ash during cooling. After cooling sufficiently to allow comfortable handling (about twenty to thirty minutes) the ash samples were placed in cuvetts and immediately scanned.

Cuvet filling

The materials used to prepare a sample for scanning are shown in Figure 7.6. Using a piece of creased weighing paper as a funnel, dry ash was transferred into a 4.5mL methacrylate cuvet¹¹, filling the cuvet to about 50 percent height (normally requiring between 2 to 3g ash), and the container was sealed with putty¹² leaving an air volume above the ash of about 25 percent of the height of the cuvet (Figure 7.7). Care was taken to ensure that no putty extended beyond the clear container walls to allow the cuvet to lie flat on the scanner glass. It was important to handle the cuvet carefully and to wear gloves to avoid impairing the optical clarity of the cuvet walls. An identifying self-adhesive label was placed on one of the four sides, and any ash, putty or finger marks were carefully removed from the cuvet, leaving three clean, clear, and scan-able surfaces.

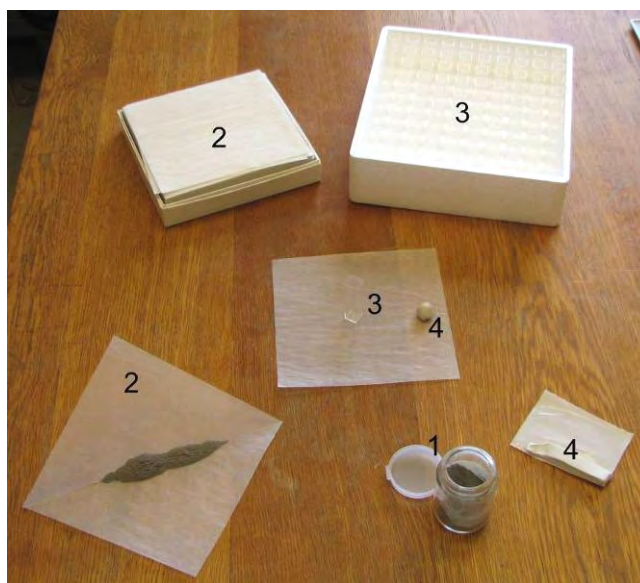


Figure 7.6: Fly ash sample scanning materials: 1) oven-dried fly ash, 2) weighing paper, 3) cuvetts, and 4) putty.

¹¹ 12 mm x 12 mm x 45 mm with 1 mm thick walls with four clear sides (These cuvetts are normally used for holding liquid samples for ultra violet-visible light spectrographic analysis, manufactured by Fisher Scientific Company L.L.C., Cat. No. 14-386-21.)

¹² Putty as used to hanging posters was used (available in office supply stores). Other similar materials could be used.

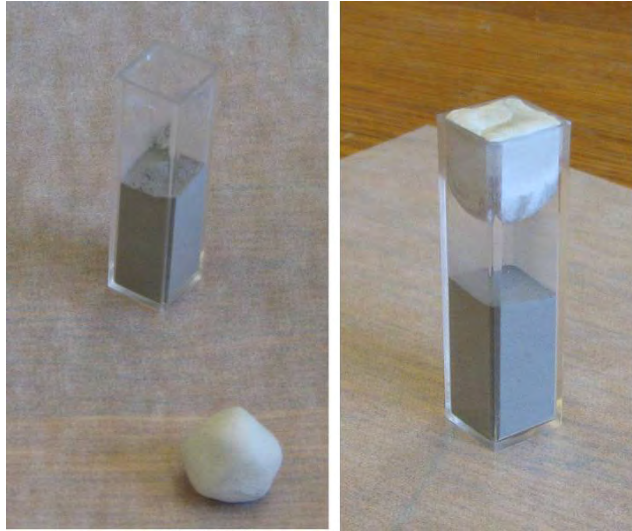


Figure 7.7: Cuvet filling and stopping with putty plug.

Sample consolidation

Before placing the sample on the platen, the cuvet was shaken 10 times (vertical displacement about 120 to 150 mm, frequency about 2 to 3 shakes/s, holding the cuvet by the base and plugged end between finger and thumb) to dislodge any compacted material. The cuvet was then tapped ten times by holding the cuvet (between finger and thumb as described for the shaking process) horizontally about 20 to 25 mm above a table top and allowing it to free fall, scanned side down, onto the table to consolidate the ash against the scanned side of the cuvet. (Tapping in the manner described was found to not impair the cuvet scanning surfaces provided the table top was clean and the scanning surfaces were not touched by hand.) After tapping, the cuvet is left in the horizontal position with the scanned side down to avoid disturbing the scanning surface before the scan was performed.

Image scanning

Cuvets were scanned one at a time (although the process could be modified for simultaneous scanning of multiple samples if scanner variability were demonstrated to be acceptable over multiple locations on the scanner bed.) The scanner lid remained open in the 180° position. After tapping, the cuvet was placed in the template window, and for consistency, the plugged end was always nearest the edge of the scanner glass (Figure 7.8-left).

The entire scanner was covered with a cardboard box to block ambient light as shown in Figure 7.8-right. (Other methods for blocking ambient light, a heavy cloth for example, could likely be used as well. However, it was determined that the entire platen must be covered, not just the location of the scan, because of the influence of reflected light on the image color.)



Figure 7.8: Position of cuvet during scanning (left) and blocking ambient light with a cardboard box (right).



Figure 7.9: Typical scanned image of ash sample in cuvet held in place by the paper template (left), selection of the region of interest for color analysis (right).

The imaged was scanned using the scanner’s “color image” option with a resolution of 400 ppi. The scanned image was saved as a 24-bit-depth JPG file. An example of a typical JPG scanned image is shown in Figure 7.9-left.

Steps 7.2.1.3 and 7.2.1.4 were performed two more times to capture images of all three unmarked sides of the cuvet. Consolidation of the ash described in step 7.2.1.3.3 was repeated prior to each scan.

7.1.5 Treatment of scanned image data

Image analysis

To obtain numerical indices of ash color, a sub-region within the scanned image of the cuvet (Figure 7.9-right) was selected and then analyzed for its Red (R), Green (G) and Blue (B) content. The sub-region was approximately 7 mm wide by 20 mm high, and selected to not include the putty or walls and base of the cuvet.

Analysis of the RGB content of selected sub regions was performed using a software package available in the public domain.¹³ Due to the large number of images collected in this study a specially developed script software tool was written to automate the handling of files and the insertion of analysis output into a master spreadsheet file. (Details are provided in Harris, 2007) The final output for a given ash sample consisted of three separate sets of the means for Red, Green and Blue values (0 to 255), corresponding to the three scanned sides of the cuvet. Mean values for each of the three scanned sides were averaged to produce a single set of (R,G,B) values used to characterize the sample.

Although a great deal more information is contained in the (R,G,B) data set for any given ash, these three parameters were converted to a single grayscale value for subsequent analysis and comparison. The method of conversion is described next. Additional study of the full color analysis could provide additional useable information and is recommended for future study.

Converting a Color Image to a Grayscale Image

For the phase of the research reported here, 24-bit ash color values were converted to 8-bit grayscale values. This simplified comparison of ash samples by reducing three color parameters to one, at the expense of reduced information content. The color-to-grayscale conversion method used in this study, (Equation 7.1), is similar to methods used in many commercial image processing software packages and applies weights, ranging between 0 and 1, to the red, green and blue color components and then rounds the sum of the weighted values to the nearest whole number.

$$\text{Grayscale value} = rR + gG + bB \qquad \text{eqn. 7.1}$$

The variables R, G and B are the average 8-bit color components of a 24-bit color image and *r*, *g* and *b* are the applied weights. The sum of *r*, *g* and *b* is equal to 1. The values of the weights used in this study are given in Table 7.1, are similar to those used in several digital image editing software programs. Variations in the weight values exist but the values are generally similar to those shown in Table 7.1 with the greatest weight applied to the green component.

Table 7.1: Twenty-four-bit color conversion weights

Weight	Value
r	0.25
g	0.625
b	0.125

¹³ UTHSCSA ImageTool developed by C. Donald Wilcox, S. Brent Dove, W. Doss McDavid and David B. Greer of the Department of Dental Diagnostic Science at The University of Texas Health Science Center, San Antonio, Texas. ImageTool executable and source code can be downloaded free of charge at <http://ddsdx.uthscsa.edu/dig/download.html>.

7.1.6 Sources of Variability in the Scanning and Image Analysis Procedure

During the development of the test procedure described above, experiments were devised to isolate and quantify sources of variability that could influence the results. The sources of variability discussed here can be divided into two groups: variability in the flatbed scanner or scanning procedure and variability in the scanned sample.

Scanner and Scanning Procedure Variability

Scanner Model

An experiment was performed to identify differences in ash grayscale value as produced by two commercial scanners. For the experiment, fourteen ash samples were first scanned with the model used in the development of the method (Scanner 1, see footnote 3) and again with a different commercial scanner model (Scanner 2)¹⁴. Scanner 2 was produced by the same manufacturer and used the same type of scanning array (LED light source and contact image sensor) as Scanner 1 but was a different generation model with different operation software. The standard procedures for scanning and grayscale analysis described above were used for all ash samples.

The resulting grayscale values are compared in Figure 7.10, showing a strong linear correlation ($R^2 > 0.99$), with scanner 2 consistently resulting in average grayscale values 13.6 units higher (lighter) than scanner 1, with a standard deviation of 1.3. It is therefore clear that scanner calibration is required prior to conducting these analyses, especially when two different labs do the work, or when one lab changes scanners, or perhaps due to changes that may occur over time in the operation of a single scanner. This also means that any correlations to properties have to be re-corrected for a specific scanner.

¹⁴ Canon CanoScan LiDE 20 color scanner, Canon Inc., Tokyo, Japan.

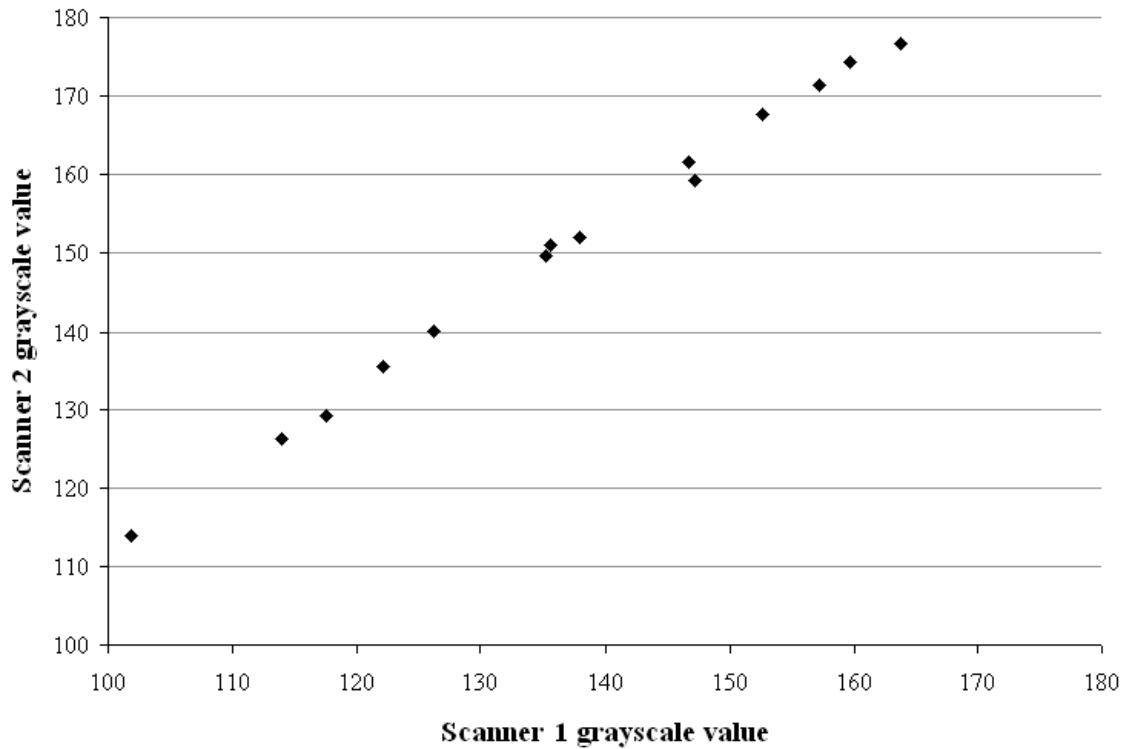


Figure 7.10: Comparison of grayscale values between two different scanner models.

It is proposed that a standard color card be used to calibrate differences between scanners. One method is to use a standard paint chip containing a range of values similar to those of fly ash that can be scanned at the beginning of each session to determine if analysis values should be corrected for comparison.

A correction could be performed by first scanning a range of standard colors on a standard scanner, analyzing the colors and computing the grayscale values, $g_{\text{standard-1}}, g_{\text{standard-2}}, \dots, g_{\text{standard-n}}$. Next the same standard colors are scanned using a non-standard scanner and quantified, g_1, g_2, \dots, g_n . The regression equation that best fits the relationship of g_x versus $g_{\text{standard-x}}$ for $x = 1$ to n , can then be used to correct the values of the scanner to the standard, provided the color fall within the range of the measured standard.

Given the equipment-dependent variability in quantifying grayscale, the Kodak IT8.7/2 Q-60R1 reflection target, shown in Figure 7.11, was used as a standard in this study. The target has 24 gray “patches” numbered 0 to 23 (called G0 to G23 here). The R, G, B and grayscale values of the target gray patches G3 to G13 (which represent the range of fly ashes used in this study) were determined using the Canon CanoScan LiDE 500F and are shown in Table 7.2. The calibration gray numbers are plotted with the analysis grayscale values in Figures 7.4 and 7.20 to allow comparison to other scanners.

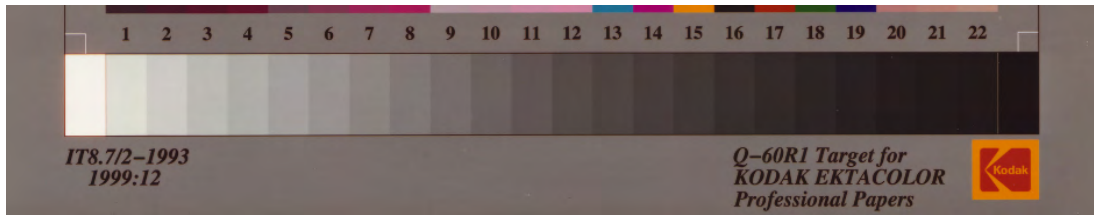


Figure 7.11: Grayscale band of Kodak IT8.7 calibration target.

Table 7.2: RGB and grayscale values of selected Kodak IT8.7 gray patches as determined by author's scanner.

Target gray value	Red mean	Green mean	Blue mean	Gray mean
G3	186.6	185.7	179.7	185.2
G4	173.7	172.6	167.6	172.2
G5	162.4	159.2	156.4	159.6
G6	150.9	145.8	143.3	146.8
G7	138.4	131.9	128.3	133.0
G8	128.0	119.8	119.2	121.8
G9	117.3	108.8	107.2	110.7
G10	106.2	97.1	95.2	99.2
G11	96.4	84.9	84.5	87.7
G12	84.7	74.8	73.0	77.1
G13	77.9	68.7	66.5	70.7

Sample Location on Platen

The effect of location of the ash sample holder on the scanner platen was first studied by scanning the entire platen surface while empty, with the scanner lid closed. The scanned image of the white lid revealed faint yellow lines parallel to the long edge of the platen nearest the lid hinges. These lines progressively diminished towards the center of the platen and were no longer visible beyond 35 mm from the edge. In subsequent testing using gray paint chips at various locations on the platen it was observed that as long as the sample location was 35 mm or more from the hinged edge of this scanner, the maximum difference in computed gray scale value was ± 1 unit, a specimen-location error associated with about $\frac{1}{2}$ to 1 percent of the gray scale value for typical ash samples. Nevertheless the sample location was fixed in all tests via the template as previously described.

Size of scanned area

The mean grayscale value determined by analysis of an ash sample is dependent on the location and size of the sample area that is analyzed. Generally speaking, the greater the size of the analysis region the more representative the sample will be of the mean ash color. Therefore, using as much of the scan-able surface as possible is preferable, though care should be taken to avoid including areas where the ash color is distorted, such as near the edges of the cuvet and the putty plug. The minimum acceptable analysis region size was measured by scanning a sample of ash and analyzing the scan ten times with different sized analysis regions. The computed mean grayscale values versus analysis area are shown in the Figure 7.12.

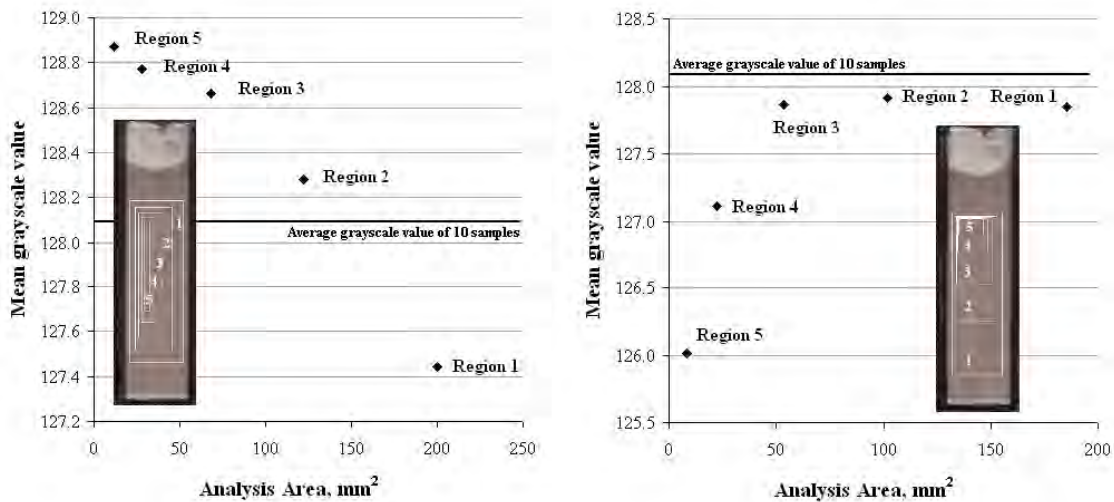


Figure 7.12: Mean grayscale value versus analysis area.

Figure 7.12 shows that changing the size of the analysis region effects grayscale value. The direction and magnitude of the influence on grayscale depends on the location of the analysis region. The left-hand plot in the figure shows an increasing grayscale value with decreasing area while the right-hand plot shows the opposite trend. The variability due to area of analysis was approximately 0 to 2 grayscale values.

It is concluded that as the analysis region decreases, less of the sample is analyzed and the analysis becomes increasingly sensitive to local variability in the sample. Based on the information shown in Figure 7.12, the analysis region should be greater than approximately 100 mm² or one-third of area of the available sample area.

Background Color

The effect of background color was investigated by analyzing a 10 by 20 mm sub region within a single 25 mm by 50 mm paint chip, scanned within a 90mm by 90 mm colored background. Colored construction paper was used for the backgrounds. In each case the 90mm x 90mm scanned region was fixed in location away from the hinged edge of the platen, and the scanner lid was closed to create constant lighting conditions. (The effects of ambient light on scanning are discussed in the following section.) After scanning, the average red, green, blue and

grayscale values of the paint chip and background colors in each image were then analyzed as described earlier.

As shown in Figure 7.13, the color of the background (as indicated by grayscale) did influence the computed grayscale value of the sub-region, even when the background portion of the scanned image was excluded from the analysis. In general, the lighter the background the lighter the computed grayscale value for the same sub region of the same gray-colored paint chip, with about a 1 grayscale unit increase as background color varied from non-glossy black construction paper to non-glossy white. It was concluded that although background color was a minor factor, it should be consistent for all ash analyses. The black construction paper was selected as described earlier.

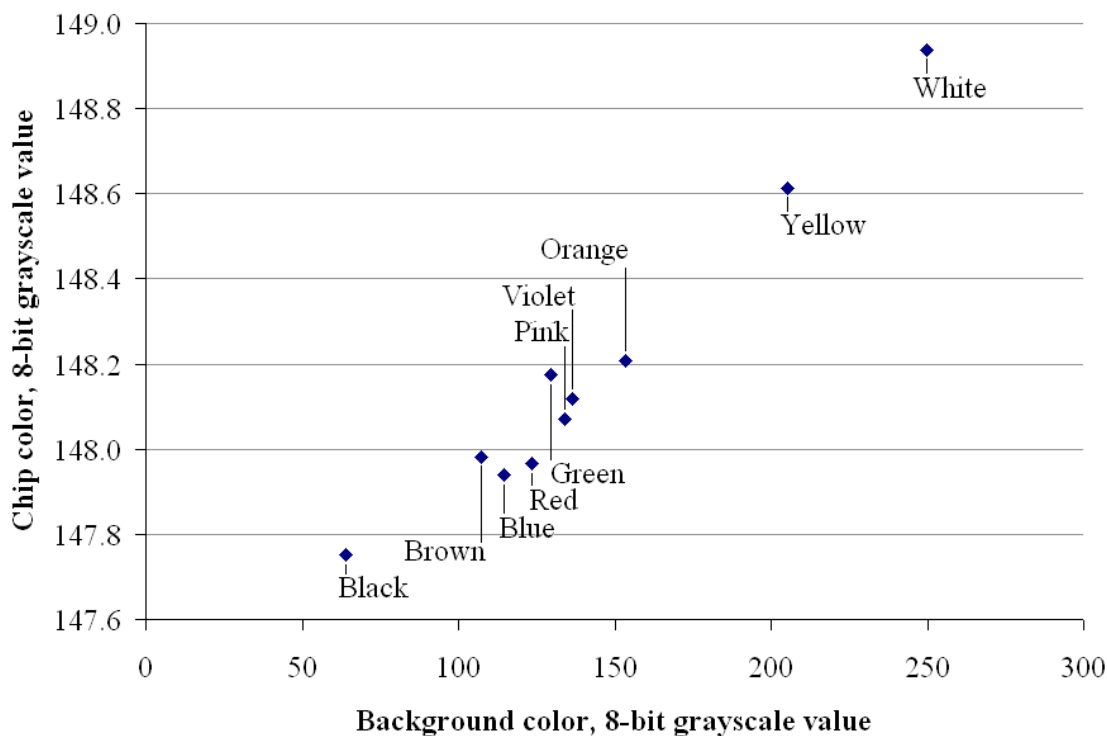


Figure 7.13: Effect of background color on chip scan.

Optical Sampling Rate (Resolution)

In multiple scans at “resolutions¹⁵” ranging from 75 to 1200 ppi (both x and y-directions), no clear influence on computed grayscale value was evident. The difference between the minimum and maximum computed result was approximately 1 gray scale value, similar to the variation observed with multiple scans of the same chip in various locations on the glass. Based on these results and general experience with the test procedure, a resolution of 400 ppi was chosen for all scans since scanning could be performed relatively quickly and file size was

¹⁵ Resolution is dependent not only on optical sampling rate (ppi) but also scanner optics, scanner operation, image processing, etc. (Gann, 1999)

manageable. Further, a resolution of 400 ppi was adequate to produce images with fine details visible.

Ambient Lighting

A sample of fly ash in a cuvet was scanned in the template according to the procedure described above with the exception that no box or other object was placed over the platen to block ambient light other than the template. The sample was then scanned again with the box covering the scanner to block ambient light. The scanned images are shown in Figure 7.14. The sample scanned without ambient light produced an average ash grayscale value of 127.5. The sample scanned with ambient light blocked produced an average ash grayscale value of 119.1. When ambient light was not blocked computed grayscale values of the ash sample were found to change as the lighting in the naturally lighted laboratory changed from morning to evening. Simply closing the scanner lid on top of the sample was determined to be insufficient in blocking the ambient light since the cover could not be closed completely. It was therefore concluded that blocking ambient light by means of the cardboard box (or some similarly effective cover¹⁶) was necessary for consistent results.

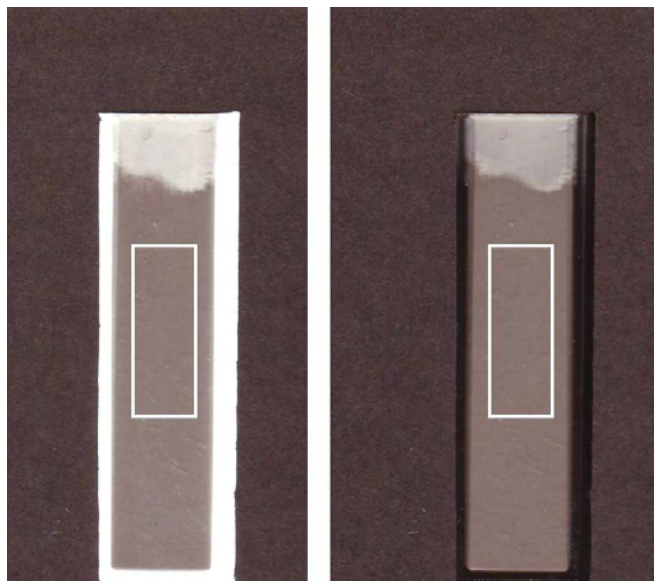


Figure 7.14: Ash sample scan with background ambient light (left) and with ambient light blocked (right).

Sample Variability

Moisture Content

The moisture content of fly ash samples was determined to influence ash color. Similar to many sands or clays which appear to darken when wetted, the color of an ash sample darkens

¹⁶ Note that the construction paper used to create the template was not completely opaque, and use of the template and a cover on the cuvet alone was not sufficient to block the effects of ambient light. If a completely opaque material were used to create the template that completely blocked ambient light from reaching the platen, then only the cuvet would need to be covered.

when moisture is present. Samples of a single ash source were placed into 200 mL porcelain bowls, each containing 5 to 6 g of ash. The bowls were then exposed to different moisture environments for about twenty four hours. The various moist environments used were 1) 105°C drying oven, 2) a sealed container used to store the ash sample, 3) the countertop of an air-conditioned laboratory, 4) a closed container containing room-temperature water and 5) a container containing boiling water. For locations 4 and 5, the ash was placed above the water level and received water by condensation from the atmosphere.

After exposure, the ash was used to fill two cuvetts from each test environment. The cuvetts were then sealed with clay plugs and immediately scanned. The cuvetts were then emptied into clean crucibles and the moisture contents of the samples determined by oven-drying at 105°C for twenty-four hours. The moisture content of the ash samples and corresponding grayscale color measurement are shown in Figure 7.15.

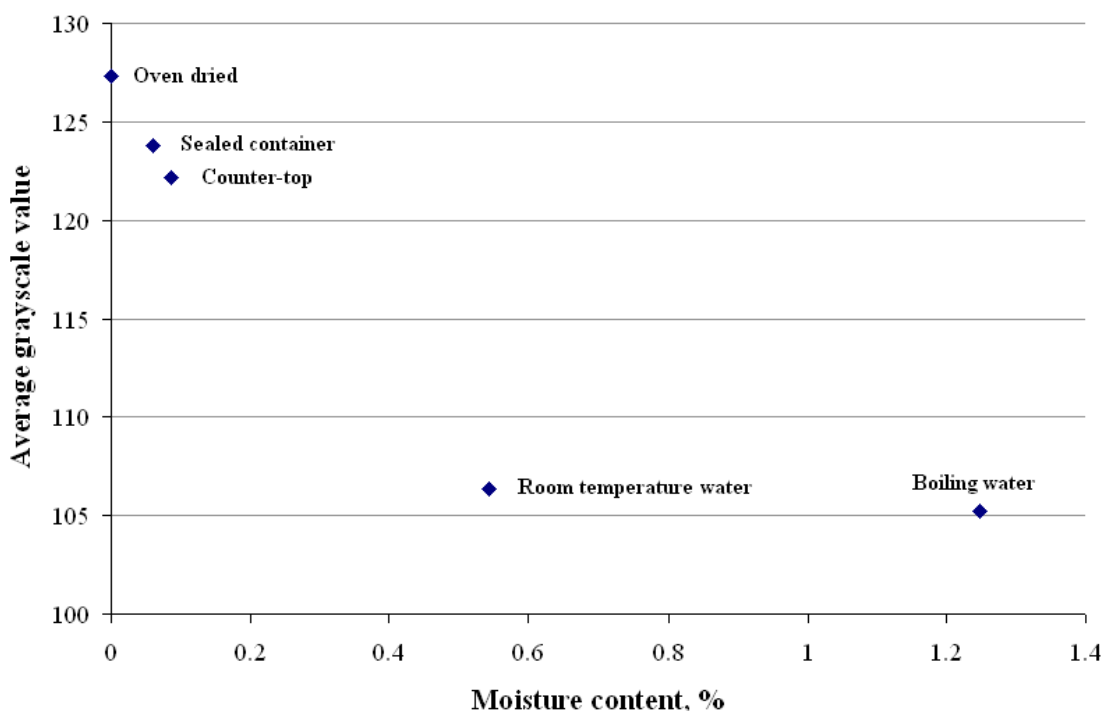


Figure 7.15: Average 8-bit grayscale value ash samples versus sample moisture content, points are labeled by ash environment.

An approximate 30-point grayscale change occurs between the sample with the greatest moisture content (1.25%) and the oven-dried sample. As the moisture content decreases, the grayscale value of the ash increases until all moisture is removed. It was therefore determined that prior to grayscale analysis 5g ash samples should be oven-dried at 105°C for 24 hours. Samples should be cooled and stored in desiccators between drying and scanning.

Sample Compaction

Oven-dried fly ash samples from five different sources were compacted prior to scanning using methods A, B, C and D as described in Table 7.3. Each cuvet was scanned on three sides,

with the average grayscale values shown in Table 7.4. The relative change in grayscale value compared to method A are shown in Table 7.5.

Table 7.3: Compaction method description.

Compaction Method	% Cuvet filled with Ash	% air space between ash and plug	Agitation/Compaction
A	~50%, no compaction upon filling or plugging	~25%	Vertical shake 10 times, cuvet held horizontally, scanned-face down.
B	~50% no compaction upon filling or plugging	~25%	Vertical shake 10 times, vertical tap against table top 4 times, cuvet held horizontally, scanned-face down.
C	~75% no compaction upon filling or plugging	~0%*	None
D	~75% in three equal layers, no compaction upon filling or plugging	~0%, putty plug pressed into contact with ash with a small rod.	Vertical tap against table top 20 times for each layer (60 total), cuvet held vertically.

*The size of the gap was small enough that when the cuvet was tipped on its side, the ash in contact with the cuvet walls was unable to redistribute

Table 7.4: Grayscale values of ash samples prepared with differing degrees of compaction.

Compaction Method	A	B	C	D
Description	Partially filled, no tapping	Partially filled, tapped	Completely filled, no tapping	Completely filled, tapped
Ash sample 1	95	95	93	94
Ash sample 2	154	159	158	159
Ash sample 3	175	176	176	176
Ash sample 4	125	128	128	128
Ash sample 5	113	112	111	112

Table 7.5: Relative change in grayscale values compared to method A

Compaction Method	A	B	C	D
Average increase in grayscale relative to method A	0	1.6	0.8	1.4
Average % increase in grayscale relative to method A	0.0%	1.1%	0.3%	0.9%

The results suggest that while the compaction effect is small, compaction methods B, C and D generally produce similar ash color results. For ash samples 1, 3 and 5, there is no significant difference between the results. Method A, however, produced lower gray scale values (darker gray) for ash samples 2 and 4 in comparison to the other methods.

During the experiment it was found that filling the cuvet in layers can, with certain samples, produce visible color changes at the layer boundaries. If the cuvet is filled completely so that the ash cannot be disturbed by shaking, the boundaries will be visible in the scanned image. Rodding the sample can cause striations in the ash along the cuvet walls. Complete filling and rodding are thus not recommended. Method B was chosen as the standard compaction method in this study because the sample could be shaken and redistributed to remove any visible layering due to sample preparation.

Sample Container

During scanning of fly ash samples, light generated by the scanning array passes through the glass platen, then through the sample holder (a plastic cuvet in the standard procedure) where it is reflected off the ash surfaces back through the sample holder and platen and finally to the image sensor. As light passes from one medium to another, some is reflected at the interface while the speed and direction of the residual light which enters the material typically changes (refraction) depending on the optical properties of the materials. The change in light characteristics can be observed when a glass microscope slide is placed over a uniformly colored paint chip; the color of the chip under the glass slide is darker than the uncovered portion. Since the path of the light in the scanner enters and exits different materials, it is likely that the nature of the light is changed before it reaches the optical sensor. To better understand how this might affect scanned images, an experiment was performed where colored paint chips were scanned through different materials and the effects of the materials on image color were compared.

Paint chips of seven differing shades of gray were scanned through different materials and the computed grayscale values were compared. To provide a reference color, the chips were first scanned directly on the glass platen and the resulting images analyzed as described above. The same paint chips were then scanned through a 1mm glass slide, a 0.2 mm glass slide cover, a 1 mm thick single wall of a methacrylate cuvet and one layer of kitchen-style plastic wrap. For each scan the platen location, resolution, background lighting and background color were controlled as previously described.

As shown in Figure 7.17, the nature of the material between the scanner glass and the ash has a significant effect on computed grayscale, generally darkening the resulting value (reducing grayscale value). The thickness of the material appears to have a lesser effect. The various materials produced very similar shifts in grayscale for the darkest paint chip, but as the paint chips got lighter in color the effects of the various materials diverged. In the case of using these methods to analyze typical cementitious materials that can represent a wide range of grayscale

values, standardizing the container material and thickness for lighter colored samples is more important than for darker samples. While glass containers may be preferable due to a reduced impact on the scanned image, the photometric cuvetts described earlier were used due to their availability and low cost, and because they are convenient to fill, scan and store.

Sample to sample variability

An experiment was performed to measure the variability in the scanning method from sample to sample. Ten cuvetts were filled with oven-dried ash from the same source. The ten samples were then scanned and analyzed according to the method described in Section 7.2.1.3.

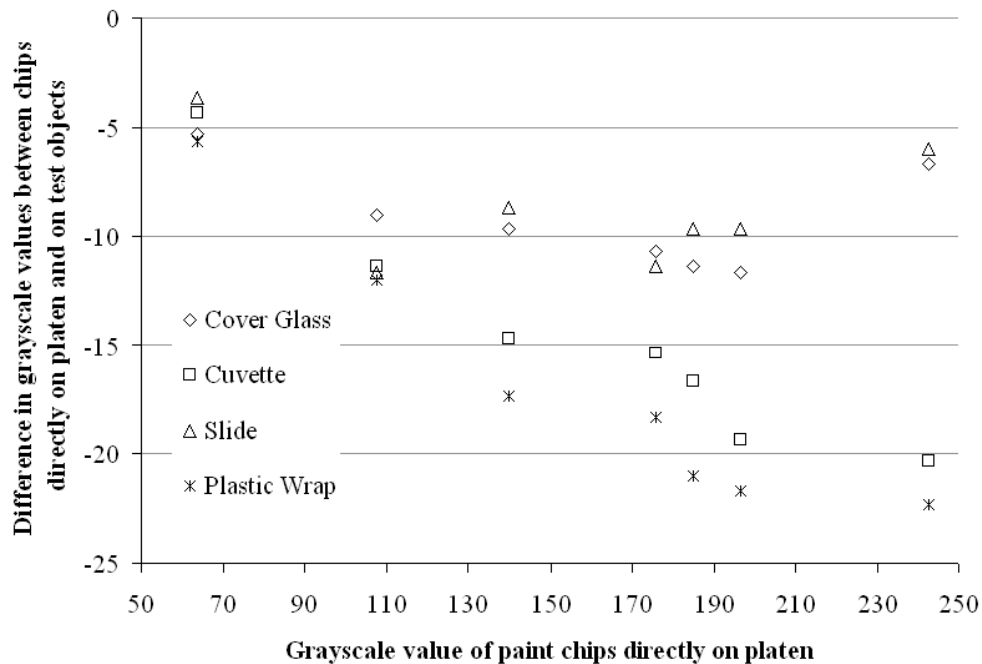


Figure 7.16: Deviation from the reference color of paint chips scanned through different materials.

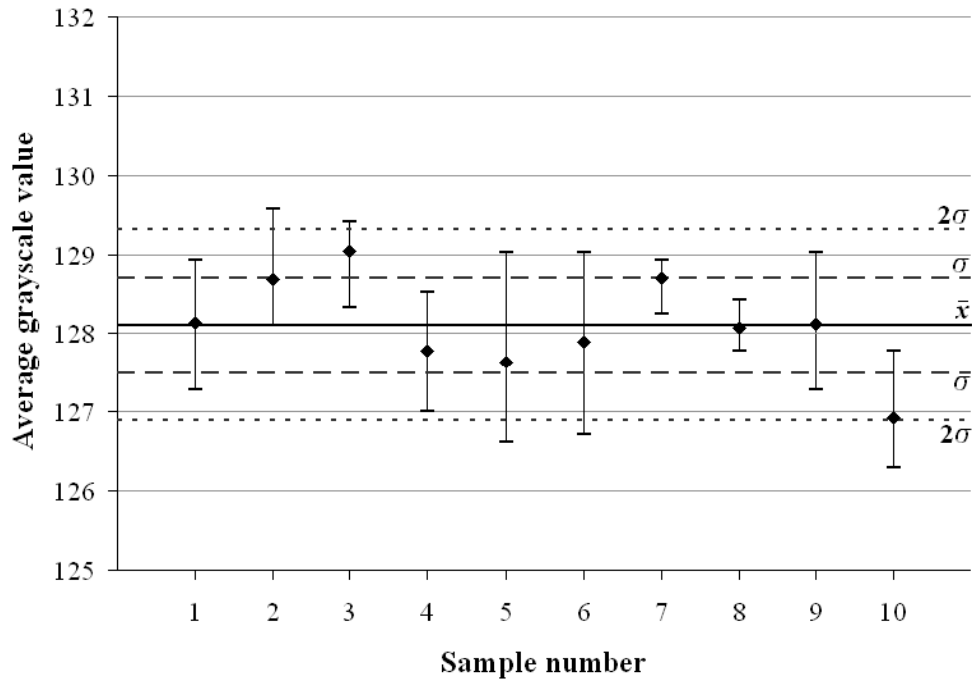


Figure 7.17: Variability in grayscale of 10 samples. The bars on each data point show the minimum and maximum grayscale values of the three scanned sides of each sample.

The results of the test, shown in Figure 7.17, contain information on 1) the variability in three sides of a single cuvet sample, and 2) the variability in ten cuvet samples. First, the variability in three scanned sides is shown by the maximum and minimum bars for each test. The greatest difference between the maximum and minimum values, sample no. 5, is equal to about 2.4 grayscale units. The average difference between minimum and maximum scans in a single sample is 1.5 grayscale units. Second, for the ten samples, the standard deviation was equal to 0.6 grayscale units. The greatest deviations from the mean (samples 3 and 10) differed by +0.9 and -1.2 grayscale units. All ten samples were located within two standard deviations of the mean (± 1.2 grayscale units).

When the same side of a single cuvet sample (left undisturbed) was scanned ten times and analyzed, the variability in grayscale value of the scanned images was 0.2 grayscale units. It can be concluded that this variability is due to the performance of the scanner only. The greater variability observed in the above experiment is likely due to variability in the cuvet and ash. Based on these experiments, it can be concluded that an error of $\pm 1.0 - 1.5$ grayscale units is typical for the test procedure. When comparing ash samples, changes in average grayscale values of approximately one unit or less are likely not significant due to the variability from other factors in the test. Such factors may include inhomogeneity in the parent ash sample, segregation of ash size fractions or components during sample filling, cuvet variability, etc.

Loss of information in converting RGB color data to grayscale

The simple but common technique used here to convert RGB data to a single grayscale valued loses information in the process. Consider that in a 24-bit “color space” composed of 8-

bit R, G, and B values, the entire spectrum of colors from black (no colors present) to white (all colors present) is divided into about 16.8 million discrete colors (256^3). The 8-bit grayscale “color space” divides the spectrum into only 256 unique colors. When the 24-bit RGB colors are converted to grayscale values using the typical weighting technique described here, it is observed that a single grayscale value can represent a large number of different combinations of R, G, and B values. This is shown in Figure 7.18, in which discrete grayscale values from 90 to 170 can each be obtained from about 105,000 different sets of RGB values. This is important since this range coincides closely with the range of grayscale values represented by the eighteen fly ashes studied. On the other hand, even though a grayscale value does not uniquely define color, each grayscale value in the range of 90 to 170 represents only 0.6 percent of the population of all possible 24-bit colors. Further, since the stimulus for the work was quantification of color differences as detected by the human eye, it is noted that many visually satisfactory computer displays use only 64 grayscales to represent 256 steps. Ash values that differ by 5 grayscale units or less are very difficult or impossible to differentiate visually. Thus the color-to-grayscale conversion here is considered to be similarly satisfactory, while recognizing that even more discernment may be possible by retaining the more cumbersome yet detailed red, green, and blue values.

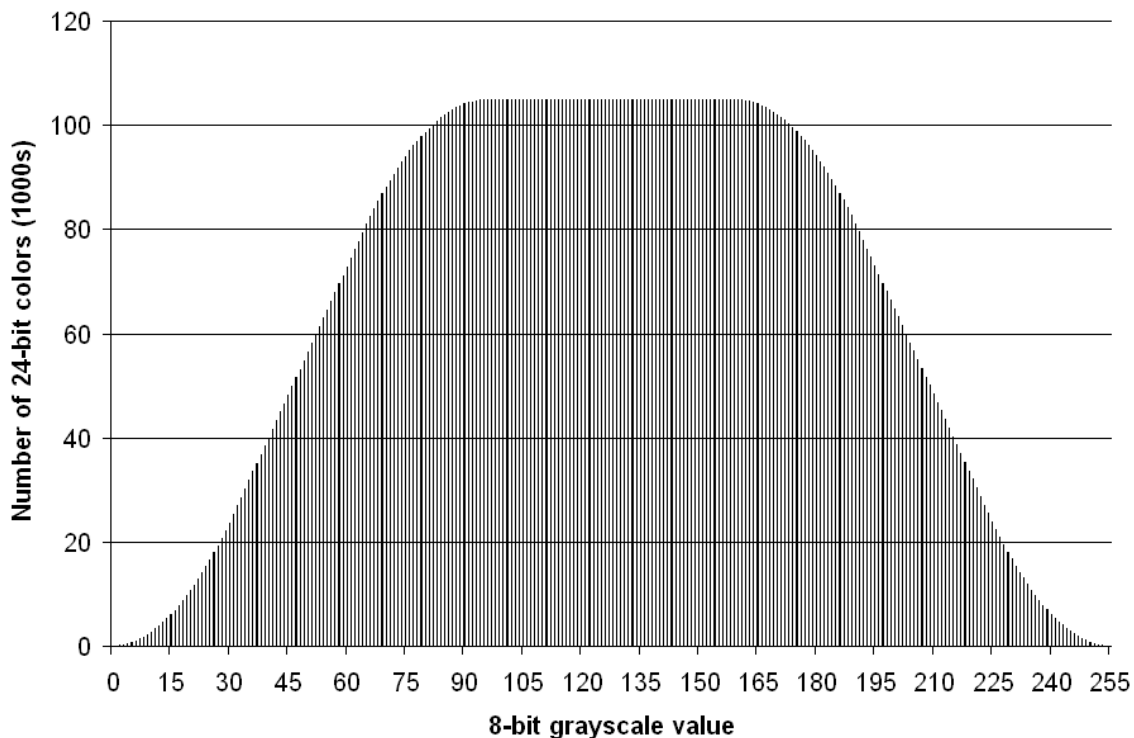


Figure 7.18: The number of individual 24-bit RGB colors per single 8-bit grayscale value.

Variability Summary

Several sources of variability in the test procedure have been identified and are summarized in Table 7.6. When the recommendations made in this section to control variability are followed, the test is capable of producing repeatable results with standard deviations of about 0.6 grayscale unit.

Table 7.6: Sources of variability in the test procedure and their effects on measured grayscale values.

Experimental Factor, in decreasing order of influence	Influence, Approximate computed grayscale value
Ash Moisture Content	5 to 20
Container material and thickness	5 to 20
Choice of Scanner	13
Ambient light	8
Size of scanned area	1 to 2
Background color	1 to 2
Location on Scanner glass	1 to 2
Compaction	1 to 2
Scanner Resolution	1 to 2
Repeatability, Same sample, same scanner, same operator	1 to 1.5

7.1.7 Correlations among ash color, AEA dosage in concrete

As introduced earlier, the development of a method to measure ash color was stimulated by the observation that ash samples that required relatively larger doses of AEA to produce a given air content in fresh concrete were generally darker in color than those that required relatively smaller doses of AEA for the same air content. The technique described above was used to obtain grayscale values of ash samples collected in “as-received” condition at batch plants with no further treatment other than oven-drying. The average grayscale values from analysis of the scanned images are shown in Figure 7.19. The ash samples vary in shades of gray with ash F-B1 the darkest ash having a gray value of 91 and ash F-R1 the lightest having a gray value of 172. All the ashes to the right of and including sample C-D1 meet the ASTM C618 requirements for Class C, and all those to the left meet the requirements for Class F. With the exception of F-R1, all Class F samples had lower gray values (were darker) than the Class C samples. Within this population the Class F samples also have the greatest range in gray values, from gray 91 to gray 172 compared with gray 144 to gray 166 for the Class C ash samples.

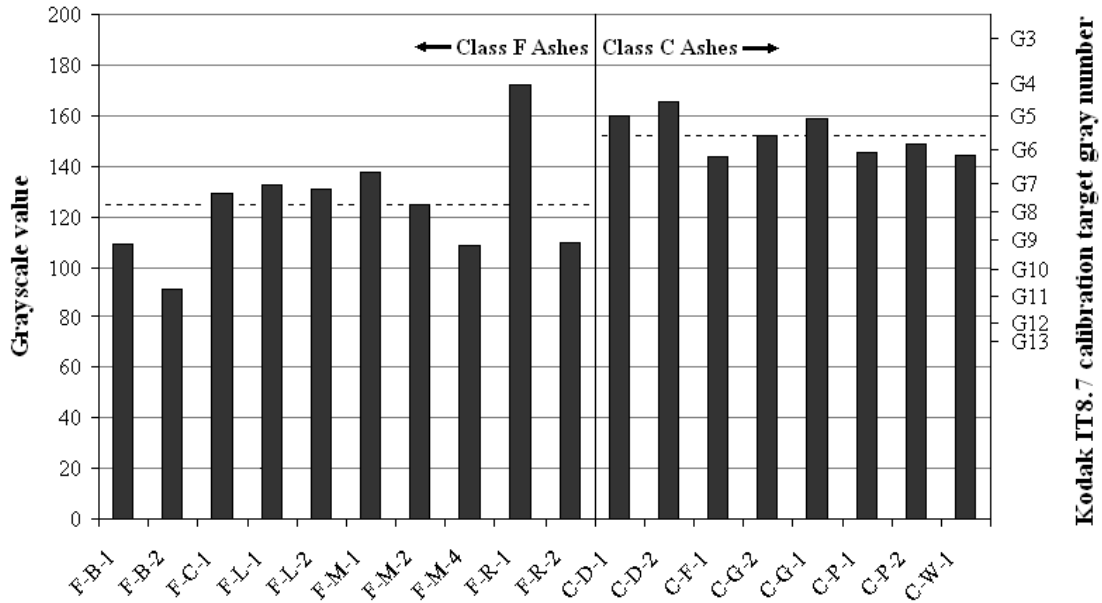


Figure 7.19: Average grayscale values of the Texas ash set. Dotted lines show the average grayscale values of the Class F and C ashes.

Figure 7.3 plots these computed grayscale values against AEA dosages required for 6 percent air as determined by Ley at The University of Texas (Ley, 2007). Figure 7.3 shows a general trend of decreasing AEA dosage with increasing gray values (i.e., lighter colored ash). Power functions fitted to the data (shown by the dashed lines) produce R^2 values of 0.5 for concrete dosage.

In a practical application of this tool, ash samples similar in origin to those tested here which possess gray values lower than 110-120 may indicate to a producer that AEA doses can rise to double or triple the doses needed for lighter colored ashes. For the ashes studied, gray values of 110-120 indicated doses of 60 mL of the wood rosin based AEA per 100 kg CM or more are required to produce 6 percent air content in concrete that incorporates the ash. Gray values of ash samples greater than 120 would indicate that the AEA dosage requirement is in the range of 20 to 50 mL per 100 kg CM.

7.1.8 Discussion

Test method

Grayscale analysis of fly ash using the presented method was simple to perform and did not require sophisticated equipment or expertise. Common commercially available scanners were used to perform the tests and no modification to the scanner hardware was required other than attaching the paper template shown in Figure 7.5. Scanning the ash samples according to the method described above did not mar or damage the scanner platen.

The most robust aspect of this method was the ability to produce repeatable results using a single scanner model insofar as the recommendations for controlling variability were followed. These sources were identified and measured in Section 7.2.3 and recommendations for controlling them are incorporated in the procedure described in Section 7.1.3. With the

fundamental method in place, further enhancements can be made in the future to reduce error and streamline the process (reducing ash drying time, scanning and analyzing multiple samples simultaneously, continuous or spot scans during the manufacturing process, etc.)

The difference in performance between commercial scanners is the most variable aspect of this method. However, it was shown in one case that analysis values obtained using one scanner can be converted to values obtained from another scanner and vice versa. Scanner calibration must be performed if the procedure is to be used in multiple labs.

Ash and color

Bulk ash color is a composite of the contributions of numerous individual ash particles. With the aid of an optical microscope, it can be observed that ash is composed of particles of a variety of shades and hues. While the majority of ash particles are clear or white in color, many dark brown to black particles are also present. The color of an individual particle is dependent on its composition and formation environment. All the individual particles contribute to the macroscopic color of the bulk ash.

Changes in ash color indicate that certain characteristics of the ash has also changed, such as moisture content to other changes that may affect behavior in a concrete mix or other system. Color change can serve as an indication of source consistency and can be useful at source, or at a concrete batch plant. The principles and test method would apply equally to condensed silica fume, ground granulated blast furnace slag, other SCMs, or portland cement itself.

Correlation between concrete air and grayscale value

The trend of increasing AEA requirement for concrete with decreasing grayscale shown in Figure 7.3 indicates that increased AEA requirement is partly dependent on the presence of dark material in ash. The work of several researchers have concluded that organic coal residuals composed primarily of carbon char present in ash increases AEA dosage of concrete (Larson, 1964; Gebler and Klieger, 1983; Freeman et al., 1997; Gao et al., 1997; Baltrus and LaCount, 2001; Hill et al., 1997; Kulaots et al., 2003; Kulaots et al., 2004). Residual coal particles are brown to black in color and were present in varying amounts in all of the samples tested. While residual coal may be a major factor contributing to ash darkness, the influence of residual coal alone or other individual components on ash color cannot be identified by the basic method described in this study.

Test Use

The basic test procedure for imaging and quantifying ash color can be used as a quick method for assessing the quality of fly ash with respect to AEA dosage in concrete. Based on the relationship shown in Figure 7.3, ash samples with grayscale values less than about 120¹⁷ may require AEA dosages 2 to 3 times higher than lighter colored ashes. AEA dosage increases with decreasing grayscale value.

One notable aspect of the relationship in Figure 7.3 is that all of the ash samples used in this study represented different power plants or burner configurations, and therefore were produced from different coal sources and in differing combustion environments. There is much

¹⁷ Grayscale values must be calibrated to the values given in Table 2.

potential for use of this test to monitor variability in ash produced at a single electric utility where the coal source and/or operating conditions are fairly constant with time.

Future work

The subsequent section presents correlations between ash color, ash composition, and ash behavior in concrete. A method for measuring carbonaceous organic coal residuals content in ash using a variation of the grayscale analysis method described here is also presented.

The ash samples tested in this study were representative of the ashes produced in a narrow geographical region of the U.S. Additional study should be done to measure differences that may exist among ash samples produced from coals and plants in different regions. It is recommended that a study of the variations in color with time of ash sample from a single source be conducted to identify the usefulness of this tool in such an application. A study of the influence of particle morphology (size and shape) on ash color should be studied to identify potential effects on grayscale analysis results.

7.1.9 Conclusions

1. A standard procedure for characterizing ash color has been developed. The procedure includes ash sample preparation, sample imaging with a common desktop color image scanner and image analysis to quantify image color information.
2. Various factors in the test procedure—such as scanner model, analysis region size and location, scanned background color and ambient light—have the potential to introduce variability in the tests and should be controlled as described herein.
3. Different scanner models image samples differently. If a correlation between scanners can be described by a mathematical function, then a correction between scanners can be easily made.
4. Characteristics of the sample preparation—such as moisture content, sample compaction and sample container material—can cause variability in the test method and should be controlled according to the guidelines given.
5. Four-clear-sided, methacrylate cuvetts were found to be satisfactory for containing ash samples during scanning. Use of containers composed of different materials can be used, however, the influence on the scanned image must be considered.
6. Use of 8-bit depth grayscale values to quantify ash color contains less information than full color (24-bit depth) values; however, grayscale values were used to adequately differentiate the ash samples tested in this study.
7. A trend between decreasing grayscale value (darkening) of ash and increasing AEA dosage for concrete containing the ash exists for the ash samples studied.
8. The scanning and grayscale analysis method presented here can be used as a quality control tool to identify ashes that may require increased AEA dosage in concrete.
9. The test could be used as a low-tech indicator for the need to perform additional testing for ash-AEA interactions. For example if ash sample grayscale value is greater than 120-130 (as measured by the author's scanner) i.e., lighter than grayscale patches G7 to G8 of the Kodak IT8.7 standard, then the influence of the ash on AEA dosage in concrete will

likely be relatively low. However, if the ash grayscale value is less than 120-130 (darker than patches G7 or G8), then the ash may significantly increase AEA dosage in concrete and additional testing should be performed to identify the magnitude of the influence.

7.2 Analysis of Fly ash by flatbed color scanner: Part II-Change in grayscale as method for identifying organic carbon in fly ash

7.2.1 Introduction

Fly ash color can vary considerably from source to source. While typically 90 percent or more of the mass of fly ash is composed of oxide compounds that are light tan to white in color, carbon in various forms, and oxides of iron, act as “pigments” such that fly ash meeting the chemical and physical requirements of ASTM C618 can range in color from nearly white to dark gray or black (Yu et al., 2000; FHWA, 2007). The research reported here investigated the ability to a.) reliably and repeatedly characterize the color of fly ash using a desktop flatbed color scanner, b.) correlate ash color to ash performance, particularly in regard to impact on air entrainment, and c.) correlate ash color to ash composition. The results suggest that the technique may be a useful tool for rapid detection of fly ash characteristics. Section 7.1 concentrated on the development of the color analysis method and conversion of color data to grayscale, and Section 7.2 presents correlations between ash color and compositional properties, specifically the presence of organic carbon.

7.2.2 Research significance

The fly ash color analysis method described in Part I can be used to reliably and repeatedly quantify fly ash color. Correlations made between fly ash color and fly ash composition could be useful for making color-based predictions on ash/concrete interactions. The presence of organic carbon in ash can influence the air entraining admixture dosage of concrete which incorporates the ash (Harris, 2007). Use of the fly ash color analysis method to estimate organic carbon content in ash could aid concrete producers in estimating the proper air entraining admixture dosage for concrete.

7.2.3 Background

Basic procedure

In Section 7.1 of this work, a procedure for quantifying ash color as a single numerical grayscale value was presented. The procedure consisted of filling a four-clear-sided, methacrylate cuvet¹⁸ with oven-dried ash to approximately half-full (without compaction). A putty plug was inserted completely into the top of the container leaving an air-filled gap about one-quarter of the height of the container above the ash. The cuvet was then shaken and tapped in a prescribed manner to lightly consolidate the ash against one of the four clear walls of the cuvet. The cuvet was then placed on a flatbed scanner with fitted scanner holding template and scanned as a color image. The consolidation and scanning procedure was repeated for two other sides of the cuvet. During scanning, ambient light was blocked from reaching the scanner.

¹⁸ 12 mm x 12 mm x 45 mm with 1 mm thick walls with four clear sides (The cuvetts are normally used for holding liquid samples for ultra violet-visible light spectrographic analysis, manufactured by Fisher Scientific Company L.L.C., Cat. No. 14-386-21).

Numerical indices of ash color were found by averaging the individual Red (R), Green (G) and Blue (B) components of all pixels in a sub-region of the ash image. Analysis of the RGB content was performed using a software package available in the public domain.¹⁹ The final output for a given ash sample consisted of three separate sets of the means for Red, Green and Blue values (0 to 255), corresponding to the three scanned sides of the cuvet. Mean values for each of the three scanned sides were averaged to produce a single set of (R,G,B) values used to characterize the sample. The three parameters were converted to a single grayscale value for subsequent analysis and comparison. The method of conversion is given by equation 7.2.

$$\text{Grayscale value} = rR + gG + bB \quad \text{eq. 7.2}$$

The variables R, G and B are the average 8-bit color components of a 24-bit color image and *r*, *g* and *b* are the applied weights. The sum of *r*, *g* and *b* is equal to 1. The values of the weights used in this study are given in Table 7.7. A grayscale value of 0 indicates pure black and a grayscale value of 255 indicates with pure white.

Table 7.7: Twenty-four-bit color conversion weights

Weight	Value
r	0.25
g	0.625
b	0.125

Variability

Several sources of variability were identified in Section 7.1 of this chapter. The sources include: variation between scanner models, ambient lighting and sample moisture content to name a few. The detailed test procedure described in Section 7.1 was designed to minimize variability in the test.

Correlation between grayscale values and fly ash-AEA interaction

A trend between decreasing grayscale value (darkening) of ash and increasing AEA dosage for concrete containing the ash was identified for the ash samples studied in Section 7.1. Based on the correlation, the color analysis method was suggested for use as a quality control tool to identify ashes that may require relatively high AEA dosage in concrete. This study seeks to improve the correlation between AEA dosage and ash color and identify the factors that influence grayscale values.

¹⁹ UTHSCSA ImageTool developed by C. Donald Wilcox, S. Brent Dove, W. Doss McDavid and David B. Greer of the Department of Dental Diagnostic Science at The University of Texas Health Science Center, San Antonio, Texas. ImageTool executable and source code can be downloaded free of charge at <http://ddsdx.uthscsa.edu/dig/download.html>.

Scope

In this study, the relationship between ash grayscale value and ash organic carbon content is explored. Materials in ash that may include organic carbon are coal char (Freeman et al., 1997; Hill et al., 1997; Kulaots et al., 2003; Kulaots et al., 2004), volatile organic compounds (Fan and Brown, 2001; Helmuth 1987) and possibly soot (Gao et al. 2007). The contribution of organic carbon to ash grayscale value could be measured by analyzing ash color before and after organic carbon removal. Organic carbon can be removed from ash by heating the ash in air to sufficient temperatures as will be shown.

There is no clear consensus on the classification of carbon forms as either “organic” or “inorganic,” and the definition of organic substances has changed over time (Zumdahl, 1993). Nevertheless a working definition for carbon classification for this study is based on the output of the TOC analyzer. The TOC analyzer measures what is referred to as “inorganic” carbon by decomposing carbonates with acid to produce carbon dioxide which is then detected and measured by the apparatus. The total carbon content (organic AND inorganic) of a fresh sample is measured by heating a sample to 900°C to remove all carbon present either by calcination of carbonates or by oxidation of organic carbon. The oxides of carbon are then measured to determine the total carbon removed from the sample. The so called “organic” carbon content is simply the difference between total carbon content and the inorganic carbon content. Therefore, for this work inorganic carbon is considered to be the carbon that is acid-soluble, such as the carbon in carbonates. All other carbon forms which oxidize at temperatures of 900°C and are not acid-soluble are taken as organic carbon. Forms of carbon that are neither decomposed by reaction with acid nor oxidized by heating at 900°C are not detected or measured by the TOC analyzer and are not considered in the definitions.

In this work, correlations between ash organic carbon content and ash grayscale values are presented. The technique measures the changes in grayscale values of ash which occur as the ash is heated between 300 and 500°C. Contributions from other materials such as calcium containing minerals in ash on grayscale change are considered. Relationships between change in ash grayscale value and concrete AEA dosages are given.

7.2.4 Experimental procedures

Fly ash samples

Seventeen commercially-available ash samples obtained from eleven power plants across Texas were used in this study. In this work, the samples are identified by two letters followed by one or more digits. The first letter is either a “C” or “F” denoting the classification of the ash by ASTM C618.

Seven additional samples were “processed” by dry sieving one sample (Ash FR-2). U.S. standard sieves numbers 120, 140, 170, 200, 230 and 325 were used (opening sizes 125, 106, 90, 75, 63, 45 μm). These samples are labeled FR-#* where the “#” corresponds to the opening size of the sieve from which the sample was collected (Sample FR-0* was collected from the pan). Sieving was performed to increase the organic carbon content of the largest size fractions.

Ash grayscale change due to heating in air

Seven Class F and three Class C ashes were heated in an air-atmosphere muffle furnace at temperatures between 105 and 800°C. For each temperature and ash sample, 3 g of ash was

heated in a porcelain bowl for 60 min then removed from the furnace and cooled in a desiccator for about 20 min. After cooling, the sample was immediately placed in a standard sample holder and the grayscale value analyzed according to the method described in Section 7.1 of this study. Organic carbon contents of heat-treated samples of Ash FB-2 and FR-2 were measured as described in Section 7.2.4.3.

The seventeen commercially available ashes were oven-dried at 105°C for 24 hr, scanned and analyzed according to the method described in Section 7.1 of this chapter²⁰. The samples were then heated to 750°C (ASTM C311 fly ash loss on ignition test temperature) in a muffle furnace and scanned and analyzed. The difference in grayscale values of the ashes between 105 and 750°C was calculated as the 750°C grayscale value minus the 105°C grayscale value. Positive grayscale changes indicate that the ash became lighter toned between 105 and 750°C. Concrete AEA dosage values for the ash samples were determined as described in Section 7.1 of this work.

The same experiment performed above was repeated for the seventeen ash samples and the sieved ash fractions except that temperatures of 300 and 500°C were used in place of 105 and 750°C. Changes in grayscale values were computed by subtracting the grayscale value of the ash exposed to 300°C from the grayscale value of the ash exposed to 500°C.

Organic carbon measurement

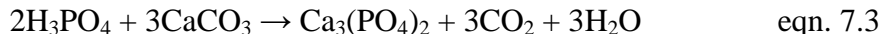
The organic carbon contents of the seventeen commercially-available samples and the sieved ash fractions were measured using a two step process with a Shimadzu TOC-VCPN with solid sample combustion unit (SSM-5000A). The two steps were, first, determination of the total carbon content, and second, the determination of the inorganic carbon content. The organic carbon content was then determined by subtracting the inorganic carbon content from the total carbon content.

The total carbon content is measured by heating the samples to 900°C in the TOC solid sample module furnace. Inside the furnace (which has a high purity air atmosphere, very low carbon oxides) organic carbon is oxidized and inorganic carbon is decomposed. The gaseous carbon, in the form of carbon dioxide then passes through a carbon measurement device that consists of an infrared light source, flow cell and infrared sensor (NDIR method). As a carrier gas (pure oxygen) flows through the flow cell, the gaseous carbon driven off the sample is carried between the infrared source and sensor. The sensor detects a change in the intensity of the light due to the absorption of the light by the carbon in the flow cell. The sensor unit then converts the change in light detected into an output voltage. The change in voltage over time is used to produce an area (of voltage multiplied by time) proportional to the amount of carbon measured. The amount of carbon detected can be determined by calibrating the instrument with a material with established carbon content. Pure solid glucose was used to establish the calibration for coal fly ash residual carbon.

The inorganic carbon content of the ash is determined by immersing the sample in 33 percent phosphoric acid and heating the sample to 200°C in the furnace of the TOC solid sample module. The acid causes the decarbonation of the carbonates present in the sample, as shown by the example of calcium carbonate in equation 7.3. The carbon dioxide released in the reaction passes through the flow cell of the detector and the absorption of the infrared light by the carbon

²⁰ A Canon CanoScan LiDE 500F color scanner, shown in Figure 4, was used for all scanning tests done in this study.

is quantified as discussed above. Reagent grade solid calcium carbonate was used to calibrate the inorganic carbon measurements. The results of the analyses on the ash samples are given in Table 3.3.



Bulk chemical analysis by x-ray fluorescence

The elemental composition of the fly ash samples was determined by x-ray fluorescence (XRF) spectroscopy at the Materials Analysis and Research Laboratory at Iowa State University, using a Philips PW2404 XRF spectrometer.

7.2.5 Results

The grayscale values versus temperature of maximum exposure for seven Class F ashes and three Class C ashes are shown in Figures 7.20 and 7.21. (The G-values shown at the right of the plot correspond to the scanner’s identification of the gray blocks of a Kodak IT8.7 calibration target, see Section 7.1.6.1.1.) The two figures show varying magnitudes of increases and decreases in grayscale values occurring at different exposure temperatures, but the changes are generally consistent with in ash class. The two ash classes differ in change in grayscale value behavior. Virtually no grayscale increases occur in the Class C ashes up to 500°C while the Class F ashes show much larger increases in the range. All of the ash samples show decreases in grayscale value (darkening) at temperatures above 500 to 600°C.

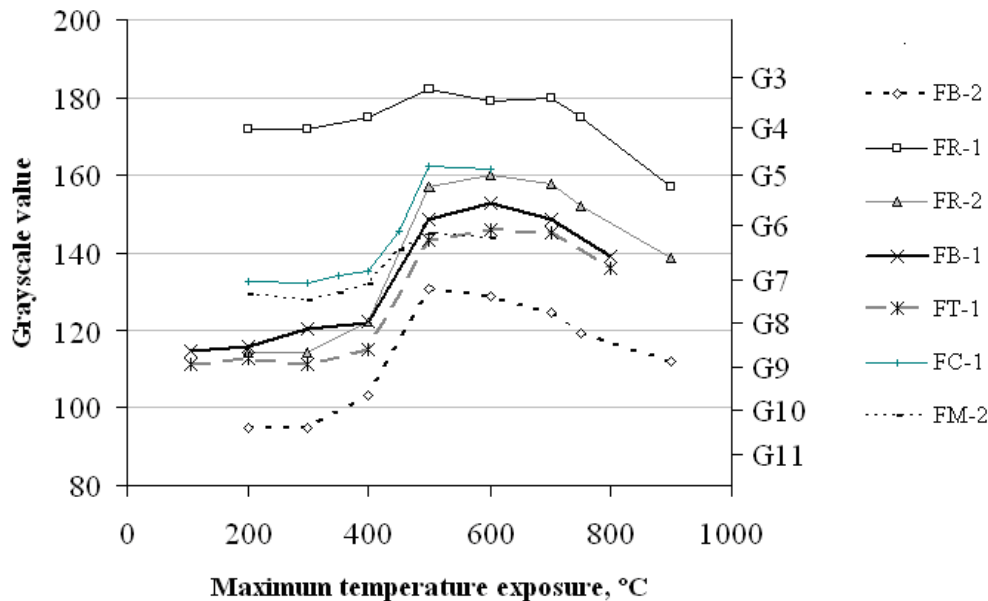


Figure 7.20: Ash average grayscale value versus temperature exposure for seven Class F ash samples.

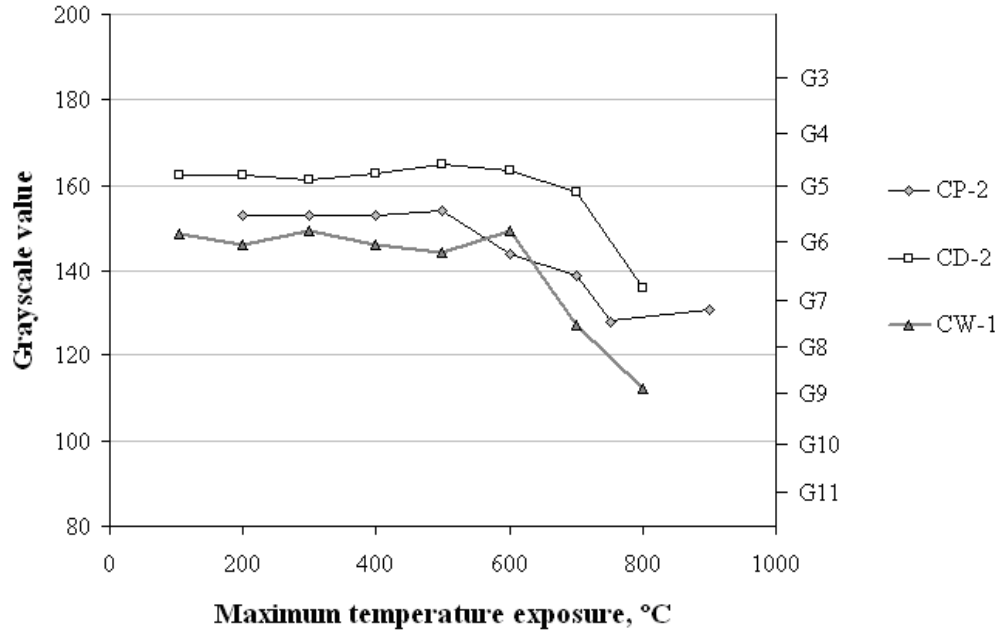


Figure 7.21: Ash average grayscale value versus temperature exposure for three Class C ash samples

The organic carbon content versus exposure temperature for ash samples FR-2 and FB-2 are shown in Figure 7.22. The figure shows that 86 percent (Ash FB-2) and 92 percent (Ash FR-2) of organic carbon content of the two ash samples is removed between 300 and 500°C. The organic carbon content of Ash FB-2 was reduced to 0.05 percent (approximately 13 percent of the organic carbon present at the beginning of the test) after exposure to 500°C. After exposure to 600°C, 0.02 percent carbon remains. For Ash FR-2, after exposure to 500°C, 0.03 percent carbon (approximately 4 percent of the organic carbon present in the as-received ash) remains. By 600°C, the remaining organic carbon is reduced to 0.02 percent.

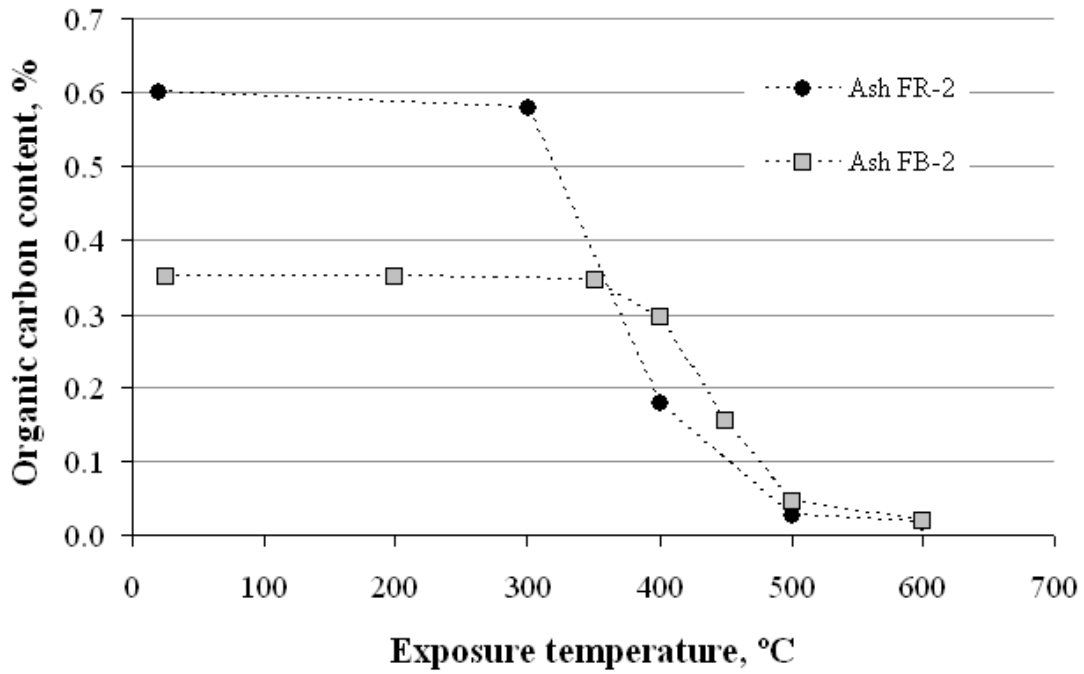


Figure 7.22: Organic carbon content versus temperature exposure for two fly ash samples.

The grayscale values of the seventeen commercially-available ash samples after exposure to 105 and 750°C are shown in Table 7.8. The difference in grayscale values from 105 to 750°C and concrete AEA dosage for 6 percent air content are also given.

Table 7.8: Grayscale values, and grayscale difference after exposure to 105 and 750°C, and concrete AEA dosages.

Ash name	Grayscale value after temperature exposure		105-750°C grayscale difference	Concrete AEA dose, mL/100kg cm
	105°C	750°C		
FB-1	109	138	29	64
FB-2	91	118	27	91
FC-1	129	139	10	52
FL-1	133	118	-15	28
FL-2	131	119	-12	39
FM-1	137	130	-7	41
FM-2	125	131	6	49
FR-1	172	173	0	24
FR-2	110	151	41	147
FT-1	109	133	24	42
CD-2	166	133	-33	50
CF-1	144	119	-25	34
CG-1	159	133	-26	38
CG-2	152	122	-30	39
CP-1	145	110	-35	36
CP-2	149	127	-22	29
CW-1	144	110	-34	44

The results of the 300 to 500°C color change analyses and organic carbon analyses of the ash samples are shown in Table 7.9. From Table 7.9 it can be observed that the organic carbon contents of the non-sieved ashes range between 0.02 and 0.72 percent. The organic carbon contents of the sieved fractions range between 0.29 and 5.31 percent. Grayscale changes between 300 and 500°C vary from -3.8 to 36 units for the non-sieved fractions and 40.3 to 87.6 for the sieved fractions. It is interesting to note that all the ash samples with negative grayscale change are ASTM C618 Class C ash samples.

Table 7.10 presents the oxide contents of the ashes determined by XRF. Fly ash sample FL-2 and the sieved fractions of ash FR-2 were not included in the bulk chemistry analysis. Multi-linear regression analysis was performed to identify possible contributions from the oxides of Table 7.10 and organic carbon contents to a correlation with change in grayscale value between 300 and 500°C. The analysis showed that organic carbon and calcium oxide contents made statistically significant contributions to the correlation. Results of the analysis are shown in Table 7.11.

Table 7.9: Change in grayscale values between 300 and 500°C and organic carbon content of ash samples.

Ash name	Change in grayscale value between 300-500°	Organic carbon content, %
FB-1	27.0	0.38
FB-2	33.5	0.38
FC-1	26.0	0.32
FL-2	3.0	0.07
FL-1	5.0	0.09
FM-2	5.0	0.11
FM-1	12.5	0.17
FT-1	30.8	0.28
FR-1	7.0	0.02
FR-2	36.0	0.72
CD-2	0.2	0.05
CF-1	-1.7	0.06
CG-2	2.6	0.13
CG-1	2.8	0.14
CP-2	-0.9	0.04
CP-1	-2.0	0.12
CW-1	-3.8	0.12
Sieved ashes		
FR-125*	87.6	5.31
FR-106*	80.2	2.09
FR-90*	74.3	1.79
FR-75*	68.3	1.11
FR-63*	62.3	0.93
FR-45*	46.6	0.47
FR-0*	40.3	0.29

Table 7.10: Fly ash bulk chemistry by X-ray fluorescence (XRF), note sample FL-2 is not included.

Sample name	Na ₂ O (%)	MgO (%)	Al ₂ O ₃ (%)	SiO ₂ (%)	P ₂ O ₅ (%)	SO ₃ (%)	K ₂ O (%)	CaO (%)	TiO ₂ (%)	Fe ₂ O ₃ (%)
FB-1	0.68	3.2	19.4	52.2	0.21	0.91	1.07	14.0	1.14	4.7
FB-2	0.52	2.9	18.6	50.8	0.19	0.94	0.91	14.0	1.22	7.9
FC-1	1.63	3.6	22.5	47.2	1.50	0.62	0.77	14.3	1.13	4.7
FL-1	0.47	2.7	19.2	55.0	0.18	0.57	0.91	11.1	1.25	7.2
FM-2	0.50	2.7	20.6	54.4	0.12	0.46	1.16	8.6	1.15	8.4
FM-1	0.67	3.0	20.1	50.9	0.09	0.70	1.07	11.7	1.17	8.1
FT-1	0.39	2.0	17.9	63.2	0.19	0.16	1.12	7.7	1.22	4.0
FR-1	0.22	2.5	24.5	48.3	0.18	0.69	0.68	15.6	1.61	3.4
FR-2	0.25	2.1	23.3	51.9	0.18	0.77	0.77	12.4	1.48	4.5
CD-2	1.72	4.8	19.9	34.8	1.26	1.71	0.45	26.3	1.65	5.7
CF-1	1.88	5.9	18.4	33.7	1.13	1.88	0.37	27.2	1.38	6.8
CG-2	1.58	4.3	20.2	37.4	0.99	1.20	0.44	24.6	1.72	6.2
CG-1	1.58	4.5	20.5	38.2	1.30	1.09	0.51	23.8	1.61	5.6
CP-2	1.72	4.6	19.2	35.7	1.30	2.63	0.47	24.4	1.49	6.6
CP-1	1.84	5.5	17.8	33.4	1.15	2.77	0.29	27.4	1.44	6.8
CW-1	2.12	6.6	17.5	30.9	0.83	3.74	0.30	28.7	1.44	6.1

Table 7.11: Regression analysis results (from JMP²¹), Y= change in grayscale value, parameters organic carbon and calcium oxide

Summary of fit					
RSquare			0.87		
RSquare Adj			0.86		
Root Mean Square Error			5.4		
Mean of Response			11.3		
Observations (or Sum Wgts)			16		
Analysis of variance					
Source	DF	sum of squares	mean square	F Ratio	
Model	2	2659	1329	45.5	
Error	13	380	29	Prob > F	<0.0001
C. Total	15	3039			
Parameter estimates					
Term	estimate	std error	t Ratio	Prob> t	
Intercept	14.3	5.0	2.9	0.013	
Organic carbon content,%	54.0	8.6	6.3	2.81E-05	
CaO, %	-0.74	0.21	-3.6	0.003	
Effects test					
Source	Nparm	DF	sum of squares	F Ratio	Prob > F
Organic carbon content,%	1	1	1155	39.5	2.81E-05
CaO, %	1	1	371	12.7	0.003

7.2.6 Discussion

Factors influencing grayscale change

Figures 7.23 and 7.24 show that the ash grayscale values change (increase and decrease) in certain temperature ranges. For the Class F ashes in Figure 7.23, grayscale values increase between 200°C and 500-600°C and then decrease thereafter. For the Class C ashes, grayscale values remain relatively stable until 500 to 600°C and then decrease thereafter.

It is hypothesized that the increases in grayscale value of the ashes due to elevated temperature exposure are caused by the removal of the organic coal residuals in the ash. The

²¹ SAS Institute Inc., 2006.

forms of organic carbon possibly present in ash (coal char, VOCs and soot) are generally dark brown to black in color. Removal of organic coal residuals would be expected to cause increases in grayscale ash grayscale value. The hypothesis is supported by Figure 7.25, which shows that for two of the ash samples, approximately 90 percent of the organic carbon is removed from the ashes between the temperatures of 300 and 500°C. This range corresponds to significant lightening of the ash samples seen in the 300 to 500°C range shown in Figure 7.23.

Further evidence is given in Figures 7.26 and 7.27. The figures show the correlations between grayscale value change between 300-500°C and organic carbon content (based on the test values shown in Table 7.9). Figure 7.26 contains the values for the seventeen commercial ashes and Figure 7.27 contains values for the seventeen ashes and the sieved ash fractions. In both graphs, a similar logarithmic-shaped trend is observed. The magnitude of the grayscale change increases with increasing organic carbon content. Values of organic carbon contents less than about 2 percent are clearly differentiated by change in grayscale value in Figure 7.24. For organic carbon contents greater than about 2 percent, differentiation by change in grayscale value is more difficult due to the flattening slope in the data.

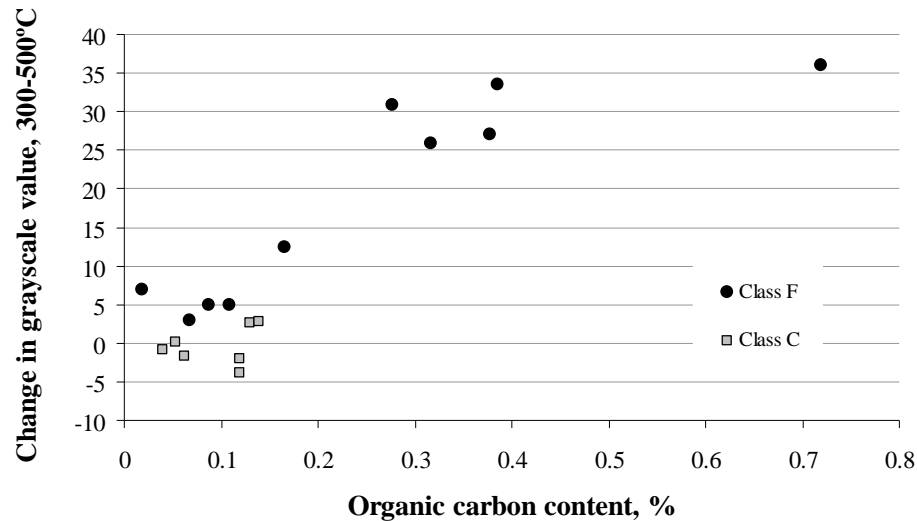


Figure 7.23: Change in grayscale value versus organic carbon content for the non-sieved ash samples.

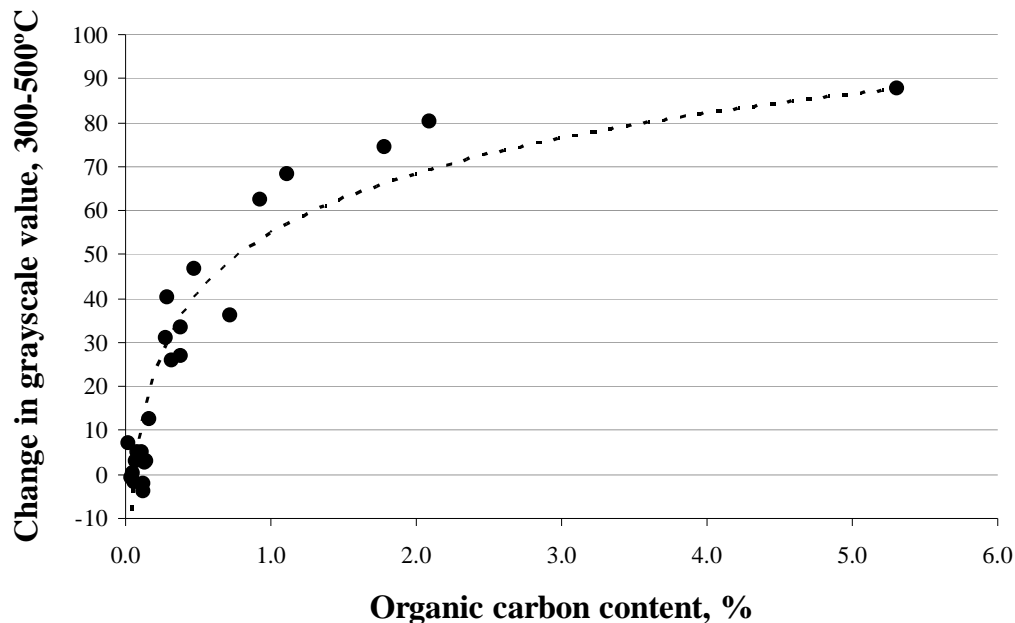


Figure 7.24: Change in grayscale value versus organic carbon content for all samples.

As evidenced by the grayscale decreases which occur, other factors in addition to organic carbon content also play a role in grayscale value change due to heating. Multi-linear regression analysis was performed to identify other factors in addition to organic carbon content which might influence the change in ash grayscale value between 300 and 500°C. The analysis results, shown in Table 7.11, suggested that only organic carbon content and calcium oxide content (shown as CaO) provided statistically significant contributions to grayscale change. Based on the regression parameter estimates for organic carbon and calcium oxide (CaO) shown in Table 7.11, organic carbon appears to have a positive influence on ash grayscale change (regression coefficient equal to 54) while calcium oxide shows a negative influence on ash grayscale change (regression coefficient equal to -0.74). These results are physically manifested in the color change values shown in Table 7.9. All but four of the ash samples show positive grayscale changes. Ash samples CF-1, CP-1, CP-2 and CW-1 experienced net darkening (between -0.9 and -3.8 grayscale units) in the temperature range of test. These samples, all Class C, have relatively high CaO contents between 24 and 29% but relatively low organic carbon contents between 0.04 and 0.14%. The result is that the contribution from sample darkening was greater than the contribution from lightening resulting in a net decrease in grayscale value.

The R^2 value for the regression (0.87) suggests that other parameters not identified also influence grayscale change. One possibility is that calcium can be present in ash in many forms including calcium hydroxide, calcium sulfate, tricalcium aluminate, calcium carbonate or in a calcium-containing glass (Helmuth, 1987; Joshi and Lohtia, 1997). It is possible that some form or forms of calcium may contribute to negative grayscale change while others do not. The forms of calcium present in the ash samples were not identified in this work. Another possible factor that may influence grayscale change is the presence of differing forms of organic carbon in ash. Differing organic carbon forms may affect ash color differently. For example, char and soot are present in discrete separable particles (though as demonstrated by Gao et al., (1997) individual

soot particles are sized on the order of about 40 nm). VOCs, however, are condensed on fly ash surface and impart a dark, oily appearance (Fan and Brown, 2001). Other sources of scatter in the data may be due to differences within a single form of organic carbon. Maroto-Valer et al. (1999a,b) identified microscopically three types of coal char present in ash: inertinite, isotropic coke and anisotropic coke. Maroto-Valer et al. showed the differing forms to vary in properties, such as density and specific surface area.

The contributions of the different forms of organic carbon in the ash samples were not identified in this work. It is recommended that methods of measuring the contributions of the different forms of organic carbon in ash be identified so that the influence of carbon form on color can be assessed.

Correlations between color change and concrete AEA dosage

Organic coal residuals in fly ash have been correlated to elevated fly ash-AEA interactions (Gebler and Klieger, 1983; Freeman et al., 1997; Whiting and Nagi, 1998; Hurt et al., 2001; Harris, 2007). Because ash grayscale change is influenced by organic carbon content, measurements of ash grayscale change could provide a method for estimating ash influence on AEA dosage values.

The ASTM C311 loss on ignition test for fly ash is generally considered in industry to be a measurement of ash “carbon” content (Schlorholtz, 2006) (note that this claim is not made by the ASTM C618 specification or ASTM C311 test procedure). The test procedure measures the change in ash mass which occurs between oven drying at 105°C and 750±50°C. Figure 7.25 shows concrete AEA dosages plotted against the change in grayscale values of the ashes due to heating between 105 and 750°C (values are also given in Table 7.8). It is seen in Figure 7.25 that heating the ash to 750°C can cause a net decrease in ash color for all of the Class C ashes and three of the Class F ashes. Figures 7.23 and 7.24 suggest that decreases in grayscale values occur in both Class C and F samples above 500 to 600°C; however, the grayscale decreases in many Class F ash samples are offset by the increases that occur up to about 500°C. The Class F ashes ranged in behavior from some darkening (-15) to significant lightening (+41). A trend of increasing AEA dosage with increasing change in grayscale value exists in the Class F ash samples. The opposite trend appears to exist for the Class C ash samples.

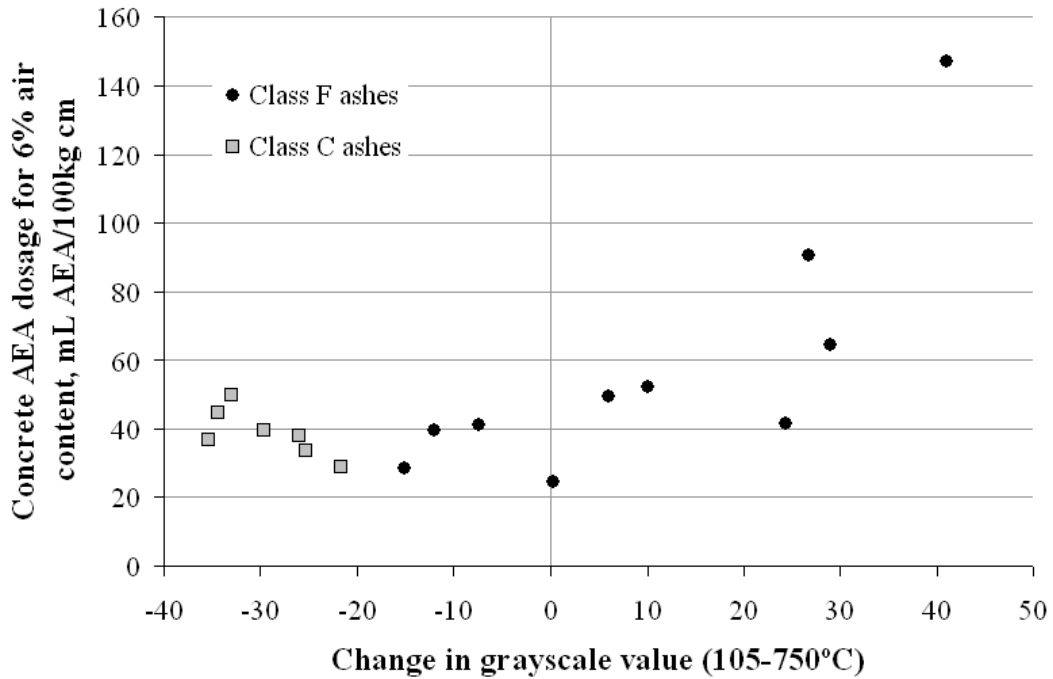


Figure 7.25: Concrete AEA dosages required for 6 percent air in concrete versus change in grayscale values between 105 and 750°C.

Figure 7.26 shows the relationship between concrete AEA dosage and ash 300 to 500°C grayscale-value change. Figure 7.26 shows fewer ashes with negative grayscale changes (in comparison to Figure 7) since net grayscale that occur up to 500°C are much lower relative to grayscale decreases that occur at temperatures of 750°C and higher. The figure shows little change in concrete AEA dosage with increasing grayscale value for grayscale changes between -4 and 25. Then for grayscale changes greater than about 25, concrete AEA dosage increases rapidly with increasing grayscale change.

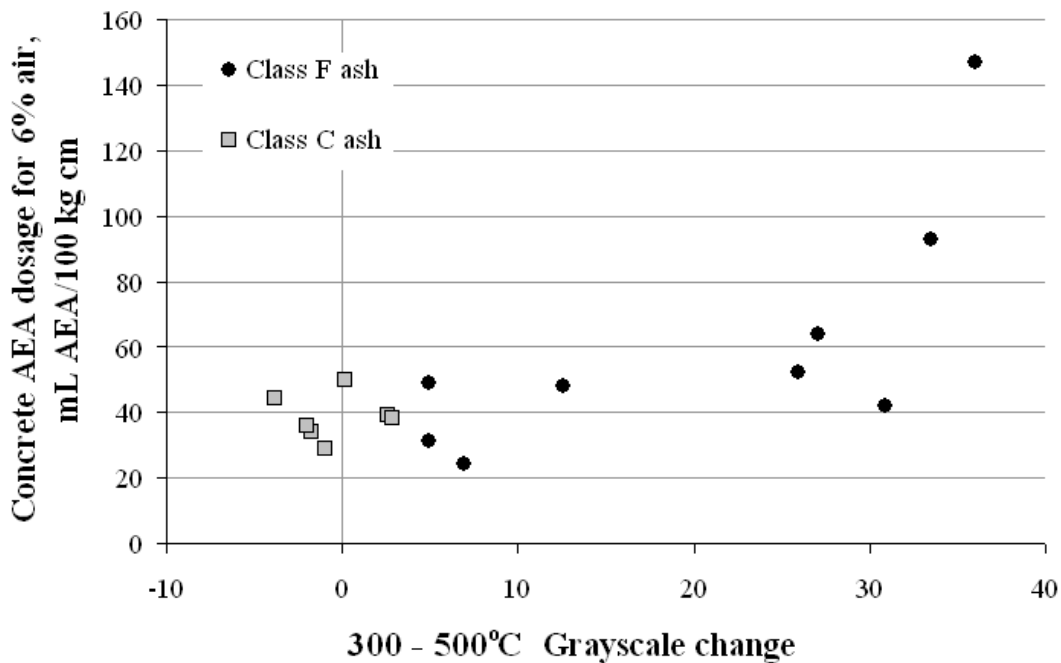


Figure 7.26: Concrete AEA dosages required for 6 percent air in concrete versus change in grayscale values between 300 and 500°C.

7.2.7 Practical applications

It is proposed that the change in grayscale analysis test be used as an inexpensive method for estimating organic carbon contents of particulate matter. The method could find use as an assessment of organic carbon in the ash stream of coal fired boilers as a measurement of operating efficiency.

Fly ash marketers could use the test in addition to the ASTM C311 LOI test for assessing organic carbon content of marketable ash. For example, ashes that may have relatively high ignition losses but relatively low grayscale changes would indicate that losses from sources other than organic carbon are influencing the LOI value. Harris (2007) and others (Brown and Dykstra, 1995; Fan and Brown, 2001; Paya et al. 2002) have shown that in addition to forms of carbon, other materials in fly ash also influence the LOI measurement.

The change in grayscale value (either between 300-500°C or 105-750°C) could be used as an estimate of the organic carbon content of ash for assessing the potential influence of fly ash on air entraining admixture (AEA) dosages in concrete.

7.2.8 Conclusions and future work

1. A procedure for measuring change in ash grayscale value has been proposed. The procedure consists of exposing ash to elevated temperatures in a muffle furnace and measuring the ash color before and after heating. The sample imaging and color analysis portion of the procedure is identical to the basic method described in Section 7.1 of this work.

2. Multi-linear regression analysis suggests that organic carbon content (which has a positive or lightening influence) and calcium oxide content (which has a negative or darkening influence) are primarily responsible for ash grayscale change between 300 and 500°C.
3. Grayscale values of Class F ash samples were shown to increase (lighten) due to exposure to increasing temperature in air up to 500-600°C. Class C ash samples showed little or no increase in grayscale values in the same temperature range. The grayscale values of all ashes decrease (darkened) at temperatures greater than about 600°C.
4. A non-linear (logarithmic) correlation between ash grayscale change and organic carbon content was established. The trend shows grayscale change varying from 0 to 80 units for ash samples having organic carbon contents of 0 to 2.0 percent. For organic carbon contents up to 5 percent, further change in grayscale was about 10 units. Since change in grayscale value was used for the correlation, the influence of individual scanner type on the value is minimized. However, it should be noted that differences between scanners (described in Section 7.16.1.1) may influence the correlation.
5. The change in grayscale method could be used in industry as a rapid and inexpensive approximation of organic carbon content in ash. The applications of this measurement could be beneficial to boiler operators as a measurement of combustion efficiency. The method could also be employed by fly ash marketers as a method of assessing potential influence of fly ash on air entraining admixture dosage.

Additional value could be gained from the change in grayscale value test if the individual forms of organic carbon present in coal could be quantified. Fan and Brown (2001) proposed a qualitative method for identifying VOCs in ash by means of dissolving the organic compounds in benzene and visually comparing the change in solvent color. This method could be improved using an ultra violet-visible light spectrophotometer to quantify VOC presence in solvent by light absorbance. Methods for quantifying soot content in ash should also be identified.

Additional work is recommended to determine the suitability of the color change test on ash produced in other geographical regions. The possibility exists that differing source coal or combustion conditions may produce differences in ash properties with respect to color.

Additional further study should be done to determine what, if any, other materials may be removed or changed in ash when subjected to temperatures up to 500°C. The influence of other changes in properties besides organic carbon removal would need to be considered when analyzing color change results.

Chapter 8. Synthesis

8.1 Main objectives

The main objectives of this work were introduced in Chapter 2 and are repeated below.

1. Identify and characterize the properties of fly ash that influence interaction with the industrial surfactants known as air entraining admixtures (AEA's) in concrete, so as to better understand fundamental behavior and predict performance.
2. Identify or develop effective methods for measuring the interactions between fly ash and AEAs so that variability in the fly ash can be detected and the AEA dosage of concrete incorporating the ash can be adjusted to compensate.
3. Develop a plan for industry implementation of the test methods.

During the pursuit of the first two objectives multiple tests were performed and multiple lessons were learned as outlined in Tables 8.1 and 8.2 below, which serves as a guide to the discussions included in the first part of this chapter. Previous chapters have described the outcome and lessons learned from various analyses and test methods, generally taken one at a time. The purpose of this chapter is to explore the degree to which data from multiple types of tests and analyses synergistically combine and support one another to provide additional insight.

8.2 Lessons learned regarding fly ash-AEA interactions

Table 8.1 shows five lessons regarding fly ash-AEA interactions that were learned during this research. Lesson 1, which is that a weak correlation exists among concrete AEA dosage, ASTM C311 LOI and the non-standard foam index tests, was learned through the literature survey of Chapter 3 and firsthand by the studies of the standard LOI test and foam index test variations discussed in Chapters 5 and 6. Lesson 2, which is that the 3-way correlation is improved by tightening the LOI test procedure and standard foam index test, was learned through the study of the procedural factors influencing the LOI test measurements (Harris et al., 2006) and by application of the standard foam index test to the Texas fly ash samples (shown and discussed later in this chapter). Lesson 3, which is that color analysis shows a reasonable correlation with concrete AEA dosage, was learned by the study of ash color described in Chapter 6. Lesson 4, which is that improved correlations are observed between concrete AEA dosage and the modified LOI and 300 to 500°C color change, was learned by the application of these tests to the Texas ash samples described in Chapters 4 and 6. Lesson 5, which is that ash composition (primarily along the lines of the two ash classes) affects the reliability of the correlations, was shown for the modified LOI, standard foam index and color change test described in Chapters 5 through 7. The fundamental factors (shown in Table 8.2) which influenced these five lessons are discussed in this chapter.

8.3 Fundamental factors influencing fly ash-AEA interactions

As shown in Table 8.2, five fundamental factors (numbered 6 through 10) were identified which influence fly ash-AEA interactions. The factors are supported by the results from several tests (Figures 8.5 and 8.6) used to assess the properties of the ash. The five factors and the tests that support them are described in detail in this section.

8.3.1 The influence of organic carbon content

Organic carbon content (mass) of fly ash was determined to correlate strongly with concrete AEA dosage. Organic carbon content was also found to be the common thread that ties the three proposed fly ash tests to concrete AEA dosage. The relationship between AEA dosage in concrete and organic carbon content, and the link between organic carbon content and the three test methods are described below.

Table 8.1: Lessons learned regarding fly ash-AEA interactions and the tests that contributed to the learning.

	Lessons Learned	Concrete AEA dosage	ASTM C311 LOI	C311 with Harris**	Modified LOI	Non-Std foam index	“Std” Foam index	Bulk chemistry	Total Carbon	Color analysis	Sieve Analysis	BET	UV Vis	Micro TGA	Macro TGA
1	There is a weak correlation among concrete AEA dose, LOI, and non-standard foam index test subject to large errors and outliers	●	●			●									
2	This 3-way correlation is improved by tightening the LOI test procedure and standard foam index test	●		●			●								
3	Color analysis further enhances this correlation	●		●			●			●					
4	The correlation further improves when we connect concrete AEA dose to modified LOI and 300 to 500°C color change	●			●					●*					
5	Ash composition affects the reliability of correlations	●			●		●	●		●					
* After heat exposure															
** Harris, Hover, Folliard, Ley, “Variables Affecting the ASTM C 311 LOI Test,” <i>JAI</i> , Vol 3, Issue 8, 2006															

Table 8.2: Fundamental factors that influenced the lessons learned in Table 8.1

	Fundamental Factors influencing Fly Ash— AEA Interactions	Concrete AEA dosage	ASTM C311 LOI	C311 with Harris	Modified LOI	Non-Std foam index	“Std” Foam index	Bulk Chemistry	Total Carbon	Color analysis	Sieve Analysis	BET	UV Vis	Micro TGA	Macro (furnace) TGA
6	Organic carbon has a strong influence on AEA interaction, Std foam index, mod LOI and color change are linked by organic carbon content	●			●		●		●	●				●	●
7	ASTM C311 LOI is an unreliable estimator of organic carbon			●	●				●	●				●	●
8	Several differing forms of carbon may be present in ash and each may influence AEA interactions differently	●	●		●			●	●					●	●
9	Calcium appears to have an effect, but the scope of project did not allow us to track it very far									●			●		
10	Surface area may play a role in AEA interactions								●	●	●	●			

Relationship between concrete dosage and organic carbon content

Figure 8.1 shows the correlation between concrete AEA dosage and organic carbon content (measured by TOC analysis) of the Texas ash samples. The relationship can be described by a linear function (R^2 equal to 0.85 and standard error equal to 12 mL AEA/100 kg cm). Based on the relationship (and the specific concrete mix used) when ash possessing no organic carbon is utilized, a baseline AEA dosage of about 20 mL AEA/100 kg cm is necessary to achieve 6 percent target air content. As organic carbon content increases, the AEA dosage also increases by about 15 mL AEA/100 kg cm for each 0.1 percent increase in organic carbon (Slope established by regression analysis is equal 150 mL AEA/100 kg cm per percent organic carbon.)

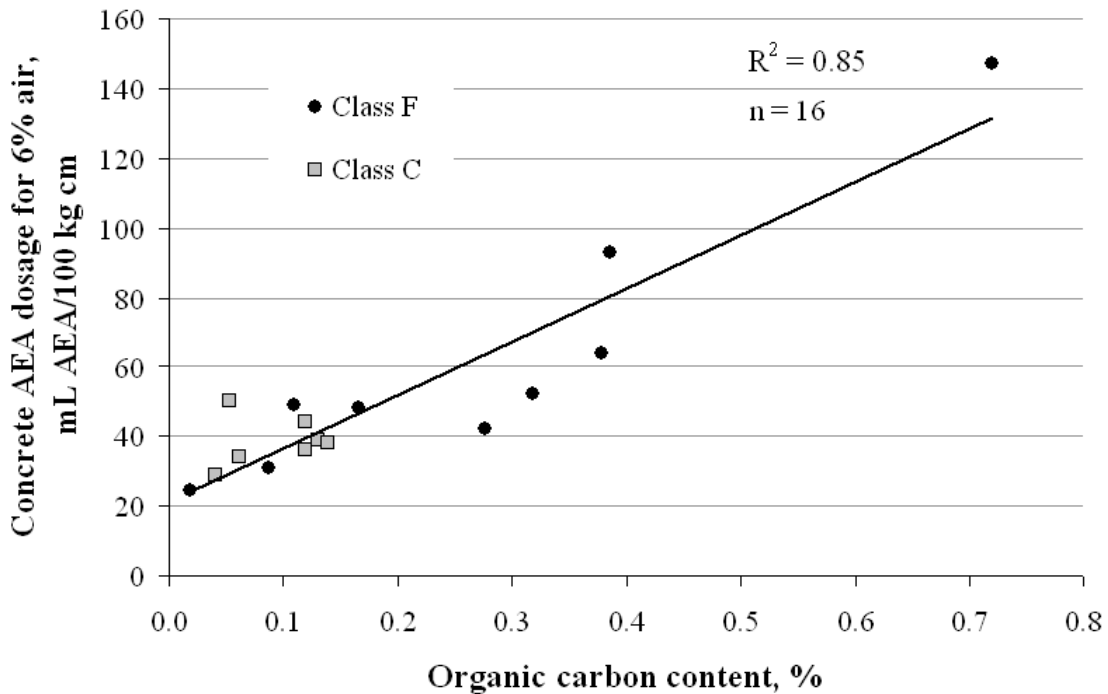


Figure 8.1: Correlation between concrete AEA dosage and organic carbon content of Texas fly ash samples.

The sensitivity of concrete AEA dosage to organic carbon content highlights the need for accurate measurement of organic carbon content for predictive purposes. Figure 8.1 shows that an increase in organic carbon content from zero to approximately 0.7 percent increases the AEA dosage by a factor of greater than 7. From this perspective it becomes apparent that seemingly minor fluctuations in ash organic carbon content can have major impacts on AEA dosage.

Due to the demonstrated influence of organic carbon content on fly ash-AEA interactions, evaluation of fly ash by Total Carbon Analysis would be preferred on a technical basis. However, such apparatus may be inaccessible to much of the industry due to the approximately \$30,000 initial investment to purchase the equipment, and the need for technical expertise to perform tests and interpret results. Less expensive, simpler, and more readily

available test methods are required so that the test can be performed in laboratories, power plants, or batch plants. The three methods recommended are discussed below.

Modified LOI test

Development of the modified LOI test arose from the assessment of the utility of the standard LOI test as a predictor of fly ash-AEA interactions (discussed further in Section 8.3.2). Compared with the standard LOI test, the proposed modification to the ASTM C 311 LOI test was found to provide an improved correlation with concrete AEA dosage. The relationship between concrete AEA dosage and modified LOI is shown in Figure 8.2 (a comparable graph showing concrete dosage versus standard LOI values is shown in Figure 8.1).

Figure 8.2 compares closely with concrete AEA dosage versus organic carbon content shown in Figure 8.1 for the Class F ash samples. (The slope of the fitted curve in Figure 8.2 is equal to 160 mL AEA/100 kg cm per percent modified LOI loss while the slope in Figure 8.1 is 150 mL AEA/100 kg cm per percent organic carbon.) The ability of the modified LOI test to estimate AEA dosage for concrete containing Class C ash is difficult to assess due to the limited breadth of experimental data for Class C ashes. Further research on the relationship between Class C ash modified LOI and concrete AEA dosage is recommended.

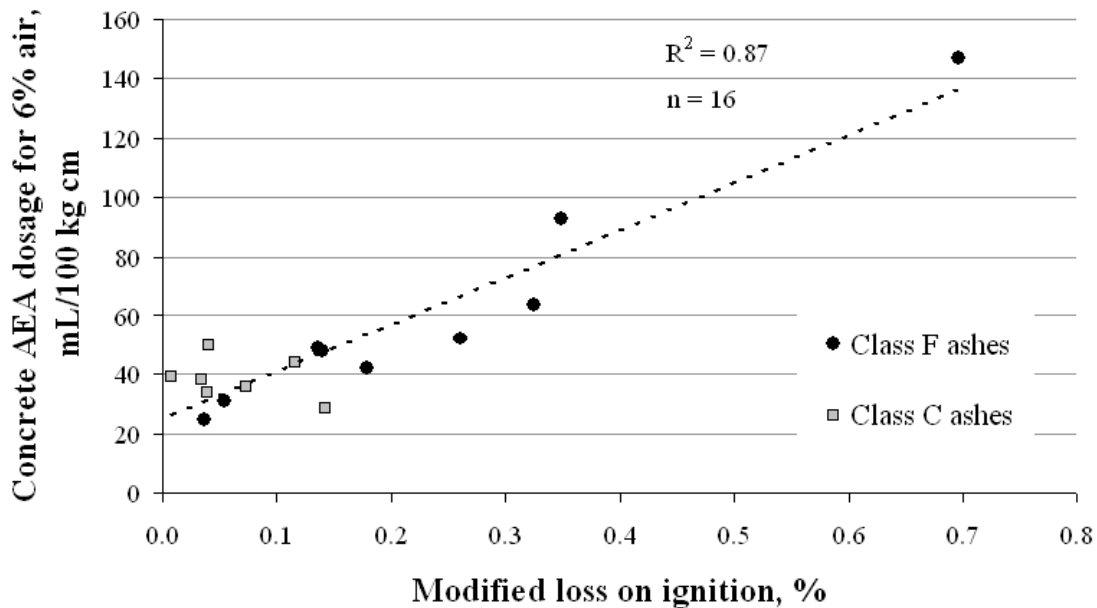


Figure 8.2: Relationship between modified LOI and Concrete AEA dosage for 6 percent air.

As described in Chapter 5, the modified LOI test is directly linked to organic carbon content since the test was designed to focus on the temperature range in which 92 percent or more of the organic carbon content of ash is removed (when heated at 500°C for 60 min). Figure 8.3 shows the relationship between the modified LOI content and the organic carbon content of the Texas ash samples. In general, the modified LOI test is a better predictor of organic carbon content for Class F ashes than Class C ashes. Possible explanations for influence of ash composition on the measurements were given in chapter 5.

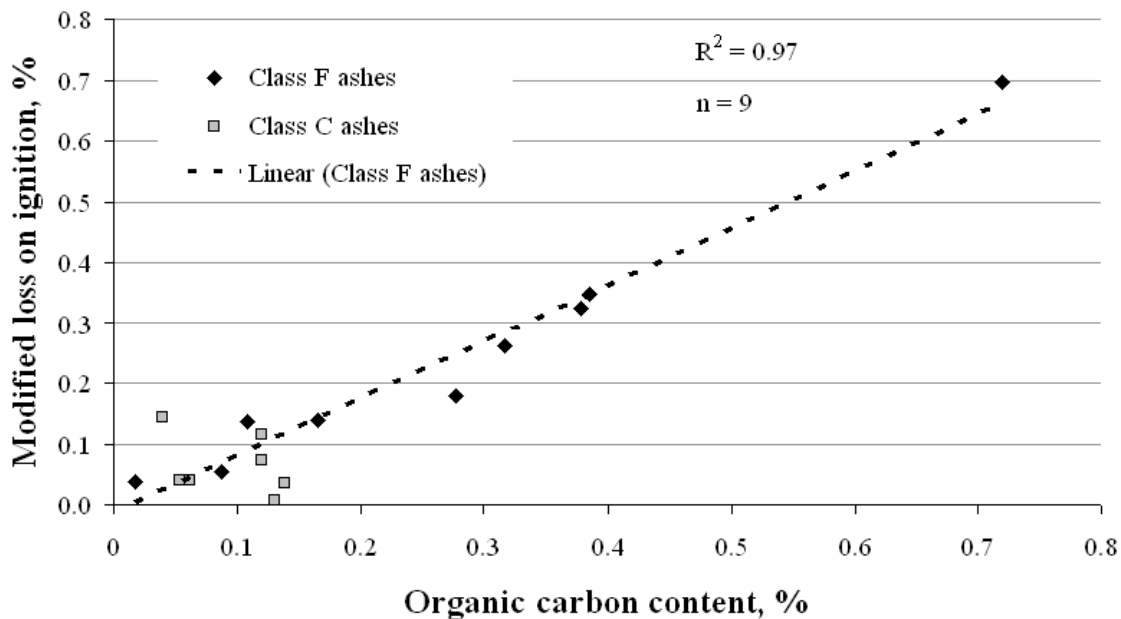


Figure 8.3: Relationship between modified LOI and organic carbon content of Texas ash samples.

Foam Index Test

Two major limitations of the foam index test are, first, the mixture of water, cement and ash used in the test is not representative of actual concrete in several ways: 1) the water-to-cement ratios is 5 or more times larger than actual concrete, 2) chemical admixtures (other than AEAs) which are commonly present in concrete are not included, 3) no aggregates are present and 4) the time scale of the test is on the order of 1 to 10 min, while in fresh concrete the materials are in contact for up to several hours. As a result of these differences, the test may not allow realistic comparisons. The second major limitation of the test is that many variations of the test have been used (seven were identified in Chapter 6) and no standard test method currently exists.

The second limitation of the foam index test was the primary focus of Chapter 6. During this study, the major factors influencing the test were identified and the practical limits of the test were defined. Based on the study a standard test method was proposed for industry use.

The first limitation of the test is explored by comparing the foam index results of the Texas fly ash samples to the concrete AEA dosage data (shown in Figure 8.4). The “mix-specific” application of the foam index tests was used, i.e. the same cement type, ash to cementitious ratio and AEA type were used in the concrete mixes and the foam index tests. The description of the foam index test parameters and R_{min} of the tests are given in Section 8.2.4.2. The chemically treated ash samples, excluded in most of the tests in this work, were included in the comparison.

Several observations can be made from Figure 8.4. First, when restricting the population to un-treated, Class F ash samples, a strong linear correlation exists (R^2 equal to 0.93 and standard error equal to 10 mL AEA/100 kg cm). Second, the foam index test did not distinguish

differences among the Class C ashes. Third, foam index test values did not consistently correlate with concrete AEA dosages for the chemically treated ash samples. This primarily applies to the ash sample showing a concrete AEA dosage of about 140 mL AEA/100 kg cm and foam index value of about 20 mL AEA/100 kg cm. For the samples, the foam index test predicts relatively little AEA interaction in contrast to the concrete dosage value. Since the three other treated ashes are a better fit to the predicted relationship, more information would be needed about the apparent outlier, but such is not available due to the proprietary nature of the treatment chemical and process.

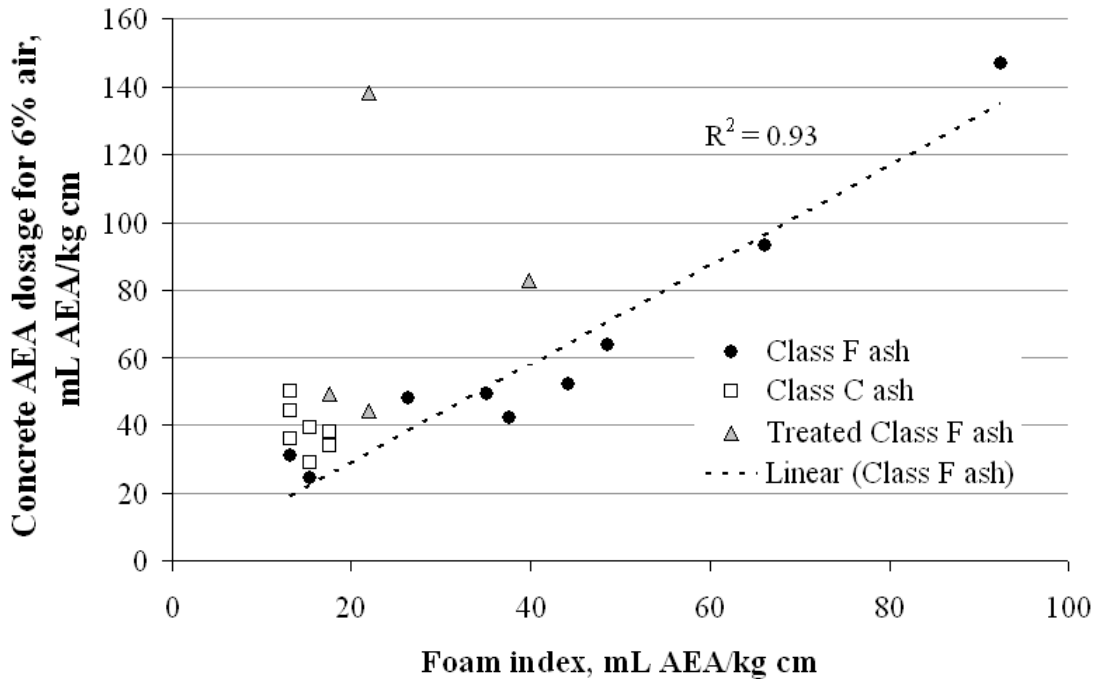


Figure 8.4: Correlation between concrete AEA dosages and foam index values for all Texas fly ash samples.

For the ash samples, foam index procedure and concrete mixtures used in this study, the AEA dosage of concrete incorporating Class F ash could be estimated by multiplying the specific foam index value obtained for the ash sample by a factor of 1.5.

Factors influencing the foam index test

Chapter 5 showed that the foam index test results can be influenced by the procedural factors in the test. However, use of the recommended standard test removes much of the variability and allows examination of the impact of the test materials on the result. Studies of the fly ash properties which correlate with the foam index test have shown organic carbon content to be a major factor. The correlation is shown through the sequence of Figures 8.5 to 8.8. The foam index values of two ash samples, Ashes FB-2 and FR-2, differ by about 45 mL AEA/100 kg cm (Figure 8.5). When heated, the foam index values of the two ashes converge to virtually the same values at temperatures of 400°C and above. A similar pattern is shown for the organic carbon

contents of the ash samples when exposed to elevated temperatures (Figure 8.6). When heated between 300 and 500°C, the organic carbon contents of the samples decrease to near zero.

The correlation between foam index values and organic carbon contents for the heat treated ash samples is shown in Figure 8.7. The figure shows a strong linear correlation (R^2 is equal to 0.98 and standard error equal to 7 mL AEA/100 kg cm) between foam index and organic carbon content. The correlation between foam index and organic carbon content for the set of Texas fly ash samples (excluding the chemically treated ashes) is shown in Figure 8.8. Similar to the heat-treated ashes, the set of Texas ashes also shows a linear correlation (R^2 equal to 0.91 and standard error equal to 7 mL AEA/100 kg cm) with organic carbon content.

The correlations between foam index values and organic carbon contents in Figures 8.7 and 8.8 provide evidence that organic carbon content is an important factor influencing fly ash-AEA interactions.

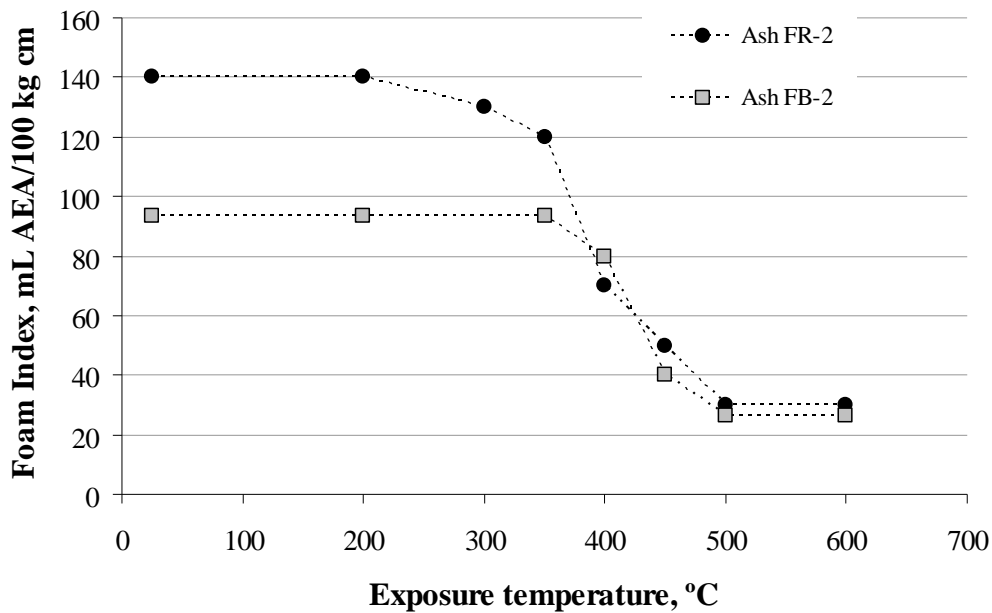


Figure 8.5: Foam index versus temperature exposure for two ash samples.

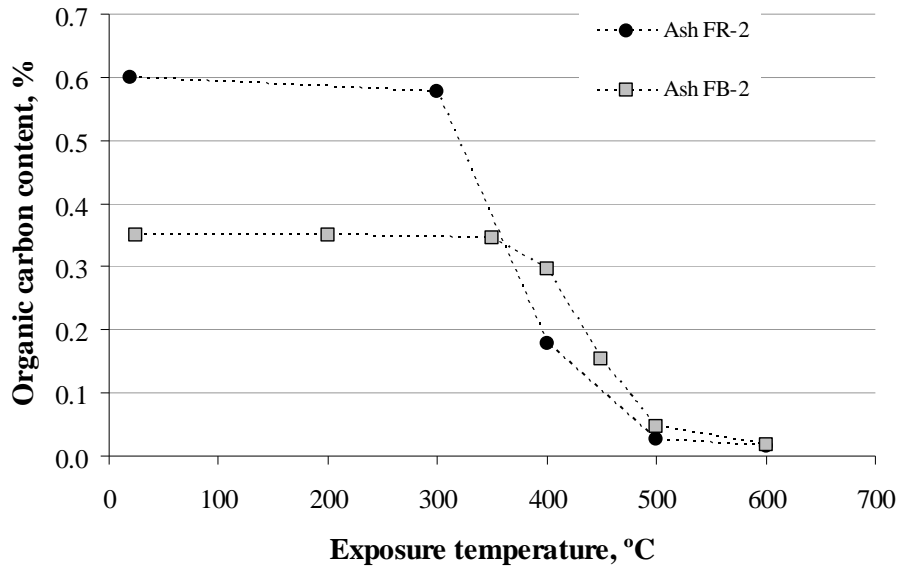


Figure 8.6: Organic carbon content versus temperature exposure for two fly ash samples.

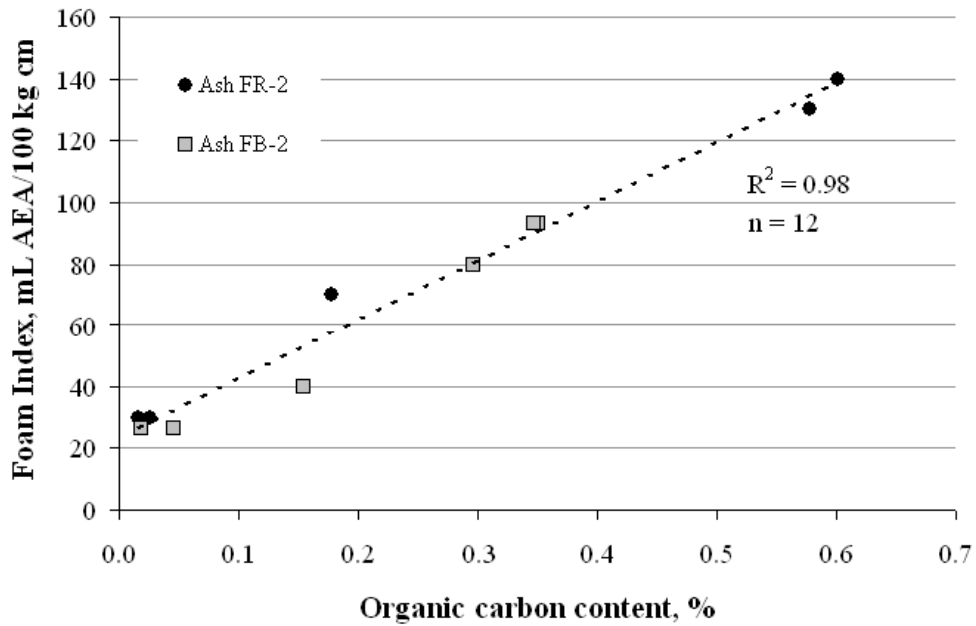


Figure 8.7: Foam index versus organic carbon content for two ash samples.

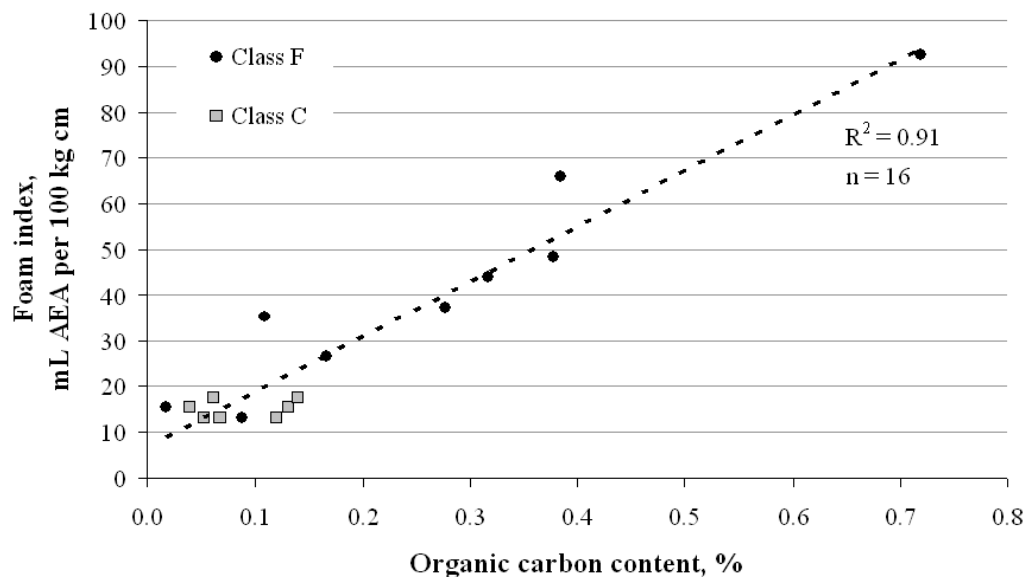


Figure 8.8: Foam index values versus organic carbon content for all Texas fly ash samples.

Figure 8.4 showed that the foam index test did not distinguish differences in the Class C ashes relative to AEA dosage in concrete. Figure 8.8 however, shows a reasonable correlation for both ash Classes. Still, lack of a perfect fit in the correlation suggests that other factors are involved. One of the major differences between the two ash classes is that Class C ashes tend to have higher calcium oxide (and lower silica) contents than Class F ashes. This was verified for all of the Texas ash samples in Section 4.2.2.1. To explore whether calcium (or any other major oxide) may be an influencing factor in the foam index test, multi-linear regression analysis on the foam index test data as a function of organic carbon, all oxide contents and soluble calcium ion concentration (see Chapter 4 Section 4.2.2.2 for test details) was performed. The analysis showed no statistically significant influence from any oxide or soluble calcium on concrete AEA dosage. No positive identification of the other variables was achieved in this work; however potential factors which were identified for future study include organic carbon type, organic carbon surface area. These other factors are discussed later.

It is interesting to note that an apparent “sag” is repeated in the Class F ash sample data in correlations between concrete AEA dosage and organic carbon content (Figure 8.1), modified LOI (Figure 8.2) and foam index (Figure 8.4). The sag is not as prominent in the correlation between modified LOI and organic carbon content (Figure 8.3) and between foam index and organic carbon content (Figure 8.8). The three samples that consistently fall below the trend lines in the middle of the three formerly mentioned correlations are Ashes FT-1, FC-1 and FB-1. Study of the properties reported in Chapter 4 of the three ashes did not identify any consistent differences in the ash samples from the other Class F ashes. Possible explanations for the inconsistent behavior could be traced to the other factors that are mentioned later in this chapter such as organic carbon form and organic carbon surface area/size distribution. Since the inconsistent behavior is not observed in the Figures 8.3 and 8.8, it is possible that the differences are related to the methods used to measure concrete AEA dosages for the ash samples.

Color analysis

The colorimetric analysis method is used to quantify ash color. Two methods were proposed for its use with regard to assessing ash quality for air-entrained concrete. The first method is the color analysis of oven-dried ash. The grayscale value obtained by this method can be used to assess general ash behavior by comparing the value to the trend between ash grayscale value and concrete AEA dosage shown in Figure 8.9. This method could also be used to monitor changes with time in ash produced from a single source. The second method measures the change in grayscale value that occurs upon heating the ash between 300 and 500°C. The change in grayscale values is shown in Figures 8.10 and 8.11 to be correlated with ash organic carbon content.

It was shown in Chapter 7 that fly ash grayscale value may be influenced by several factors including organic carbon content. It was also shown that the contribution of organic carbon to ash grayscale value could be estimated by measuring grayscale value before and after heat treatment to remove organic carbon (some changes in color possibly linked to calcium content also occur).

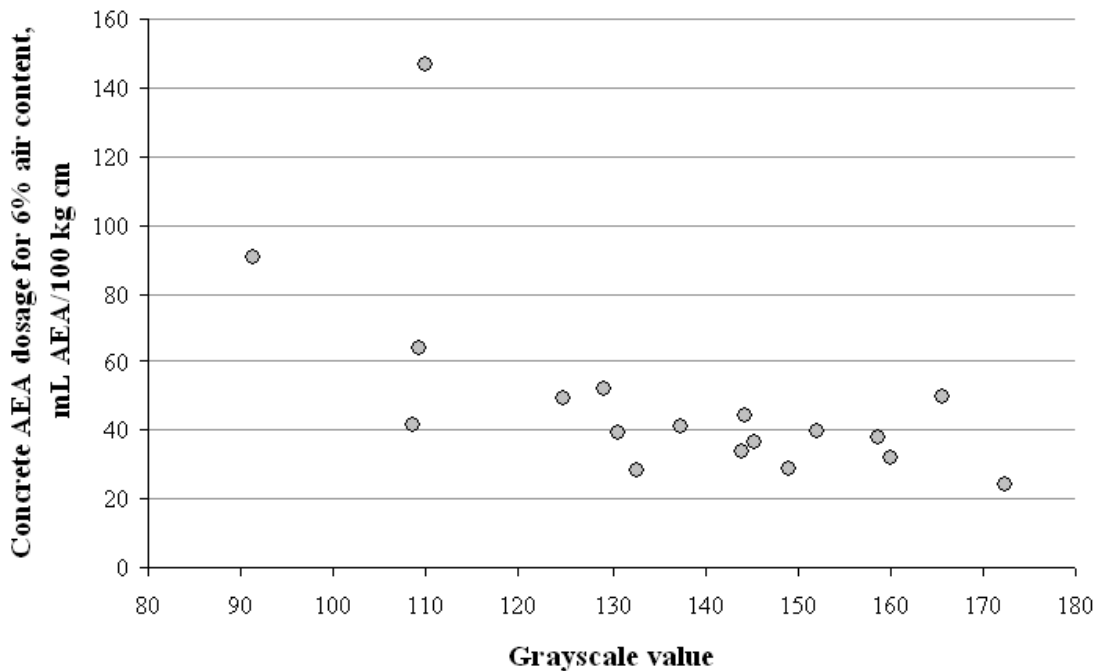


Figure 8.9: Concrete AEA dosages vs. ash grayscale change for the Texas fly ash samples.

Carbon losses of Figure 8.10 shows the changes in grayscale values of two Texas fly ash samples due to heat treatment in air (the testing procedures used to determine these values are provided in Section 4.2.5.2). The two ash samples in Figure 8.10 show significant positive grayscale change in the temperature range of 300 to 500°C. When compared with Figure 8.6 it is apparent that the change in organic carbon content may be a primary factor causing the change in grayscale value.

The hypothesis that grayscale change is dependent on organic carbon content is supported by the comparison of grayscale change between 300 and 500°C of the set of Texas ashes with

organic carbon content in Figure 8.11. (Recall that the organic carbon content of all of the Texas ashes was less than 1 percent. To evaluate ashes with carbon contents as high as 5.3 percent, a sample of ash FR-2 was sieved into size fractions as reported in Chapter 7, Section 7.2. This procedure concentrated carbon in the largest size fractions, thus yielding a set of surrogate or “processed” ashes, each from the same source, but with widely varying carbon content).

Figure 8.11 shows that the relationship between change in grayscale value and organic carbon content resembles a logarithmic function shown by the dotted trend line. Values of organic carbon contents less than about 2 percent are clearly differentiated by change in grayscale value. For organic carbon contents greater than about 2 percent, differentiation by change in grayscale value is more difficult due to the flattening slope in the data. It should be noted that while the relationship in Figure 8.11 does not conclusively identify organic carbon as the sole source of color change, a useful correlation is nevertheless demonstrated.

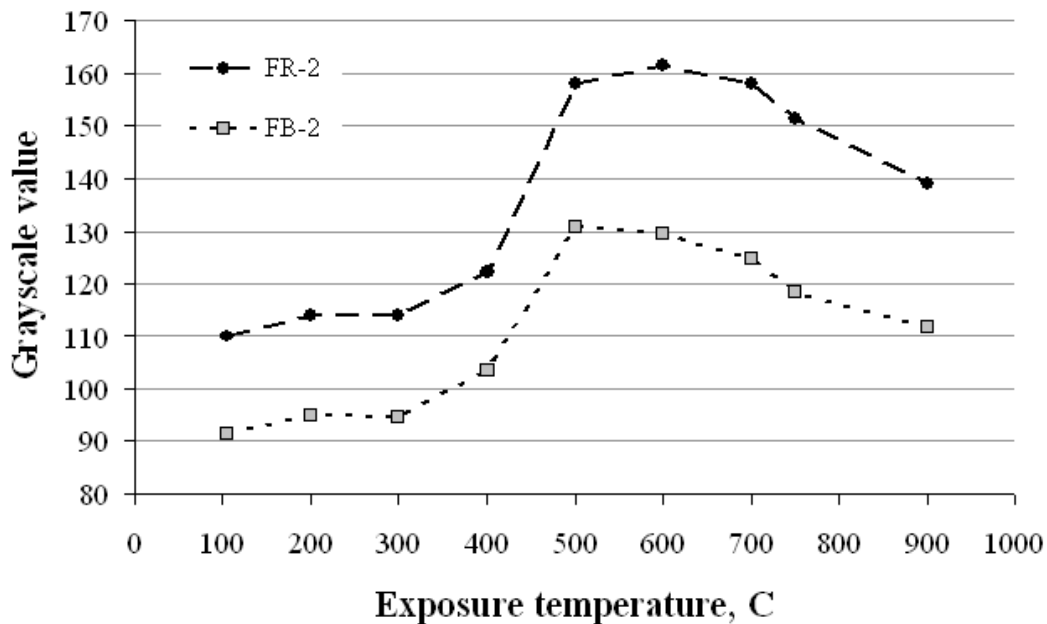


Figure 8.10: Grayscale value versus exposure temperature for two Texas ash samples.

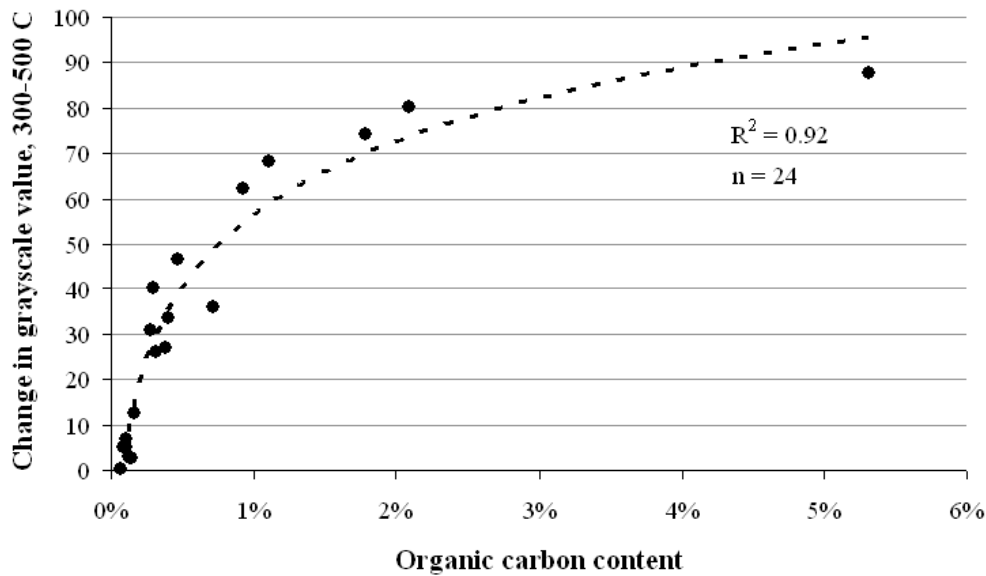


Figure 8.11: Relationship between change in grayscale value of Texas ash samples and sieved ash fractions when heated from 300 and 500°C and organic carbon content.

The total organic carbon contents of “processed” fractions of Ash FR-2 are plotted against the oven-dry grayscale value of the samples prior to any heat treatment in Figure 8.12. The “processed” ash samples happen to be shown in order of particle size, as shown by the labels in the figure, however the focus is not particle size but grayscale values versus organic carbon content.

The “flattening” of the slope in the data seen in organic carbon contents above 2 percent (shown in Figure 8.12) could be interpreted as un-removed organic carbon remaining in ash after being heated at 500°C for 60 min. However, limited observations suggest that as the organic carbon content increases, the ash “darkness” reaches a limit where additional residual carbon may not darken the ash any further. The ash grayscale spectrum is limited to 256 possible discrete values. However, the lightest of all Texas ashes, Ash FR-1 has a grayscale value of 172 which represents an approximate “practical” upper limit. The grayscale value of pulverized charcoal (containing about 7 percent ash) is 36, which represents a lower estimate. Therefore, in reality the practical ash grayscale spectrum likely exists between about 40 and 170 grayscale units. As shown in Figure 8.12, a change in organic carbon content from approximately 0.3 percent to 5.3 percent corresponds to a grayscale change of about 50 units. Thus, a 5 percent change in organic carbon content resulted in a nearly 40 percent change in the practical ash spectrum. It is hypothesized that as the organic carbon content increases beyond 5 percent, the corresponding change in darkness must decrease at a slower rate until the grayscale of 100 percent organic carbon is reached (near a value of 36). Whether this phenomenon is the cause of the shape of the graph in Figure 8.11 cannot be determined based on the limited data here. Further study of color properties of ash samples with carbon contents greater than those used in this study is recommended.

Grayscale values of sieved ash fractions (Ash FR-2)

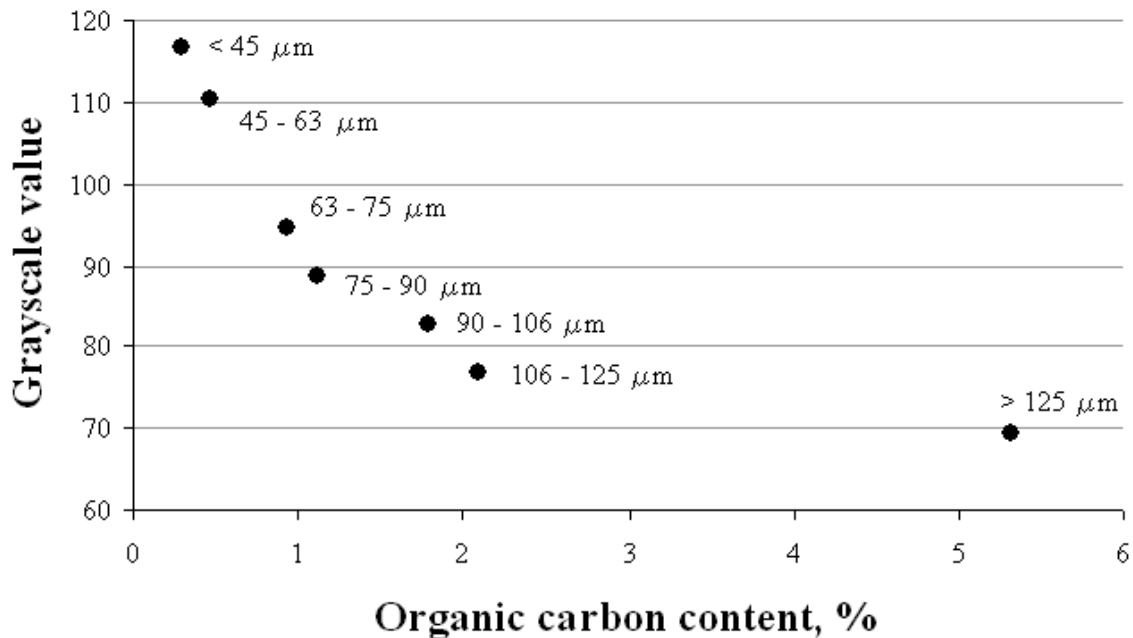


Figure 8.12: Grayscale values for size fractions sieved from ash FR-2

Summary of methods

The three methods described above, the modified LOI test, standard foam index and color analysis test, are recommended for implementation in the industry for the following reasons:

1. The test methods were shown to correlate with fly ash-AEA interactions.
2. The methods are each unique in the approach taken to measure potential fly ash-AEA interactions and together provide a suite of complementary tests.
3. The test methods are simple to perform and require no sophisticated apparatus or training.

8.3.2 ASTM C311 LOI test is an unreliable estimator of organic carbon

The next fundamental factor influencing the lessons learned in this research (shown as factor number 7 in Table 8.2) is that the ASTM C311 loss on ignition test is an unreliable estimator of organic carbon content.

The current use of the LOI test as an indicator of ash-AEA interactions in industry is based on two assumptions: 1) that “carbon” in ash is the primary factor in ash-AEA interactions and 2) that the results of the ASTM C 311 LOI test can be reliably interpreted as a measurement of the carbon content of ash. As previously described, the validity of the assumptions is called into question by the conflicting conclusions in literature and industry regarding the correlation between ash LOI content and AEA interactions (Hurt et al. 2001; Hill et al., 1997).

The correlation between concrete AEA dosage and organic carbon content shown in Figure 8.1 suggests that the first assumption is valid yet imprecise since carbon has been shown to be present in ash in forms that influence AEA interactions (coal char) and forms that appear to be benign (carbonates).

In answer to the second assumption, critical assessment of the standard LOI test (described in Chapter 5) concluded that the interpretation of the standard LOI test is complicated by the fact that carbon may be present in ash in multiple forms and these forms react differently under testing conditions. In addition, reactions of non-carbon materials in ash and variability in test procedure cause mass changes during the test. These factors and their potential influence on the LOI test are summarized in Table 8.3. The contributions to mass change in the test cannot be individually distinguished. When the ash contains forms of carbon that are not removed at temperatures up to 750C, and/or non-carbon minerals that change mass at temperatures up to 750C, the standard test is an unreliable measurement of the total carbon content.

As shown in Figure 8.1, the slope of the correlation between concrete AEA dosage and organic carbon content is 150 mL AEA/100 kg cm per percent organic carbon. It is clear that even small contributions from reactions other than loss of organic carbon in the standard LOI test can lead to significant errors when using the results of that test to predict AEA dosage in concrete.

Table 8.3: Factors influencing ASTM C311 LOI results.

Factor	Potential content in fly ash	Range of effect on LOI values
Carbon forms		
Organic carbon		
Char	0-23% ¹	3-97% ¹
Volatile organic compounds	0-12% ¹	0-97% ¹
Soot	Trace to “significant” ²	--
Inorganic carbon(carbonates)	0-2% ³	0-90% ³
Mineral Dehydration	0-2% ³	3-40% ³
Other mineral losses	0-0.25% ⁴	0-50% ⁵
Mass gains	0-0.15% ⁴	0-30% ⁵
Test Procedure		
Cooling	NA	0-20% ^{5,6}
Handling	NA	See Chapter 4
Furnace variability	NA	See Chapter 4

1. Fan and Brown, 2001
2. Gao et al., 1997
3. Brown and Dykstra, 1995
4. Chapter 4
5. Based on LOI of 0.5%
6. Harris et al., 2006

This sensitivity analysis highlights the need for a suite of tests which can be used to assess fly ash instead of a single gravimetric-type test. The three tests identified for implementation use differing techniques to predict fly ash-AEA interactions to better provide a user with information than a single test. For example, outliers which may occur in the modified LOI test may be identified by the foam index or color analysis tests as such. The three tests in combination would allow a user to avoid misinterpreting a single result and provide a measure of confidence for conclusions regarding an ash sample’s influence on AEA dosage.

8.3.3 Carbon forms

The next fundamental factor influencing the lessons learned in this research (shown as factor number 8 in Table 8.2) is that different forms of carbon may be present in ash and each

may influence AEA interactions differently. Two classification of carbon in ash were identified in Chapter 4: organic carbon and inorganic carbon. As shown previously in this chapter, ash organic carbon content correlates with AEA dosage in concrete. Inorganic carbon in the form of carbonates does was not found to influence AEA interactions but can influence standard LOI results (as shown in Table 8.3).

Three forms of organic carbon in ash were identified in Chapter 4: solid coal char, volatile organic compounds and soot. The test methods utilized in this research were unable to conclusively identify the presence of volatile organic compounds or presence of soot in the ash samples studied. As described in Chapter 5 Section 5.6.5, a “solvent stain” test for qualitative analysis of the presence of VOCs did not identify any present in the Texas ashes. Therefore it is recommended that further research be performed to both identify the forms of organic carbon in ash and study the contribution of each to AEA interaction. Recommendations for how such a study might be performed are given in Chapter 9.

8.3.4 Calcium content

The presence of calcium in one or more forms (factor 9 in Table 8.2) in ash may play a role in fly ash-AEA interactions. This general hypothesis is result of observations that differences in the behaviors of Class C and Class F ashes appear in certain analyses such as the correlation between foam index and concrete AEA dosage (Figure 8.4) and the correlation between modified LOI and organic carbon (Figure 8.2). In addition, as discussed in Chapter 7, Section 7.3, calcium oxide was shown to correlate with ash grayscale change. In ultra-violet visible-light spectrophotometry tests discussed in Chapter 4 Section 4.2.4.3, dissolved calcium ions (and likely magnesium ions) were suspected to play a major role in removing AEA from solution.

Attempts to correlate calcium content (using either the bulk chemistry oxide data or soluble calcium test data) with AEA interactions were unsuccessful in either concrete or foam index tests. This may be because calcium can be present in ash in several different forms as discussed in Chapter 4 Section 4.2.2.1. While some of these forms may influence AEA interactions, the ability to differentiate the forms was limited in this work. Future work on the influence of calcium content is recommended.

8.3.5 Surface area

The final fundamental factor identified in this research which may influence AEA interactions is ash surface area (factor 10 in Table 8.2). Relationships between fly ash surface area and fly ash-AEA interactions have been suggested by several researchers (Freeman et al., 1997; Gao et al., 1997; Hurt et al. 2001). In this present work the influence of ash surface area on AEA interactions was studied using two methods: 1) correlating BET specific surface area of ash with concrete AEA dosage data and 2) comparing foam index values to estimates of exterior surface area of solid coal char in sieved ash fractions.

BET specific surface area

The specific surface areas of eleven different ash samples (measurement method is described in Section 4.2.3.4) are plotted versus concrete AEA dosage in Figure 8.13. Two sets of data are shown in the graph, the overall specific surface area of the ash as measured by nitrogen adsorption (BET), and the specific surface area excluding the contribution from micropores

(pores less than 2 nm in diameter) as described in Section 4.2.3.4. A general trend of increasing concrete AEA dosage with specific surface area is apparent, though no improvement in the trend is visible when the contribution from micropores is excluded (based on R^2 values shown in the figure). Note that the mass of fly ash used was constant (67 kg/m^3) for all AEA dosage experiments; thus the total ash surface area available for AEA is proportional to the specific surface values reported.

Multi-linear regression analysis was performed with AEA dosage in fresh concrete as the dependent variable and specific surface, organic carbon content, and the product of specific surface and organic carbon content as independent variables. The regression showed no statistically significant contribution from specific surface area or the product of the two variables on concrete AEA dosage.

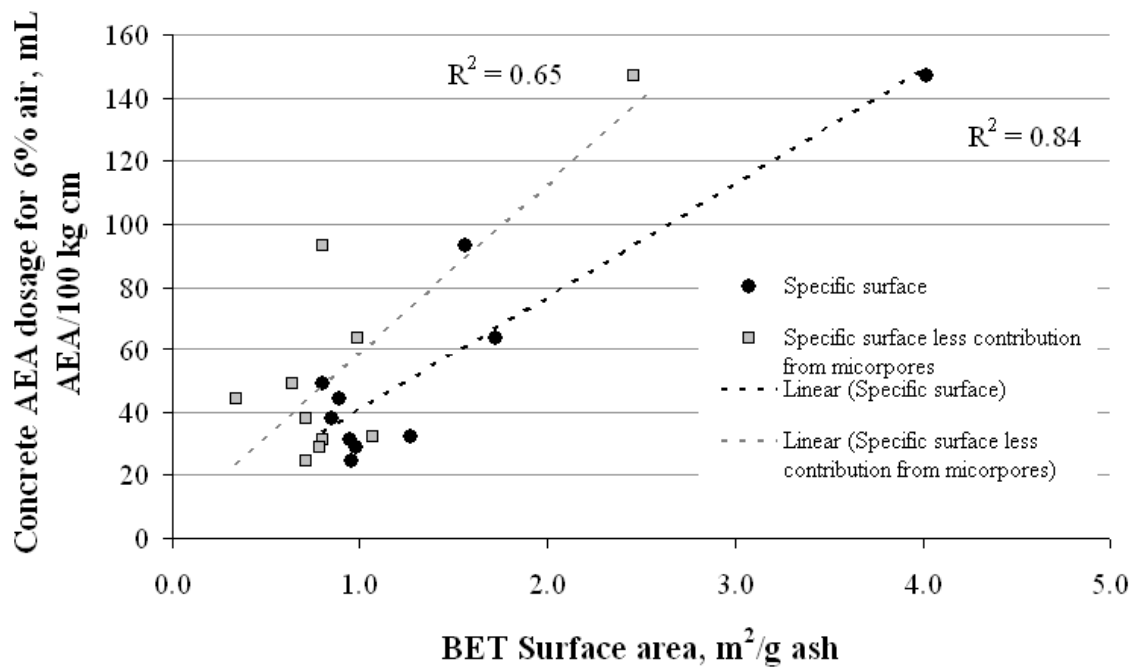


Figure 8.13: Relationship between concrete AEA dosage and BET specific surface area for selected fly ash samples. This pattern mimics the clearer pattern for AEA dose versus organic carbon.

An exponential relationship is observed between BET surface area and organic carbon content shown in Figure 8.14. This relationship may be the main factor influencing the BET specific surface and concrete AEA dosage relationship observed in Figure 8.13. Even though the BET surface area grows exponentially with organic carbon content, the concrete AEA dosage does not appear to follow the same trend. No conclusive relationship between BET surface area and AEA interactions was identified based on the data collected.

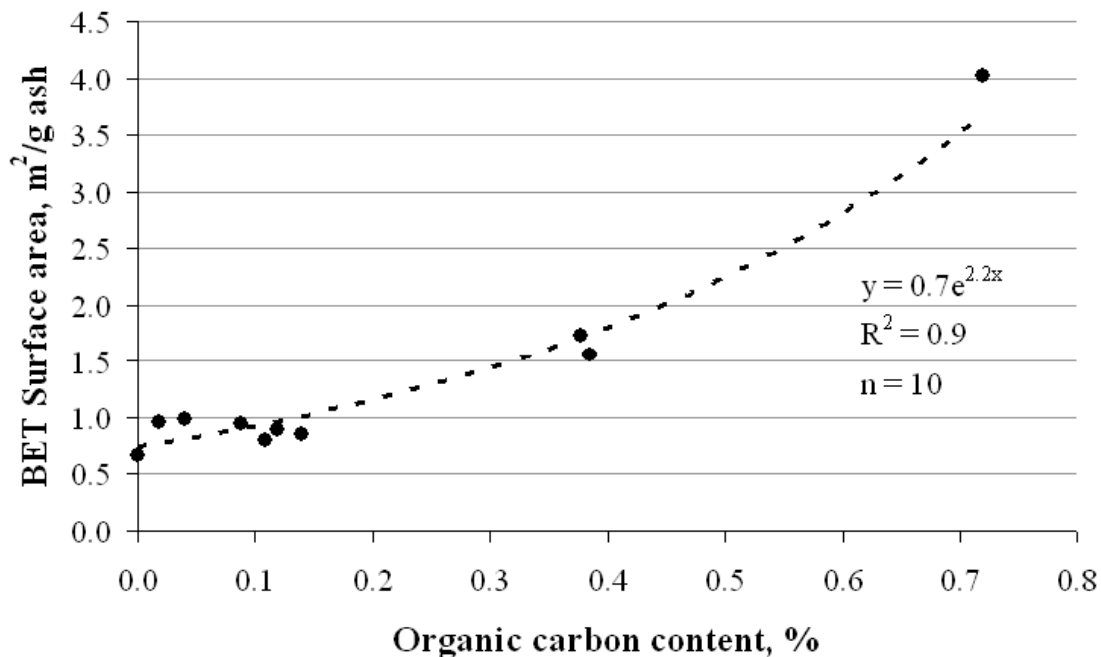


Figure 8.14: Correlation between organic carbon content and BET surface area.

It is interesting to observe, however, that Figure 8.14 suggests a specific surface of about $0.7 \text{ m}^2/\text{g}$ for the non-carbon constituents of the ash, and one can compute specific surface of the organic carbon on the basis of a weighted-average approach. Using this approximate method one can estimate that the specific surface of the organic carbon alone is between 300 and $500 \text{ m}^2/\text{g}$, which is at the low end of the range reported for activated carbon (Cheremisinoff and Morresi, 1980). Under the assumption of a fixed specific surface for the organic carbon (and knowing that all foam index tests and concrete air tests used a constant ash content) a comparison of foam index or concrete air as a function of carbon surface area would have the identical shape as the previously displayed graphs with organic carbon as the independent variable.

Particle size

The previous discussion focused on the total external and internal surface area of solid and porous constituents of ash, and the very high BET values of ash (up to $4 \text{ m}^2/\text{g} = 4000 \text{ m}^2/\text{kg}$ or about 10 times greater than the typical portland cement or fly ash particles) and estimates of organic carbon specific surface about 10 times higher again indicate the dominance of internal surface area of pores. Other researchers have suggested that the external surface at the geometric boundaries of the organic coal residuals may play a role in AEA interactions (Gao et al., 1997; Hachmann et al., 1998; Hurt et al., 2001; Kulaots et al., 2004). External surface area is related only to particle size and not to porosity.

The hypothesis that external surface area influences AEA interactions was studied by analysis of the sieved fractions of ash samples FB-1 and FR-2. The ash samples were separated into seven size fractions as shown in Tables 8.4 and 8.5. The organic carbon contents and specific foam index values were then determined for each of the various size fractions. The results of the tests are shown in the two tables.

As shown in Row A of both Tables 8.4 and 8.5, about 70 to 80 percent of the particles (by mass) are less than about 63 microns in size. The organic carbon contents of the sieved fractions (as percent mass of the size fractions) increase with increasing particle size (Row B) with the smallest size fraction containing 0.18 percent for Ash FB-1 and 0.29 percent for Ash FR-2, and the largest size fraction containing 2.7 percent for Ash FB-1 and 5.3 percent for Ash FR-2. (For comparison, the organic carbon contents of the un-sieved ashes are 0.38 percent for ash FB-1 and 0.72 percent for ash FR-2.)

Table 8.4: Properties of sieved fractions of Ash FB-1.

Ash FB-1		< 45	45 - 63	63 - 75	75 - 90	90 - 106	106 - 125	> 125
Size range, μm								
A	Fraction of ash mass, % retained	41.0	32.0	11.0	5.5	2.1	2.2	5.1
B	Organic carbon content, % of mass of size fraction	0.18	0.19	0.25	0.37	0.45	0.62	2.71
C	Contribution to ash TOC content, % mass of unsieved ash	0.07	0.06	0.03	0.02	0.01	0.01	0.14
D	Fraction of total organic carbon in unsieved ash, %	19.4	16.3	7.2	5.4	2.5	3.6	36.4
E	Specific foam index, mL AEA/100 kg cm for the size fraction	150	120	90	80	100	160	320
F	Specific foam index per mg organic carbon in test	16.6	12.4	7.2	4.3	4.5	5.2	2.4
G	Computed specific surface for model particle, mm^2/g	1.1e5	5.0e4	3.9e4	3.3e4	2.8e4	2.4e4	1.8e4
H	Estimated exterior carbon surface area in foam index test, mm^2	1663	828	834	1031	1055	1239	4172

Table 8.5: Properties of sieved fractions of Ash FR-2.

Ash FR-2		< 45	45 - 63	63 - 75	75 - 90	90 - 106	106 - 125	> 125
Size fraction								
A	Fraction of ash mass, % retained	63.5	19.0	4.0	3.3	2.0	2.1	4.8
B	Organic carbon content, % of mass of size fraction	0.29	0.47	0.93	1.11	1.79	2.09	5.31
C	Contribution to ash TOC content, % mass of unsieved ash	0.19	0.09	0.04	0.04	0.04	0.04	0.25
D	Fraction of total organic carbon in unsieved ash, %	25.9	12.4	5.2	5.2	5.0	6.1	35.1
E	Specific foam index, mL AEA/100 kg cm for the size fraction	200	160	120	140	200	260	400
F	Specific foam index per mg organic carbon in test	13.6	6.8	2.6	2.5	2.2	2.5	1.5
G	Computed specific surface for model particle, mm ² /g	1.1e5	5.1e4	4.0e4	3.4e4	2.8e4	2.4e4	1.9e4
H	Estimated exterior carbon surface area in foam index test, mm ²	2706	2006	3103	3113	4208	4182	8175

The contributions of each sieved fraction to the total organic carbon content of the ashes are shown in Rows C and D. Row C shows the mass of organic carbon present in the size fraction as a percent of the mass of the un-sieved ash (Row A values multiplied by Row B values). Row D shows the mass of organic carbon in each size fraction relative to the total organic carbon content in the un-sieved ash sample (Row B values divided by the total organic carbon content). For both ashes the greatest contribution to organic carbon content (35 to 36%) is found in the >125 μm size fraction. This is likely to be in the form of porous carbon char. Other forms of organic carbon, such as VOC's and soot may be distributed on the surface of larger particles, or may be retained in the smallest size fraction.

The data in Row D of both tables is shown in Figure 8.15. The figure shows that the organic carbon content of the two ash samples is distributed so that 50 percent or more of the carbon is less than 45 μm and greater than 125 μm . These results differ from those reported by Kulaots et al. (2004) (summarized in Section 2.5.2.6). Kulaots et al. (2004) reported that 40 to 60 percent of the total LOI losses (called "carbon" by Kulaots et al.) in five Class F ash samples were present in the size range between 45 and 106 μm with relatively minor contribution from the largest size fractions. The distribution of *organic* carbon in the Texas ash samples shown in Figure 8.15 more closely resembles Kulaots et al.'s Class C ash "carbon" distribution. This difference may be the results of Kulaots et al.'s use of the standard LOI test to estimate organic carbon content. Another possibility is that the Texas ash samples used in this study have fundamental differences in physical properties from those studied by Kulaots et al. (ashes from

the Midwest U.S. and New England). In any case, additional study of ash organic carbon size distribution in ash is recommended.

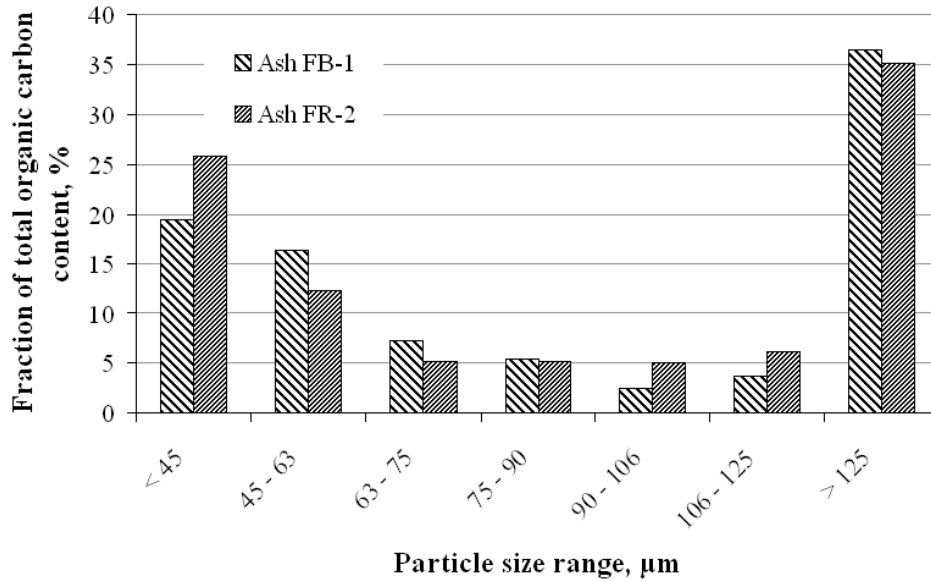


Figure 8.15: Organic carbon size distributions in two ash samples.

As described in Section 8.2.4.2, foam index tests were performed on the sieved fractions. The results of the tests are given in Row E of Tables 8.4 and 8.5. The foam index values are shown versus the organic carbon contents for each size fraction in Figure 8.16 (though the largest ash fraction, $> 125 \mu\text{m}$, is not shown in the graph to focus on the organic carbon range of 0 to 2 percent). Figure 8.16 shows that the smallest and largest size fractions correspond to the highest foam index values, while the middle-sizes fractions have the lowest foam index values. This is of particular interest because this behavior differs from the foam index versus organic carbon content behavior shown for all the ashes in Figure 8.8.

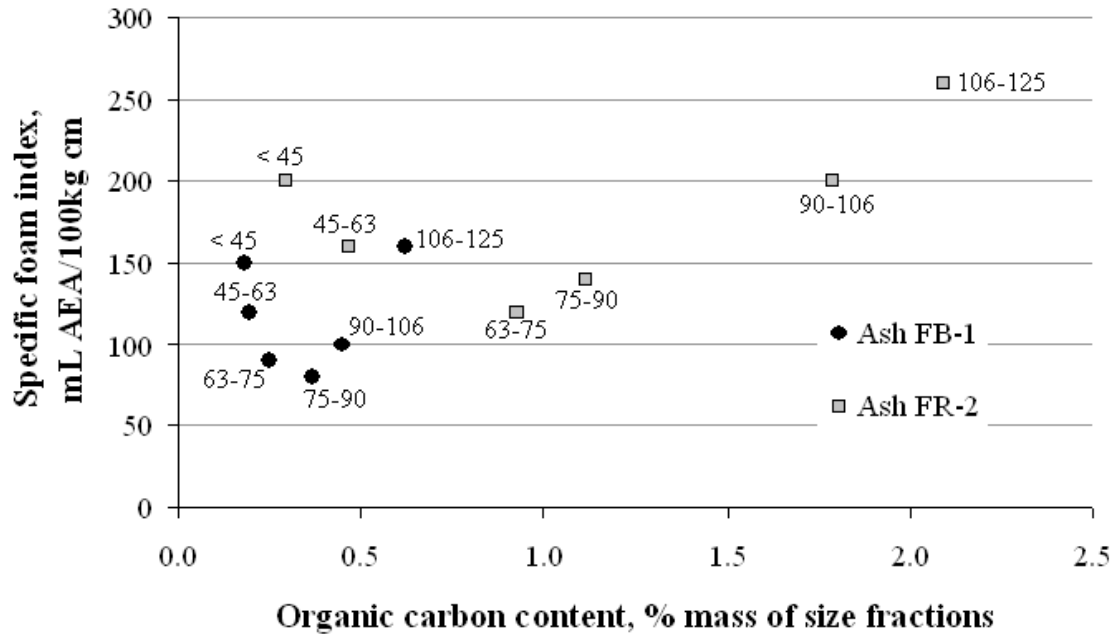


Figure 8.16: Specific foam index values of sieved ash fractions versus organic carbon content of the size fractions (Row B in Tables 8.4 and 8.5), size labels are shown in micrometers.

In Figure 8.8, foam index was shown to increase linearly with increasing organic carbon content. (Note that direct comparison of foam index values cannot be made between Figures 8.8 and 8.16 due to differences in the testing parameters which included unequal container sizes and ash to cementitious materials ratio. However trends and relative differences in values can be compared between the two graphs.) As shown in Row B in Tables 8.4 and 8.5 and in Figure 8.16, organic carbon content decreases with decreasing particle size, therefore the smallest size fractions appear to be influenced by factors other than organic carbon mass. This observation is supported by dividing the foam index values by the mass of organic carbon present in the tests. These values are shown in Row F of Tables 8.4, 8.5 and in Figure 8.17. Figure 8.17 confirms that the smallest size fractions show the greatest AEA dosage per mass of organic carbon.

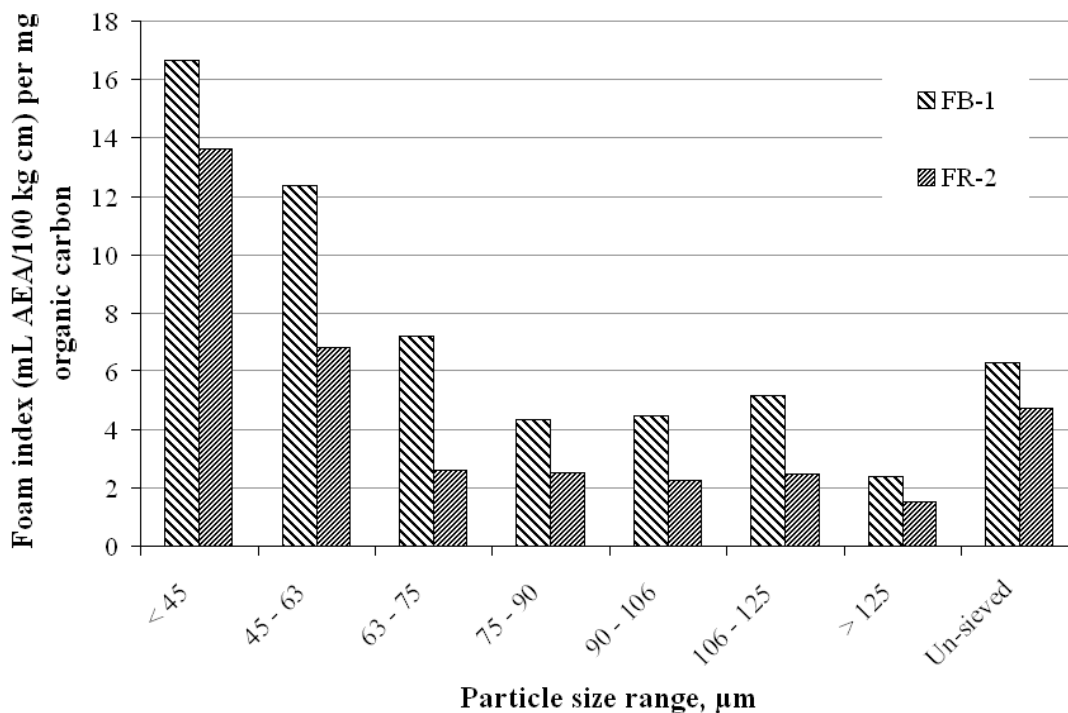


Figure 8.17: Foam index per mg organic carbon content for sieved fractions of two ash samples.

One possible reason for the behavior is that the exterior surface area of the organic carbon is a factor in AEA interactions. To study this hypothesis, an estimate of the external surface area of particles comprising the organic carbon in each size fraction was determined from organic carbon mass. To convert organic carbon mass to organic carbon particle surface area the following assumptions were made: 1) the organic carbon particles were solid and spherically shaped, 2) all particles in a given size fraction were equal to the average of the upper and lower sieve-opening sizes (except the smallest fraction was equal to 25 μm and the largest was equal to 150 μm), 3) the specific gravity of solid char was equal to 1.3 (Reid, 1981) for all size fractions, and 4) the organic carbon in all size fractions was uniform in physical and chemical properties and only differed in size.

The estimated specific exterior surface area of the combined organic and inorganic portions of the ash for each size fraction are shown in Row G of Tables 8.4 and 8.5. The estimated organic carbon external surface areas of 5 g ash (the amount used in the foam index tests) are shown in Row H of Tables 8.4 and 8.5. The values show that the organic carbon surface area decreases with decreasing particle size for the six largest fractions but then increases for the smallest size fraction.

The relationships between foam index and estimated organic carbon external surface area for the ash samples are shown in Figure 8.18. The relationships can be modeled with linear functions with the R^2 values shown in the Figure. The correlations give support to the hypothesis that organic carbon external surface area may be a factor influencing AEA interactions. If this is accurate, then analysis of the organic carbon size distribution could lead to improved correlation between organic carbon and AEA dosage in concrete relative to the correlation shown in Figure

8.1. The scope of the research did not allow for further testing of this hypothesis; however, it is recommended that future research be performed to identify relationships between organic carbon size distribution and organic carbon external surface area with ash-AEA interactions.

It is noted that the slopes of the two ash data sets are not equal, suggesting that other factors are also influencing AEA interactions as measured by the foam index test. One possibility is the presence of differing forms of organic carbon (such as VOCs and soot) in the two ash samples and in the different sizes may influence AEA interaction. This emphasizes the need for further study on the forms of organic carbon present in ash and their influences on AEA interactions. Also, it should be noted that the organic carbon external surface area estimate relies on several questionable assumptions.

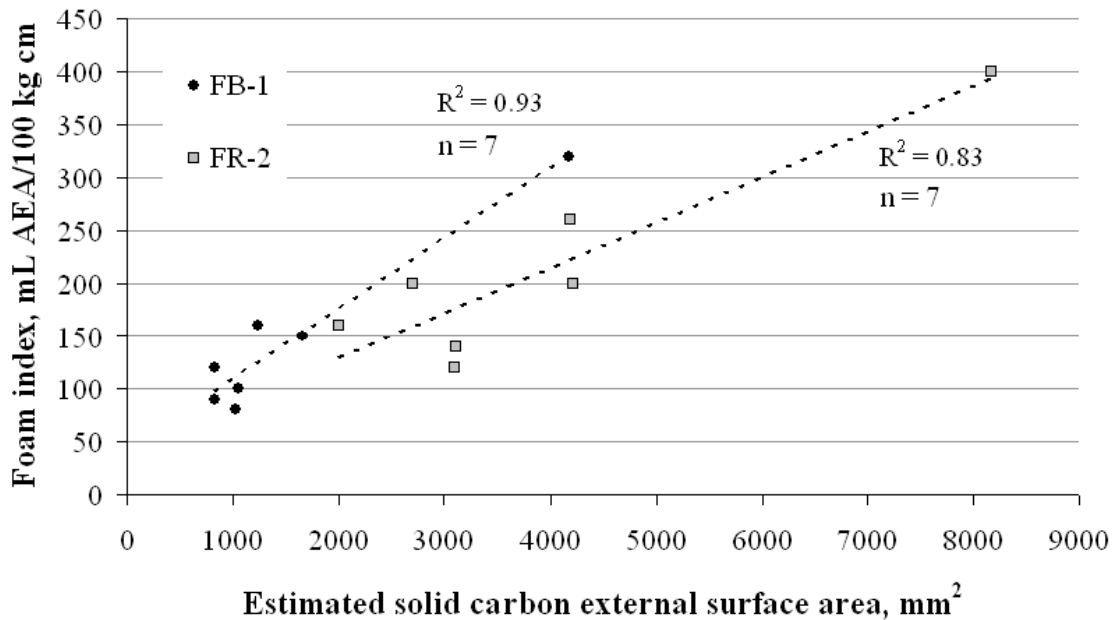


Figure 8.18: Foam index versus estimated solid carbon external surface area for seven fly ash size fractions from two samples.

BET surface area measurements showed the interior and exterior organic carbon specific surface area to be approximately 300 to 500 m²/g. The estimated exterior surface area of the organic carbon in the ash samples FB-1 and FR-2 was determined to be only 3 to 6x10⁻⁴ m²/g. Despite this considerable difference, correlations were found in both scales as shown in Figure 8.13 for BET internal and external surface and in Figure 8.18 for external surface. Additional work should be performed to study the correlations between organic carbon content, organic carbon surface area and AEA interactions.

8.3.6 Summary of fundamental factors

Five fundamental factors possibly influencing ash-AEA interactions were identified in this study. First, the mass of organic carbon in ash was shown to correlate strongly with AEA dosage in concrete. The correlation was repeated in each of the three recommended tests for measuring interactions despite the fundamental differences in the tests. This behavior appears to

contradict the conclusions of some researchers that have suggested that “carbon” mass does not correlate with AEA interactions (as typically measured by some variant of the foam index test) (Freeman et al., 1997). However, these researchers used the standard ASTM C311 LOI test to assess carbon content. As shown in this study, the LOI test is not a reliable tool for measuring organic carbon, (the second fundamental factor) and therefore the results of the other study cannot be directly applied here.

The third fundamental factor learned during this study is that several forms of carbon are present in fly ash as either inorganic or organic forms. Inorganic carbon in the form of carbonates can be present in ash but appear to have no measurable influence on AEA interactions, though they do influence the standard LOI test value. The various forms of organic carbon may influence AEA interactions differently and cannot be separated by the recommended tests for industry. Further research into the forms of organic carbon present in ash is recommended.

The fourth fundamental factor learned in this study is that calcium content appears to influence certain test results. Evidence supporting this observation was gained from the UV-Vis spectrophotometry study described in Section 8.2.4.3 and from the color change analysis described in Chapter 7. Also, the inability to correlate foam index and modified LOI test results between Class C ashes and concrete AEA dosage may be linked to this issue.

Studies on the influence of surface area on AEA interactions showed that BET surface area correlates with organic carbon mass; however, BET surface area did not improve the correlations between organic carbon and concrete AEA dosage. Particle size was shown to affect AEA interactions as measured by the foam index tests. Estimates of organic carbon surface area in sieved ash fractions showed reasonable correlations with foam index values. Improved correlations between AEA dosage and organic carbon may be improved if carbon size distribution is taken into account. Further study of the influence of particle size on AEA interactions is recommended.

8.4 Industry implementation plan

It is recommended that the test procedures developed for quality control of fly ash be implemented at the three major points of fly ash handling: 1) the ash producer, 2) the ash distributor’s materials testing lab and 3) the concrete producer. Not all tests are of equal value at each point and are therefore selectively applied.

8.4.1 Fly ash producer

Efficiency of power plant operation is of primary importance to a fly ash producer. The LOI test is generally used as a method for monitoring organic coal residuals in ash as an indicator of the efficiency of the combustion system (Fan and Brown, 2001). Minimizing LOI content of ash is desirable for reasons of combustor efficiency and for potential sale of ash to the concrete industry, and therefore frequent assessment of the ash stream is a necessary component of plant operation. The fly ash producer could benefit from the use of the modified LOI and colorimetric analysis tests to aid in monitoring fly ash organic carbon content.

Implementation of the modified LOI test

The fly ash producer could utilize the modified LOI test as a more accurate measurement of organic carbon in coal in comparison to the standard LOI test. Improved accuracy in the

measurement would provide the producer with a better assessment of combustor efficiency and allow for more informed decisions on changes that may be necessary to improve operations. The modified LOI test would provide the producer with an indication of the potential for ash marketability. Additionally, some ashes that do not meet ASTM C 618 standard LOI specification may qualify if modified LOI is used to replace the test, however this would require a change to the standard specification (ASTM C618).

Implementation of the color analysis test

Color analysis could be used as a rapid method for assessment of organic carbon. Ash could be sampled directly from the point of collection (in dry state or if wet after oven drying) and scanned and analyzed. When monitored on a regular basis, changes in color could be used to indicate combustion efficiency and/or changes in the potential for sale to the concrete industry.

8.4.2 Fly ash distributor/material testing lab

The ash distributor collects ash from the ash producers and then distributes the ash to concrete producers and other users. Because the concrete industry requires consistent quality ash, several tests (such as standard LOI) are performed to assess various ash properties. The three recommended tests could be beneficial to the fly ash distributor for identifying the suitability of a given ash source for use in concrete and provide the distributor with information about the potential effects of the ash on concrete AEA dosage which the distributor can pass along to the concrete producer.

Implementation of the modified LOI test

The modified LOI test can be used in conjunction with the standard LOI test to provide valuable information regarding potential fly ash-AEA interactions. The modified LOI test can be performed in any testing laboratory that currently performs the standard LOI test since no additional testing apparatus is necessary. The two tests can be combined as is described in Chapter 5.

It is recommended that fly ash distributors assess both the modified LOI and standard LOI contents of ash regularly to identify changes in ash properties that might influence behavior in concrete. The test results should be reported to the concrete producer upon delivery of the ash.

Implementation of the standard foam index test

The proposed standard foam index test could be used as a general measurement of fly ash-AEA interactions. A standard test would be consistent in the container geometry, filled-height, ash to cementitious materials ratio, water to cementitious materials ratio, cement type and titrant type. When a standard is used, different ash sources and test values obtained in different laboratories could be directly compared. It is recommended that the fly ash distributor pass on the foam index value (in addition to standard and modified LOI) to the concrete producer upon delivery of the ash.

Implementation of the color analysis test

Because the standard LOI and modified LOI tests require several hours to perform (modified LOI requires a minimum of 2 h after drying) use of the color analysis test may be used

as rapid method for assessing changes in ash quality from a single source. When regularly monitored, the color analysis test could indicate potential changes in ash quality, prompting the distributor to perform additional tests to verify the potential impact of the changes.

The color analysis test could be used as a low-tech indicator for the need to perform additional testing on ash quality with respect to ash-AEA interactions. For example if ash sample grayscale value is greater than 120-130 (as measured by the author's scanner) i.e., lighter than grayscale patches G7 to G8 of the Kodak IT8.7 standard, then the influence of the ash on AEA dosage in concrete will likely be relatively low. However, if the ash grayscale value is less than 120-130 (darker than patches G7 or G8), then the ash may significantly increase AEA dosage in concrete and additional testing, such as the modified LOI and foam index, should be performed to identify the magnitude of the influence.

Use of the change in ash grayscale value (by heat treatment) test could be used as a complimentary test to the modified LOI test for estimating organic carbon content. While the change in grayscale value is limited in the amount of organic carbon which can be measured (generally less than 2 percent as shown by Figure 8.11), the test could find use in situations where small mass changes (such as those measured in the modified LOI test) are difficult to measure accurately.

8.4.3 Concrete producer

It is recommended that the concrete distributor provide the modified LOI, standard LOI and standard foam index test results to the concrete producer upon delivery of fly ash. For the concrete producer to benefit from the tests, it is essential that a careful log of fly ash performance relative to the test values be kept. It is proposed that the concrete producer's ash performance log include the test values provided by the distributor and the details of the various mixes produced using the ash including: percentage of fly ash used in the cementitious system, the AEA dosage requirements and percent air content as determined by trial mixes, additional mineral and chemical admixtures used and other factors that may influence air content. As information is collected, trends between the test and concrete AEA dosages should become apparent.

It is recommended that the concrete producer make use of mix-specific foam index tests for predicting AEA dosages in individual mixes. The mix specific foam index tests would incorporate the same fly ash, cement, ash to cementitious materials ratio and AEA type used in the proposed mix. All other parameters of the test would remain fixed. Recording both the mix-specific test results and actual AEA dosage of the concrete would provide data that could be used to establish a correlation between mix-specific foam index tests and AEA dosages for mixes which incorporate local materials.

8.4.4 Application of the conclusions made in this study to local ash

It is noted that the fly ash samples studied in this research were obtained from power plants within a limited geographical region of the U.S. that nevertheless represented coal produced over a far broader geographic range. Therefore it is possible that the results and general rules for ash influence on AEA dosages determined from this study may not directly apply to regions where fly ash properties, particularly those properties related to residual carbon type and quantity, differ significantly. In regions where this is the case, the recommended tests can still be utilized when correlated with local data to establish general rules and guidelines for use.

8.5 Contributions of this research to the state of the art

This research has produced several contributions to the current state of knowledge concerning fly ash-AEA interactions in concrete and current testing practices.

8.5.1 Organic carbon is the key

The industry assumption that carbon in the form of solid char is the primary factor affecting ash-AEA interactions was shown to be imprecise. Evidence gathered in this research suggests that the organic carbon content, defined as the forms of carbon that are not acid soluble but are removed in the form of carbon oxides when heated to 900°C in air, correlate strongly with ash-AEA interactions. Other forms of organic carbon that may in fact interact with AEA's but are not indicated in the results of the 300-500°C modified LOI test include volatile organic compounds and soot.

8.5.2 Organic carbon mass

While some researchers have hypothesized that properties of “residual carbon” in ash such as surface area and surface charges affect ash-AEA interactions, it was shown during the course of this research that the mass of organic carbon appears to be the primary contributor to AEA interaction among the factors and ash samples studied. A linear relationship between AEA dosage in concrete and organic carbon mass content in fly ash was established. Furthermore, it was shown that relatively small changes in organic carbon mass measurements are accompanied by significant changes in required AEA dosages in concrete to produce target air contents (150 mL AEA/100 kg cm per percent organic carbon). Because of the variable nature of fly ash, within-source variations in organic carbon content on this small scale are likely.

8.5.3 Limitations of current testing methods

Current industry methods for predicting ash influence on concrete AEA dosage can be unreliable. The standard LOI test can measure the contributions of several materials in addition to organic carbon content on mass change. Because the contributions from other materials cannot be distinguished from organic carbon content, establishment of reliable relationships between standard LOI and ash-AEA interactions can be difficult or impossible.

Lack of a standard foam index test limits the potential of the test as an estimator of AEA dosage in concrete. This research identified that variations on the test can lead to different conclusions regarding the potential influence of ash on AEA dosage. Several factors in the test were identified which could potentially cause significant variability in the test results of a single test procedure.

8.5.4 Improved quality control methods

Three techniques for estimating fly ash influence on AEA dosage are recommended for industry implementation, modified loss on ignition, a “standard” foam index test, and color analysis. The three test methods, though fundamentally different, are linked by their apparent sensitivity to organic carbon content. The tests are recommended for implementation at the three points of ash handling.

Chapter 9. Conclusions and Future Research

9.1 Conclusions

9.1.1 Conclusion from the assessment of the of the ASTM C311 loss on ignition test

- The ASTM C311 LOI test measurement for fly ash is routinely interpreted as a measure of carbon content. This may not always be an accurate interpretation.
- Several forms of carbon are present in ash including: carbon char, volatile organic compounds, soot and carbonates. The various forms of carbon behave differently under LOI test conditions. The temperatures at which carbon containing materials are oxidized or decompose vary.
- Carbon in the form of soot may not be measured by the LOI test. Carbon black, a form of manufactured soot, did not readily oxidize under the conditions of the LOI test.
- Certain non-carbon materials can be removed from ash under LOI test conditions. Calcium hydroxide, calcium sulfate hemi-hydrate and gypsum, which may be present in ash, were shown to dehydrate under LOI conditions. Oxides of silicon, iron and aluminum were also shown to lose mass (between 0.1-0.3 percent measured at 750°C) when exposed to LOI test conditions.
- Some fly ash samples were shown to gain mass under LOI test conditions. The mass gains typically occurred at temperatures greater than 600°C. Thermo gravimetric analysis of Ash FR-2 showed that mass gain does not occur in an inert (nitrogen) environment suggesting that mass gain may be due to oxidation of ash materials.
- The individual contributions of different materials in ash to mass change are not differentiated by the LOI test; instead the LOI value is the sum of mass losses and gains that occur during the test.

9.1.2 Conclusions pertaining to the modified LOI test

- Manufactured charcoal, which is similar in nature to coal char found in ash, can completely oxidize in air at 500°C provided sufficient time is allowed for the reaction to complete (220 minutes for 1.7 g samples in a muffle furnace).
- The organic carbon content of two fly ash samples was shown to be at least 85 percent removed at temperatures between 300 and 500°C in air (1 g samples and 30 min exposure at each temperature interval).
- A modified LOI test was proposed which measures the change in ash mass between 300 and 500°C.
- The modified LOI test which measures mass loss of 1 g samples in the temperature range of 300 to 500°C (60 min exposure at each temperature) correlates more reliably with ash organic carbon content than the standard LOI test.

- The modified LOI test correlates more reliably with concrete AEA dosage data than the standard LOI test.
- The modified LOI may not indicate the presence of either VOCs or soot.
- The modified LOI test is sensitive to several sources of variability including, handling effects on mass measurements, furnace variability and ash source.
- The modified LOI test is recommended for implementation in industry. The modified LOI procedure can be combined with the standard LOI procedure currently in regular use. Fly ash distributors should regularly assess ash quality by use of both the standard LOI and modified LOI to detect potential changes in properties. Modified LOI measurements could be used to estimate potential influence of fly ash on concrete AEA dosages.

9.1.3 Conclusions from the assessment of the foam index test

Comparison of existing foam index test methods

- Foam index test results are sensitive to the method used, i.e., variations in foam index test methods lead to materials- and test-specific variations in results. One should not expect the same or necessarily comparable results from different foam index test methods, even though they may be conceptually similar in general procedure and apparatus.
- A predictive correlation between foam index test result and the dose of AEA required to stabilize 6 percent air in fresh concrete could be established for any of the four foam index methods studied. The reliability of that correlation varied among test methods and materials, however.
- Foam index values should be reported in consistent units that normalize cumulative amount and concentration of AEA and the mass of cementitious materials present. Units of mL of AEA per 100 kg cementitious materials (or US Customary equivalent), as commonly used in the industry for AEA dosages in fresh concrete, are recommended.
- Test variations can rank ash interaction with AEA differently and can lead to different decisions concerning influence of fly ash or other mix constituents on air content.
- For the fly ash samples tested in this study, the Bottle Shake test resulted in the strongest correlation with concrete air data followed by the Vial Shake test, Test Tube Shake and finally the Blender test.
- Of the four foam index test variants studied, the most reliable correlation between foam index and concrete results was obtained with the Bottle Shake test. This was also the most repeatable and easiest to perform
- A systematic study of the effects of variation in the foam index parameters on test results was required for the development of a proposed standard test method.

9.1.4 Study of the influence of procedural factors on the foam index test

Several variations of the foam index test have been used successfully to predict the required dose of AEA in air entrained concrete, but such predictive correlations depend on the specific combination of materials and the specific foam index test method. This is true whether one is using the foam index to evaluate a single component with all other ingredients standardized, or to evaluate a specific combination of materials unique to a particular concrete mixture. If the foam index is to have broader application, allowing comparison of results among multiple users, standardization of the following aspects of the test method is recommended.

- Test results should be reported in units of mL AEA /100 kg cm (or is US customary equivalent) to account for drop volume, AEA concentration, and mass of cementitious materials, yielding a unit that is numerically compatible with that commonly in use for AEA proportions in concrete mixtures.
- Results are specific to the container used. Foam index values, in units of mL AEA/100 kg cm, can only be compared when the filled height of paste in the test containers are equal.
- For a simple hand-test, as can be performed in any lab or plant site, the geometry of prismatic, sealable containers is defined by limits on interior height, maximum and minimum fill ratio, volume of paste at filled-height, minimum resolution, and convenience, as described in Figures 6.11 and 6.12. An ideal container is described in Chapter 6, Section 6.2, Table 6.16.
- While agitation by hand has been shown to be practical and reproducible, foam index test results are sensitive to the number and frequency of shaking cycles. A shaking duration of 10 s and shaking frequency of 4 ± 0.5 shakes/sec is recommended.
- For the AEA and cementitious materials used in this study the duration of the rest period was not a significant factor when kept between 15 and 45 seconds. A 20 second rest period is recommended.
- AEA effectiveness can degrade with storage time. AEA solutions should be tightly capped in filled containers, stored in the dark, and discarded after 2 weeks.
- The mean and standard deviation of the drop volume as dispensed by the pipette affects precision of the foam index test. Pipette standard deviation should be no more than about 10 percent of the mean drop volume.
- The minimum resolution of the test can be adjusted based on drop volume, AEA concentration, and mass of cementitious materials. R_{\min} should be computed and reported with test results.
- Drop volumes of 20 microliters (dispensed with a pipet) and AEA concentrations of 5 percent were determined to be suitable in the tests performed in this study. Repeatability of the test among three independent operators in the same lab is within the minimum resolution.

9.1.5 Study of the influence of material proportions on foam index values

- Because the specific foam index of a fixed combination of cementitious materials increases with water to cementitious materials ratio, w/cm must be fixed in a standard test. Required values of w/cm are considerably higher than those in ordinary portland cement concrete to achieve adequate mixing and to form a stable, discernable endpoint. A value of 1.5 is an absolute lower bound for a hand-agitated test, and a value of 2.0 is recommended.
- Values of ash to cementitious materials will vary depending on the test application. In regards to a standard test in which all proportions are fixed, ash/cm equal to 0.33 is recommended. With regard to mix-specific testing, ash/cm should match that of the specific mixture being evaluated
- Normalization of specific foam index values by the air/paste ratio (air volume is estimated as to the volume of foam at the paste surface) at the test endpoint, as shown by eqn. 1 in Chapter 6, Section 6.2.3, is necessary for comparison of tests performed with differing volumes of paste or differing containers. When the same container and paste volume (and thus same filled height) is used, specific foam index values can be compared directly.

9.1.6 Conclusions from color analysis for fly ash properties

Color analysis test procedures

- A standard procedure for characterizing ash color has been developed. The procedure includes ash sample preparation, sample imaging with a common desktop color image scanner and image analysis to quantify image color information.
- Various factors in the test procedure—such as scanner model, analysis region size and location, scanned background color and ambient light—have the potential to introduce variability in the tests and should be controlled as described herein.
- Different scanner models image samples differently. If a correlation between scanners can be described by a mathematical function, then a correction between scanners can be easily made. Alternatively, a commercially available grayscale target is proposed as a calibration standard.
- Characteristics of the sample preparation—such as moisture content, sample compaction and sample container material—can cause variability in the test method and should be controlled according to the guidelines given.
- Four-clear-sided, methacrylate cuvetts were found to be satisfactory for containing ash samples during scanning. Use of containers composed of different materials can be used, however, the influence on the scanned image must be considered.
- Use of 8-bit depth grayscale values to quantify ash color contains less information than full color (24-bit depth) values; however, grayscale values were used to adequately differentiate the ash samples tested in this study.

- A trend between decreasing grayscale value (darkening) of ash and increasing AEA dosage for concrete containing the ash exists for the ash samples studied.
- The scanning and grayscale analysis method presented here can be used as a quality control tool to identify ashes that may require increased AEA dosage in concrete.

9.1.7 Correlations between ash grayscale value and chemical properties

- A procedure for measuring change in ash grayscale value has been proposed. The procedure consists of exposing ash to elevated temperatures in a muffle furnace and measuring the ash color before and after heating. The sample imaging and color analysis portion of the procedure is identical to the basic method described in Section 7.1 of this work.
- Multi-linear regression analysis suggests that organic carbon content has a positive or lightening influence on ash grayscale change in the 300 to 500°C range. This is hypothesized to be due to the removal of the organic carbon content by heating. The regression analysis also showed that calcium oxide content correlated with a negative or darkening influence of ash grayscale change between 300 and 500°C. The mechanisms behind this correlation are not known and deserve further study.
- Grayscale values of Class F ash samples were shown to increase (lighten) due to exposure to increasing temperature in air up to 500-600°C. Class C ash samples showed little or no increase in grayscale values in the same temperature range. The grayscale values of all ashes decrease (darken) at temperatures greater than about 600°C.
- A non-linear (logarithmic) correlation between ash grayscale change and organic carbon content was established. The trend shows grayscale change varying from 0 to 80 units for ash samples having organic carbon contents of 0 to 2.0 percent. For organic carbon contents up to 5 percent, further change in grayscale was about 10 units.
- The change in grayscale method could be used in industry as an inexpensive approximation of organic carbon content in ash. The applications of this measurement could be beneficial to boiler operators as a measurement of combustion efficiency. The method could also be employed by fly ash marketers as a method of assessing variations in ash in general, and more specifically, potential influence of fly ash on air entraining admixture dosage.

9.1.8 Synthesis summary

- The industry assumption that carbon in the form of solid char is the primary factor affecting ash-AEA interactions was shown to be imprecise. Evidence gathered in this research suggests that the organic carbon content, defined as the forms of carbon that are not acid soluble but are removed in the form of carbon oxides when heated to 900°C in air, correlate strongly with ash-AEA interactions. Other forms of organic carbon that may in fact interact with AEA's but are not indicated in the results of the 300-500C modified LOI test include volatile organic compounds and soot.

- While some researchers have hypothesized that properties of “residual carbon” in ash such as surface area and surface charges affect ash-AEA interactions, it was shown during the course of this research that the mass of organic carbon appears to be the primary contributor to AEA interaction among the factors and ash samples studied. A linear relationship between AEA dosage in concrete and organic carbon mass content in fly ash was established. Furthermore, it was shown that relatively small changes in organic carbon mass measurements are accompanied by significant changes in required AEA dosages in concrete to produce target air contents (150 mL AEA/100 kg cm per percent organic carbon). Because of the variable nature of fly ash, within-source variations in organic carbon content on this small scale are likely. It is noted, however, that if the specific surface of the carbon in these ashes is about constant, and given the constant mass of ash in the foam index and concrete air tests, the influence of carbon mass and carbon surface area would be directly proportional to one another, and thus indistinguishable from each via the methods used here.
- Current industry methods for predicting ash influence on concrete AEA dosage can be unreliable. The standard LOI test can measure the contributions of several materials in addition to organic carbon content on mass change. Because the contributions from other materials cannot be distinguished from organic carbon content, establishment of reliable relationships between standard LOI and ash-AEA interactions can be difficult or impossible.
- Lack of a standard foam index test limits the potential of the test as an estimator of AEA dosage in concrete. This research identified that variations on the test can lead to different conclusions regarding the potential influence of ash on AEA dosage. Several factors in the test were identified that could potentially cause significant variability in the test results of a single test procedure.
- Three techniques for estimating fly ash influence on AEA dosage are recommended for industry implementation, modified loss on ignition, a “standard” foam index test, and color analysis. The three test methods, though fundamentally different, are linked by their apparent sensitivity to organic carbon content. The tests are recommended for implementation at three points of ash handling: the ash producer, ash distributor and concrete producer.

9.2 Future research recommendations

9.2.1 ASTM C311 Loss on ignition and modified loss on ignition

Future work should identify and examine the inorganic components of ash that change with exposure to LOI temperatures. Methods for precisely identifying minerals that dehydrate, decompose or increase in mass could allow for better analysis of the net changes in mass which occur during the LOI test.

Evaluation of the proposed modified LOI procedure on a group of ash samples possessing a larger range of organic carbon content than the Texas ashes is necessary to identify the ability of the test to measure organic carbon in ashes produced at other sources. It is possible that ashes with larger organic carbon content may require greater exposure time to complete the test.

The ability of the modified LOI test to predict fly ash-AEA interactions in concrete should be studied for a variety of ashes from different coal sources to identify whether the relationship observed in this study is directly applicable to other ash types.

9.2.2 Foam index

The next major steps that must be taken before the foam index test can be reliably used in industry are 1) to further compare foam index results with actual concrete AEA dosages for a variety of ash samples to identify correlations that would allow the test to predict AEA dosages in real concrete, 2) examine the influence of chemical admixtures in addition to AEA on the test and compare the results to real concrete data, and 3) inter-laboratory testing to identify the repeatability of the test performed by multiple users.

Further study of the combined effects of agitation frequency and duration with a variety of containers and fill ratios should be performed. Development of a mechanically agitated foam index could help to reduce the variability and labor-intensiveness of agitation by hand.

9.2.3 Color analysis methods

The ash samples tested in this study were representative of the ashes produced in a narrow geographical region of the U.S. Additional study should be done to measure differences that may exist among ash samples produced from coals and plants in different regions. It is recommended that a study of the variations in color with time of ash samples from a single source be conducted to identify the usefulness of this tool in such an application. A study of the influence of particle morphology (size and shape) on ash color should be studied to identify potential effects on grayscale analysis results.

Additional value could be gained from the change in grayscale value test if the individual forms of organic carbon present in coal could be quantified. A proposed method for qualitatively identifying VOCs in ash by means of dissolving the organic compounds in benzene and visually comparing the change in solvent color was described in Chapter 5. Perhaps this method could be improved using an ultra violet-visible light spectrophotometer to quantify VOC presence in solvent by light absorbance. Methods for quantifying soot content in ash should also be identified.

Additional work is recommended to determine the suitability of the color change test on ash produced in other geographical regions. The possibility exists that differing source coal or combustion conditions may produce differences in ash properties with respect to color.

Additional study should be performed to identify the influence of changes in inorganic ash contents due to heating on ash color. Use of the RGB values in addition to the grayscale values may provide more information for identifying ash properties.

9.2.4 Further study of the factors influencing fly ash-AEA interactions

Organic carbon forms

Three forms of organic carbon were identified in this research: coal char, volatile organic compounds and soot. The individual contributions of these materials to the total organic carbon content of the ash samples were not identified in this study. It is recommended that methods of assessing the forms of organic carbon in ash be identified.

One possible method for identifying the contribution of VOCs to organic carbon is to perform macro thermo gravimetric analysis of ash in an inert atmosphere (such as nitrogen) and

measure the change in organic carbon content with temperature. Changes in organic carbon content of the heated ash could be attributed to the loss of carbon in the volatiles. This could shed light on the presence of VOCs that may be driven off in the LOI test or modified LOI temperature ranges. Methods for measuring the soot content of ash should also be developed.

In addition to studies on measuring the contents of various forms of organic carbon in ash, study of the influence of the individual forms on AEA behavior should be performed. If the varying forms of organic carbon influence AEA-interactions differently, then correlations between AEA-interactions and organic carbon content could be improved by considering the relative influences of the individual organic carbon forms.

Fundamental mechanisms behind fly ash-AEA interactions

The hypothesis that fly ash-AEA interactions are the result of the adsorption of AEA molecules on the surface of organic coal residuals has not been conclusively proven. This research identified a relationship between organic carbon content and fly ash AEA interactions and also suggests that particle size and/or surface area may play a role which may support the hypothesis; however, the fundamental mechanisms behind the interactions were not established.

Further work should be performed to identify the underlying mechanisms causing the correlation between AEA dosage in concrete and organic carbon content. The use of ultra-violet visible-light spectrophotometry could provide useful data on the adsorption of AEA from solutions containing fly ash in carefully controlled experiments. One possible method for avoiding AEA precipitation due to divalent cations (described in Section 4.2.4.3) is to use a nonionic or cationic surfactant in the test.

Carbon separation techniques (such as electrostatic precipitation or froth floatation) that do not alter the properties of the ash mineral content but could increase or decrease the amount of organic carbon present in ash could be used to isolate the organic carbon for studies on AEA interactions.

Calcium and Class C fly ash

Correlations between modified LOI and foam index tests and concrete AEA dosages were not identified for the Class C ashes used in this study. The causes behind this behavior were not determined in this study. One possible reason is that the Class C ashes used had relatively uniform properties, and therefore lack of variability did not allow for correlations to be established. It is recommended that the tests performed in this study to correlate concrete AEA dosage with organic carbon content, modified LOI, and foam index tests be done with a set of Class C ashes which exhibit greater variability in properties (particularly organic carbon content) than those used here. Additional work is required to determine if the observations regarding Class C ash performance made in this study apply to Class C ashes generally. Furthermore, given that the ASTM C 618 Class F/C distinction is somewhat arbitrary, and that silicon, aluminum, and calcium contents in fly ash are distributed on a continuum, more study is needed on the underlying compositional variables that caused the ashes studied here to fall into the “F” or “C” categories.

Surface area and particle size

The results of this study suggested that neither BET surface area (including internal pore area) nor external surface area inferred from particle size could be used to fully explain ash-AEA

interactions, despite general correlations with concrete air or foam index. It is likely that some forms of carbon are porous and BET measurements are useful, and that other forms are not porous and external surface areas are useful. Further study should be performed to identify the influence of organic carbon size distribution on AEA interactions. Improved methods of measuring fly ash particle size distribution could provide additional information.

9.3 Closing items

The organic coal residuals that appear to be at the root of the fly ash-AEA interaction problems represent lost potential energy that was initially intended to heat steam in a boiler to generate electricity. The residual energy content of organic coal residuals is lost when the ash is incorporated in concrete.

Consider that if an ash containing 1 percent by mass of organic coal residuals is incorporated in concrete as 30 percent of cementitious materials, then about 170 lbs of the ash is present per cubic yard of concrete. Thus, about 2 lbs of organic coal residuals is present per cubic yard. At an energy content of about 20,000,000 BTU per ton of coal, 2 lb of coal is 20,000 BTU of heat energy lost per cubic yard of concrete. (The energy content in 2 lb of coal is equivalent to about 500 mL of diesel motor fuel.) This may be an important factor in the problem—there is not enough potential heat energy in the ash to make scavenging it financially worthwhile, therefore the fly ash is sold to the concrete industry as is.

Nevertheless, the cleaner and more efficient (with respect to complete oxidation of coal organics) the operation of the boiler, the more coal organic material will be consumed and the less problem there will be with air entrained concrete. If in the future the cost of energy increases to the point that recovering the organic coal residuals becomes economically viable, then the issue of fly ash quality with respect to air entraining concrete may disappear.

VOLUME II

Chapter 10. The Effects of Fly Ash on the Ability to Entrain and Stabilize Air in Concrete

10.1 Introduction

Concrete is the most widely used engineering material (Mehta and Monteiro, 2006). Furthermore, it is the most used manmade material (Lomborg, 2001). It is estimated that 6 billion cubic meters are placed every year (Mehta and Monteiro, 2006). This amounts to approximately 1 cubic meter of concrete placed every year for every living human on the earth.

If concrete is going to be utilized in a location where it is exposed to high amounts of moisture and subjected to freezing temperatures, then the concrete should be air-entrained to make it resistant to freezing and thawing (and salt scaling, if applicable). Furthermore, the air-void system in the hardened paste of the concrete should be made up of small and somewhat uniformly spaced voids. An extensive list of items has been provided by Whiting and Stark (1983) that have been shown to impact the ability to entrain and stabilize air-voids in concrete. The totality of this list suggests that almost every aspect of material selection, mixture proportioning, and concrete construction have the ability to impact air-entrainment. While past research has investigated many of these influencing factors, questions still remain about the underlying causes of air-entrainment problems and methods of preventing such problems. Because of this, it can be very challenging to produce satisfactory air-entrained concrete. A better understanding of these systems and their performance would greatly benefit the concrete industry.

The work presented herein was funded by the Texas Department of Transportation (TxDOT) Research Project 5207, "Effects of Texas Fly Ash on Air-Entrainment in Concrete." The research project was a joint effort by The University of Texas and Cornell University. This project was undertaken because a large number of construction problems were being encountered with air-entrained concrete. The majority of these problems were initially attributed to the use of fly ash in concrete. Fly ash is a by-product from the coal-fired power plant industry that is widely used in concrete and has shown the ability to improve the material properties of concrete. The variable interactions between fly ash and air-entrainment are attributed to changes in the burning process at coal-fired power plants in Texas in order to reduce emissions and comply with new standards.

One method that is commonly used in Texas to reduce emissions is to install a different type of coal combustion burner. This burner allows greater control over the amount of oxygen and burning temperature during the combustion process. As this burning process was changed, so was the resulting fly ash. It is often reported that there are changes in the carbon in the fly ash and this has an impact on the performance of air-entraining agents (AEAs) in concrete; carbon present in the fly ash products tends to preferentially absorb AEAs. It is still unclear what aspects of the carbon or other materials in the fly ash are important in determining the demand of the material for the AEAs.

10.1.1 Research Objectives

The main tasks of this research were to:

- Investigate test methods for assessing fly ash and effects on air entrainment
- Investigate test methods to estimate air-void system using fresh concrete
- Develop guidelines for managing air content when using fly ash
- Develop guidelines for air content tolerances, rejection criteria, and mitigation techniques
- Further objectives were to:
 - Provide a recommendation of some simple test methods that can be used to predict the impact of a given fly ash on AEA demand
 - Investigate the reported discrepancy between fresh and hardened properties in concrete
 - Investigate the occurrence of air-void clustering in air-entrained concrete

These tasks constitute a very diverse set of research topics that are not only fundamental to properties encountered in the state of Texas but throughout the world where air-entrained concrete is used.

10.1.2 Overview of Study

In this portion of this research project, work is presented that contributes to a number of the bulleted items above.

- Chapter 11 reviews several existing test methods that can be utilized to assess the AEA demand of different fly ashes from Texas and compares these tests to the performance of the same ashes in concrete.
- In the 12th chapter more simple tests are investigated. The focus of this chapter is on an existing and a newly designed mortar test to investigate the AEA demand of fly ash.
- Chapter 13 presents a method to assess the AEA demand of fly ash from a single concrete mixture. The work presented in this chapter serves as a base method against which the other methods of assessing the AEA demand of fly ash in concrete can be compared. This work also explores the impact of different AEA, water reducer, fly ash volume, and mixing temperature on the performance of fly ash concrete with different AEA demands.
- Chapter 14 describes challenges of using two testing methods aimed at measuring the fresh properties of concrete to predict the air-void system and performance in a rapid freezing and thawing test. The use of a device advertised to assess the air-void system in fresh concrete is investigated and comparisons are made to results from a hardened air-void analysis.

- Chapter 15 presents a new experimental technique that was developed to make visual observations of air-voids in the bleed water of cement pastes. These observations suggest that a shell is present around these voids and that this shell may be relevant to resisting changes in the air-void system of concrete.
- Finally, chapter 16, the air-void shells are investigated with several different analytical techniques in order to relate some of the physical properties observed to the chemical properties of the shells.
- Volume II: Appendix A shows an investigation of the sensitivity of different parameters on an automated hardened air-void analysis.
- Volume II: Appendix B provides the procedure used to prepare samples for the hardened air-void analysis utilized in this research.
- Volume II: Appendix C presents a master collection of the fly ash investigated in project 5207 and their relevant chemical and physical properties.

Chapter 11. Investigation of Air-Entraining Admixture Dosage in Fly Ash Concrete

11.1 Introduction

Fly ash is a waste material from the coal combustion process that is typically sent to a landfill if another use is not identified. Fly ash has proven to be a useful supplementary cementing material (SCM) in concrete. Some of the benefits of fly ash include a reduction of cement, improved workability of fresh concrete, decreased permeability, and increased long term strength. Because of these improvements in material performance and sustainability, fly ash is a common SCM for concrete.

The production of a small and well distributed air-void system in concrete is necessary to resist damage from freezing and thawing cycles. To obtain this void distribution, an air-entraining agent (AEA) is added to the fresh concrete mixture to encourage formation and stabilization of these voids. The volume of air in the fresh concrete needed to prevent damage varies, but is often specified in the range of about 6 percent of the concrete volume.

This project was initiated in response to reported increases in AEA dosages of up to 500 percent in the presence of certain fly ashes, discrepancies of up to 5 percent between fresh and hardened air contents, and problems with reduced strength concrete due to air void clustering around aggregates (Lukefahr, 2004). It was also reported that these problems were encountered in the state of Texas in greater frequency after the incorporation of low-NO_x burners in several coal-burning power plants. Similar observations have been reported in the literature (Freeman et al. 1996; Kulaots 2004; Hill and Folliard 2006). Among the objectives of the research project was an evaluation of the loss-on-ignition (LOI) test (ASTM C 311), and the as yet non-standard foam index test (Dodson, 1990) for predicting the potential for interaction between AEA and a given fly ash. This was done by testing ten separate fly ashes from six separate sources using LOI and the foam index test, and comparing those results to the dose of a conventional AEA required to produce an air content of 6 percent in fresh concrete. This test series was augmented with a limited number of nitrogen adsorption tests on fly ash to gain insight on the possible effects of surface area of either fly ash particles, contaminants, or both. An exciting but coincidental aspect of the work reported here is that fly ash samples were collected from four of the six sources both before and after modification of the burning process to meet U.S. Environmental Protection Agency (EPA) emission standards (via retrofitting with low-NO_x burners). While the results are interesting, a lack of information about the input coal or the burning processes themselves prevents the drawing of firm conclusions about the effect of low-NO_x burners

11.2 Research Significance

In recent years, concrete producers in Texas have faced difficulties with air-entrainment in concrete containing some fly ashes. Specifically, the AEA demand has increased sharply for certain fly ash sources, especially ASTM C 618 Class F fly ashes. In some cases, the use of affected fly ashes have been banned due to the daily variability of the ashes produced and the lack of a consistent test method to assess these changes. The work contained in this chapter is in response to this need for improved test methods to measure AEA-fly ash interactions.

11.3 Experimental

11.3.1 Samples

Fly ash samples were collected from six different coal-fired electrical power plants in Texas that produce fly ash commercially used in concrete. These samples are labeled numerically, 1-6. Fly ash samples were obtained from four of these locations (1-4) both before and after the modification of the burning process to reduce NO_x emission levels, but without sufficient control of samples it is not possible to associate any changes in ash behavior directly with the burning process alone. These samples have been labeled with an “A” or a “B”; “A” label corresponds to ashes after the modification and the “B” label to the ashes before. Samples 5 and 6 are representative ASTM C 618 Class F and Class C fly ashes from the same region whose burning process was not altered. Please note that fly ash samples 2A and 5 are used for testing throughout the report and are labeled as fly ash 7 and 1, respectively, in all other chapters.

11.3.2 Chemical Properties

A chemical analysis of the fly ashes and ASTM C 618 classification are given in Table 11.1. A graphical comparison is shown in Fig. 11.1 and 11.2. The compositional analysis was done using x-ray fluorescence spectroscopy.

Table 11.1: Chemical and physical properties of fly ashes

Fly Ash Number	14	26	7	7	24	5	23	10	27	1	2	
Sample Number	1A	1B	2A	2A ig*	2B	3A	3B	4A	4B	5	6	
Chemical Tests	Silicon Dioxide (SiO ₂), %	50.98	52.56	52.07		48.48	34.47	34.62	37.16	38.07	56.18	30.76
	Aluminum Oxide (Al ₂ O ₃), %	18.84	19.82	23.65		25.01	20.35	21.16	20.55	20.75	20.37	17.75
	Iron Oxide (Fe ₂ O ₃), %	7.87	4.72	4.55		3.56	5.65	5.69	6.06	5.50	6.77	5.98
	Sum of SiO ₂ ,Al ₂ O ₃ ,Fe ₂ O ₃ ,%	77.69	77.10	80.27		77.05	60.47	61.47	63.77	64.32	83.32	54.49
	Calcium Oxide (CaO), %	14.39	14.35	12.76		15.92	26.50	25.35	24.76	23.78	9.95	28.98
	Magnesium Oxide (MgO), %	2.91	3.16	2.02		2.50	4.70	4.62	4.29	4.42	2.55	6.55
	Sulfur Trioxide (SO ₃), %	0.95	0.92	0.78		0.72	1.71	1.55	1.23	1.11	0.53	3.64
	Sodium Oxide (Na ₂ O), %	0.57	0.73	0.31		0.30	1.76	1.74	1.63	1.65	0.47	2.15
	Potassium Oxide (K ₂ O), %	0.94	1.11	0.80		0.71	0.46	0.47	0.45	0.52	1.08	0.30
	Total Alkalies (as Na ₂ O), %	1.19	1.46	0.84		0.77	2.06	2.05	1.93	1.99	1.18	2.35
	Classification (ASTM C 618)	F	F	F		F	C	C	C	C	F	C
+Physical Tests	mL AEA/100 kg cm for 6% air in concrete	93	64	147		24	50	32	39	38	31	44
	LOI (ASTM C 311)	0.26	0.39	0.79		0.63	0.11	1.12	0.07	0.13	0.12	0.35
	Foam Index (μLAEA /g fly ash)	3.3	2.5	5	1	1	1	1	1	1	1	1
	Surface Area (m ² /g)			4.02	0.66	0.96					0.89	0.95

*A sample of Fly Ash 2A after the completion of the LOI test.

+A wood rosin AEA was used in all tests presented.

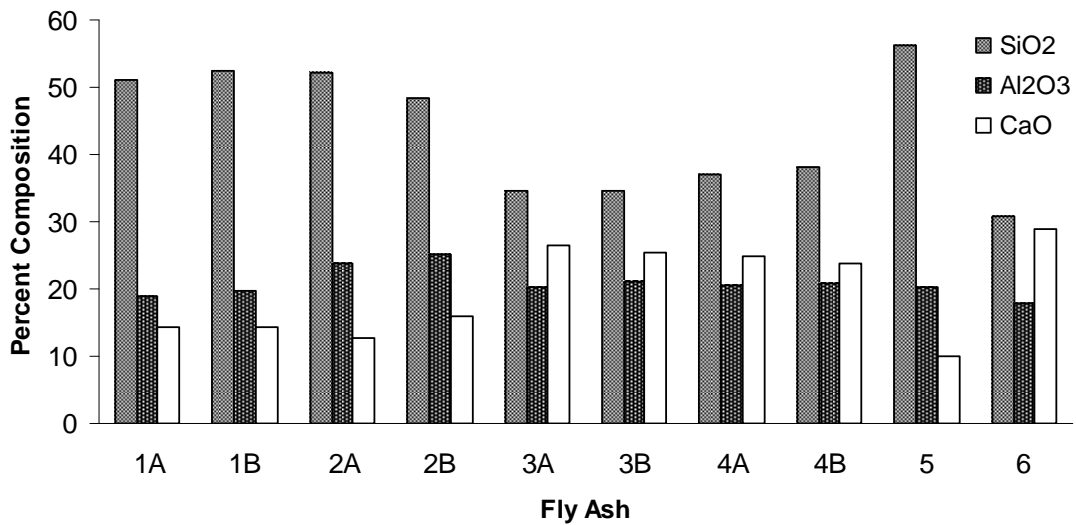


Figure 11.1: Fly ash compositions: major components

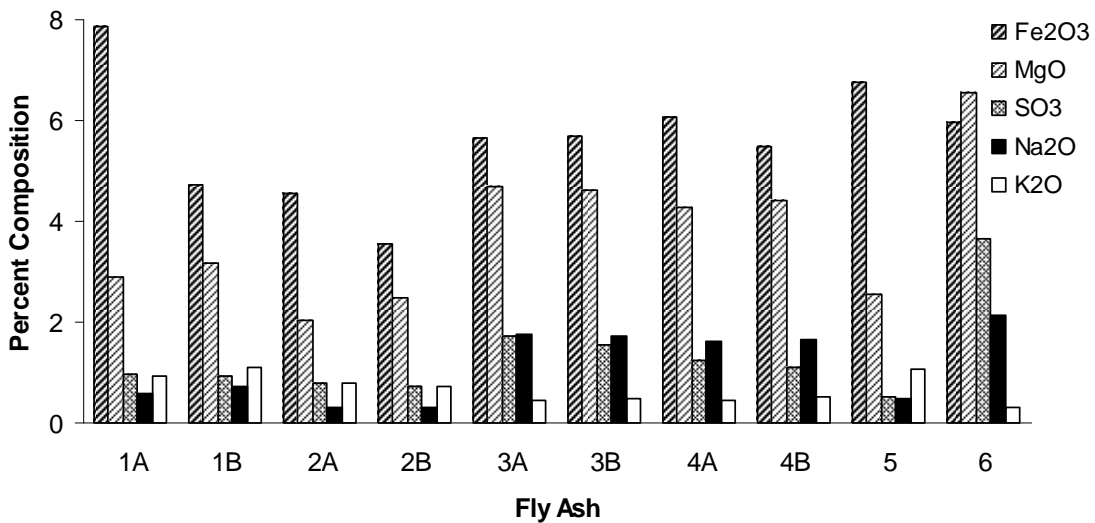


Figure 11.2: Fly ash compositions: minor components

11.3.3 Concrete Mixtures

To develop a baseline for comparison, a series of concrete mixtures was prepared in the laboratory in which the ten different fly ashes were incorporated using the same mass of ash. The mixture proportions are in Table 11.2. During the mixing process, the amount of AEA used was incrementally increased and the air content monitored via the ASTM C 138 unit weight method. Frequent mix-specific calibrations between the unit weight method and the ASTM C 231 pressure meter method produced a series of trend lines indicating air content as a function of wood rosin AEA dosage. From these data the dose required to stabilize 6 percent air in the fresh concrete was interpolated for each mixture. Further details on this mixing process follow.

Initially a 64-L batch of concrete was made in an 85-L drum mixer. All of the material for the mixture was stored in the mixing room for at least 24 hours at 23°C prior to mixing to keep the fresh concrete temperature constant. The mixture, shown in Table 11.2, used a water-to-cementitious materials ratio (w/cm) of 0.45 with 335 kg/m³ (equivalent to six sacks of cement) of total cementitious materials, of which 80 percent was ordinary portland cement that met the requirements for ASTM C 150 Type I and Type II with a 0.53 alkali content (Na₂O_{eq}), and 20 percent was the fly ash to be investigated. Local river gravel and sand were used for the aggregate. Coarse and fine aggregates were brought in from the stock piles and individually mixed. A moisture correction for each was used to adjust the batch weights. The gravel and sand were added to the mixture first, and then 2/3 of the mixing water was added. The mixture was agitated for 1 minute. Next, the cement, fly ash and the remaining mixing water were added and mixed for 3 minutes. At this point the mixer was stopped and any material gathering on the sides or back of the mixer was removed. During the final 3-minute mixing period the mixture was brought to a constant slump (ASTM C 143) of 75 mm +/- 25 mm using a normal water reducer. Due to water demand differences of the fly ash mixtures the dosage of normal water reducer varied between 45 and 85 mL/100 kg of cementitious material. The normal water reducer met the requirements of ASTM C 494 as a Type B and Type D. It is expected that different results would be obtained with the same materials when mixed for different durations, at different mixing speeds, or with different mixing energy per unit volume of mixture. Nevertheless, this method allows useful comparisons for the fly ashes investigated.

Table 11.2: Standard concrete mixture proportions

Components	Mass (kg/m ³)
Cement	268
Fly Ash	67
Coarse Aggregate	1098
Fine Aggregate	742
Water	151

11.3.4 LOI

The most common hypothesis to explain the fly ash and AEA interaction is that AEA is adsorbed to the surface of unburned carbon particles in the fly ash. It is also commonly understood that LOI is generally a useful indicator of unburned carbon. ASTM C 618 specifies a maximum LOI value of 6 percent for fly ash, and Texas DOT specifies a maximum limit of 3 percent (TxDOT DMS 4610 2006). Such specifications are based on work such as that by Gebler and Kleiger (1983). In this project all ten fly ash sources were tested in accordance with ASTM C 311 standards with the procedure published by Harris et al. (2006). Two samples were measured and averaged for each data point reported.

11.3.5 Foam Index

Given the obvious desirability for a test that directly measures fly ash and AEA interaction, researchers such as Dodson (1990) and others (Gebler and Kleiger 1983, Kulaots et al. 2003) have proposed multiple versions of what has been called a foam index test. In the many variations of this test, a mixing container is partially filled with water-and-fly ash slurry, with or

without cement or other admixtures. AEA is incrementally added, followed by vigorous agitation of the container. The amount of AEA required to stabilize a foam layer that just covers the surface of the slurry is reported as the foam index, and is a simple but a useful indicator of slurry-AEA interaction as influenced by the specifics of the container, agitation, and other details of the method. Currently there is no established standard for the foam index test. After investigations were made of several different methods the procedure used in this study was chosen due to ease of use and good repeatability of measurements.

For this testing, 25 mL of distilled water, 5.0 g cement, and 5.0 g fly ash were added to a 120 mL glass vial (O.D. x H: 50 x 95mm). The mixture was shaken for 20 seconds and 0.10 mL was added of a solution of 2.5 vol.% wood rosin AEA and distilled water. The mixture was subsequently shaken for 10 seconds and then allowed to rest for 20 seconds and the foam produced was inspected for stability. The AEA solution is incrementally added and shaken until a stable foam is formed that completely covers the liquid surface after sitting statically for 20 seconds. At this point the volume of the AEA added was recorded and the value reported as μL of AEA/g fly ash. For this testing, the same cement and AEA were used as was used in the concrete testing.

11.3.6 Nitrogen Gas Adsorption

It has been hypothesized that the ash-AEA interaction is influenced by the surface area of an adsorbent within the ash (Kulaots et al. 2004, Hill et al. 1997). If unburned carbon is the primary adsorbent of the AEA, then the carbon surface area may be more influential than the carbon content by mass. A comprehensive examination of this effect would require identifying the critical adsorbent, measuring both its mass and surface area, and comparing these results with indicators such as AEA dose to stabilize 6 percent air in fresh concrete or foam index values.

Preliminary work in this project included nitrogen adsorption tests in conjunction with Brunauer, Emmet and Teller (BET) analysis on a subset of the ash samples. All BET isotherms were obtained using a Micrometrics ASAP 2000 automated gas adsorption system. The samples were outgassed at 200 °C for 24 hours prior to analysis.

11.4 Results

All test results are included in Table 11.1, and displayed graphically in Fig. 11.3. Data in Fig. 11.3 have been normalized relative to the values obtained for fly ash 6. This fly ash was arbitrarily selected as the control sample. Perhaps the clearest and most meaningful findings are: 1) there is significant variation in AEA demand to produce 6 percent air in fresh concrete (varying from 24 to 147 ml/100 kg cementitious material) and 2) there is a lack of correlation between AEA demand and any of the other test results. Relative to source 6, in only 2 of the 10 series does an increase in LOI correspond to an increase in the amount of AEA required to stabilize 6 percent air in fresh concrete. In only 3 of the 10 series does an increase in foam index correspond to an increased required dose of AEA in concrete.

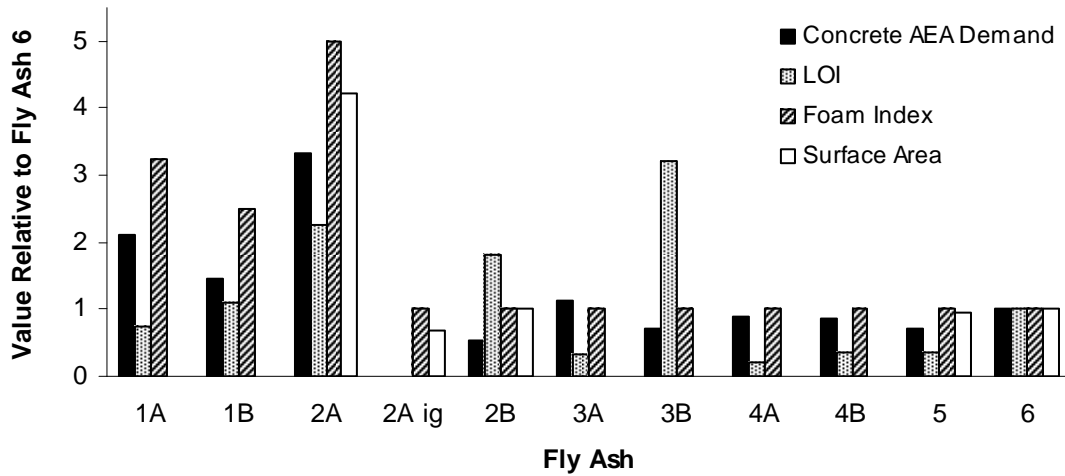


Figure 11.3: Physical test results for fly ashes and concrete mixtures normalized to the values for fly ash 6

11.4.2 LOI

A comparison is made in Fig. 11.4 between the LOI values and the AEA dosages required in concrete to produce 6 percent air content for the fly ash samples in this study. There appears to be no correlation between the two tests. This suggests that the amount of material removed during the 750 °C ignition of the fly ash is not a reliable predictor of AEA demand. These findings are similar to those found by Hill et al. (1997) and conflict with work done by Gebler and Klieger (1983).

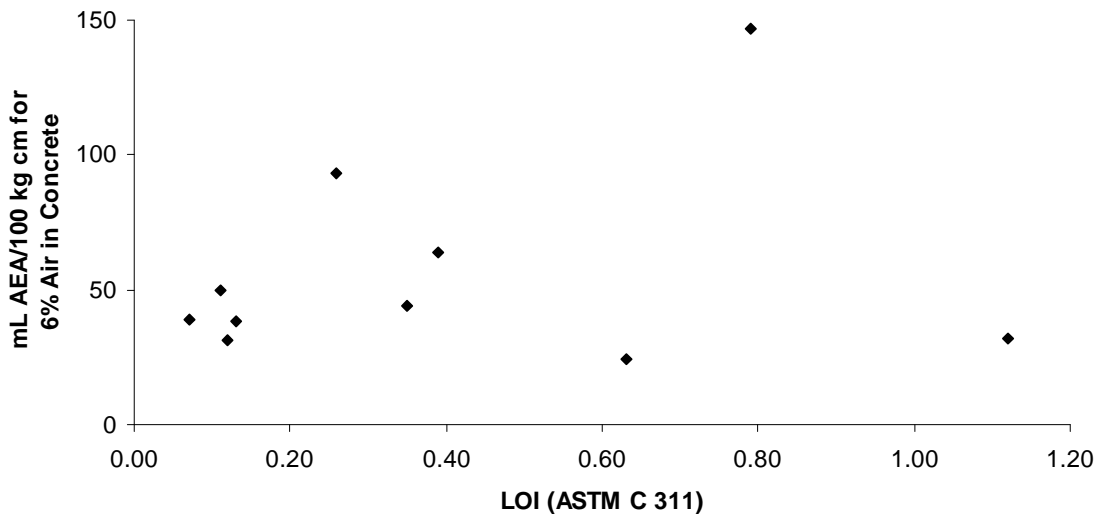


Figure 11.4: Dosage of AEA required to achieve 6% air in concrete versus the LOI value of the fly ash.

11.4.3 Foam Index

As shown in Fig. 11.5, this test is able to predict AEA demand when large dosages of AEA are required for fly ash samples but it is not able to distinguish between the fly ash samples that require less AEA (with required dosages less than 60 mL/100 kg of cementitious materials).

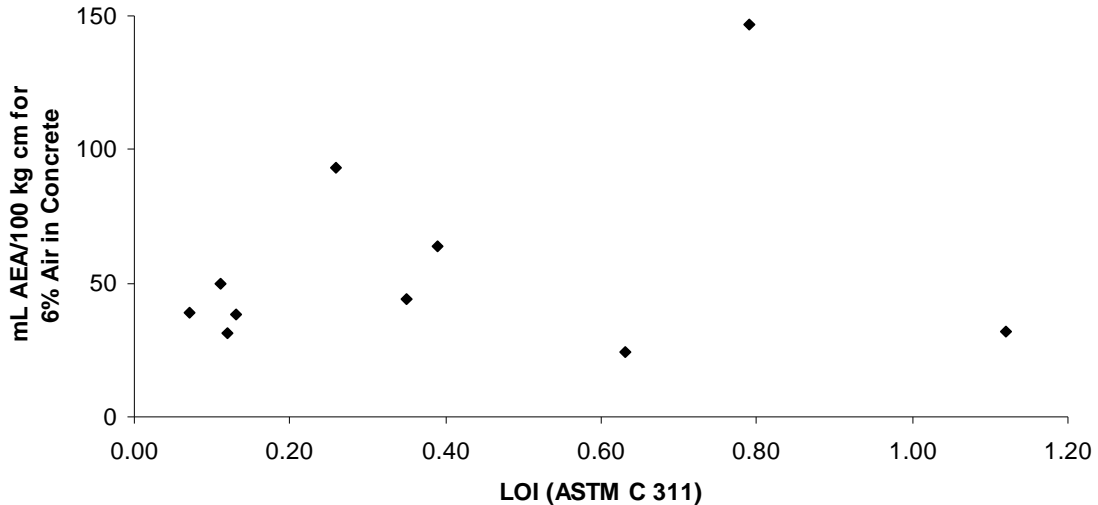


Figure 11.5: Dosage of AEA required to achieve 6 percent air in concrete versus the LOI value of the fly ash.

11.4.4 Nitrogen Gas Absorption

For a limited number of specimens, the surface area was determined by nitrogen gas absorption. The results can be found in Table 11.1. From the samples investigated it appears that a correlation may exist between the AEA demand in concrete and the surface area per unit mass of fly ash. As the surface area per unit mass increases, the AEA dosage requirement in concrete also increases.

In order to examine the effect of the material removed by the LOI test on the surface area per unit mass, the remaining material from fly ash 2A after the LOI test was analyzed with nitrogen gas adsorption. The result is shown in Table 11.1. It is interesting to note that after the high-temperature (750 °C) ignition, the surface area per unit mass of the fly ash was reduced to a value similar to a fly ash with a low AEA demand in concrete. Furthermore, when foam index testing is done with a fly ash sample that has been ignited, the amount of AEA required to form a stable foam is also reduced to the amount required for a low surface area fly ash. This finding supports the hypothesis that it is the removal surface area, not mass, in the LOI test that controls AEA demand.

11.4.5 Comparison of Fly Ash

Fly Ash 1A and 1B

When inspecting the chemical properties of fly ash 1 before and after the altering of the burning process, one can see that there was a 66 percent increase in the iron oxide levels and an increase of more than 20 percent in the sodium oxide levels. These changes are significant

enough to suggest that a change in the characteristics of the source coal may have occurred between the sampling periods (in addition to potential changes in the nature of the fly ash imparted by the changed burning process). Foam index values increased 32 percent and LOI actually decreased 33 percent after the new burning processes were implemented. AEA dosage increased 40 percent. The change in AEA demand was the largest; however, one should note that the initial sample obtained from this source had the highest AEA demand of any of the other initial samples from the other fly ashes. The change in AEA needed in concrete appears to correlate better with the increase with foam index than with carbon content since the LOI value actually decreased.

Fly Ash 2A and 2B

The chemical characteristics of the fly ash from source 2 showed approximately a 20% increase in the iron oxide, calcium oxide, and magnesium oxide contents between the two sampling periods. The foam index increased 500%, suggesting that a significant increase in AEA demand should be expected. However, the LOI results from the two samples were similar. The AEA demand in concrete again correlates best with the foam index; this was the largest change between the sampling periods for any of the sources examined (613% increase).

Fly Ash 3A and 3B

The chemical properties for fly ash from source 3 did not change significantly between the sampling periods, likewise there was no significant change in foam index test results. There was actually a 90% decrease in the measured LOI between sampling periods. Surprisingly, the AEA demand of the fly ash in concrete increased by more than 60% between fly ash 3B and 3A. Therefore, there is no correlation between AEA demand and any of the fly ash characteristics tested for this fly ash source.

Fly Ash 4A and 4B

The chemical properties, foam index, and AEA demand for source 4 did not change significantly between sampling periods, although there was a significant decrease in measured LOI values.

11.5 Conclusions

This section provides information about the chemical and physical characteristics of fly ashes from various coal-burning power plants. These ashes are commonly used in concrete. Among the problems reported from the field are increases in the required dose of AEA at some time after various power plants installed low NO_x burners. A full investigation of such reports would require rigorous comparison of both the input coal and the output ash immediately before and after burner change-over, along with careful monitoring of all other coal-to-ash processing and handling steps, coupled with documentation of specific burner types and burning parameters. Such a comprehensive investigation is beyond the scope of this study. Nevertheless, for four different power plants this study was able to document a change in ash-AEA interaction occurring after low NO_x burners were installed and any other unknown changes were made to coal-processing, burning, and ash recovery.

Samples 1-4A were obtained from 4 power plants prior to installation of low NO_x burners, while corresponding samples 1-4B were obtained from the same plants after installation

of the burners. No accompanying samples of coal (pre- or post grinding) were obtained, and no data were recorded relative to the type of burner, feed rate, or burning temperature. No data were recorded concerning any other changes or maintenance that may have accompanied the installation of the low NO_x burners, or any changes to the ash-recovery processes. But against this background, fly ashes from power plants that have been modified with low-NO_x burners generally tend to increase the AEA demand in laboratory testing, and this observation generally agrees with the field reports of increased AEA dosages. But what cannot be said with certainty is that the installation of the low NO_x burners, per se, is responsible for these observed changes in the ash. It is clear, however, that for the four plants evaluated, ash-AEA interaction changed significantly over the time period associated with a change in the burning process. It is not known whether similar changes would have been observed over a similar time period for ash recovered from plants where no such process changes were made. Given the unquestioned need to control harmful emissions and at the same time produce fly ash that adds value when used as an integral component of concrete, detailed study of how power plant processes affect ash properties is urgently needed.

With regard to screening tests aimed at evaluating fly ash samples, it was observed that LOI measurements did not correlate strongly with the AEA demand in concrete. The foam index test used in this study showed a satisfactory correlation to the AEA demand in concrete; however, it was unable to differentiate fly ashes with low AEA demand (less than 60 ml AEA/100 kg cm for 6% air in fresh concrete air tests). More work is necessary to refine this test so that it can better resolve differences in these materials. Lastly, limited work was shown in this study with regard to measurements of surface area of fly ash (using BET nitrogen absorption). The results suggest that surface area is a good indicator of AEA demand, especially for the ashes that have been obtained from power plants after the incorporation of low-NO_x burners. Furthermore, surface area measurements taken before and after igniting the ash (using LOI procedure) showed a significant decrease in surface area measured on the ignited samples compared to the as-received ashes. These ignited ashes were then found to respond better to AEAs in foam index testing, suggesting that the carbon lost (along with other impurities/organics) and its associated surface area contributed to AEA demand. Significant follow-up work to this study has been performed or is in progress, and the findings from these studies, including mechanistic work, will be reported in future publications.

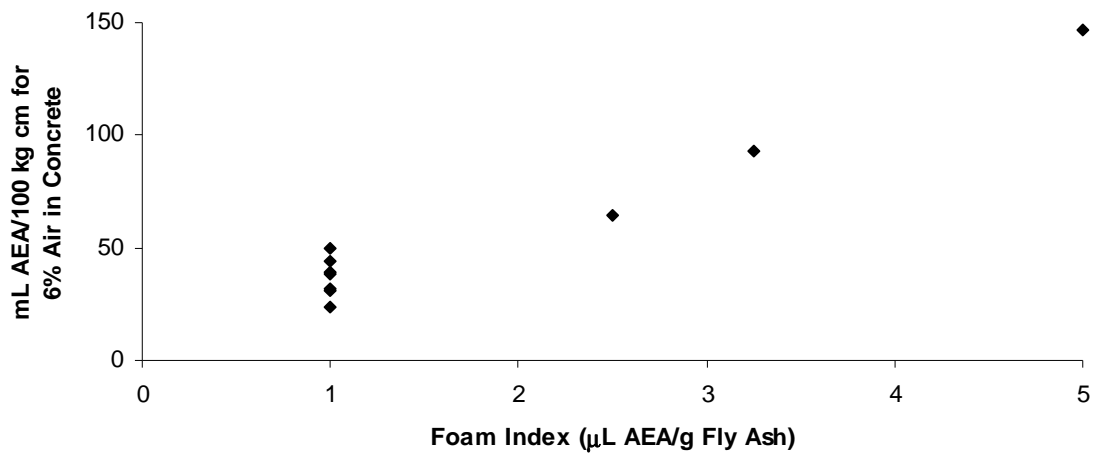


Figure 11.6: The results from the foam index test versus the dosage of AEA to achieve 6% air in concrete.

Chapter 12. Evaluation and Improvement of the ASTM C 311 Air Entrainment of Mortar with Fly Ash Test

This chapter examines test methods for assessing air-entrainment in fly ash-containing concrete. A mortar test described in ASTM C 311 “Standard Test Methods for Sampling and Testing Fly Ash or Natural Pozzolans for Use in Portland-Cement Concrete” is currently specified by ASTM C 618 “Standard Specification for Coal Fly Ash and Raw or Calcined Natural Pozzolan for Use in Concrete” to evaluate the ability to entrain air in fly ash-containing concrete. The work presented here shows the variability of this test to be significant. This variability is attributed to the variable water content and air-entraining agent (AEA) dosage specified in the test. A modified version of the test is developed that has a fixed water content and AEA dosage. The results for this modified test method are evaluated for 15 different fly ashes and an acceptable amount of variability was found. Guidance is given on means to implement this test method with different materials.

12.1 Introduction

The presence of an adequate air-void system is paramount to the durability of concrete placed in moist environments that undergo freezing and thawing cycles. Although the role of air entrainment in providing frost resistance is undisputed, there are a large number of variables that have been suggested to be detrimental to the formation of an adequate air-void system in concrete. Understanding how various parameters and factors, such as materials, mixture proportions, and construction practice, impact the air-void system is essential in producing frost-resistant concrete.

One of the common problems with the use of fly ash in concrete is that it can impact the dosage of AEA required to produce the desired air content in concrete. Past work has suggested that the amount of residual carbon in the fly ash is the primary cause of the problem (Gebler and Klieger, 1983). Work presented in this report suggests that the mass of carbon in a fly ash has limited correlation to the ability to entrain air in concrete containing certain fly ashes, and that the mechanism is more complicated.

Tools are needed to accurately evaluate the interactions between concrete mixture ingredients that do not require making a concrete mixture as this is time consuming and costly. Currently, there are only a handful of tools that are designed to evaluate the impact of a fly ash on the ability to entrain air in a mixture. One of these tools is the “Air-Entrainment of Mortar” test described in sections 25 and 26 of ASTM C 311 “Standard Test Methods for Sampling and Testing Fly Ash or Natural Pozzolans for Use in Portland-Cement Concrete.” This test is currently specified by ASTM C 618 “Standard Specification for Coal Fly Ash and Raw or Calcined Natural Pozzolan for Use in Concrete” to evaluate the ability to entrain air in fly ash containing concrete.

12.1.1 Background

ASTM C 618 specifications

Certain uniformity requirements are suggested by ASTM C 618 for fly ash used in concrete. One of these requirements is that the dosage of AEA in fly ash concrete should not vary excessively. The current method of evaluating this requirement, according to ASTM C 618,

is to limit the loss on ignition (LOI) (ASTM C 311) of a fly ash as to less than 6%, and to determine the amount of Vinsol resin AEA needed to produce 18% air in an ASTM C 311 mortar mixture containing the fly ash in question. It is suggested by ASTM C 618 that the fly ash should not be used in concrete if the required dosage to produce 18% air in the mortar test varies by more than 20% from an established average determined from previous testing results on the material.

ASTM C 311 Procedure

In the mortar test presented in ASTM C 311, a standard mixture is prepared with prescribed amounts of cement, fly ash, and standard sand. Proportions for this test are given in Table 12.1. This mixture uses the fly ash to be investigated at a 20% replacement by mass of the portland cement along with an ASTM C 778 standard sand meeting the 20-30 gradation. Water and an AEA are added to produce a flow between 80 and 95 after ten drops on the ASTM C 230 flow table and an air content of 18%. Because it is difficult to produce exactly 18% air content in a mixture, the test suggests that a mixture be produced that contains between 15 and 18% air and another with an air content between 18 and 21%. Then interpolation can be used between the AEA dosages to determine the dosage to produce 18%. The air content of the mixture is determined by the unit weight method with a standard 400 mL measure as specified in ASTM C 185.

Table 12.1: Mortar mixture design

	ASTM C 311	Modified Mixture
portland cement	300 g	312.5 g
fly ash	75 g	78 g
standard sand 20-30	1125 g	1395 g
water	A	164 g
AEA	B	0.5 mL*

A - Amount to produce a flow of 80-95 in ten drops on the ASTM C 230 flow table

B - Amount of Vinsol resin to produce an air content of 18%

* - equivalent to 128 mL of AEA/100 kg of cm

In this test the amount of water and AEA needed to meet the flow and the air requirements are unknown and work by Bruere (1956) suggests that these are dependent on one another. Bruere's work suggests that as the water content of a mixture increases so does the air content for mortar mixtures. Due to the test containing two unfixed and interdependent variables, several iterations may be required before a satisfactory combination is found. Furthermore, it may be possible that the difference in water needed to produce a flow at the high and low end of the test method is large enough that it could cause an increase significant increase in the air content. If this were the case then the resulting AEA dosage to produce 18% air content in the mortar mixture and the hence the results of the ASTM C 311 test.

Criticisms of the ASTM C 311 test have been published by Lane (1991). In this work Lane commented that when a mortar mixture is evaluated at 18% air content, the change in the air content for increasing dosage of AEA is small and is therefore not sensitive to changes in the required air content. The work went on to suggest that the dosage of AEA required in the test is significantly higher than what is typically required in concrete and that because of this higher

concentration of AEA the ingredients in the mortar mixture may behave differently than in concrete. In a broad statement about ASTM mortar based testing, Struble (2006) questioned why the flow of a test could not be measured with a standard water content instead of the water content being determined by the flow in the test.

12.1.2 Objectives

This chapter presents an examination of the reliability of the ASTM C 311 “Air Entrainment of Mortar” test with goal of finding a mortar based test that provides a simple, economical and precise way to evaluate the AEA demand of a fly ash.

12.2 Experimental Methods

12.2.1 Materials

In this investigation, a portland cement meeting the ASTM C 150 specifications for Type I and II with 0.53 alkali content ($\text{Na}_2\text{O}_{\text{eq}}$) and a Blaine fineness of $3630 \text{ cm}^2/\text{g}$ was used. The crystalline phases of the cement were determined by a Rietveld analysis and are reported in Table 12.2. Two fly ashes were investigated that are commercially used in concrete and meet the ASTM C 618 classification for a Class F fly ash. The oxide analysis and the dosage of AEA to produce 6% air in concrete for these fly ashes are given in Table 12.3. The two fly ashes were chosen because they represent samples requiring a high and low dosage of AEA in concrete to produce 6% air. At least two mixtures were prepared for each investigation presented in order to ensure reproducibility and the results were averaged.

Table 12.2: Composition of the Type I/II cement as determined by RQXRD

phase	percentage
C_3S	68.0
C_2S	15.7
C_3A	2.7
C_4AF	8.7
gypsum	1.3
CaCO_3	2.6

Table 12.3: Oxide analysis, LOI, and AEA demand in concrete with fly ash

Fly Ash	1	7
Silicon Dioxide (SiO ₂), %	56.18	52.07
Aluminum Oxide (Al ₂ O ₃), %	20.37	23.65
Iron Oxide (Fe ₂ O ₃), %	6.77	4.55
Sum of SiO ₂ , Al ₂ O ₃ , Fe ₂ O ₃ , %	83.32	80.27
Calcium Oxide (CaO), %	9.95	12.76
Magnesium Oxide (MgO), %	2.55	2.02
Sulfur Trioxide (SO ₃), %	0.53	0.78
Sodium Oxide (Na ₂ O), %	0.47	0.31
Potassium Oxide (K ₂ O), %	1.08	0.80
Total Alkalies (as Na ₂ O), %	1.18	0.84
Classification (ASTM C 618)	F	F
LOI (ASTM C 311)	0.12	0.79
mL AEA/100 kg cm for 6% air in concrete	32	147

12.2.2 Evaluation of ASTM C 311

In order to separate the effects of the water content and the AEA dosage in the testing, a constant dosage of AEA was used in the mixture shown in Table 12.1 and then different water contents were tested until the flow was within the acceptable range. At this point the air content of the mixture was recorded. Mixtures with water contents to produce flows at the high and low limits of the test were investigated to examine how the resulting air content changed.

12.2.3 Modification to ASTM C 311

Modifications to the ASTM C 311 test were investigated. A mortar test is needed that:

- highlights the difference between fly ashes with significantly different AEA demand in concrete
- minimizes the number of mixtures to be investigated to complete a test
- has an acceptable variability
- utilizes a representative water-to-cementitious materials ratio (w/cm) of practical concrete
- is compatible with various commercial AEAs
- utilizes a standard mixing procedure and aggregate

Key variables in the ASTM C 311 test were altered to investigate a new version of the test. These variables were: the method of flow testing, the amount of material, and w/cm.

12.2.4 Comparisons to AEA Demand in Concrete

The ultimate validation of a simplified screening test is to compare the results to the impact on AEA demand of a concrete mixture. To make this comparison, a series of concrete mixtures were prepared in the laboratory with 15 different fly ashes at a 20% replacement of cement by mass, with a 0.45 w/cm and normal water reducer to obtain a slump (ASTM C 143) of 75 mm +/- 25 mm. The mixture proportions are given in Table 12.4.

Table 12.4: Composition of the Type I/II cement as determined by RQXRD

phase	percentage
C ₃ S	68.0
C ₂ S	15.7
C ₃ A	2.7
C ₄ AF	8.7
gypsum	1.3
CaCO ₃	2.6

During mixing the amount of wood rosin AEA in the mixture was incrementally increased and the air content was monitored via the ASTM C 138 unit weight method. Frequent mix-specific calibrations between the unit weight method and the ASTM C 231 pressure meter produced a series of trend lines indicating air content as a function of AEA dosage. From these data the AEA dose required to stabilize 6% air in the fresh concrete was interpolated for each mixture. Further details on this test procedure can be found in Chapter 13 in this report.

12.3 Results and Discussion

12.3.1 Evaluation of ASTM C 311

Because the test results are dependent on both the flow and the air content of the mixture it was decided that mixtures would be prepared with a constant dosage of Vinsol resin AEA and then the water content would be varied until the flow was within the range specified by ASTM C 311. This approach was necessary as it is commonly understood that the workability or flow and air content of a mixture have been shown to be related (Bruere, 1956). After the desired flow was obtained the resulting air content was recorded. This process was continued until a mixture was found with air content between 15% to 18% and 18% to 21%. At this point interpolation was used between two data points to determine the dosage of AEA required for the mixture to produce 18% air content. Results of the ASTM C 311 testing are shown in Fig. 12.1. This plot shows the air content and AEA dosage along with the corresponding w/cm needed to produce the desired flow for two different fly ashes. A horizontal line is included to highlight the 18% air content required in ASTM C 311. Red lines are also included that correspond to mixtures that are at the high end of the allowable flow with air contents between 18% and 21%. The results of the test are shown with vertical lines and circles show the results of the test. The average percent difference between these two results for fly ash 1 is 48%. A large difference between the results for the Fly Ash 7 was not found. As Lane (1991) suggested because the results of the test are not sensitive at this high air content that differences in water content of the mixtures have an ability to increase the air entrained in the mortar mixture as suggested by Bruere (1958). Because these

results are interpolated to find the amount of Vinsol resin AEA needed to produce 18% air inside concrete this difference in air content can skew the results.

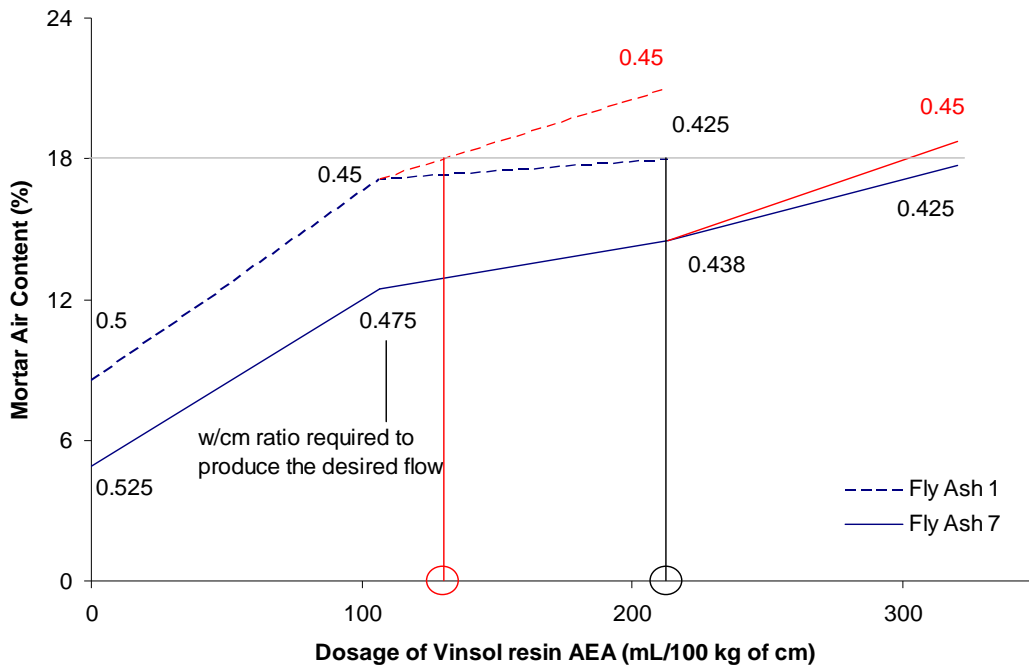


Figure 12.1: ASTM C 311 results with fly ash 1 and 7

The variability in the test results are larger for fly ash 1 than is allowed between two separate grab samples that are to be compared to itself as specified in ASTM C 618. This large variability brings the usefulness of this test into question. Furthermore, it is time consuming to obtain valid data points as several mixtures are required to determine a mixture with an adequate flow and air content between 15% and 18% and then again for 18% and 21%. This test could be improved if this dependence on flow was removed as it not only appears to be a source of the variance but also requires a large number of mixtures to be prepared to investigate a fly ash.

12.3.2 Modifications to ASTM C 311

At the outset of the modification it was decided that certain parameters should not be changed as they help ensure repeatability in the test. It was decided that the mixing procedure and sand specified in ASTM C 311 should not be changed. From preliminary testing it was determined that the flow specified in the test can lead to wide variations in the water content in the test. Furthermore, the wide variation in the flow in the original test was shown to cause the large variability in the standard test method. Therefore, it was decided that the water content utilized in the test should no longer depend on flow and instead be fixed at 0.42 w/cm and the flow would just be measured as suggested by Struble (2006). It was also decided that the measurement of the flow should be modified to be measured in accordance with ASTM C 1437. The primary difference between the two procedures is that the flow would be measured after 25 drops instead of the 10 required previously. By using a larger number of drops more energy is imparted on the mortar before it is evaluated and the material is able to reach a flow that is near

the maximum for the material. The amount of material in the test was increased because there was concern that the original test did not ensure that enough properly mixed material is available to evaluate the air content and flow of the mortar. The mass of cement and fly ash were increased 5% compared to the original ASTM C 311 mixture.

Ratio of cementitious materials to sand

In order to optimize the mixture to highlight the performance in air entrained in the test different ratios of cementitious materials to sand (cm/sand) were investigated as the first step to find a mixture proportion that showed the most significant sensitivity to the amount of AEA in the mixture. In Figs. 12.2 and 12.3, the air content and flow of the mortars with different cm/sand (0.25 to 0.31) were investigated with different dosages of tall oil AEA (0 to 290 ml AEA/100 kg cm). In each of the mixtures fly ash 1 was used and the mixture proportions were adjusted to provide approximately the same mixing volume. In both Figs. 12.2 and 12.3 one can see that the air content increases in the mixture as the AEA dosage increases and as the cm/sand decreases. There was very little change in the percent flow at the different AEA dosages but the flow increased as the cm/sand increased. The flow of the non air-entrained sample was not measurable when the cm/sand is decreased below 0.28.

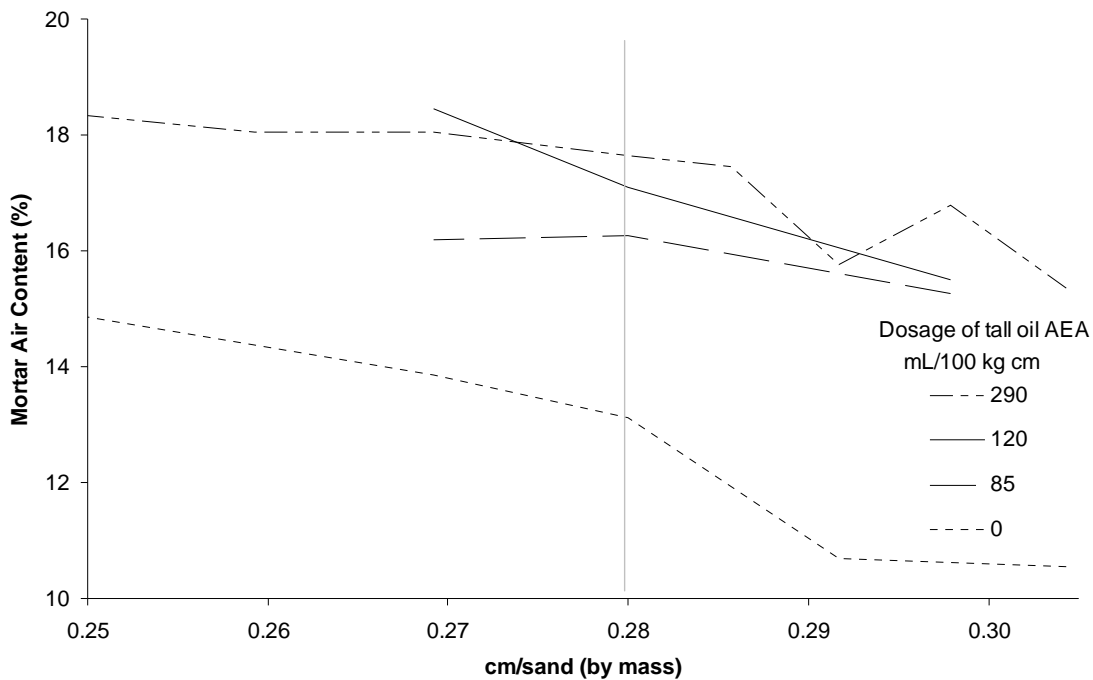


Figure 12.2: The change in air content for different cm/sand and different dosages of tall oil AEA with fly ash 1.

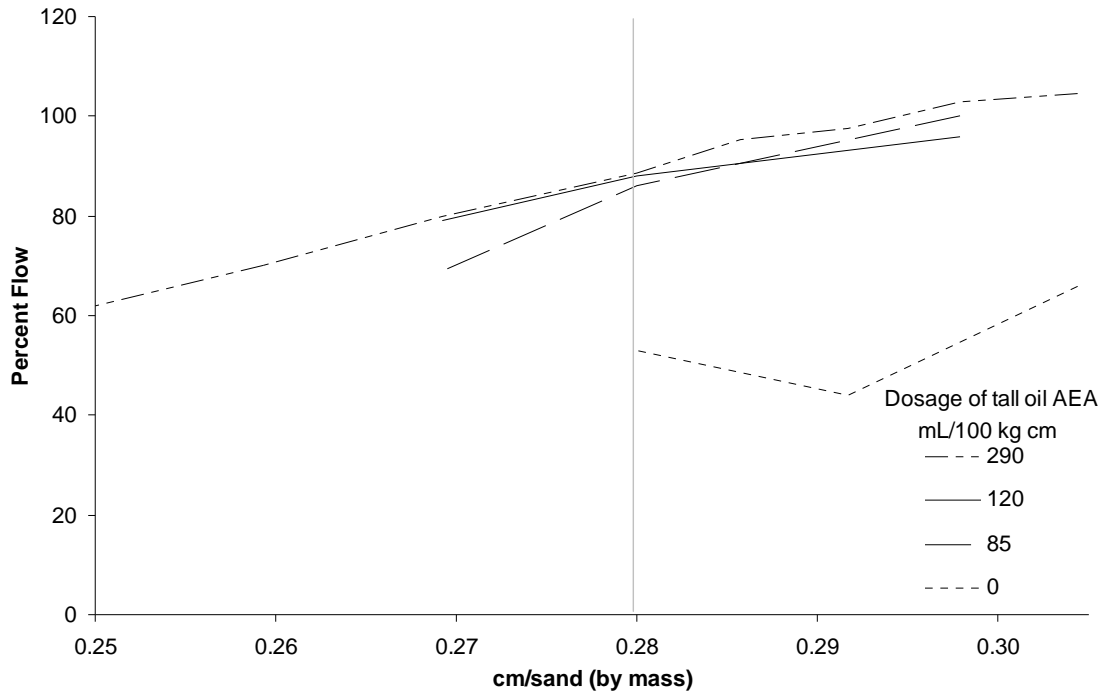


Figure 12.3: The change in flow for different cm/sand and different dosages of tall oil AEA with fly ash 1.

In designing a test it is beneficial to use a mixture that shows the largest difference between the variables of interest. For this reason a cm/sand of 0.28 was chosen to be investigated further. A line is provided in Fig. 12.2 and 12.3 to highlight the flow and air content at this ratio. The resulting proportions of the mixture are presented in Table 12.1 as the modified mixture.

Dosages of AEA

Different dosages of a tall oil AEA were investigated and the air content and flow of the mortar mixture are shown in Figs. 12.4 and 12.5 for fly ash 1 and 7. For both fly ashes the air content and flow start from a low value and increase with increasing AEA dosage to some limiting value. Fly ash 1 starts at an air content of around 14% and increases with increasing dosages of AEA to a limiting value of around 18% air in the mixture. This seems to be the maximum amount of air that is able to be produced as the values do not drastically change with increased amounts of AEA. The mixture with fly ash 7 starts at an air content of around 10.5% and builds at a slower rate compared to the other mixtures and ultimately gets to the same limiting air content of around 18%; however, the dosage required to get to this point is much larger. The behavior of the flow follows a similar trend and seems to reach a limiting value of 100.

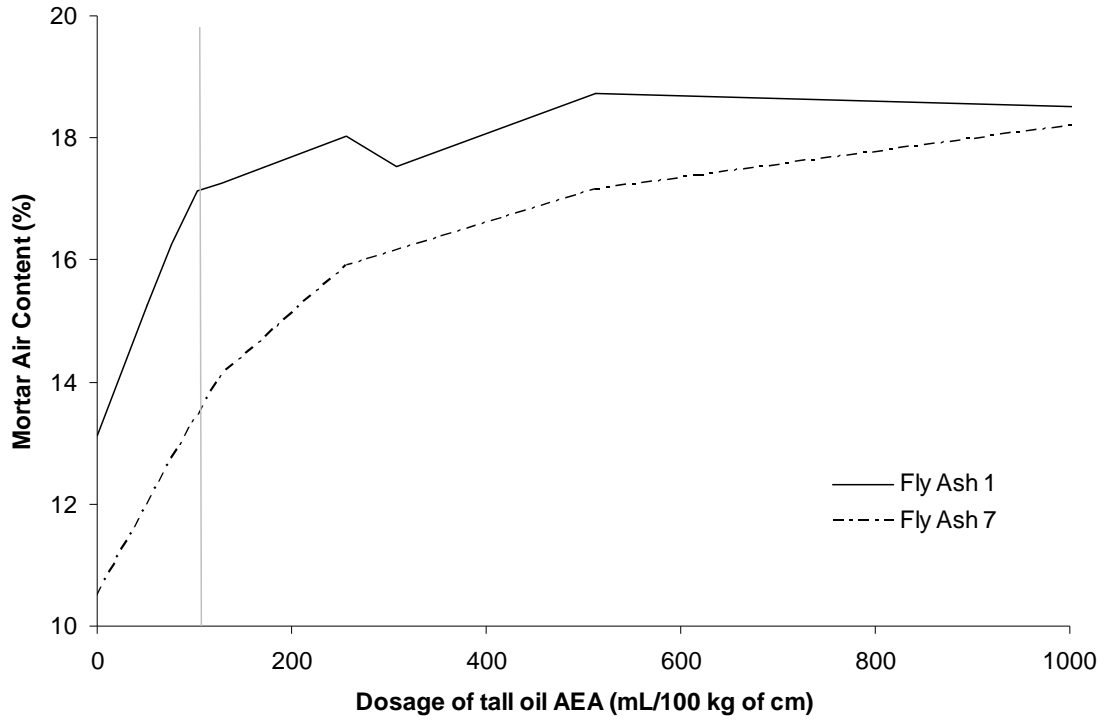


Figure 12.4: Air content of a modified mortar mixture with various dosages of tall oil AEA.

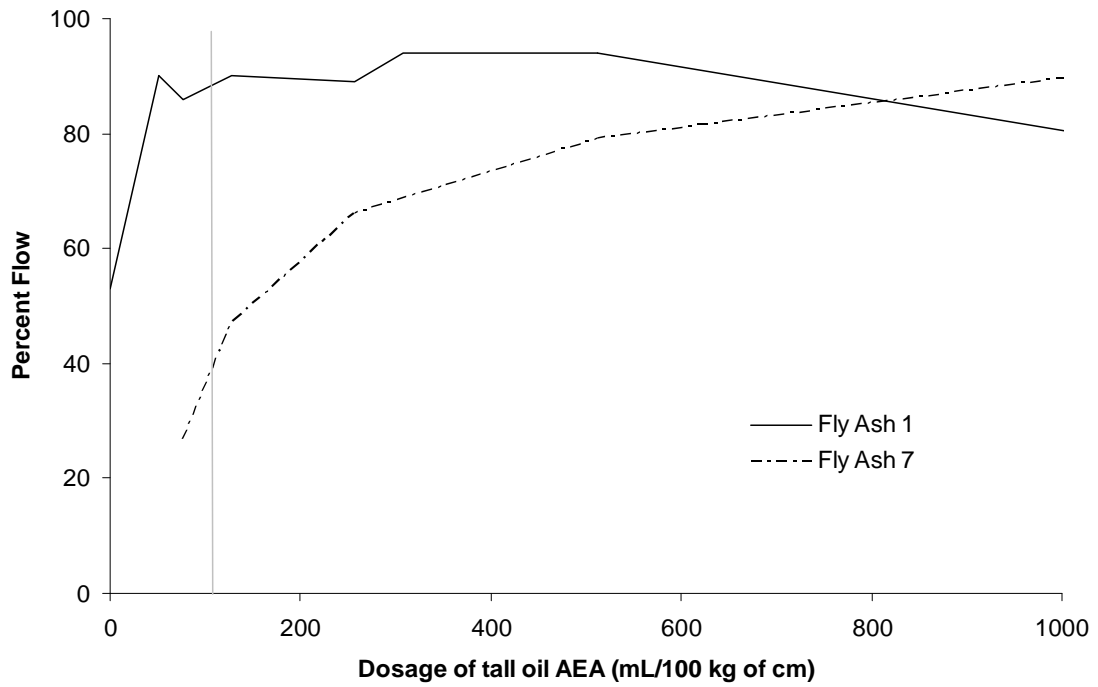


Figure 12.5: Flow of a modified mortar mixture with various dosages of tall oil AEA.

As shown in Table 12.3 there is a large difference in the AEA required to entrain 6% air in concrete between the two fly ashes and so one would anticipate a large difference in response between the test results of these two materials in a mortar mixture. By testing these two fly ashes an investigation can be made of the most significant difference in behavior in the test to be observed. This point appears to be at a dosage of tall oil AEA of 128 mL AEA/100 kg of cement. This dosage is highlighted with a line on Figs. 12.4 and 12.5. By focusing on the air content and flow produced in a mixture at this dosage of AEA there is the widest difference in performance between these two fly ashes. By preparing mixtures at this fixed dosage of AEA a direct assessment of the AEA demand of a fly ash can be assessed by comparing the air content in the mixture at this fixed dosage of AEA against some established average. While other points of comparison may be possible, especially if different sand contents, mixing methods, or mixture proportions are utilized, this combination was chosen as it satisfies the goals established for the modified test method.

In order to investigate different commercially available AEAs in the modified mortar test, mixtures containing fly ashes 1 and 7 were investigated at AEA dosages of 0, 128 and 512 mL of AEA/100 kg of cement for a tall oil, synthetic, wood rosin, and Vinsol resin AEA. These dosages were chosen as they showed the most promise from the investigations with the tall oil AEA. As can be seen in Fig. 12.6 and 12.7 the air content and flow increased as the AEA dosage increased for all of the AEAs investigated. It was noticed in the air-entrained mortar mixtures that the air content of the mixtures increase at different rates and each had different maximum values depending on the AEAs used. This performance is as expected as the manufacturer-suggested dosage rates for these AEAs are different and hence their effectiveness to entrain air and reach a certain maximum value are different depending on the product. However, for all of the AEAs investigated there is a measurable difference in the amount of air entrained at a dosage of 128 mL of AEA/100 kg cm. This dosage of AEA will still be able to serve as a useful point of comparison of the AEA demand for different fly ashes. However, if one were to use a different AEA than what was investigated in this study then a different dosage may be needed. Some care should be taken in investigating different AEAs to be sure the dosage rate used in the test provides a meaningful difference in performance between a fly ash with a high and low AEA demand.

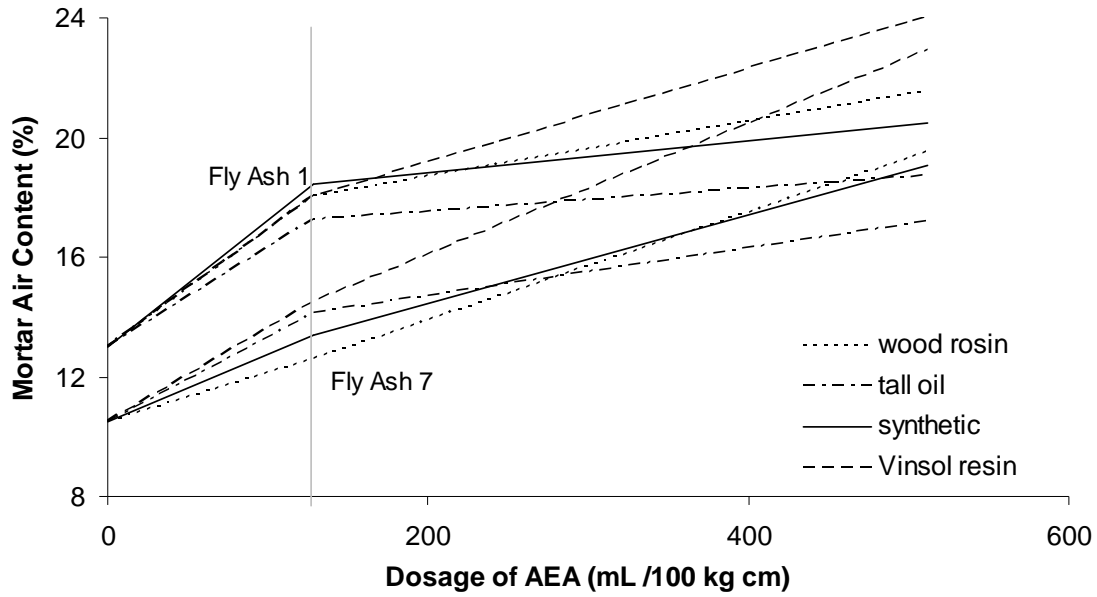


Figure 12.6: The air content of a modified ASTM C 311 test with various AEA at a dosage of 0, 128, and 512 mL/100 kg of cm.

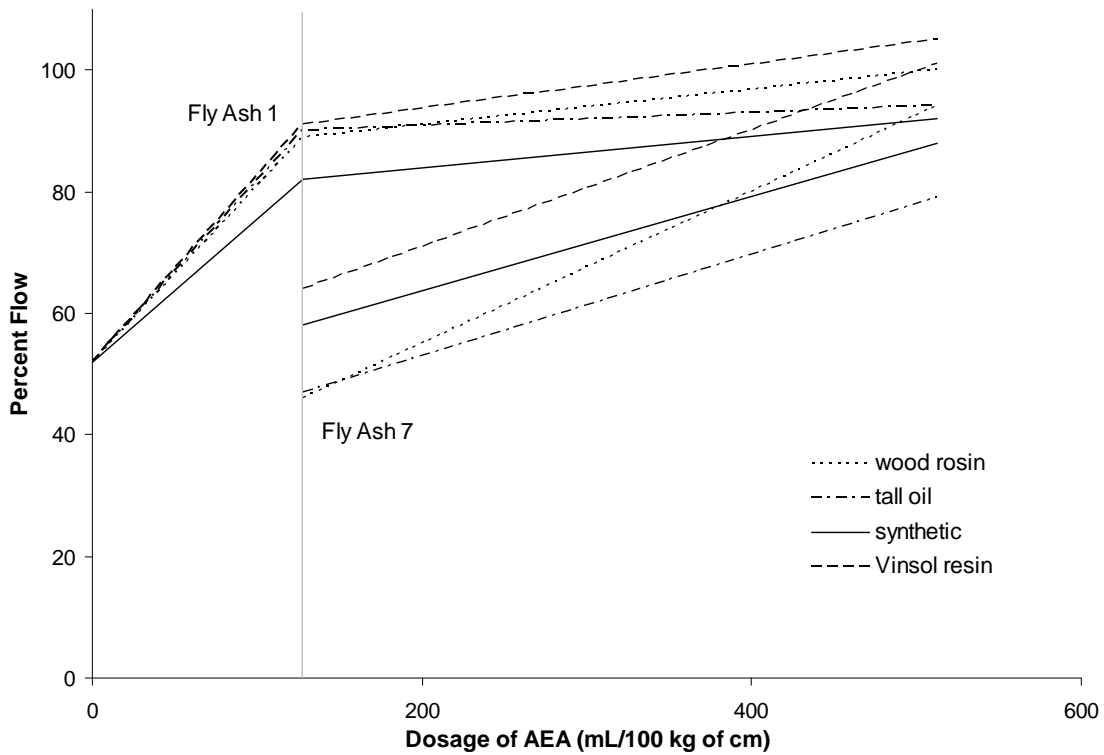


Figure 12.7: The flow of a modified ASTM C 311 test with various AEA at a dosage of 0, 128, and 512 mL /100 kg of cm.

Variability of Modified ASTM C 311 with a Wood Rosin AEA

Finally, the average percent difference is shown in Table 12.5 for replicate mixtures made with 15 different fly ashes using the modified mixture proportion shown in Table 12.1 with a wood rosin AEA. Low average percent differences are shown for the flow and air content determined by the modified mortar test method. The average percent difference of 2.3% for the air content is much improved over the 48% as determined for ASTM C 311.

Table 12.5: The average percent difference for the percent air content and flow of replicate mixes of 15 different fly ashes with a wood rosin AEA with the modified mixture.

	average % difference	
	air content	flow
average	2.3	7
maximum	5.4	16
minimum	0.5	0

12.3.3 Comparison of Modified ASTM C 311 to AEA Demand in Concrete

In Fig. 12.8 the dosage of wood rosin AEA to produce 6% air content in concrete is plotted against the air content produced in the mortar mixture for a 128 mL of AEA/100 kg of cm using the same fly ash and wood rosin AEA in each test for 15 different fly ashes. The correlation shown in the graph shows that as the AEA demand of the fly ash in concrete increases the air content produced in the modified mortar air test decreases for a standard dosage of AEA. There appears to be a general correlation of the performance of the mortar air test and the impact the fly ash has on the ability to entrain air in concrete.

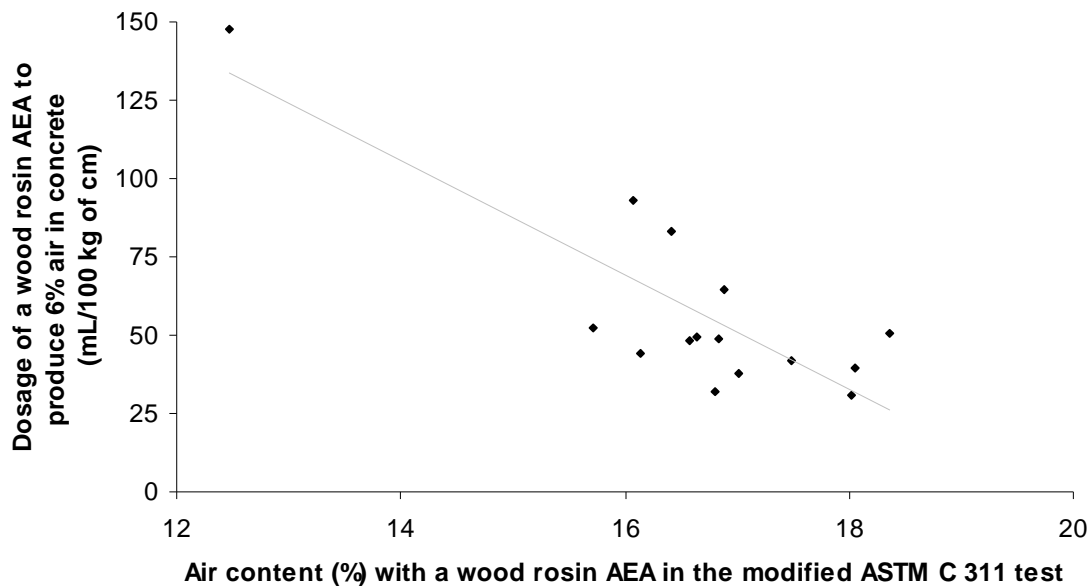


Figure 12.8: A comparison between the results of the modified ASTM C 311 test and the dosage of wood rosin AEA in concrete to produce 6% air for 15 different fly ashes.

12.4 Implementation

This modified test method could be used in several ways to evaluate the changes of AEA demand of fly ash to be used in concrete. However, the most probable method is to use this test as a substitute for the ASTM C 311 mortar test. This would allow the air content of a fly ash in question to be determined with a fixed AEA dosage and w/cm to be compared against a historical average established for that material. If changes of the air content determined by the test were larger than two standard deviations or 0.60% then this would provide a greater than 95% confidence interval that the AEA demand of the fly ash has changed. A confidence interval of 95% is widely used in the specifications to establish reasonable limits of the test results.

While materials were chosen in an attempt to bracket the practical combinations of cement, fly ash, and AEA that may be utilized in this test it may be possible that a material combination is investigated that does not give satisfactory results. If this occurs then the same development steps presented should be taken with those materials and the mortar mixture proportions adjusted so that satisfactory results are obtained. This may involve using different cm/sand, water content, or AEA dosages as these have been determined to be the major variables affecting the performance of the test besides the mixing procedure and the sand type and gradation.

12.5 Applications of Finding to Other ASTM Mortar Tests

It is common in ASTM methods that utilize mortar to prescribe a flow in order to standardize the water content in the mixtures investigated. It would be beneficial if other ASTM tests that utilize mortar were evaluated to investigate the variability of the test by investigating the results at the extremes of the allowed flow. One test that should be evaluated is ASTM C 185 as this test is very similar to the ASTM C 311 test but is used to evaluate the impact of cement on the ability to entrain air in mortar. This test has the same dependence on flow and air content that was shown to cause the large variability in the ASTM C 311 test.

12.6 Conclusions

This work has shown that the current version of the “Air Entrainment of Mortar” test described in section 25 and 26 of ASTM C 311, “Standard Test Methods for Sampling and Testing Fly Ash or Natural Pozzolans for Use in Portland-Cement Concrete” is variable. It appears that because the flow and air content are allowed to vary that the results in the test has been shown to have an average percent difference of 48% between two valid results of the investigated fly ash. While there is no precision and bias statement included in ASTM C 311, ASTM C 618 suggests that the fly ash mortar mixtures investigated in ASTM C 311 should not vary by more than 20% from an established average for the fly ash being investigated. This suggests that changes need to be made to the current test as the variation in the test is capable of being larger than suggested limits for the established average.

Work has been presented in this section concerning improvements on this ASTM C 311 test. These improvements were made by establishing a standard mortar mixture and AEA dosage that highlighted the difference in performance of two fly ashes known to have high and low AEA demand in concrete. The performance of this test has been evaluated with 4 different commercially available AEAs and 15 different fly ashes. The results of the test have been compared to the wood rosin AEA dosage requirements for concrete mixtures with 15 different fly ashes and satisfactory correspondence was shown. An average percent difference in the

modified test of 2.3% and 7% was shown to exist for the air volume and flow measurements respectively. This is an improvement over the 48% shown for the existing method. Furthermore, the modified test reduces the number of mixtures required to evaluate the performance of a fly ash in a mixture from approximately six to two. Finally, some guidance is given on possible methods to implement the test. This guidance is structured so that this new test method could be substituted in place of the previous methods with minimal changes.

Chapter 13. Determining the Air-Entraining Admixture Dosage Response from a Single Concrete Mixture

Currently there is no standardized test method to determine the interaction of the ingredients of a concrete mixture with a dosage of air-entraining admixtures (AEA). Typically, to investigate the AEA demand multiple concrete mixtures are made with varying dosages of AEA and the resulting air contents are measured. This method is not ideal as it is time consuming, uses large amounts of material, and allows several variables to change that could cause changes in the dosage response of the mixture. A method is presented that is able to measure the air content of a mixture through a correlation between the gravimetric (ASTM C 138) and pressure method (ASTM C 231) with only minimal changes to the volume of the mixture. This allows the AEA demand to be determined from a single concrete mixture rather than sequential mixtures. Testing results are also provided for concrete mixtures containing fly ashes with various AEA demands. These mixtures are evaluated for changes in AEA demand with water reducer (WR), mixing temperature, fly ash replacement level, and type of AEA.

13.1 Introduction

While there are several existing methods available to design a concrete mixture, all of them require making a trial mixture with the actual materials to verify the assumptions of the design method and to make any adjustments to the mixture. One issue that is not able to be easily answered with a single trial mixture is the response of the mixture to admixture dosage.

One admixture whose dosage is exceptionally difficult to characterize in a concrete mixture is air-entraining admixture (AEA). The addition of AEA during the mixing of concrete is a common method to provide concrete with resistance to salt scaling and freezing and thawing. There are a large number of variables that have the ability to affect the air void system in concrete. Some of these include: cement chemistry, mixture water chemistry, aggregate gradation, supplementary cementitious materials (SCM) and other chemical admixtures (Whiting and Stark, 1983).

The current method of examining the response of a mixture to AEA is to prepare several trial batches with different dosages of AEA and then examine how the mixtures respond. This method is useful as it allows a direct observation of how these materials perform in concrete. In creating each one of these mixtures it is difficult to ensure that no unintentional variables have been introduced that can affect the results. Any of the following changes between batches could cause differences in results: moisture content of the aggregates, batch weights, sand gradation and mixing methods.

Practitioners and researchers would benefit considerably if a new method to determine the response of a mixture to AEA demand could be developed from a single batch of material. This would minimize the efforts to create the mixtures, while also removing the variability between mixtures. This method must allow the mixture to be evaluated without substantially changing the volume of the mixture in order to keep the mixing action at a constant level, as this could lead to changes in the resulting air content. Furthermore, this method must provide a good correlation to individual mixtures cast at discrete dosages of AEA.

13.1.1 Methods of Measuring Air Content in Concrete

To examine the total volume of air content in fresh concrete there are currently three common methods: gravimetric (ASTM C 138), pressure (ASTM C 231), and volumetric (ASTM C 173).

In the gravimetric method a container of a known volume is filled with the concrete to be investigated and consolidated in a standard manner. This volume of concrete is then weighed and from this weight, material properties, and theoretical batch weights the total volume of air can be calculated for that mixture. Some problems with this method have been pointed out by Roberts (2006). These problems include the need for very accurate batch weights, material properties, and moisture content. It is difficult, in the laboratory or in the field, to get an accurate measure of air content with the gravimetric method. One advantage to this method is that it allows the concrete utilized in the test to be reused. This concrete can either be returned to the mixer or used for other tests. Care should be taken though to return this material to the mixer and agitating the mixer so that the material is well mixed.

The pressure and volumetric methods of measuring air content do not rely on an accurate characterization of the mixture materials and instead attempt to directly measure the amount of air in the mixture. However, both of these methods require water to be added to the concrete specimen. This addition of water changes the water content and forces the concrete analyzed in the test to be discarded. When using either of these methods the volume of the mixture that is being investigated will decrease in size. While this size change is not a concern when a large truck or central batch mixer is used, this volume decrease is significant for a laboratory mixer. By using either one of these methods to evaluate the air content of a laboratory mixer it is likely that the mixture volume will change from 10% to 25%. Therefore, after investigating the air content of the laboratory mixture the remaining material would have to be discarded if the dosage did not yield the required air content.

Criticisms have been made of both the pressure and volumetric methods of measuring the air content of concrete. However, the pressure meter seems to be the test that is most widely used to evaluate the air content of fresh concrete. For this reason this test method was used in this research. The methods presented though should work accurately for either meter but was not verified with this work.

13.1.2 Combining the Gravimetric and Pressure Method

If one were able to accurately measure the air content of a mixture while holding the volume of the mixture constant then it would be possible to prepare a single concrete mixture and evaluate how the air content of that mixture changes as AEA is added. However, none of the existing methods, at least individually, allow this to happen.

By combining the results of a gravimetric and either the pressure or volumetric method, one should be able to correlate the volume of air in a mixture to a measured density. Assuming that both of these tests are performed properly then the unknowns in the gravimetric test are no longer significant as the air-void content has been tied to the density of the mixture. After this correlation is made, the air content of the mixture can be evaluated by only monitoring changes in the density of the mixture as long as no other variables are allowed to change.

By using the gravimetric method to monitor the density change and then returning the materials to the mixer it allows successive AEA dosages to be made to a mixture and the resulting changes in the air content to be measured. A method similar to this is suggested by

Roberts (2006) to verify the results of the pressure method on several successive concrete batches with the same mixture design.

13.1.3 Objectives

The objectives of this work are to develop a test method that is able to utilize a single concrete mixture to determine the impact on AEA demand of the ingredients. This test method will then be utilized to investigate the impact of several variables commonly reported to cause an impact on the AEA demand of a concrete mixture. While past literature does exist about the impact of several of these variables on the ability to entrain air in concrete this data is presented to show the abilities of this test to investigate the performance of different variables in a concrete mixture.

13.2 Experimental

13.2.1 Materials

In all of the mixtures presented in this study, Type I/II cement (conforming to ASTM C 150) was used, with equivalent alkali content ($\text{Na}_2\text{O}_{\text{eq}}$) of 0.53 and a Blaine fineness of 3630 cm^2/g . The phases of the cement are reported in Table 13.1 as determined by a Rietveld quantitative x-ray diffraction (RQXRD) (Rietveld, 1969; Stutzman, 1996) completed with the Topas Academic Software. The aggregates used in the mixtures were locally available river gravel and sand that are commercially used in concrete. All of the AEAs were obtained from commercial sources and meet ASTM C 260. The WR used in this research met the requirements of ASTM C 494 as a type A and D.

Table 13.1: Composition of the Type I/II cement as determined by RQXRD

phase	percentage
C_3S	68.0
C_2S	15.7
C_3A	2.7
C_4AF	8.7
gypsum	1.3
CaCO_3	2.6

The AEA demand for 17 different fly ashes (all meeting ASTM C 618) were investigated in this report. Material properties for these fly ashes can be found in Appendix C. However, additional testing was completed on a subset of three fly ashes. These three fly ashes (all ASTM C 618, Class F) were chosen as they exhibited drastically different AEA demands in prior laboratory testing. Fly ashes 6 and 7 were obtained from the same source; however, fly ash 6 had been treated with a sacrificial surfactant to improve the AEA demand in concrete (Hill et al. 2004). No information was provided by the manufacturer about the amount of sacrificial surfactant that was added to the fly ash. Therefore, all results for fly ash 6 are likely dependent on the amount of this additive. If the concentration is changed then the results for fly ash 6 may also change. An oxide analysis completed with x-ray fluorescence spectroscopy and loss-on

ignition (LOI) measurements from ASTM C 311 is reported in Table 13.2 for each of the three fly ashes.

Table 13.2: Oxide analysis and LOI data for three fly ashes

Fly Ash Name	1	6	7
Silicon Dioxide (SiO ₂), %	56.18	52.07	52.04
Aluminum Oxide (Al ₂ O ₃), %	20.37	23.65	23.75
Iron Oxide (Fe ₂ O ₃), %	6.77	4.55	4.59
Sum of SiO ₂ , Al ₂ O ₃ , Fe ₂ O ₃ , %	83.32	80.27	80.38
Calcium Oxide (CaO), %	9.95	12.76	12.63
Magnesium Oxide (MgO), %	2.55	2.02	2.01
Sulfur Trioxide (SO ₃), %	0.53	0.78	0.79
Sodium Oxide (Na ₂ O), %	0.47	0.31	0.28
Potassium Oxide (K ₂ O), %	1.08	0.80	0.81
Total Alkalies (as Na ₂ O), %	1.18	0.84	0.81
ASTM C 618 Classification	F	F	F
LOI (ASTM C 311)	0.12	0.79	0.79

13.2.2 Concrete Mixture Methodology

The following methodology was used to investigate the response of a single concrete mixture to increases in AEA dosage. Initially, a 64-L batch of concrete was prepared in a 85-L drum mixer. The mixture used a 0.45 w/cm with 335 kg/m³ (equivalent to 6 sacks of cement) of total cementitious materials (cm), with a 20% replacement of the fly ash (by mass of cement). Proportions for the mixture can be found in Table 13.3.

Table 13.3: Concrete Mixture Design

Components	Mass (kg/m ³)
Cement	268
Fly Ash	67
Coarse Aggregate	1098
Fine Aggregate	742
Water	151

All of the materials for the mixture were stored at 23°C for 24 hours prior to mixing to keep the mixing temperature constant. Coarse and fine aggregates were brought in from the stock piles and individually mixed. A moisture correction for each was used to adjust the batch weights. The rock and sand were added to the mixture first and 2/3 of the mixing water. The mixture was agitated for one minute. Next the cement, fly ash and the remaining mixing water were added and mixed for three minutes. At this point, the mixer was stopped and any material gathering on the sides or back of the mixer was removed. During the final three minute mixing period a normal water reducer (WR) was added to the mixture in either a desired dosage or to

bring the mixture to a desired slump (ASTM C 143). It was found for the materials used in this study that there was interplay between the efficiency of the AEA and the WR dosage used. In order to compare results between mixtures it was necessary to have mixtures that had a similar WR dosage and workability. These issues are discussed in detail in later sections.

The following samples were taken after the mixing was completed: a 7-L sample for a gravimetric test, a slump test, and a 1-L rectangular prism for hardened air void analysis. The air content of the gravimetric sample was determined by the pressure method establishing the relationship between the air content and the density of the mixture. The concrete used for the slump test was returned to the mixer leaving the volume of the batch equal to 56-L. Next a commercially available AEA was added to the mixture and mixed for three minutes. Slump and gravimetric measurements were taken and the concrete was returned to the mixer. A 1-L rectangular prism was also taken for hardened air void analysis. These steps were repeated in regular dosage increments and the gravimetric measurement was taken until the change in the density from the initial sample was approximately 6%. A final slump, air content by the pressure meter, and rectangular prism were taken from the mixture.

Throughout this report the terms slump and workability have been used interchangeably. However it has been shown that the slump test, although widely used because of its simplicity, is not able to accurately measure the plastic viscosity of a mixture (Tattersall and Banfill, 1983). Plastic viscosity has been shown to be an important variable in the rheology of concrete. Furthermore, ASTM C 143 reports that the single operator and multi-laboratory acceptable range for a slump of 85 mm to be +/- 25 mm. This would indicate that the test may not be precise enough to determine the workability differences in the mixtures investigated. Had this study been completed using a method of measuring the rheology of the concrete instead of the slump test, then a better understanding of the relationship between a rheological parameter of the mixture, WR dosage and AEA demand may have been determined.

13.3 Results and Discussion

By using the combination of results from the gravimetric and pressure methods it was possible to measure the initial density and total air content of a mixture and correlate them. This correlation was then used to monitor the density change in the mixture with increased dosages of AEA and mixing. The percent change between the initial density and the density being investigated for a given AEA dosage is essentially equal to the change in air content for the mixture. Since these measurements were able to be made without significantly decreasing the volume of the mixture, additional AEA dosages could be added to the mixture and the mixture could be re-evaluated. After the unit weight of the concrete mixture had changed by approximately 6%, a final pressure meter reading was taken from the mixture. The predicted air content at that AEA dosage from the initial pressure meter reading and the unit weight measurements were compared to the final pressure meter reading. The difference between these values were found and the measured results were adjusted to correct for this difference. This correction was made by dividing the difference by the number of measurements and making an equal adjustment to each of the measurements. This difference between the air content predicted and measured by the final pressure meter reading was typically less than 0.5%. A linear trend was then fit to the estimated air content versus the AEA dosage. In Fig. 13.1 a sample data set is shown for this method. This figure shows a discrete set of data points with a linear trend fit to the data. Several data points are also shown from individual mixtures that did not use the multiple dosage method to compare the difference. By using the linear trend one is able to compare the

AEA demand between different concrete mixtures. This comparison can be made by comparing the amount of AEA required to produce a certain air content or the slope of the trend-line provides information on the change in air content for a given dosage of AEA. In this chapter the dosage of AEA required to produce an air content of 6% was used. A value of 6% air content was chosen as it is a common value required in specifications for concrete.

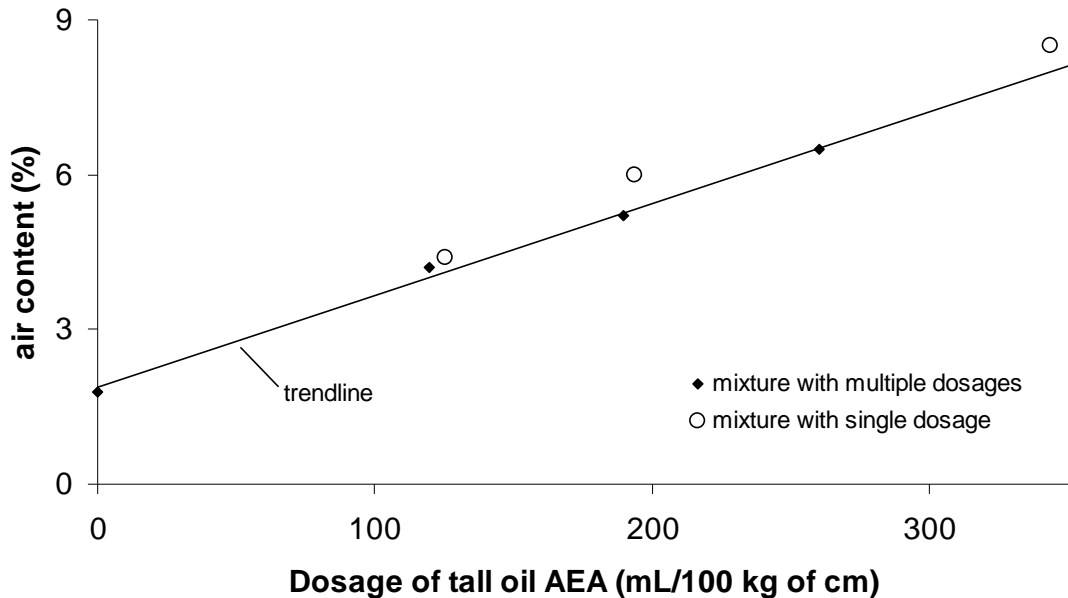


Figure 13.1: Air content versus AEA dosage from single mixture method compared to several individual mixtures with a trend line fit to the single mixture method results.

It was found for these mixtures that even though the air content changed by 7% with increased AEA dosage, the slump of the mixture did not increase by more than 25 mm. It is expected that different results may be obtained with the same materials if the mixture were prepared with different mixing durations, speeds, or energy per unit volume of mixture. Nevertheless, this method allowed a useful comparison for the response of concrete mixtures to AEA dosages.

13.3.2 Validation

The average correlation coefficient (r^2 value) for the linear fit to the discrete air contents measured from a single mixture for more than 130 concrete mixtures created with this method was 0.98, with a standard deviation of 0.04. This shows that the response of the mixture to increases in AEA dosage as measured by this method seems to consistently fit a linear trend. In order to examine how well this method is able to represent the performance of mixtures made with individual dosages of AEA, a comparison was made between the air content measured in single dosages and the values predicted by the linear trends from the mixtures of multiple doses. This comparison was made between mixtures that contained different AEAs and fly ashes. The results of this comparison are shown in Table 13.4. The measured air contents closely match those predicted. The largest difference in air content was found to be 0.8% between the two methods with an average difference of 0.0% and a standard deviation of 0.4%. This shows that

there is a good correspondence between the air content measured in several individual mixtures and the air content predicted by correlating the density and air content determined by the pressure method in a single mixture and using multiple dosages of AEA.

Table 13.4: Comparison of measured air content in mixtures with single dosages of AEA and that predicted by a mixture using multiple dosages of AEA.

Fly Ash	AEA Product	Slump (mm)	normal WR mL/100 kg cm	AEA mL/100 kg cm	Percent Air Content		
					Measured	Predicted	Difference
1	tall oil	89	170	50	5.7	5.2	0.5
1	tall oil	89	170	100	7.8	8	-0.2
1	wood rosin	70	44	27	6	6	0
1	wood rosin	51	46	47	6.2	6.3	-0.1
6	synthetic	76	166	36	3.2	3.2	0
6	synthetic	76	166	89	5.6	5.4	0.2
6	synthetic	76	166	140	7.3	7.5	-0.2
6	tall oil	70	169	194	6	5.3	0.7
6	tall oil	76	169	344	8.5	9.3	-0.8
6	tall oil	70	169	125	4.4	4.6	-0.2
6	wood rosin	89	83	30	2	2.6	-0.6
6	wood rosin	89	83	93	5.4	5.2	0.2
7	wood rosin	51	108	32	3.2	3.2	0
7	Vinsol resin	95	33	124	4.5	4.5	0
15	wood rosin	76	72	44	5.3	5.4	-0.1
15	wood rosin	76	72	69	7.3	7.2	0.1
average							0.0
standard deviation							0.4

13.3.3 Effect of Water Reducer Dosage on Air-Entraining Agent Dosage

In order to investigate the affect of the WR dosage on AEA demand for a fly ash concrete mixture with wood rosin AEA, several mixtures were prepared with different dosages of WR. The AEA demand was determined in a single mixture as previously described. The results are shown in Table 13.5 and in Fig. 13.2. One would expect that as the WR dosage was increased between mixtures that the slump of the mixture would also increase. This trend follows for fly ash 1 and 7. Even though the slump of the mixture does not correspond to the WR dosage directly, it seems the AEA dosage required in concrete to produce 6% air content shows a good correlation. As shown in Table 13.5 as the WR dosage increases, the AEA demand to produce 6% air content in concrete decreases for both fly ashes 1 and 7.

Table 13.5: AEA demand for two fly ashes with different dosages of WR.

fly ash	slump (mm)	AEA demand ^y (mL/100 kg cm)	WR (mL/100 kg cm)
1	51	62	0
	102	53	44
	102	31	84
	102	35	98
	121	29	102
	102	28	169
	127	37	194
	7	64	238
83		192	46
89		139	83
102		112	84
102		108	103
70		95	167
83		78	196

^y - Dosage of wood rosin AEA required to produce 6% air content in the mixture. These values are interpolated from the dosage response curve.

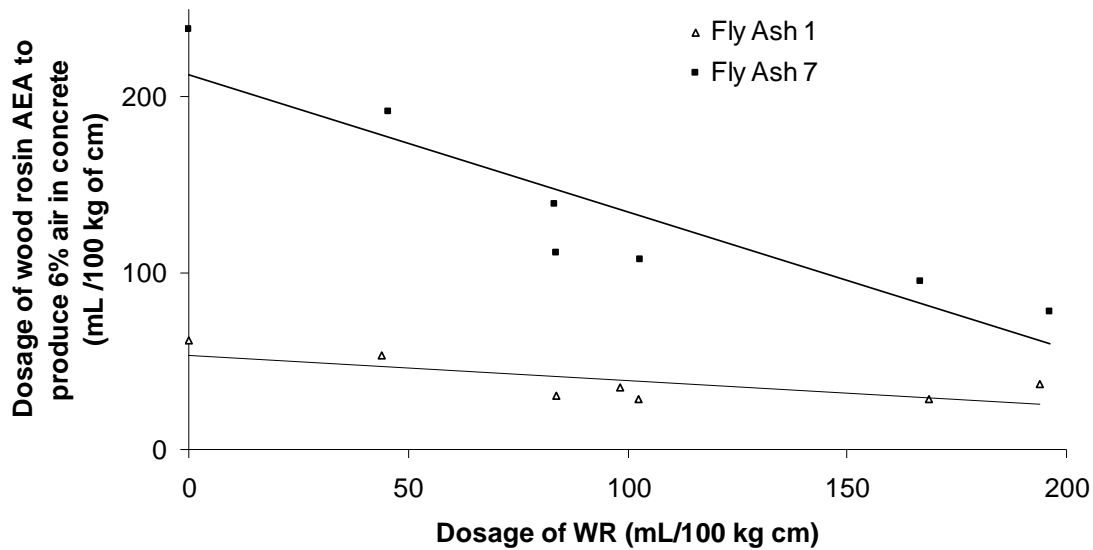


Figure 13.2: AEA demand interpolated from single mixture method for two different fly ashes with different dosages of WR.

These results suggest that if two mixtures are to be compared to one another, it is more important to have a similar WR dosage in the mixture than a similar slump. However, in preliminary testing it was found that a minimum workability was needed to efficiently entrain air in concrete. Other research suggests that when the workability of a mixture becomes too high

then it is difficult to stabilize the entrained air bubbles (Dodson, 1990). Because of this it was decided that the concrete mixtures should have a slump between 50 and 100 mm to be accurately investigated.

13.3.4 Evaluation of AEA Demand of Fly Ash Concrete

By using a correlation between the pressure and gravimetric methods, one is able to evaluate the AEA demand of a fly ash concrete in a single mixture. These differences in AEA demand can occur for any number of reasons, but are usually attributed to the amount of carbon in the fly ash remaining after the burning process (Gebler and Kleiger, 1983). Reports of the variability of AEA demand in fly ash concrete have increased as the coal fired power plant sources have been required to reduce emission levels (Freeman et al. 1996; Kulaots 2004; Hill and Folliard 2006). To reach these reduced emissions several modifications to the coal burning process can be made. It is unclear how each of these modifications impact the AEA demand of fly ash in concrete, and more research is needed before conclusions can be made. However, the ability to assess the AEA demand of a fly ash concrete mixture has been important in the past and continues to become more relevant.

This method was used to evaluate the AEA demand of 19 different fly ashes that were produced in power plants in Texas and the results are reported in Table 13.6. In order to make a fair comparison between fly ash samples it was decided that the slumps and WR should be within a certain range. Each mixture was prepared with a target WR dosage between 45 and 85 mL/100 kg cm and target slump between 50 and 100 mm. However, the WR dosage had to be adjusted for two of the fly ash mixtures due to insufficient slump of the concrete caused by differences in water demand. Both of these mixtures required dosages of over 110 mL/100 kg cm and have been reported with an asterisk in Table 13.6. These mixtures contained fly ashes that were treated with a sacrificial surfactant to decrease the AEA demand of the fly ash. It is possible, but not certain that this treatment contributed to this increase in water demand observed.

Table 13.6: A ranking of several fly ashes commercially used in concrete by the AEA demand from the single mixture method

fly ash	slump (mm)	WR (ml/100 kg cm)	AEA demand ^x (mL/100 kg cm)
1	100	83	31
23	95	45	32
19	95	66	34
11	70	81	36
27	64	45	38
10	95	46	39
8	89	64	42
2	76	51	44
9*	57	132	44
25	64	58	48
15	95	68	49
20	70	46	49
5	64	46	50
16	76	72	52
26	89	48	64
4	83	47	83
14	83	50	93
6*	57	111	138
7	83	71	147



Increasing AEA Dosage

* These mixtures required high dosages of WR to obtain an acceptable slump. This increase in WR could cause a response in the AEA demand of the mixture.

^x – Dosage of wood rosin AEA required to produce 6% air content in the mixture. The value is interpolated from the dosage response curve.

13.3.5 Effects of Mixing Temperature, Percent Fly Ash Replacement, and AEA Type on AEA Demand

In this section the effects of mixing temperature, percent fly ash replacement, and AEA type are reported for three fly ashes. The results are contained in Tables 13.7 and 13.8. For each of these mixtures the WR dosage was held constant where possible in order to investigate the effects of each variable. Care should be taken in extrapolating comparisons beyond what is presented in the table as the WR dosage was not held constant between all variables due to the large differences in water demand between the mixtures. Ratios larger than 1 in Tables 13.7 and 13.8 show an increased AEA demand.

Table 13.7: Effects of mixing temperature and fly ash replacement on AEA demand in concrete for three fly ashes.

Details of Mixture	Fly Ash					
	1		6		7	
	AEA Demand ^A	Ratio to Standard ^B	AEA Demand ^A	Ratio to Standard ^B	AEA Demand ^A	Ratio to Standard ^B
Mixing Temperature						
32°C	32	1.03	187	1.35	224	1.16
23°C	31	1.00	138	1.00	192	1.00
10°C	29	0.94	60	0.43	80	0.42
Fly Ash Replacement						
50%	44	0.71	203	-	368	1.54
35%	40	0.65	196	-	267	1.12
20%	63	1.00	-	-	239	1.00

^A – The amount of wood rosin AEA (mL/100 kg cm) required to produce 6% air in concrete. The value is interpolated from the dosage response curve.

^B – The ratio of the AEA demand for the variable being investigated and fly ash compared to a mixture prepared with wood rosin AEA at 23°C, with a fly ash replacement of 20%, and with a 0.53 Na₂O_{eq} cement. Note: The WR dosage was held nearly constant between fly ashes for each variable investigated. However WR dosage was not able to be held constant for the entire table and so comparisons should not be taken past those presented.

Table 13.8: Effects of AEA type on AEA demand in concrete for three fly ashes.

AEA	Fly Ash					
	1		6		7	
	AEA Demand ^A	Ratio to Standard ^B	AEA Demand ^A	Ratio to Standard ^B	AEA Demand ^A	Ratio to Standard ^B
Synthetic	33	1.00	-	-	104	3.12
Tall Oil	67	1.00	181	2.72	231	3.47
Vinsol Resin	40	1.00	73	1.84	142	3.57
Wood Rosin	29	1.00	95	3.32	147	5.14

^A – The amount of wood rosin AEA (mL/100 kg cm) required to produce 6% air in concrete. The value is interpolated from the dosage response curve.

^B – The ratio of the AEA demand for the variable being investigated and fly ash compared to a mixture prepared with wood rosin AEA at 23°C, with a fly ash replacement of 20%, and with a 0.53 Na₂O_{eq} cement. Note: The WR dosage was held nearly constant between fly ashes for each variable investigated. However WR dosage was not able to be held constant for the entire table and so comparisons should not be taken past those presented.

Mixing Temperature

To compare the effects of different mixing temperatures on fly ash concrete with different AEA demand, mixtures were prepared with the constituent materials initially conditioned to 10, 23, and 32° C. For each mixture, the AEA demand was determined by the

dosage of AEA required to produce 6% air content in the mixture. These results are presented in Table 13.7. In each one of these comparisons a constant WR dosage was used for all of the mixtures containing a given fly ash and the results of each mixture is compared back to a mixture at 23° C.

It appears that the change in temperature had little effect on the AEA demand for mixtures with fly ash 1. However, the AEA demand decreased for the mixtures with fly ashes 6 and 7 as the mixing temperature increased. Past research has suggested that as the mixing temperature increases, the efficiency of the AEA decreases (Gay, 1985). The response of the fly ash with the sacrificial surfactant (fly ash 6) seemed more sensitive to the temperature than the others investigated.

Fly Ash Replacement

The amount of wood rosin AEA required to produce 6% air in concrete for mixtures utilizing fly ashes 1, 6 and 7 at replacement levels of 20%, 35%, and 50% is shown in Table 13.7. Fly ash 1 shows a reduction in the amount of AEA demand required in the mixture as a higher fly ash replacement is used. For fly ash 6, a complete data set was not obtained as the slump of the mixture at a 20% replacement level was not comparable to the mixtures at 35% and 50% replacement and WR dosage used. However, there was very little change in the AEA demand as the amount of fly ash in the mixture increased. This behavior is different than what was observed with mixtures containing fly ash 7 as the AEA demand increased as the amount of fly ash replacement increased. This increase in AEA demand was not linear.

Response of Fly Ash Concrete to Different AEAs

Several different commercial AEAs were used in concrete mixtures with the different fly ashes to investigate the AEA demand. The results are shown in Table 13.8. For all of the AEAs investigated fly ash 1 showed the lowest AEA demand, fly ash 6 showed more AEA demand than fly ash 1 and fly ash 7 showed the highest AEA demand. When comparing the difference in AEA demand between fly ashes 1 and 7, it was determined that the largest change was for the wood rosin AEA and the smallest change was for the synthetic AEA. The AEA demand for the tall oil and Vinsol resin fell in between these values but were closer to the values for the synthetic AEA at 3.47 and 3.57 times higher than the AEA demand for fly ash 1. When investigating the change in AEA demand between mixtures containing fly ashes 1 and 6 it was found that the wood rosin still showed the highest change in demand and the Vinsol resin showed the least. It should be noted that a mixture with fly ash 6 and the synthetic AEA was not investigated.

Comparison of Results for Fly Ash 1, 6, and 7

One significant finding from the testing was that fly ash 6 behaved notably different than fly ashes 1 and 7 in the testing. As reported earlier fly ash 6 is a sample from the same source as fly ash 7 but was treated with a sacrificial surfactant of an unknown dosage to reduce the AEA demand of the fly ash. As can be seen from the results that this treatment does consistently reduce the AEA demand of the concrete mixture over the variables investigated when compared to fly ash 7. Other notable behavior is that fly ash 6 seems to show a greater change in AEA efficiency when the mixing temperature is raised. The material also shows a consistent dosage requirement in concrete as the percent replacement of the fly ash is increased with respect to the

cement. This is significantly different to the behavior of fly ash 7 as the AEA demand of this mixture increased non-linearly with fly ash replacement. The significant decrease in AEA efficiency with increase in temperature, and the behavior of the AEA demand to remain constant with increasing levels of fly ash replacement are likely attributable to the sacrificial surfactant that was added to the fly ash.

The mixtures containing fly ash 1 at different replacement levels show a decrease in AEA demand with increasing replacement levels of fly ash. Fly ash 1 was shown to have a very low AEA demand when used at 20% replacement in concrete. When larger replacements are used in a mixture then one would expect the workability to increase. This increase in workability appears to have caused a decrease in the AEA demand as it has made it easier to entrain air in the mixture.

Fly ash 7 was found to consistently require a higher AEA dosage than either fly ash 1 or 6 and was found to have the highest of the 19 fly ashes investigated. This larger dosage requirement is likely caused by increased levels of high activity carbon in fly ash 7. This increase in high activity carbon could also cause an increase in variability in slump obtained by the different mixtures shown in Table 13.5. The high activity carbon could lead to a reduced efficiency of the WR or an increase in fineness of the mixture that affected the workability of the mixture.

From the results of the different AEAs used in combination with the different fly ashes it appears that the change in AEA demand between fly ash 1 and 7 was very similar for all of the AEAs investigated except for the wood rosin AEA. This suggests that the wood rosin AEA may be more sensitive to changes in AEA demand (from fly ash) than the other commercial AEAs investigated with the normal WR used in this study.

As a whole, this study shows that every fly ash is different, and its response to changes in dosage, temperature, and AEA dosage/type can vary considerably from source to source (and presumably from time to time for a given source). This reinforces the need to have available simple, but accurate, test methods to evaluate the AEA demand for a given concrete mixture containing a particular fly ash. The work presented in this chapter, coupled with other work presented in this report and parallel efforts at Cornell University, are aimed at providing such tools to allow for accurate assessments of any fly ash source, with regard to AEA dosage response.

13.4 Conclusions

This report has presented a method to produce an AEA dosage response curve for a concrete mixture while only using a single mixture. The method was then compared to the AEA dosage response of several sequential mixtures and the results were found to be closely comparable for air contents up to 7%. Next, the method was utilized to build a large data set to compare several variables that affect the AEA demand of concrete that are not easily measurable by using single mixtures. These include: effects of WR dosage on AEA demand, ranking the AEA demand of several fly ashes, mixing temperature, fly ash replacement, and comparison of different commercially available AEAs. This data set provides insight into how mixing temperature, percent fly ash replacement and AEA type affects fly ash concrete with high and low AEA demand as well as a fly ash utilizing a commercially available sacrificial surfactant to reduce the AEA demand in fly ash concrete.

The results of this study suggest:

- The WR used in this study showed the ability to reduce the wood rosin AEA demand in fly ash concrete with increasing dosages.
- A sacrificial surfactant that is used on fly ash with high AEA demand can decrease the AEA demand of fly ash concrete
- The mixing temperature had a larger impact on the AEA demand of a fly ash treated with a sacrificial surfactant than the other fly ash mixtures investigated
- As the percent fly ash replacement increases in a concrete mixture the AEA demand in fly ash concrete decreased if the AEA demand of the fly ash was low or increased if the AEA demand of the fly ash was high. This increase occurred in a nonlinear fashion.
- The AEA demand of fly ash treated with a sacrificial surfactant did not change as the percent fly ash replacement increased
- A wood rosin AEA is the most sensitive of the AEAs examined to a fly ash with a high AEA demand in concrete

Chapter 14. Investigation of the Frost Resistance of Concrete through Measurement of Fresh and Hardened Properties and Resistance to Rapid Freezing and Thawing Cycles

Although it is widely understood that the size and spacing of the air-void system inside concrete is crucial to providing freeze-thaw durability, it is common for specifications to instead require measurement of the total air volume in fresh concrete. This practice is followed because there are no established or standard methods to evaluate the size and spacing of the air-void system in fresh concrete. This chapter highlights some of the challenges of using a pressure method (ASTM C 231) and a commercial Air-Void Analyzer (AVA) to evaluate the air-void parameters of fresh concrete. Correlations are made between these two methods, hardened air-void analysis, and rapid freeze-thaw testing (ASTM C 666).

14.1 Introduction

In order to produce concrete that is durable to exposure to moist freezing and thawing environments, it is well understood that an adequate air-void system must exist in the paste of the concrete. This air-void system is traditionally produced in concrete by adding an air-entraining agent (AEA) during mixing. This admixture gathers at the interface between the air and water and reduces the surface tension. This alteration of the surface tension improves the probability of trapping and stabilizing air-voids or forming smaller bubbles when a larger bubble is sheared during mixing (Powers, 1968). The number, size, and distribution of these small air voids are currently thought to be the key parameters in imparting freeze-thaw durability to concrete.

The most common methods to directly evaluate concrete durability in a cold climate are ASTM C 666 (resistance to rapid freezing and thawing) and ASTM C 672 (surface scaling resistance). ASTM C 666 and ASTM C 672 tests force a saturated specimen into a harsh freezing environment and evaluate the damage to the specimen after several cycles of freezing and thawing. These tests have the ability to provide insight into the resistance of concrete to freezing and thawing. However, the results of these tests require months to obtain. Another common method of investigating the frost durability of a concrete is to microscopically investigate the air void system using a test described in ASTM C 457 (hardened air-void analysis). While this test does not require the months required by the previously mentioned tests, it is quite labor intensive.

The inability to obtain rapid results from these tests does not make them easy to use in construction specifications. Instead, specifications often require a satisfactory volume of air to be required in the fresh concrete. This air content is typically specified to be measured at the point of placement and consolidation. However it is commonplace to take these measurements at a different convenient time and place during the construction process. A myriad of methods exist to evaluate the total air content including tests described in ASTM C 231 (pressure method), ASTM C 173 (volumetric or “roller” meter), or ASTM C 138 (gravimetric method). While the method of evaluating the total volume of air in fresh concrete as a means for acceptance of materials is common, it has been shown in previous research that it is possible to obtain air-void parameters that are not satisfactory at air contents commonly specified (Saucier et al., 1991; Plante et al., 1989). Due to this lack of correlation between the fresh air content and hardened air-void parameters a method to better evaluate the air-void system in fresh concrete is needed. The Air Void Analyzer (AVA) is a device advertised to measure the air-void parameters in fresh

concrete. This device was evaluated for this project and the results are then compared to air-void analyses and performance tests on hardened concrete.

14.1.1 Objectives

This chapter reports on laboratory testing performed to evaluate the air-void system in fresh concrete, as measured by pressure meter to obtain total air volume and by the AVA to attempt to quantify air-void parameters, and hardened concrete, as measured by use of Rapid-Air 457 system for measurement of key air-void parameters in hardened concrete) and compares these results to the performance of selected mixtures subjected to freeze-thaw cycles as per ASTM C 666. Only minimal emphasis was placed on evaluating frost resistance (ASTM C 666) as it was not the prime focus of this research project; however, a limited number of mixtures were cast and tested to focus on specific issues related to concrete with low specified air contents as these mixtures were identified as being particularly relevant in the state of Texas. Specifically, for paving mixtures, relatively low air contents are allowed (e.g., 3.5 to 4 percent total air, as per pressure or roller meter), and it was decided to evaluate mixtures in this low range of air content. Relevant issues that were addressed included (1) the use (or in actually, lack of use) of the aggregate correction factor when using the pressure meter to measure air at the jobsite; (2) the use of high dosages of water-reducing admixture that generate enough air to often pass the low air content specifications; and (3) the use of fly ash treated with a sacrificial surfactant to help offset high absorption tendency of carbon in ash.

14.1.2 Background

Background information is provided on the methods utilized in this research to evaluate the air-void system of different concrete mixtures.

Concrete Pressure Meter (ASTM C 231)

The concrete pressure meter is the most common method utilized to assess the total air-void content of concrete. This method uses a 7 L sample of concrete that is consolidated in a standard manner. The response of the sample to an increase in pressure is measured and the air content in the mixture is estimated by using Boyle's Law.

Questions have been raised about the inaccurate simplifying assumptions made in the test and the ability of the test to measure the air content in very small air-voids (Gay, 1982). However, numerical simulations by Hover (1988) have suggested that these concerns are insignificant for the air-void distributions commonly found in concrete. This test method was used in this research despite some concerns because of its widespread use in industry.

One challenge in using the concrete pressure method is that the pressure changes used in the method force water to be displaced into the pores of the aggregate in the mixture. Erroneously high air content is reported in the results of the test from this displacement of water. If the porosity of the aggregate becomes very high, as in lightweight aggregate, then the pressure method is not recommended to be used to measure the air content of the mixture. A method is outlined in ASTM C 231 that is intended to provide a correction for this aggregate-related issue—namely, the aggregate correction factor. Unfortunately this method is rarely utilized in the field as the results are dependent on aggregate type, moisture content, mixture proportions, and target air content of the mixture.

As stated previously the pressure method does not give any indication of the air-void size, distribution, and spacing, only the total volume of air contained in the concrete. However, past research has shown that as the air content of a mixture increases, the air-void system improves (Saucier, et al., 1991; Backstrom, et al., 1958; Klieger, 1952). Work done by Klieger (1952) examining the results from a large number of ASTM C 666 tests with different size aggregates suggested that an air content between 8% and 10% is required in the mortar fraction of concrete if it is to be durable against freezing and thawing damage.

Currently, ACI 201.2R-01 “Guide to Durable Concrete” and ACI 318-05 “Building Code Requirements for Structural Concrete” recommends that the acceptable volume of air in a concrete mixture should be based on the maximum nominal aggregate size in the mixture despite this parameter having nothing directly to do with the freeze-thaw durability of concrete. These suggested air contents are often adopted into specifications without realizing that this recommendation is made with the assumption that the concrete mixture has been designed by the ACI 211 mixture design method. In ACI 211 the maximum nominal aggregate size is used to determine the total amount of water used in the mixture for a desired workability. This selection of water then leads to the total amount of cementitious materials based on the needed water-to-cementitious material ratio. Finally the volume of fine aggregate is chosen to fill the remaining volume in the mixture. Therefore, the maximum nominal aggregate size has some bearing on the percentage of mortar in a mixture designed by ACI 211. While this method can be used as a starting point it rarely produces a mixture that is optimized for use with local materials. If a mixture is not designed according to ACI 211, or if the mortar content of the mixture is adjusted during the trial batches, then the correspondence between the air content required in the mixture and the maximum nominal aggregate size is no longer meaningful. Furthermore, specifications are often written assuming that a larger aggregate size will be used for the construction of an element (e.g. pavement) when this might not be the case. Care should be taken to insure that an air content of at least 8% is provided in the mortar fraction of the concrete regardless of the aggregate size utilized.

Air Void Analyzer (AVA)

The AVA (Jensen, 1990) is a device for analyzing the air-void system in the mortar that uses a 20 cm³ of mortar that has been extracted from concrete so as to exclude material larger than 6 mm. The analysis is performed by injecting the extracted mortar into the base of a column containing de-aerated water and a special blue liquid. In order for the test to be valid the temperature of the water column must remain between 21 and 25° C and the air content in the concrete mixture must be between 3.5% and 10%. A stirring rod is used in the bottom of the column to agitate the mixture for 30 seconds. An inverted Petri dish is suspended in the water at the top of the column to catch the bubbles that rise upwards. The change in the buoyancy force on the Petri dish is monitored by a balance and computer with time. According to Stokes’ Law, larger diameter bubbles rise at a faster rate than smaller ones. Changes in buoyancy measured in the test at different time periods give an indication of the volume of different size air-voids. From these measurements, and from inputs provided by the user about the mortar and paste content of the mixture, an estimate is made of the air volume, size, and distribution in the concrete. The data produced by the AVA is manipulated mathematically so that it can be directly comparable to the results from a hardened air-void analysis.

The AVA’s goals of providing a rapid measurement of the air-void size and spacing in fresh concrete are drastically needed in the concrete industry. However, the AVA and its ability

to accurately generate a measurement of the air void system of the subject concrete has been called into question (Desai et al., 2006; Distlehorst and Kurgan, 2006; Magura, 1996). Despite its potential drawbacks, the raw data collected by the AVA is a fundamental property of the mixture that should provide some indication of the actual air-void size distribution in concrete. What remains to be seen is if and how this fundamental property is able to give an accurate indication of the air-void parameters in concrete.

Hardened Air-Void Analysis (ASTM C 457)

Currently the most common method to examine the air-void spacing and size distribution in concrete is hardened air-void analysis performed according to ASTM C 457. This method inspects the area of a hardened concrete slab that is cut from a larger element and polished until the voids are clearly observable with a stereomicroscope at a magnification that is between 50x and 125x. The edges of the voids should be clearly observable with no differences in relief between the paste and aggregate on the sample surface.

Two different techniques are described by this method: the linear traverse and modified point count methods. In the modified point count method, locations on the sample are analyzed at regular intervals. At each one of these points the location is categorized as to whether it is an aggregate, paste, or air void. In the linear traverse method the area is investigated in a similar manner, but instead of investigating the sample at discrete points the specimen is analyzed by a continuous line or traverse. As the traverse covers the specimen the length of paste, aggregate, and air-void chords can be recorded. One advantage with the linear traverse technique is that it is possible to record the chord lengths of the air-voids intersected to determine the frequency of each chord size covered in the analysis. Both methods are able to provide general estimates of the air content and air void parameters of the area analyzed.

Two of the most common parameters used to assess the quality of an air-void system in concrete are the spacing factor and specific surface. Both of these parameters are not directly measured in the ASTM C 457 analysis and are instead estimated from the parameters measured in the analysis. The specific surface is a measure of the surface area of voids divided by their volume. A higher specific surface of two samples with equal volume of air indicates that there is on average a larger number of small air bubbles in the sample with the higher specific surface. The spacing factor is a parameter developed by Powers (1949) that estimates the average maximum distance from a point in the cement paste and an air-void. The reported precision of the method for samples prepared and measured in the same laboratory is 1.61% difference in the total air volume and a maximum error of 22.6% for the spacing factor (ASTM C 457). Even higher values are reported for samples prepared and analyzed in different laboratories. This implies that the sample surface preparation techniques has an effect on the results of the test. Recommended values for the specific surface ($24 \text{ mm}^2/\text{mm}^3$) and spacing factor (0.200 mm) were obtained from a comparison of length change of specimens in freezing and thawing tests to the air void parameters in the hardened concrete from two different mixtures (Powers, 1954; Backstrom et. al, 1958). Publications since have investigated the performance of multiple of different concretes in the test method and a spacing factor in the hardened concrete between 0.200 mm and 0.250 mm (Ivey and Torrans, 1970).

Resistance to Rapid Freezing and Thawing (ASTM C 666)

The most common method of determining the freeze-thaw resistance of concrete is to subject saturated specimens to rapid freeze-thaw cycles and to monitor the degradation by

monitoring the change in the relative frequency of the specimen (and/or length change) of the specimen. In ASTM C 666, concrete prisms are subjected to 300 temperature cycles between 5 and -18°C with certain allowable rates of heating and cooling. There are two different procedures outlined in the test method. Procedure A, the procedure utilized in this research, specifies that the specimens are stored in a metal box and allowed to freeze and thaw while completely surrounded by water. Procedure B requires specimens to freeze in air and to thaw in water. The samples are measured at regular intervals and the change in the resonant frequency (ASTM C 215), and weight of the specimens is monitored. Typically, results from the test are reported as a parameter called the durability factor. This value is equal to the square of the ratio of the relative frequency after 300 cycles to relative frequency at 0 cycles. The failure criteria for the test is not specified in the method and is intentionally left open to interpretation. However, several admixture specifications (ASTM C 260, ASTM C 494, and ASTM C 1017) recommend that the reduction in the ASTM C 666 durability factor of a mixture with and without an admixture should not be more than 20%. If this criterion is used to evaluate the performance of a mixture in the ASTM C 666 test then the limiting durability factor would be between 70 and 80.

Concerns have been stated (Pigeon and Pleau, 1995) that the ASTM C 666 test is much more severe than would be expected in nature and that the difference in laboratory testing methods could provide increased variability in results. Furthermore, the period of freezing that the specimen experiences in the test is very short and may not be representative of actual freezing. Also, the test results are shown to be sensitive to the surface scaling of the specimen (Pigeon and Pleau, 1995). Despite all of these drawbacks, this test continues to be widely used to evaluate the freeze-thaw durability of a concrete mixture.

14.2 Experimental

14.2.1 Materials

In all of the mixtures presented in this chapter, a Type I/II cement (as per ASTM C 150) was used, with equivalent alkali content ($\text{Na}_2\text{O}_{\text{eq}}$) of 0.53 and a Blaine fineness of 3630 cm^2/g . The phases of the cement are reported in Table 14.1 as determined by a Rietveld quantitative x-ray diffraction (RQXRD) (Rietveld, 1969; Stutzman, 1996) completed with the Topas Academic Software.

Table 14.1: Composition of the Type I/II cement as obtained through RQXRD

phase	percentage
C_3S	68.0
C_2S	15.7
C_3A	2.7
C_4AF	8.7
gypsum	1.3
CaCO_3	2.6

The aggregates used in the mixtures were locally available river gravel, limestone and natural sand. All aggregates are commercially used in concrete. All of the AEAs were obtained from commercial sources and meet ASTM C 260. The water reducer (WR) used in the majority

of this research met the requirements of ASTM C 494 (Type A and D). A midrange water reducer (MWR) was used in the mixtures containing a limestone aggregate meeting the requirements of ASTM C 494 as a type A and F. The product information sheet classifies the MWR as a lignosulfonate with triethanolamine.

The mixtures presented in this chapter were primarily cast with three different fly ashes (all meeting ASTM C 618) with varying AEA demand, based on prior laboratory experience. In this study, fly ashes 6 and 7 were obtained from a coal fired power plant utilizing a Low NOx burner technology. No information was obtained about the coal type, chemistry or burning conditions. Both of these fly ashes have a high AEA demand in concrete despite having a low LOI (less than 0.8%). In order to reduce the AEA demand, fly ash 6 was treated with a commercially used sacrificial surfactant (Hill, et al. 2004) that has been suggested to improve the AEA demand in concrete by preferentially absorbing on the carbon in the fly ash. No information was provided by the manufacturer about the amount or specific chemical nature of the sacrificial surfactant that was added to the fly ash. Therefore, all results for fly ash 6 are likely dependent on the amount and chemical nature of this additive. Oxide analyses completed with x-ray fluorescence spectroscopy and loss-on-ignition (LOI) measurements from ASTM C 311 are reported in Table 14.2 for each fly ash.

Table 14.2: Oxide analysis and LOI data for three fly ashes

Fly Ash Name	1	6	7
Silicon Dioxide (SiO ₂), %	56.18	52.07	52.04
Aluminum Oxide (Al ₂ O ₃), %	20.37	23.65	23.75
Iron Oxide (Fe ₂ O ₃), %	6.77	4.55	4.59
Sum of SiO ₂ , Al ₂ O ₃ , Fe ₂ O ₃ , %	83.32	80.27	80.38
Calcium Oxide (CaO), %	9.95	12.76	12.63
Magnesium Oxide (MgO), %	2.55	2.02	2.01
Sulfur Trioxide (SO ₃), %	0.53	0.78	0.79
Sodium Oxide (Na ₂ O), %	0.47	0.31	0.28
Potassium Oxide (K ₂ O), %	1.08	0.80	0.81
Total Alkalies (as Na ₂ O), %	1.18	0.84	0.81
ASTM C 618 Classification	F	F	F
LOI (ASTM C 311)	0.12	0.79	0.79

14.2.2 Mixture Preparation

All of the mixtures presented in this chapter contained a river gravel aggregate, with the exception of two mixtures that were used to analyze the aggregate correction factor and hence contained a limestone aggregate with a higher aggregate correction factor. The mixture proportions for these are shown in Table 14.3. In all cases the mixtures were prepared by the following method. A 64-L batch of concrete was made in an 85-L drum mixer. All of the material for the mixture was stored in the mixing room for at least 24 hours at 23° C prior to mixing to keep the mixing temperature constant. Coarse and fine aggregates were brought in from the stock piles and individually mixed. A moisture correction for each was used to adjust the batch weights. The coarse aggregate and sand were added to the mixture first and then 2/3 of

the mixing water was added. The mixture was agitated for one minute. Next the cement, fly ash and the remaining mixing water were added and mixed for three minutes. At this point the mixer was stopped and any material gathering on the sides or back of the mixer was removed. During the final three minute mixing period the mixture was brought to a constant slump (ASTM C 143) of 87.5 mm +/- 37.5 mm using a water reducer. Due to water demand differences of the fly ash mixtures the dosage of the WR and MWR varied. It is expected that different results would be obtained with the same materials when mixed for different durations, at different mixing speeds, or with different mixing energy per unit volume of mixture. Nevertheless, this method allowed for useful comparisons of the variables investigated.

Table 14.3: Concrete Mixture Composition

Components	Mass (kg/m ³)	
Cement	268	208
Fly Ash	67	89
Coarse Agg.	1098	1075
Fine Agg.	742	772
Water	151	113
total cm	335	297
Coarse Aggregate Type	River Gravel	Limestone
Agg. Correction Factor	0.55%	1.75%
w/cm	0.45	0.38

14.2.3 Determining Aggregate Correction Factors

As mentioned previously, ASTM C 231 specifies a method to determine the impact that an aggregate has on the air content of a mixture. In this method an equivalent amount of coarse and fine aggregate is used in the moisture condition that matches the material that is to be used in the concrete mixture. This material and water are then added to the pressure meter chamber and the mixture is stirred and consolidated in order to remove any trapped air voids. After the chamber has been filled to capacity then a certain volume of water is removed from the slurry equal to the volume of air for which the mixture is designed.

ASTM C 231 states that the aggregate correction values are not directly related to the absorption capacity of the rock. However, limited results in this study showed that the aggregate with a higher absorption capacity also showed an increased aggregate correction factor. The aggregate correction values for the mixtures utilizing the river gravel and natural sand and the limestone and natural sand were found to be 0.55% and 1.75%, respectively. The aggregate correction was not applied to the data reported for the pressure meter analysis as one goal of this testing is to best replicate the field application of the test method. However, all but two of the mixtures investigated were prepared with river gravel aggregate and so the correction factor is low. The aggregate correction factors for the aggregates used in the study are shown in Table 14.4 with various moisture contents investigated at 5% air content. Each value is an average of two measurements. All measurements were completed with either just the coarse or fine aggregate so that the individual contribution of each material could be investigated.

Table 14.4: Aggregate correction factor for three aggregate sources with various moisture content.

aggregate description		moisture content (%)	percent saturated (%)	ASTM C 231 correction factor (%)
river gravel	oven dry	1	0	0.4
	stock pile	0.68	68	0.3
	SSD	0	100	0.1
limestone	oven dry	4.5	0	1.8
	stock pile	2.5	56	1.5
	SSD	0	100	1
natural sand	stock pile	1.02	59	0.25

14.2.4 Hardened Air-Void Analysis

All of the hardened air-void analysis was completed in this study by using an automated air-void analysis with the Rapid-Air 457 instrument (Concrete Experts International). In order for samples to be analyzed in this machine the surface of the sample is prepared according ASTM C 457 and then painted black. Next a fine white powder ($< 1 \mu\text{m}$) is added to the samples surface and forced into the voids. This technique is described in EN 480-11. After the extra powder is removed from the surface any voids that are found inside the aggregate that became filled with powder must be painted black. The machine uses the contrast between the surface of the sample and the powder contained in the voids to measure the air-void chord lengths with a linear traverse measurement technique. This analysis technique is not able to measure the paste content of the sample as the machine cannot distinguish the difference from the paste and aggregate. Therefore, this information is required to be input from the mixture proportions or a manual modified point count method. For this study this value was obtained from the mixture proportions and fresh air content. The results of the hardened air-void analysis are not able to be classified as meeting the specifications of ASTM C 457 as the test requires the analysis to be completed by a human. Because of this, the results for the test will be referred to as the “hardened air-void analysis” in the remainder of the document. Several publications have shown outstanding repeatability of measurement and a good correlation between the analysis determined by the automated system and ASTM C 457 linear traverse (Pade et al., 2002, Jakobsen et al., 2006).

All of the samples presented in this study were analyzed by utilizing a traverse length of 7240 mm over an area of 77 cm^2 . This is equal to a length 3.17 times larger and an area of 1.08 times larger than is required in a traditional ASTM C 457 analysis with a maximum nominal aggregate size of 19 mm. Because of the larger traverse length that was utilized the analysis should provide a more thorough investigation of the air-void system of the sample. While a precision statement was not prepared for the use of the hardened air-void analysis as utilized in this study, data by Pleau et al. (1990) suggests that when three analyses are completed on a sample that the maximum error decreases from 20% to 12% for the spacing factor, 24% to 15% for the specific surface, and 27% to 16% for the total air content measured. While these precision values were not determined for this analysis technique one would expect a similar decrease in maximum error as the length of analysis increased.

The Rapid-Air 457 requires that the user choose a threshold value for the sample. This portion of the analysis is somewhat subjective. There is little guidance provided by the documentation or training with the Rapid-Air 457 to guide a user on how to accurately choose a threshold value for a sample. However, it has been shown with a limited data set that the threshold value chosen does not have a large impact on the results of the analysis as long as a consistent method is utilized to evaluate the appropriate value for the specimen (Volume II: Appendix A). All of the threshold values for the specimens in this study were between 158 and 174.

For the results of the hardened air-void analysis reported in this chapter the chords smaller than 30 μm were not included in the analysis as they are not able to be detected by a human during the ASTM C 457. By excluding these chords the air-void parameters determined by the hardened air-void analysis are better comparable to other reported values of ASTM C 457 results.

14.3 Results

14.3.1 AVA

To examine the repeatability and comparison between the results obtained in the AVA and the hardened air-void analysis ten different mixtures were examined with fresh air contents from 3.2% up to 9.75%. For five of these mixtures two samples were taken from each mixture and the results compared to one another. Table 14.5 provides a summary of the maximum, minimum and average standard deviations between each one of the measurements. The average percent differences between each AVA measurements for the air content, specific surface, and spacing factor were 36%, 48%, and 36%, respectively.

Table 14.5: Repeatability of five different mixtures each analyzed twice with the AVA

	air content (%)	specific surface (mm^2/mm^3)	spacing factor (mm)
maximum difference	2	29	0.092
minimum difference	0.50	7.6	0.030
average percent difference	36	48	36

In Table 14.6, results are presented for the analysis of ASTM C 231 fresh air content (pressure method), hardened air content, and the AVA. Testing was completed with four different fly ashes and four different AEAs. If more than one sample was taken from a mixture then the average results were reported. Note that the air content reported by the AVA is only for bubbles with diameters less than 3 mm. Because of this, the air content of the hardened air-void analysis was also only reported for voids less than 3 mm in size. The average percent differences between the AVA and hardened air-void analysis for the air content, specific surface, and spacing factor are 56%, 30%, and 63%, respectively.

Table 14.6: Comparison of estimates from the pressure meter, hardened air-void analysis and the air void analyzer.

ASTM C 231 pressure meter	hardened air-void analysis			AVA		
air content (%)	air content* (%)	specific surface (mm ² /mm ³)	spacing factor (mm)	air content* (%)	specific surface (mm ² /mm ³)	spacing factor (mm)
3.2	3.66	24.81	0.209	4.2	35.2	0.143
4.2	3.27	23.37	0.232	2.75	30.4	0.198
4.5	5.61	17.16	0.240	6.05	32.4	0.14
5.7	6.98	25.92	0.127	2.3	22.6	0.280
6.0	3.83	23.24	0.216	2.05	21.0	0.329
6.1	5.73	23.12	0.172	3.5	16.3	0.319
6.4	6.08	24.99	0.149	2.6	16.3	0.368
8.5	9.99	27.54	0.081	3.7	18.4	0.293
9.0	7.66	29.46	0.098	4.3	22.1	0.213
9.75	11.47	30.63	0.062	4.7	34.4	0.131

* The air content only includes voids that are less than 3 mm in size.

14.3.2 Impact of Mixture Ingredients on an Air-Void System

Figure 14.1 shows a comparison between the hardened air content and the results of the pressure meter for 39 different mixtures that contained 7 different fly ashes, 5 different AEAs, and two different coarse aggregate. The line of equality between the two is shown as well as a linear trend line. The average difference between the hardened air void analysis and the pressure meter was found to be 0.19% with a standard deviation of 1.18%.

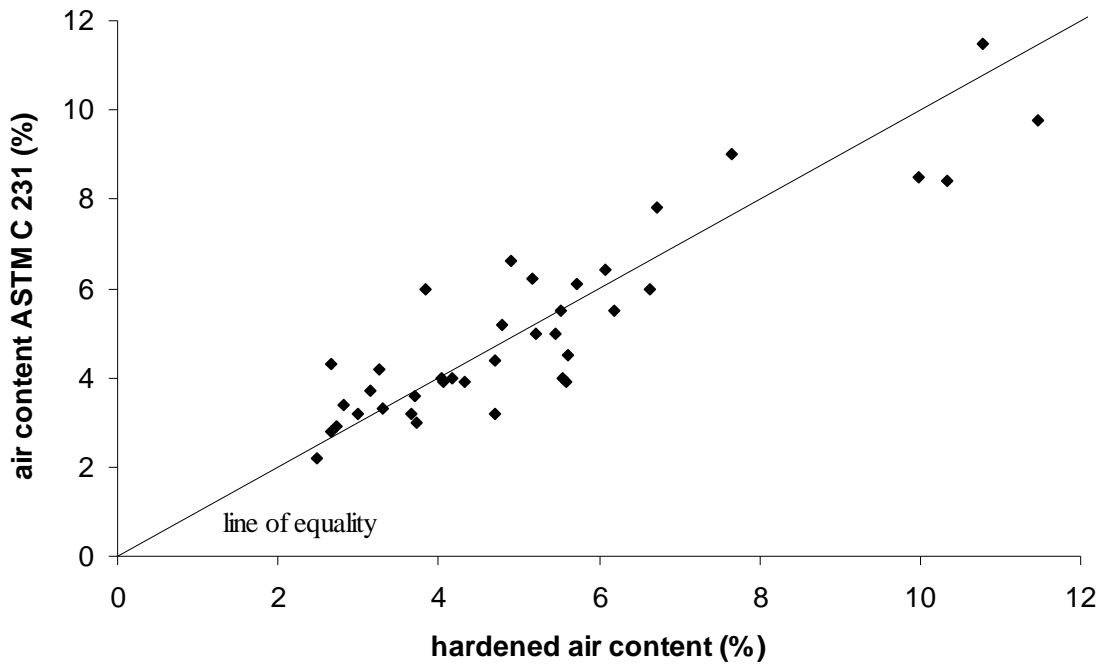


Figure 14.1: Comparison of air content from the ASTM C 231 pressure method and the hardened air content

In order to assess the freeze thaw durability of mixtures between 3% and 5% of fresh air content as determined by ASTM C 231, a hardened air-void and ASTM C 666 analysis were completed to determine how certain parameters affect the performance in the rapid freeze-thaw test and the air-void parameters. A summary of the data is shown in Table 14.7.

Table 14.7: Comparison of mixture information, fresh air volume, hardened air-void analysis, and rapid freeze-thaw testing.

specimen	fly ash	AEA type	AEA dosage (mL/100 kg cm)	WR/MWR dosage (mL/100 kg cm)	ASTM C 231 air content (no correction) (%)	ASTM C 231 air content (w/ correction) (%)	hardened air-void analysis					ASTM C 666		
							air content (%)	specific surface (mm ² /mm ³)	spacing factor (mm)	void freq. (mm ⁻¹)	avg. chord (mm)	durability factor	standard deviation	
1	1	wood resin	18	44	3.3	2.8	3.31	26.72	0.203	0.221	0.150	93	5.2	
2	1		21	98	4.5	4.0							90	4.9
3	7		87	46	3.7	3.2	3.31	20.30	0.266	0.168	0.197	94	0.2	
4	7		83	83	4.5	4.0	2.48	26.68	0.233	0.165	0.150	93	2.1	
5	7		36	177	4.0	3.5	2.73	17.64	0.336	0.121	0.227	16	0.0	
6	6		32	108	3.2	2.7							18	9.9
7	6		32	90	3.6	3.1	3.70	17.85	0.288	0.165	0.222	40	10.7	
8	6		61	110	4.0	3.5	4.16	19.10	0.254	0.199	0.209	67	1.2	
9	6		95	105	5.0	4.5	5.22	20.45	0.214	0.267	0.196	94	2.4	
10*	1		8	111	4.2	2.5	3.27	23.37	0.232	0.191	0.171	75	4.2	
11*	1		15	136	5.0	3.3	4.46	18.69	0.225	0.255	0.214	96	0.7	
12	1	Vinsol resin	9	33	4.0	3.5	4.68	23.65	0.196	0.277	0.169	93	0.1	
13	6		41	34	3.2	2.7	4.33	18.44	0.260	0.200	0.217	26	3.5	
14	6		66	33	3.9	3.4	4.71	19.71	0.234	0.232	0.203	62	0.6	
15	6		124	32	4.5	4.0	5.61	17.16	0.240	0.241	0.233	93	1.4	
16	6	synthetic	23	33	3.2	2.7	2.99	16.28	0.350	0.122	0.246	18	8.5	
17	6		27	33	3.9	3.4	5.59	19.65	0.211	0.275	0.204	91	1.6	

These mixtures contain limestone coarse and natural sand fine aggregate with an aggregate correction factor of 1.75%.

The other mixtures contain a river gravel coarse and natural sand fine aggregate with an aggregate correction factor of 0.55%.

14.4 Discussion

14.4.1 AVA

No previous data has been published indicating the repeatability of measurement for the values of the specific surface and air content reported by the AVA from a single mixture analyzed multiple times by the same machine. There has been work published by Distlehorst and Kurgan (2006) about the repeatability of the spacing factor. This work suggested that the single operator variance using the same machine is not expected to be more than 43%. The average difference between values of 36% obtained in this study is within this range for the spacing factor and so the variance of the other two parameters is likely characteristic of measurements taken by the AVA. The variance of measurement between devices has been suggested to be significant enough that the use of the AVA has not been recommended to be implemented in a construction specification (Desai et al., 2006).

When one compares the results between the estimates of the hardened air-void analysis and AVA shown in Table 14.6 the difference between the results is quite variable. The results between the two methods for the air content, specific surface and spacing factor show little agreement. The air content reported in the AVA and the hardened air-void analysis were on average different by more than 50%. In only three cases out of ten was the air content within 1%. The parameter that showed the closest correlation to the hardened air-void analysis was the specific surface measurement at an average difference of 30%. It is encouraging that this parameter shows the closest correlation as it is the one most directly calculated from the measurements of the AVA.

Thus, the overall findings of this study show that the AVA showed poor repeatability and that the estimated air-void parameters measured did not correlate well to air-void parameters estimated by the hardened air-void analysis from the same mixtures.

14.4.2 Impact of Mixture Ingredients on an Air-Void System

Figure 14.1 shows a comparison between the air content measured by ASTM C 231 and the hardened air-void analysis is shown in Fig. 14.1. This figure shows a good correlation between the two methods; however, one should keep in mind that both of these tests can have significant variance. It should also be noted that the vast majority of the samples analyzed contained air contents less than 6%.

Although the data in Table 14.7 allow for many different trends to be investigated, the discussion in this chapter will focus on the impact of different mixture ingredients on the quality of the air-void parameters and performance in the ASTM C 666 with air contents between 3.2 and 5% as measured by ASTM C 231. These ranges of air contents were chosen as they allow the performance of mixtures with different ingredients to be investigated at the low end of specified air contents (as described earlier in this chapter). Some of the variables investigated include: different aggregate correction factors, impact of WR dosage on the air-void system, and the impact of a high AEA demand fly ash that has been treated with a sacrificial surfactant to improve the AEA demand. Each variable was investigated with a range of air contents in order to find the threshold value of fresh air content that was needed to provide a performance in the ASTM C 666 test similar to the requirements specified in ASTM C 260, ASTM C 494, and ASTM C 1017. It was decided that a durability factor of 75 would be used as the point of failure for the testing in this study.

14.4.3 Aggregate Correction Factor

As can be seen in Table 14.4, the aggregate correction factor seems to be dependent not only on the aggregate porosity but also on the moisture content. Therefore, the difference between the air content in the matrix and the amount reported by the pressure meter for the limestone aggregate mixtures is significantly different and will vary based on the moisture condition of the aggregate during the test. This may lead to a situation where an operator that is only investigating the air content of a mixture with the ASTM C 231 method to determine that the mixture has a large enough volume of air to provide satisfactory freeze-thaw performance when it does not. An example of this can be seen if one compares the results from specimens 2 and 10 in Table 14.7. The aggregate correction factor for specimens 10 and 11 was determined to be 1.75% while the aggregate correction factor for the remainder of the mixtures was 0.55%. In both of these specimens similar air content was determined by fresh air content analysis of 4.5% and 4.2% by ASTM C 231 with no aggregate corrections applied; very different air content results when the aggregate correction factor is applied of 3.95% and 2.45%. It seems that this amount of air was not enough in mixture 10 as a durability factor of 75 was obtained in the rapid freeze-thaw tests, while specimen 2 had a durability factor of 90. In specimen 11 the AEA dosage was increased, which corresponded to an increase in the corrected air content to be 3.25% which exhibited an improvement of the air-void parameters and performance in the ASTM C 666 test. However if one does not apply the aggregate correction factor then an air content of 5% in the ASTM C 231 test was needed to ensure adequate performance in the ASTM C 666 test with the limestone aggregate mixture, while the 3.3% air content in specimen 1 was enough to ensure satisfactory performance. It is unclear how differences between mixtures of the w/cm, type of WR, and paste content may have affected the results of the ASTM C 666 tests. However, these data do suggest that the use of a high porosity aggregate can lead to unsatisfactory frost performance in the ASTM C 666 test with air contents less than 4.2% as measured with by ASTM C 231 if the aggregate correction factor is not applied.

14.4.4 Impact of WR Dosage

The impact of WR dosage has been shown to improve the effectiveness of an AEA to produce a larger volume of air in a concrete mixture for a similar dosage (chapter 13). In this study the impact on the hardened air-void system and performance of the mixtures in the rapid freezing and thawing tests is examined. In specimens 3, 4, and 5 the amount of AEA and WR was varied in each mixture containing a fly ash with a high AEA demand, due to high activity carbon to examine the impact on the hardened air-void analysis, and the performance in the rapid freeze-thaw test.

Between specimens 3 and 4 the dosage of AEA was held constant while the WR dosage was 180% larger in specimen 4. With this increase in WR dosage the air content measured in the ASTM C 231 test increased and an improvement was obtained in the specific surface. However the spacing factor did not change. Furthermore, both specimens performed adequately in the ASTM C 666 test. In specimen 5 a WR dosage was used that was 380% larger and an AEA dosage that was 59% less than what was used in specimen 3. The air-void content and distribution measured was very different despite a similar air content measured by ASTM C 231. The performance in the rapid freeze thaw test was also different as specimen 5 showed very poor performance in the ASTM C 666 test. Furthermore, if one looks at the difference between the hardened air content and that measured by ASTM C 231 for specimen 4 and 5 it can be seen that the amount of air in the hardened concrete has decreased between the fresh and hardened state.

This decrease in air content implies that there may be an air-void stability problem in concrete with high dosages of WR. This observation is in line with results reported by Plante et al. (1989) where mixtures with large dosages of WR when compared to AEA showed a decrease in air content with time. These data along with the 36 mixtures provided by Plante et al. (1989) suggest that a WR is capable of increasing the measurement of air content in the fresh concrete above levels that would be produced with an AEA alone and yet produce unsatisfactory performance in ASTM C 666 test.

14.4.5 High Activity Carbon Fly Ash Treated with a Sacrificial Surfactant

As stated previously a sacrificial surfactant has been used to reduce the AEA demand of fly ash 6 in concrete. This fly ash was investigated with three different AEAs as shown in Table 14.7. In each case a range of air contents was investigated and it was common to find that higher total air volumes were needed in the fresh and hardened air content for fly ash 6 before the durability factor determined by the ASTM C 666 was above 75 when compared to mixtures that did not contain a sacrificial surfactant. The spacing factors and specific surfaces as determined by the hardened air-void analysis were not sufficient to satisfy the recommended values of 0.200 mm and $24 \text{ mm}^2/\text{mm}^3$ and yet satisfactory durability factors were obtained in the ASTM C 666 test. One other observation is that all mixtures containing fly ash 6 with a hardened air content greater than or equal to 5% showed satisfactory performance in the ASTM C 666 for all AEAs used. These data imply that the use of a sacrificial surfactant may cause an increase in the air-void sizes produced in air-entrained concrete and therefore, a larger volume of air was needed in the mixture to obtain a satisfactory number of small air-voids and performance in the ASTM C 666 test. This difference in void size can be clearly seen when one compares the average chord lengths of specimens 1, 3, 4, and 7 or 12 and 14.

This behavior is especially clear when one compares specimen 4 with specimen 7. The fly ash in specimen 4 is the same as used in specimen 7 except for the sacrificial surfactant. In both mixtures all other parameters were held the same except for the AEA dosage and the air content. Specimen 4 is shown to have a satisfactory durability rating with a hardened air content of 2.48% and specimen 7 did not show a satisfactory durability rating with an air content of 3.70%. As stated previously the reason for the difference in behavior is that specimen 7 appears to have a coarser air-void system. This can be seen directly when one compares the average chord lengths, specific surface, and spacing factor between the two samples. The average chord length suggests an increase of 39% between the two samples. Despite this apparent coarsening of the air-void system, when sufficient air was entrained in these mixtures (5% or more), satisfactory frost resistance was obtained.

14.5 Conclusions

This work presented in this chapter examined the challenges of relying on a fresh air-void specification to determine the ability of a mixture to provide satisfactory freeze thaw resistance in the ASTM C 666 test. An evaluation of the AVA was presented that investigated the repeatability of measurement with the device and also the difference in values compared the hardened air-void analysis with the Rapid-Air 457. Although the results of this testing are based on a small number of mixtures that had a similar workability and mixture proportions the results obtained suggested that the AVA has significant variability between two measurements examined from the same mixture, and significant differences were found between air-void parameters estimated by the hardened air-void analysis and the AVA. More work is needed to

determine the causes of these discrepancies; however, the variability between the two measurements from the same mixture was similar to values obtained by Distlehorst and Kurgan (2006), and significant discrepancies between the hardened air-void analysis and the AVA measurements were also observed by Desai et al. (2006) and Magura (1996).

One of the primary concerns of the authors with the AVA is the ability to obtain a meaningful representation of a concrete mixture from a 20 cm³ sample. Furthermore, the version of the AVA investigated utilized a balance that was only accurate to 0.01 g. It is unclear if this is precise enough to measure the buoyancy change in the Petri dish as it collects air bubbles.

Several concrete mixtures with relatively low total air contents were evaluated, and it was shown that concrete with total air content greater than or equal to 5% was generally frost resistant. Some mixtures with lower air contents were not frost resistant (using ASTM C 666), especially mixtures containing high amounts of WR (and lower AEA dosages), mixtures for which aggregate correction factors were not applied, or mixtures containing a fly ash treated with a sacrificial surfactant. However, none of these variables listed previously were investigated in combination; combinations of these variables could require a larger volume of air to be contained in the mixture.

For mixtures containing a fly ash treated with a sacrificial surfactant, a coarsening of the air-void system was observed when compared to mixtures prepared with similar types of AEA and volume of air. This coarsening was directly observed as an increase in the average chord length of air voids, increase in the spacing factor and decrease in the specific surface. However, once the air content was increased to 5% or more, satisfactory frost resistance was obtained. It should be stated that no details were provided nor were they obtained about the concentration or chemical nature of the sacrificial surfactant. If either one of these parameters change then the results may also change.

Chapter 15. Observations of Air-Bubbles from Fresh Cement Paste

Recent experimental work is also presented using a new technique to observe bubbles that have escaped from pastes and suspended in the bleed water. These experiments suggest that the stability of an air-entrained bubble may be related to the integrity of this shell. This chapter also reviews literature dealing with changes to air bubbles with time in fresh air entrained cement paste and concrete. Coverage is also given to the existence of a shell surrounding these bubbles.

15.1 Introduction

Development of an air void system in hardened concrete through the use of an air entraining admixture (AEA) to stabilize air bubbles in fresh concrete is the primary method of producing freeze-thaw-resistant concrete. Although AEAs are widely specified and used to obtain frost and salt scaling resistance, practitioners still face significant problems in reliably and reproducibly stabilizing and maintaining an effective air-void system in concrete. Existing literature, based on laboratory and field observations, suggests that all aspects of the concrete construction process can affect the air void system in concrete (Whiting and Stark, 1983). In addition to the influence of dynamic processes such as batching, mixing, transporting, placing, consolidating and finishing the concrete, it has been reported that air bubbles in fresh concrete can change while the plastic material is at rest (Mielenz et al., 1958; Fagerlund, 1990). The purpose of this paper is to report several experimental observations of air bubbles that have escaped from cement paste and observed over time.

The goal of this chapter is to resolve some of the conflicts presented in previous research. This was achieved by developing a new experimental method that uses microscopy to examine the changes in bubbles separated from 0.42 w/cm paste. While these observations are not numerous enough to obtain an understanding of the behavior, they do provide insight. Follow up testing is planned to examine the air-void stability of concrete.

15.1.1 Background

While there has been a large amount of research completed on the bulk properties of air-entrained concrete there has not been a large amount of work done to fundamentally investigate the air-voids themselves or how they change with time. One classic and frequently cited collection on air-entrained concrete is the series of four papers by researchers at the U.S. Bureau of Reclamation (Mielenz et al., 1958A, Backstrom et al., 1958A; Backstrom et al., 1958B; Mielenz et al., 1958B). The first (Mielenz et al., 1958A) of these papers included data suggesting that due to a pressure gradient between large and small bubbles, gas transfer can occur between bubbles. This transfer leads to a change in volume of the air entrained in pastes with time. Photos of air-entrained bubbles in dilute water-to-cementitious materials ratio (w/cm) pastes were also shown to change while sitting statically. Bruere (1962) attempted to replicate some of the behavior previously described by Mielenz et al. (1958A) with a different experimental setup, and found no air bubble instability. In a review of both sets of experiments Powers (1968) states that it is doubtful that bubbles will be able to expand in fresh cement paste because of the restraint provided by the cement paste. Other researchers identified a “transition zone” around bubbles that had been frozen during the first 3 hours of hydration and observed cryogenically with a low temperature scanning electron microscope (LTSEM) (Ahmad and Williamson, 1991A, 1991B; Corr et al., 2002). This transition zone was suggested to be filled with water (Ahmad and

Williamson, 1991A) or of a phase with a high porosity (Corr et al., 2002). The size of the transition zone was suggested to increase with an increase in w/cm and shrink with hydration. A summary of previous work is provided in Table 15.1.

Table 15.1: Summary of previous research completed on air-void stability and the bubble shell.

reference and year	samples	method of observation	key observation	primary conclusion
Meilenz et al., 1958A	paste w/cm 30 AEA/lime/sand/cement combinations paste w/cm 0.3 - 0.6 prepared in drum mixer concrete w/cm 0.45 prepared in drum mixer	stereoscope ASTM C 457 ASTM C 231	bubbles change size with time and appear to have precipitates on the surface hardened air volume was higher than fresh; discrepancy was larger with higher w/cm hardened air volume lower than fresh	pressure differential exists between bubbles gas interchange is occurring between bubbles
Bruere, 1962	paste 0.45 w/cm prepared with 1000 RPM stirrer set of mixture modified to 5 min, 3, and 8 hours	ASTM C 457	no difference in air-void system between samples	no gas interchange between bubbles
Powers, 1968	---	---	how can bubbles increase in size if they are confined by paste?	doubtful if bubbles change size in paste
Rashed and Williamson, 1991A, 1991B	mortar w/cm 0.30 concrete 0.29-0.49 w/cm 3 hr-3 day w/ and w/o silica fume	frozen in liquid nitrogen and observed in LTSEM (mortar), SEM (concrete)	hydration products around air-void appear to be different morphology than bulk paste; shell observed at 5 min and 3 hour; shell made up of fine particles; gap between particles and shells vary in size and appear to contain water during hydration	shell likely made up of hydration products
Corr et al., 2002	bubbles isolated by AVA less than 30 min paste w/cm 0.4 at 5 min	frozen in liquid nitrogen and observed in LTSEM	"mineral" shell seen on individual bubbles and in the paste high porosity transition zone "often" observed around bubbles with a 10-15 μm thickness	shell observed in individual separation technique similar to one found in paste transition zone may be increased by freezing

15.2 Experimental Methods

To augment the studies described above, an experimental program was initiated to observe in-situ changes in air bubbles that had escaped from cement pastes, and were monitored over time as the bubbles resided in a static bleed-water solution. For this testing, a 0.42 w/cm paste was made using 1.37 kg of a cement meeting the ASTM C 150 specifications for Type I and II with a 0.53 alkali content ($\text{Na}_2\text{O}_{\text{eq}}$). Table 15.2 presents a summary of the admixture combinations investigated. The mixer and mixing procedure used in this study met ASTM C 305. After the mixing cycle was completed, a funnel was used to transfer the paste into a 70 ml bottle that was filled in thirds by volume and consolidated by agitation and taping on the desktop. Care was taken to ensure the bottle did not have any large air-voids and was filled until it reached capacity. At this point the cap was tightened and the bottle was turned on its side. After about 10 minutes it was possible to observe a layer of bleed water forming at the surface of the paste. In this bleed water air bubbles could be found that had worked their way to the inside face of the bottle wall due to buoyancy. These bubbles were then observed under a stereo microscope at magnification of 50X, fitted with a 5 megapixel, high resolution digital camera. A computer program was written to capture images of the changes in these bubbles with time. These images were measured with the AxioVison AC software from Carl Zeiss. This software allows the user to count pixels between any two designated locations on the image and converts pixels to units of length via an image-specific calibration. Accuracy of the measuring system had been checked and calibrated by the instrument manufacturer. When objects of fixed size were subsequently measured twenty times the software reported coefficients of variation ranging from 0.3% for lengths of 700 microns to 1.3% for lengths of 30 microns. For bubbles sizes reported in this chapter a representative coefficient of variation (COV) is about 0.4%, including any effects of distortion by the plastic bubble wall.

Table 15.2: Mixtures investigated

mixture	admixture	dosage (ml/100 kg cm)	setup
1	none	---	1,2
2	synthetic	47	1,2
3	tall oil	143	1,2
4	wood rosin	48	1,2,3
5	Vinsol resin	18	1,2
6	Vinsol resin	26	3
	water reducer	81	

15.2.2 Setup #1

Setup #1 is shown in Fig. 15.1. In preliminary tests it was found that the paste in the bottle swelled as hydration progressed. Since the bottle was filled to capacity the change in volume of the paste disturbed the voids that had escaped the paste and these were then caught on the surface of the bottle in the bleed water. The swelling of the paste was likely related to temperature increase (due in part, perhaps to heat of hydration, and in part to a high-intensity light source), as swelling of the paste was no longer observed once the sample was maintained in

isothermal conditions. (A plot of the average temperature from two thermocouples in the ambient room, in a specimen under the point light source, and in a specimen in the ambient temperature is shown in Fig. 15.2. These measurements were taken on two different occasions and the results did not vary by more than 1°C between the measuring periods. The average temperature changes with time for the different specimens can be found in Fig. 15.2.) While this swelling was unexpected it proved to be useful as the bubbles could be inspected as they were pushed by the paste from below.

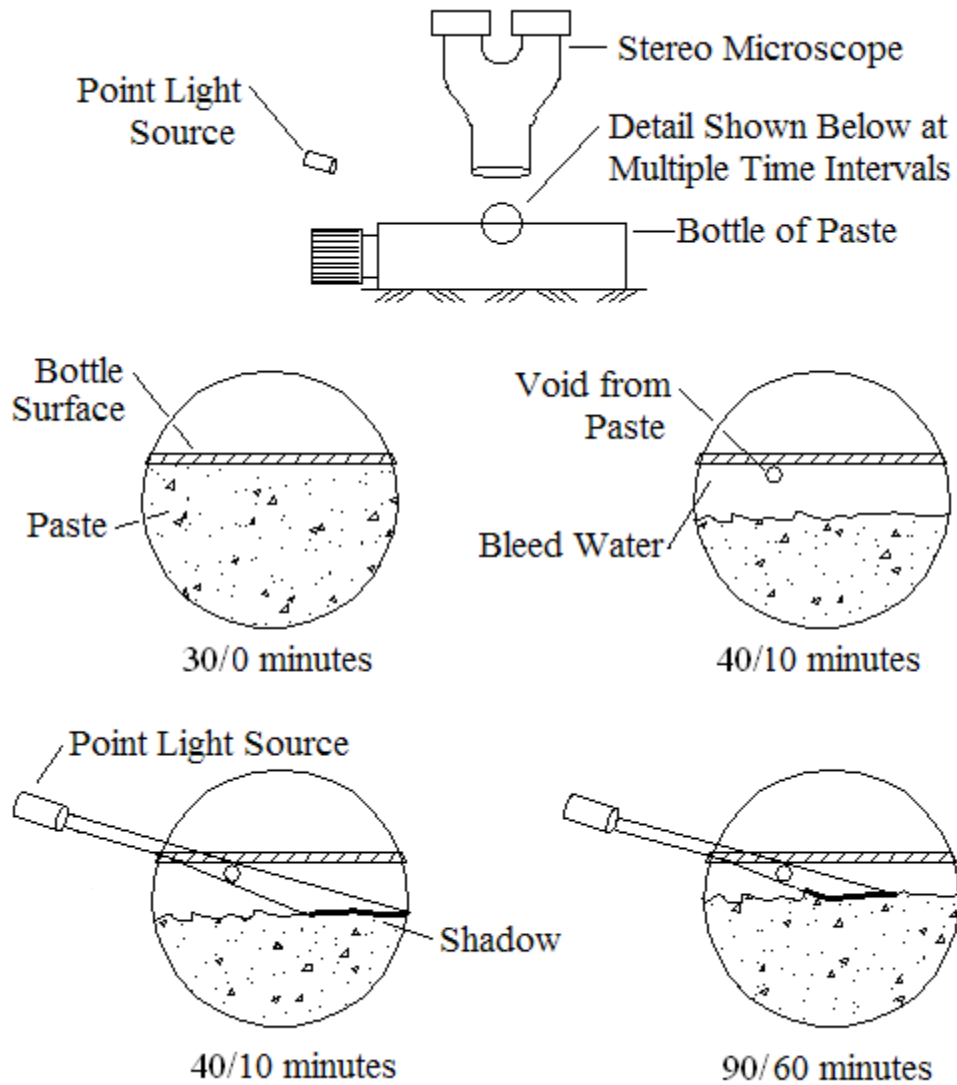


Figure 15.1: Setup #1 showing orientation of bottle, stereoscope, and point light source.

The time is displayed in minutes after initial mixing and time after the bottle was placed on its side.

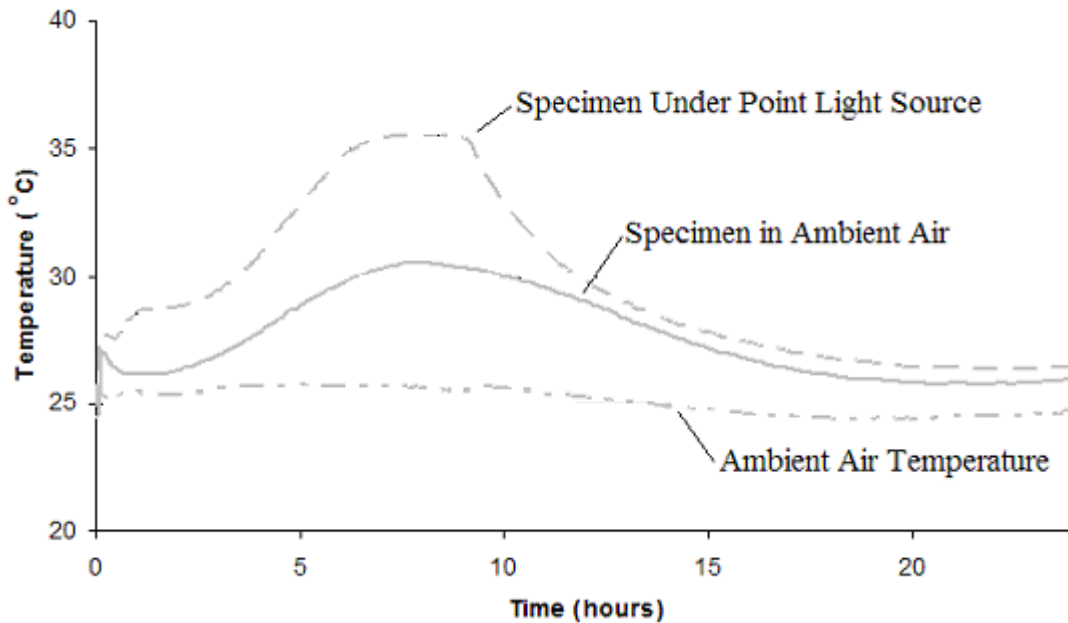


Figure 15.2: Time and temperature for the ambient temperature, a specimen under the point light source, and a specimen in the ambient temperature.

In order to monitor the upwards movement of the paste as it swelled, with respect to the air-bubbles, a single point light source was used at a sharp angle so that the shadow of the bubble could be monitored with time. Since the bubble was stationary at the underside of the bottle wall, an apparent movement of the shadow towards the bubble means that the surface of the paste is moving upwards.

15.2.3 Setup #2

In order to isolate the changes in the bubbles without contact from the paste an alternate setup was used. The only difference in this test setup from the previous is that the bottle of paste was filled to 75% of capacity and the balance of the volume kept full of a surrogate bleed water solution by means of a tube connected to the cap as shown in Fig. 15.3. The surrogate pore or bleed water solution (water and cement at $w/cm = 60$) was carefully added so that it filled the remaining portion of the bottle and the tube, and minimized mixing with the paste in the process. Some agitation was needed to remove air bubbles trapped during filling with the bleed water solution, accomplished by flicking the tube of the bottle with a finger. After this solution was added the bottle was carefully turned on its side and the paste formed a slope as shown in Fig. 15.3. After 10 minutes in this position air bubbles were seen to escape from the 0.42 w/cm paste, and floated up to the underside of the bottle. Changes in the bubbles were then observed with time as previously described. Because the bottle was not filled to capacity, once it was put on its side the bleed-water filled gap isolated the bubbles from contact with the paste, and allowed this migration to the underside of the glass surface. This ensured that any changes in bubble diameter with time were solely due to interactions between the bubbles and the surrounding fluid in combination with any effects of temperature-changes in the air within the bubbles.

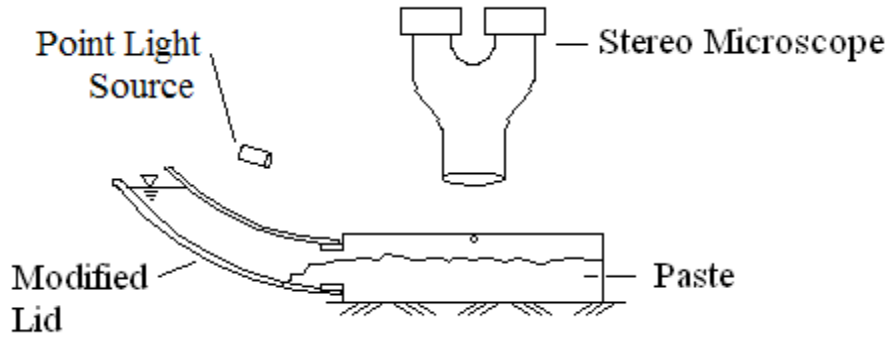


Figure 15.3: A cross section of setup #2 showing the reduced paste level and additional water provided by the tube with the modified lid.

15.2.4 Setup #3

A final setup was used to investigate the effect of pressure on escaped air bubbles from cement paste. While additional work is underway in this area, these test results were included because the stability of static air-bubbles as the surrounding fluid pressure is influenced by concrete placing methods, consolidation, and by the static head of the fresh concrete. For this test the fluid surrounding the air-bubbles was increased to 0.7 bar above atmospheric pressure in 10 equally-spaced steps and then decreased back to atmospheric pressure in three equal steps. It should be noted that the pressure regime was chosen based on limitations of the available equipment.

15.3 Results and Discussion

15.3.1 Results of Setup #1-paste expansion

Air bubbles from Air-Entrained Cement Paste

The images of escaped air bubbles from an air-entrained cement paste with a tall oil AEA as per mixture 1 in Table 15.2 (per setup #1) are shown in Fig. 15.4. These experiments have been completed 3 times with a Vinsol resin, wood rosin, and synthetic AEA at dosages typical of air entrained concrete, and similar behavior was observed for all. A summary of experiments is shown in Table 15.2. These images were chosen as they are a representative set that clearly shows the behavior. The bubbles in Fig. 15.4 appear to have a textured surface similar to that observed by Mielenz, et al. (1958A) and Corr (2002). If one compares Fig. 15.3A and 15.3B the shadow of the air-voids from the point light source has moved towards the bubble with time. The point of focus of the microscope was never changed and the bubbles have remained in focus the entire time; therefore, the depth between the bottle surface and the bubble did not change beyond the depth of focus, which for this instrument at this magnification is about 1 mm. As shown previously in Fig. 15.1 this is only possible if the paste is expanding towards the bottle surface. Once the paste swells enough to touch the bubble, the shell appears to crack in a brittle manner. As the paste swells further one can see a much smaller bubble that appears to emerge from the inside of the cracked shell. This emerging bubble seems to have a different, much smoother surface than the shell that was previously observed. As the paste continues to swell and the bubbles are forced to interact no coalescence is observed as the bubbles touch one another

(15.4D and 15.4E). In Fig. 15.4E one can see that as bubble B and A come into contact with each other the surface of bubble B appears to have curved away from the surface of bubble A. As further paste expansion occurs in Fig. 15.4F bubble A appears to have surrounded bubble B without coalescence.

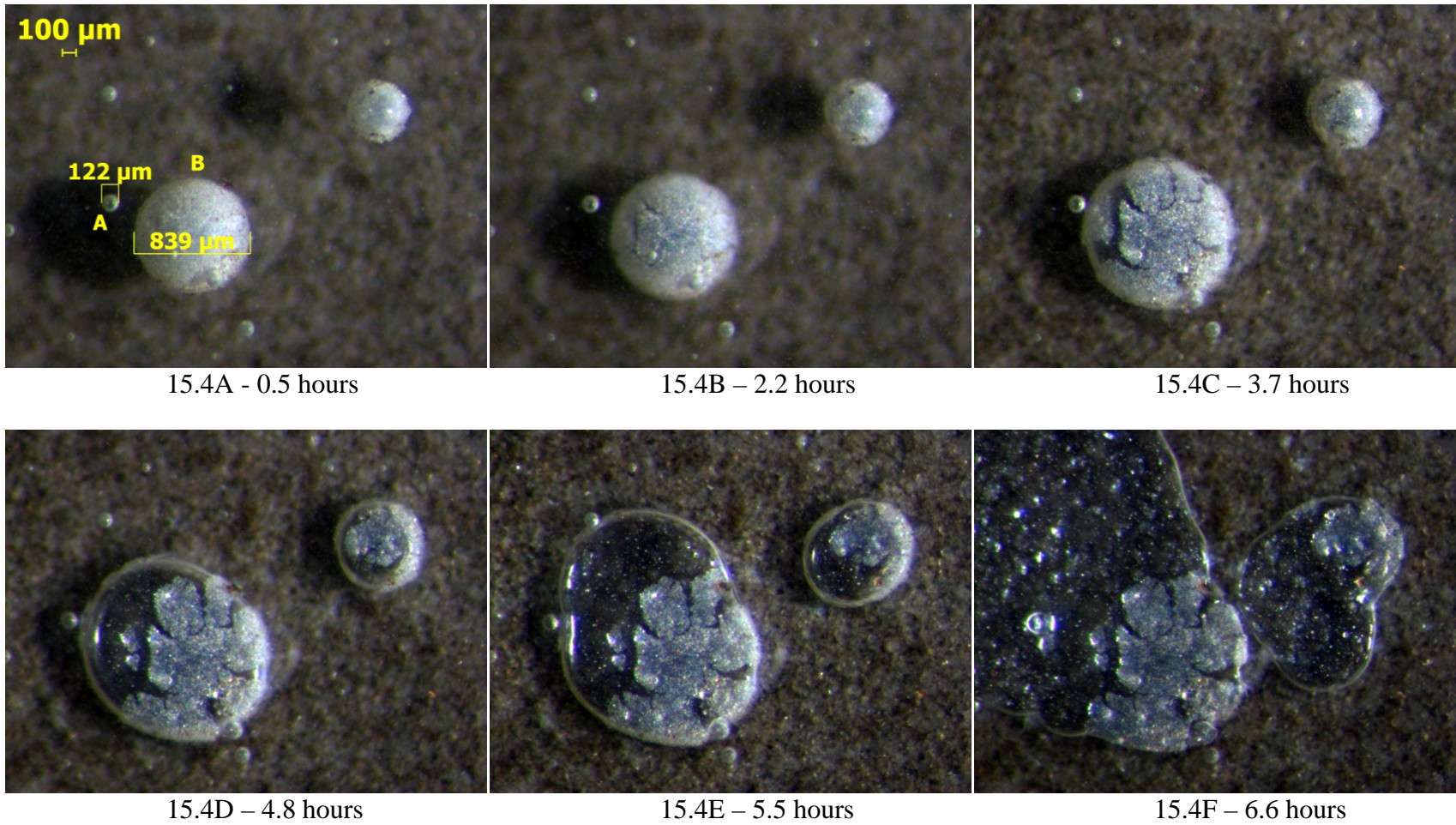
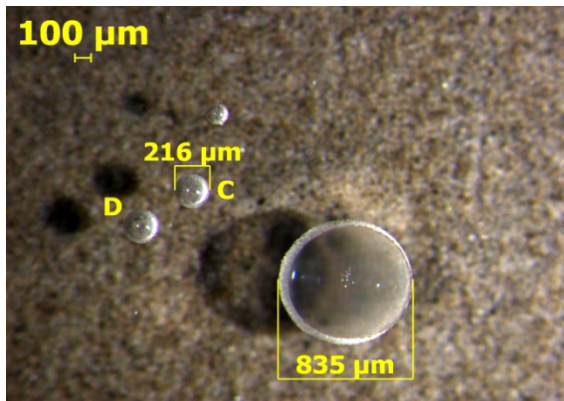


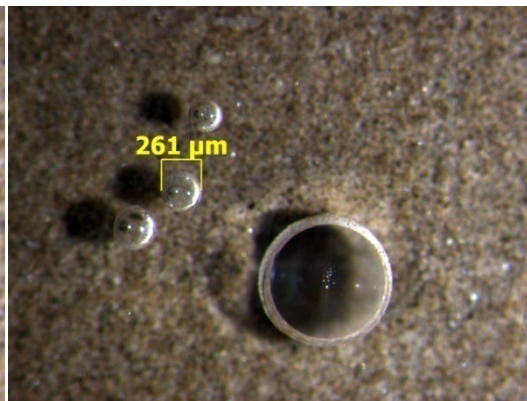
Figure 15.4: An air-entrained paste containing a tall oil AEA at 143 mL/100 kg cm in setup #1 whose bubbles are pushed by the paste below.

Air bubbles from Non-Air-Entrained Cement Paste

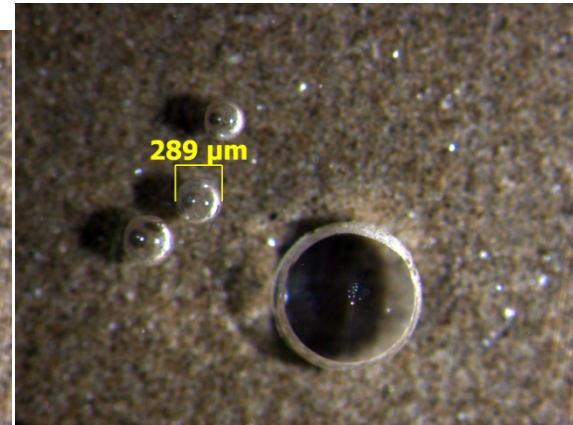
The images from a non air-entrained cement paste observed in test setup #1 are shown in Fig. 15.5. The bubbles in this system appear to be translucent-to-transparent and do not have the rough or opaque surface texture previously observed with bubbles escaped from air-entrained paste. Again the shadows of the bubbles from the point light source move closer to the bubble with time while the bubble is stationary, and so again the paste appears to be rising upwards. Once the paste contacts the bubble, one can see that the bubble diameter begins to expand without an apparent change in the bubble surface. As paste expansion and the accompanying bubble deformation continues, Fig. 15.5E shows that once bubbles C and D come into contact they coalesce and form a larger void. This behavior contrasts with that observed in the previous experiment in which bubbles that escaped from air-entrained paste appeared to resist coalescence. Several dimensions are given for bubble C in Fig. 15.5A, 15.5B, and 15.5C showing that this bubble did change diameter with time before it came into contact with the expanding paste (as indicated by the shadow technique described earlier.) This is discussed further in Setup #2. This test was repeated three times with similar behavior each time.



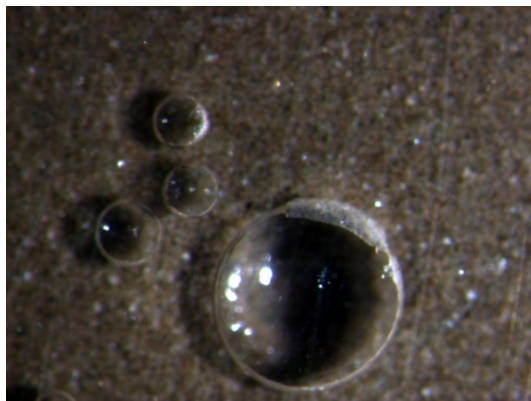
15.5A – 0.5 hours



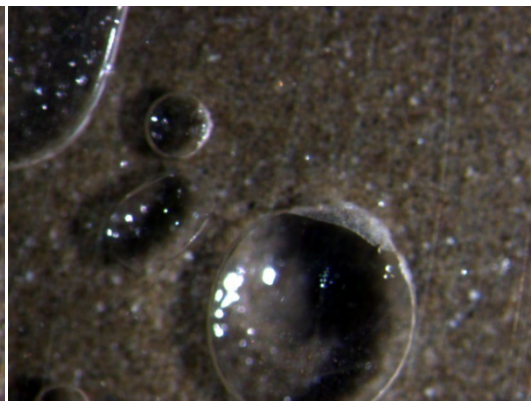
15.5B – 3.7 hours



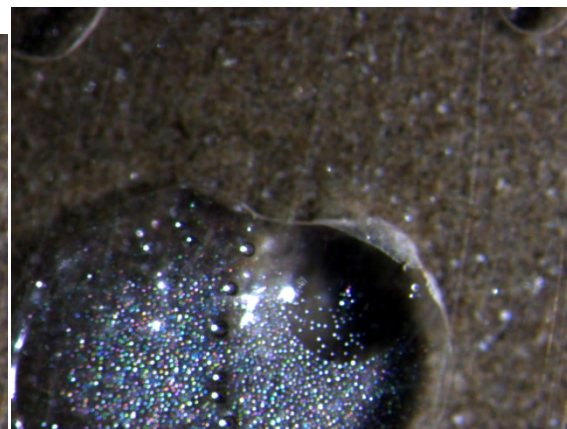
15.5C – 5.3 hours



15.5D – 6.8 hours



15.5E – 7.3 hours



15.5F – 7.8 hours

Figure 15.5: A non-air-entrained paste sample in setup #1 whose bubbles are pushed by the paste below.

15.3.2 Results of Setup #2-no paste expansion

Bubbles from Air-Entrained Cement Paste

When air-entrained cement paste was tested in this setup, there was no measurable change in the diameters of the bubbles that had escaped into the fluid above the paste over the 8-hour period of observation. This test was repeated four times with a similar size distribution of observed bubbles and little to no diameter change was observed for the following AEAs investigated: tall oil, Vinsol resin, wood rosin, or so-called “synthetic” as reported in Table 15.2.

Bubbles from Non Air-Entrained Cement Paste

When bubbles from non air-entrained cement paste were examined over time in setup #2, it was found that there was a significant change in bubble diameter for the first 3.5 hours after hydration. A picture of the layout of the bubbles is shown in Fig. 15.6 at 0.6 and 3.6 hours of hydration, and the same translucent-to-transparent bubble walls are evident as seen earlier when the bubbles originated in non air-entrained paste. A graph summarizing the average change in diameter with time is shown in Fig. 15.7. For the diameters reported in Fig. 15.7, two measurements were taken that were perpendicular to one another and then averaged. As can be seen bubble “I” begins to decrease in size from the initial observation until about 1 hour of hydration. Bubbles “M” and “K” begin to decrease in size at about 2 hours after initial hydration and stabilize after about 3 hours. Bubbles “J” and “L” begin to increase in size from the initial observation and stabilize at 2 hours of hydration. The smaller bubbles appear to decrease in size initially while the larger bubbles appear to increase in size. The mid-sized bubbles remain a constant diameter initially, and then start to decrease in size. A proposed explanation for the size change of different diameter voids has been suggested by Fagerlund (1990), who hypothesized that the smallest (higher-pressure) bubbles lose air to the largest (lower pressure) bubbles while intermediate sized bubbles would show no volume change. (Thus all bubbles in the system tend towards an equilibrium pressure and size). Fagerlund went on to propose that the bubble-size distribution would continuously change until such equilibrium is reached. The observations of this present experiment not only support Fagerlund’s ideas, but are also similar to the observations by Mielenz et al. (1958A) for air-entrained paste with a w/cm of 30. The experiments reported here were repeated 4 times and each time many, but not all, of the smaller bubbles decreased in size over time while the larger bubbles increased in size.

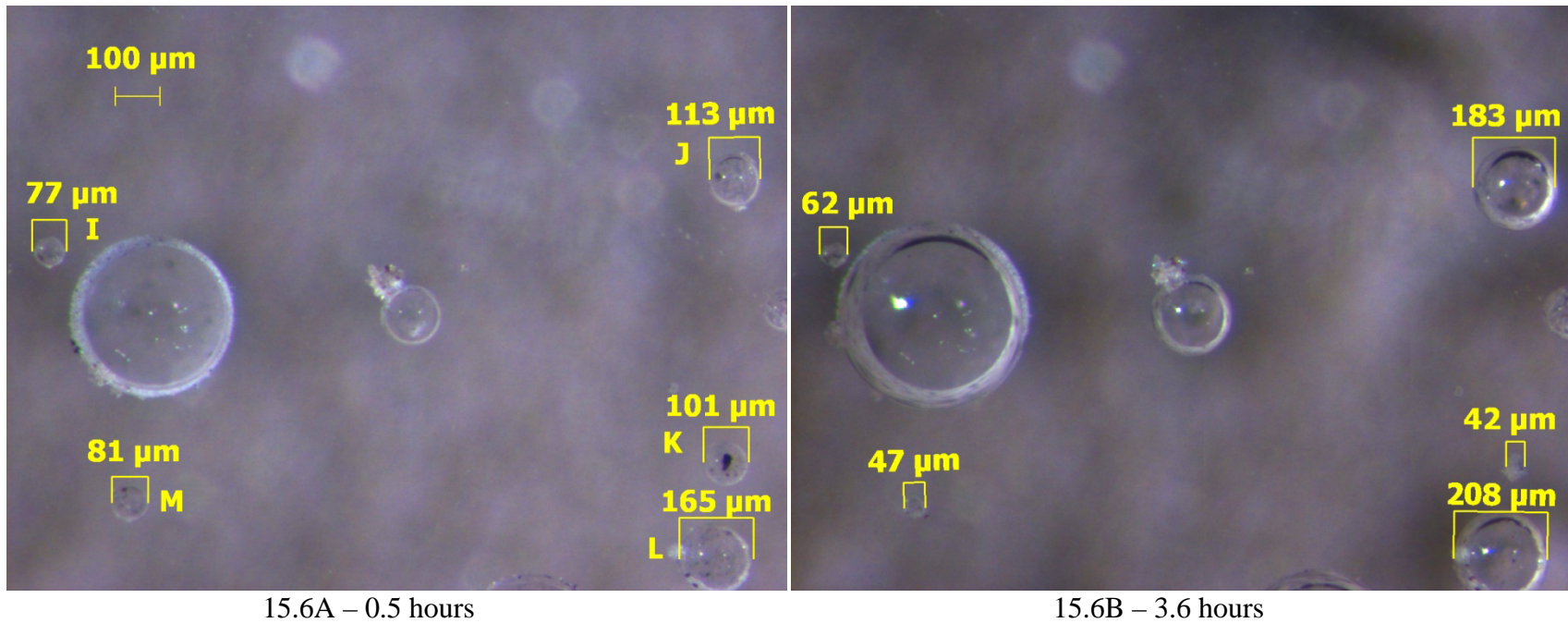


*Figure 15.6: A non-air-entrained paste sample in setup #2.
15.6A is taken 0.5 hours and 15.6B is taken 3.6 hours after hydration began.*

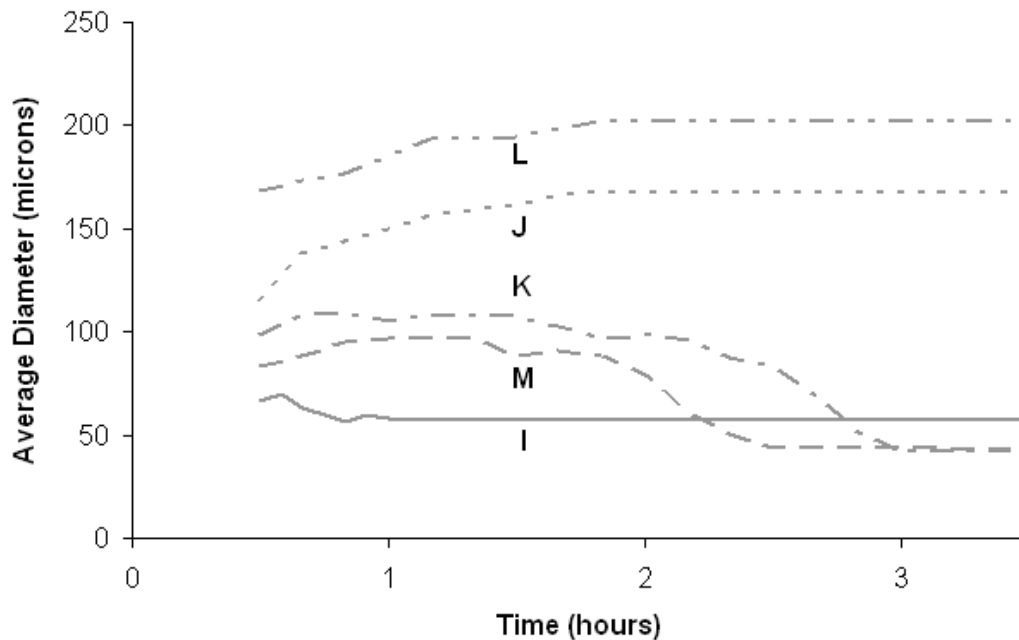


Figure 15.7: Average diameter of bubbles in a non-air-entrained paste specimen as shown in Fig. 15.6 in setup #2.

15.3.3 Setup #3-Varying Fluid Pressure

Response of an Air Bubbles to Pressure

In Fig. 15.8A an approximately 400 μm diameter bubble from mixture 6 is shown at atmospheric pressure. One first notices that the bubble shell with the Vinsol Resin and water reducer used here appears to be different from the shell observed in Figure 15.4, which had been stabilized with a tall oil AEA and no water reducer. This difference is stark and is likely to be important, but is beyond the scope of this study. Further, in Fig. 15.8A through 15.8D the fluid pressure around the bubble is being increased. In Fig. 15.8D one can see that the air bubble has decreased in diameter such that bubble volume at 0.7 bar overpressure is 58% of the volume of the same bubble at 0 bar overpressure. Since simple application of Boyle's Law would have predicted 59%, it appears that this particular bubble is behaving as an elastic, gas-filled body with no significant surface tension effects. (The degree to which this finding can be generalized to other bubble sizes, stabilized with other AEA's deserves further investigation, some of which is already in progress.) Further, it is interesting to note that the shell around the bubble does not appear to be distressed by the significant decrease in diameter during the pressurization phase. In Figs. 15.8E and 15.8F the fluid pressure is reduced to atmospheric pressure. As this is taking place one can see in Fig. 15.8E that the shell of the large air bubble cracks as the bubble is increasing in volume during the depressurization phase. These cracks widen in Fig. 15.8F as the fluid returns to atmospheric pressure. It can be seen that the void is no longer covered by the shell. Furthermore, it appears that some air contained in the bubble has been lost to the surrounding fluid during the overall pressure cycle as the final diameter does not match the initial diameter (net reduction in diameter of 6%, which would correspond to about a 17%

reduction in air volume if the internal pressure was the same before and after the pressure cycle was applied). This experiment has been repeated over 10 times with Vinsol resin and wood rosin AEAs at dosages shown in Table 15.2 and each time many but not all bubbles with diameter of 200 μm or greater were observed to crack while the pressure was decreased. (These images were chosen for their clarity.) From observations at this magnification it is difficult to observe if the shells of smaller bubbles are also damaged upon depressurization.

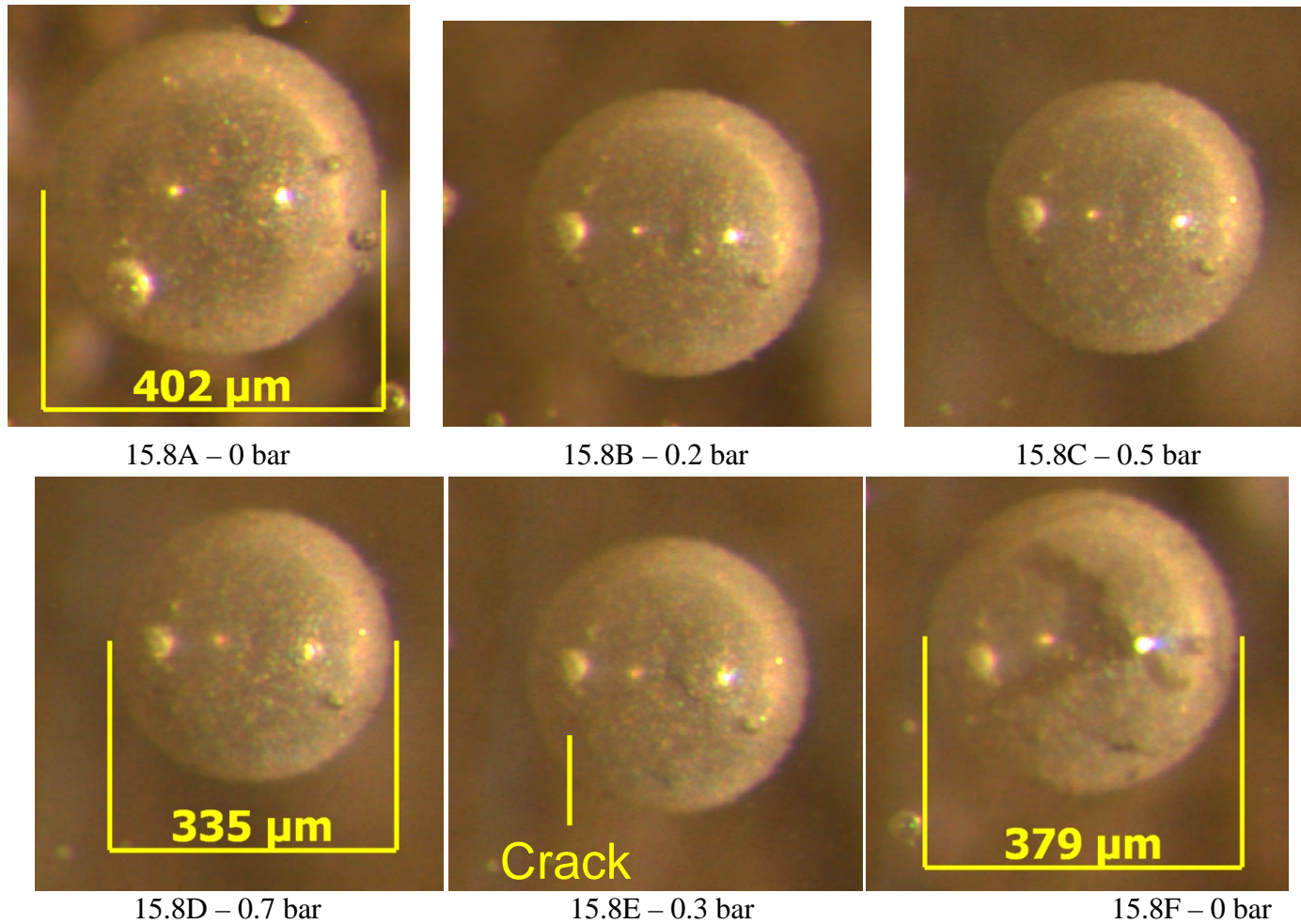
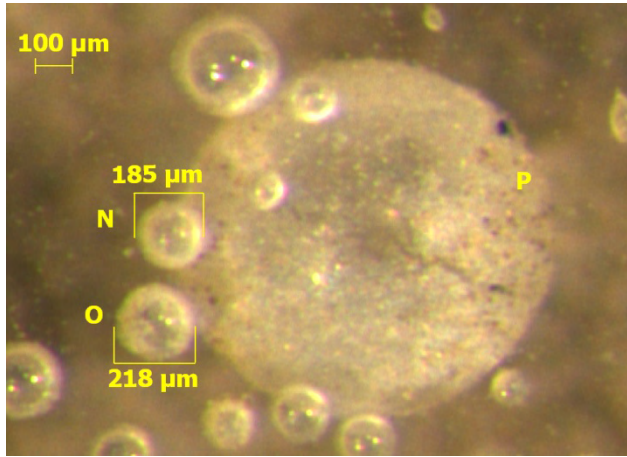


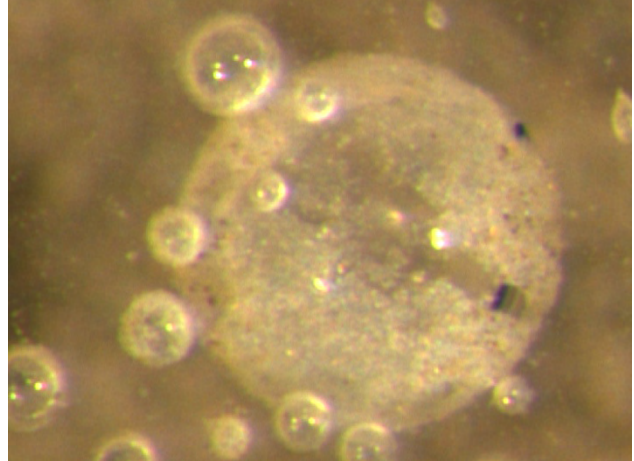
Figure 15.8: The response of bubbles escaped from a mixture containing 26 mL/100 kg cm of Vinsol resin and 81 mL/100 kg cm of normal WR subjected to a pressure 0.7 bar above atmospheric and then returned back to atmospheric pressure.

Changes in a Bubble with Time after the Shell Has Been Damaged

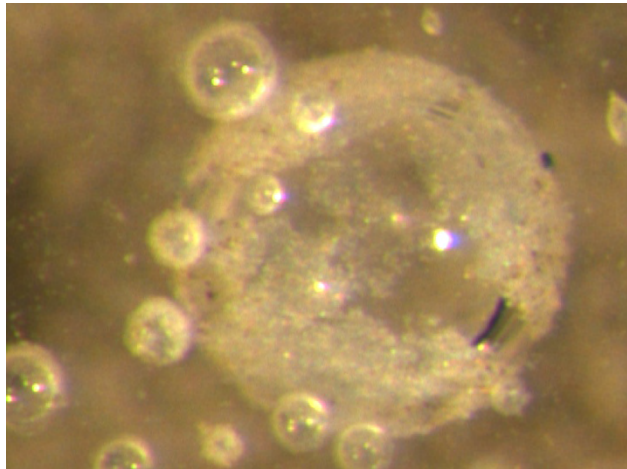
Pictures in Fig. 15.9 show the changes in a collection of bubbles stabilized with a wood rosin AEA from mixture 4 over approximately three hours after being subjected to a pressure of 0.7 bar and returned to atmospheric pressure. The pictures in Fig. 15.9 show the changes in the collection of bubbles at the conclusion of pressure cycle. As can be seen the shell of the bubble labeled P in Fig. 15.9 has been damaged during the depressurization phase and appears to be “shedded” by the bubble over time. Also the smaller bubbles N and O surrounding the large bubble P appear to shrink in diameter as P appears to expand. It should be noted that several other bubbles very close to bubble P do not show a change in size. It is unclear why only bubble N and O decreased in size. Perhaps only the shells of these bubbles were damaged during the change in pressure or perhaps as Fagerlund (1990) suggested, bubbles of this intermediate size are not yet affected by the pressure differential. Furthermore, voids N and O decreased to a certain size and then stabilized. This is the same general behavior observed in the non air-entrained paste shown in setup #2 and had been observed by Mielenz et al. (1958A). While cracking of air-bubble shells was observed many times in this present experimental series, there were insufficient observations to conclude that a change in bubble diameter is typically associated with cracking of the shells.



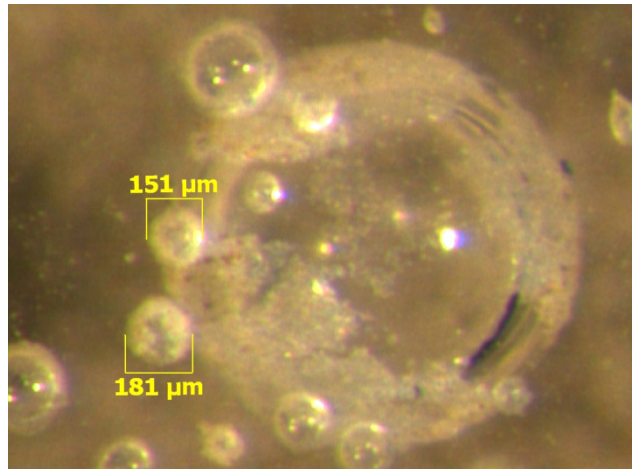
15.9A – 0.75 hours



15.9B – 1.4 hours



15.9C – 1.8 hours



15.9D – 3.4 hours

Figure 15.9: An air-entrained paste sample with wood rosin AEA at 48 mL/100 kg cm in setup #3.

As an interesting potential consequence of the observation of changes in bubble size, consider that the air bubbles observed here in water-suspension may be similar to those in cement paste that are surrounded in-place by a water filled “gap,” as observed by others (Rashed and Williamson, 1991A, 1991B; Corr et al., 2002) . It would then seem plausible that gas permeability of the bubble shell would influence gas interchange among bubbles of various sizes and internal pressures as also proposed by Mielenz (1958A) and Fagerlund (1990). This interchange could lead to a decrease in volume of the smaller bubbles and an increase in volume of the larger bubbles as observed in the experimental work in this chapter. This change in void volume could ultimately lead to a higher overall air content in the mixture as first suggested by Mielenz et al. (1958A). This phenomenon could be an explanation for observations of increased air contents (i.e., higher air contents measured in hardened concrete as compared to air contents measured in fresh concrete using a pressure meter (ASTM C 231) as reported in field concrete (Hover, 1989) and in past research (Mielenz et al., 1958A; Gay, 1982).

15.4 Summary of Key Observations

In this paper, some background is presented on the changes in a static air-void system in concrete and paste. Results from three different setups are presented that may provide insight into the fundamental behavior of air bubbles in water that have escaped from air-entrained and non air-entrained pastes. The degree to which these observations pertain to actual air bubbles fully surrounded by cement paste remains to be determined. It is pointed out, however, that the Air Void Analyzer (Jensen, 1990), the relatively new and interesting method for evaluating air bubbles in fresh concrete, liberates air bubbles into a water-glycerine solution in a far more energetic manner than was done in these experiments, and the bubbles thus liberated are considered by proponents of the method to be representative.

1. An opaque “shell” was observed on the exterior of air bubbles that had escaped from air entrained paste. The appearance of the shell changed as different AEA admixtures were used.
2. In these experiments with bubbles in bleed water, bubbles with an opaque shell appeared to resist coalescence, whereas translucent-to-transparent bubbles coalesced readily. Similarly, the shell appeared to take on structural properties such as stiffness, resistance to deformation, and eventual cracking. The role of these properties in stabilizing air bubbles within cement paste has not been identified.
3. When the shell appeared to be fully intact over observable portions of the bubble surface, the diameter of the bubbles did not change with time for the conditions of setup #2. When a readily discernible shell was not present as in the specimen of non air-entrained paste in setup #2, the diameter of the air bubbles was observed to change with time. Likewise, of those bubbles with a readily observed shell, only those that had cracked changed diameter with time.
4. In pressurized experiments shown in setup #3 it was observed that the air-bubble shell was damaged during depressurization from 0.7 bar to atmospheric pressure. This may be important in construction applications in which the concrete pressure is increased and decreased. It is not known, however, whether the experimental observations made here under a relatively mild and slow pressure change apply equally to the much higher pressure differences and rates of pressure change experienced in concrete pumping, for example.
5. A single shell-covered bubble that had escaped from air-entrained paste was observed to decrease in volume under pressure precisely as would be predicted by Boyle’s Law, with no apparent influence of the shell.

The observations reported here have been of air bubbles suspended in surrogate bleed water above paste. These observations may or may not be valid in concrete, and more research is clearly needed in this interesting and critical area of the stability of air bubbles in fresh concrete. Nevertheless the role played by what appears to be a shell of sorts at the periphery of air bubbles in air entrained concrete deserves attention.

Chapter 16. The Physical and Chemical Characteristics of the Shell of Air-Entrained Bubbles in Cement Paste

Recent research has suggested that the shell of an air-entrained void is important for resisting coalescence between air-voids and diffusion of gas from the surrounding fluid. The current chapter describes the physical and chemical properties of an air-void shell during the first two hours of hydration and chemical characteristics at 60 days. Results from this research suggest that the air-void shells found in air-entrained paste have varied physical properties and the crystalline material of these shells is largely made up of fine cement particles and calcium carbonate (CaCO_3) during the first two hours of hydration. Observations of paste at 60 days of hydration suggest that the shell is made up of calcium silicate hydrate (C-S-H) with a morphology and stoichiometry different from that in the bulk paste.

16.1 Introduction

Air-entrainment is the primary method to provide resistance to damage from freezing and thawing and salt scaling in concrete in North America. Extensive research has been performed on the bulk properties of air-entrained concrete and the distribution and volume of air-entrained bubbles. However, very little work has been done to investigate the fundamental behavior and properties of an air-entrained void and its surrounding shell. These shells have been suggested in Chapter 15 to be important in resisting the diffusion of gas into an air-entrained void from the surrounding fluid. This diffusion of gas is important as it suggests the small air-voids may diminish with time in fresh cement paste and lead to the increase in size of the more coarse air-voids and total volume of air (Mielenz, et al., 1958A). This phenomenon could explain the occasional discrepancy between the measurements of the total volume of fresh and hardened air content as reported by several workers (Hover, 1989; Gay, 1982).

The goal of the present study was to investigate possible changes in air-void size and volume in fresh paste as suggested by Mielenz et al. (1958A). A further goal was to characterize the nature of the air-void shell that governs this behavior. This chapter presents investigations of the relevant physical properties of air-entrained voids and their response to outside stress. Furthermore, x-ray diffraction (XRD), scanning electron microscopy (SEM), and energy-dispersive x-ray analysis (EDXA) are used to determine the chemical properties and morphology of the air-void shell at times of less than two hours and at 60 days.

16.1.1 Background

A review of the limited literature on the composition of air-void shells yields various hypotheses of their origin and makeup. Unfortunately very little supporting experimental work exists on this topic. In some of the earliest work done to investigate the fundamental characteristics of an air-void system in concrete, Mielenz et al. (1958A) photographed air-entrained voids in dilute pastes (i.e. high water-to-cementitious material ratio (w/cm)) with the aid of an optical microscope. These pictures showed that the perimeter of the air-entrained voids was covered by an early hydration shell. It was suggested that these shells could be made up of either a precipitated solid or gelatinous film from the calcium salts of the air-entraining agent (AEA) or metal ions contributed from the hydrating cement paste. The mechanism suggested by Mielenz et al. (1958A) to describe the shell formation is that the calcium salts of the AEA are

soluble when the material is mixed in the bulk paste but could precipitate once concentrated around the air-water interface. To demonstrate this behavior, common AEAs were mixed with saturated lime-water and a white and brown insoluble precipitate formed. It was suggested that this insoluble material comprises the air-void shells. Mielenz et al. (1958A) also observed that cement particles were attracted to the surface of the air-entrained void.

Dodson (1990) pointed out that all commercially available AEAs are anionic in nature. This suggests that the hydrophilic portions of the surfactant molecules align themselves preferentially around the perimeter of an air-void and that these molecules are negatively charged. Dodson also suggested that the calcium ions, with their high charge density, are attracted to the negatively charged, hydrophobic ions stabilizing the bubble and these react to form an insoluble calcium salt, which was suggested to be a calcium rosinate. However, Dodson did not provide any experimental evidence to support this hypothesis. A study by Pigeon and Plante (1990) that utilized SEM with microprobe analysis on specimens prepared with high dosages of alkaline salts suggested that there were increased concentrations of sodium and potassium ions around air-entrained voids. The concentration was much larger than would be expected to be provided from the AEA and larger than that measured in the bulk cement paste. However, calcium ion concentration was not investigated in this study and the methods utilized did not allow observations of the bulk paste.

Several other studies investigated the mechanisms of freeze-thaw damage and the characteristics of air-void shells (Rashed and Williamson, 1991A, Rashed and Williamson 1991B; Corr et al., 2002). These studies featured samples whose hydration had been stopped by cryogenic freezing. The samples were then investigated in a low temperature scanning electron microscope (LTSEM). A technique was also developed that allowed the air-voids to be separated from the paste and then frozen and investigated with the LTSEM. Upon freezing, these air-voids were largely irregular in shape and seemed to be made up of heterogeneous fine particles that were between 1 and 5 μm . The researchers hypothesized that the particles surrounding the air-voids at least partially consist of unhydrated cement particles (Corr et al., 2002). Observations were also made of the morphology and interface between the air-void shells and the bulk paste (Rashed and Williamson, 1991B, Rashed and Williamson 1991B; Corr et al., 2002). The hydration products were suggested to be very dense over the 1-2 μm shell and a 10-15 μm water-filled space seemed to exist between the shell and the bulk paste. This gap was reported to increase in size as the w/cm of the mixtures increased and decreased in size with increased hydration.

16.2 Experimental Methods

Due to the lack of available information regarding the basic physical and chemical properties of the air-void shells in concrete, an experimental program was developed to better characterize this material. In this study, several physical properties of the shells were investigated using a novel technique of isolating the bubbles in bleed water and then examining their response to stress. The behavior of the bubbles was captured with a digital camera fitted to a stereomicroscope at 50x magnification.

Chemical properties of the shell were also evaluated over the first 2 hours of hydration and at 60 days of hydration with the use of XRD and SEM with EDXA. The goal of this study was to investigate the microstructure and composition of the air-void shell and how they change with time with the hopes that this would lead to a better understanding of the behavior of the air-void shell and how it can ultimately be improved.

All of the specimens in this study were produced with a 0.42 w/cm paste using 1.37 kg of cement meeting the ASTM C 150 specifications for Type I and II with a 0.53 alkali content ($\text{Na}_2\text{O}_{\text{eq}}$). The phases of the cement were determined by Rietveld quantitative x-ray diffraction (RQXRD) (Rietveld, 1969; Stutzman, 1996) analysis and are reported in Table 16.1 as the specimens at zero minutes of hydration. The mixer and mixing procedure used in this study met requirements of ASTM C 305. All other details of the specimens are given in the respective sections.

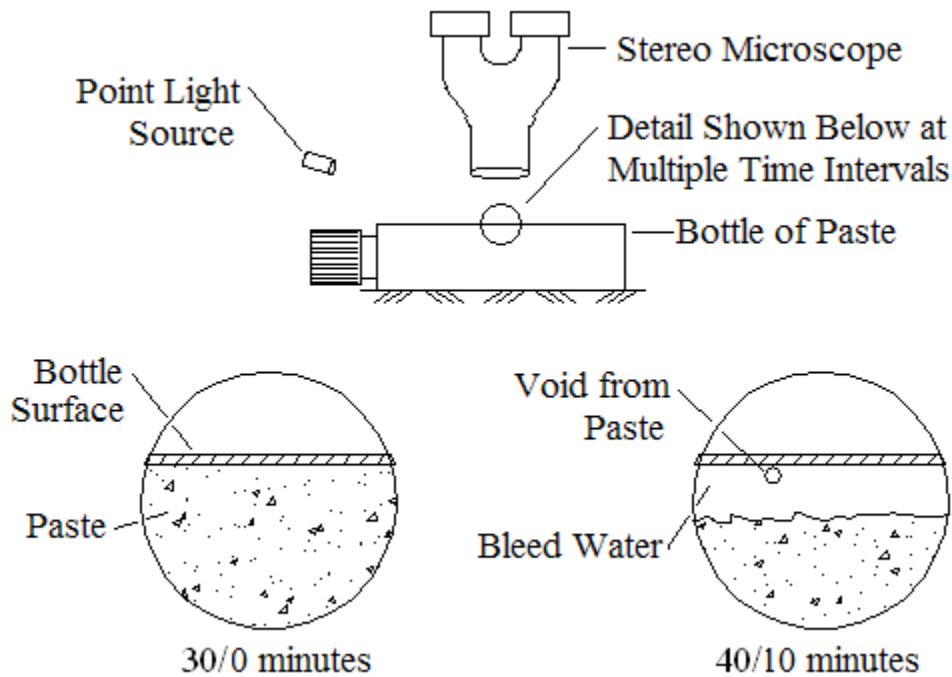
Table 16.1: Summary of the RQXRD analysis for the air-void shells and bulk paste.

	Time	C_2S %	C_4AF %	C_3A %	CaCO_3 %	C_3S %	Ettringite %	Gypsum %
wood rosin	0	15.7	8.7	2.7	2.6	68.0	0.8	1.3
	8	17.6 (0.8)	13.6 (1.2)	5.6 (0.9)	8.0 (0.8)	50.5 (2.4)	2.6 (2.1)	2.0 (1.4)
	30	20.9	16.4	4.3	12.7	38.2	5.3	2.2
	45	18.9 (4.0)	14.7 (0.6)	5.8 (1.6)	14.7 (3.0)	41.6 (0.4)	1.3 (0.3)	3.2 (0.1)
	90	20.7 (1.5)	16.5 (0.5)	5.5 (1.2)	14.1 (0.9)	38.3 (0.5)	2.2 (2.5)	2.8 (0.4)
	120	22.5 (3.9)	16.5 (1.6)	5.2 (1.2)	14.6 (2.7)	35.5 (6.5)	4.1 (3.3)	1.6 (0.8)
synthetic	0	15.7	8.7	2.7	2.6	68.0	0.8	1.3
	8	18.2 (0.2)	18.8 (2.7)	4.7 (0.4)	21.9 (5.7)	33.1 (9.5)	0.9 (0.4)	2.4 (1.0)
	30	16.0 (0.7)	14.6 (1.4)	6.6 (0.4)	20.8 (3.9)	36.1 (5.5)	3.8 (0.1)	2.1 (1.2)
	45	15.4 (0.4)	18.0 (5.8)	5.0 (1.3)	18.6 (6.2)	38.7 (12.8)	1.7 (1.1)	2.7 (2.8)
	60	18.7 (3.9)	15.8 (2.1)	5.0 (1.2)	18.0 (8.0)	38.5 (8.1)	3.0 (1.2)	1.1 (0.5)
bulk paste	0	15.7	8.7	2.7	2.6	68.0	0.8	1.3
	10	10.1	7.1	2.7	4.7	67.7	2.6	5.1
	45	13.0 (3.7)	8.2 (0.9)	2.9 (1.2)	6.4 (2.5)	60.3 (1.4)	1.6 (0.5)	7.6 (2.4)
	90	13.7	8.7	3.8	6.6	60.0	1.6	5.6
	120	13.6	12.5	4.2	4.7	58.4	0.7	6.0

The values at 0 minutes of hydration correspond to the unhydrated cement. All values shown are the percentage of crystalline material analyzed. The standard deviation is shown in parenthesis.

16.2.2 Physical Properties

All of the observations of physical properties of the air-void shells were made by using a novel technique to investigate air-voids in the bleed water of cement paste contained in a bottle as shown in Fig. 16.1.



The detail cross-section is at two time intervals. The time is displayed in minutes after initial hydration/time after the bottle was placed on its side.

Figure 16.1: The experimental setup for the physical testing showing the orientation of bottle, stereoscope, and point light source.

The following is a short summary of the experimental technique:

After the mixing of the paste was completed, a funnel was used to transfer the material into a transparent polystyrene bottle. The bottle was filled in three equal volumes and agitated after each addition of paste by tapping on a table top. Care was taken to ensure the bottle did not have any large air-voids, and was filled to capacity. At this point, the cap was tightened and the bottle was placed horizontally. After sitting for approximately 10 minutes it was possible to observe a layer of bleed water forming at the surface of the paste (Fig. 16.1). In this bleed water, air-voids could be found that had worked their way to the surface of the paste due to their buoyancy. These voids were then observed and documented using a stereomicroscope fitted with a digital camera. A computer program was written to automatically capture images of the changes in these voids at specified intervals of time.

For some of the specimens, the same preparation technique was used; but an air pump was attached to the bottle of paste with a pressure regulator and gage. This allowed the fluid pressure inside of the bottle to be increased or decreased in any manner while the bubbles were investigated with the stereomicroscope and digital camera. The air-voids were investigated while they were subjected to an increase and then sudden decrease in fluid pressure similar to what might be imposed by a concrete pump.

With these experimental setups, the following physical properties of air-entrained bubbles were investigated: adhesion of cement particles, transparency, the response of bubbles to fluid pressure, and the ability of the air-void shell to repair after being damaged.

16.2.3 Chemical Properties during the First Two Hours of Hydration

In order to determine the chemical consistency of the air-void shell, the air-voids were separated from the paste at different time periods, in this case from eight minutes to two hours of hydration by injecting a 20 cm³ sample of air-entrained paste into the bottom of a tall column of water utilized by the Air-Void Analyzer as this provided an useful method to liberate the bubbles from the paste. A stirring rod at the bottom agitated the paste and the bubbles rose up the column. The bubbles were caught at the top of the column with an inverted watch glass. After collecting bubbles for three minutes, the watch glass was removed. The majority of the bubbles collected adhered to the watch glass surface. The excess water was removed from the watch glass with a syringe and the specimen was placed in a vacuum desiccator overnight. The dried material was scraped from the watch glass and stored under vacuum until the crystalline material could be analyzed by RQXRD. Because so little material was collected during the bubble separation (approximately 5 mg) it was necessary to use a standard height low-background quartz-disk specimen holder. The specimen holder was covered with a thin layer of petroleum jelly to insure the material would adhere to the holder. The sample was sprinkled onto the jelly and then spread out so a thin layer of material covered the surface. Care was taken to ensure that a low profile of powder was used for the sample, such that proper specimen height was maintained, thus minimizing sample-displacement error. A sample holder was also analyzed that was only covered in petroleum jelly and was found to give only slight background noise at low angles of investigation. This was determined to not impact the accuracy of the quantitative analysis.

This technique was utilized to analyze air-voids from pastes containing wood rosin and synthetic AEA dosed at 48 mL/100 kg of cement at various time intervals, up to two hours of hydration. A non air-entrained paste was also investigated after 30 minutes of hydration. The same cement was used for this testing as was used for examination of the physical properties of the air-voids.

Another set of tests was conducted on samples of hydrated cement paste obtained from a bulk cement paste containing 48 mL/100 kg of cement of a wood rosin AEA which was allowed to hydrate in the mixing bowl and was stirred by hand prior to a sample being extracted at time intervals of hydration from 8 minutes to 2 hours. No petroleum jelly was used for this analysis as the paste was placed directly on the low-background sample holder at the reported time of hydration and then placed in a drying vacuum. It is unclear how long it took the water to be removed from the sample. While visual observations of the color change of the sample indicate that drying was complete within 5 minutes under vacuum, drying was allowed to continue overnight. A low-background sample holder was used so that the sample preparation between the two methods was kept as similar as possible. After the specimens were dried, the height of the sample was reduced to the clearance of the zero background sample holder in order to minimize the sample displacement.

Cement samples were also analyzed by preparing approximately 2 g of cement in a standard powder-mount sample holder. The RQXRD analysis was performed with a Siemens D500 x-ray diffractometer equipped with a DACO_MP digital controller and analog-to-digital signal converter. All samples were analyzed from 20° to 80° 2θ, with a step size of 0.02° and dwell time of 4 seconds/step. The atypically lengthy step provided a sufficient x-ray signal-to-noise ratio for rigorous quantitative analysis. A traditional 2200 watt copper (Cu) x-ray tube was used. The diffractometer was configured with a 1° divergent slit, a 4° soller slit, and a 1° antiscatter slit on the incident-beam side. A 1° antiscatter slit, a 4° soller slit, a single-crystal

monochromator, a 0.15mm receiving slit, and a 0.6 mm detector slit were used on the divergent-beam side. Each pattern was analyzed using the whole-pattern fitting method developed by Rietveld (1969) and demonstrated for use in cementitious materials by Stutzman (1996) using the TOPAS-Academic software package.

16.2.4 Chemical Properties after 60 Days of Hydration

Air-entrained paste made with wood rosin AEA at 48 mL/100 kg of cement was allowed to hydrate inside of a bottle shown in Fig. 16.1 in a 100% RH environment for 60 days. The sample was fractured and a small flake about 2 mm thick of the now exposed, interior surface was examined for air-entrained voids using a SEM with EDXA. The SEM used was a LEO 1530 Field Emission SEM equipped with an IXRF solid-state energy dispersive spectrometer. The operating voltage was 15kV, working distance = 11 mm, X-ray count rate = 400 cps, and EDXA dwell time = 60 seconds. The sample was sputter-coated with a 20 nm thick layer of silver to provide conductive continuity.

16.3 Results and Discussion

16.3.1 Physical Properties

Adhesion of Cement Particles

In Fig. 16.2, a paste made with wood rosin AEA at a dosage of 48 mL/100 kg of cement is shown after 10 minutes of hydration. When the void leaves the cement paste and rises to the surface, one can clearly see a significant portion of cement paste is adhering to the air-entrained void and is also carried up to the surface of the bottle. While it is difficult to determine the volume of the paste that is attached to the void, it is obvious that the quantity is significant. This implies that the attraction between the cement particles and the air-entrained bubble is significant and may be measurable. This observation is not an anomaly and the adhesion of cement to air-entrained bubbles is regularly observable in the specimens investigated for this study. This observation confirms previous work by Mielenz et al. (1958A) and hypothesized by Corr et al. (2002).

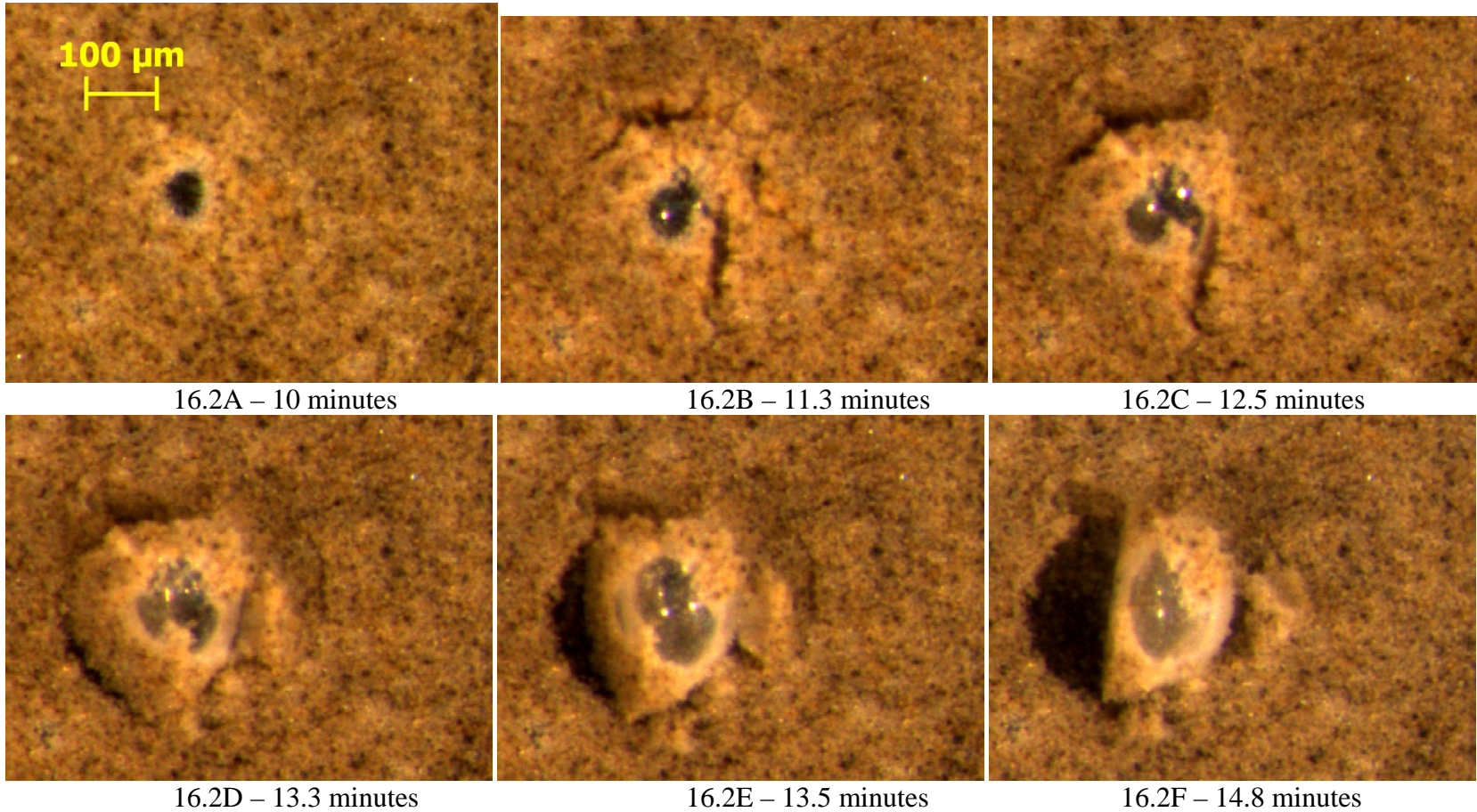
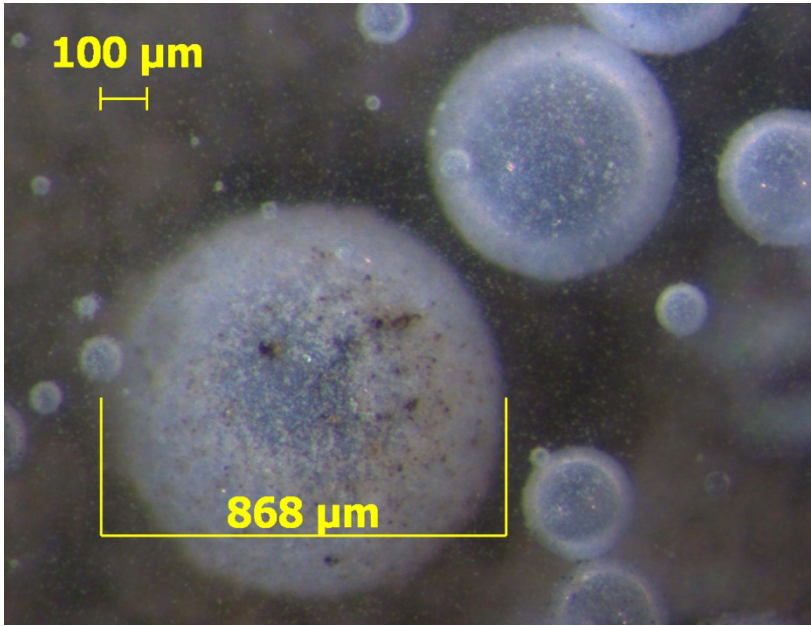


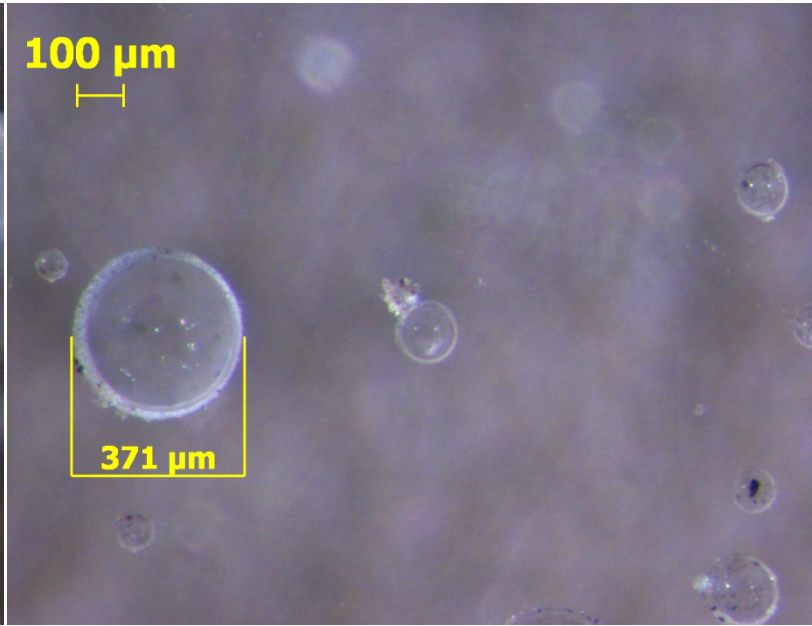
Figure 16.2: An air-entrained void is shown emerging from a cement paste surface due to buoyancy with cement grains attached. The paste was made with 48 mL/100 kg of cm of wood rosin AEA.

Transparency

Air-voids from a paste with wood rosin AEA used at a dosage of 48 mL/100 kg of cement are shown in Fig. 16.3A. The air-voids shown in Fig. 16.3B are from a paste with no AEA. Both pictures were taken approximately 45 minutes after mixing. There is a significant difference in the transparency of voids in air-entrained and non air-entrained pastes, the former are translucent while the latter are transparent. This difference in transparency is likely attributable to the shell material that has been shown to exist around voids in air-entrained paste and is missing from voids in a non air-entrained paste. These shells seem to be present at AEA dosages typically used in concrete. The translucent air-void shells were regularly observed for the following AEAs: wood rosin, Vinsol resin, tall oil, and synthetics. The appearance of the shells is different for each of the AEAs. Very little difference was observed for different dosages of AEA, but more work is needed in this area.



16.3A



16.3B

Figure 16.3: A. Air-entrained void (48 mL/100 kg of cm wood rosin AEA) after 45 minutes of hydration, B. Non air-entrained voids after 45 minutes of hydration.

Bubble Response to Fluid Pressure

Vinsol Resin AEA

An air-void in the bleed water of an air-entrained paste with 26 mL/100 kg of Vinsol resin AEA and 81 mL/100 kg of a polymer-based normal range water reducer is shown at atmospheric pressure in Fig. 16.4A after 45 minutes of hydration. For this test, the fluid surrounding the air-void system was increased to 0.7 bar above atmospheric pressure in 10 equally spaced steps and then decreased back to atmospheric pressure in three equal steps. A selected number of images are shown in Fig. 16.4 with Figs. 16.4A-D showing the results of increasing pressure and Figs. 16.4E and F showing voids while the pressure is decreasing.

In Fig. 16.4D, one can see that the air-void has decreased in diameter by almost 20% at a pressure of 0.7 bar and yet the bubble does not appear to be distressed. As the pressure began to be released, it can be seen in Fig. 16.4E that the shell of the large air-void cracked as the volume of air increased inside the void. These cracks widen in Fig. 16.3F as the fluid was brought back to atmospheric pressure. This is significant as it has been previously proposed that after the air-void shell has been damaged, it is possible for an interchange of air to occur from the surrounding fluid, then a change in the air-void distribution and volume can occur (Mielenz et al., 1958A). It appears that some amount of air was lost to the surrounding fluid during the increase in fluid pressure as the final diameter is 6% lower than the initial diameter. Similar behavior was found for voids of a similar size stabilized by wood rosin AEAs. This behavior has been witnessed regularly for voids that are larger than 200 μm . However, it is difficult to say whether the behavior occurs in voids that are smaller as they are difficult to observe at the magnification used.

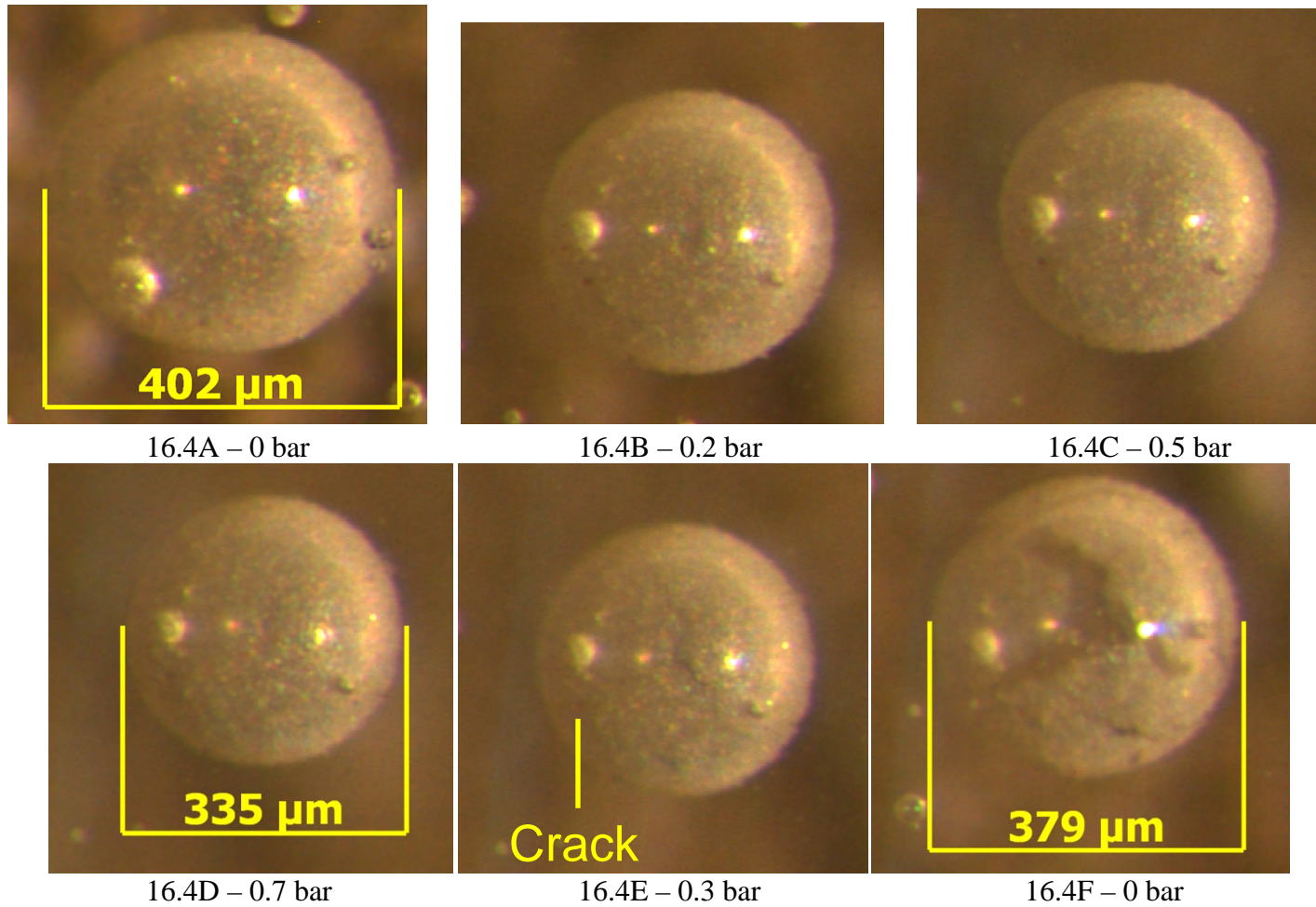


Figure 16.4: The response of a mixture containing 26 mL/100 kg cm of Vinsol resin and 81 mL/100 kg of normal range water reducer subjected to a pressure 0.7 bar above atmospheric and then returned back to atmospheric pressure.

Synthetic AEA

A void in the bleed water of air-entrained paste with 47 mL/100 kg dosage of a synthetic AEA and 85 mL/100 kg of normal range water reducer is shown in Fig. 16.5A after 45 minutes of hydration. The surrounding fluid pressure was increased to 0.7 bar in 5 equal pressure steps and then decreased back to atmospheric pressure in three equal pressure steps. Selected images are shown in Fig. 16.5.

At a pressure of 0.3 bar, the shell of the air-entrained void began to distort as shown in Fig. 16.5B. As the fluid pressure increased, so did the distortion of the void. It can be seen in Fig. 16.5C that the bubble was no longer spherical and had a significant crease at the center. Whenever the air pressure was reduced back to atmospheric the shell returned to a size within 5% of the original diameter. Also, during this increase and decrease in pressure, the shell of the void was never permanently damaged. This test was performed five times and the behavior was similar for voids larger than 40 μm . Voids smaller than this did not appear to show the same buckling of the shell; but it is very difficult to observe small voids at this magnification.

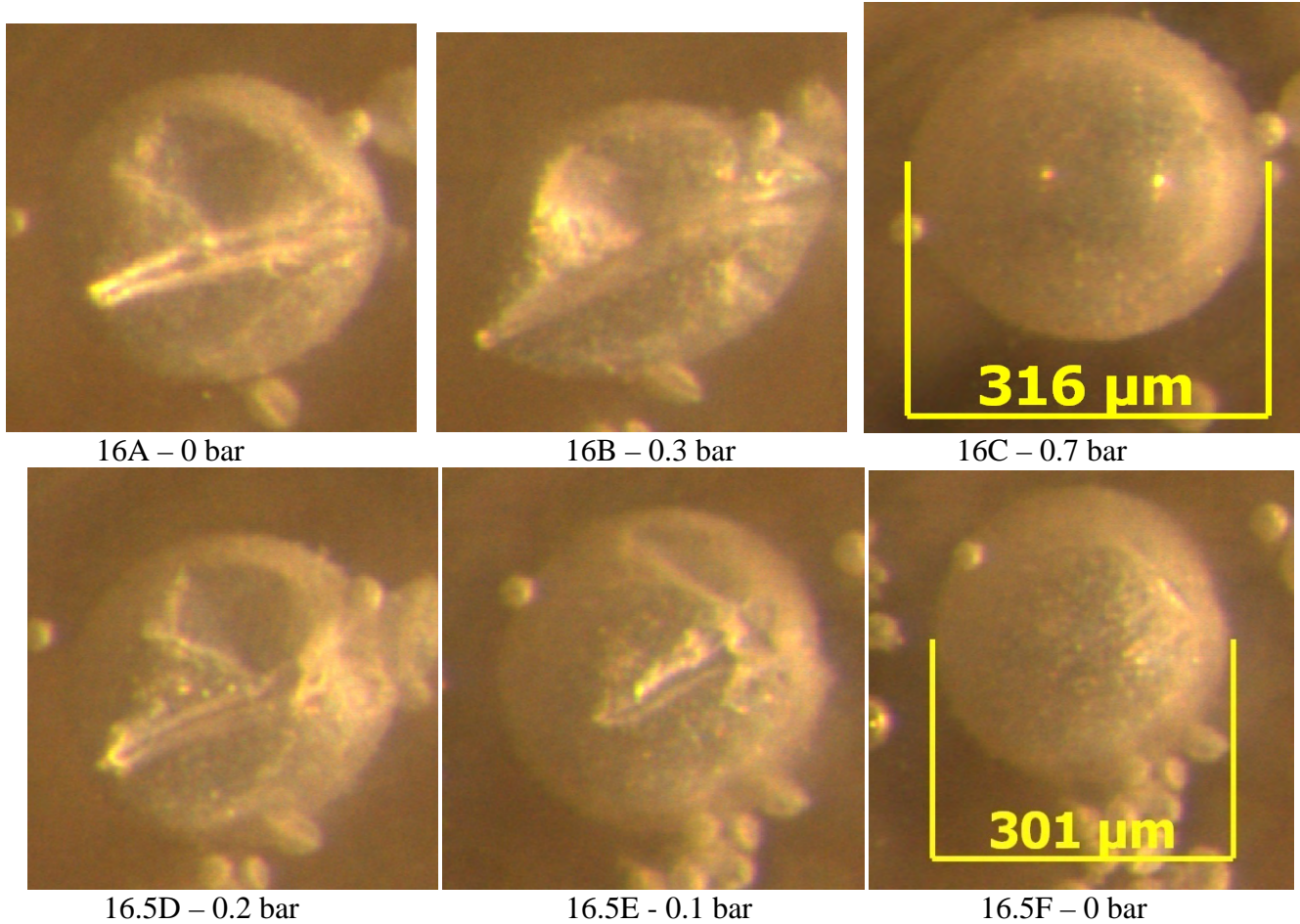


Figure 16.5: The response of an air-entrained void in a mixture (47 mL/100 kg of cm of synthetic AEA and 81 mL/100 kg of normal range water reducer) subjected to a pressure 0.7 bar above atmospheric and then returned back to atmospheric pressure.

Differences in AEAs

It is clear that there is a significant difference in behavior between the synthetic and the Vinsol resin and wood rosin AEAs. The air-void stabilized with the synthetic AEA seemed to buckle as the surrounding fluid pressure was increased. This seems to imply that the air-void shell has some stiffness in compression and a substantial amount of elasticity in tension as the void did not crack when the fluid returned to atmospheric pressure. On the other hand, the air-void stabilized with the Vinsol resin was very elastic when the fluid pressure was increased and seemed to be very weak in tension. It is unclear why there is such a large difference in behavior between the two products. However, this difference in behavior is possibly attributable to the difference in the molecular structure of the AEA or the resulting air-void shell, and thus the surrounding hydration products.

Self Repairing

In Fig. 16.6 an air-void above a paste containing 48 mL/100 kg of wood rosin AEA that has been pressurized to 0.7 bar and then depressurized to atmospheric pressure is shown over a 5.7 hour time period. As stated previously, the shell of air-voids in wood rosin systems crack while being depressurized. Fig. 16.6A shows a void with a cracked shell immediately after the return to atmospheric pressure. Over the next 0.4 hours the shell continues to crack and expose more of the underlying bubble, Fig 16.6B. This occurred while the bottle sat undisturbed. At 3.6 hours after hydration began, the shell around the air-void begins to reform, Fig. 16.6C. Pictures are shown of the shell reforming over the next 2.8 hours. In Fig. 16.6F an image is shown after 6.4 hours of hydration and it appears that the shell has repaired itself completely and no cracks are present.

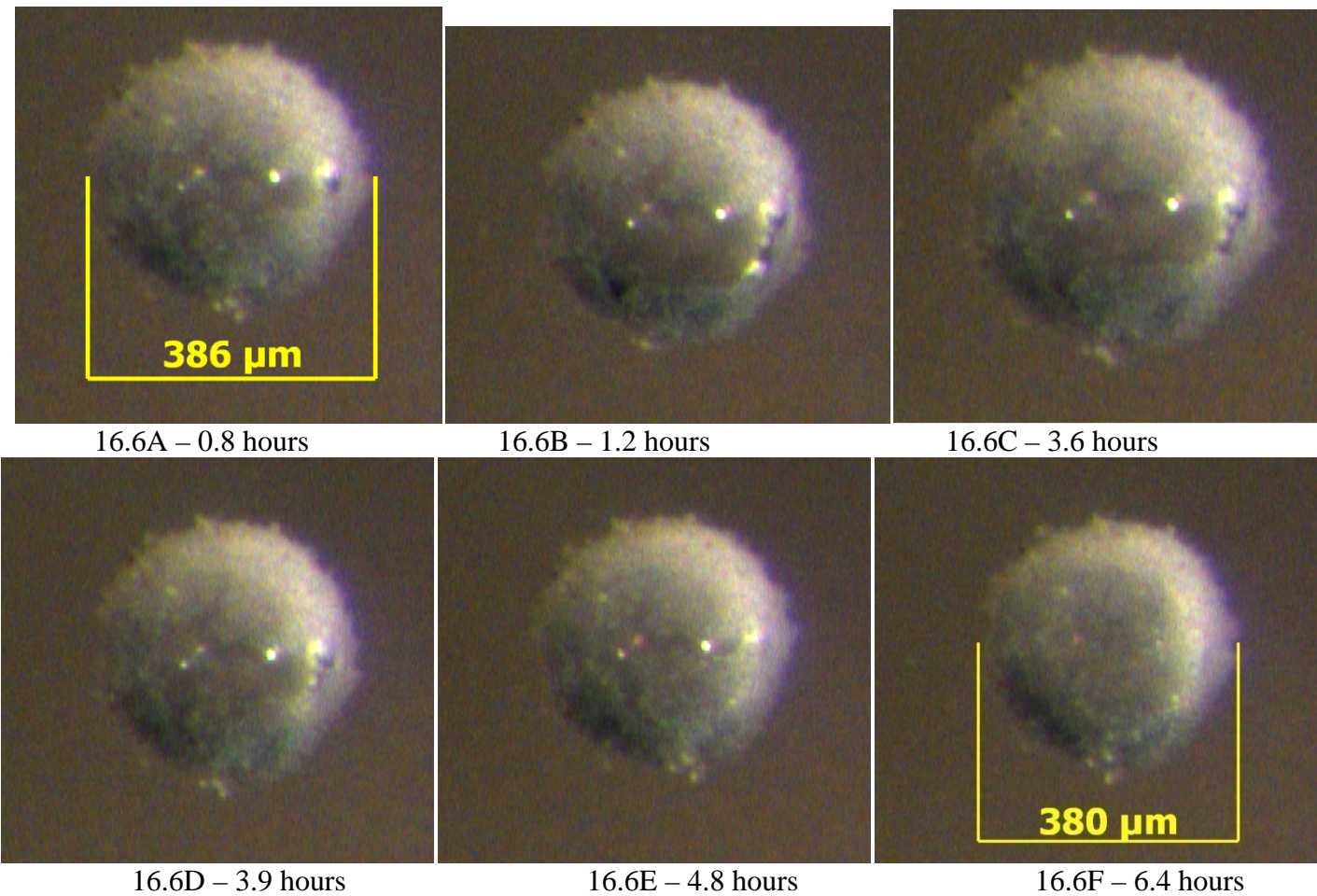


Figure 16.6: A void in bleed water above a cement paste (48 mL/100 kg of cm of a wood rosin AEA) was subjected to a pressure 0.7 bar above atmospheric and then returned back to atmospheric pressure.

If an air-void shell were able to self heal itself, then this behavior could provide a method for the air-void to recover from damage to the surrounding shell as previously shown with changes in pressure. One reason why the shell in Fig. 16.6 may have taken such a long period of time to repair itself was the large amount of damage that was done to it. If this damage had been less severe, then the repair might have taken less time. These observations may also help provide insight into the mechanisms of the initial air-void shell formation. Three other observations of self healing have been observed but none as dramatic as the one shown in Fig. 16.6. On the majority of the tests completed it was very difficult to see the shells being repaired as the cracks in the bubbles are small and the repairs seem to take less time.

16.3.2 Chemical Properties

Chemical Properties during the First Two Hours of Hydration

Table 16.1 contains a summary of the crystalline material analyzed in the air-void shells in pastes containing wood rosin and synthetic AEAs over time. Table 16.1 also contains results from analysis of the crystalline materials in the bulk paste. These data were obtained through RQXRD analysis. The data for the unhydrated cement indicate the composition of the starting material. Repeat specimens were run for the majority of the data points and the values presented in Table 16.1 are averages with standard deviations in parenthesis. While some variability was found, it was determined to not be significant for phases that were present in quantity greater than 10% of the overall crystalline material of the sample. Variability in RQXRD is generally on the order of at least 3% (Chancey, 2007).

All of the specimens analyzed contained the same crystalline phases; however, the amount of each phase present in the sample varied with sample type and time. The results indicate that there is very little change in the crystalline phases present in the bulk cement paste over the first two hours of hydration. This is not surprising since the onset of significant C_3S hydration is not expected in this time period at room temperature in the absence of accelerators. The increase in gypsum content may be a reflection of the hydration of hemihydrate and anhydrite. The changes in quantities of the other phases are within error and can be considered negligible.

For the specimens taken from the air-void shell material it was found that there was a significant change in the amounts of anhydrous material and $CaCO_3$ with time in the samples. The C_3S and $CaCO_3$ contents are shown graphically in Fig. 16.7. In each of the types of air-void shells it appears that there is less C_3S than in the original cement. In the wood rosin AEA shells, the C_3S content appears to decrease between 8 and 30 minutes, then remains constant. In the synthetic AEA shell, the amount of C_3S decreases from the initial amount found in the cement and then is constant with time.

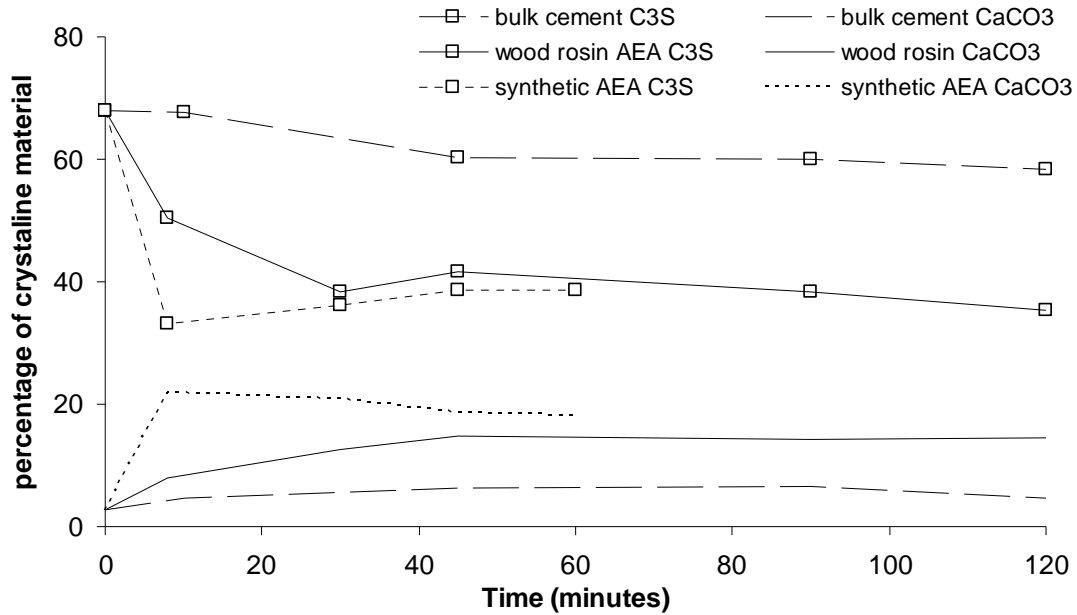


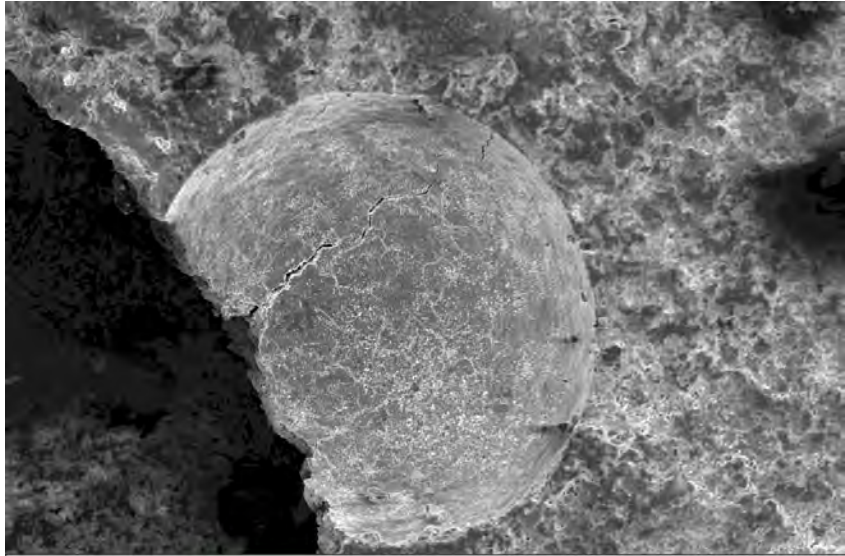
Figure 16.7: Change in C_3S and $CaCO_3$ content with time is shown for the bulk cement paste and the air-void shells created with wood rosin and synthetic AEAs

Correspondingly, the percentage of other phases crystalline phases present are observed to increase with time. This is expected if dissolution of C_3S is occurring. Another interesting observation is that the amount of $CaCO_3$ is higher in the air-void shells than in the original cement and increases with time up to 30 minutes. After 30 minutes the amounts of $CaCO_3$ remain constant. The increase in $CaCO_3$ seems to occur at an increased rate when the specimen is made with the synthetic AEA compared to wood rosin AEA, but they reach the same constant level with time.

The changes in anhydrous phases and the presence of so much $CaCO_3$ in the air-void shell material are unexpected. More discussion on these observations appears later in the chapter. However, whatever the mechanism for the increase in $CaCO_3$ is it is likely tied to the reduction in the C_3S as they occur simultaneously and proportionately.

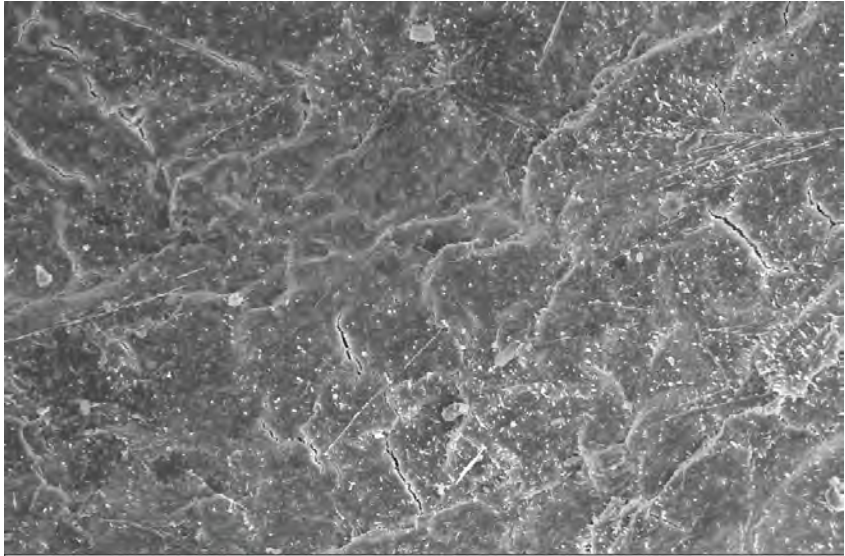
Chemical Properties at 60 days of Hydration

An air-entrained void approximately 550 μm in diameter was found on a fractured hardened cement paste surface and investigated with a SEM with EDXA. A top view of the air-void is shown in Fig. 16.8A and magnified pictures of the air-void wall are shown in Figs. 16.8B-D. The interface between the air-void shell and the bulk paste is shown in Fig. 16.9A and at increased magnification in Fig. 16.9B. From Fig. 16.9 it appears there is a 1 μm thick shell of hydration product surrounding the air-void. Just adjacent to the shell there appears to be a discontinuity between the phases in the shell and the bulk paste of the sample, similar to the observations mentioned previously (Rashed and Williamson, 1991A, Rashed and Williamson 1991B; Corr et al., 2002). The shell seems to be made of a very dense hydration product. Furthermore, it seems small crystals are growing on the surface of the void. Visual and EDXA analysis suggest that these crystals are ettringite.



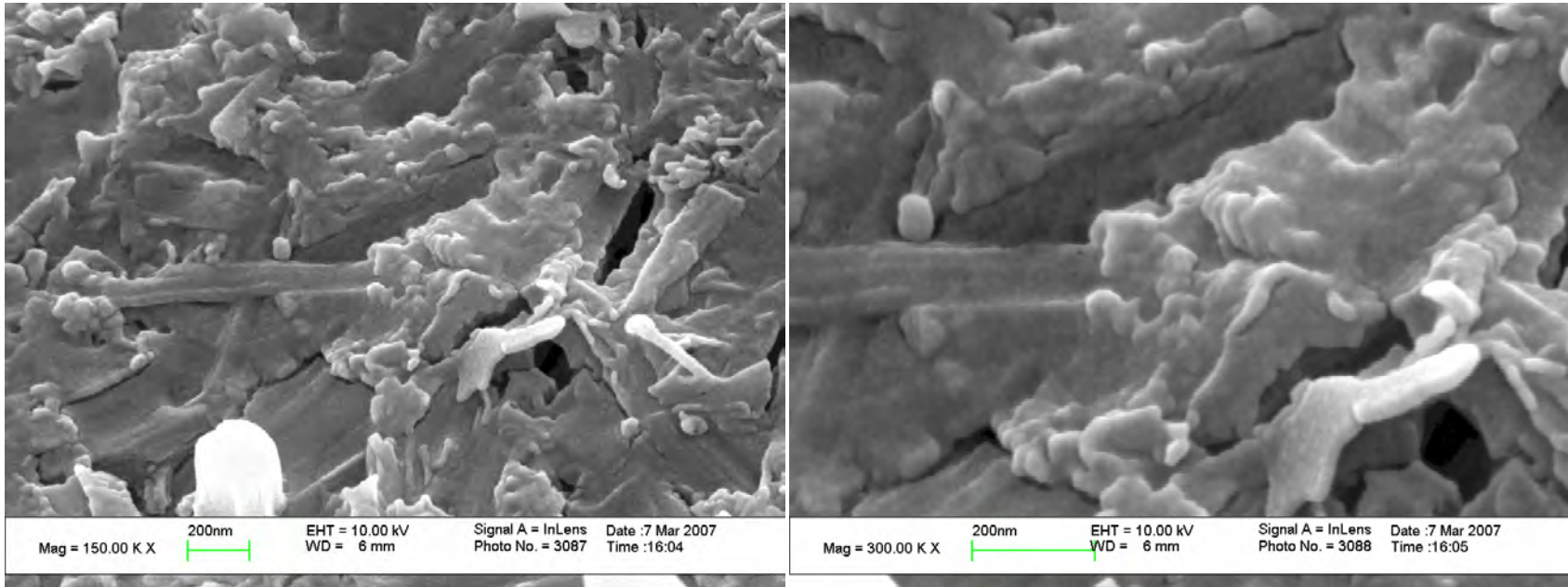
Mag = 375 X 100µm EHT = 10.00 kV Signal A = InLens Date :7 Mar 2007
WD = 12 mm Photo No. = 3103 Time :17:31

16.8A



Mag = 2.05 K X 10µm EHT = 10.00 kV Signal A = InLens Date :7 Mar 2007
WD = 11 mm Photo No. = 3090 Time :16:17

16.8B



16.8C

16.8D

Figure 16.8: SEM image of an air-entrained void from a mixture containing wood rosin AEA at 48 mL/100 kg of cement that was allowed to hydrate for 60 days before examination. An overview of the void is shown in Fig. 16.8A. The surface of the air-void is shown in Fig. 16.8B. Fig. 16.8C and 16.8D show the voids surface under increased magnification.

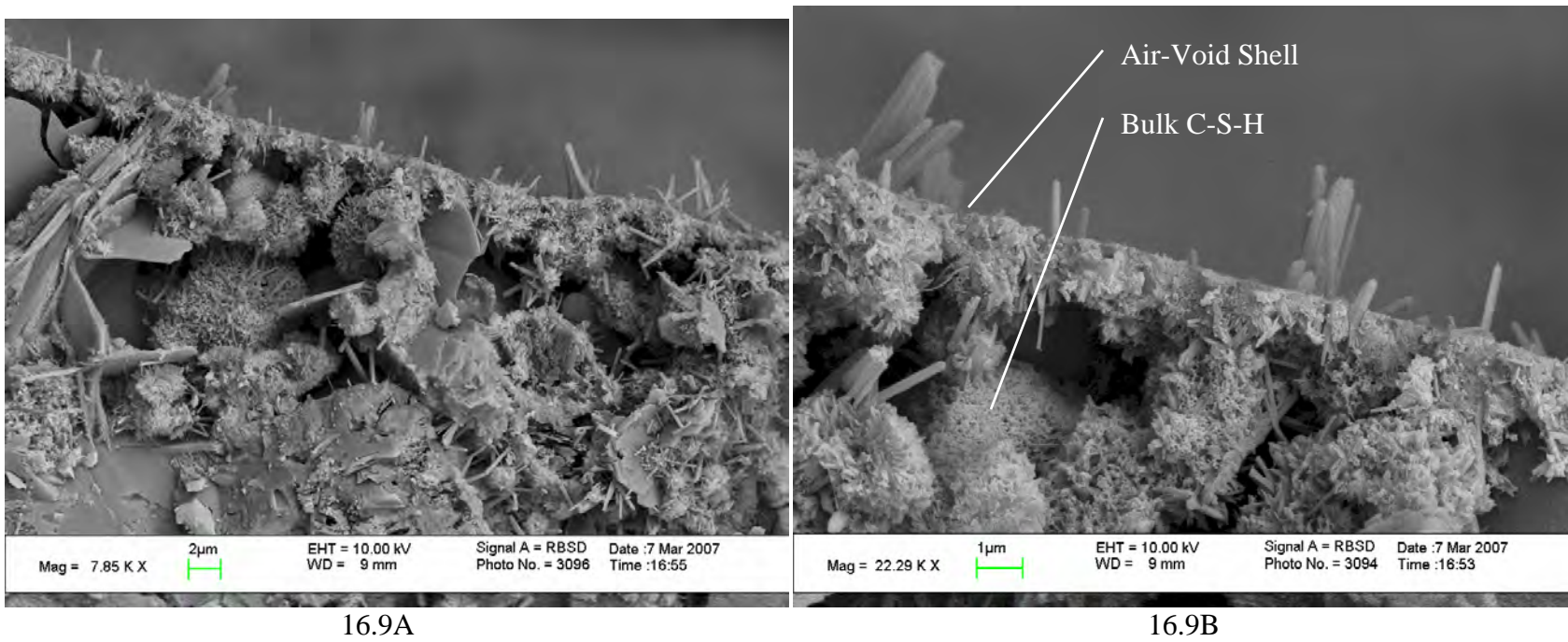


Figure 16.9: A SEM image of the interface between the air-void in Fig. 16.8 and the bulk paste. In Fig.16.9B a closeup is shown of Fig. 16.9A.

The air-void surface in Fig. 16.8B is shown in Fig. 16.8C and 16.8D under increasing magnification. At this high magnification one is able to closely examine the very dense microstructure of the air-void shell. To investigate the chemical composition of the shell, the area shown in Fig. 16.8B was investigated with EDXA. The surface analyzed was approximately $185\ \mu\text{m} \times 135\ \mu\text{m}$. Since this analysis is taken over a large area it should be representative of the chemical makeup of the void surface. EDXA gives information on the relative amounts of the elements present. The ratios of the peak heights can be compared to find the relative quantity of each element. It was determined that the majority of the sample was made primarily of calcium and silicon. Trace amounts of aluminum and sulfur were also found. The ratio of calcium-to-silicon of the air-void shell was equal to 1.1. This is lower than what is expected for a typical C-S-H found in bulk cement paste. When the EDXA was used to investigate C-S-H found in the bulk paste of this sample, the calcium-to-silicon ratio was found to be 1.5. The ratio for the C-S-H of the bulk paste agrees with numbers given by Pigeon and Plante (1982) and Diamond (1976) for the method used.

EDXA seems to indicate that the air-void shells consist of C-S-H with small amounts of ettringite needles on the surface of the void. The air-void hydration shell shown in Fig. 16.9 seems to be denser than the C-S-H found in the bulk paste. This can be seen in Fig. 16.9 if one looks at the large number of voids in the hydration product formed adjacent to the shell in comparison to the shell itself. The shell thickness and presence of a “transition zone” confirms results from Corr et al. (2002).

16.4 Discussion of Mechanisms

RQXRD showed that the early composition of the air void shell is very similar to the bulk cement paste but with a lower C_3S content, higher amounts of other anhydrous phases, and higher CaCO_3 content. These differences are unexpected and merit further discussion. The ability to understand the chemistry of these air void shells is critical in order to improve the performance of air entraining agents and understand the observed behavior.

The charge imparted by the anionic AEA on the outside of the air-entrained void may be significant in explaining the composition of the air void shell. This anionic charge likely contributes to the adhesion of cement particles to the air void. The surfaces of cement particles are charged, causing an attraction between the particles and the outside of the bubble. This attraction results in cement particles adhering to the bubble as shown in Fig. 16.1 and as suggested by others (Mielenz, 1958A; Corr et al., 2002). This also results in the high quantities of anhydrous cement phases measured in the bubble shell at early ages through RQXRD. The only way that anhydrous phases would be present in the shell is through adhesion of the particles to the bubble.

If the early hydration shell were made up completely of adhered cement particles, then the shell composition would be identical to the unhydrated cement and, correspondingly, the bulk paste since it does not differ significantly from the unhydrated cement at the times examined. However, the amount of C_3S in the shells is much lower than the amount of C_3S in the anhydrous cement and bulk paste. If all anhydrous phases were present in lower amounts in the shell, then one could assume that the ratio of cement-to-reaction products in the shell is lower than in the paste. However, the relative proportions of the other anhydrous phases are higher in the shell than in the original cement. One possible explanation for this difference is that the C_3S dissolves more rapidly in the cement particles attached to the air void. This explanation is consistent with the decrease in C_3S and increase in all other analyzed phases. Since all analyzed

phases must add up to 100%, a decrease in one phase must be matched by increases in all of the others.

The anionic surface charge may also play a significant role in the mechanism of this rapid decrease in C_3S . The dissolution of C_3S into solution initially occurs rapidly in water. This dissolution has been suggested to subside when the surface of the C_3S changes, beginning the induction period (Gartner et al., 2002). While different theories exist about the mechanism of the reduction in the rate of early C_3S dissolution, one by Barret and Menetrier (1980) suggests that the dissolution of the C_3S surface results in a net positive charge on the particle. In the bulk cement paste this surface charge is thought to be balanced by hydroxyl ions which block further dissolution until a critical concentration of calcium and silicon is reached. If this were the case, then the negative charge of the air-void surface may neutralize this surface charge and allow C_3S dissolution to continue in this region without an induction period. This would explain the observed rapid decrease in C_3S content in the air void shell. As the C_3S dissolves, an early C-S-H may be nucleating on the air void, giving the shell the physical characteristics observed. With time, the surface charge on the air-void shell is likely reduced from this C-S-H formation, decreasing the ability to control the surface charge of the C_3S and the induction period begins. This would explain the reduced rate of dissolution and the beginning of the induction period for the C_3S .

As explained previously it appears the C_3S is dissolving or leaving the surface of the air-void as all other phases in the analysis are shown to increase. However, the $CaCO_3$ in the analysis showed a much more significant increase compared to the other phases and this increase appears to be proportional to the decrease in C_3S . It is unclear the source of this increase but they appear related. One possibility is that calcium ions released from the dissolving cement may concentrate at the charged air-void shell surface, since it is negatively charged, as discussed earlier. These free calcium ions may react with carbon dioxide that is dissolved in the mixing water, water column used to separate the air-voids from the paste, or from the air contained in the air-void to form the $CaCO_3$. For this mechanism to be satisfactory then the C_3S in cement would need to contribute calcium ions to the formation of $CaCO_3$ and to the formation of other hydration products. This may be possible as the EDXA on the 60 day old air-void shell suggests that the C-S-H formed on the air-void shell has a low calcium content which could allow the remaining calcium ions to contribute to the formation of the $CaCO_3$. It should also be noted that there was no portlandite (CH) in the air-void shell or in the paste during the two hour fresh testing period. This is not surprising, since the induction period had not ended and CH generally does not precipitate during this period. Therefore, CH formation is not competing with $CaCO_3$ for calcium ions which would permit it to form.

It was also observed in this study that the use of a synthetic AEA resulted in a much more rapid decrease in C_3S content than with the wood rosin AEA and displayed different physical properties. This difference in performance is likely attributable to differences in the chemical nature of the surfactants used in the different AEA products. This could be from differences in surface chemistries that promote the hydration or dissolution of C_3S . However, without detailed knowledge of the nature and concentration of the compounds utilized in these products it is difficult to make comments on their difference in performance. The ability to understand how differences in these surfactants change the performance of the air-void shell is crucial to improving the performance of existing products.

It should be noted that the explanations offered for the changing composition of the air void shells are speculative and it is possible that the chemistry of the shells is controlled by

mechanisms other than those suggested here. This is an area that certainly merits further research.

16.5 Conclusions

This chapter presents the results of an investigation into the physical and chemical properties of air-void shells. The results are not meant to be conclusive; a large amount of information remains unknown. However, several new insights have resulted from this work.

- It has been shown that there is a strong adhesion between cement particles and air-voids beginning at the first minutes of hydration.
- It appears that there is a large difference in transparency between the air-entrained and non air-entrained voids as well as a difference in the ability of the voids to resist size changes with time.
- There is a significant difference in performance between the resulting shells with different AEA admixtures when the fluid pressure surrounding voids is increased and then decreased again to atmospheric pressure. Voids made with synthetic AEA sustain no permanent damage, while voids made with Vinsol resin and wood rosin crack on depressurization.
- The cracks in a wood rosin void shell were observed to self-heal.
- The amount of C_3S present in the air-void shell is lower than in the original unhydrated cement and the bulk paste. This effect may be due to delays in the induction period for the C_3S particles at the air-void surface.
- The increase in $CaCO_3$ in the air-void shell in the first two hours of testing may be an artifact of the sample preparation technique as it was not observed in the SEM analysis of the 60 day old air-void shell.
- The rate of C_3S decrease and $CaCO_3$ increase is faster for synthetic AEA than for wood rosin AEA. It is likely that this difference in hydration rate is related to the difference in behavior of the air-void shells of the different AEAs.
- SEM observations and EDXA of the air-voids in the 60-day-old cement paste showed that the surface of the air-void seems to be predominately made up of a C-S-H phase that is of a different stoichiometry than that found in the C-S-H of the bulk paste as the ratio of the calcium-to-silicon of the air-void shell is around 1.1 compared to 1.5 as found in the bulk paste.

While this chapter showed several unique physical characteristics of air-entrained void shells, more work is needed to better characterize the chemical makeup of this material. The majority of the work done in this chapter to chemically characterize the air-void shells focused on the crystalline material found in the shell. While the findings are helpful, no data are presented regarding the amorphous materials involved as no analytical techniques are currently readily available to the authors to analyze early amorphous hydration products in these shells. Characterization of the amorphous material is needed before any final conclusions can be drawn. If one were able to fully and accurately characterize the shell material then it may be possible to explain why the AEA voids have their respective physical properties that change with time,

pressure, and AEA composition. It may also be possible to engineer new surfactants that could improve the performance of air-entrained concrete.

Chapter 17. Conclusions

The research presented in this report provides a multi-scale approach to achieving a better understanding of the challenges of entraining and stabilizing air-voids in concrete. While several questions remain, it is hoped that the information provided some new insight into air-entrained concrete, an amazingly complicated and useful building material.

17.1 Investigation of Air-Entraining Admixture Dosage in Fly Ash Concrete

- Fly ashes from power plants that have been modified with low-NO_x burners generally led to increases in AEA demand in laboratory testing, and this observation generally agrees with the field reports of increased AEA dosages during this time period. However, it cannot be said with certainty is that the installation of the low NO_x burners, per se, is responsible for these observed changes in the ash.
- Loss-on-ignition (LOI) (ASTM C 311) measurements did not correlate with the AEA demand in concrete for most of the fly ashes studied in this project.
- The foam index test used in this study showed a satisfactory correlation to the AEA demand in concrete; however, it was unable to differentiate fly ashes with low AEA demand (less than 60 ml AEA/100 kg cm for 6% air in fresh concrete air tests)
- Limited results suggest that surface area, as indicated by nitrogen absorption using Brunauer-Emmet-Teller (BET) analysis, is a good indicator of AEA demand, especially for ashes with highly active carbon.
- BET surface area measurements were taken before and after igniting the ash (using LOI procedure), with a significant decrease in surface area measured on the ignited samples (compared to the as-received ashes). These ignited ashes were then found to respond better to AEA in foam index testing, suggesting that the loss of carbon (along with other impurities/organics) and the associated surface area contributed to AEA demand

17.2 Evaluation and Improvement of the ASTM C 311 Air-Entrainment of Mortar with Fly Ash Test

- For the work performed under this project, an average percent difference of 48% was measured for the mortar air test specified in ASTM C 311. This large variation was found to be a result of the fixed flow rate and air content of the mortar investigated.
- The ASTM C 311 test was modified to remove the iterations in the test and to reduce the variation. This was done by fixing the water content and AEA dosage in the test. This test has been shown to have a satisfactory variability but the correlation of the testing results to concrete could be improved.

17.3 Determining the Air-Entraining Admixture Dosage Response From a Single Concrete Mixture

- A method was presented to produce an AEA dosage response curve for a given fly ash/AEA combination using only using a single mixture. The method was then compared to the standard test for AEA dosage response that uses several sequential mixtures and the results were found to be closely comparable for air contents up to 7%.

- The water reducer (WR) used in this study was shown to reduce the AEA demand (to achieve a target air content) as the WR dosage was increased.
- A sacrificial surfactant that is applied to fly ash with high AEA demand can decrease the AEA demand of fly ash concrete.
- The mixing temperature had a larger impact on the AEA demand of a fly ash treated with a sacrificial surfactant than on the AEA demand of the other fly ash mixtures investigated.
- As the percent fly ash replacement increased in a concrete mixture, the AEA demand in fly ash concrete decreased if the AEA demand of the fly ash was low or increased if the AEA demand of the fly ash was high. This increase occurred in a nonlinear fashion.
- The AEA demand of fly ash treated with a sacrificial surfactant did not change as the percent fly ash replacement increased.
- Wood rosin AEA is the most sensitive of the AEAs examined to a fly ash with a high AEA demand in concrete.

17.4 Investigation of the Frost Resistance of Concrete through Measurement of Fresh and Hardened Properties, and Resistance to Rapid Freezing and Thawing Cycles

- Based on a small data set of mixtures with a similar mixture design but different air content as determined by ASTM C 231 (pressure method), the commercially available Air-Void Analyzer (AVA) was determined to have significant variability between two measurements examined from the same mixture. Significant differences were found between air-void parameters obtained from the hardened air-void analysis and the AVA.
- It was found that concrete mixtures with an air content greater than or equal to 5% was generally frost resistant (using ASTM C 666). Some mixtures with lower air contents were not frost resistant, especially mixtures containing high amounts of WR (and lower AEA dosages), mixtures with porous aggregates for which the aggregate correction factors were not applied, or mixtures containing a fly ash treated with a sacrificial surfactant. However, none of the variables listed previously were investigated in combination.
- For mixtures with relatively low air contents (e.g., less than 4.5% air) and containing a fly ash treated with a sacrificial surfactant, a coarsening of the air-void system was observed, manifested in an increase in the average chord length of air voids. However, once the air content was increased to 5% or above, satisfactory frost resistance was obtained.

17.5 Observations of Air Bubbles from Fresh Cement Paste

- An opaque “shell” was observed on the exterior of air bubbles that had escaped from air entrained paste. The appearance of the shell changed as different AEA admixtures were used.
- In these experiments with bubbles in bleed water, bubbles with an opaque shell appeared to resist coalescence, whereas translucent-to-transparent bubbles coalesced readily. Similarly, the shell appeared to take on structural properties such as stiffness, resistance to deformation, and eventual cracking. The role of these properties in stabilizing air bubbles within cement paste has not been identified.

- When the shell appeared to be fully intact over observable portions of the bubble surface, the diameter of the bubbles did not change with time for the conditions of setup #2. When a readily discernable shell was not present as in the specimen of non air-entrained paste in setup #2, the diameter of the air bubbles was observed to change with time. Likewise, of those bubbles with a readily observed shell, only those that had cracked changed diameter with time.
- In pressurized experiments shown in setup #3 it was observed that the air-bubble shell was damaged during depressurization from 0.7 bar to atmospheric pressure. This may be important in construction applications in which the concrete pressure is increased and decreased. It is not known, however, whether the experimental observations made here under a relatively mild and slow pressure change apply equally to the much higher pressure differences and rates of pressure change experienced in concrete pumping, for example.
- A single shell-covered bubble that had escaped from air-entrained paste was observed to decrease in volume under pressure precisely as would be predicted by Boyle's Law, with no apparent influence of the shell.
- If a water-filled gap does exist between the air-void shell and the surrounding paste as observed by others in concrete (Rashad and Williamson, 1991A; Rashad and Williamson, 1991B; Corr et al., 2002), then it seems plausible that gas interchange could occur between air-voids whose shells were either inadequate or damaged. This interchange could lead to a decrease in volume of the smaller bubbles and an increase in volume of the larger bubbles as observed in the experimental work in this chapter. This change in void volume would ultimately lead to a higher overall air content in the mixture as the gas is under a lower pressure in the larger air-voids than the small; therefore, the air would take up a larger volume on transfer as first suggested by Mielenz et al. (1958A). The above explanation is based on observations of air-void behavior in the bleed water of cement paste and has not been proven in concrete mixtures.

17.6 The Physical and Chemical Characteristics of the Shell of Air-Entrained Bubbles in Cement Paste

- It has been shown that there is a strong adhesion between cement particles and air-voids beginning at the first minutes of hydration.
- It appears that there is a large difference in transparency between the air-entrained and non air-entrained voids as well as a difference in the ability of the voids to resist size changes with time.
- There is a significant difference in performance between the resulting shells with different AEA admixtures when the fluid pressure surrounding voids is increased and then decreased again to atmospheric pressure. Voids made with synthetic AEA sustain no permanent damage, while voids made with Vinsol resin and wood rosin crack on depressurization.
- The cracks in a wood rosin void shell were observed to self-heal.
- The amount of C_3S present in the air-void shell is lower than in the original unhydrated cement and the bulk paste. The effect may be due to delays in the induction period for the C_3S particles at the air-void surface.

- The increase in CaCO_3 in the air-void shell in the first two hours of testing may be an artifact of the sample preparation technique as it was not observed in the SEM analysis of the 60 day old air-void shell.
- The rate of C_3S decrease and CaCO_3 increase is faster for synthetic AEA than for wood rosin AEA. It is likely that this difference in hydration rate is related to the difference in behavior of the air-void shells of the different AEAs.
- SEM observations and EDXA of the air-voids in the 60-day-old cement paste showed that the surface of the air-void seems to be predominately made up of a C-S-H phase that is of a different stoichiometry than that found in the C-S-H of the bulk paste as the ratio of the calcium-to-silicon of the air-void shell is around 1.1 compared to 1.5 as found in the bulk paste.

17.7 Recommendations

One of the major goals of this research project was to recommend test methods that have the ability to determine the AEA demand of fly ash in concrete. One criterion of these methods was for them to be simple and applicable in the field as well as in a quality control laboratory.

The foam index test shows the most promise of the tests investigated. This test does not require any complicated equipment and has been shown at least for the mixture proportions investigated to provide a reasonable prediction of the AEA demand of the fly ash in concrete. One problem with this test is that the results are based on human subjectivity in the mixing and evaluation. This subjectivity may be overcome if the tests are completed by experienced technician. More data are presented in Volume I.

- The modified mortar air test developed in Volume II showed a lower variability than the current ASTM C 311 mortar test and requires significantly fewer mixtures to be created. This test is useful in that it does not rely on human subjectivity for mixing or evaluation. However, this test requires somewhat specialized equipment and the correlation to the performance of the concrete mixtures was better for the foam index test.
- The BET nitrogen surface area testing, for the limited data set presented, showed a satisfactory ability to examine the AEA demand of a fly ash in concrete. However, this test requires very expensive equipment. Additional work completed at Cornell University should be consulted before recommending this test. However, the high expense for the equipment does not meet the requirements set by TxDOT.
- The LOI test showed little or no correlation to the AEA demand of a fly ash in concrete for the fly ashes evaluated in this particular study and requires specialized equipment. While this test is a standard in the concrete industry it is not recommended to evaluate the AEA demand of fly ashes in this study.

The previously mentioned tests have been shown to be useful when examining the AEA demand of fly ash in concrete. However, for the mixtures investigated, a large number of factors can impact the ability to entrain air in concrete. Because these previously mentioned tests were completed on simplified systems or measured physical properties of the fly ash they are unable, and should not be expected, to describe all of the different combinations that may impact the ability to entrain air in concrete. However, the best method to investigate the impact of different mixture ingredients on the ability to entrain air in concrete is to create a trial concrete mixture. In the past this would have required the creation of several mixtures that may have unintentional differences that impact the ability to entrain air in concrete. However, the methodology outlined

in allows the impact on the AEA demand of these variables to reliably be investigated from a single concrete mixture. While this test is not as simple as the ones described previously and does not satisfy the initial requirements set by the problem statement it does provide a direct measurement of the impact of different mixture ingredients on the ability to entrain air of the mixture in question.

A number of variables were investigated which have the ability to impact the AEA demand and resulting air-void system in concrete. It has been shown that in a limited number of tests that the following variables may not provide satisfactory frost durability at air contents lower than 4.5% as determined by the ASTM C 231 (pressure method). Because of this it is recommended that an air content of at least 5% is provided in a hardened concrete that is desired to be resistant to freeze-thaw damage, as this was shown as the threshold air content that performance was satisfactory. However, it should be said that no combination of these variables were investigated and that the results of an investigation may yield different recommendations. It would be prudent to require that a minimum dosage of AEA be required in a concrete mixture. One possibility is to utilize the manufacturer's minimum suggested dosage until other limits can be established.

The Air Void Analyzer was shown to have a significant difference between the air-void parameters in the hardened air-void analysis and for this reason is not recommended to be utilized to evaluate the air-void system in concrete as a construction specification until a better understanding is obtained of how the measurements of the machine correspond to the air-void system in the sampled concrete.

While no evidence is presented in this report of the air-void system changing with time in concrete, optical observations of the air-void system in pastes suggest that it is possible for air-voids to change in size with time as first suggested by Mielenz et al. (1958A). These observations suggest that the hydration shell formed around air-entrained voids may be important to the stability of the air-void system. This shell was shown to form in concrete with AEA and not shown in concrete without AEA. The relevance of these observations to concrete deserves more attention. However, these observations reinforce the need for the quality control testing of the air content in concrete to be completed as close to the point of placement as is feasible in order to best measure the in-place air content.

17.8 Research Needs

This project was one that was quite ambitious in scope. Volume II provided new information not currently in the state of the art on testing methods, performance of different ingredients in concrete, the characteristics of the air-void shell, and the chemical properties of this shell. It is unfortunate but inevitable that some research needs still remain. The following is a list of the most pressing research needs.

- Different combinations of water reducer dosage, sacrificial surfactant, and aggregates with different correction factors should be investigated that are typically used in concrete construction to investigate the air-void systems produced with different air contents.
- The vast majority of the mixtures performed for this research focused on a concrete mixture that would be typical of a bridge deck mixture. Other mixture proportions representative of other applications should be investigated to monitor the impact of different variables on the resulting air-void content and distribution.

- A subset of the most critical mixture combinations from the previous recommendations should be investigated in a set of full scale mixtures created in a ready-mix concrete plant and the resulting air content and air-void distribution should be evaluated.
- A survey of the aggregate correction factor of aggregates should be completed in locations where freeze-thaw durability is specified. Different moisture contents of these aggregates should also be investigated to determine the impact on the accuracy of the ASTM C 231 pressure method to measurements made on hardened concrete.
- A detailed study is needed to examine how the air-void shells impact the change in the air-void distribution in concrete.
- More work is needed to further characterize the chemistry of the air-void shells. The focus of this research is to isolate several of the variables and develop a less intrusive technique to separate the air-voids from the paste and compare the results to previous testing. Also more work is needed with different AEAs to understand why they show distinctly different physical properties.

VOLUME III

Chapter 18. Clustering of Air Voids Around Aggregates in Air-Entrained Concrete

18.1 Introduction

There are numerous factors that can affect the compressive strength (or flexural/tensile strength) of concrete. Typically, some of the first factors looked for when determining the cause of low compressive strengths are the quantity of mixing water added and the air content. Increases in the water content and/or total air content can significantly reduce concrete strength. In recent years, several state departments of transportation (DOTs), including Texas DOT, have reported compressive strengths lower than expected in concrete that was reasonably well proportioned with air contents in the range typically specified and used in field applications. After several comprehensive investigations, the cause of the low compressive strengths was attributed to clustering of air voids around aggregate particles (Cross et al. 2000, Kozikowski et al. 2005).

The clustering of air voids around aggregates reduces the bond between the paste and the aggregate and results in a weak interface. Recent research suggests that the phenomenon of air void clustering is linked to several factors. Research funded by the Portland Cement Association (PCA) has found that air void clustering primarily occurs when a non-vinsol resin air-entraining admixture (AEA) is used and when the concrete is re-tempered with water (Kozikowski et al. 2005). This research, conducted in a laboratory, has reported up to 22% additional compressive strength loss due to clustering of air voids around the aggregates. Re-tempering with water is often done in the summer months to regain workability lost due to high concrete temperatures causing loss of water through evaporation and/or increased hydration of the cement. Most of the reported cases of air void clustering in the field have occurred during the summer months when re-tempering concrete, even though not recommended, occurs quite often.

Volume III describes research conducted at the University of Texas at Austin to determine the effects re-tempering air-entrained concrete has on concrete properties.

18.2 Research Objectives

The main objectives of this research were as follows:

- Determine if it is possible to reproduce clustering of air voids around the aggregates under laboratory conditions.
- Determine the effect air void clustering has on hardened concrete properties (e.g. strength loss).
- Determine the severity of the air void clustering (if any) before and after re-tempering the concrete mixtures.
- Determine if coarse aggregate properties (mineralogy, shape, texture, etc.) affect clustering of air voids.
- Determine the affect re-tempering has on the hardened air void system.
- Determine if a correlation between air void clustering in field concrete and re-tempering exists.

18.3 Project Scope

The research plan involved evaluating three different types of air-entraining admixtures. Two non-vinsol resin AEAs and one vinsol resin AEA were used. The concrete mixtures targeted either low air content (3%-4%), medium air content (4%-7%), or high air content (7%-10%). A Type I/II low alkali cement (as per ASTM C 150) was used for all the mixtures. Siliceous river gravel and crushed limestone coarse aggregates were used to evaluate the effects of aggregate type on air void clustering. Samples of the fresh concrete were taken at various stages during mixing and subsequently evaluated to determine the presence and effects of air void clustering around the aggregates.

This project also included a thorough review of reported cases of low strength concrete. Texas DOT project files and databases were searched for cases of low strength concrete, and all available data was found to determine if a correlation exists between re-tempering field concrete and air void clustering.

The remaining chapters of Volume III include a literature review of air-entrained concrete discussing factors affecting air-entrainment and recent air-entrainment issues, description of the materials used in the research, a detailed research plan, results and discussion of the research conducted in the laboratory, and a study of low strength concrete field cases reported by Texas DOT.

Chapter 19. Literature Review

19.1 Air-Entrained Concrete

Air-entrainment is mainly used to improve concrete's freeze-thaw durability. Concrete is porous material containing numerous capillary pores (microscopic voids). The size and quantity of these pores are dependent on the original water-cementitious (w/c) ratio and the degree of hydration of the cementitious material. The amount of water-filled pores prior to drying impacts the rate and amount of water that penetrates into concrete during its service life. As the temperature decreases to a point in which water freezes in the concrete, water expands to form ice and tensile stresses are generated. If these stresses are greater than the tensile strength of the concrete, cracks will develop. Upon thawing, the damaged concrete allows more water to enter which can result in further damage during the next freezing cycle.

There are several theories that try to explain the mechanism of freeze-thaw damage. It was originally theorized that hydraulic pressures are generated as water freezes in the pores of the concrete (Powers 1953). As water freezes, it expands by approximately 9% and forces the unfrozen water through the pores (and away from the freezing water), and the movement of water through the pores generates large hydraulic pressures. Later, the osmotic pressure theory was developed which suggests that the concentration of dissolved alkalis in the pores increases when ice begins to form (Powers, 1975). Unfrozen water from smaller pore migrates to higher concentration regions to reach equilibrium. This migration of water generates osmotic pressures. One of the more recent theories states that water in the capillary pores cannot freeze in situ, due to changes in the vapor pressure, and will travel to external surfaces to freeze (Litvan 1972, 1973, 1975, 1980). If the path to an external surface is too long, the freezing rate too fast, or the duration of the freeze cycle too long, rapid drying of the concrete occurs and high internal stress are generated.

Regardless of the theory considered, the presence of microscopic air voids in the concrete matrix has been shown to improve concrete's resistance to freeze-thaw damage. Accidentally discovered in the mid-1930s, air-entrainment has become the leading method used to improve concrete freeze-thaw resistance in cold weather regions. Air-entrainment is the stabilization of microscopic air voids in the concrete and is accomplished by introducing a chemical admixture to the concrete during mixing. Air voids in hardened concrete act as pressure relief sites that allow water to migrate without generating pressure or ice crystals to form, depending on which theory is considered.

Fresh air content is the easiest and most common air void characteristic determined. Many DOTs use this value as an acceptance or rejection criteria but, as will be discussed later, the fresh air content may sometimes be misleading. Other air-void parameters are evaluated by performing hardened air void analysis by following ASTM C 457: "Standard Method for Microscopical Determination of Parameters of the Air-Void System in Hardened Concrete." Since air voids vary in size, usually in the 0.0004 in. to 0.004 in. range with an average diameter of 0.002 inches, other factors have been developed to characterize the air void system. The specific surface is a measure of the average size of the air voids in terms of surface area per unit volume. The larger the specific surface, the larger number of smaller the voids in the concrete. The most important air void characteristic is the spacing factor. The spacing factor is a measure of the largest distance of any point in the paste to the edge of a nearby air void (Powers 1954).

The key is to determine if the air content is capable of producing the proper spacing factor to resist freeze-thaw damage, which was determined to be about 0.008 to 0.010 inch (Powers 1954). However, the spacing factor can be highly variable for a given air content and is dependent on the specific surface of the air voids (Saucier et al. 1991).

19.2 Air-Entraining Admixtures

Air-entraining admixtures (AEAs) are surface active agents or surfactants. These surfactants typically have a hydrophilic head on one end that has a strong attraction to water. The other end is a hydrophobic tail that has less of an attraction to water. Air is initially present between grains of cement and aggregates or dissolved in mixing water, and it can also be introduced in the concrete during mixing by the shearing action of the mixer blades and by the folding action of concrete falling onto itself. AEA's perform several functions. The main function is to reduce the surface tension of the water (Pigeon and Pleau 1995). The reduction in surface tension reduces the amount of energy needed to form air voids. The reduction in surface tension also makes it easier breakdown larger air voids to form smaller air voids. AEA's form elastic films around the air voids which prevent bubbles from combining and forming larger air voids when colliding during mixing (Pigeon and Pleau 1995). The hydrophilic head usually carries a negative charge and tends to get absorbed onto the cement grains. The cement grains help disperse the air voids throughout the mixture and keep the air voids from floating to the surface. The buoyancy of the air voids also reduce the rate of settlement of the cement grains and thus reduce bleeding of the concrete (Du and Folliard 2005).

There are a number of chemicals that are used to produce air-entraining admixtures, and many of them are by-products of the paper or petroleum industries. Table 19.1 list some of the more common chemicals used and their performance characteristics.

Table 19.1: Classification and Performance Characteristics of Air-Entraining Admixtures (adapted from Kosmatka et al. 2002)

Classification	Performance Characteristics
Wood resin and rosin	Quick air generation. Minor air gain with initial mixing. Air loss with prolonged mixing. Mid-size air bubbles formed. Compatible with most other admixtures.
Tall oil	Slower air generation. Air may increase with prolonged mixing. Smallest air bubbles of all agents. Compatible with most other admixtures
Synthetic detergents	Quick air generation. Minor air loss with mixing. Coarser bubbles. May be incompatible with some HRWR. Also applicable to cellular concretes.
Vegetable oil acids	Slower air generation than wood rosins. Moderate air loss with mixing. Coarser air bubbles relative to wood rosin. Compatible with most other admixtures.

19.3 Factors Affecting Air-entrainment

The characteristics of the air-void system (air content, spacing factor, specific surface, etc.) are affected by the properties of the materials used to produce the concrete and the handling,

consolidation, and placement operations. The following are a few of the factors that affect the air void characteristics.

For a given dosage of AEA, finer cements will entrain less air. This can be attributed to more of the AEA being absorbed on the cement grains making less AEA available to stabilize bubbles. Type III cements usually require double the dosage of AEA to entrain an equal amount of air compared to a Type I cements with the same cement content (Whiting and Nagi 1998).

The use of supplementary cementitious materials (SCMs) can also have an effect on the air content. In most, if not all cases, SCMs increase the AEA demand needed to obtain a target air content. One of the more recent problems stems from coal burning power plants changing to low-NO_x burners to meet the requirements of the Clean Air Act (Hill et al. 1997). These burners operate at lower temperature, which results in fly ashes that contain large amounts of unburned highly absorptive carbon, some of which has a very high surface area. The AEAs are absorbed by the carbon, requiring large dosages to entrain the desired amount of air. Several fly ash producers have begun treating problem fly ashes with sacrificial surfactants which are preferentially absorbed by the carbon, thus leaving the AEAs to stabilize the air voids.

The grading, shape and fineness of aggregates also affects the air voids formed during mixing. Fine aggregates with high amounts of material passing the #100 sieve tend to decrease the air content. Fine aggregates that have proper gradations between the #30 and #100 sieve promote the formation of air voids and increased amounts of this fraction size tends to entrain more air (Whiting and Nagi 1998). Coarse aggregates with crushed faces tend to entrain more air than rounded gravels, due to the increase of impact and shearing during mixing (Du and Folliard 2005).

The type of mixer, mixing time, and size of load can either increase or decrease the quantity of air-entrained in concrete. The speed of the mixer, blade orientation, etc. dictate the type of mixing action. The shearing and folding of the concrete generates air in the concrete while the mixing action distributes the air void throughout the mixture. The time needed to entrain the maximum air content is dependent on the mixer characteristics. Energetic mixers require less time to generate air voids (Du and Folliard 2005). Small loads tend to have less air-entrained voids due to the high impact forces when the concrete falls from the top of the mixer to the bottom. This essentially beats the air out of the concrete.

Workability of the concrete can affect the amount of air-entrained voids in the concrete. Slump is typically used as a measure of workability, and in most cases there is a very good correlation to actual workability. However the viscosity of the paste, which can be directly tied to w/c, is the more important factor. Mixtures that tend to have higher viscosity paste (low w/c) will generate smaller voids because the air voids are less prone to colliding and forming larger air voids (Pigeon and Pleau 1995). Lower viscosity paste mixtures allow air bubbles to easily move through the paste and collide and form larger air voids, which tend to move upward to the surface resulting in lower air contents.

As the concrete temperature increases, the ability to entrain air decreases. This is due to the fact that it is easier to form and stabilize air at lower temperatures, and also, in hot weather, water demand increases and mixtures can become stiffer, thereby making it more difficult to entrain air. During the winter months, AEA dosages are typically reduced because the workability improves as the concrete temperature decreases and air-entrainment becomes easier. The reduction of the dosage results in higher spacing factors because changes in temperature only affects the air content and not spacing factors or specific surfaces (Gay 1983, Saucier et al. 1990).

Transportation, consolidation, and pumping all tend to cause loss of air. Long hauls can result in loss of air contents in the range of 1-2% (Kosmatka et al. 2002). Proper vibration has little effect on the air void system. However, over vibration with high frequency vibrators results in additional air loss. Pumping concrete can result in the loss of 1-1.5% air content (Hover and Phares 1996). The orientation of the pump boom and pump pressures can change also affect the air void characteristics (Lessard et al. 1996).

19.4 Effect of Air-entrainment on Concrete Properties

Air-entrainment has a substantial effect of many of concrete's fresh and hardened properties. Workability of air-entrained concrete is generally improved. The spherical shape and the repulsion properties of the air voids make air-entrained concrete more cohesive and easier to handle and place. Air-entrained concrete generally requires less water and sand than non-air-entrained concrete to maintain the same workability. Reduction in water and sand can help in overcoming the strength loss issues. However, high air contents can result in sticky mixtures which are difficult to finish.

Both compressive and flexural strength are negatively affected by air-entrainment. Compressive strengths can decrease by 2-6% for every percent increase in air content, and flexural strengths can decrease by 2-4% for every percent increase in air content (Kosmatka et al. 2002).

As previously mentioned, the primary reason for producing air-entrained concrete is to improve its resistance to freeze-thaw damage. Along with improved freeze-thaw resistance, salt scaling is drastically improved, and sulfate resistance can also be improved (Kosmatka et al. 2002).

19.5 Issues with Air-entrained Concrete

One of the most common problems with air-entrained concrete is low strength. There are several factors that can cause low strength in concrete. High w/c, high air contents, improper mixing, transporting and placing techniques, and the mishandling of test specimens can all be viable causes for low strength concrete. However, when air-entrained concrete is used; low strength is typically attributed to higher than normal air contents. Intrinsically, air-entrained concrete will be weaker than non-air-entrained concrete (when both mixtures have the same w/c), due to its higher porosity, but this is offset in concrete mixture proportioning by using a lower w/c for air-entrained concrete. When the target air content is exceeded, strength losses can be significant, especially when total air contents exceed 7 to 8 percent.

As mentioned previously, fly ashes from coal burning power plants with low-NOx burners may contain large amounts of unburned highly absorptive carbon. The AEA's are absorbed by the carbon, requiring large dosages of AEAs to entrain the desired amount of air. Problems in controlling air contents with these types of problem fly ashes can be due to inconsistency of the carbon in the fly ash. One dosage of AEA may only be viable for one shipment of fly ash. Research is currently being performed to develop test methods that will allow concrete or fly ash producers to try and get a better grasp on how the fly ash will affect the concrete (Folliard and Ley 2006). Discussion of these methods is beyond the scope of this report.

Many researchers have noted discrepancies between air contents measured in fresh concrete and the air contents measured microscopically in hardened concrete with air contents greater than 10 percent, with the hardened measurement usually higher than the fresh air content (Pigeon and Pleau 1995). The cause of this discrepancy is still debated and currently being

investigated. It has been suggested that this discrepancy can be attributed to the air void size distribution (Gay 1982). If large quantities of small, less compressible air voids are present in high air content concretes, the fresh air content measured by the pressure method will be lower than the actual air content (Gay 1982). Mielenz et al. (1958) suggested that the high internal pressure of the smaller air voids causes them to dissolve into the surrounding water and reform later as larger air void. The formation of the larger air voids will then be recorded as higher air contents during hardened air content analysis. There also have been numerous reports of instances where the air content measured on hardened concrete samples is drastically higher than what was measured in the fresh concrete using the pressure method. One explanation is that the increase in air content is due to inadequate mixing of the concrete and the addition of more AEA at the jobsite which results in large amounts of unactivated air-entraining admixture. The AEA will become active later when the concrete is mechanically spread (paver screw, etc.) which causes the now active AEA to form additional air bubbles and increase the air content. (Eickschen, 2003).

In recent years, several state DOTs have reported the occurrence of air voids clustered around the aggregates. The clustering was typically noted when air-entrained concrete was produced with synthetic AEAs and was identified due to problems with low concrete strengths. Most of the reported cases occurred during the summer construction seasons, which indicated that temperature of the concrete could have a role. Also, the use of crushed ice to control concrete temperature has also been suggested as a factor in leading to discrepancies in air between fresh and hardened air contents. The mechanism of the air void clustering is unknown; however, recent research has suggested that re-tempering concrete containing non-vinyl resin AEAs promote clustering and results in significant strength loss (Kozikowski et al. 2005). The research in this chapter focuses on the effects re-tempering has on concrete properties and the air void system.

19.6 Re-tempering Air-Entrained Concrete

Re-tempering is the late addition of water and/or admixtures to the concrete, and is usually not recommended, but it is a common practice in the field. Concrete often arrives at jobsites with a lower than desirable workability or air content. The loss of workability is typically due to evaporation, absorption of water by the aggregates, or from hydration during long hauls. In order to make the concrete useable, water or chemical admixtures are sometimes added on site to increase the slump. Some concrete producers purposely hold back a calculated amount of water that can be added to the concrete to make any necessary workability adjustments at the jobsite. This is an acceptable practice provided that the mixing trucks have working and calibrated water meters and that the design w/c is not exceeded. Unfortunately, the amount of re-tempering water added is sometimes not properly monitored or controlled, and there is thus uncertainty as to the final w/c. When air contents are below the required percentage, air-entraining agents are sometimes added to increase the air content to the desired percentage. Numerous studies have been performed to determine how re-tempering concrete with water, or water plus air-entraining admixtures, affects concrete properties and air void characteristics, as described next.

Langan and Ward (1976) performed a laboratory study of concrete re-tempered to modify air content and workability. The intent of this study was to determine the effects re-tempering with water and water plus air-entraining admixtures had on the air-void system. The mixing procedure consisted of three phases: initial mixing, agitation, and re-tempering. Test results

showed that during the agitation phase, both air content and slump decreased and compressive strength increased. The increase in compressive strength was attributed to the loss of air. During the re-tempering phase, the w/c was increased by 0.02-0.05 depending on the degree of slump loss. Test results showed that the specific surface for mixtures re-tempered with water plus air-entraining admixture remained constant and the spacing factor significantly decreased with increased air content. When only re-tempering with water, the air content increased and the spacing factor decreased. The compressive strength testing did not indicate anything other than what was expected due to the changes in w/c and air content.

Burg (1983) sampled and tested freshly mixed concrete from fifteen trucks at various stages; as mixed at the plant, as received at the jobsite, and after re-tempering with water. The air content and slump decreased from the as-mixed value when tested at the jobsite before re-tempering. Similar to Langan and Ward's findings, Burg also noted an increase in compressive strength, approximately 400 psi, in the as-received concrete, prior to re-tempering. Approximately 10 lb/yd³ of water was added to the trucks to increase the slump about 1 inch. The added water and additional mixing increased the average air content by 0.56 percent. Hardened air void analysis indicated that the microscopically measured air content was either equal to or slightly greater than the air content measured in the fresh concrete and that spacing factors were all lower than 0.008 inches. Burg also stated that the difference between fresh air content and hardened air content was greater in concrete with higher air contents. Burg concluded that 8 to 10 percent of the original amount of water could be added as re-tempering without drastically changing the properties of the concrete.

Pigeon et al. (1990) also studied the effects of re-tempering field and laboratory mixed concrete with water or water and an air-entraining admixture. In this study, the concrete was re-tempered 45 minutes after initial mixing with an amount of water that increased the w/c from 0.45 to 0.48. Test results showed that the added water increased the air contents slightly but had no significant effect on the spacing factor or the specific surface. Pigeon et al. also noted that when the air contents measured on fresh concrete was high, the hardened air tended to be slightly higher.

19.7 Past Research on Air Void Clustering

As mentioned previously, clustering of air voids around the aggregate particles has been reported by several DOTs. During the 1997 construction season, South Dakota DOT reported an unusually high number of low concrete strengths statewide. After an extensive investigation, it was determined that the low concrete strengths could be attributed to air void clusters around the aggregates, which resulted in weak paste-aggregate bonding (Cross et al. 2000). The clustering of air voids was noted in mixtures that contained synthetic or vinsol resin AEAs, but was more pronounced in the synthetic AEA mixtures. Foam drainage testing also indicated that non-vinsol AEAs drain water faster than vinsol resin AEAs, which results in thinner walled bubbles and a low quality paste at the aggregate surface. These combined factors resulted in the reduction in compressive strength. Depending on the quantity of aggregates that have clustering, the compressive strength could potentially be reduced by 1000 psi. South Dakota DOT made revisions to their specification in 1998 by requiring the use of vinsol resin AEA. This reportedly resulted in the reduction of low strengths during the 1999 construction season.

Kozikowski et al. (2005) performed a laboratory investigation on the potential causes of air void clustering around the aggregates. A large number of factors were investigated to determine the cause of the clustering. They reported that concrete mixed with vinsol resin AEAs

did not have any clustering of the air voids. Also, re-tempering with water and additional mixing promoted clustering in mixtures containing non-vinsol resin AEAs. These mixtures also showed significant loss in compressive strength that was not related to the increase in w/c. In order to correlate strength loss with clustering, a rating system was developed to evaluate the severity of the clustering. Concrete mixtures that had cluster ratings of 1 or greater generally had substantial compressive strength loss. Mixtures containing limestone tended to have larger strength losses than mixtures with river gravel aggregate. As will be discussed later in more detail, the study performed by Kozikowski formed a starting point for the research described in this chapter, although the mixing procedure was slightly modified.

The common factor between the two projects discussed was the determination that the use of a non-vinsol resin based air-entraining admixture caused low compressive strength problems and that the use of vinsol resin air-entraining admixtures resulted in no clustering of the air voids. It should be mentioned that Gutman (1988), while performing research to improve the air-entraining admixtures, noted that vinsol resins tended to have clusters of air voids within the paste and clusters of air voids surrounding the aggregates. It was also noted that clustering and the presence of thin wall bubbles were possibly the cause of lower compressive strengths, rather than simply being caused by the use of newer or synthetic air-entraining admixtures.

Texas DOT has also reported several cases of low compressive strengths where clustering of air voids around the aggregates was noted. Review of available field data and petrographic reports is discussed in Chapter 23.

Chapter 20. Materials

20.1 Cement

A Texas DOT-approved low-alkali Type I/II cement (as per ASTM C 150) was used for all of the mixtures included in this research. Two shipments of cement were received during the duration of this research. The cement properties are listed in Table 20.1. The first shipment was used for Phase I of the project, and the second shipment was used for Phase II. Table 20.1 shows that there was very little difference between the two shipments of cement.

Table 20.1: Cement Chemical Analysis

Oxides	Shipment 1	Shipment 2
SiO ₂	20.18	20.75
Al ₂ O ₂	5.18	4.92
Fe ₂ O ₃	3.59	3.57
CaO	62.55	62.17
MgO	1.02	1.07
Na ₂ O	0.08	0.07
K ₂ O	0.76	0.70
SO ₃	3.20	3.15
LOI	2.77	2.93
Total Alkalies as Na ₂ O _e	0.57	0.53
Bogue Calculated Phases		
C ₃ S	52.22	48.31
C ₂ S	18.47	23.04
C ₃ A	7.66	7.00
C ₄ AF	10.91	10.86

20.2 Aggregates

Siliceous river gravel and crushed limestone coarse aggregates were used for this research. Both aggregates are from the central Texas region and are on Texas DOT's approved aggregate producer list. The fine aggregate used was also a Texas DOT's approved material from the central Texas region and consisted of natural siliceous river sand. The aggregate properties and gradations are shown in Table 20.2 and Table 20.3.

20.3 Admixtures

Three air-entraining admixtures (AEAs) were selected for evaluation and are listed in Table 20.4. One of the most predominantly used AEA in Texas is a wood and gum rosin based

admixture. The majority of the mixtures in this study contained this particular AEA. As mentioned in several past research reports, vinsol resin AEAs tended not to promote clustering, so a commercially available vinsol resin was also evaluated. The last AEA was a synthetic AEA and was only evaluated in Phase I of the research. All three AEAs met the requirements of ASTM C 260. A normal range water reducing admixture, ASTM C 494 Type A, was used to achieve the desired workability.

Table 20.2: Aggregate Properties

	Coarse Aggregate		Fine Aggregate
	River Gravel	Limestone	
Specific Gravity (SSD)	2.61	2.59	2.56
Absorption	1.02%	1.43%	0.55%
Unit Weight	101.2 lb/ft ³	87.16 lb/ft ³	-
Fineness Modulus	-	-	2.63

Table 20.3: Aggregate Gradation

Sieve Size	% Passing		
	Limestone	River Gravel	Fine Aggregate
1 1/2	100	100	100
1	100	83	100
3/4	95	44	100
5/8	88	30	100
1/2	71	17	100
3/8	38	5	100
No. 4	0.2	0.5	97
No. 8	0	0	86
No. 16	0	0	71
No. 30	0	0	49
No. 50	0	0	27
No. 100	0	0	7
No. 200	0	0	1

Table 20.4: Air-entraining Admixtures

Air-entraining Admixture ID	Type
A	Wood and Gum Rosin
B	Vinsol Resin
C	Salt of Fatty Acid

Chapter 21. Research Plan

As previously mentioned, re-tempering is common practice at the jobsite and it is important for contractors and owners to understand the potential problems and risks that may result when re-tempering air-entrained concrete. To attempt to quantify the effects of re-tempering on concrete for a range of different materials, this study was launched. The main objectives of this project follow:

- Determine if it is possible to reproduce clustering of air voids around the aggregates under laboratory conditions.
- Determine the effect air void clustering has on hardened concrete properties (e.g. strength loss).
- Determine the severity of the air void clustering (if any) before and after re-tempering the concrete mixtures.
- Determine if coarse aggregate characteristics (mineralogy, shape, texture, etc.) affect clustering of air voids.
- Determine the effect re-tempering has on the hardened air void system.

In order to achieve these objectives, a research plan was devised as described below.

21.1 Mixing Procedure

Several days before mixing, the coarse and fine aggregates were taken from the stockpiles and put into five gallon buckets. This was done at least one day before mixing to allow all the material to come to room temperature. The number of buckets needed was determined by the number of mixtures scheduled and volume of each concrete mix. These buckets were then taken to the mixing room for batching.

The coarse aggregates were batched by loading all of the aggregate into a nine cubic foot drum mixer and mixed for several minutes. A small amount of water was then added to the mixer to ensure that the aggregate was beyond saturated surface dry (SSD) condition. The aggregate was then mixed for several more minutes to uniformly distribute the moisture. Once all of the aggregate was well coated with water, two samples for moisture corrections were taken and placed in an oven to dry for at least twelve hours. The aggregate in the mixer was then placed into five gallon buckets and weighed until the desired weight was obtained. Each bucket was sealed and labeled with the appropriate mix number.

The fine aggregate was batched in an identical manner as the coarse aggregate. Moisture corrections were calculated and weighed before mixing. The corrected amount of water and required admixtures were weighed just prior to mixing. The cement was also weighed and sealed in five gallon buckets.

A modified version of the mixing procedure used by Kozikowski et al. (2005) was used for this project. The initial stage of the mixing procedure did not contain an AEA as in Kozikowski et al.'s procedure. This was to ensure that all of the mixtures started with approximately the same slump. Cycle 2 of Kozikowski et al.'s procedure (agitation period) was eliminated since preliminary test results showed that this cycle did not have strength loss or clustering of the air voids around the aggregates. It was also noted that very little strength loss was observed between cycles 3 and 4. Therefore, these two cycles were combined since the

largest strength losses were found after final cycle. The final mixing procedure used was comprised of three stages as shown in Figure 21.1 and detailed in the following sections.

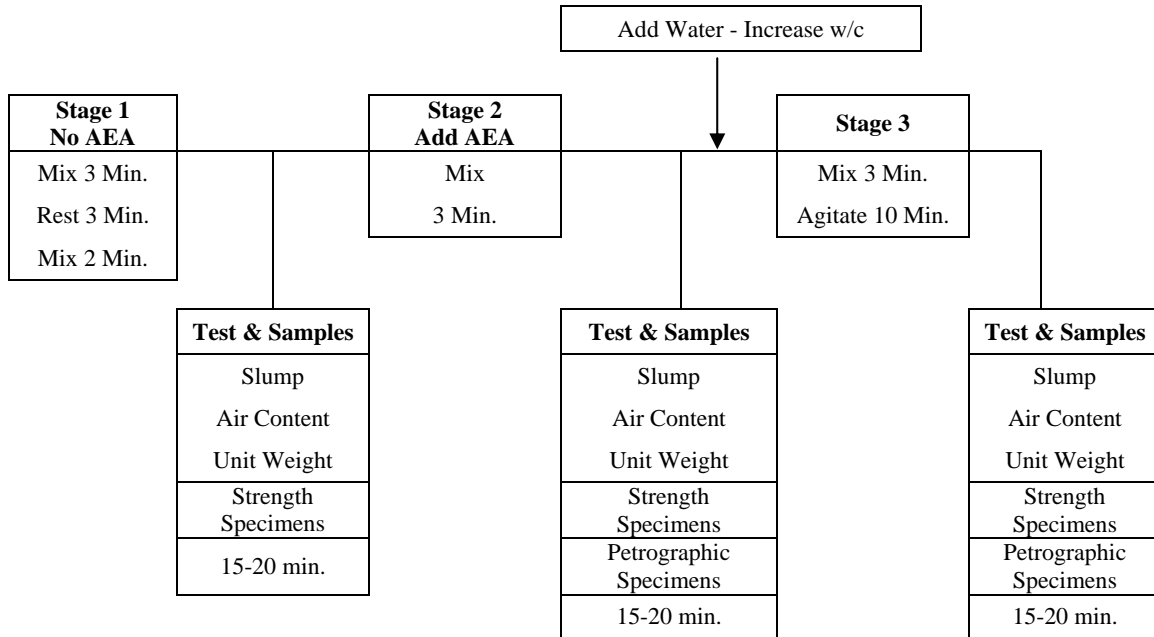


Figure 21.1: Mixing Procedure

21.1.2 Mixing Stage 1

All of the aggregates were loaded into the mixer with approximately two-thirds of the mixing water. The mixer was turned on and allowed to mix the aggregates and water. Once the coarse and fine aggregates were blended together, the water-reducing admixture, if necessary, was added and mixed for approximately one minute. The cement and the remaining water were added to the mixer and mixed for three minutes and then allowed to rest for three minutes. During the rest period, any unmixed material adhering to the drum was scraped off. After the rest period, the concrete load was then mixed for two more minutes. After all of the mixing was completed, slump, unit weight, and air content were determined. Four 4 x 8 in. cylinders for compressive strength testing (7 day and 28 day), were cast. Performing fresh concrete tests and molding the test specimens usually took fifteen to twenty minutes.

21.1.3 Mixing Stage 2

After the stage 1 test specimens were molded, a dosage of air-entraining admixture was added to produce the desired air content. The concrete was then mixed for three minutes. After the additional mixing was complete, slump, unit weight, and air content were determined. Four 4 x 8 in. cylinders for compressive strength testing (7 day and 28 day), and one specimen for petrographic analysis were cast. Performing fresh concrete tests and molding the test specimens usually took fifteen to twenty minutes.

21.1.4 Mixing Stage 3

After the stage 2 test specimens were molded, re-tempering water was weighed and added to concrete and the load was mixed for three minutes. After the three minutes of mixing, the angle of the mixer was increased so the concrete was no longer falling onto itself and very little shearing action occurred. This resulted in the concrete being agitated at the back of the mixer. The agitation period lasted for ten minutes. Once the agitation period was over, slump, unit weight, and air content were determined. Four 4 x 8 in. cylinders for compressive strength testing (7 day and 28 day), and one specimen for petrographic analysis were made. Performing fresh concrete tests and molding the test specimens usually took fifteen to twenty minutes.

21.2 Mix Design

Texas DOT specifications limit concrete suppliers to a maximum water-cementitious ratio of 0.45 for concrete used in bridge deck construction. Therefore, a 0.45 w/c was selected as the initial w/c for the mix design. As mentioned before, past research conducted on re-tempering air-entrained concrete added water to increase the w/c by a few hundredths. During stage 3, re-tempering water added increased the w/c from 0.45 to 0.48. A few mixtures were re-tempered with less and more water which resulted in a final w/c of 0.47 and 0.50, respectively.

Previous research had concluded that the increase in w/c in the 0.03 range had very little effect on compressive strength and was considered negligible and a 4% loss of strength for every percent of entrained air was assumed for all types of AEAs (Kozikowski et al. 2005). To determine the effect of w/c and air content, several series of non-re-tempered mixtures with w/c of 0.48, and 0.5 were also mixed to compare against the re-tempered mixtures. Table 21.1 lists the weights of each concrete component used. The proportions of this mix design were selected to represent a typical Texas DOT Class S concrete which is typically used for bridge deck construction. The target slump range for the 0.45 w/c mixtures was 1-3 inches. A dosage of 1.25 oz/cwt of a normal range water reducing admixture is used in all 0.45 w/c mixtures. The water reducing admixture was not used in the non-re-tempered mixtures with the higher w/c.

Table 21.1: Mix Design Proportions

Mixture Proportions	
Component	Weights, lbs/yd ³
Water	254*
Cement	564
Coarse Aggregate	1850
Fine Aggregate	1174
w/c	0.45

* Higher w/c mixtures used same proportions except water was increased accordingly.

21.3 Phase I

The main objectives of Phase I were to determine:

- if clustering of air voids around the aggregates is possible with the modified mixing procedure,
- the severity of air void clustering (if any),

- the extent of compressive strength loss due to clustering, and
- the effect re-tempering has on the air void system.

The three different AEAs were evaluated in Phase I with the siliceous river gravel coarse aggregate.

A three cubic foot mixer was used for all Phase I concrete mixtures. One concern was the removal of concrete after each mixing stage and its effect on subsequent stages. The initial batch size was selected to ensure that there would be approximately 1.5 ft³ of concrete (50% of mixer capacity) remaining in the mixer at the beginning of stage 3. An initial batch size of 2.5 ft³ allowed for the removal of 0.5 ft³ of concrete for air content test and specimens after stages 1 and 2, and left 1.5 ft³ of concrete in the mixer at the start of stage 3.



Figure 21.2: 3 ft³ Drum Mixer

21.3.2 Testing Procedures

During mixing operations, slump, unit weight, and air content tests were performed after every stage according to ASTM C 143, ASTM C 138, and ASTM C 231. After performing the slump test, the concrete used was returned to the mixer once all other tests were performed and specimens molded. The unit weight of the concrete was determined by using the 0.25 ft³ bottom portion of the pressure meter. Once the unit weight was determined, the air content was determined on the same concrete. This concrete was then discarded. Compression and petrographic specimens were then molded according to ASTM C 192.

The compression and petrographic specimens were left undisturbed and uncapped for approximately one hour or until bleeding stopped. The specimens were then capped and left in a 73 °F room for 24 hours for initial curing. After the initial curing period was finished, the specimens were stripped from the molds, labeled, and placed in a fog room (73 °F, 100% RH) until the required age for testing. The preparation of the petrographic specimens will be discussed in later sections.

Compressive strength specimens were tested in accordance with ASTM C 39. Compression tests were performed at 7 days and 28 days of age. The average of two cylinders was used as the final compressive strength for each age. All cylinders were tested with unbonded neoprene pads on a 600 kip capacity Forney compression machine.

21.3.3 Petrography

As previously mentioned, one sample from stage 2 and 3 of every mix was made for petrographic analysis. Paper cartons with wax coating on the interior, typically used for carry-out food, were used as the molds for these samples. This type of mold was used because it provided an adequate area for hardened air analysis and required less concrete than a 4 x 8 inch cylinder. These specimens were used for determining the severity of the clustering and for hardened air void analysis.

Sample Preparation

The petrographic specimens were kept in the fog room for a minimum of 7 days to ensure that they had achieved enough strength to withstand the concrete saw and subsequent polishing. After 7 days, these specimens were removed from the fog room. A slab approximately 3/4 inches thick was cut from each specimen using a concrete saw with a continuous diamond blade. The specimens were cleaned to remove any cutting oil and debris from the sawing and then relabeled. The specimens were then lapped on progressively finer grit plates.

In order to make the lapping process more efficient, a novel method was devised that allowed four specimens to be lapped simultaneously. This was done by making four holding rings that attached to the side of the lapping machine. Each ring was cut from a plastic 6 x 12 inch cylinder mold and had two wooden arms attached. Specimens were then placed in the rings. Pressure on the specimens was applied by placing a 6 x 12 inch concrete cylinder in each holding ring. The bottom portion of the concrete cylinder was made with a slightly smaller diameter when it was molded so that it fit loosely in the holding ring. Once the system was setup, the lapping machine was turned on. Every 2 to 5 minutes, the cylinders were rotated 90° to reduce the unidirectional lapping marks on the specimens.

Specimens were first lapped on a coarse grit plate (60 grit) to remove any saw marks and to plane the specimen. To ensure a plane surface, a grid was marked on the surface with a construction crayon (grease pencil). The specimen was lapped until the grid was completely removed. A machinist ruler (small metal ruler) was used to check the flatness of the specimen. The ruler was placed on edge on the lapped surface and held up to the light. Low or high area could be seen by the passing of light between the specimen and the ruler. If the specimen was not plane, the grid was reapplied and placed on the lapping machine.

Once the operator was satisfied with the flatness of the specimen, it was then lapped on progressively finer grit plates. The plates included 60 grit, 80 grit, 100 grit, 180 grit, and 260 grit. After being lapped on each plate, the specimen was checked for flatness as detailed above. Before being lapped on the 180 and 260 grit plates, a coat of a 1:5 lacquer to acetone solution was applied to strengthen the paste.

After the final lapping was completed, each sample was examined under a stereo microscope to ensure adequate sample preparation. The microscope had a light source on each side. One light was taken off the specimen and the other positioned so that the light was parallel to specimen. With this light configuration, the operator could determine if the specimen was flat by looking for shadows on the backside of the aggregates. Also, with this light configuration the air voids should look like crescent shapes with sharp edges. If shadows were not present and the air voids looked good, the specimen was deemed acceptable. The samples were then soaked in acetone to remove the lacquer/acetone solution in the voids.

Clustering Rating System

The severity of the clustering was determined by using a rating system developed by Kozikowski et al. (2005). Once the lapping procedures were completed, a 3 1/2 in. by 3 1/2 in. area was marked on the lapped surface. Approximately 50 coarse aggregates with diameters greater than 1/4 in. within the selected area were numbered. Each numbered aggregate was examined under a stereo microscope and was given a rating from 0 to 3 (Figure 21.3). A “0” rating indicates no air void clustering around the aggregate. A “1” rating indicates minor air void clustering. Minor clustering is defined as intermittent occurrences of clustering around the aggregate particle. A “2” rating indicates moderate air void clustering, and is defined as the majority of an aggregate’s perimeter is surrounded by air voids. A “3” rating indicates severe air void clustering with several layers of air voids surrounding the aggregate. The ratings of each aggregate are summed and divided by the number of aggregates examined in the particular specimen. This composite clustering rating was then used to determine the severity of the clustering. Sample calculations of the composite rating are shown in Table 21.2.

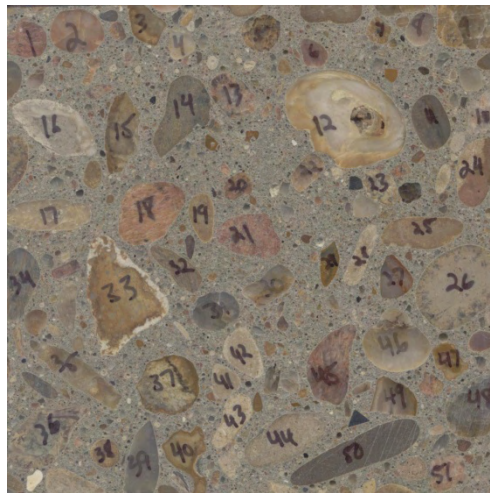


Figure 21.3: Sample Prepared for Composite Rating Evaluation

Table 21.2: Sample Calculations of Composite Rating

Mix #	Stage	Rating				Composite Rating
		0	1	2	3	
A	2	13	33	3	0	0.80
	3	6	17	17	0	1.28

Hardened Air Void Analysis

Hardened air void analysis was performed on a selection of specimens from Phase I to determine the effects re-tempering had on the air void system.

Hardened air void characteristics were determined by using the Rapid-Air 457 machine manufactured by Concrete Experts International. RapidAir 457 is an automated image analysis system that performs air void analysis on hardened concrete according to ASTM C 457, Method A. Rapid-Air uses contrasting images to determine air void characteristics and is capable of

performing up to ten lines of traverse per analysis frame. One line of traverse (95 in.) can be performed in about 15 minutes, which is a substantial time reduction from the manual analysis which can take several hours to perform. For the same traverse length, the analysis time can be reduced by increasing the number of lines of traverse per analysis frame. However, Jakobsen et al. (2006) found that using three lines per analysis frame and tripling the traverse length resulted in better statistical data in the same time one line of traverse is performed. All the specimens were analyzed using this technique (three lines per analysis frame and tripled traverse length).

Before performing hardened air void analysis, the contrasting operation had to be performed. Lapped surfaces of the specimens were first colored with a black marker pen. The specimens were colored in one direction and then rotated 90° and colored again. The ink was allowed to dry for at least twenty four hours. The intent of the drying time is to minimize the smearing of the black ink into powder filled the voids. Once the ink was dried, white barium sulfate powder was spread on the specimen and pressed into the voids with a small rubber stopper. When all of the voids were filled, the surface was leveled off with a wooden straight edge. The surface was then buffed with the palm of the hand to enhance to black/white contrast. Voids within the aggregates and cracks within the paste that contained barium sulfate powder were then colored black with a fine tip marker. Figure 21.4 shows two color-contrasted samples with different air contents.

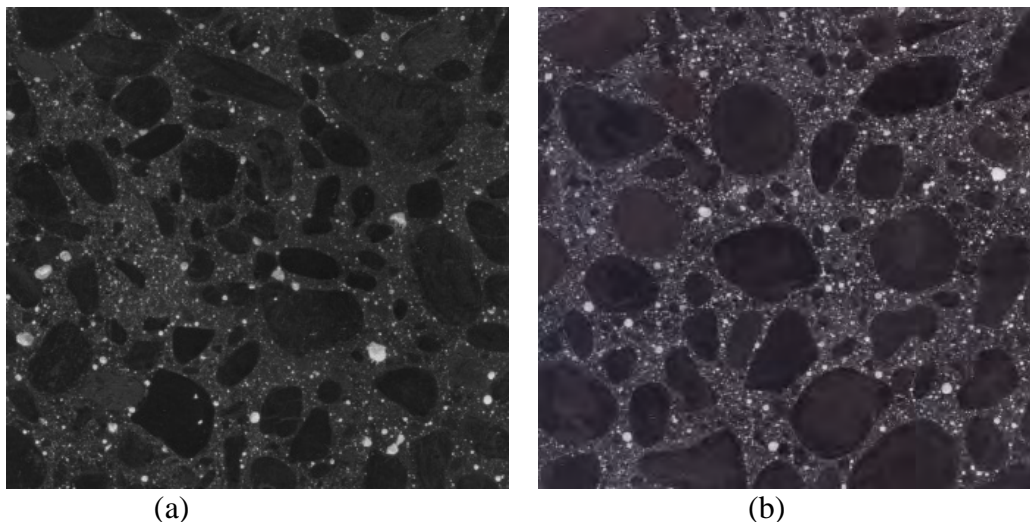


Figure 21.4: Samples prepared for hardened air void analysis. (a) Low air content, (b) high air content

After the contrasting procedure was completed, a specimen was placed and secured on the traverse stage according to the Rapid-Air 457 instructions. The camera was focused and a threshold value set. The threshold value is dependent on room lighting, contrast and light settings of the system, and the type of ink used to color the specimen (Jakobsen et al. 2006). An average threshold value for each specimen was determined in the following manner. After the specimen was in focus and positioned in the upper left hand corner, a threshold value was set for this frame and recorded. The stage was then moved horizontally to the middle to the specimen and a new threshold value was set and recorded. The stage was once again moved horizontally to the far edge of the specimen and a new threshold value was set and recorded. This process was repeated two more times for the middle and opposite end of the specimen. Two additional randomly

selected locations on the specimen were also given threshold values. This resulted in a total of twelve threshold values. The high and low values were discarded and the remaining ten values averaged. The average threshold value was used to analyze the specimen. The average threshold value ranged from 148 to 153. The results of the hardened air void analysis are discussed in Chapter 22.

21.4 Phase II

The objectives of Phase II were to determine:

- if the severity of clustering increases with the use of limestone aggregate,
- the effects re-tempering has on the of flexural and splitting tensile strength, and
- the effect re-tempering has on the air void system.

Phase II focused on evaluating two AEAs with limestone coarse aggregate, and with one AEA with river gravel coarse aggregate. Phase II included flexural and splitting tensile testing in addition to compressive strength testing.

Because more test specimens were needed, the batch size was increase and a 9 ft³ mixer (Figure 21.5) was used for all the mixtures. An initial batch size of 6.25 ft³ allowed for the removal of 1.63 ft³ after stage 1 and 2 which left 3 ft³ in the mixer at the beginning of stage 3.



Figure 21.5: 9 ft³ Drum Mixer

21.4.2 Test procedures

Fresh concrete tests were performed in an identical manner as in Phase I. In addition to the four compressive strength specimens molded for each stage of mixing, four splitting tensile strength specimens (4 x 8 in. cylinders) and two flexural strength specimens (6 x 6 x 20 in. beams) were cast according to ASTM C 192.

The strength and petrographic specimens were left undisturbed and uncovered for approximately one hour or until bleeding stopped. The cylindrical specimens were then capped and flexural specimens were covered with a plastic tarp and left in a 73 °F room for 24 hours for initial curing. After the initial curing period was over, the specimens were stripped from the molds, labeled, and place in a fog room until the required age for testing.

Compressive and splitting tensile strength specimens were tested in accordance with ASTM C 39 and ASTM C 496. These tests were performed at 7 days and 28 days of age. The average of two cylinders was used as the final strength for each age. Compression strength specimens were tested with unbonded neoprene pads on a Forney compression machine. Flexural

strength specimens were test at 7 days of age in accordance with ASTM C 78 on a Tinius Olsen testing frame.

21.4.3 Petrography

Petrographic specimens from Phase II were prepared and analyzed in an identical manner as the Phase I specimens.

21.5 Case Studies

Over the past several years, Texas DOT has reported a number of low strength air-entrained concrete cases occurring in the field, but has never performed a study to determine if any correlation existed between the cases. The objective of this case study was to determine if any correlation between re-tempering field concrete and air void clustering existed. Texas DOT project files and databases were searched, and field cases were selected for review based on the following criteria:

- Failing strength of field specimens.
- Air-entrained concrete.
- Evidence of re-tempering.
- Failing strengths of laboratory tested referee specimens.
- Notation of clustering of air void around the aggregate in the petrographic report.

Available field data, concrete batch tickets, results of laboratory testing and petrographic reports of samples taken from these cases were collected, and a thorough review of each case meeting the selection criteria was performed.

Chapter 22. Test Results and Analysis

22.1 Phase I

Phase I consisted of twenty re-tempered mixtures and fourteen non-re-tempered mixtures. Tables listing the details of the re-tempered and non-re-tempered mixtures are shown in Volume III: Appendix A. The following sections will discuss the fresh and hardened concrete properties of the mixtures from Phase I.

22.1.1 Fresh Concrete Tests Results

After every stage of mixing, slump, unit weight, and air content (pressure method) tests were performed. To recall, stage 1 was the initial mixing, AEA dosage was added during stage 2, and stage 3 consisted of re-tempering and agitation of the concrete. Figure 22.1 shows the results of the slump tests. The addition of AEA “A” and “B” during stage 2 resulted in an average increase of 2.1 inches in slump from stage 1. The addition of AEA “C” resulted in an average increase of 1.4 inches in slump from stage 1. This increase in slump demonstrates the increase in workability air-entrained concrete has over non-air-entrained concrete.

Mixtures 1 through 7 contained AEA “A” and were re-tempered to a final w/c of 0.48, an addition of 17 lb/ft³ of water. The addition of water and extended mixing from stage 3 resulted in an average increase of 2.0 inches of slump from stage 2. This increase corresponds to the rule of thumb of 10 lb/ft³ of water for an approximately 1-inch increase of slump (Burg 1983). Mixtures 14 through 17 contained AEA “B” and were also re-tempered to a final w/c of 0.48. These mixtures had an average increase of 2.6 inches of slump from stage 2. Mixtures 18 through 20 contained AEA “C” and were re-tempered to a final w/c of 0.48 and had an increase of 1.9 inches of slump from stage 2. AEA “A” was also used in mixtures 8 through 10 and 11 through 12 which were re-tempered with 8 lb/yd³ and 28 lb/yd³ which resulted in final w/c of 0.47 and 0.5 respectively. As would be expected, mixtures 8 through 10 had the lowest average increase in slump and mixtures 11 through 13 had the largest average slump increase from stage 2. Every mix in their respective mix group targeted low, medium, or high air contents. The results of the slump tests suggest that the dosage or type of AEA used had only a minimal effect on the increase in slump before or after re-tempering the concrete and slump was mainly dependent on the amount of re-tempering water added.

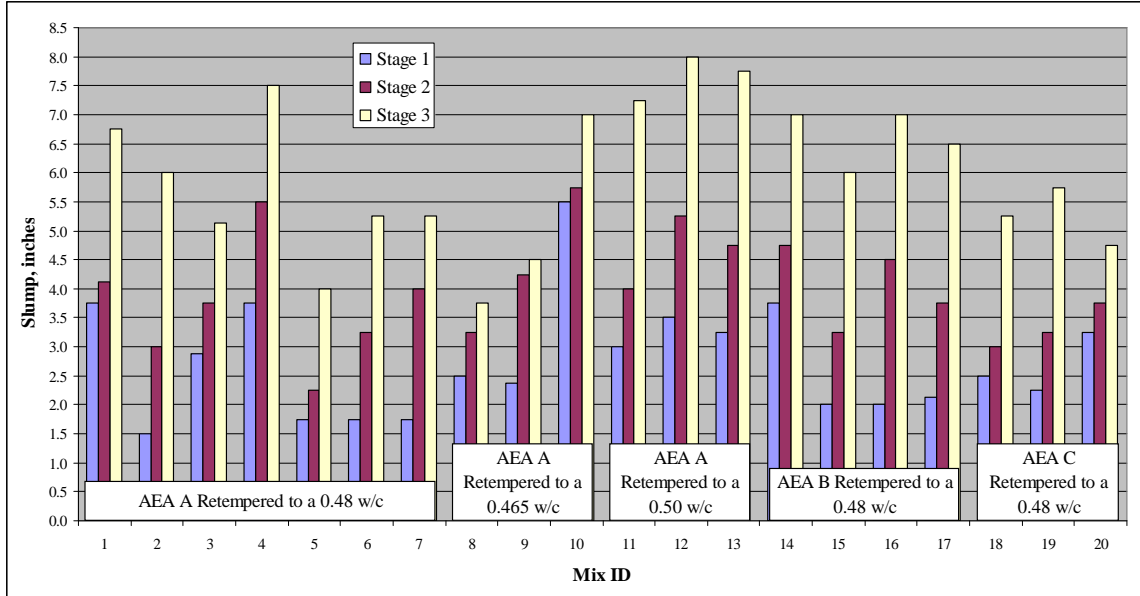


Figure 22.1: Change in Slump for Phase I Mixtures

Unit weight and fresh air content of concrete were determined after every mixing stage. Figure 22.2 shows the results of the unit weight vs. air content (pressure method) for all the mixtures in Phase I. This plot shows that the unit weight and fresh air have a linear relationship with a very good R^2 value of 0.99. As the fresh air content increased, the unit weight decreased for all stages of the mixing procedure.

Figure 22.3 plots the air contents (determined by gravimetric method) vs. the air contents (determined by pressure meter) for all the mixtures in Phase I. The linear correlation also has a very good R^2 value of 0.99. However, the air content (pressure method) tended to result in higher air contents, typically about 1% higher than the gravimetric air contents. Determination of air content by the gravimetric method has been found by other researchers to be somewhat inaccurate (Pigeon and Pleau 1995). Reasons for the inaccuracies can stem from errors in determining the specific gravities of the aggregates or errors in the batch weights of each component. The correction for moisture content can also affect the results of the test. Errors in any of these values are sufficient enough to cause differences in the air content.

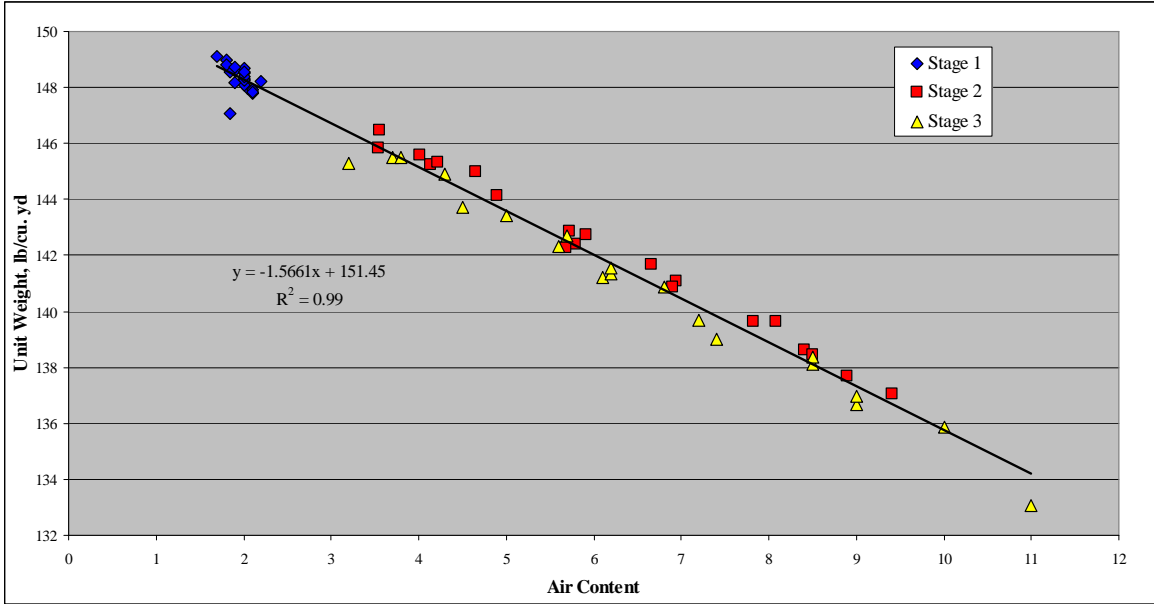


Figure 22.2: Unit Weight vs. Fresh Air Content

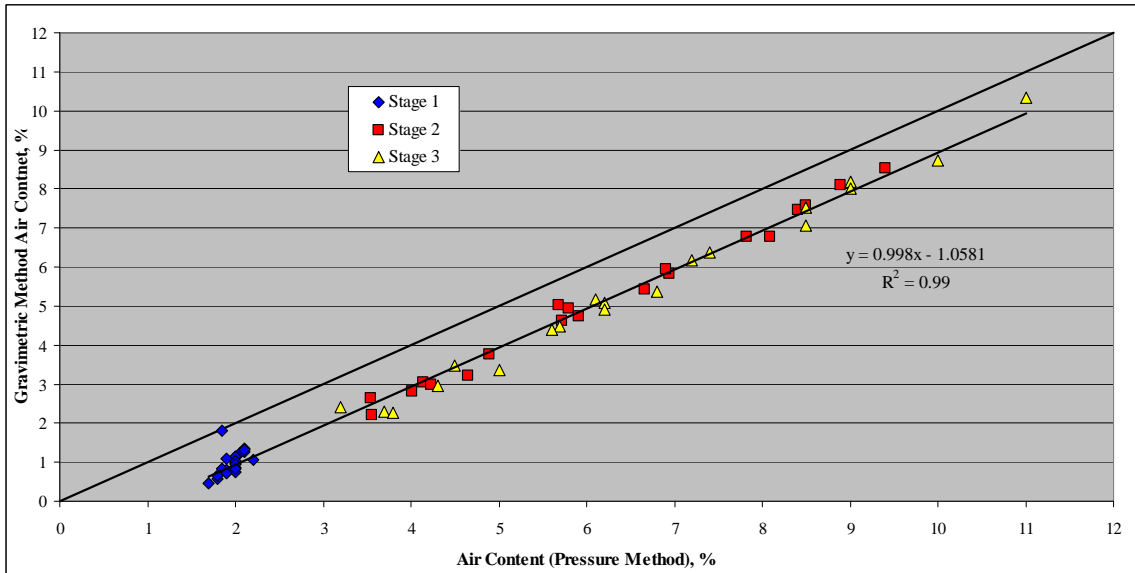


Figure 22.3: Gravimetric Air Content vs. Air Content (pressure method)

The change in air content after re-tempering and additional agitation varied for each mix group (Figure 22.4). Mixtures 1 through 7 had five mixtures with slight increases (< 1%) in air content and two mixtures that had minor decreases (< 1%) in air content. Mix 8 was re-tempered with less water and had a very little increase in air content, while mixtures 9 and 10 lost about 1% air content after stage 3.

Mixtures 11 through 13 also exhibited increases in air content after stage 3. The largest increase in air content occurred in the mix with the highest dosage of AEA. This may be explained by the phenomenon called micelle formation. A micelle is a buildup of extra

surfactants at the air-water interface which does not contribute toward the reduction in surface tension of the water (Du and Folliard 2005). This usually occurs with high dosages of AEAs, and explains why there is an upper dosage at which AEAs will no longer produce entrained air regardless of mixing time. The addition of re-tempering water may reduce the micelle concentration and make more surfactant available to form additional entrained air voids.

Mixtures 14 through 17 showed similar increases in air content as mixtures 1 through 7. These mixtures contained a vinsol resin AEA, and three of the four mixtures had minor increases in air content. Mixtures which contained AEA “C” (synthetic AEA) had significant increases in air content at the higher air contents. This indicates that the type and dosage of AEA, along with the amount of re-tempering water added can affect the change in fresh air content. It was hypothesized that the mixtures with the larger increases in air content would potentially have substantial strength loss due to clustering; this is discussed next.

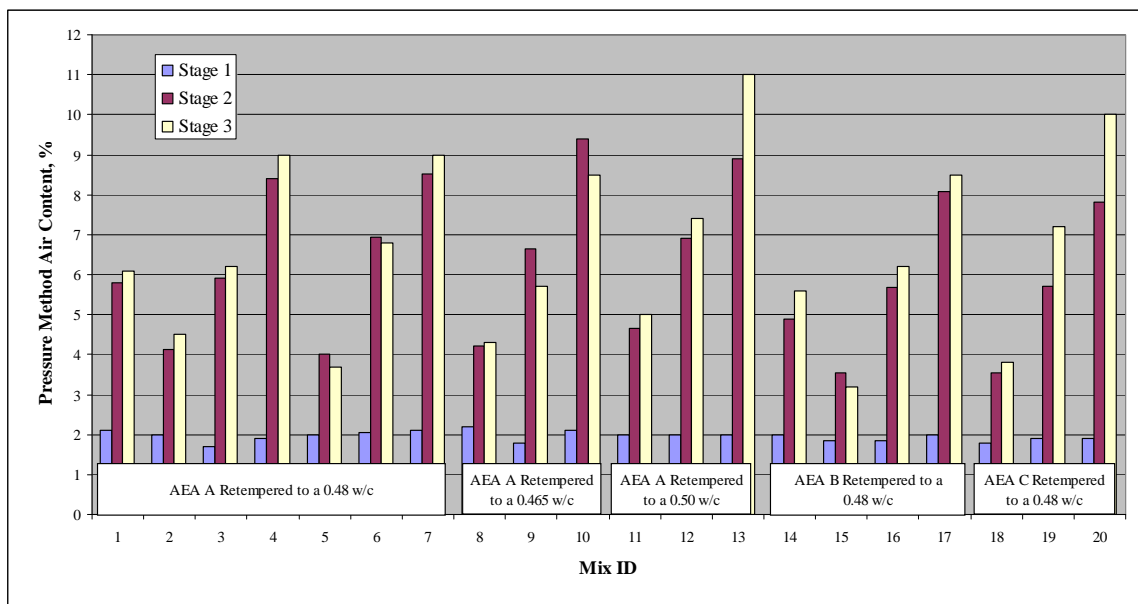


Figure 22.4: Changes in Air Content for Phase I Mixtures

22.1.2 Compressive Strength Results

As discussed in Chapter 19, the effect of re-tempering air-entrained concrete on compressive strength is still unclear. Langan and Ward (1976) stated that the loss of compressive strength due to re-tempering “followed accepted relationships” with increased w/c, while Kozikowski et al. (2005) noted significant losses in compressive strength after re-tempering and agitating the concrete in mixtures that contained non-vinsol resin AEAs, and the strength loss was not attributed to the increase in w/c. In order to determine the effects of re-tempering on compressive strength, cylinders were tested at 7 and 28 days of age for each stage of every mix. The intent of this testing was to determine the loss of compressive strength for every percentage of air content and to determine the reduction in compressive strength due to re-tempering and compare the strength loss to mixtures with the same w/c that were not re-tempered.

Figure 22.5 shows 28-day compressive strengths vs. air content (determined by the pressure method) for mixtures 1 through 7, which contained AEA “A” (wood and gum rosin) and started with an initial w/c of 0.45 and were re-tempered to a final w/c of 0.48. For stages 1 and 2

(0.45 w/c), these mixtures had a loss of compressive strength per percent air content of approximately 6.4%. The re-tempered stage also had an approximate 6.4% of strength loss for every percent of air content. The control mixtures (0.48 w/c) had an approximate strength loss of 5.3% for every percent of air content. The 7-day compressive strength plots can be found in Volume III: Appendix B, and followed the same trends described here.

The loss of compressive strength per percent air content is significantly higher than the assumed value of 4% used in previous research to determine the effects of air void clustering and is slightly outside the typical range of 2% to 6% (Kosmatka et al. 2002) reported in literature. The assumption of a 4% compressive strength loss could have skewed the results of the previous research and made it appear that clustering had a larger effect on compressive strength than it actually did. This is not to say that clustering does not affect compressive strength, only that its effect may not be as significant as previously thought.

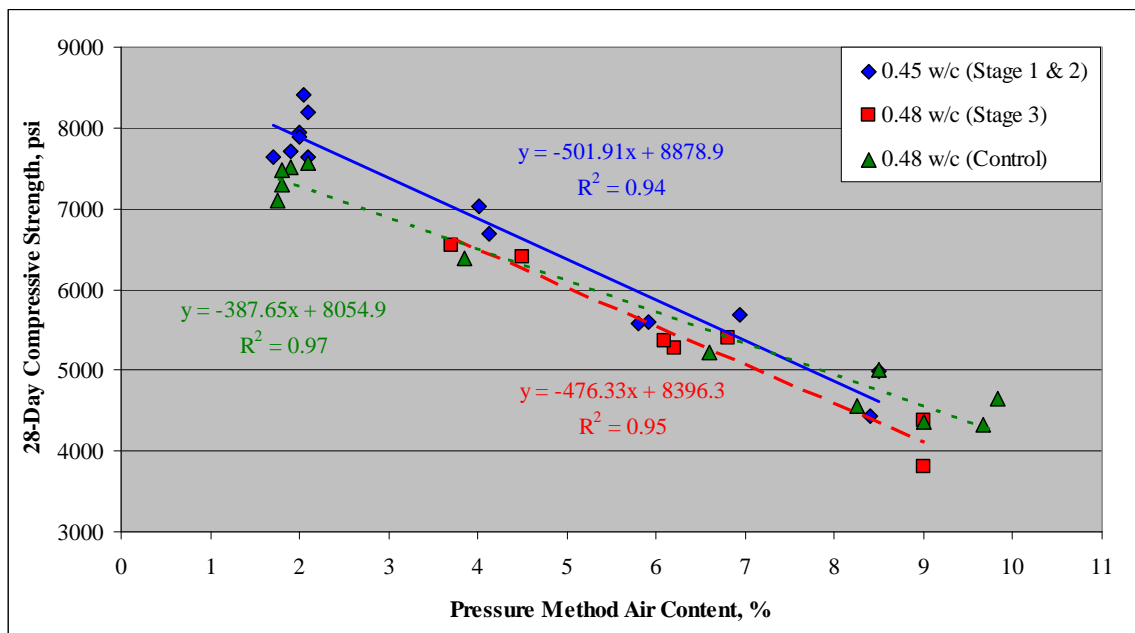


Figure 22.5: 28-Day Compressive Strength vs. Air Content (Pressure Method) for Mixtures Containing AEA “A”

As a whole, the compressive strength of the re-tempered stage falls in line with the control mixtures. This indicates that the only strength loss observed was due to the increased w/c. There was some deviation from the control mix at higher air contents. Each mix was evaluated separately to determine the percent loss of compressive strength that could potentially be attributed to clustering. The actual compressive strength for each stage of every mix was compared to an adjusted compressive strength. Stage 1 compressive strengths were used as a base line and adjusted for the changes in air content (6.4% for every 1% percent air content) and increase in w/c. It was determined that the increase of 0.03 in w/c resulted in an average 470 psi decrease in compressive strength. Table 22.1 shows the results of this evaluation.

Table 22.1: Compressive Strength Loss due to Air Void Clustering for Mixtures 1-7

Mix #	Stage	Air Content, %	Actual Compressive Strength, psi	Adjusted Compressive Strength, psi	Strength Change Potentially due to Clustering, %
1	1	2.1	7630	7630	
	2	5.8	5580	5820	-4.3
	3	6.1	5370	5210	3.0
2	1	2.0	7940	7940	
	2	4.1	6700	6860	-2.4
	3	4.5	6410	6200	3.3
3	1	1.7	7640	7640	
	2	5.9	5600	5580	0.4
	3	6.2	5280	4970	5.9
4	1	1.9	7710	7710	
	2	8.4	4430	4500	-1.6
	3	9.0	3810	3740	1.8
5	1	2.0	7880	7880	
	2	4.0	7030	6860	2.4
	3	3.7	6790	6560	3.4
6	1	2.1	8400	8400	
	2	6.9	5680	5770	-1.6
	3	6.8	5400	5380	0.4
7	1	2.1	8190	8190	
	2	8.5	4990	4830	3.2
	3	9.0	4380	4110	6.6

Based on the evaluation in Table 22.1, there was no significant loss of strength that could be attributed to clustering. The actual compressive strengths were equaled to or higher than the adjusted compressive strengths. All the actual compressive strengths were within about 5% of the adjusted compressive strengths.

Figure 22.6 shows 28-day compressive strengths vs. air content determined by the pressure method for mixtures 14 through 17, which contained AEA “B” (vinsol resin) and started with an initial w/c of 0.45 and were re-tempered to a final w/c of 0.48. For stages 1 and 2 (0.45 w/c), these mixtures had a loss of compressive strength per percent air content of approximately 6.6%. The re-tempered stage also had an approximate 6.4% of strength loss for every percent of air content. The control mixtures (0.48 w/c) had an approximate strength loss of 5.9% for every percent of air content. The 7-day compressive strength plots can be found in Volume III: Appendix B, and followed the same trends described here.

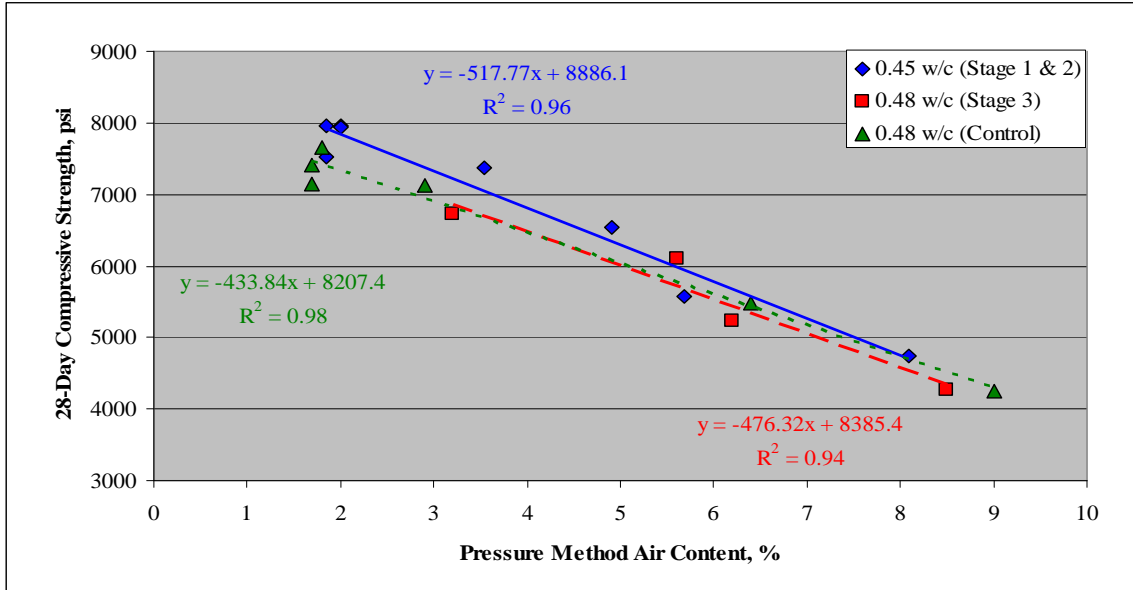


Figure 22.6: 28-Day Compressive Strength vs. Air Content (pressure method) for Mixtures Containing AEA “B”

Of the three types of air-entraining admixtures evaluated in Phase I, the synthetic AEA showed the highest loss of compressive strength per percent air content (Figure 22.7). Mixtures 18 through 20 were re-tempered to a final w/c of 0.48 and contained AEA “C.” For stages 1 and 2 (0.45 w/c), these mixtures had a loss of compressive strength per percent air content of approximately 7.9%. The re-tempered stage had an approximate 7.3% of strength loss for every percent of air content. The control mixtures (0.48 w/c) had an approximate strength loss of 7.2% for every percent of air content. The 7-day compressive strength plots can be found in Volume III: Appendix B, and followed the same trends described here.

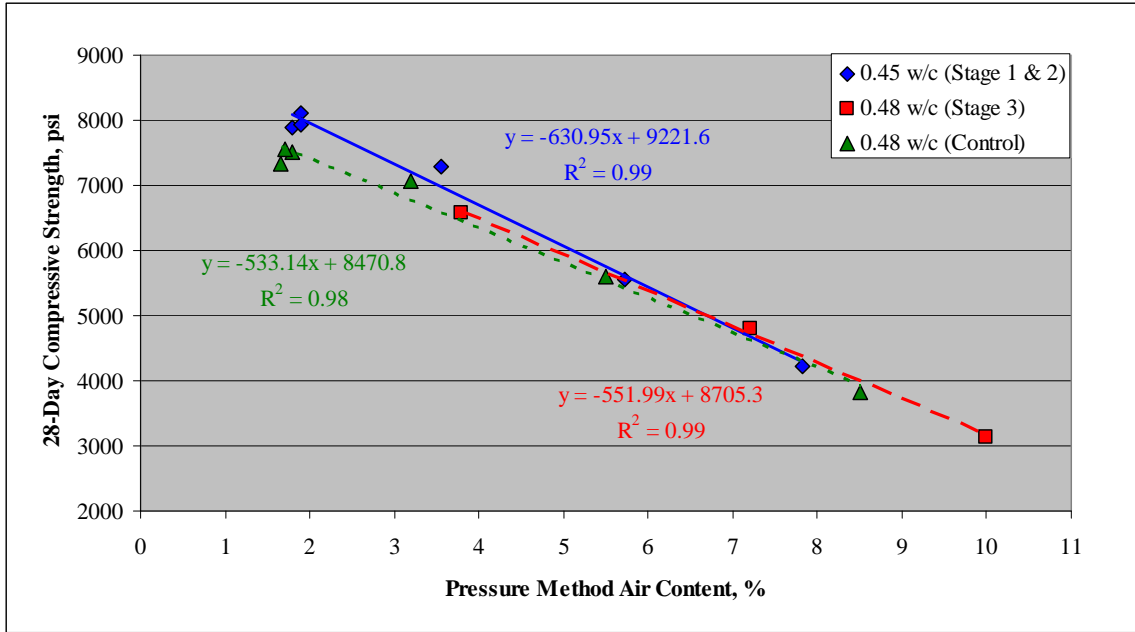


Figure 22.7: 28-Day Compressive Strength vs. Air Content (pressure method) for Mixtures Containing AEA “C”

Again, it seems that the re-tempered stages of mixtures 14-17 and 18-20 falls in line with the control mixtures. There is a slight deviation from control mixtures at higher air contents in mixtures 14-17, but mixtures 18-20 show no deviation from the control mixtures. The compressive strengths for these mixtures were also compared to the adjusted compressive strength and again showed no loss of compressive strength due to clustering. The results are shown in Table 22.2

Table 22.2: Compressive Strength Loss due to Air Void Clustering for Mixtures 14-20

Mix #	Stage	Air Content, %	Actual Compressive Strength, psi	Adjusted Compressive Strength, psi	Strength Change Potentially due to Clustering, %
14	1	2.0	7930	7930	
	2	4.9	6530	6410	1.8
	3	5.6	6100	5640	7.5
15	1	1.9	7530	7530	
	2	3.5	7370	6690	9.2
	3	3.2	6740	6410	4.9
16	1	1.9	7960	7960	
	2	5.7	5580	5950	-6.6
	3	6.2	5240	5280	-0.8
17	1	2.0	7960	7960	
	2	8.1	4740	4760	-0.4
	3	8.5	4270	4180	2.1
18	1	1.8	7880	7880	
	2	3.6	7300	6790	7.0
	3	3.8	6570	6260	4.7
19	1	1.9	8110	8110	
	2	5.7	5560	5660	-1.8
	3	7.2	4810	4510	6.2
20	1	1.9	7930	7930	
	2	7.8	4230	4220	0.2
	3	10.0	3140	2770	11.8

With the only variable changing between the mixture groups 1-7, 14-17, and 18-20 being the type of air-entraining admixture used, the above figures show that AEA “A” (wood and gum rosin) and AEA “B” (vinsol resin) have comparable compressive strength loss per every percentage of air content. The use of AEA “C” (synthetic) results in significantly higher losses of compressive strength per percent air content. *Therefore, a single value for compressive strength loss should not be used to estimate the loss of compressive strength per percent air content when evaluating different air-entraining admixtures.*

The amount of re-tempering water was also varied in a few of the Phase I mixtures to determine if the amount a re-tempering water affected the strength loss due to clustering. Mixtures 8 through 10 were re-tempered with water to increase the w/c from 0.45 to 0.47. Mixtures 11 through 13 were re-tempered to increase the w/c from 0.45 to 0.50. Figure 22.8 shows the result of the compressive strength for mixtures 11 through 13. As seen in all the other previous plots, there is little difference between the re-tempered mixtures and the control mixtures.

The percent strength loss was also calculated as described earlier and is listed in Table 22.3. Mix 8 had the highest percentage of strength loss, however it was only slightly greater than 5% which is very reasonable.

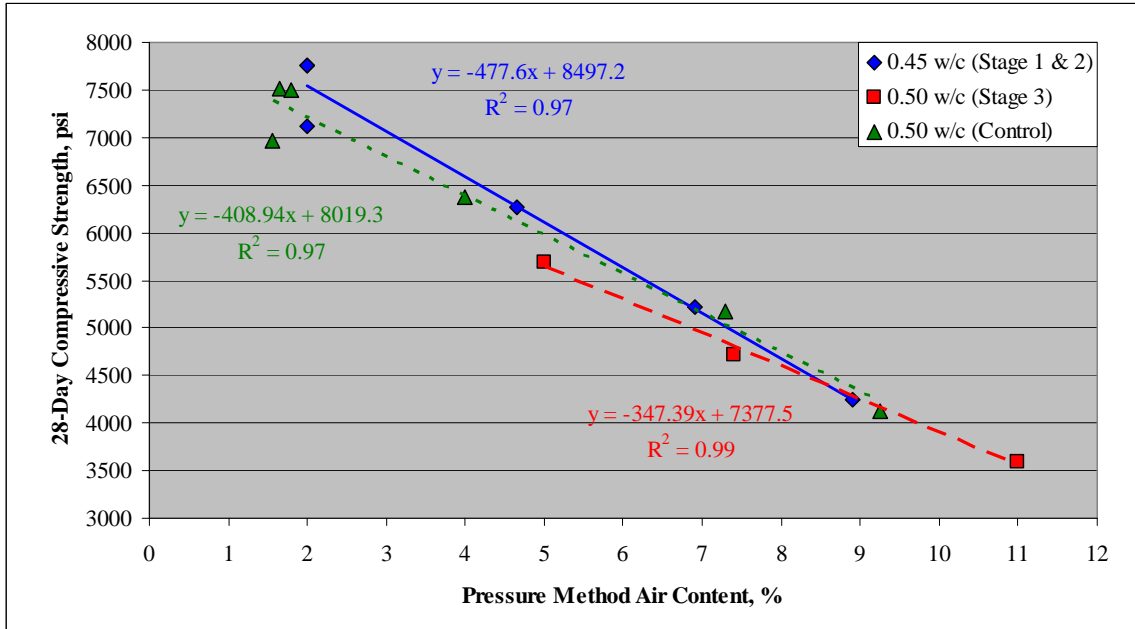


Figure 22.8: 28-Day Compressive Strength vs. Air Content (pressure method) for Mixtures Re-tempered to a 0.50 w/c and Containing AEA “A”

Table 22.3: Compressive Strength Loss due to Air Void Clustering for Mixtures 8-13

Mix #	Stage	Air Content, %	Actual Compressive Strength, psi	Adjusted Compressive Strength, psi	Strength Change Potentially due to Clustering, %
8	1	2.20	8050	8050	
	2	4.22	6750	6990	-3.6
	3	4.3	6160	6500	-5.5
9	1	1.8	7880	7880	
	2	6.66	5300	5390	-1.7
	3	5.7	5880	5250	10.7
10	1	2.1	7900	7900	
	2	9.40	4190	4150	1.0
	3	8.5	3700	3720	-0.5
11	1	2.00	7120	7120	
	2	4.65	6260	5930	5.3
	3	5.0	5690	5230	8.1
12	1	2	7750	7750	
	2	6.90	5220	5360	-2.7
	3	7.4	4720	4800	-1.7
13	1	2	7760	7760	
	2	8.90	4240	4390	-3.5
	3	11.0	3590	3350	6.7

22.1.3 Air Void Clustering Analysis

The results of the compressive strength testing indicated that the only loss of compressive strength was due to the increase in w/c. However, it was uncertain if clustering of air voids around the aggregate occurred. In order to determine the severity of air void clustering (if any), petrographic specimens were prepared and evaluated for clustering as described in Section 21.3.2.2 and Section 21.3.2.3. Tables detailing the composite cluster rating for each mix are included in the appendices of this report.

Figure 22.9 shows the composite cluster ratings for stage 2 and stage 3 for Phase I re-tempered mixtures. Every mix in mix group 1 through 7 showed an increase in the composite cluster rating from stage 2 to stage 3. Mixtures in this group with air contents higher than 6% seemed to have the greatest increase in cluster rating, even though the change in air content between stages only slightly increased.

Mixtures 8 through 10, which were re-tempered with the least amount of water, had small increases in the clustering rating, and the changes did not seem to be dependent on the air content. Mixtures 11 through 13, which were re-tempered to a w/c of 0.50, had substantial increases in the cluster rating especially at high air contents. The differences in the change in clustering rating between these two mix groups would suggest that a higher dosage of re-tempering water promotes the formation of air void clustering around the aggregate. It also seems that the dosage of AEA is important as all the high air content mixtures in both mix groups had severe clustering rating (greater than 1).

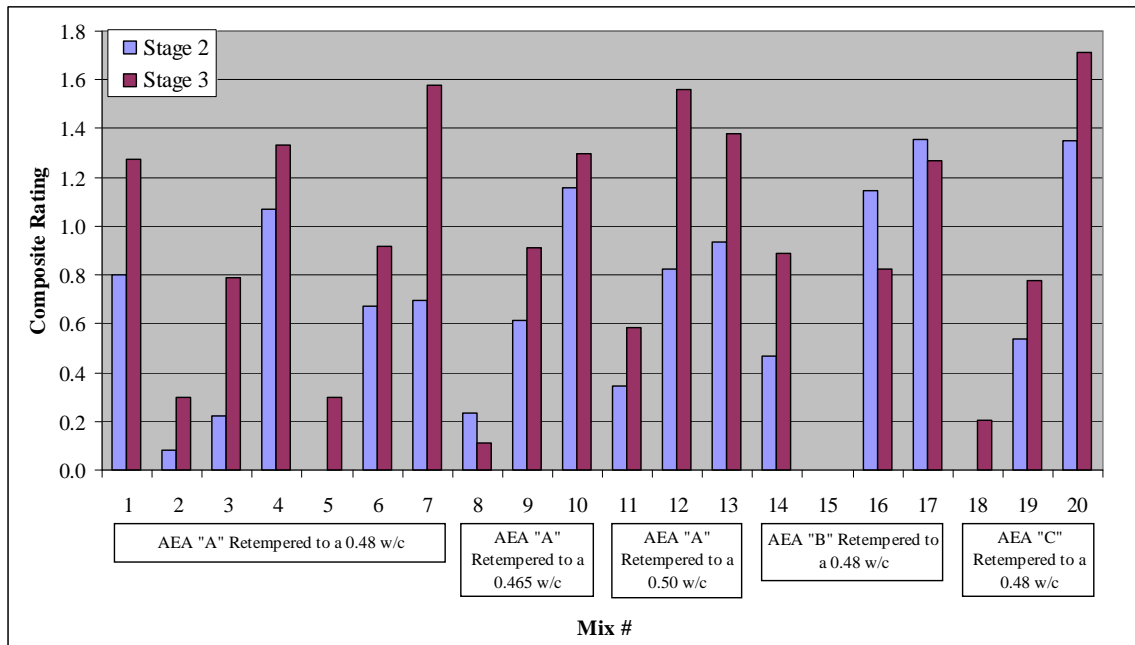


Figure 22.9: Changes in Composite Rating after Re-tempering Phase I Mixtures

Mixtures that contained vinsol resin showed interesting results. Mix 14, which had air content around 5%, had a significant increase in the cluster rating after re-tempering. However, mixtures 16 and 17 had higher air contents and had a decrease in the cluster rating after re-tempering. Mix 15, which had low air content showed no signs of clustering in either stage. It is difficult to draw conclusions from only a few mixtures, but the variability of mixtures with vinsol resin may be a clue to why these types of AEAs have not been associated with for clustering of air void around the aggregates and strength loss.

Mixtures 18 through 20 seem to have a well-defined trend. As the air content increased from low to high, the severity of the clustering also increased. Mixtures that had the largest change in air content from Stage 2 to Stage 3 also seem to have greater changes in the clustering rating. Mix 20 which had the largest change in air content between stages also had the largest change in the clustering rating.

The exercise of determining the composite rating confirmed that the modified mixing procedure used did indeed produce clustering of air void around the aggregates. Approximately 50% of the mixtures also had composite cluster ratings greater than 1, which was determined to be the critical rating to predict potential compressive strength losses (Kozikowski et al. 2005). As discussed in the previous section, none of the mixtures showed any sign of significant strength losses (beyond that caused by increased w/c).

The composite cluster rating was also plotted against the air content determined by the pressure method (Figure 22.10). There was a general trend of higher composite cluster rating with increased air content. The 0.45 w/c mixtures typically had more scatter for a given air content than the re-tempered stage and the control mixtures. Results of stage 3 plotted higher than the 0.48 w/c control mixtures. This may indicate that re-tempering and/or the additional agitation of the concrete promoted more clustering of air voids around the aggregates.

Composite cluster rating and compressive strength are also correlated (Figure 22.11). As the composite cluster rating increases, the compressive strength decreases. However, as shown in Figure 22.10, higher air contents also result in higher composite cluster ratings, and since no loss of strength could be attributed to clustering, it appears that air content rather than the severity of air void clustering has a greater effect on the compressive strength.

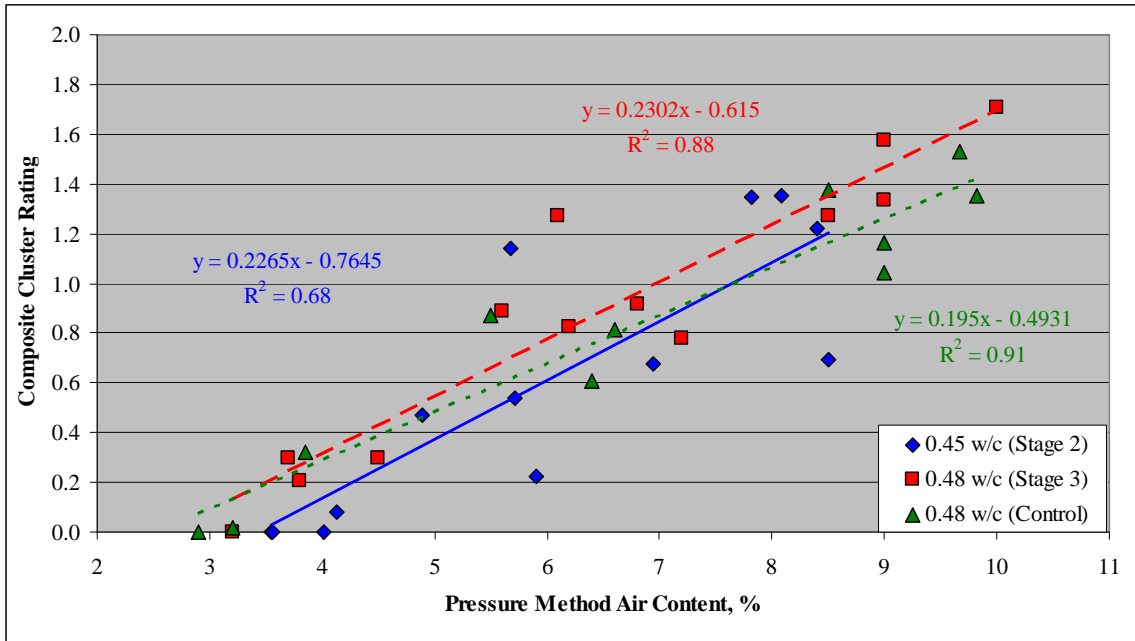


Figure 22.10: Composite Rating vs. Air Content (pressure method) for Phase I Mixtures

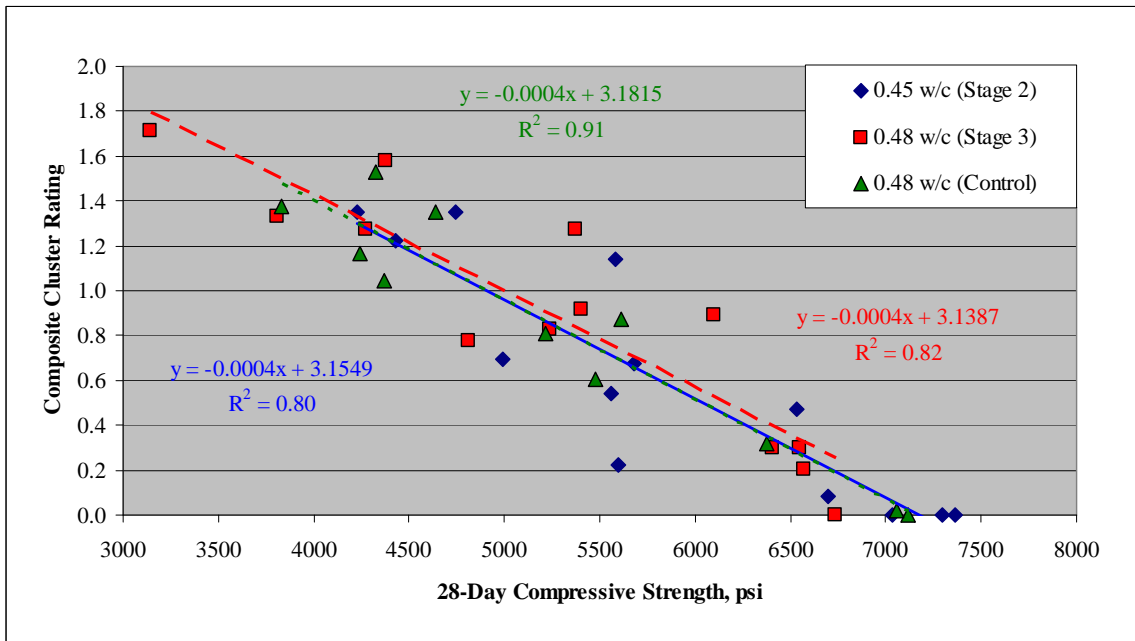


Figure 22.11: Composite Rating vs. 28-Day Compressive Strength for Mixtures Re-tempered to a 0.48 w/c for all AEA Types

The calculated percent strength loss was plotted against the composite cluster rating (Figure 22.12) and compared to data reported by Kozikowski et al. (2005) and Camposagrado (2004). Kozikowski et al.'s data clearly show a sharp increase in percent strength loss at a composite cluster rating around 1 and with the largest reported percentage of strength losses approximately 22%. It was concluded that concrete that had cluster ratings of 1 or greater would experience significant strength loss. Camposagrados' data showed greater strength loss at the lower cluster rating when compared to the other data. Unlike Kozikowski et al., there is not an abrupt increase in strength loss around the 1 composite rating, but the percent strength loss remains constant at the higher composite ratings. The data collected for this research had similar results to the Kozikowski et al. data at composite cluster ratings below 1. However, specimens with composite cluster ratings above 1 showed no increase in the percentage of strength loss, and the calculated percentage of strength loss stayed fairly constant regardless of the composite cluster rating. The inability to reproduce similar data may be an indication that the materials (cement, aggregate, etc.) used may have a big role in the effect of strength loss due to clustering of the air voids since all three researchers were able to produce clustering and some degree of strength loss.

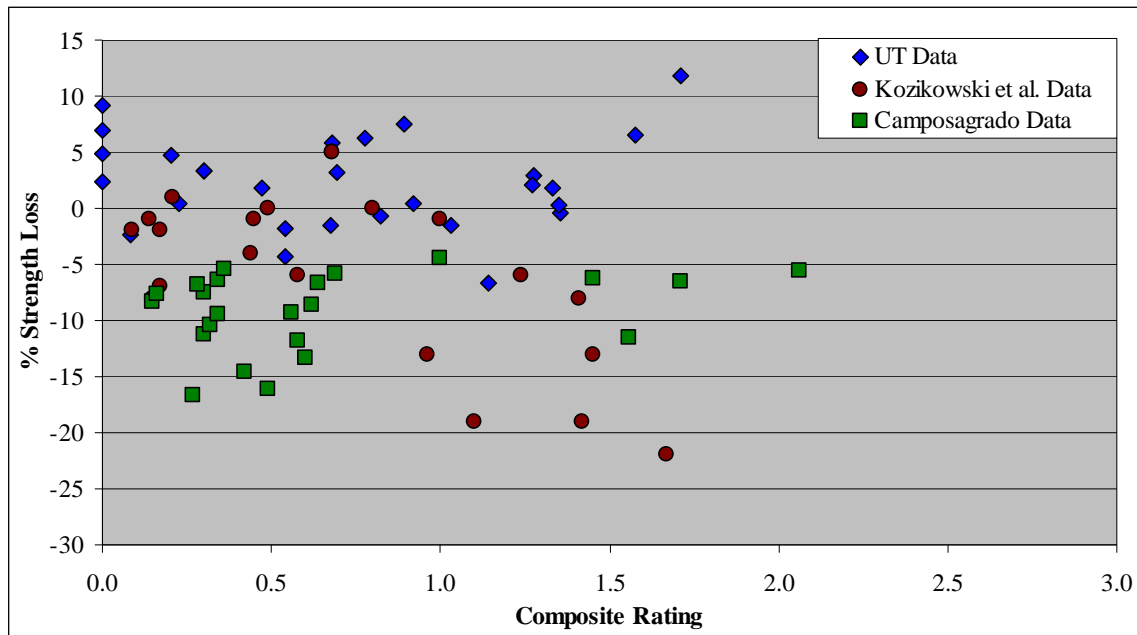


Figure 22.12: Calculated % Strength Loss vs. Composite Cluster Rating

22.2 Phase II

The results of Phase I indicated that clustering of the air voids around the aggregates did not have an effect of the compressive strength of concrete. Since the air voids around the aggregates would potentially reduce the bond strength between the paste and the aggregates, it was concluded that compressive strength testing may not be significantly affected by lack of bond. Therefore, splitting tensile and flexural testing were conducted in Phase II, with the rationale that bonding may impact these strength parameters more substantially.

Phase II consisted of six re-tempered mixtures and three non-re-tempered mixtures. Four of the re-tempered mixtures also used limestone coarse aggregates since it was reported that re-

tempering air-entrained concrete that contained limestone aggregate resulted in more severe reduction in strength than mixtures with siliceous river gravel (Kozikowski et al. 2005). The remaining re-tempered mixtures used siliceous river gravel. Only AEA “A” and AEA “B” were evaluated in Phase II. Detailed tables of the mixture designs and testing results for Phase II mixtures are included in Appendix C and D.

Phase II mixtures were mixed in a larger mixer than Phase I mixtures because more concrete was needed to cast the additional test specimens. The mix proportions were kept constant and only the batch size was increased. Due to the potential differences in mixing action of the two mixers and the differences in batch size, the Phase II data were not combined with Phase I data and the two data sets were only compared to note any differences the mixers or batch size may have had on the concrete.

22.2.1 Fresh Concrete Test Results

After every stage of mixing, slump, unit weight, and air content (pressure method) tests were performed. Figure 22.13 shows the results of the slump tests for the re-tempered mixtures. In all mixtures, the addition of air-entraining admixture during stage 2 resulted in a slight increase in slump (average of 0.3 inches) from stage 1. This is a substantial decrease from Phase I mixtures which had an average increase of 2 inches. The decrease in slump change can potentially be attributed to the use of limestone which can reduce the workability of the mix, and the reduced mixing energy of the larger mixer and the increased batch size.

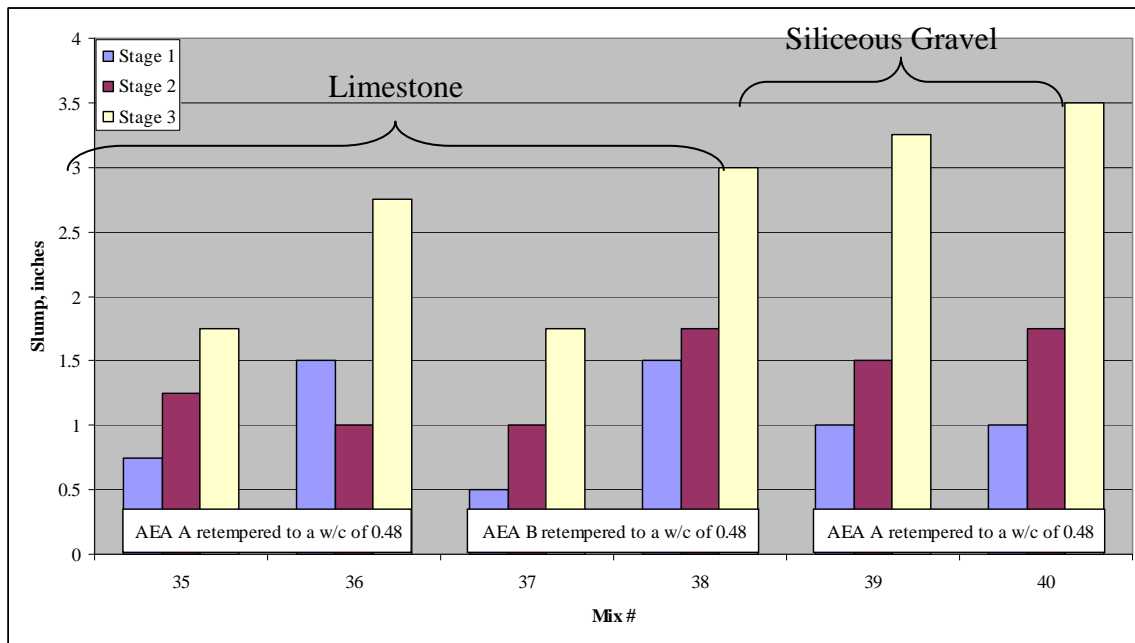


Figure 22.13: Change in slump for Phase II Mixtures

All of the Phase II mixtures were re-tempered to a final w/c of 0.48, an addition of 17 lb/ft³ of water. The addition of water and extended mixing from stage 3 resulted in an average increase of 1 inch of slump from stage 2 for mixtures that contained limestone coarse aggregate. This increase in slump is less than expected with the amount of water added. The mixtures that contained the siliceous river gravel had an average increase of 1.75 inches of slump which is

closer to what was observed in Phase I. This is an indication that limestone coarse aggregate has a more pronounced effect on the workability of the concrete than siliceous river gravel coarse aggregates.

Unit weight and fresh air content of concrete was determined after every mixing stage. Figure 22.14 shows the results of the unit weight vs. air content (pressure method) for all the mixtures in Phase II. This plot shows that the unit weight follows that general trend expected with a very good R^2 value of 0.97. As the fresh air content increased the unit weight decreased for all stages of the mixing procedure.

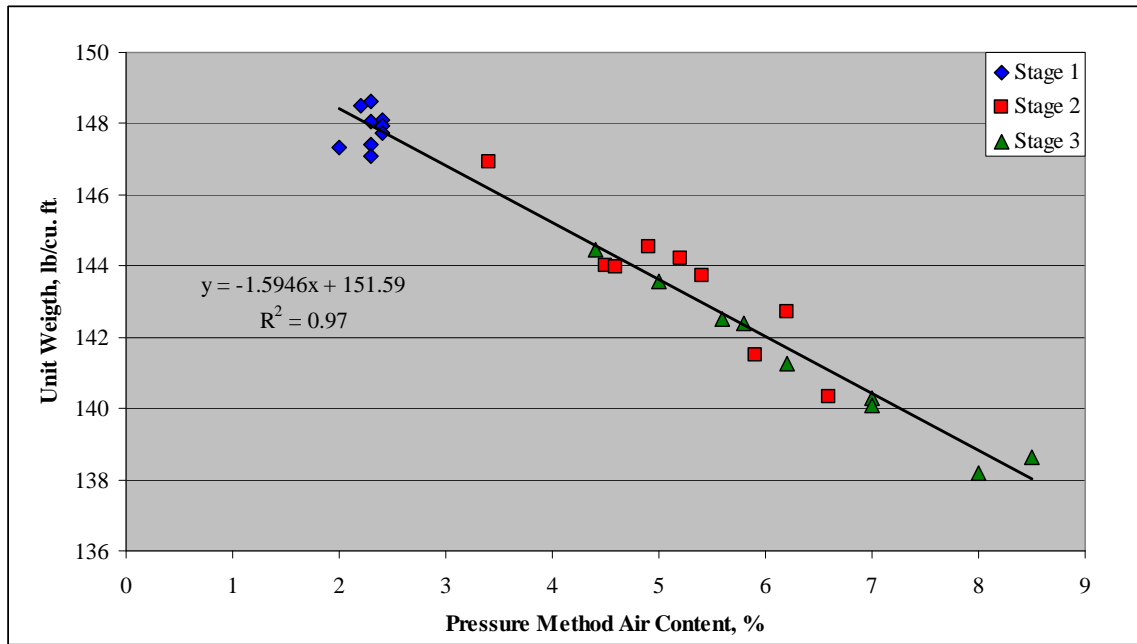


Figure 22.14: Unit Weight vs. Air Content (pressure method) for Phase II Mixtures

Figure 22.15 plots the air contents (gravimetric method) vs. the air contents (pressure method) for all the mixtures in Phase II. The linear correlation has a very good R^2 value of 0.97. However, the air content (pressure method) tended to result in air contents about 1% higher than the gravimetric air contents. As explained in the previous section, determination of air content by the gravimetric method has been found to be somewhat inaccurate (Pigeon and Pleau 1995).

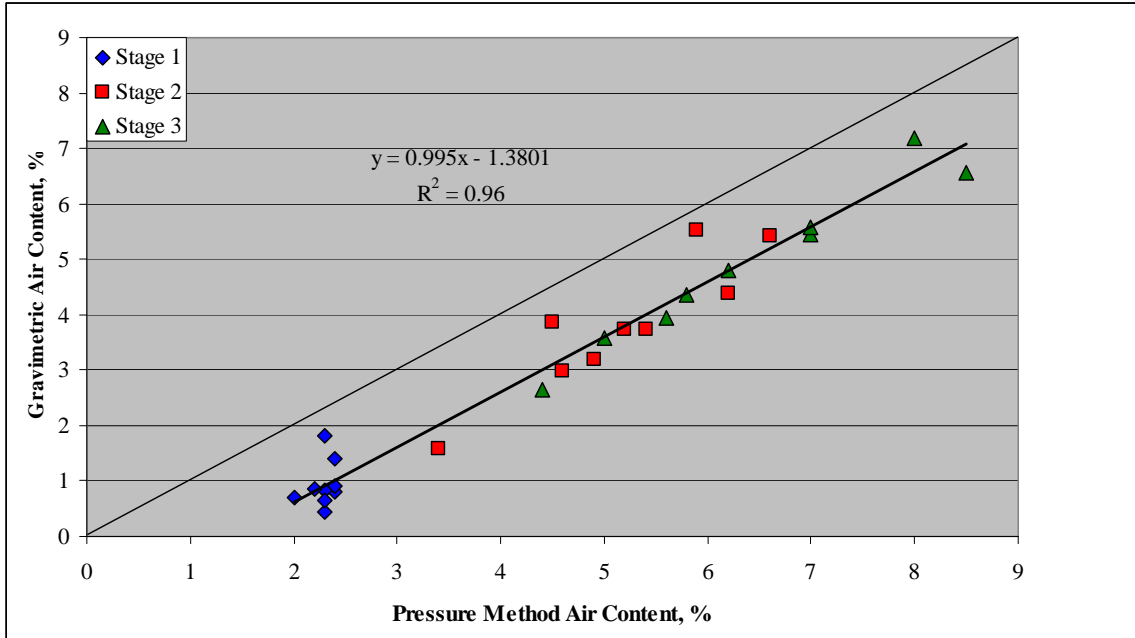


Figure 22.15: Gravimetric Air Content vs. Air content (pressure method) for Phase II Mixtures

The changes in air content after re-tempering and additional agitation varied and seemed to be dependent on the air content before re-tempering (Figure 22.16). Mixtures that had stage 2 air contents around 5% and less had an increase in air content of less than 1% after adding the re-tempering water and performing the additional agitation. The other mixtures, which had air contents greater than 5%, had an increase in air contents around 2%. This trend holds true regardless of the type of AEA and type of aggregate used in the mix. This is similar to what was observed in Phase I where high stage 2 air contents tended to have larger increases in air content after re-tempering.

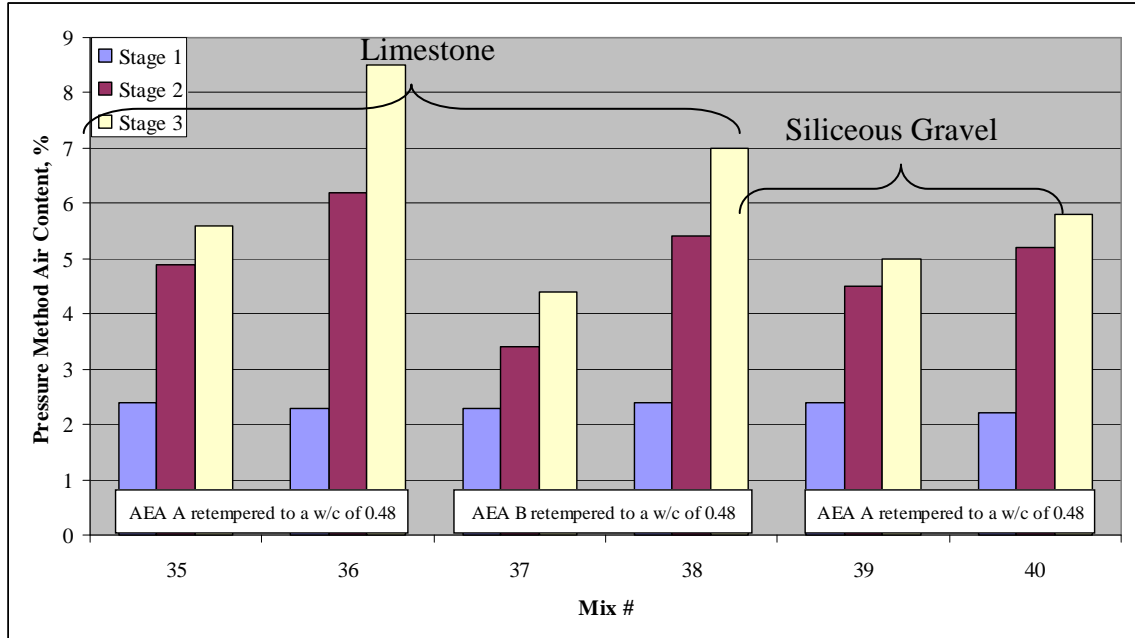


Figure 22.16: Changes in Air Content for Phase II Mixtures

22.2.2 Compressive Strength Test Results

The main objective of Phase II was to evaluate the effects re-tempering had on splitting tensile and flexural strength, but compressive strength specimens were also cast to determine if there were any differences in the trends noted in Phase I. Compressive strength cylinders were tested at 7 and 28 days of age for each stage of every mix. The intent of this testing was to determine the reduction in compressive strength due to re-tempering and compare the strength to mixtures with the same w/c that were not re-tempered.

Due to the limited data set for each of these mixtures, the percent loss of compressive strength per percent air content could not be determined with any confidence. However Figures 22.17, 22.18, and 22.19 all show the same general trend observed in Phase I. The compressive strength of the re-tempered stages of each mix was higher than the control mixtures that contain limestone coarse aggregate for both the non-vinsol AEA and the vinsol resin AEA. This would suggest that clustering of air voids, if achieved, did not affect the compressive strength, a similar conclusion as in Phase I. This trend also suggests that concrete mixtures with limestone coarse aggregate do not experience larger strength losses than concrete mixtures with siliceous river gravel coarse aggregate as previously reported by others.

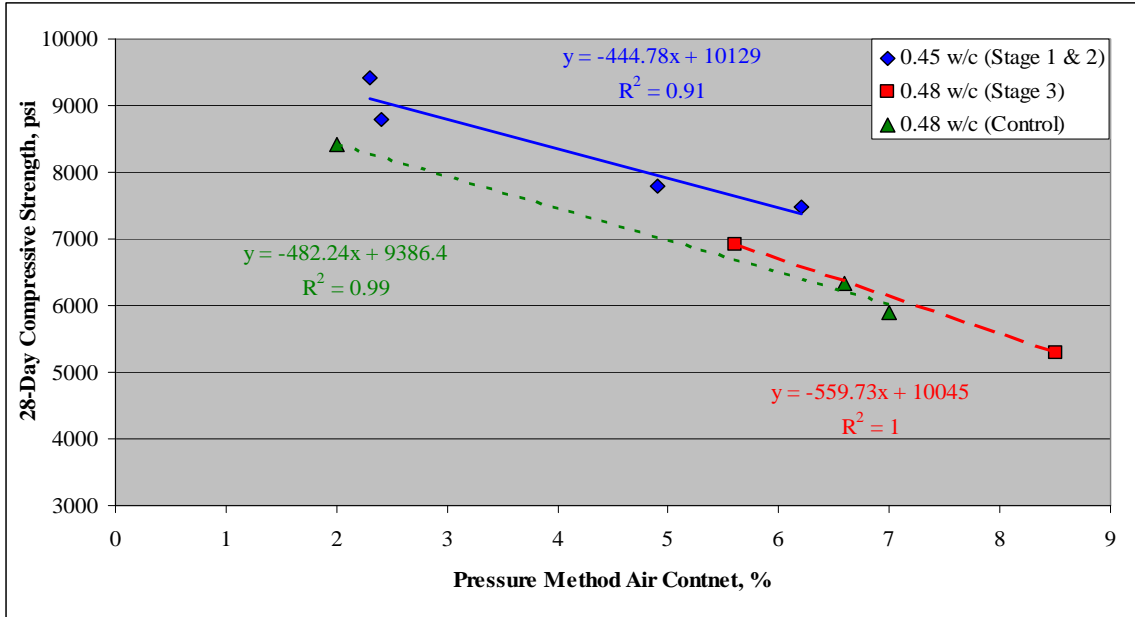


Figure 22.17: 28-Day Compressive Strength vs. Air Content (pressure method) for Mixtures Containing AEA "A" and Limestone Coarse Aggregate

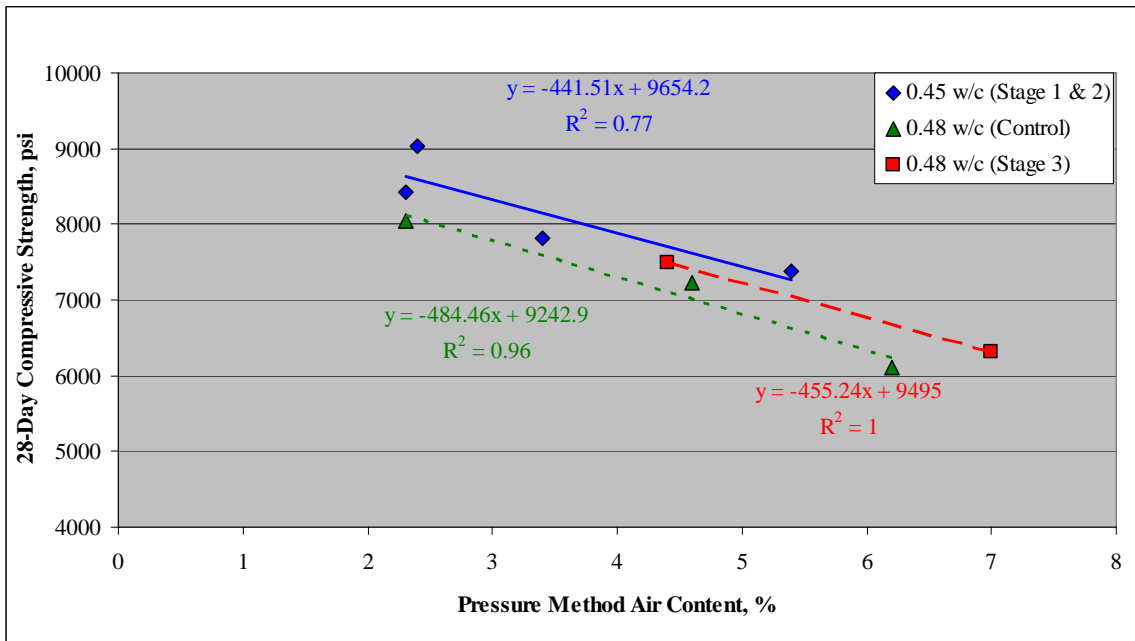


Figure 22.18: 28-Day Compressive Strength vs. Air Content (pressure method) for Mixtures Containing AEA "B" and Limestone Coarse Aggregate

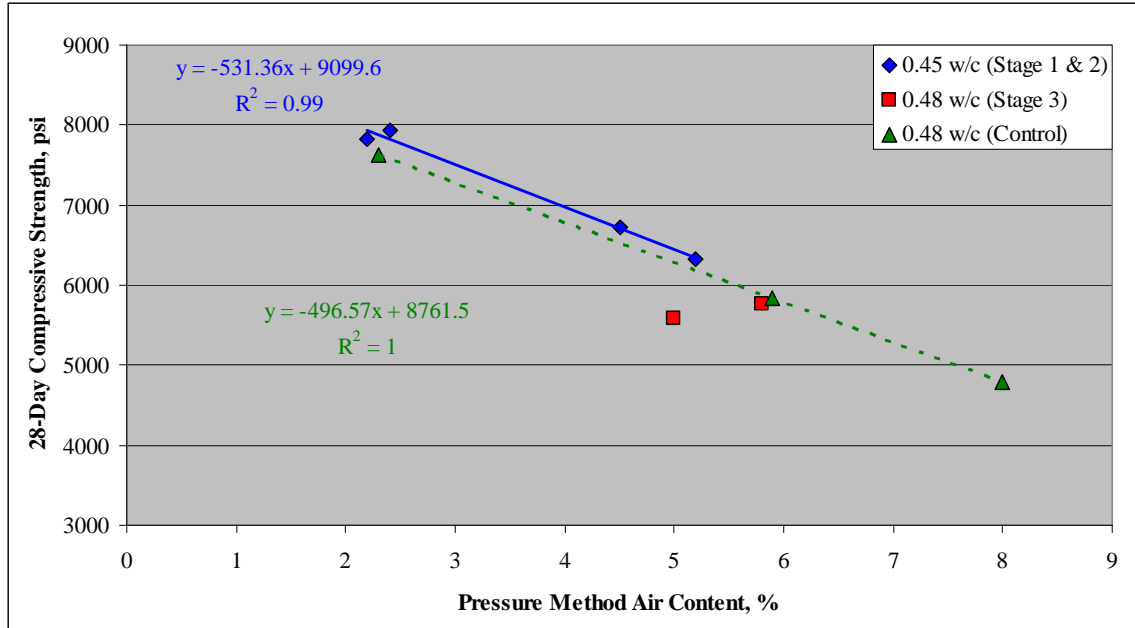


Figure 22.19: 28-Day Compressive Strength vs. Air Content (pressure method) for Mixtures Containing AEA “A” and Siliceous Coarse Aggregate

22.2.3 Splitting Tensile Strength Test Results

The results of the compressive strength testing conducted in Phase I and Phase II clearly demonstrated that the clustering of air voids did not dramatically affect compressive strength. Splitting tensile testing was conducted to determine if other strength properties of the concrete were affected.

The 28-day splitting tensile strength of the re-tempered stage for mixtures with limestone coarse aggregate and a non-vinsol resin AEA (Figure 22.20) indicated that the splitting tensile strength of the re-tempered stage was about 100 psi lower than the control mixtures splitting tensile strength. This was thought to be the long sought strength loss, but as will be discussed later, this strength loss was not due to clustering of air voids around the aggregate. The 7-day splitting tensile strength for this series of mixtures (Figure D.3) shows a better correlation between the mixtures. This leads to the conclusion that there was some unknown error in the testing of these 28-day splitting tensile specimens.

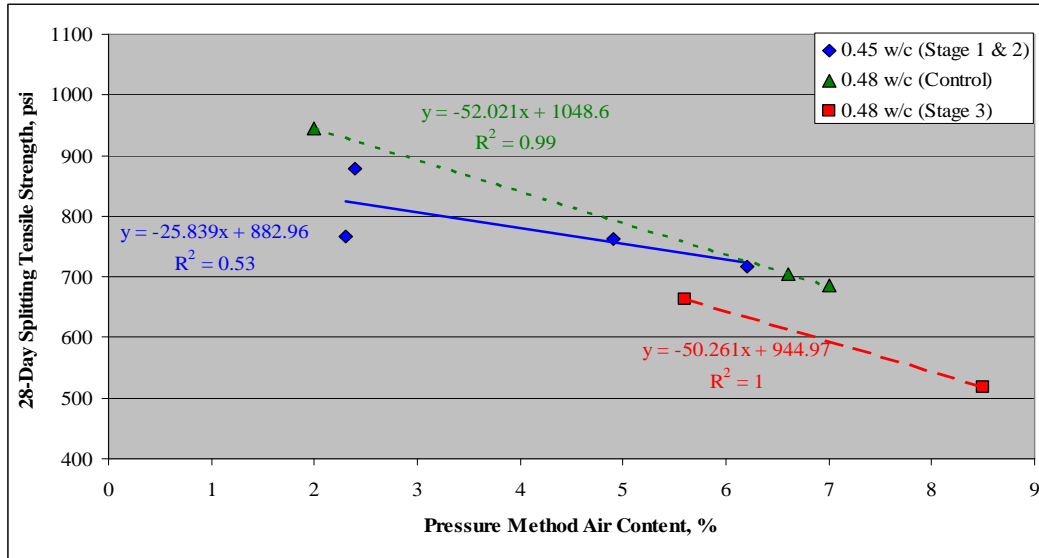


Figure 22.20: 28-Day Splitting Tensile Strength vs. Air Content (pressure method) for Mixtures Containing AEA “A” and Limestone Coarse Aggregate

Figures 22.21 and 22.22 show similar trends to the compressive strength trends already discussed. The splitting tensile strength of the re-tempered stages of these mixtures had strengths that were equal to or higher than the control mix’s splitting tensile strength. The use of limestone coarse aggregates resulted in slightly higher splitting tensile strength than siliceous river gravel mixtures, and none of the mixtures showed any signs of significant strength loss.

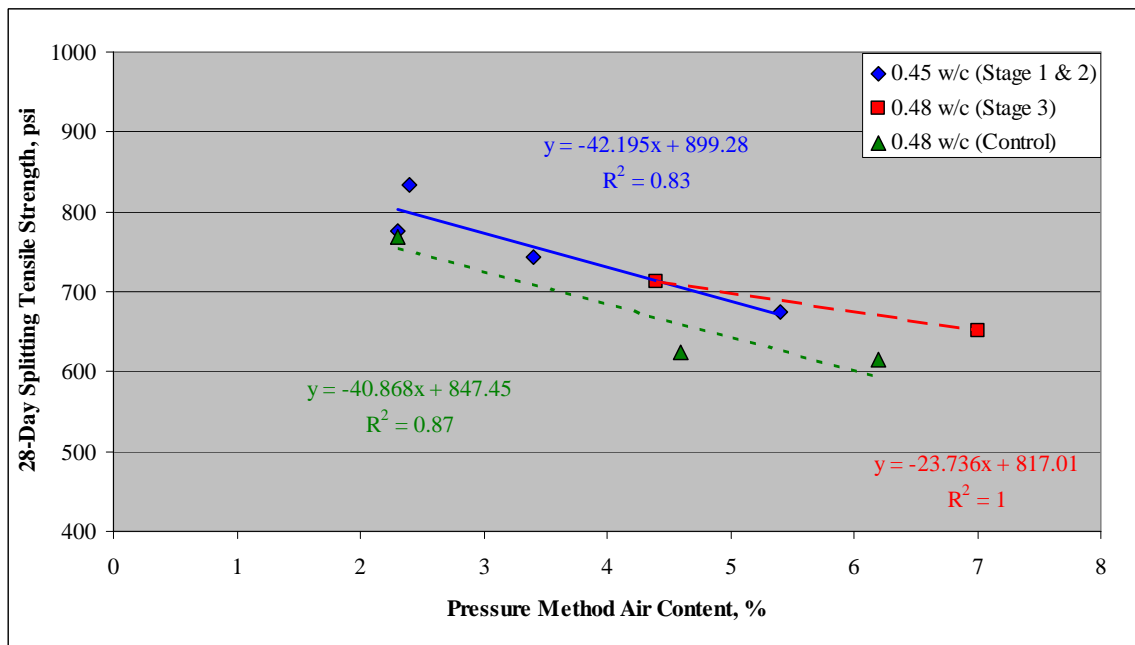


Figure 22.21: 28-Day Splitting Tensile Strength vs. Air Content (pressure method) for Mixtures Containing AEA “B” and Limestone Coarse Aggregate

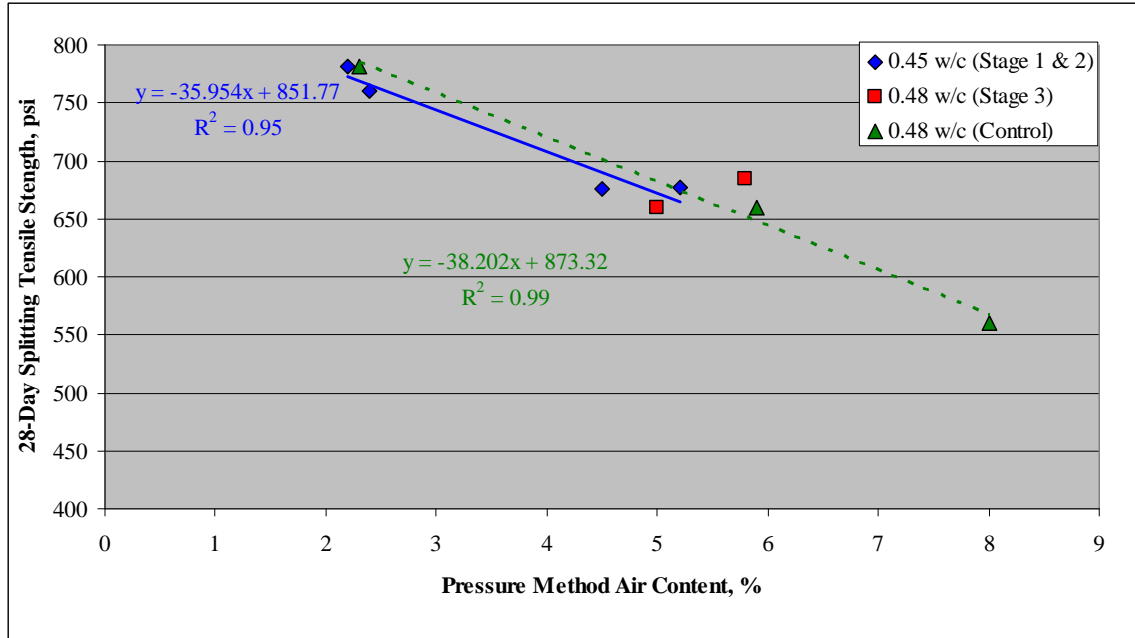


Figure 22.22: 28-Day Splitting Tensile Strength vs. Air Content (pressure method) for Mixtures Containing AEA “A” and Siliceous Coarse Aggregate

22.2.4 Flexural Strength Test Results

Flexural strength specimens were tested at 7 days of age for each stage of every mix and conducted according to ASTM C 78. The intent of this testing was to determine the reduction in flexural strength due to re-tempering and compare the strengths to mixtures with the same w/c that were not re-tempered. If the bond strength between the aggregate and the paste was affected by the presence of air voids, the re-tempered stages of these mixtures should have lower flexural strengths than the control mixtures.

Figures 22.23, 22.24, and 22.25 all show the same general trend. The flexural strength of the re-tempered stages of each mix falls in line with the flexural strengths of the control mixtures. The use of limestone coarse aggregates resulted in slightly higher flexural strength than siliceous river gravel mixtures. Assuming that clustering of air voids around the aggregate was achieved, it does not appear that re-tempering had any effect on the concrete other than the reduction of strength due to the increase in w/c. Mixtures with AEA “A” and limestone coarse aggregate (Figure 22.24) showed no strength reduction due to the increase in w/c in the re-tempered stage or the control mixtures. All splitting tensile strengths were similar to the 0.45 w/c stages.

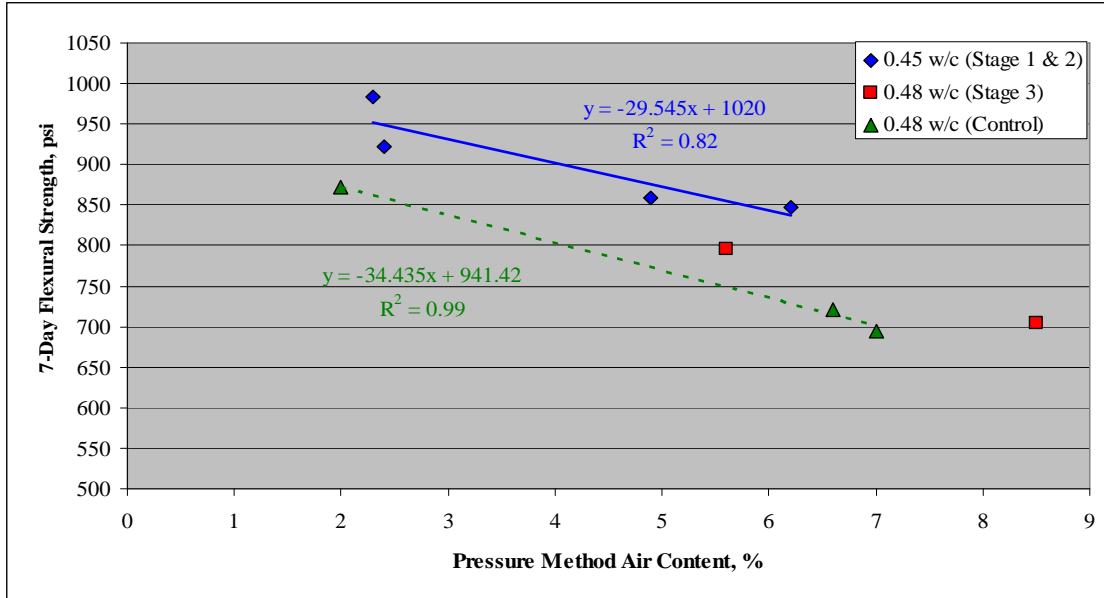


Figure 22.23: 7-Day Flexural Strength vs. Air Content (pressure method) for Mixtures Containing AEA "A" and Limestone Coarse Aggregate

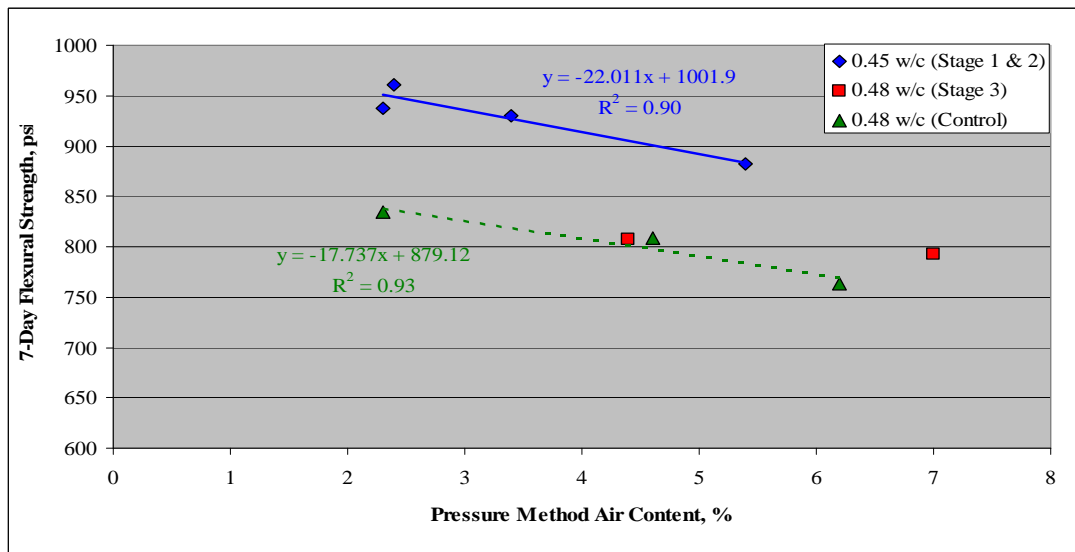


Figure 22.24: 7-Day Flexural Strength vs. Air Content (pressure method) for Mixtures Containing AEA "B" and Limestone Coarse Aggregate

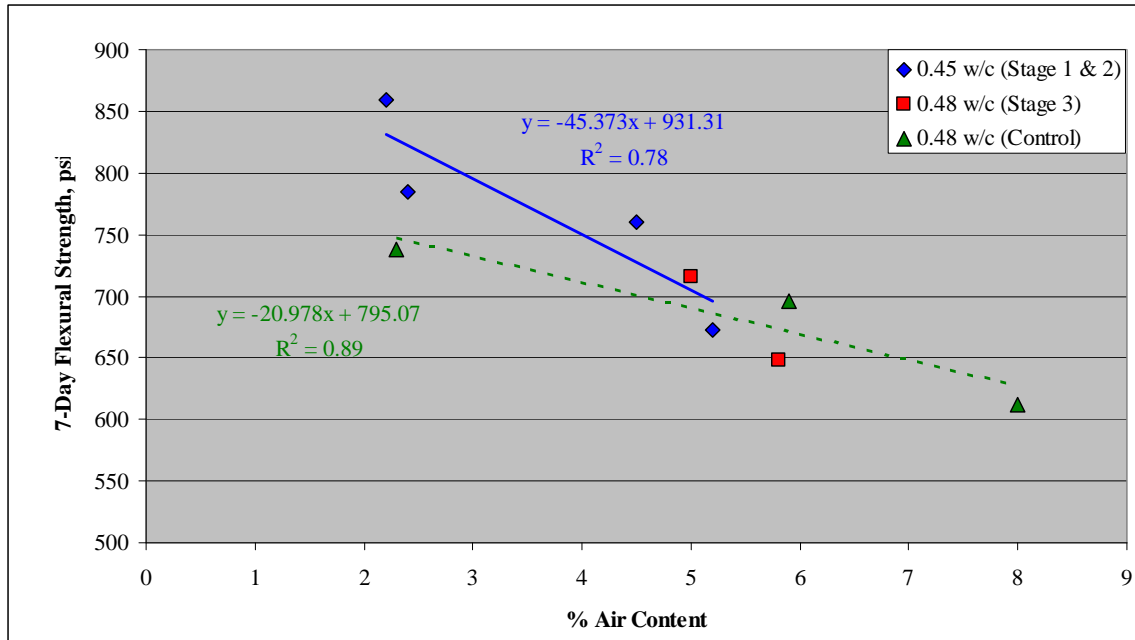


Figure 22.25: 7-Day Flexural Strength vs. Air Content (pressure method) for Mixtures Containing AEA “A” and Siliceous Coarse Aggregate

22.2.5 Air Void Clustering Analysis

The results of the Phase II strength testing indicated that the only loss of compressive strength was due to the increase in w/c. However, the severity of air void clustering around the aggregates needed to be determined in order to confirm that clustering was achieved with the larger mixer and increased batch size. Petrographic specimens were prepared and evaluated for clustering as described in Section 21.3.2.2 and Section 21.3.2.3. Tables detailing the composite cluster rating for each mix are included in Volume III Appendices B and D.

Mixtures 35 and 36 contained a non-vinsol resin AEA and limestone coarse aggregate and stage 2 of each mix showed no signs of clustering of the aggregate even with air content above 5% (Figure 22.26). Stage 3 of mix 35 also did not have any clustering of air void around the aggregate, and stage 3 of mix 36 had an increase in the clustering rating, but the rating was still below the critical rating. Because these mixtures did not experience severe clustering of the air void around the aggregate, the low 28-day splitting tensile strengths for these mixtures could not be attributed to clustering.

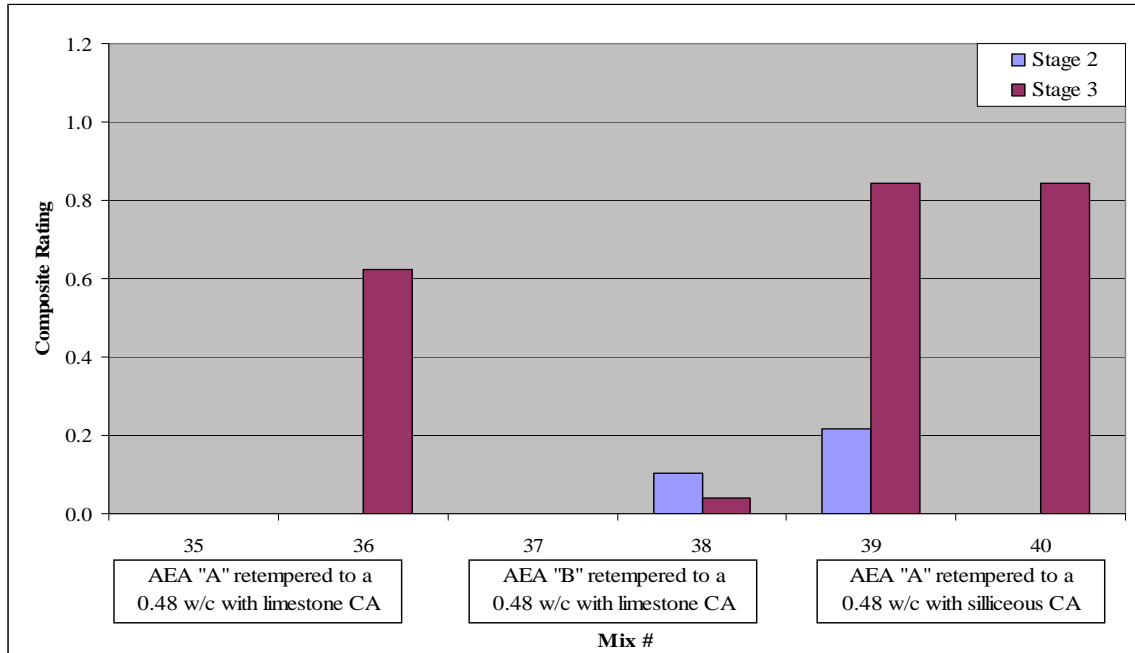


Figure 22.26: Changes in Composite Cluster Ratings for Phase II Mixtures

Mixtures 37 and 38 also used a limestone coarse aggregate and a vinsol resin AEA. These two mixtures also showed no signs of severe clustering before and after re-tempering. Mixtures 39 and 40 used AEA “A” and siliceous river gravel coarse aggregate and were similar to mixtures in mix group 1 through 7 in Phase I. The composite cluster ratings for stage 2 were slightly lower than the Phase I mixtures with the same air contents. The stage 3 composite cluster ratings were very close to Phase I mixtures that had the same air content.

The composite cluster rating was plotted against the air content determined by the pressure method (Figure 22.27). There was more scatter in these mixtures than in Phase I. There was a general trend of higher composite cluster rating with increased air content. With the limited number of mixtures, it is difficult to determine if these scatter was due to the use of the larger mixer or the increased batch size.

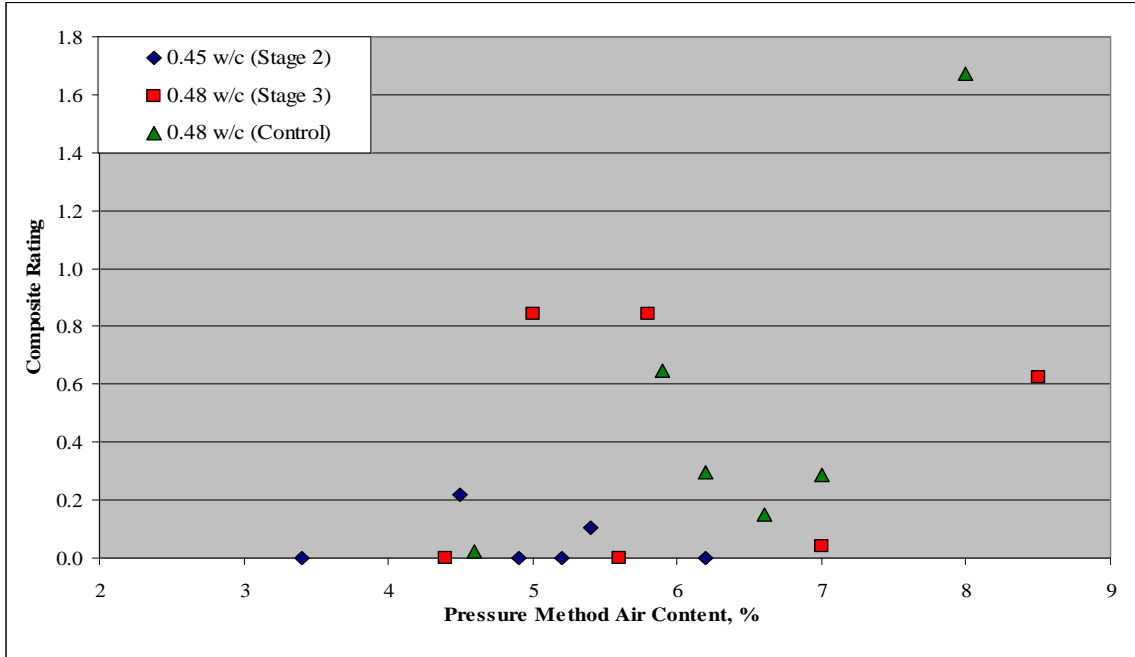


Figure 22.27: Composite Cluster Ratings vs. Air Content (pressure method)

There is also a trend of composite cluster rating and compressive strength (Figure 22.28). As the composite cluster rating increased, the compressive strength decreased. The stage 3 compressive strengths seem to follow this trend quite well. However, several of the control mixtures that had low composite cluster rating also had low compressive strengths. Again, as noted in Phase I, the air content may play a bigger role than the clustering rating.

Figure 22.29 shows composite cluster rating versus the 28-day splitting tensile strength. It is difficult to note any trends due to the amount of scatter in the data. Figure 22.30 shows there is a good correlations between the cluster rating and the 7-day flexural strength. As the composite cluster rating increase, the flexural strength decreases.

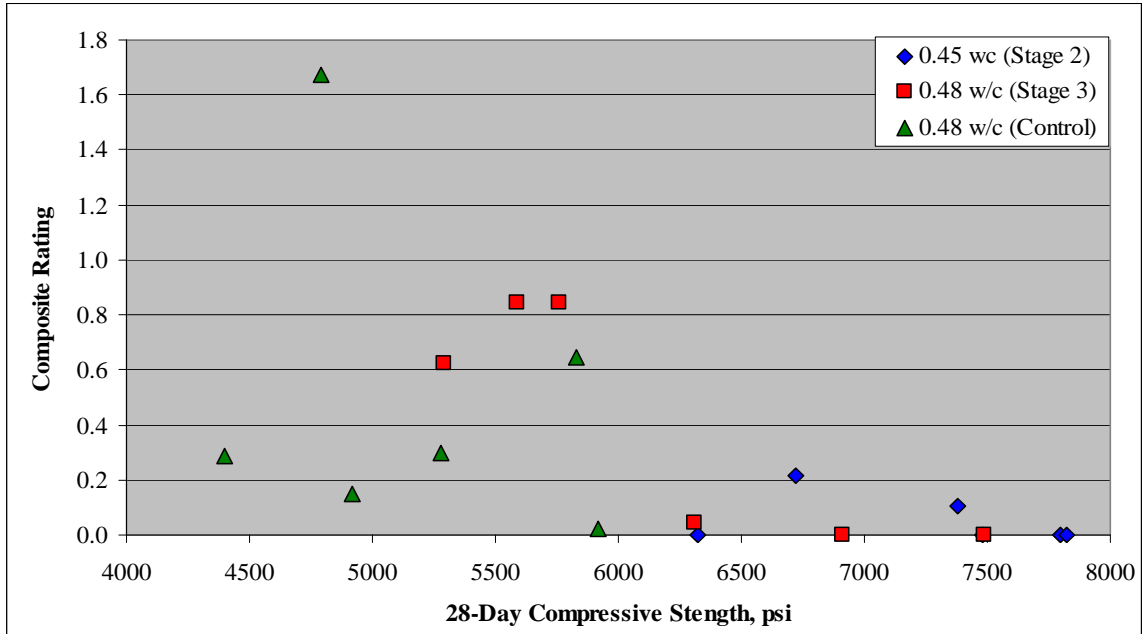


Figure 22.28: Composite Cluster Ratings vs. 28 Day Compressive Strength

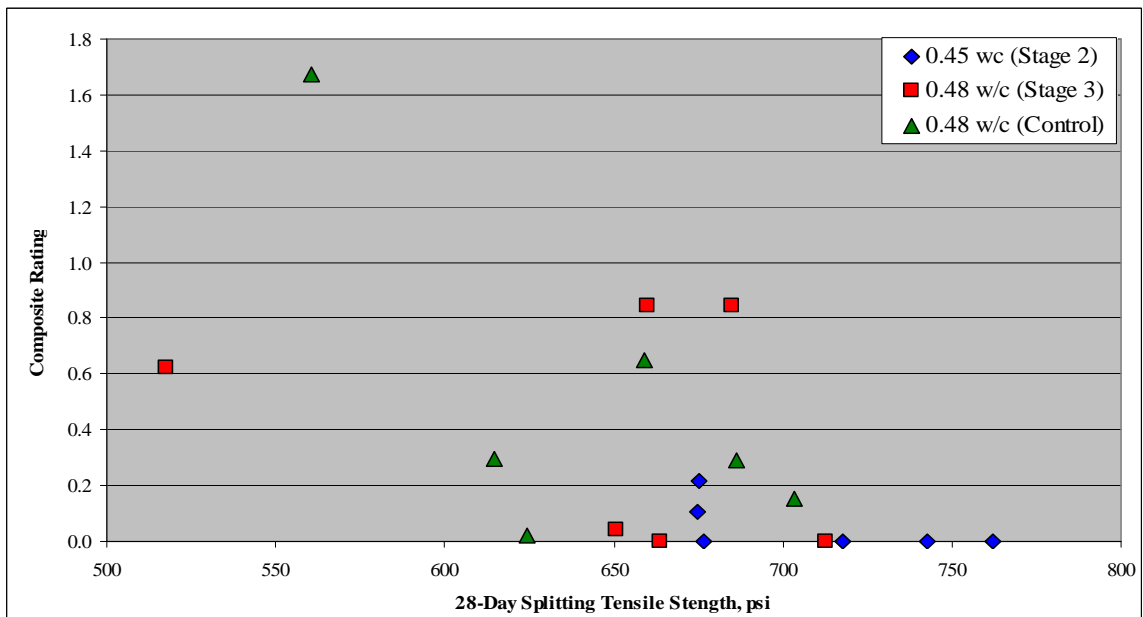


Figure 22.29: Composite Cluster Ratings vs. 28 Day Splitting Tensile Strength

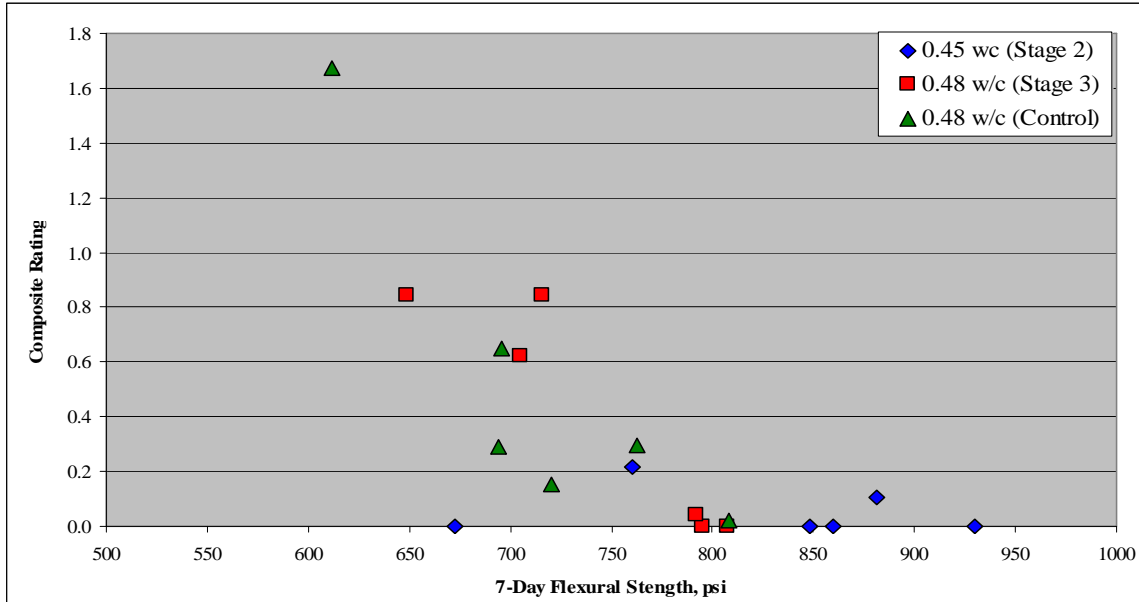


Figure 22.30: Composite Cluster Ratings vs. 7-Day Flexural Strength

22.3 Hardened Air Void Analysis

It has been proposed that clustering of air voids around the aggregates is directly connected to the fineness of the air void system (Kozikowski 2005). Concretes that have high specific surfaces and low spacing factors are considered to have finer air void systems. It should be noted that clustering of the air voids around the aggregate, or even out in the bulk paste may potentially skew the results of the hardened air void analysis towards the finer side. The close spacings of the clustered air voids may falsely indicate a finer air system. In order to properly determine the effect of clustering on the air void system, the characteristics of the voids around the aggregate should be subtracted from the total air void characteristics to determine the air void system of the bulk paste. The difference between the total air void system and the corrected air void system would be the effect of clustering. To do this would be extremely difficult, if not impossible, and is well beyond the scope of this project.

Hardened air void analysis was performed on a selection of mixtures from Phase I and Phase II to determine the effect re-tempering had on the air void system. Hardened air void analysis was performed according to ASTM C 457 and as described in Section 21.3.2.4. Since strength test results did not indicate any obvious signs of strength loss due to clustering, the specimens were selected based on the fresh air contents. Specimens having air content in the range of 3% to 9% were chosen for hardened air void analysis. The results of the hardened air void analysis are presented in Appendix E.

The fresh air content showed reasonable agreement with the hardened air content in Phase I (Figure 22.31). There were a few discrepancies at the higher air contents. The hardened air void analysis calculated higher air content than the measured fresh air content. The possible reasons for this were explained in Chapter 19. Phase II mixtures had more scatter than the Phase I mixtures however; all but two of the results are within the typical 2% deviation (Whiting and Nagi 1998).

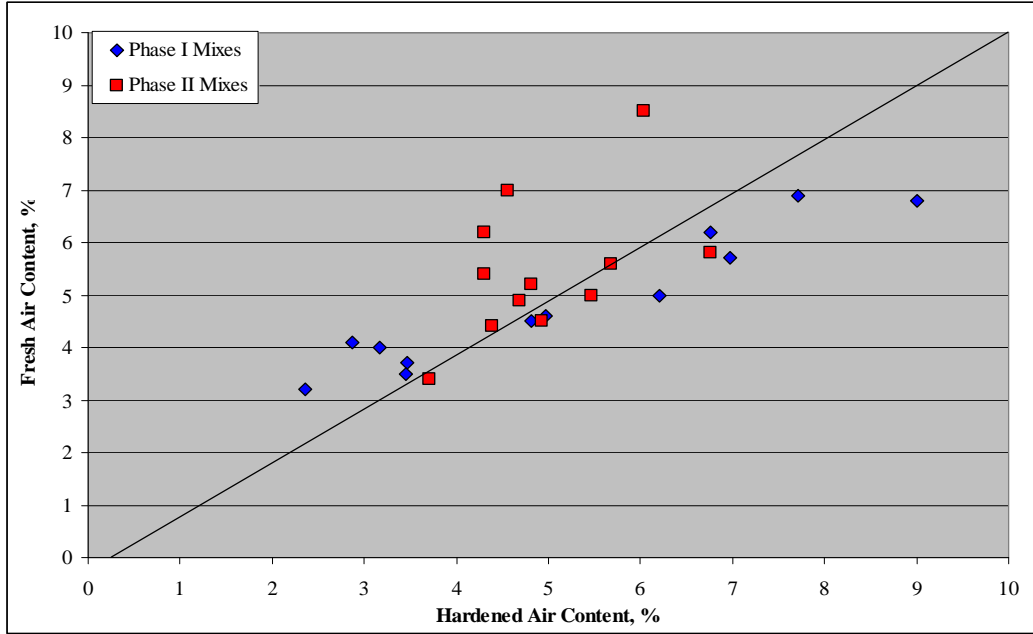


Figure 22.31: Fresh Air Content vs. Hardened Air Content

It has been well documented that re-tempering air-entrained concrete has little to no effect on the spacing factor and specific surface. The same trend was also noted in this research. In all but three of the mixtures, the spacing factor decreased from the stage 2 value (Figure 22.32). The decrease may potentially be attributed to the additional agitation which may have cause a better distribution of the air voids. All of the spacing factors were also well below the 0.008 in limit to be considered freeze-thaw durable.

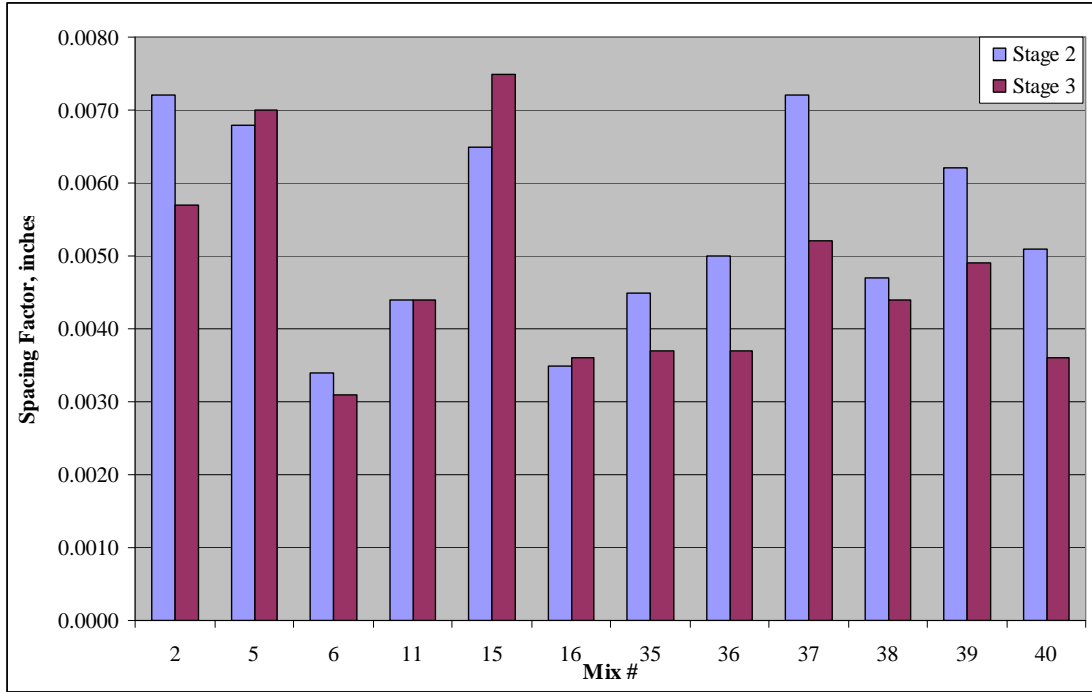


Figure 22.32: Changes in Spacing Factor

Figure 22.33 shows the changes in the specific surface after re-tempering and agitation of the concrete. Similar to the documented trends, there was very little change in the specific surface of the air void system. Phase I mixtures only had small changes in the specific surface where as Phase II mixtures had slightly larger changes. However, the changes are still relatively minor.

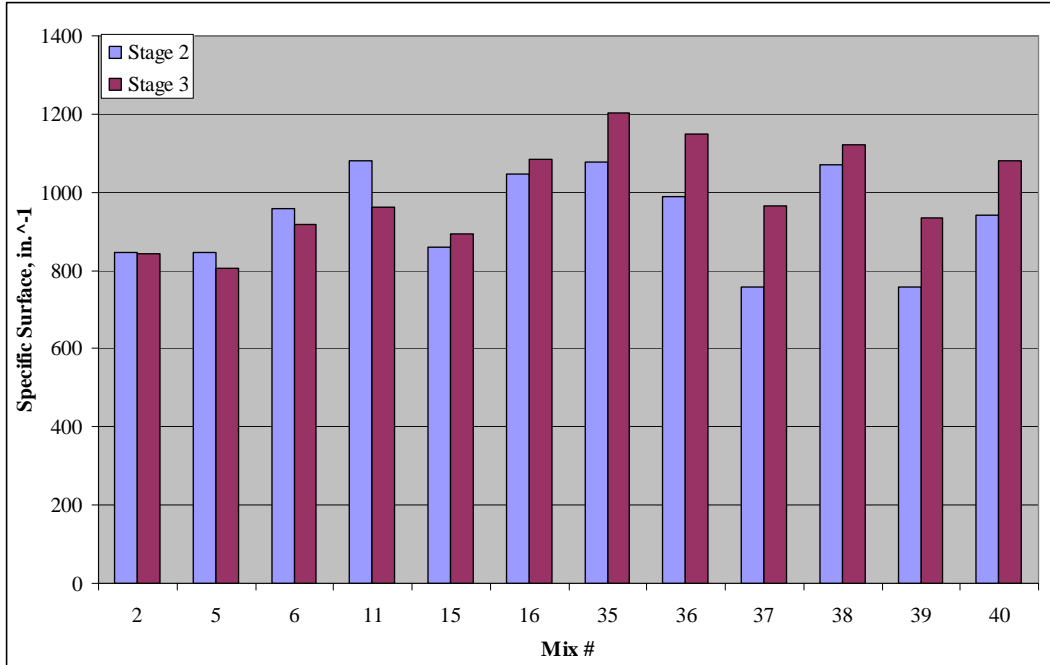


Figure 22.33: Changes in Specific Surface

Figure 22.34 plots the composite cluster rating against the spacing factor for Phase I and Phase II mixtures. This plot indicates that as the air void system get finer (lower spacing factors), the degree of clustering increases. However, for reasons already discussed, this may not actually be an accurate trend, and there is no way to quantitatively determine the effect of clustering on the air void system.

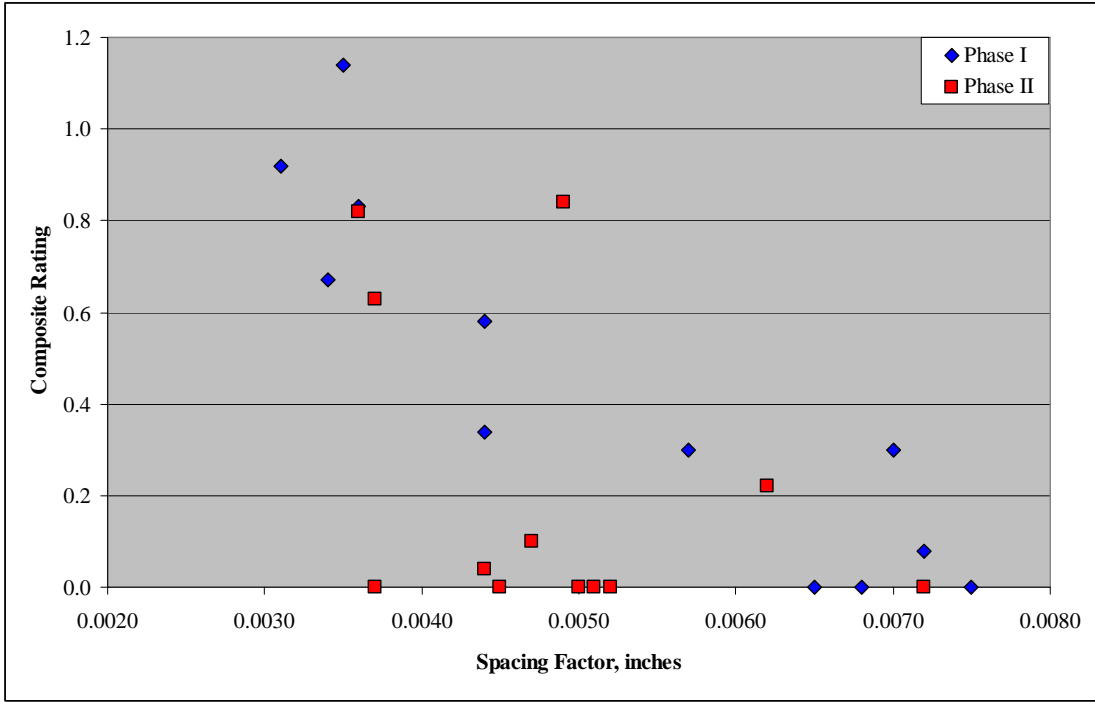


Figure 22.34: Composite Rating vs. Spacing Factor

Chapter 23. Field Case Studies

As previously mentioned, over the past several years, Texas DOT has reported several case of low concrete compressive strength which also had signs of clustering of air voids around the aggregate. The follow sections are a review of the available field data and petrographic reports for several of the reported low concrete strength cases to determine if any correlations between air void clustering in field concrete and re-tempering exists. The information contained in these sections was provided by Texas DOT, and the petrographic analysis presented in this chapter was performed by Texas DOT.

23.1 Case Study #1

County: Nueces	CSJ: 0671-02-046
Structure Type: Bridge Deck	Location: Humble Bridge
Sample Type: Cores	Date: June 2003
Type of Coarse Agg.: River gravel	Type of AEA: Unknown

Compressive strength cylinders taken during casting operations of the bridge deck failed to meet the 28-day compressive strength requirement of 4000 psi (Table 23.1). Fresh concrete air contents did indicate that several of the air contents were high, but still within specification tolerance.

Table 23.1: Field Test Results

Span	Set #	Slump, inches	Air Content	28-Day Compressive Strength, psi
2	1	4	7%	3550
	2	4	6%	3780
6	1	4 1/2	8%	2665
	2	4 1/2	6%	3261
8	2	4 1/2	8%	3020

A review of the available concrete batch tickets indicated that every load of concrete contained 80 lbs/yd³ of ice, and multiple loads of concrete were re-tempered with water. During the casting of span 2, concrete loads were re-tempered with 4 lbs/yd³ to 9 lbs/yd³ of water. It was not possible to determine from which loads the compressive strength specimens were taken. During casting of span 6, concrete loads were re-tempered with 2 lbs/yd³ to 8 lbs/yd³ of water. During casting of span 8, concrete loads were re-tempered with 4 lbs/yd³ to 10 lbs/yd³ of water. Concrete used in the other spans were also re-tempered, but were able to meet the required compressive strengths. The concrete was also pumped, and it is uncertain if the sampling of the concrete occurred before or after pumping.

Twelve concrete cores were taken from spans 2, 6, and 8 to verify compressive strengths and perform petrographic analysis. The results of the compressive strengths are listed in Table 23.2 as well as the hardened air content. The compressive strengths of the cores also failed to meet the 28-day compressive strength requirements.

Table 23.2: Core Test Results

Spans	Air Content	Compressive Strength, psi
2	15.7%	3120
6	8.9%	3265
6	13.4%	3035
8	12.4%	3425

Petrographic analysis revealed that the air content was extremely high in all the cores, and that the air void system was finer than normal. The air voids were, for the most part, uniformly distributed except for regions around the aggregates. Clustering of air voids was noted at numerous aggregate-paste interfaces (Figure 23.1). There were no obvious signs of re-tempering, which suggest that the addition of water was performed relatively soon after mixing.

The contractor was given the option of removing and replacing the bridge deck or applying a dense concrete overlay over all eight spans. The contractor chose to overlay the structure at his expense.

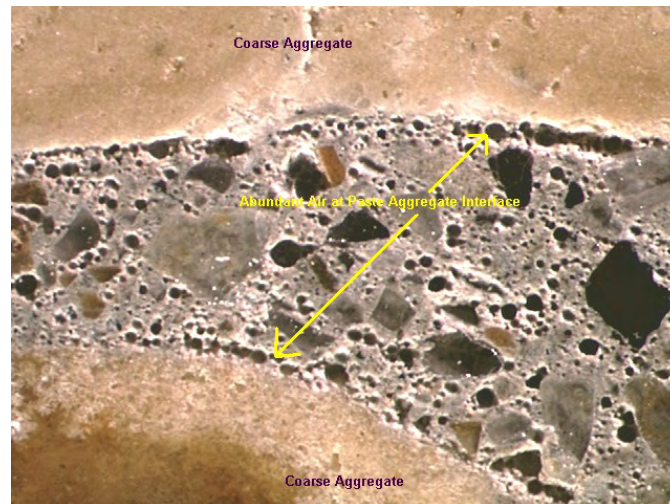


Figure 23.1: Clustering of the Air Voids Around the Aggregate (Photo courtesy of E. Morgan)

23.2 Case Study #2

County: Burleson

Structure Type: Bridge Deck

Sample Type: Cores from Flexure Beams

Type of Coarse Agg.: Limestone

CSJ: 0116-02-027

Location: State Highway 21

Date: August 2005

Type of AEA: Unknown

Twelve flexural beams halves (six beams) were submitted to determine the cause of low flexural strength concrete used in a bridge deck. Core samples were taken from each beam half and tested for compressive strength at 28 day of age. The required 28-day compressive strength was 4000 psi. The remaining portions of the beams were used for petrographic analysis. Table 23.3 lists the compressive strengths of the cores and the air content determined by hardened air analysis.

Table 23.3: 28-Day Compressive Strengths and Hardened Air Contents of Core Samples

Core #	Compressive Strength, psi	Air Content, %
1	3300	13.2
2	2890	11.0
3	3690	9.4
4	3110	10.3
5	3030	7.5
6	2580	11.0

Petrographic analysis indicated possible re-tempering with evidence of lower w/c paste adjacent to the aggregates (Figure 23.2). It was concluded that the low strength was attributed to the excessive air contents and the clustering of air voids around the aggregates along with the increased in water-cement ratio due to re-tempering. It should also be noted that clustering of the air voids is not present along the perimeter of the aggregate within the low w/c paste. This may indicate that clustering may be caused by the late addition of water.

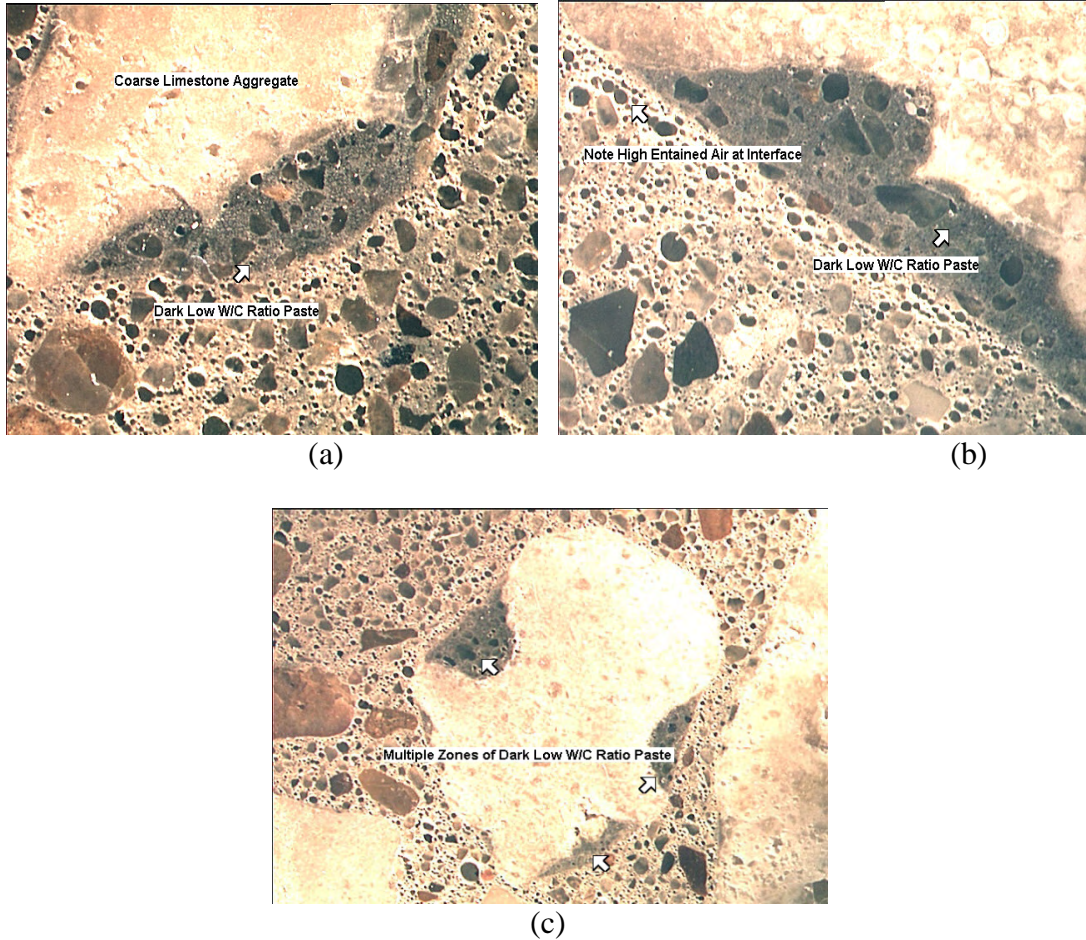


Figure 23.2: (a), (b), and (c) show evidence of re-tempering, (a) and (b) show clustering of the air void around the aggregate, but not within the low w/c paste (Photos courtesy of E. Morgan)

23.3 Case Study #3

County: Robertson

CSJ: 0049-06-061

Structure Type: Box Culvert

Location: State Highway 6

Sample Type: Cores

Date: September 2005

Type of Coarse Agg.: Limestone and Siliceous

Type of AEA: Unknown

Flexural beams were taken to represent the day concrete production of a cast in place box culvert. The 7-day flexural strengths, listed in Table 23.4, failed to meet the 510 psi requirement. Fresh concrete tests indicated that the slump was 4 inches and the air content (pressure method) was 5%.

Table 23.4: 7-Day Flexural Strengths of Concrete

Beam ID	Flexural Strength, psi
C4-A	435
C4-B	390
C4-C	390
C4-D	430

Four cores were then taken from the structure to verify the strength. The 44-day compressive strengths of the cores (Table 23.5) also failed to meet the 28-day specification requirement of 3600 psi, and one core had a compressive strength 1000 psi lower than the required strength. It was noted that the very few of the coarse aggregate particles were fractured after testing. The concrete cores were submitted for petrographic analysis to determine the cause for low compressive strengths.

Table 23.5: Compressive Strengths of Concrete Core Samples

Core #	Compressive Strength, psi
1	3460
2	2910
3	2510
4	3200

Petrographic analysis revealed that concrete had been re-tempered. There were numerous low w/c paste remnants (dark colored paste) observed along many of the coarse aggregate particles which is indicative of re-tempered concrete (Figure 23.3).

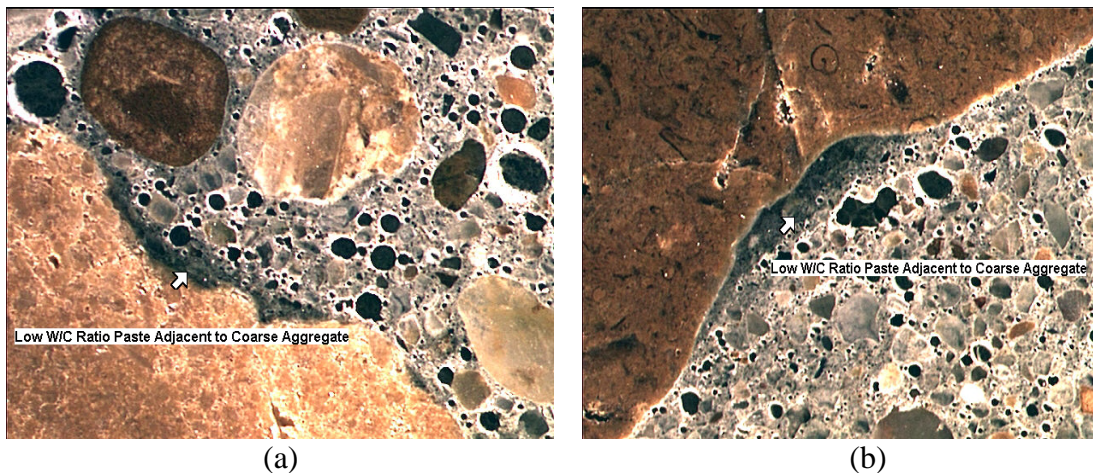


Figure 23.3: Evidence of Re-tempered Concrete. (a) Area of low w/c paste in core #1, (b) Area of low w/c paste in core #3 (photos courtesy of E. Morgan)

Hardened air void analysis performed on core #1 and core # 3 determined that air contents were 5.2% and 7.5% respectively. It was also noted that the overall air void system was not uniformly distributed and clustering of air voids was found at numerous coarse aggregate paste interfaces and also within the paste (Figure 23.4 and Figure 23.5)

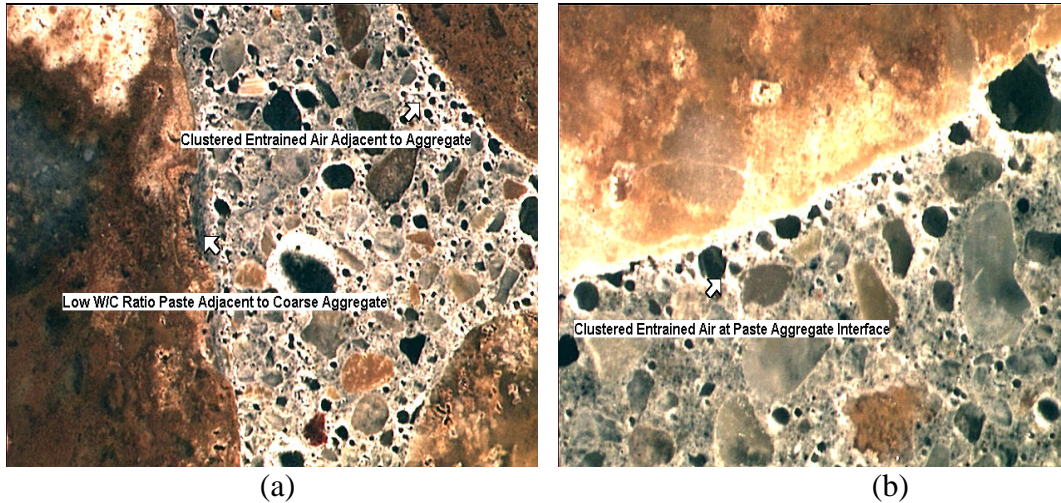


Figure 23.4: Clustering of Air Voids Around the Coarse Aggregate (a) Core #1, (b) Core #3 (Photo Courtesy of E. Morgan)



Figure 23.5: Clustering of Air Void within the Paste (Photo Courtesy of E. Morgan)

It was concluded that the low strength were attributed to the air void clustering along aggregate paste boundaries which resulted in weak bonding characteristics between the paste and aggregate and the increase of water-cement ratios caused by re-tempering the concrete. Failure to meet the specified strength requirement resulted in a 22% reduction in payment for the structure.

23.4 Case Study #4

County: Ennis

CSJ: 0918-22-072

Structure Type: Bridge Deck

Location: Brushy Creek Bridge

Sample Type: Cylinders and Cores

Date: September 2005

Type of Coarse Agg.: Limestone

Type of AEA: Unknown

Cylinders tested at 7 days and 28-day failed to meet the required compressive strength (Table 23.6). Fresh concrete tests indicated that the slump was 4 inches and the air content (pressure method) was 5%.

Table 23.6: Compressive Strengths of Concrete Cylinders

Cylinder ID	Age, Days	Compressive Strength, psi	Average, psi	Required Comp. Strength, psi
S-2	7	2292	2240	2960
S-2		2184		
S-2	28	2958	2990	4000
S-2		3014		

The two concrete cores from the bridge deck were submitted to determine the possible cause of low compressive strengths. The cores were fractured as a result of compression testing and did not have any abnormal features other than the lack of broken coarse aggregate along the fracture planes. The w/c in both cores was consistent with the design w/c of 0.45. However, there were a few areas of lower w/c paste adjacent to many of the coarse aggregates which are indications of re-tempering.

Hardened air void analysis determined that the air content was high in both cores. Core # 1 had 8.9 % air content and core # 2 had 8.2 % air content which was 3% greater than fresh concrete air content. Both cores also had concentration of air voids at many of the paste aggregate interfaces (Figure 23.6).

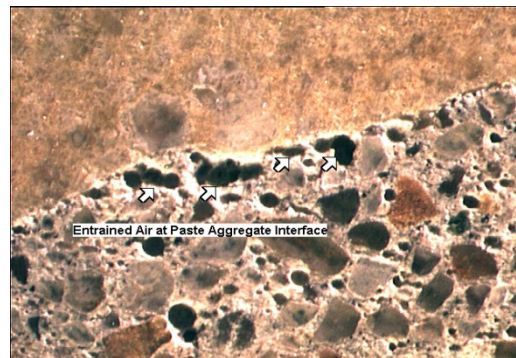


Figure 23.6: Air Void Cluster at Aggregate Paste Interface (Photo courtesy of E. Morgan)

It was concluded that the primary causes for the low compressive strength in this concrete was a combination of the excessive entrained air content and the clustering of entrained air at the paste aggregate interfaces. The contractor received a reduction in pay for this structure.

23.5 Case Study #5

County: Nueces	CSJ: 1069-01-029
Structure Type: Bridge Deck	Location: State Highway 357
Sample Type: Cores & Cylinders	Date: September 2005
Type of Coarse Agg.: River Gravel	Type of AEA: Unknown

Compressive strength cylinders for the bridge deck of this project failed to meet the required of compressive strength of 4000 psi. To verify compressive strength of the concrete, four cores were taken from the structure. Table 23.7 lists the results of the 31-day compressive strengths of the cores. The strengths of the cores were well below the required compressive strength.

Table 23.7: 31-Day Compressive Strengths of Core Samples

Core #	Compressive Strength, psi
1	3300
2	2890
3	3690
4	3110
5	3030
6	2580

Two cylinders from that days casting had not been tested and were submitted for petrographic analysis. Hardened air void analysis determined that the hardened air content in both cylinders was excessively high. Cylinder #5 had an air content of 11.8% with a spacing factor of 0.0019 inches and a specific surface of 764 in²/in³. Cylinder #11 had an air content of 10.3% with a spacing factor of 0.0024 inches and a specific surface of 552 in²/in³. Stereomicroscopy indicated the both cylinders had excessive amounts of air voids along the perimeter of the aggregates (Figure 23.7). There were no evident signs of re-tempering.

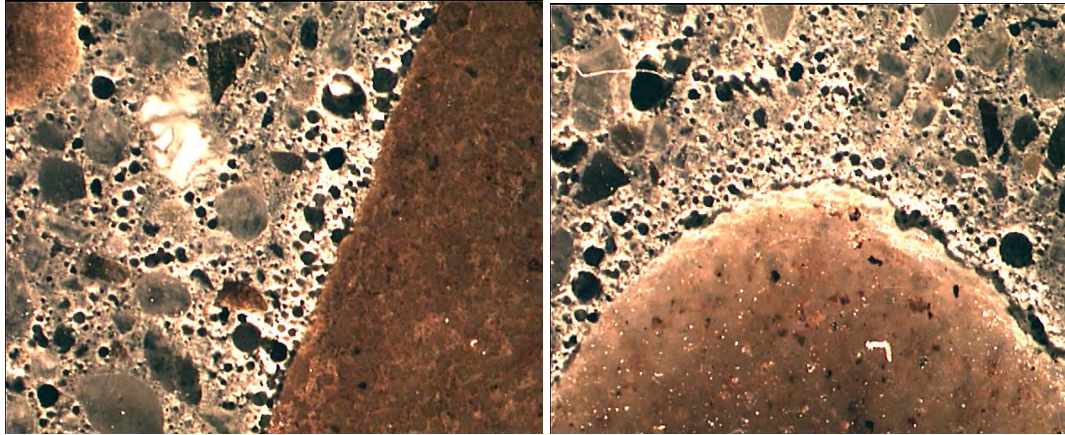


Figure 23.7: Excessive Air Voids Around Aggregates (Photo courtesy of E. Morgan)

23.6 Case Study #6

County: Bandera

Structure Type: Drill Shaft

Sample Type: Fractured Cylinders

Type of Coarse Agg.: Limestone

CSJ: 0915-11-015

Location: Bandera

Date: March 2006

Type of AEA: Unknown

Compressive strength specimens tested a 7-days of age failed to meet the 7-day target strength of 2820. The structure was cored and the cores were tested at 16-days and 28-days, and both failed to meet compressive strength requirements of 3600 psi (Table 23.8).

Fragments of compressive strength test specimens were submitted to determine the cause of low compressive strengths. It was apparent that very few of the coarse aggregate had been fractured during the compression testing. Due to the size and condition of the samples, hardened air analysis could not be performed, but the air content was estimated to be between 12% and 14%. Stereoscopic microscopy concluded that the cause for low strength was connected with excessive entrained air content. There was also clustering of air voids at the paste-aggregate interfaces (Figure 23.8). It could not be determined if the concrete had been re-tempered.

Table 23.8: Compressive Strengths of Concrete

Specimen ID	Age, Days	Compressive Strength, psi	Required, psi
C-13	7	1630	2820
C-14		1620	
#1	16	1990	2820
#2		1970	
#3	28	2740	3600
#4		2240	

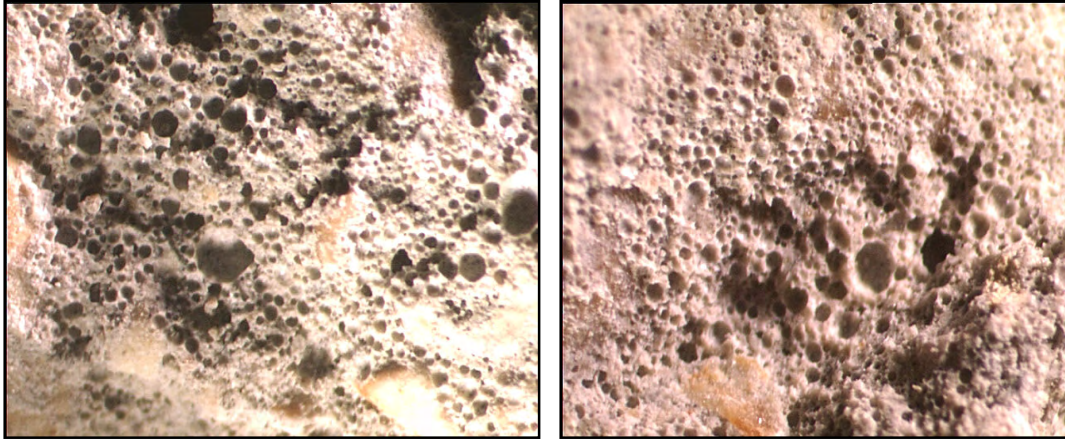


Figure 23.8: Clustering of the Air Voids Along Aggregate Sockets (Photo courtesy of E. Morgan)

23.7 Case Study #7

County: Smith	CSJ: 3487-01-002
Structure Type: Drill Shaft	Location: Shackleford Creek Bridge
Sample Type: Cores	Date: June 2006
Type of Coarse Agg.: Limestone	Type of AEA: Unknown

Six cores were submitted for determination of low compressive strengths. The estimated w/c for the cores was .38 to .42. Petrographic Analysis performed on core C5 did not find any deficiencies in proportioning when compared to the theoretical volumes from the concrete batch design. Numerous areas of low w/c paste were noted around many coarse aggregate particles in core C5 which is a good indicator of re-tempered concrete (Figure 23.9).

Hardened air void analysis determined that core C5 had 7.0% air content, a spacing factor of 0.0041 in. and a specific surface of 815 in²/in³. The remainder of the cores had similar entrained air contents. Clustering of the air voids was observed around numerous coarse aggregates especially in cores C5 and C6. Cores C1 and C2 had fewer areas of clustering than C5 and C6. Cores C3 and C4 had isolated clustering of the air voids at the aggregate paste interface.

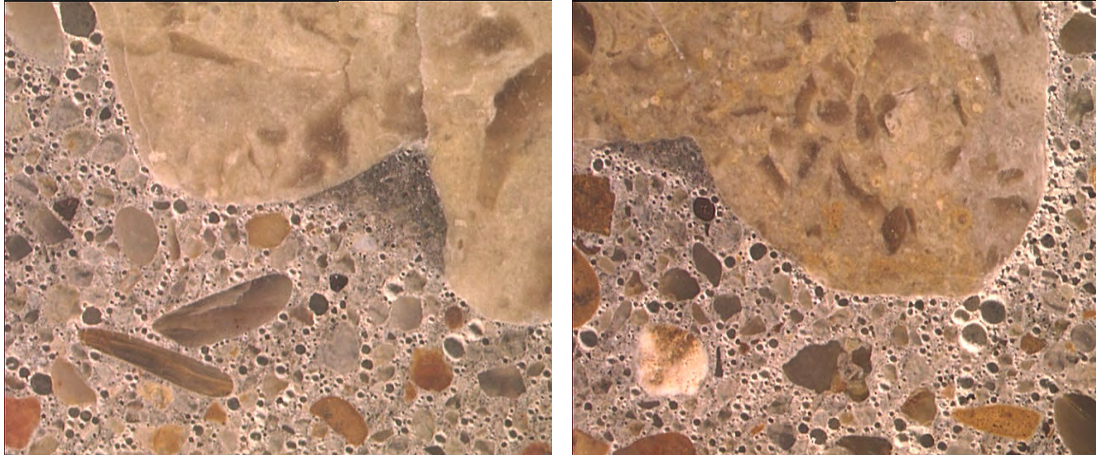


*Figure 23.9: Evidence of Re-tempering and Clustering of the Air Voids Around the Aggregate
(Photo courtesy of E. Morgan)*

Based on the features observed, the cause of the low compressive strength was attributed to re-tempering the concrete which caused excess amount of entrain air to collect at the paste aggregate interfaces. This caused weak zones at the paste aggregate interfaces resulting in compression strength losses.

23.8 Summary

There seems to be a fairly good correlation between re-tempering and clustering of the air voids in these field cases. All but two of the case showed signs of re-tempering. The extent of clustering did seem to vary as indicated in the photos, and concretes with the higher air contents seem to have higher degrees of clustering. Most of these cases also occurred during the summer construction season, which in Texas is quite long and hot, and when re-tempering would most likely be preformed to reestablish workability lost due to high summer temperatures. From these case studies and the research conducted, it still is not clear what role the temperature of the concrete plays in the clustering mechanism.

Unfortunately, due to the limited field data, the type of air-entraining admixture used in these mix designs could not be determined. However, a survey of concrete producers and admixture representatives conducted by others as part of a larger air-entrainment project found that most major concrete producers in the state of Texas use non-vinsol resin air-entraining admixtures (typically gum rosin based), and there is not a vinsol resin sold on the Texas market. Therefore, it can be safely stated at that the type of air-entraining admixture used in these concrete was a non-vinsol resin which furthers the case that non-vinsol resin concretes are prone to clustering when re-tempered.

Again, due to the lack of field compressive strength data, it is difficult to determine what effect air void clustering had on the compressive strengths. Most of these cases had extremely high air contents that in themselves could cause substantial strength loss. It also seems that clustering is mainly associated with higher air contents. This is not to say that clustering does not occurred at normal range air contents (case #1), but those concretes will generally not have lower than expected compressive strengths. This may be an explanation as to why clustering seems to correlate to higher air contents; only low compressive strength cases are typically investigated.

Chapter 24. Conclusions, Recommendations, and Future Research Needs

Based on the research conducted in the laboratory and on the field case studies, the following conclusions can be reached about air void clustering.

24.1 Fresh Concrete Properties

1. The late addition of water, re-tempering, to air-entrained concrete increased the workability, as expected. Workability increase (slump) was constant for a given re-tempering amount regardless of the type or dosage of air-entraining admixture used.
2. The type of coarse aggregate affected the increase in workability after re-tempering of the concrete. Siliceous river gravel mixtures had larger increases in slump compared to limestone mixtures
3. There was a good correlation between the unit weight of concrete and the air content (pressure method).
4. The increase in air content was dependent on the amount of re-tempering water, dosage of air-entraining admixture, and the type of air-entraining admixture used, with synthetic type air-entraining admixtures having the largest increase in air content after re-tempering.

24.2 Strength Properties

1. The effect of re-tempering on the compressive strength followed established trends with increased air contents and increased w/c. There was no strength loss that could be attributed to clustering of air void around the aggregate.
2. Loss of compressive strength per 1% air content varied for each AEA used, and was higher than the traditionally reported range of 2%-6%. Loss of compressive strength per 1% air content noted in this research ranged from 5.3% to 7.9%.
3. A single value for compressive strength loss should not be used to estimate the loss of compressive strength per percent air content when evaluating different air-entraining admixtures.
4. Splitting tensile and flexural strengths also followed the same trends as the compressive strength results.

24.3 Clustering of Air Voids

1. The mixing procedure used was capable of producing clustering of air voids around the aggregate, as verified by the microscopic examination and the clustering rating procedure.
2. There was a good correlation between air content and the composite cluster rating. The increase in air content was proportional to the composite cluster rating.
3. Generation of air void clusters around the aggregate was possible with all types of air-entraining admixtures before and after re-tempering.
4. The change in the composite cluster rating was somewhat dependent on the type of air-entraining admixture used. Non-vinsol air-entraining admixtures tended to have

- higher composite cluster rating after re-tempering, whereas the changes in composite cluster ratings for vinsol resin mixtures were more variable.
5. All mixtures were preformed under laboratory conditions, so the role of concrete temperature is still unclear.

24.4 Hardened Air Void Characteristics

1. Fresh air content generally showed reasonable agreement with the hardened air content, although there were some discrepancies evident.
2. Re-tempering had very little effect on the spacing factor and the specific surface of the air void system.
3. There was a general trend between clustering and finer air void systems. However, it is difficult to determine the actual affect clustering has on the air void system.

24.5 Field Case Studies

1. Clustering of the air voids around the aggregate does occur in field concrete and may have some affect on the compressive strength.
2. There is a correlation between re-tempering and clustering of the air voids in the field cases.
3. Most of these cases also occurred during the summer construction season when ambient temperatures are high; however, it still is not clear what role the concrete temperature plays in the clustering mechanism.

24.6 Recommendations

Since a vinsol resin air-entraining admixture is not currently available in Texas, restricting the use of non-vinsol resin AEAs would not be in the best interest of owners and producers. Instead of focusing on materials, the focus should be directed to construction practices and concrete mix designs.

Restricting the late addition of water in air-entrained concrete would reduce the incidences of low concrete strength caused by an increase in water-cement ratio and the potential effect of air void clustering. However, this restriction would increase the number of concrete loads rejected due to poor workability. It may also force contractors to use unworkable concrete and create other unwanted problems such as unconsolidated concrete or cold joints.

Texas DOT's current specification prohibits re-tempering concrete with water after discharging of concrete has begun. However, the concrete producers are allowed to add hold water when the concrete arrives at the jobsite. The addition of hold water would be considered re-tempering as defined in this research. Depending on the concrete producer's practices, a substantial amount of water can be withheld and added to make adjustments at the jobsite. Concrete producers use this procedure to avoid rejection of concrete because low slump concrete is traditionally rejected less than concrete exceeding the maximum specified slump. To avoid the late addition of hold water, it would be recommended that Texas DOT consider increasing the acceptable slump range. This increase in slump range would allow concrete producers add the majority of water during the initial mixing and make re-tempering less likely to occur at the jobsite.

The quantity of rejected concrete loads would be directly related to concrete mix design. Mix designs that tend to lose workability rapidly are excellent candidates for re-tempering.

Concrete producers should try to optimize their mixtures for longer slump retention, in addition to strength, to ensure that re-tempering is less likely to occur. Prior to approving concrete mix designs, Texas DOT should require the concrete producers to provide additional information (i.e. slump retention data) for selected concrete mix designs. It is extremely important to ensure that the data provided reflects the mixing practices (hold water/re-tempering), and the environmental conditions (i.e. temperature).

24.7 Future Research Needed

This research indicated that clustering had no effect on the strength properties of concrete. However, an in depth field evaluation of air-entrained concrete needs to be performed to determine other potential factors that may promote the formation of air void clustering. The effect of mixer size and type needs to be determined. It is well understood that smaller laboratory mixers are more energetic than truck mixers and distribute cement and air voids much more efficiently, which may be a reason why laboratory concrete did not experience any strength loss other than what was expected. Additional research should also focus on both non-re-tempered and re-tempered air-entrained field concrete with lower air contents since very little field data is available on concrete that did not cause problems. The practice of re-tempering concrete with plasticizing agents instead of water should also be investigated.

Chapter 25. Overall Conclusions and Recommendations for Future Research

25.1 Summary

This report summarized a comprehensive joint-research project, funded by TxDOT and performed by researchers at the University of Texas at Austin and Cornell University. This three-volume report is perhaps the most complete study to date on this important topic, and it is expected that the key findings from this study will be of immediate benefit to practitioners in Texas and beyond. Each of the three volumes of this report presented, as a last chapter in each volume, the main conclusions of the studies and recommendations for future research. For convenience, the current chapter presents the main conclusions and recommendations from each of the volumes.

25.2 VOLUME I – Conclusions and Recommendation for Future Research

25.2.1 Conclusions

- The industry assumption that carbon in the form of solid char is the primary factor affecting ash-AEA interactions was shown to be imprecise. Evidence gathered in this research suggests that the organic carbon content, defined as the forms of carbon that are not acid soluble but are removed in the form of carbon oxides when heated to 900°C in air, correlate strongly with ash-AEA interactions. Other forms of organic carbon that may in fact interact with AEA's but are not indicated in the results of the 300-500C modified LOI test include volatile organic compounds and soot.
- While some researchers have hypothesized that properties of “residual carbon” in ash such as surface area and surface charges affect ash-AEA interactions, it was shown during the course of this research that the mass of organic carbon appears to be the primary contributor to AEA interaction among the factors and ash samples studied. A linear relationship between AEA dosage in concrete and organic carbon mass content in fly ash was established. Furthermore, it was shown that relatively small changes in organic carbon mass measurements are accompanied by significant changes in required AEA dosages in concrete to produce target air contents (150 mL AEA/100 kg cm per percent organic carbon). Because of the variable nature of fly ash, within-source variations in organic carbon content on this small scale are likely. It is noted, however, that if the specific surface of the carbon in these ashes is about constant, and given the constant mass of ash in the foam index and concrete air tests, the influence of carbon mass and carbon surface area would be directly proportional to one another, and thus indistinguishable from each via the methods used here.
- Current industry methods for predicting ash influence on concrete AEA dosage can be unreliable. The standard LOI test can measure the contributions of several materials in addition to organic carbon content on mass change. Because the contributions from other materials cannot be distinguished from organic carbon

content, establishment of reliable relationships between standard LOI and ash-AEA interactions can be difficult or impossible.

- Lack of a standard foam index test limits the potential of the test as an estimator of AEA dosage in concrete. This research identified that variations on the test can lead to different conclusions regarding the potential influence of ash on AEA dosage. Several factors in the test were identified which could potentially cause significant variability in the test results of a single test procedure.
- Three techniques for estimating fly ash influence on AEA dosage are recommended for industry implementation, modified loss on ignition, a “standard” foam index test, and color analysis. The three test methods, though fundamentally different, are linked by their apparent sensitivity to organic carbon content. The tests are recommended for implementation at three points of ash handling: the ash producer, ash distributor and concrete producer.

25.2.2 Recommendations for Future Research

ASTM C311 Loss on ignition and modified loss on ignition

Future work should identify and examine the inorganic components of ash that change with exposure to LOI temperatures. Methods for precisely identifying minerals that dehydrate, decompose or increase in mass could allow for better analysis of the net changes in mass which occur during the LOI test.

Evaluation of the proposed modified LOI procedure on a group of ash samples possessing a larger range of organic carbon content than the Texas ashes is necessary to identify the ability of the test to measure organic carbon in ashes produced at other sources. It is possible that ashes with larger organic carbon content may require greater exposure time to complete the test.

The ability of the modified LOI test to predict fly ash-AEA interactions in concrete should be studied for a variety of ashes from different coal sources to identify whether the relationship observed in this study is directly applicable to other ash types.

Foam index

The next major steps that must be taken before the foam index test can be reliably used in industry are 1) to further compare foam index results with actual concrete AEA dosages for a variety of ash samples to identify correlations that would allow the test to predict AEA dosages in real concrete, 2) examine the influence of chemical admixtures in addition to AEA on the test and compare the results to real concrete data, and 3) inter-laboratory testing to identify the repeatability of the test performed by multiple users.

Further study of the combined effects of agitation frequency and duration with a variety of containers and fill ratios should be performed. Development of a mechanically agitated foam index could help to reduce the variability and labor-intensiveness of agitation by hand.

Color analysis methods

The ash samples tested in this study were representative of the ashes produced in a narrow geographical region of the U.S. Additional study should be done to measure differences

that may exist among ash samples produced from coals and plants in different regions. It is recommended that a study of the variations in color with time of ash samples from a single source be conducted to identify the usefulness of this tool in such an application. A study of the influence of particle morphology (size and shape) on ash color should be studied to identify potential effects on grayscale analysis results.

Additional value could be gained from the change in grayscale value test if the individual forms of organic carbon present in coal could be quantified. A proposed method for qualitatively identifying VOCs in ash by means of dissolving the organic compounds in benzene and visually comparing the change in solvent color was described in Section 5.2.3.1. Perhaps this method could be improved using an ultra violet-visible light spectrophotometer to quantify VOC presence in solvent by light absorbance. Methods for quantifying soot content in ash should also be identified.

Additional work is recommended to determine the suitability of the color change test on ash produced in other geographical regions. The possibility exists that differing source coal or combustion conditions may produce differences in ash properties with respect to color.

Additional study should be performed to identify the influence of changes in inorganic ash contents due to heating on ash color. Use of the RGB values in addition to the grayscale values may provide more information for identifying ash properties.

Further study of the factors influencing fly ash-AEA interactions

Organic carbon forms

Three forms of organic carbon were identified in this research: coal char, volatile organic compounds and soot. The individual contributions of these materials to the total organic carbon content of the ash samples were not identified in this study. It is recommended that methods of assessing the forms of organic carbon in ash be identified.

One possible method for identifying the contribution of VOCs to organic carbon is to perform macro thermo gravimetric analysis of ash in an inert atmosphere (such as nitrogen) and measure the change in organic carbon content with temperature. Changes in organic carbon content of the heated ash could be attributed to the loss of carbon in the volatiles. This could shed light on the presence of VOCs that may be driven off in the LOI test or modified LOI temperature ranges. Methods for measuring the soot content of ash should also be developed.

In addition to studies on measuring the contents of various forms of organic carbon in ash, study of the influence of the individual forms on AEA behavior should be performed. If the varying forms of organic carbon influence AEA-interactions differently, then correlations between AEA-interactions and organic carbon content could be improved by considering the relative influences of the individual organic carbon forms.

Fundamental mechanisms behind fly ash-AEA interactions

The hypothesis that fly ash-AEA interactions are the result of the adsorption of AEA molecules on the surface or organic coal residuals has not been conclusively proven. This research identified a relationship between organic carbon content and fly ash AEA interactions and also suggests that particle size and/or surface area may play a role which may support the hypothesis; however, the fundamental mechanisms behind the interactions were not established.

Further work should be performed to identify the underlying mechanisms causing the correlation between AEA dosage in concrete and organic carbon content. The use of ultra-violet visible-light spectrophotometry could provide useful data on the adsorption of AEA from solutions containing fly ash in carefully controlled experiments. One possible method for avoiding AEA precipitation due to divalent cations (described in Section 4.2.4.3) is to use a nonionic or cationic surfactant in the test.

Carbon separation techniques (such as electrostatic precipitation or froth floatation) that do not alter the properties of the ash mineral content but could increase or decrease the amount of organic carbon present in ash could be used to isolate the organic carbon for studies on AEA interactions.

Calcium and Class C fly ash

Correlations between modified LOI and foam index tests and concrete AEA dosages were not identified for the Class C ashes used in this study. The causes behind this behavior were not determined in this study. One possible reason is that the Class C ashes used had relatively uniform properties, and therefore lack of variability did not allow for correlations to be established. It is recommended that the tests performed in this study to correlate concrete AEA dosage with organic carbon content, modified LOI, and foam index tests be done with a set of Class C ashes which exhibit greater variability in properties (particularly organic carbon content) than those used here. Additional work is required to determine if the observations regarding Class C ash performance made in this study apply to Class C ashes generally. Furthermore, given that the ASTM C 618 Class F/C distinction is somewhat arbitrary, and that silicon, aluminum, and calcium contents in fly ash are distributed on a continuum, more study is needed on the underlying compositional variables that caused the ashes studied here to fall into the “F” or “C” categories.

Surface area and particle size

The results of this study suggested that neither BET surface area (including internal pore area) nor external surface area inferred from particle size could be used to fully explain ash-AEA interactions, despite general correlations with concrete air or foam index. It is likely that some forms of carbon are porous and BET measurements are useful, and that other forms are not porous and external surface areas are useful. Further study should be performed to identify the influence of organic carbon size distribution on AEA interactions. Improved methods of measuring fly ash particle size distribution could provide additional information.

25.3 VOLUME II – Conclusions and Recommendation for Future Research

25.3.1 Conclusions

- Fly ashes from power plants that have been modified with low-NO_x burners generally led to increases in AEA demand in laboratory testing, and this observation generally agrees with the field reports of increased AEA dosages during this time period. However, it cannot be said with certainty is that the installation of the low NO_x burners, per se, is responsible for these observed changes in the ash.

- Loss-on-ignition (LOI) (ASTM C 311) measurements did not correlate with the AEA demand in concrete for most of the fly ashes studied in this project.
- The foam index test used in this study showed a satisfactory correlation to the AEA demand in concrete; however, it was unable to differentiate fly ashes with low AEA demand (less than 60 ml AEA/100 kg cm for 6% air in fresh concrete air tests)
- Limited results suggest that surface area, as indicated by nitrogen absorption using Brunauer-Emmet-Teller (BET) analysis, is a good indicator of AEA demand, especially for ashes with highly active carbon.
- BET surface area measurements were taken before and after igniting the ash (using LOI procedure), with a significant decrease in surface area measured on the ignited samples (compared to the as-received ashes). These ignited ashes were then found to respond better to AEAs in foam index testing, suggesting that the loss of carbon (along with other impurities/organics) and the associated surface area contributed to AEA demand
- For the work performed under this project, an average percent difference of 48% was measured for the mortar air test specified in ASTM C 311. This large variation was found to be a result of the fixed flow rate and air content of the mortar investigated.
- The ASTM C 311 test was modified to remove the iterations in the test and to reduce the variation. This was done by fixing the water content and AEA dosage in the test. This test has been shown to have a satisfactory variability but the correlation of the testing results to concrete could be improved.
- A method was presented to produce an AEA dosage response curve for a given fly ash/AEA combination using only using a single mixture. The method was then compared to the standard test for AEA dosage response that uses several sequential mixtures and the results were found to be closely comparable for air contents up to 7%.
- The water reducer (WR) used in this study was shown to reduce the AEA demand (to achieve a target air content) as the WR dosage was increased.
- A sacrificial surfactant that is applied to fly ash with high AEA demand can decrease the AEA demand of fly ash concrete.
- The mixing temperature had a larger impact on the AEA demand of a fly ash treated with a sacrificial surfactant than on the AEA demand of the other fly ash mixtures investigated.
- As the percent fly ash replacement increased in a concrete mixture, the AEA demand in fly ash concrete decreased if the AEA demand of the fly ash was low or increased if the AEA demand of the fly ash was high. This increase occurred in a nonlinear fashion.
- The AEA demand of fly ash treated with a sacrificial surfactant did not change as the percent fly ash replacement increased.

- Wood rosin AEA is the most sensitive of the AEAs examined to a fly ash with a high AEA demand in concrete.
- Based on a small data set of mixtures with a similar mixture design but different air content as determined by ASTM C 231 (pressure method), the commercially available Air-Void Analyzer (AVA) was determined to have significant variability between two measurements examined from the same mixture. Significant differences were found between air-void parameters obtained from the hardened air-void analysis and the AVA.
- It was found that concrete mixtures with an air content greater than or equal to 5% was generally frost resistant (using ASTM C 666). Some mixtures with lower air contents were not frost resistant, especially mixtures containing high amounts of WR (and lower AEA dosages), mixtures with porous aggregates for which the aggregate correction factors were not applied, or mixtures containing a fly ash treated with a sacrificial surfactant. However, none of the variables listed previously were investigated in combination.
- For mixtures with relatively low air contents (e.g., less than 4.5% air) and containing a fly ash treated with a sacrificial surfactant, a coarsening of the air-void system was observed, manifested in an increase in the average chord length of air voids. However, once the air content was increased to 5% or above, satisfactory frost resistance was obtained.
- An opaque “shell” was observed on the exterior of air bubbles that had escaped from air entrained paste. The appearance of the shell changed as different AEA admixtures were used.
- In these experiments with bubbles in bleed water, bubbles with an opaque shell appeared to resist coalescence, whereas translucent-to-transparent bubbles coalesced readily. Similarly, the shell appeared to take on structural properties such as stiffness, resistance to deformation, and eventual cracking. The role of these properties in stabilizing air bubbles within cement paste has not been identified.
- When the shell appeared to be fully intact over observable portions of the bubble surface, the diameter of the bubbles did not change with time for the conditions of setup #2. When a readily discernable shell was not present as in the specimen of non air-entrained paste in setup #2, the diameter of the air bubbles was observed to change with time. Likewise, of those bubbles with a readily observed shell, only those that had cracked changed diameter with time.
- In pressurized experiments shown in setup #3 it was observed that the air-bubble shell was damaged during depressurization from 0.7 bar to atmospheric pressure. This may be important in construction applications in which the concrete pressure is increased and decreased. It is not known, however, whether the experimental observations made here under a relatively mild and slow pressure change apply equally to the much higher pressure differences and rates of pressure change experienced in concrete pumping, for example.

- A single shell-covered bubble that had escaped from air-entrained paste was observed to decrease in volume under pressure precisely as would be predicted by Boyle's Law, with no apparent influence of the shell.
- If a water-filled gap does exist between the air-void shell and the surrounding paste as observed by others in concrete (Rashad and Williamson, 1991A; Rashad and Williamson, 1991B; Corr et al., 2002), then it seems plausible that gas interchange could occur between air-voids whose shells were either inadequate or damaged. This interchange could lead to a decrease in volume of the smaller bubbles and an increase in volume of the larger bubbles as observed in the experimental work in this chapter. This change in void volume would ultimately lead to a higher overall air content in the mixture as the gas is under a lower pressure in the larger air-voids than the small; therefore, the air would take up a larger volume on transfer as first suggested by Mielenz et al. (1958A). The above explanation is based on observations of air-void behavior in the bleed water of cement paste and has not been proven in concrete mixtures.
- It has been shown that there is a strong adhesion between cement particles and air-voids beginning at the first minutes of hydration.
- It appears that there is a large difference in transparency between the air-entrained and non air-entrained voids as well as a difference in the ability of the voids to resist size changes with time.
- There is a significant difference in performance between the resulting shells with different AEA admixtures when the fluid pressure surrounding voids is increased and then decreased again to atmospheric pressure. Voids made with synthetic AEA sustain no permanent damage, while voids made with Vinsol resin and wood rosin crack on depressurization.
- The cracks in a wood rosin void shell were observed to self-heal.
- The amount of C_3S present in the air-void shell is lower than in the original unhydrated cement and the bulk paste. The effect may be due to delays in the induction period for the C_3S particles at the air-void surface.
- The increase in $CaCO_3$ in the air-void shell in the first two hours of testing may be an artifact of the sample preparation technique as it was not observed in the SEM analysis of the 60 day old air-void shell.
- The rate of C_3S decrease and $CaCO_3$ increase is faster for synthetic AEA than for wood rosin AEA. It is likely that this difference in hydration rate is related to the difference in behavior of the air-void shells of the different AEAs.
- SEM observations and EDXA of the air-voids in the 60-day-old cement paste showed that the surface of the air-void seems to be predominately made up of a C-S-H phase that is of a different stoichiometry than that found in the C-S-H of the bulk paste as the ratio of the calcium-to-silicon of the air-void shell is around 1.1 compared to 1.5 as found in the bulk paste.

25.3.2 Recommendations for Future Research

This project was one that was quite ambitious in scope. Volume II provided new information not currently in the state of the art on testing methods, performance of different ingredients in concrete, the characteristics of the air-void shell, and the chemical properties of this shell. It is unfortunate but inevitable that some research needs still remain. The following is a list of the most pressing research needs.

- Different combinations of water reducer dosage, sacrificial surfactant, and aggregates with different correction factors should be investigated that are typically used in concrete construction to investigate the air-void systems produced with different air contents.
- The vast majority of the mixtures performed for this research focused on a concrete mixture that would be typical of a bridge deck mixture. Other mixture proportions representative of other applications should be investigated to monitor the impact of different variables on the resulting air-void content and distribution.
- A subset of the most critical mixture combinations from the previous recommendations should be investigated in a set of full scale mixtures created in a ready-mix concrete plant and the resulting air content and air-void distribution should be evaluated.
- A survey of the aggregate correction factor of aggregates should be completed in locations where freeze-thaw durability is specified. Different moisture contents of these aggregates should also be investigated to determine the impact on the accuracy of the ASTM C 231 pressure method to measurements made on hardened concrete.
- A detailed study is needed to examine how the air-void shells impact the change in the air-void distribution in concrete.
- More work is needed to further characterize the chemistry of the air-void shells. The focus of this research is to isolate several of the variables and develop a less intrusive technique to separate the air-voids from the paste and compare the results to previous testing. Also more work is needed with different AEAs to understand why they show distinctly different physical properties.

25.4 VOLUME III – Conclusions and Recommendation for Future Research

25.4.1 Conclusions

- The late addition of water, re-tempering, to air-entrained concrete increased the workability, as expected. Workability increase (slump) was constant for a given re-tempering amount regardless of the type or dosage of air-entraining admixture used.
- The type of coarse aggregate affected the increase in workability after re-tempering of the concrete. Siliceous river gravel mixtures had larger increases in slump compared to limestone mixtures
- There was a good correlation between the unit weight of concrete and the air content (pressure method).

- The increase in air content was dependent on the amount of re-tempering water, dosage of air-entraining admixture, and the type of air-entraining admixture used, with synthetic type air-entraining admixtures having the largest increase in air content after re-tempering.
- The effect of re-tempering on the compressive strength followed established trends with increased air contents and increased w/c. There was no strength loss that could be attributed to clustering of air void around the aggregate.
- Loss of compressive strength per 1% air content varied for each AEA used, and was higher than the traditionally reported range of 2%-6%. Loss of compressive strength per 1% air content noted in this research ranged from 5.3% to 7.9%.
- A single value for compressive strength loss should not be used to estimate the loss of compressive strength per percent air content when evaluating different air-entraining admixtures.
- Splitting tensile and flexural strengths also followed the same trends as the compressive strength results.
- The mixing procedure used was capable of producing clustering of air voids around the aggregate, as verified by the microscopic examination and the clustering rating procedure.
- There was a good correlation between air content and the composite cluster rating. The increase in air content was proportional to the composite cluster rating.
- Generation of air void clusters around the aggregate was possible with all types of air-entraining admixtures before and after re-tempering.
- The change in the composite cluster rating was somewhat dependent on the type of air-entraining admixture used. Non-vinsol air-entraining admixtures tended to have higher composite cluster rating after re-tempering, whereas the changes in composite cluster ratings for vinsol resin mixtures were more variable.
- All mixtures were preformed under laboratory conditions, so the role of concrete temperature is still unclear.
- Fresh air content showed reasonable agreement with the hardened air content with only a few discrepancies.
- Re-tempering had very little effect on the spacing factor and the specific surface of the air void system.
- There was a general trend between clustering and finer air void systems. However, it is difficult to determine the actual affect clustering has on the air void system.
- Clustering of the air voids around the aggregate does occur in field concrete and may have some affect on the compressive strength.
- There is a correlation between re-tempering and clustering of the air voids in the field cases.

- Most of these cases also occurred during the summer construction season when ambient temperatures are high; however, it still is not clear what role the concrete temperature plays in the clustering mechanism.

25.4.2 Recommendations for Future Research

This research indicated that clustering had no effect on the strength properties of concrete. However, an in depth field evaluation of air-entrained concrete needs to be performed to determine other potential factors that may promote the formation of air void clustering. The effect of mixer size and type needs to be determined. It is well understood that smaller laboratory mixers are more energetic than truck mixers and distribute cement and air voids much more efficiently, which may be a reason why laboratory concrete did not experience any strength loss other than what was expected. Additional research should also focus on both non-re-tempered and re-tempered air-entrained field concrete with lower air contents since very little field data is available on concrete that did not cause problems. The practice of re-tempering concrete with plasticizing agents instead of water should also be investigated.

References

1. Adamson, A.W., *Physical Chemistry of Surfaces*, John Wiley and Sons, New York, 1982.
2. American Coal Ash Association, "2005 Coal Combustion Product Production and Use Survey," Aurora, CO.
3. American Concrete Institute, *Recommended practice for proportioning normal and heavyweight concrete mixtures*, ACI 211.1, Detroit, MI, 1991.
4. Averitt, P., "Coal Resources" in *Chemistry of Coal Utilization*, 2nd Supplementary Volume, Elliott, M.A., Ed., John Wiley & Sons, New York, 1981.
5. Backstrom, J. E.; Burrows, R. W.; Mielenz, R. C. and Wolkodoff, V. E., Origin, Evolution, and Effects of the Air Void System in Concrete. Part 2- Influence of Type and Amount of Air-Entraining Agent, *J. Am. Concr. Inst.* 55 (8) (1958A) 261-272.
6. Backstrom, J.E.; Burrows, R.W; Mielenz, R.C.; and Wolkodoff, V.E., Origin, Evolution, and Effects of the Air Void System in Concrete. Part 3 – Influence of Water-Cement Ratio and Compaction, *J. Am. Concr. Inst.* 55 (8) (1958B) 359-375.
7. Badogiannis, E., Kakali, G., Tsvivilis, S., "Metakaolin as supplementary cementitious material: Optimization of kaolin to metakaolin conversion," *Journal of Thermal Analysis and Calorimetry*, Vol. 81, 2005, pp. 457–462.
8. Baltrus, J.P. and LaCount, R.B., 2001, "Measurements of adsorption of air-entraining admixture on fly ash in concrete and cement," *Cement and Concrete Research*, 31, pp.819-824.
9. Barret, P. and Menetrier, D., Filter Dissolution of C₃S as a Function of the Lime Concentration in a Limited Amount of Lime Water, *Cement and Concrete Research*, 10, 4 (1980) 521-534.
10. Böhm, J., *Electrostatic precipitators*, Elsevier Scientific Pub. Co., New York, 1982.
11. Boyd, T. J. and Cochran, J. 1994. "Fly ash beneficiation by carbon burnout." *Proceedings of the American Power Conference*, 56, 937-942.
12. Bradley, B., Wilson, M.L., "Using supplementary cementitious materials," *Construction Specifier*, v 58, n 6, June, 2005, pp. 34-41.
13. Brown, R.C., Dykstra, J., "Systematic errors in the use of loss-on-ignition to measure unburned carbon in fly ash," *Fuel*, Vol. 74, No. 4, pp. 570-574, 1995.
14. Bruere, G. M., Air Entrainment in Mortars, *Journal of the American Concrete Institute*, V27, 10 (1956) 1115-1124.

15. Bruere, G.M., (1971), "Air-entraining actions of anionic surfactants in portland cement pastes" *Journal of Applied Chemistry and Biotechnology*, Vol 21, March, pp. 61-64.
16. Bruere, G.M., "Air-entraining actions of anionic surfactants in portland cement pastes" *Journal of Applied Chemistry and Biotechnology*, Vol 21, March, pp. 61-64, 1971.
17. Bruere, G.M., Rearrangement of Bubble Sizes in Air-Entrained Cement Pastes During Setting, *Australian J. of Applied Sci.* 13 (1962) 222-227.
18. Burg, G.R.U. (1983). "Slump Loss, Air Loss, and Field Performance of Concrete," *ACI Materials Journal*, 332-339.
19. Burg, R.U., Slump loss, Air Loss, and Field Performance of Concrete. *ACI Journal*, 80(4) (1983), 332-339.
20. Camposagrado, G.R. (2004). "Investigation of cause and effect of air void coalescence in air-entrained concrete mixtures," MS Thesis, Mississippi State University, Mississippi.
21. Carpenter, R.L., Chang, D.P.Y., Brummer, M., "Fly ash from electrostatic precipitators: characterization of large spheres," *Journal of the Air Pollution Control Association*, Vol. 30, No. 6, pp. 679-681, 1980.
22. Chaddha, G., Seehra, M.S., "Magnetic components and particle size distribution of coal fly ash," *J. Phys. D: Appl. Phys.*, 1983, 16, pp. 1767-1776.
23. Chancey, R., Personal Communication, 2007.
24. Chen, X., Farber, M., Gao, Y., Kulaots, I., Suuberg, E.M., Hurt, R.H., "Mechanisms of surfactant adsorption on non-polar, air-oxidized and ozone-treated carbon surfaces," *Carbon*, Vol. 41, No. 8, 2003, p 1489-1500.
25. Cheremisinoff, P.N., Morresi, A.C., "Carbon Adsorption Applications" in *Carbon Adsorption Handbook*, Cheremisinoff, P.N., Ellerbusch, F., eds., Ann Arbor Science Publishers, Michigan, 1980.
26. Cheremisinoff, P.N., Morresi, A.C., "Carbon adsorption applications" in *Carbon adsorption handbook*, Ann Arbor Science Publishers, Ann Arbor, MI, 1980.
27. Corr, D., 2002, *A Microscopic Study of Ice Formation & Propagation in Concrete*, PhD dissertation, University of California, Berkeley.
28. Corr, D.J., Lebourgeois, J, Monteiro, P.J.M., Bastacky, J. Gartner, E.M., Air Void Morphology in Fresh Pastes, *Cem Concr Res* 32 (7) (2002) pp. 1025-1031.
29. Cross, W., Duke, E., Kellar, J., and Johnston, D. (2000). "Investigation of low compressive strengths of concrete paving, precast and structural concrete," *South Dakota Department of Transportation*, Report SD98-03-F.

30. Damson, A.W., *Physical Chemistry of Surfaces*, John Wiley and Sons, New York, 1982.
31. Dean and Daylrimple, *Water Wave Mechanics for Engineers and Scientists*, World Scientific Press, 368 pp., 1991
32. Deer, W.A., Howie, R.A., Zussman, J., *An Introduction to the Rock-Forming Minerals*, Longman Group Ltd., England, 1966.
33. Desai, D.H.; Tikalsky, P.J.; and Scheetz, B.E., *Hardened Air in Concrete Roadway Pavements and Structures*, Pennsylvania Department of Transportation, FHWA-PA-2007-002-04-01 (006), 2007.
34. Diamond, S., *Cement Paste Microstructure – An Overview at Several Levels*, Hydraulic Cement Pastes: Their Structure and Properties, Cem and Concr Assoc, Slough U.K., pp. 2-30 (1976).
35. Distlehorst, J.A., and Kurgan, G.J., *Development of a Precision Statement for Determining the Air Void Characteristics of Fresh Concrete Using the Air Void Analyzer*, Transportation Research Board, 07-3479, 2006.
36. Dodson, V., 1990, *Concrete Admixtures*, Van Nostrand Reinhold, New York, NY.
37. Dodson, V.H., 1990, *Concrete Admixtures*, Van Nostrand Reinhold, New York, pp. 136-143.
38. Dodson, V.H., *Concrete Admixtures*, Van Nostrand Reinhold, New York, 1990.
39. Dolch, W.L., 1984, “Air Entraining Admixtures” *Concrete Admixtures Handbook*, ed. V.S. Ramachandran, Noyes Publications, Park Ridge, New Jersey, pp. 269-302.
40. Donnet, J.B., Bansal, R.C., Wang, M.J., *Carbon black: science and technology*, Dekker, New York, 1993.
41. Du, L., and Folliard, K.J. (2005). “Mechanisms of Air-entrainment in Concrete,” *Cement and Concrete Research*, 35(8), 1463-1471.
42. Duval, C., *Inorganic Thermogravimetric Analysis*, 2nd Edition, Elsevier Publishing Company, New York, 1963.
43. Edmeades R.M., Hewlett, P.C., 1998, “Cement Admixtures” *Lea’s Chemistry of Cement and Concrete*, 4th Edition, ed. P.C. Hewlett, Arnold Publishers, London, pp. 837-901.
44. EIA, *International Energy Annual 2002* (U.S. Department of Energy, Energy Information Administration, Washington, D.C., May 2004).
45. Eickschen, E. (2003). “Factors affecting the formation of air voids in road concrete,” *In: beton*, 53(5), 265-270

46. Energy Information Administration, "2005 Annual coal report" U.S. Department of Energy, October 2006, available at: <http://www.eia.doe.gov/cneaf/coal/acr/acr.pdf>.
47. Englund, H.M. and Beery, W.T., eds., *Fine particulate control technology*, Air Pollution Control Association, 1975.
48. Environmental Literacy Council, www.enviroliteracy.org/article.php/18.html.
49. Essenhigh, R.H., "Fundamentals of Coal Combustion" in *Chemistry of Coal Utilization*, 2nd Supplementary Volume, Elliott, M.A., Ed., John Wiley & Sons, New York, 1981.
50. Fagerlund, G., Air-Pore Instability and its Effect on the Concrete Properties, *Nordic Concrete Research*, V9 (1990) 34-52.
51. Fan, M., Brown, R.C., "Comparison of the Loss-on-Ignition and Thermogravimetric Analysis Techniques in Measuring Unburned Carbon in Coal Fly Ash," *Energy & Fuels*, 15, pp. 1414-1417, 2001.
52. FHWA, *Fly Ash Facts for Highway Engineers*, American Coal Ash Association, Federal Highway Administration Report No. FHWA-IF-03-019, available to the public at <http://www.fhwa.dot.gov/pavement/recycling/fa17007.cfm>, 2007
53. Fidjestøl, P., Lewis, R., "Microsilica as an Addition," *Lea's Chemistry of Cement and Concrete*, 4th Edition, Hewlett, P.C., Ed., Arnold, 1998, pp. 675-708.
54. Fisher, G.L., Prentice, B.A., Silberman, D., Ondov, J.M., Bierman, A.H., Ragaini, R.C., McFarland, A.R., "Physical and morphological studies of size-classified coal fly ash," *Environmental Science and Technology*, Vol. 12, No. 4, pp. 447-451, 1987.
55. Folliard, K.J, and Ley, M.T. (2006). Personal communications.
56. Freeman, E.; Gao, Y.M.; Hurt, R.; Suuberg, E., "Interactions of carbon-containing fly ash with commercial air-entraining admixtures for concrete," *Fuel*, Vol. 76, No. 8, Elsevier Science Ltd., pp. 761-765, 1997.
57. Freme, F., *U.S. Coal Supply and Demand: 2003 Review*, U.S. Energy Information Administration.
58. Gann, R. *Desktop scanners: image quality evaluation*, Hewlett-Packard Company, Prentice Hall PTR, 1999.
59. Gao, Y.; Kulaots, I.; Chen, X.; Aggarwal, R.; Mehta, A.; Suuberg, E.M.; Hurt, R.H., "Ozonation for the chemical modification of carbon surfaces in fly ash," *Fuel*, Vol. 80, No. 5, Apr, 2001, p 765-768.
60. Gao, Y.M., Shim, H.S., Hurt, R.H., Suuberg, E.M., Yang, N.Y.C., 1997, "Effects of carbon on air entrainment in fly ash concrete: the role of soot and carbon black," *Energy & Fuels*, 11, pp. 457-462.

61. Gartner, E.M., Young, J.F., Damidot, D.A., and Jawed, I., Hydration of Portland Cement, Structure and Performance of Cements, 2nd ed., Bensted, J. and Barnes, P., 2002, pp. 57-108.
62. Gay, F.T. (1982). "A factor which may affect differences in the determined air content of plastic and hardened air-entrained concrete," *Proceedings of the Fourth International Conference of Cement Microscopy*, Las Vegas, 276-292.
63. Gay, F.T. (1983). "The influence of mixing temperature on air content of hardened concrete," *Proceedings of the Fifth International Conference of Cement Microscopy*, 231-239.
64. Gay, F.T. A Factor Which May Affect Differences in the Determined Air Content of Plastic and Hardened Air-Entrained Concrete, *Proceedings of the Fourth International Conference on Cement Microscopy*, Las Vegas, Int. Cem. Microscopy Assoc. (1982) 286-292.
65. Gay, F.T., The Effect of Mix Temperature on Air Content and Spacing Factors of Hardened Concrete Mixes with Standardized Additions of Air-Entraining Agent, *Proceedings, Seventh International Conference on Cement Microscopy*, Fort Worth, International Cement Microscopy Assoc., Duncanville, TX, (1985) pp. 305-315.
66. Gebler, S.H. and Klieger, P., "Effect of fly ash on the air-void stability of concrete," *Fly Ash, Silica Fume, Slag and Other Mineral By-Products in Concrete*, SP-79, American Concrete Institute, Detroit, MI, 1983 pp. 103-142.
67. Gebler, S.H., and Klieger, P., *Effect of Fly Ash on the Air- Void Stability of Concrete* (RD085.OIT), Portland Cement Association, 1983. Preprint of Proceedings, presented at the First International Conference on The Use of Fly Ash, Silica Fume, Slag and Other Mineral By-Products in Concrete, Montebello, Quebec, Canada, July-August 1983 (American Concrete Institute publication SP-79).
68. Given, P.H., "The Distribution of Hydrogen in Coals and Its Relation to Coal Structure," *Fuel*, 39, p 147, 1960.
69. Gluskoter, H.J., Shimp, N.F., Ruch, R.R., "Coal analyses, trace elements and mineral matter" in *Chemistry of Coal Utilization*, 2nd edition, Elliot, M.A., Ed., John Wiley & Sons, New York, 1981.
70. Goodwin, R.W., *Combustion ash/residue management*, Noyes Publications, Park Ridge, NJ, 1993.
71. Gregg, S.J. and Sing, K.S.W., *Adsorption, Surface Area and Porosity*, Academic Press, New York, 1982.
72. Gutmann, P.F. (1988). "Bubble Characteristics as They Pertain to Compressive Strength and Freeze-Thaw Durability," *ACI Materials Journal*, 84(5), 361-366.

73. Hachmann, L, Burnett, A., Gao, Y.M., Hurt, R.H., Suuberg, E.M. *27th Symp. (Int.) on Combustion*, p. 2965, The Combustion Institute, Pittsburgh, 1998.
74. Harris, N. *Evaluating the influence of fly ash on air entrained concrete*, PhD dissertation, Cornell University, Ithaca, NY, 2007.
75. Harris, N.J., Hover, K.C., Folliard, K, Ley, T., “The Use of the Foam Index Test to Predict AEA Dosage in Concrete Containing Fly Ash: Part I-Evaluation of the State of Practice,” 2007.
76. Harris, N.J., Hover, K.C., Folliard, K, Ley, T., “The Use of the Foam Index Test to Predict AEA Dosage in Concrete Containing Fly Ash: Part I-Evaluation of the State of Practice,” 2007a.
77. Harris, N.J., Hover, K.C., Folliard, K, Ley, T., “The use of the foam index test to predict AEA dosage in concrete containing fly ash: Part II-Development of a Standard Test Method: Apparatus and Procedure,” 2007b.
78. Harris, N.J., Hover, K.C., Folliard, K.J., Ley, T., “Variables Affecting the ASTM Standard C 311 Loss on Ignition Test for Fly Ash,” *Journal of ASTM International*, Vol 3, Issue 8, 2006.
79. Harris, N.J., Hover, K.C., Folliard, K.J., Ley, T., “Variables Affecting the ASTM Standard C 311 Loss on Ignition Test for Fly Ash,” *Journal of ASTM International*, Vol. 3, Issue 8, 2006.
80. Haswell, S.J. (ed.), *Atomic absorption spectrometry: theory, design and applications*, New York, Elsevier, 1991.
81. Heiri, O., Lotter, A.F., Lemcke, G., “Loss on ignition as a method for estimating organic and carbonate content in sediments: reproducibility and comparability of results,” *Journal of Paleolimnology*, 25, pp. 101-110, 2001.
82. Helmuth R.A., Detwiler, R.J., 2006, “The nature of concrete” *Significance of Tests and Properties of Concrete and Concrete-Making Materials, STP 169D*, ASTM International, West Conshohocken, PA, pp. 5-15.
83. Helmuth, R., *Fly Ash in Cement and Concrete*, Portland Cement Association, Skokie, IL, 1987.
84. Hess, W.M., Herd, C.R., “Microstructure, Morphology and General Physical Properties,” *Carbon Black*, 2nd Edition, Marcel Dekker, Inc., New York, 1993.
85. Hill R., Rathbone, R., Hower, J.C., “Investigation of fly ash carbon by thermal analysis and optical microscopy,” *Cement and Concrete Research*, Vol. 28, No. 10, pp. 1479-1488, 1998.

86. Hill, L.R., Sarkar, S.L., Rathbone, R.F., Hower, J.C., “An examination of fly ash carbon and its interactions with air entraining agent,” *Cement and Concrete Research*, Vol. 27, No. 2, pp 193-204, 1997.
87. Hill, R., and Folliard, K., 2006, The Impact of Fly Ash on Air-Entrained Concrete, HPC Bridge Views, V. 43, Spring 2006.
88. Hill, R., Jolicoeur, C.R., Page, M., Spiratos, I., To, T.C., U.S. Patent No. 20,040,206,276, Jan. 2004.
89. Hill, R.L., Sarkar, S.L., Rathbone, R.F., and Hower, J.C. (1997). “An examination of fly ash carbon and its interaction with air entraining agents,” *Cement and Concrete Research*, 27(2), 193-204.
90. Hoffman, G., *Western Region Fly Ash Survey*, New Mexico Bureau of Mines and Mineral Resources, Socorro, NM.,
91. Hover, K.C., 2006, “Air content and density of hardened concrete” *Significance of Tests and Properties of Concrete and Concrete-Making Materials*, STP 169D, ASTM International, West Conshohocken, PA, pp. 288-308.
92. Hover, K.C., Analytical Investigation of the Influence of Air Bubble Size on the Determination of the Air Content of Freshly Mixed Concrete. *Cement, Concrete, and Aggregates*, 10(1) (1988), 29-34.
93. Hover, K.C., and Phares, R.J. (1996). “Impact of concrete placing method on air content, air-void system parameters, and freeze-thaw durability,” *Transportation Research Record North*, 1532, 9-14.
94. Hover, K.C., Some Recent Problems with Air-Entrained Concrete, *Cem. Concr. and Aggregates*, 2(1) (1989) pp. 67-72.
95. Howard, J.B., “Fundamentals of Coal Pyrolysis and Hydrolyrolysis,” *Chemistry of Coal Utilization*, Second Supplementary Volume, John Wiley & Sons, 1981.
96. Hower, J.C., Thomas, G.A, Trimble, A.S., “Impact of conversion to low NO_x combustion on fly ash quality: Investigation of unit burning high sulfur coal,” 1999 International Ash Utilization Symposium, CAER, Univ. of Kentucky. Paper #36.
97. <http://www.mcrcc.osmre.gov/PDF/Forums/CCB3/1-3.pdf>, accessed June 2007.
98. Hurt, R., Suuberg, E., Vernath, J., Chen, X., Kulaots, I., *Strategies and technology for managing high-carbon ash*, Final Technical Report, DOE Award Number: DE-FG26-OONT40907, 2004.
99. Hurt, R.H., and Suuberg, E.M., *Fundamental study of low NO_x Combustion fly ash utilization*, Final Report, DOE award number: DE-FG22-96PC96213, October 2001.

100. Hwang, J.Y., *Wet process for fly ash beneficiation*, U.S. Patent No. 5,047,145, Sep. 2004.
101. Ishii, K. editor, *Advanced Pulverized Coal Injection Technology and Blast Furnace Operation*. Elsevier Science Ltd. UK., 2000.
102. Ivey, D. L. and Torrains, P. H., Air Void Systems in Ready Mixed Concrete, *Journal of Materials*, Vol. 5, No. 2, (1970), 492–522.
103. Jackobsen, U., Personal Communication, 2005.
104. Jakobsen, U.H., Pade, C., Thaulow, N., Brown, D., Sahu, S., Magnusson, O., De Buck, S., and De Schutter, G. (2006). “Automated air void analysis of hardened concrete - a round robin study,” *Cement and Concrete Research*, 36, 1444-1452.
105. Jankowska, H., Swiatkowski, A., Choma, J., *Active carbon*, Ellis Horwood Ltd., England, 1991.
106. Jenkins, R., *X-ray Fluorescence Spectrometry*, Wiley, 1999.
107. Jensen, B.J., U.S. Patent No. 4,967,588, 6 Nov. 1990.
108. Joshi, R.C., Lohita, R.P., 1997, *Fly Ash in Concrete: Production Properties and Uses*, Gordon and Breach Science Publishers.
109. Joshi, R.C., Lohtia, R.P., *Fly Ash in Concrete*, OPA, Amsterdam, 1997.
110. Joshi, R.C., Lohtia, R.P., *Fly Ash in Concrete: Production, Properties and Uses*, Gordon and Breach Science Publishers, Amsterdam, 1997.
111. Khatri, R.P., Sirivivatnanon, V., Gross, W., “Effect of different supplementary cementitious materials on mechanical properties of high performance concrete,” *Cement and Concrete Research*, v 25, n 1, 1995, pp. 209-220.
112. Klieger, P., Effect of Entrained Air on Strength and Durability of Concrete Made with Various Maximum Sizes of Aggregate, Proceedings, Highway Research Board, Vol. 31, 1952, pp. 177-201; Bulletin No. 40, Research and Development Laboratory, Portland Cement Association, Skokie, IL.
113. Kosmatka, S.H., Kerkhoff, B., and Panarese, W.C. (2002). “Design and Control of Concrete Mixtures 14th ed.,” *Portland Cement Association*, Skokie Ill.
114. Kosmatka, S.H., Kerkhoff, B., Panarese, W.C., *Design and control of concrete mixtures*, 14th ed., Portland Cement Association, Skokie, IL, 2003.
115. Kozikowski, R.L., Vollmer, D.B., Taylor, P.C., and Gebler, S.H. (2005). “Factors Affecting the Origin of Air-Void Clustering,” *Portland Cement Association*, Skokie, Ill.

116. Külaots I., Hsu, A., Hurt, R.H., Suuberg, E.M., “Adsorption of surfactants on unburned carbon in fly ash and development of a standardized foam index test,” *Cement and Concrete Research*, 33, pp. 2091-2099, 2003.
117. Külaots I., Hsu, A., Hurt, R.H., Suuberg, E.M., 2003, “Adsorption of surfactants on unburned carbon in fly ash and development of a standardized foam index test,” *Cement and Concrete Research*, 33, pp. 2091-2099.
118. Külaots I., Hurt, R.H., Suuberg, E.M., 2004, “Size distribution of unburned carbon in coal fly ash and its implications,” *Fuel*, 83, pp. 223-230.
119. Kulaots, I., Hsu, A., Hurt, R. H., and Suuberg E., 2003, Adsorption of Surfactants on Unburned Carbon in Fly Ash and Development of a Standardized Foam Index Test, *Cement and Concrete Research*, V. 33 (2003), pp. 2091-2099.
120. Külaots, I., Hurt, R.H., Suuberg, E.M., “Size distribution of unburned carbon in coal fly ash and its implications,” *Fuel*, Vol. 83, pp. 223-230, 2004.
121. Lane, S.D., Testing Fly Ash in Mortars for Air-Entrainment Characteristics, *Cement, Concrete, and Aggregates*, V13, 1, 25 (1991).
122. Langan, B.W., and Ward, M.A. (1976). “A laboratory investigation for potential durability of ready-mixed concrete re-tempered for air content and workability.” *Canadian Journal of Civil Engineering*, 3, 570-577.
123. Larson, T.D., “Air entrainment and durability aspects of fly-ash concrete,” *American Society for Testing and Materials – Proceedings*, Vol. 64, 1964, pp. 866-886.
124. Lessard, M. and Baalbaki, M., and Aitcin, P.C. (1996), “Effect of pumping on air characteristics of conventional concrete,” *Transportation Research Record North*, 1532, 1-8.
125. Ley, T., *The Effects of Texas Fly Ash on the Ability to Entrain and Stabilize Air in Concrete*, PhD dissertation, The University of Texas, Austin, 2007.
126. Li, T.X., Jiang, K., Neathery, J.K. Stencil, J.M., “Triboelectrostatic process of combustion fly ash after carbon burnout,” 1999 International Ash Utilization Symposium, CAER, Univ. of Kentucky. Paper #79.
127. Litvan, G. G. (1972) “Phase transitions of adsorbates IV - Mechanism of frost action in hardened cement paste,” *Journal of American Ceramic Society*, 55(1), 38-42.
128. Litvan, G. G. (1973) “Frost action in cement paste,” *Materials and Structures*, 6(34), 293-298.
129. Litvan, G. G. (1975). “Phase transitions of adsorbates VI - Effect of deicing agents on the freezing of cement paste,” *Journal of American Ceramic Society*, 58(1-2), 26-30.

130. Lomborg, B., *The Skeptical Environmentalist: Measuring the Real State of the World*, Cambridge University Press (2001).
131. Magura, D.D., *Air Void Analyzer Evaluation*, FHWA-SA-96-062, 1996.
132. Malte, P.C. and Rees, D.P., "Mechanisms and kinetics of pollutant formation during reaction of pulverized coal" *Pulverized-coal combustion and gasification*, Smoot, L.D, Pratt, D.T., Eds., Plenum Press, New York, 1979.
133. Manz, O.E., "Coal fly ash: a retrospective and future look," *Fuel*, Vol. 78, pp. 133-136, 1999.
134. Marceau, M.L., Gajuda, J., VanGeem, M.G., "Use of fly ash in concrete: normal and high volume ranges," *Concrete: Sustainability and Life Cycle, 1994-2004*, Portland Cement Association, Skokie, IL.
135. Maroto-Valer, M.M., Taulbee, D.N., Hower, J.C., "Application of density gradient centrifugation to the concentration of unburned carbon types from fly ash," *ACS Fuel Chemistry Division Preprints of Symposia*, v. 43, pp. 1014, 1998.
136. Maroto-Valer, M.M., Taulbee, D.N., Hower, J.C., "Novel Separation of the differing forms of unburned carbon present in fly ash using density gradient centrifugation," *Energy and Fuels*, Vol. 13, pp. 947-953, 1999a.
137. Maroto-Valer, M.M., Taulbee, D.N., Schobert, H.H., Hower, J.C., "Characterization of differing forms of unburned carbon in fly ash," 1999 International Ash Utilization Symposium, CAER, Univ. of Kentucky. Paper #18, 1999b.
138. Massazza, F., "Pozzolana and Pozzolanic Cements," *Lea's Chemistry of Cement and Concrete, 4th Edition*, Hewlett, P.C., Ed., Arnold, 1998, pp. 471-632.
139. Mehta, P.K., Monteiro, P.J.M., 2006, *Concrete: microstructure, properties and materials*, McGraw-Hill, New York.
140. Mielenz, R.C., Wolkodoff, V.E., Backstrom, J.E., and Burrows, R.W., *Origin Evolution, and Effects of the Air Void System in Concrete, Part 4 – The Air Void System in Job Concrete*, *J. Am. Concr. Inst.* 55 (10) (1958B) 507-517.
141. Mielenz, R.C., Wolkodoff, V.E., Backstrom, J.E., and Flack, H.L. (1958). "Origin, evolution, and effects of the air void system in concrete. Part I - Entrained air in unhardened concrete," *Journal of American Concrete Institute*, 55, 95-121.
142. Miller, B.G., *Coal Energy Systems*, Elsevier Academic Press, Burlington MA, 2005.
143. Monteiro, P.J.M., Bastacky, S.J., Hayes, T.L., *Low-temperature scanning electron microscope analysis of portland cement paste early hydration*, *Cem. Concr. Res.* 15 (4) (1985) 687-693.

144. Moore, E.S., *Coal, Its Properties, Analysis, Classification, Geology, Extraction, Uses and Distribution*, John Willey & Sons, 1940.
145. Moranville-Regourd, M., "Cements Made from Blastfurnace Slag," *Lea's Chemistry of Cement and Concrete, 4th Edition*, Hewlett, P.C., Ed., Arnold, 1998, pp. 633-674.
146. Myers, D., 1946, *Surfaces, interfaces, and colloids: principles and applications*, VCH Publishers, Inc., New York.
147. Myers, D., 1991, *Surfaces, interfaces, and colloids: principles and applications*, VCH Publishers, Inc., New York.
148. Naranjo, A., "Clustering of Air Voids Around Aggregates in Air Entrained Concrete," M.S. Thesis, University at Texas at Austin, 2007.
149. Neavel, R.C., "Origin, Petrography, and Classification of Coal," *Chemistry of Coal Utilization, 2nd Supplementary Volume*, Elliott, M.A., Ed., John Wiley & Sons, New York, 1981.
150. Neville, A.M., 1997, *Properties of concrete*, 4th edition, John Wiley & Sons, New York.
151. Nuffield, E.W., *X-ray diffraction methods*, Wiley, New York, 1966.
152. Okoh, J.M., Doodoo, J.N.D., Diaz, A., Ferguson, W., Udinsky, J.R., "Kinetics of beneficiated fly ash by carbon burnout," USDOE Assistant Secretary for Fossil Energy, Washington, DC. Report: DOE/MT/94016-10-PT.2; CONF-970310, Dec 1997.
153. Pade, C., Jakobsen, U.H., and Elsen, J., A New Automatic Analysis System for Analyzing the Air-Void System in Hardened Concrete, Proceedings of the 24th International Conference on Cement Microscopy, 2002, 204-213.
154. Park, C., Appleton, J.P., "Shock-Tube Measurements of Soot Oxidation Rates," *Combustion and Flame*, 20, 369-379, 1973.
155. Payá, J., Monzó, J., Borrachero, M.V., Amahjour, F., Peris-Mora, E., "Loss on ignition and carbon content in pulverized fuel ashes (PFA): two crucial parameters for quality control," *J. Chem Technol Biotechnol*, 77, pp. 251-255, 2002.
156. Pigeon, M, and Pleau, R.. (1995). "Durability of Concrete in Cold Climates," London: E&Fn Spon.
157. Pigeon, M., Plante, P., Study of Cement Paste Microstructure Around Air Voids: Influence and Distribution of Soluble Alkalies, *Cement and Concrete Research* 20, (1990) pp. 803-814.
158. Pigeon, M., Saucier, F., and Plante, P. (1990). "Air-Void Stability, Part IV: Re-tempering." *ACI Materials Journal*, 87(3), 252-259.

159. Plante, P., Pigeon, M. and Foy, C., The influence of water-reducers on the production and stability of the air void system in concrete, *Cement and Concrete Research*, 19, (1989) 621-633.
160. Pleau, R., Plante, P., Pigeon, M. and Gagne, R., Practical Considerations Pertaining to the Microscopical Determination of Air Void Characteristics of hardened concrete (ASTM C 457 Standard). *Cement, Concrete, and Aggregates*, 12(2) (1990), 3-11.
161. Powers, T. C., *Properties of Fresh Concrete*, John Wiley & Sons, Inc., New York 1968
162. Powers, T. C., Void Spacing as a Basis for Producing Air-Entrained Concrete, *ACI Journal*, Proc. V. 50, (1954) 741-760.
163. Powers, T. C., Void Spacing as a Basis for Producing Air-Entrained Concrete, *ACI Journal*, Part 2, Proc. V. 50 (1954) 760-6-760-15.
164. Powers, T.C. (1954). "Void spacings as a basis for producing air-entrained concrete," *Journal of American Concrete Institute*, 50, 741-760.
165. Powers, T.C. (1975). "Freezing Effects in Concrete," *ACI Special Publication SP-47*,: American Concrete Institute, Detroit, MI.
166. Powers, T.C., 1968, *The Properties of Fresh Concrete*, John Wiley & Sons, New York.
167. Powers, T.C., and Helmuth, R.A. (1953). "Theory of volume changes in hardened Portland cement pastes during freezing." *Proceedings of the Highway Research Board*, 32, 285-297.
168. Powers, T.C., The Air Requirement of Frost-Resistant Concrete. *Proceedings of the Highway Research Board*, 29, (1949) 184-211.
169. Ramachandran, V.S., *Concrete Admixtures Handbook*, Noyes Publications, Park Ridge, New Jersey, 1984.
170. Rashed, A.I., Williamson, R.B., Microstructure of entrained air voids in concrete: Part I, *J. Mater. Res.* 6 (9) (1991A) pp. 2004-2012.
171. Rashed, A.I., Williamson, R.B., Microstructure of entrained air voids in concrete: Part II, *J. Mater. Res.* 6 (11) (1991B) pp. 2474-2483.
172. Reid, W.T., "Coal Ash- Its Effects on Combustion Systems," *Chemistry of Coal Utilization*, 2nd Supplementary Volume, Elliott, M.A., Ed., John Wiley & Sons, New York, 1981.
173. Rietveld, H., A Profile Refinement Method for Nuclear and Magnetic Structures, *Journal of Applied Crystallography*, 2 (1969) 65-71.
174. Rietveld, H.M., *Journal of Applied Crystallography*, 2 (1969) 65-71.

175. Rixom, M.R. and Mailvaganam, N.P., *Chemical Admixtures for Concrete*, 2nd Edition, E. & F.N. Spon, London, 1986.
176. Roberts, L.R., Air Content, Temperature, Density (Unit Weight), and Yield, Significance of Tests and Properties of Concrete and Concrete-Making Materials, ASTM, STP 169D, 2006, pp. 73-79.
177. Rosen, M.J., 2004, *Surfactants and Interfacial Phenomena*, 3rd Edition, John Wiley & Sons, Inc., Hoboken, New Jersey.
178. Sabanegh, N., Gao, Y., Suubergh, E., Hurt, R., "Interaction of coal fly ash and concrete surfactants: diffusional transport and adsorption," Ziegler A et al. (eds.), Proceedings ICCS '97, DGMK Tagungsberichte 9704, pp 1907-1910.
179. Saucier, F., Pigeon, M., and Cameron, G. (1991). "Air void stability, Part V: Temperature, general analysis, and performance index," *ACI Materials Journal*, 88(1), 25-36.
180. Saucier, F., Pigeon, M., and Plante, P. (1990). "Air void stability, Part III: Field test of superplasticized concrete," *ACI Materials Journal*, 87(1), 3-11.
181. Schlorholtz, S., "Supplementary Cementitious Materials," *Significance of Tests and Properties of Concrete and Concrete-Making Materials*, ASTM STP 169, ASTM International, West Conshohocken, PA, 2006, pp. 495-511.
182. Shaw, D.J., 1985, *Introduction to colloid and surface chemistry*, 3rd Edition, Butterworth and Co., London.
183. Singer, J.G. editor, *Combustion: Fossil Power Systems, Third Edition*, Combustion Engineering Inc., 1981.
184. Skinner, F.D., Smoot, L.D., "Heterogeneous Reactions of Char and Carbon," *Pulverized Coal Combustion and Gasification*, Smoot, L.D, Pratt, D.T., Eds., Plenum Press, New York, 1979.
185. Slack, A.V., "Control of Pollution from combustion Processes," *Chemistry of Coal Utilization*, 2nd Supplementary Volume, Elliott, M.A., Ed., John Wiley & Sons, New York, 1981.
186. Smith, K.A., Külaots, I., Hurt, R.H., Suuberg, E. M., The Chemical Nature of Unburned Carbon Surfaces in Fly Ash – Implications for Utilization in Concrete, Proc. of the 1997 International Ash Utilization Symposium, Lexington, KY, pp. 650, 1997.
187. Soong, Y., Schoffstall, M.R., Irdi, G.A., Link, T.A., "Triboelectrostatic separation of fly ash," 1999 International Ash Utilization Symposium, CAER, Univ. of Kentucky, Paper #10.
188. Speight, J.G., *The Chemistry and Technology of Coal*, Marcel Dekker Inc., 1983

189. Stencel, J.M., Li, T.X., Gurupira, T., Jones, C., Neathery, J.K., Ban, H., Altman, R., "Technology development for carbon-ash beneficiation by pneumatic transport, triboelectric processing," 1999 International Ash Utilization Symposium, CAER, Univ. of Kentucky. Paper #78.
190. Struble, L., Hydraulic Cements-Physical Properties, Significance of Tests and Properties of Concrete and Concrete-Making Materials, STP 169D, ASTM (2006) 435-449.
191. Stutzman, P.E., Guide for X-Ray Powder Diffraction Analysis of Portland Cement and Clinker, National Institute of Standards and Technology Internal Report 5755, (1996).
192. Tatsch, J.H., *Coal Deposits: Origin, Evolution and Present Characteristics*, Tatsch Associates, 1980.
193. Tattersall, G.H., and Banfill, P.F.G. *The Rheology of Fresh Concrete*. Marshfield, MA: Pitman Publishing. (1983).
194. TFHRC, *Coal Fly Ash- Material Description*, Turner-Fairbank Highway Research Center, <http://www.tfhrc.gov/hnr20/recycle/waste/cfa51.htm>, 2007.
195. Thomas, M., Wilson M.L., *Supplementary Cementing Materials For Use in Concrete*, CD ROM, Portland Cement Association, Skokie, IL, 2002.
196. Tsujii, K., 1998, *Surface activity: principles, phenomena and applications*, Academic Press, San Diego, CA.
197. Turns, S.R., *An Introduction to Combustion, Concepts and Applications*, McGraw-Hill Inc., 1996.
198. Van Krevelen, D.W., *Coal: Typology, Chemistry, Physics, Constitution*, Elsevier Scientific Publishing Company, 1981.
199. Walker, A., and Wheelock, T.D., 2006. "Separation of Carbon from Fly Ash Using Froth Flotation." *Coal Preparation*. 26(4):235-250.
200. Ward, C. R., editor, *Coal Geology and Coal Technology*, Blackwell Scientific Publications, 1984.
201. Whiting, D. Stark, D., Control of air content in concrete, NCHRP report 258 (May, 1983). Washington: Transportation Research Board, National Research Council.
202. Whiting, D.A., and Nagi, M.A. (1998). "Manual on Control of Air Content in Concrete," *Portland Cement Association*, Skokie Ill.
203. Whiting, D.A., Nagi, M.A., 1998, *Manual of control of air content in concrete*, Portland Cement Association, Skokie, IL.

204. Whiting, D.A., Nagi, M.A., 1998, *Manual of control of air content in concrete*, Portland Cement Association, Skokie, IL.
205. Yu J., Külaots I., Sabanegh N., Gao Y., Hurt R., Suuberg E., Mehta A., “Adsorptive and optical properties of fly ash from coal and petroleum coke co-firing,” *Energy and Fuels*, Volume 14, Number 3, pp. 591-596, 2000.
206. Yu, J., Külaots, I., Sabanegh, N., Gao, Y., Hurt, R.H., Suuberg, E.S., Mehta, A., 2000, “Adsorptive and optical properties of fly ash from coal and petroleum coke co-firing,” *Energy & Fuels*, 14, pp. 591-596.
207. Zacarias; P.S., Oates, D.B., *Carbon removal through partial carbon burn-out from coal ash used in concrete*, United States Patent 6,783,585, Oct. 2002.
208. Zumdahl, S.S., *Chemistry*, D.C. Heath and Company, Lexington MA, 3rd Edition, 1993.

Referenced Standards

1. AASHTO T-199-00. "Concrete Air Content - Chase Air Indicator Method"
2. ASTM C 114-03. "Standard Test Methods for Chemical Analysis of Hydraulic Cement", *Annual Book of ASTM Standards 2003, Volume 04.01*, ASTM International, West Conshohocken, PA, pp. 108-135, 2003.
3. ASTM C 114-06. "Standard Test Methods for Chemical Analysis of Hydraulic Cement," ASTM International, West Conshohocken, PA.
4. ASTM C 1231. "Standard Practice for Use of Unbonded Caps in Determination of Compressive Strength of Hardened Concrete Cylinders," ASTM International.
5. ASTM C 136-01. "Standard Test Method Sieve Analysis of Fine and Coarse Aggregates," ASTM International.
6. ASTM C 138/C 138M-01a. "Standard Test Method for Density (Unit Weight), Yield, and Air Content (Gravimetric) of Concrete", *Annual Book of ASTM Standards 2002, Volume 04.02*, ASTM International, West Conshohocken, PA, pp. 90-95, 2002.
7. ASTM C 138-01. "Standard Test Method for Density (Unit Weight), Yield, and Air Content (Gravimetric) of Concrete," ASTM International.
8. ASTM C 143/C 143 M-00. "Standard Test Method for Slump of Hydraulic-Cement Concrete", *Annual Book of ASTM Standards 2002, Volume 04.02*, ASTM International, West Conshohocken, PA, pp. 96-98, 2002.
9. ASTM C 143-00. "Standard Test Method for Slump of Hydraulic-Cement Concrete," ASTM International.
10. ASTM C 143-05. "Standard Test Method for Slump of Hydraulic-Cement Concrete," ASTM International, West Conshohocken, PA.
11. ASTM C 150-02a. "Standard Specification for Portland Cement", *Annual Book of ASTM Standards 2003, Volume 04.01*, ASTM International, West Conshohocken, PA, pp. 150-156, 2003.
12. ASTM C 150-04. "Standard Specification for Portland Cement," ASTM International, West Conshohocken, PA.
13. ASTM C 150-07. "Standard Specification for Portland Cement," ASTM International, West Conshohocken, PA.
14. ASTM CC 173-07. "Standard Test Method for Air Content of Freshly Mixed Concrete by the Volumetric Method," ASTM International, West Conshohocken, PA.

15. ASTM C 173/C 173M-01e1. "Standard Test Method for Air Content of Freshly Mixed Concrete by the Volumetric Method", *Annual Book of ASTM Standards 2002, Volume 04.02*, ASTM International, West Conshohocken, PA, pp. 116-124, 2002.
16. ASTM C 185-02. "Standard Test Method for Air Content of Hydraulic Cement Mortar," ASTM International, West Conshohocken, PA.
17. ASTM C 187-04. "Standard Test Method for Normal Consistency of Hydraulic Cement," ASTM International, West Conshohocken, PA.
18. ASTM C 192-02. "Standard Practice for Making and Curing Test Specimens in the Laboratory," ASTM International, West Conshohocken, PA.
19. ASTM C 230-03. "Standard Specification for Flow Table for Use in Tests of Hydraulic Cement," ASTM International, West Conshohocken, PA.
20. ASTM C 231-04. "Standard Test Method for Air Content of Freshly Mixed Concrete by the Pressure Method," ASTM International, West Conshohocken, PA.
21. ASTM C 260-06. "Standard Specification for Air-Entraining Admixtures for Concrete," ASTM International, West Conshohocken, PA.
22. ASTM C 231-97. "Standard Test Method Air Content of Freshly Mixed Concrete by the Pressure Method," ASTM International.
23. ASTM C 231-97e1. "Standard Test Method for Air Content of Freshly Mixed Concrete by the Pressure Method", *Annual Book of ASTM Standards 2002, Volume 04.02*, ASTM International, West Conshohocken, PA, pp. 146-153, 2002.
24. ASTM C 260-01. "Standard Specification for Air-entraining Admixtures for Concrete," ASTM International, West Conshohocken, PA.
25. ASTM C 305-06. "Standard Practice for Mechanical Mixing of Hydraulic Cement Pastes and Mortars of Plastic Consistency," ASTM International, West Conshohocken, PA.
26. ASTM C 311-02. "Standard Test Methods for Sampling and Testing Fly Ash or Natural Pozzolans for Use as a Mineral Admixture in Portland-Cement Concrete", *Annual Book of ASTM Standards 2002, Volume 04.02*, ASTM International, West Conshohocken, PA, pp. 318-321, 2002.
27. ASTM C 311-05. "Standard Test Methods for Sampling and Testing Fly Ash or Natural Pozzolans for Use in Portland-Cement Concrete," ASTM International, West Conshohocken, PA.
28. ASTM C 33-02a. "Standard Specification for Concrete Aggregates," ASTM International, West Conshohocken, PA.

29. ASTM C 39. "Standard Test Method for Compressive Strength of Cylindrical Specimens," ASTM International, West Conshohocken, PA.
30. ASTM C 457-06. "Standard Practice for Microscopical Determination of Air-Void Content and Parameters of the Air-Void System in Hardened Concrete," ASTM International, West Conshohocken, PA.
31. ASTM C 457-98. "Standard Test Method for Microscopical Determination of Parameters of the Air-Void System in Hardened Concrete", *Annual Book of ASTM Standards 2002, Volume 04.02*, ASTM International, West Conshohocken, PA, pp. 241-254, 2002.
32. ASTM C 494/C 494M-99ae1, "Standard Specification for Chemical Admixtures for Concrete," *Annual Book of ASTM Standards 2002, Volume 04.02*, ASTM International, West Conshohocken, PA, pp. 269-277, 2002.
33. ASTM C 494-04. "Standard Specification for Chemical Admixtures for Concrete," ASTM International, West Conshohocken, PA.
34. ASTM C 494-05. "Standard Specification for Chemical Admixtures for Concrete," ASTM International, West Conshohocken, PA.
35. ASTM C 496. "Standard Test Method for Splitting Tensile Strength of Cylindrical Concrete Specimens," ASTM International, West Conshohocken, PA.
36. ASTM C 618-02. "Standard Specification for Coal Fly Ash and Raw or Calcined Natural Pozzolan for Use as a Mineral Admixture in Concrete", *Annual Book of ASTM Standards 2002, Volume 04.02*, ASTM International, West Conshohocken, PA, pp. 198-206, 2002.
37. ASTM C 618-05. "Standard Specification for Coal Fly Ash and Raw or Calcined Natural Pozzolan for Use in Concrete," ASTM International, West Conshohocken, PA.
38. ASTM C 666-03, "Standard Test Method for Resistance of Concrete to Rapid Freezing and Thawing," ASTM International, West Conshohocken, PA.
39. ASTM C 672-03. "Standard Test Methods for Scaling Resistance of Concrete Surfaces Exposed to Deicing Chemicals," ASTM International, West Conshohocken, PA.
40. ASTM C 778-06. "Standard Specification for Standard Sand," ASTM International, West Conshohocken, PA.
41. ASTM C 1017-07. "Standard Specification for Chemical Admixtures for Use in Producing Flowing Concrete," ASTM International, West Conshohocken, PA.
42. ASTM C 78-02. "Standard Test Method for Flexural Strength of Concrete (Using Third Point Loading)," ASTM International, West Conshohocken, PA.

43. ASTM D 3172-89(2002), "Standard Practice for Proximate Analysis of Coal and Coke", *Annual Book of ASTM Standards 2003, Volume 05.06*, ASTM International, West Conshohocken, PA, pp. 309-310, 2003.
44. ASTM D 3176-89(2002), "Standard Practice for Ultimate Analysis of Coal and Coke", *Annual Book of ASTM Standards 2003, Volume 05.06*, ASTM International, West Conshohocken, PA, pp. 323-326, 2003.
45. ASTM D 388-99(2004)e1, "Standard Classification of Coals by Rank", *Annual Book of ASTM Standards 2003, Volume 05.06*, ASTM International, West Conshohocken, PA, pp. 202-208, 2003.

American Concrete Institute

1. 201.2R-01 Guide to Durable Concrete
2. 318-05 Building Code Requirements for Structural Concrete

European Norm

- 480-11.1 Admixtures for concrete, mortar and grout - Test methods - Part 11:
Determination of air void characteristics in hardened concrete

Texas Department of Transportation

DMS 4610-06 Fly Ash

Volume I—Appendix A: Supplementary Information

This appendix contains supplementary information regarding tests and analysis on fly ash color that was not presented in the two parts of Chapter 6. The information concerns digital scanner operation and digital image characteristics, color analysis of digital images using the ImageTool software, factors influencing ash color and correlations between ash color and chemical composition.

A1. Fly Ash Color

1. Ash sample imaging

Different methods of producing digital images of the ash and then quantifying ash color were tested. Initial tests for producing digital images of the ash used a digital camera to capture images of ash samples either in glass containers or in a compressed layer within a Petri dish. Despite efforts to control lighting conditions and camera settings, obtaining consistent images that clearly showed ash color proved difficult. Instead, the use of a desktop color image scanner proved to be better suited for producing color images of the ash samples with limited variability.

1.1 Ash imaging using a common desktop scanner

A desktop flatbed image scanner is a device used to convert the reflected visible light of an object, such as a document or photograph, into a digital image. Typical desktop flatbed scanners consist of a glass surface, or platen, large enough to admit ISO A4 (210 x 297 mm) size and or letter size (8.5 x 11 in) documents. The object being scanned is placed scanned-side down on the platen and remains stationary. On the underside of the platen, a scanning array travels along the length of the scanning bed progressively converting the reflected light from the object into an analog and then digital signal. The scanning array consists of a light source and optical sensor (the detector that converts the light into an electrical charge) and possibly mirrors and lenses depending on the scanner type. A variety of scanning array configurations and optical sensors exist however the basic operation is the same.

1.2 Digital images

Once a scan of an object has been completed, the digital data is transferred to the computer software to be assembled into the digital image. The image resolution and colors of the digital image are dependent on the properties, pixels per inch (ppi) and bit depth, of both the scanner and the software.

Resolution and sharpness are dependent on several factors including the pixels per inch, ppi, at which the scan is performed (Gann, 1999). A digital image is divided into many horizontal rows and intersecting vertical columns that form a structured grid. The individual elements of the grid are called pixels. Each pixel is described by a single discrete color. As the number of pixels in a given area increases so does the potential for increased resolution and sharpness. Ppi is typically described in product literature as X by Y where X is the number of individual sensors per inch in the optical sensor array (*x*-direction) and Y is the precision in fractions of an inch of the stepper motor (*y*-direction) which moves the array across the scanner bed. A 1200 by 1200 ppi scanner with an 8.5 in platen width would have 10,200 individual

optical sensors per row and the stepper motor would control the scanner array by 1/1200ths of an inch increments.

The “bit depth” of an image refers to the amount of memory used to store a numerical description of the color of a single pixel. The number of possible shades of the pixel is limited by the number of unique values that the partition of memory can contain. A single bit of memory can store a binary value, either 0 or 1. For an 8-bit depth grayscale image, each gray pixel in the image requires 8 bits (1 byte) of memory for storage, thus the pixel is limited to 256 possible shades ($2^8 = 256$). These shades range from black (0, zero) to white (255) as shown in Figure A1. The pixels in color images can be described by three numerals representing the contributions of red, green and blue (RGB) in the pixel color. In a 24-bit depth color image, the red, green and blue values are each represented by 8 bits. As with the 8-bit grayscale values, each of the three color components possess a value from 0 to 255. The total number of different possible color combinations for a 24 bit image is 16.8 million (2^{24} or $256 \times 256 \times 256 = 16.8 \times 10^6$). Typical bit depths range from 24 to 48 on desktop scanners though larger bit depths can be found in high end scanners.

Though a scanner may be capable of producing a 48 bit depth image, if the software used to open or edit the image supports only lesser bit depth images, then the bit depth of the image will be decreased and the data from the richer color palette will be lost.

1.3 Converting a color image to a grayscale image

As described in Chapter 6, for the ash color analysis done in this research 24-bit ash color values were converted to 8-bit grayscale values. This was done to simplify comparison of different ash samples based on a single numerical value instead of three. A number of mathematical methods exist for converting 24-bit color values to 8-bit grayscale values. The color conversion method used in this study, shown in equation 1, is similar to methods used in many commercial image processing software packages. This method applies weights, ranging between 0 and 1, to the red, green and blue color components then rounds the sum of the weighted values to the nearest whole number.

$$\text{Grayscale value} = Rr + Gg + Bb \quad \text{eq. 1}$$

The variables r , g and b are the 8-bit color components of a 24-bit color image and R , G and B are the applied weights. The sum of R , G and B is equal to 1. The values of the weights used in this study, given in Table A1, were selected to be the same as those used by the image analysis software used for analyzing the digital ash images. Variations in the weight values exist among software programs, but the values are generally similar to those shown in Table A1 with the greatest weight applied to the green component. Figure A1 gives an example of eight 24-bit colors and their corresponding 8-bit grayscale values.

Table A1, Volume 1. Twenty-four-bit color conversion weights.

1. Weight	2. Value
3. R	4. 0.25
5. G	6. 0.625
7. B	8. 0.125

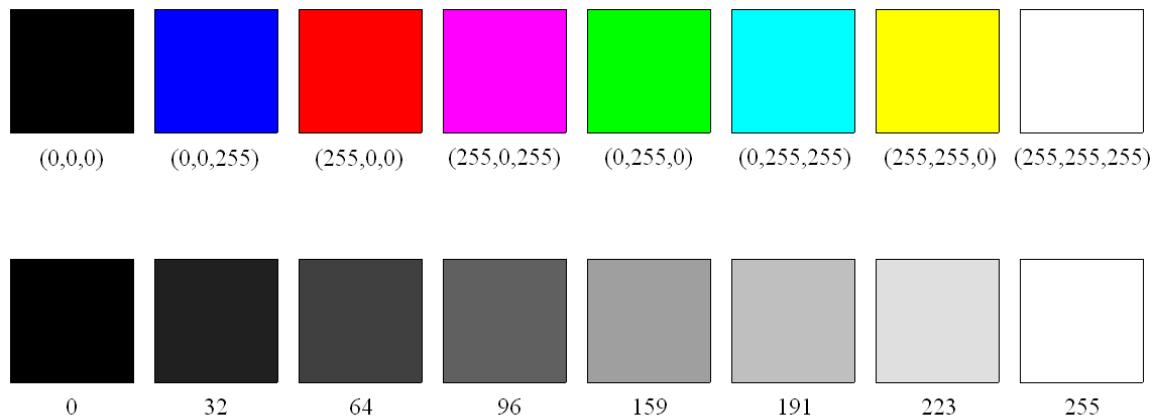


Figure A1, Volume 1. RGB and corresponding grayscale values of selected colors.

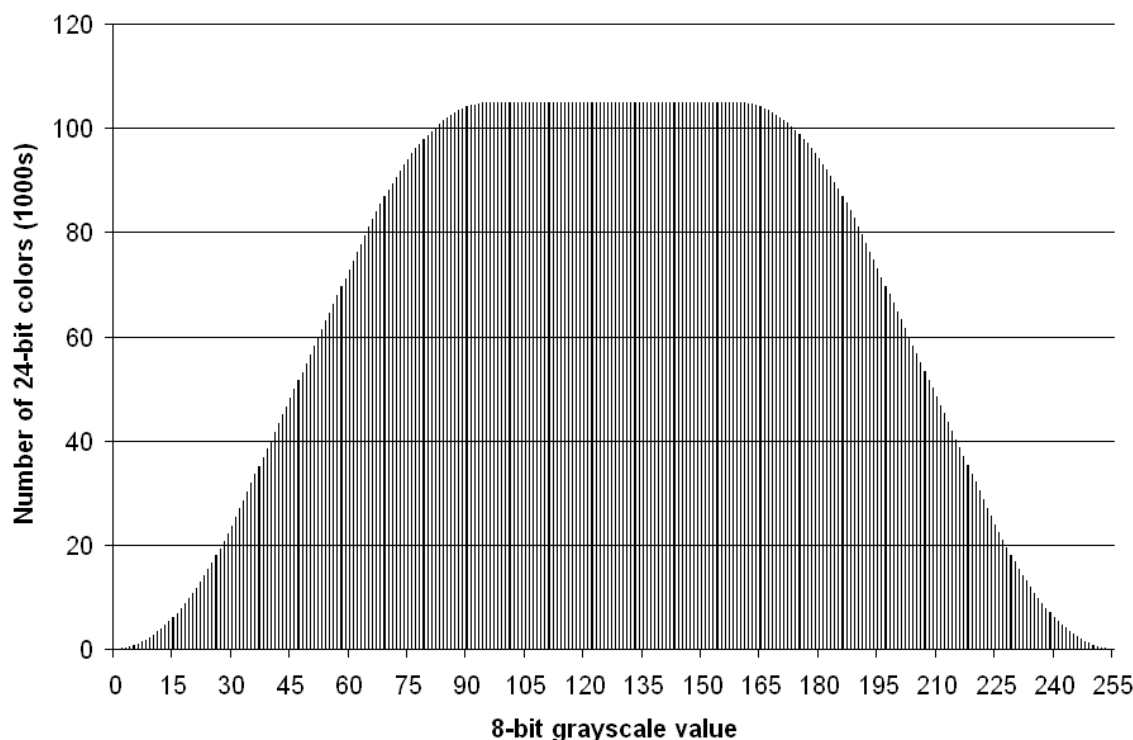


Figure A2, Volume 1. The number of individual 24-bit RGB colors per single 8-bit grayscale value.

Converting 24-bit color images to 8-bit grayscale images results in a significant loss of color data. Converting 17.8 million RGB colors to 255 gray values means that many unique color values will produce the same grayscale value. The histogram in Figure A2 shows the number of unique 24-bit colors associated with each 8-bit grayscale value, when the RGB weights from Table A1 are used. The 8-bit gray values 92 through 163 each can be created from

nearly 105,000 different 24-bit colors. The distribution of colors changes as the RGB weights change as shown in Figure A3.

Despite the loss of information due to conversion, using grayscale values to represent ash color was generally adequate in this study. In some cases, however, use of the 24-bit color information may be desired; therefore color values and corresponding grayscale values were collected from the ash samples analyzed.

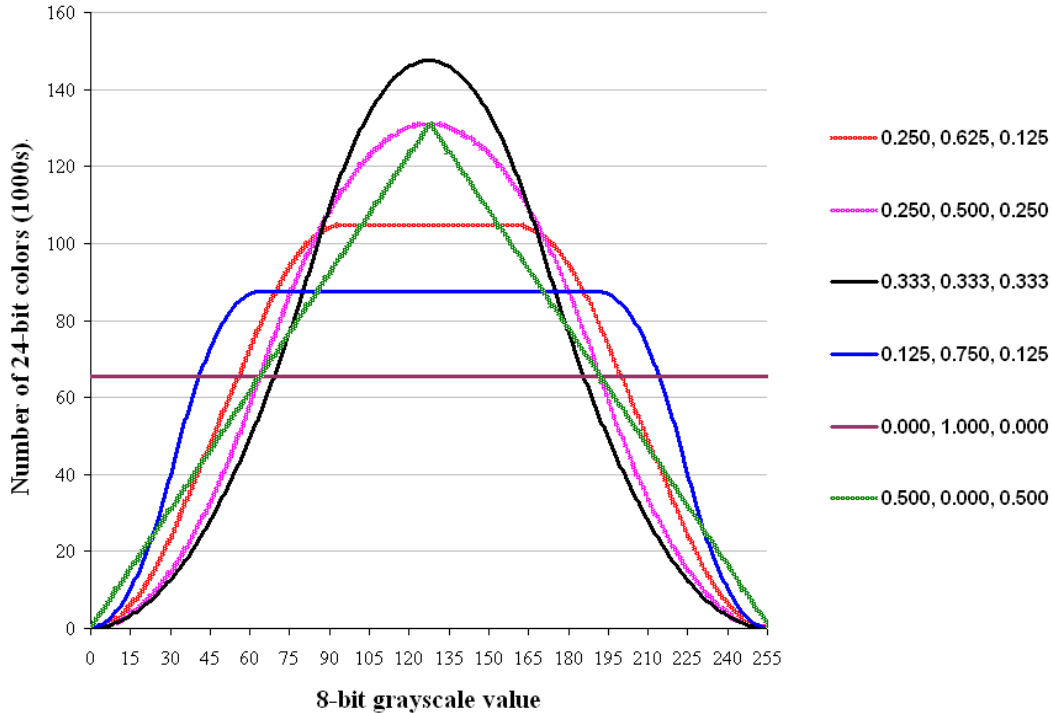


Figure A3, Volume 1. The number of individual 24-bit RGB colors per single 8-bit grayscale value for various RGB weights.

2. Fly ash image and analysis

A sample of fly ash can be scanned with a desktop scanner using a device to hold the ash sample against the scanner platen. A detailed description of the apparatus and scanning procedure used in this study is provided in a later section. After a digital image of an ash sample is produced using a scanner and computer software, an analysis of the ash color can then be performed. Several types of commercial image editing software and freeware, such as Microsoft Paint, The Gimp and Adobe Photoshop, have tools which allow users to select a single pixel within a digital image and identify its color based on RGB values and/or other schemes. Such tools can be used to analyze color, but the method is slow if many pixels are to be analyzed to obtain an average color value.

Image analysis software packages can be used to quickly analyze digital images. The UTHSCSA ImageTool²² image processing and analysis software was used in this research for image analysis. ImageTool was developed by C. Donald Wilcox, S. Brent Dove, W. Doss McDavid and David B. Greer of the Department of Dental Diagnostic Science at The University of Texas Health Science Center, San Antonio, Texas. ImageTool is an image processing and analysis program for Microsoft Windows operating systems and is available for free download. The ImageTool can acquire, display, edit, analyze, process, compress, save and print gray scale and color images. The software can read and write 22 common file formats including BMP, PCX, TIF, GIF and JPEG (UTHSCSA, 1997).

This software was selected for several reasons including: 1) the executable and source code are available for free download, 2) ImageTool has a complete scripting language built into the application with over 200 image processing and analysis functions to allow automation of repetitive tasks and extension of the program without the need for a compiler and additional language expertise, 3) it has a simple graphical user interface and 4) it is capable of automatically analyzing multiple images in succession.

2.1 Fly ash color analysis with ImageTool

All scanned images were analyzed with the use of a specially developed script for the ImageTool. The analysis was performed by 1) importing the scanned images into the ImageTool, 2) executing the script and then 3) transferring the color data to a spreadsheet. These three steps are described below.

2.1.1 Importing images to ImageTool

Scanned images were analyzed in groups to minimize analysis time. For analysis of a group of images, the images were inserted into a single “stack.” A stack contains all the imported images in a single window, with only a single image displayed at a time. As images are inserted into the stack, each is given a number designation as X/Y where X is numerical order in which the image was inserted and Y is the total number of images in the stack. The image that is displayed can be changed by using the left or right arrows on the keyboard. The number of images that can be placed in a single stack is dependent on the memory capacity of the computer. Stacks containing ninety or more images were routinely analyzed without problems on the computer system used in this study.

A new stack was created by using *File* → *New* → *Image Stack* or *Stacks* → *New* pull down menus. Images were placed into the stack using *File* → *Open Image...* or the “” icon. The images were placed into the stack in the desired order of analysis. Once the stack was complete, the zoom functions were used to size the stack window so that the complete image fit within the borders of the display. This was done so that the analysis region can be selected manually. Changing the zoom factor of the image has no effect on the analysis results.

The “RGB Analysis Stack” script is a general purpose script and does not record the image file names. Therefore, a spreadsheet file was opened and the sample names were recorded in a column of cells as the corresponding images were placed in the stack. The images were

²²UTHSCSA ImageTool executable and source code is available for free download at

<http://ddsdx.uthscsa.edu/dig/download.html>.

ordered so the first image placed in the stack corresponds to the top cell of the spreadsheet column. When the analysis is complete the data can be copied from the ImageTool results window and pasted into the spreadsheet columns beside the sample names for further analysis.

2.1.2 Running the “RGB Stack Analysis” script

The analysis was begun by selecting *Script* → *Run Script...* and selecting “RGB Stack Analysis.” The script prompted the user to select a region of interest (ROI) of the image for analysis. By default, the ROI was a rectangle with vertical horizontal and vertical sides. The script prompted the user to 1) select the top left corner, 2) the bottom left corner and 3) the top right corner of the ROI. These were selected as shown in Figure A4. The height of the analysis region was determined by the vertical difference between the first two selected points and the width determined as the horizontal difference between the first and third selected points. The ROI was selected so that the cuvet boundaries would not interfere with the analysis. The ROI is determined using the first image in the stack and then automatically repeated for the other images. The location of the cuvet in all the images was identical so that the ROI would include only the region of the image containing the scanned ash. This was ensured by using a properly fitted scanning template to hold the cuvet during the scanning process.

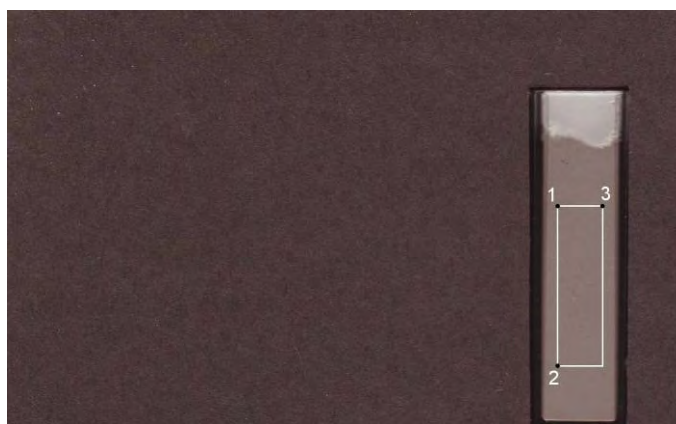


Figure A4, Volume 1. Selection of the region of interest for color analysis.

2.1.3 Transferring analysis data to spreadsheet

During the analysis, the average red, green, blue and grayscale values (each between 0 and 255) of all the pixels in the user-selected ROI were output in the “Results” window for each ash. Each row number in the “Results” window corresponded to the image stack number. When analysis is complete, the results can be copied directly from the results window to the spreadsheet containing the ash sample names. The data were copied to the spreadsheet by selecting the values in the Results window and pressing Ctrl-C then pasted in the spreadsheet by using Ctrl-V or by selecting the Paste command.

2.2 “RGB Stack Analysis” script

The “RGB Stack Analysis” script was developed specifically for the analysis of scanned fly ash images, but can be used for any similar application. The script was developed using the syntax and commands built into the ImageTool. The complete script is included below. The script first prompts the user to identify the location and extents of the ROI, then loops through

each of the images in the stack, and for each image takes the 8 bit color values for the red, green and blue contributions of every pixel in the ROI to produce average RGB and gray scale values.

The script consists of three main parts: script name (line 1), declaration of variables (lines 2-10) and the body (lines 12-63). The individual steps in the script body are explained below. First, the number of images in the stack is identified (line 13). Then the stack is “unlocked” (line 14) so that changes to the images can be made. The only changes made are the overlaying of the ROI boundaries on each image. Next, the first image (or “slice”) placed in the stack is moved to the top of the stack to be first for analysis (line 15). The stack window is then refreshed and moved to the top left of the display (lines 16-17). Any data remaining from previous analyses in the Results window are then cleared (line 19). The script then prompts the user for the three points which define the ROI and enters the user-selected points in an array of coordinates (lines 20-28). The width and height (“numrows”) of the ROI is then calculated based on the entered coordinates (lines 30, 31). The color analysis portion of the script consists of three nested *for loops* (lines 33-62). The first *for loop* (line 33) is used to guide the script through all the slices in the stack. For each slice, the ROI is constructed and drawn on the image (lines 35-37). Then the pixel counter (“counter”) and variables which hold the average color values are initialized to zero. The second *for loop* (line 44) loops the script through the horizontal rows of pixels in the ROI. The third *for loop* (line 47) loops through the individual pixels in each row. For each pixel the RGB values are determined (lines 49-51) and the running average RGB values and pixel counter are then updated (lines 53-56). After all the ROI pixels in a single slice have been analyzed, the average grayscale value is calculated based on the RGB values (line 59) and the average RGB and grayscale values are placed in columns in the results window in (lines 60-61).

RGB Stack Analysis Script for ImageTool

```
1) macro 'RGB Stack Analysis';
2) var
3) i,j,k, numstack : integer;
4) xx, yy : integer;
5) roix, roiy : array;
6) r,g,b : integer;
7) width, numrows : integer;
8) blue, green, red : integer;
9) avgblue, avggreen, avgred , avggray: real;
10) counter : integer;
11)
12) begin
13)   numstack := nSlices;
14)   Stack('unlock');
15)   SelectSlice(1);
16)   UpdateWindow;
17)   MoveWindow(50,100);
18)
19)   DiscardResults;
20)   GetUserPoint('Pick top left corner',xx,yy);
21)   roix[1] := xx;
22)   roiy[1] := yy;
23)   GetUserPoint('Pick bottom left corner',xx,yy);
24)   roix[2] := xx;
25)   roiy[2] := yy;
26)   GetUserPoint('Pick top right corner',xx,yy);
27)   roix[3] := xx;
28)   roiy[3] := yy;
29)
30)   width := roix[3]-roix[1];
31)   numrows := roiy[2]-roiy[1];
32)
33)   for i := 1 to numstack do
34)   begin
35)     SelectSlice(i);
36)     MakeRoi(roix[1], roiy[1], width+1, numrows+1);
37)     DrawBoundary;
38)
39)     counter := 0;
40)     avgblue := 0.0;
41)     avggreen := 0.0;
42)     avgred := 0.0;
43)
44)     for j:= 1 to numrows-1 do
45)     begin
46)       GetRow(roix[1]+1, roiy[1]+j, width-1);
47)       for k := 1 to width-1 do
48)       begin
49)         blue := linebuffer[k*3-2];
50)         green := linebuffer[k*3-1];
51)         red := linebuffer[k*3];
52)
53)         avgblue := (avgblue*counter+blue)/(counter+1);
54)         avggreen :=(avggreen*counter+green)/(counter+1);
55)         avgred := (avgred *counter+red)/(counter+1);
56)         counter:= counter + 1;
57)       end;
```

```

58) end;
59) avggray:= 0.25*avgred +0.625*avggreen+ 0.125*avgblue;
60) ShowResults(true);
61) AddResults('red' '\t' 'green' '\t' 'blue' '\t' 'gray',
      avgred,'\t', avggreen,'\t', avgblue,          '\t',
avggray, '\t');
62) end;
63) end;

```

2.3 Spreadsheet analysis

With the color data placed in a spreadsheet, the information can be used for tracking color change in ash samples produced from a single source, comparison of several ash samples or changes in color of a single ash sample due to high temperature exposure. These tests were performed on the ash samples studied in this research and are reported after the following discussion on the sources of variability in the test procedure.

3. Properties of ash that influence color

The color of an ash sample as seen by the human eye is a composite of the contributions from numerous individual particles. Only the largest particles in the ash, greater than approximately 120 microns, are distinguishable by the naked eye; however, particles of this size typically make up only a small percentage (up to 5%) of the total mass. Generally, ash color appears homogenous; however, when ash samples are viewed with the aid of an optical microscope, particles of many hues and shades are observed. For the samples studied in this research, the great majority of particles visible with an optical microscope at 100 times magnification were clear or white in color, this observation applied even to the darkest Texas commercial ash samples. A much smaller proportion of darkly colored particles interspersed in the ash is also visible. The dark particles have a strong influence on ash color. These particles are composed of both residual coal particles and darkly colored inorganic minerals.

3.1 Residual coal

A portion of the dark particles observed in ash consists of organic coal residuals in the form of char fragments consisting mostly of elemental carbon. The fragments can be removed from the sample by heating in air at 750°C. The colors of the particles are similar to the parent coal (lignite is dark brown to black and sub-bituminous coal is generally dull black). Relatively large char particles greater than 120 microns in width can be removed by sieving with a no. 120 U.S. standard sieve. Figure A5 shows examples of the relatively large-sized char particles viewed at approximately 90-100 times magnification. The surfaces of the particles in Figure A5 are not uniformly black in color because of the presence of fine ash particles. These particles are visible in the SEM micrograph and backscatter micrograph shown in Figure A6. Ash fractions finer than 120 microns, when viewed with an optical microscope at 100 times magnification, show black irregular shaped objects interspersed in the lighter ash spheres. These objects are difficult to isolate and analyze individually; however, when the ash sample is heated to temperatures of 750°C in an air atmosphere, many of the dark particles disappear.

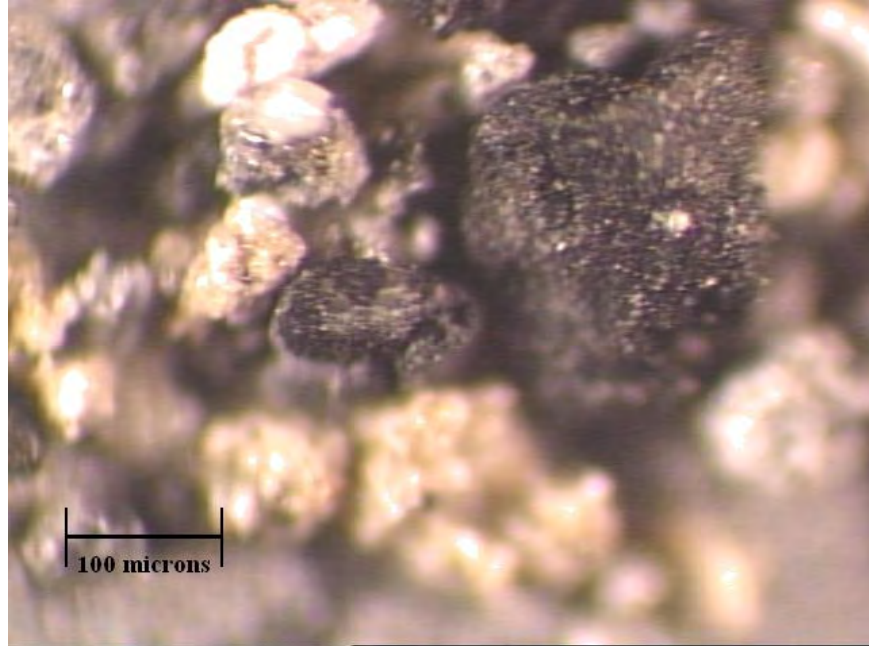


Figure A5, Volume 1. Large residual coal particles sieved from fly ash.

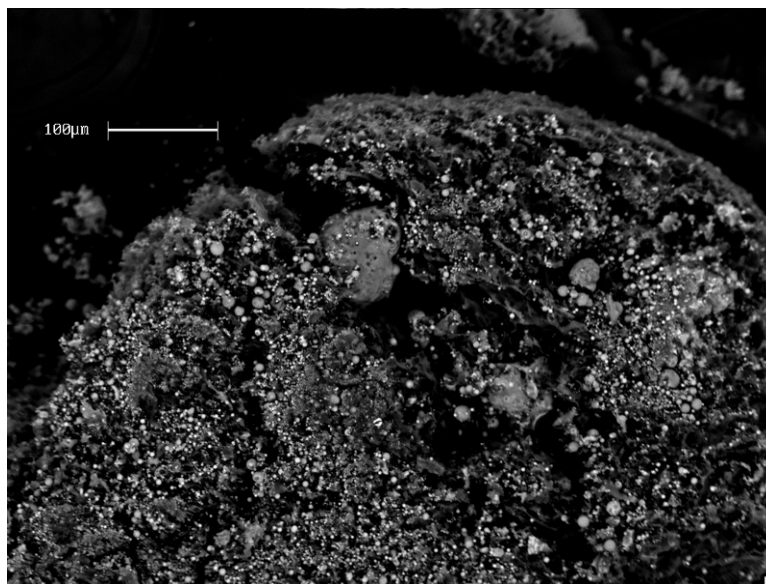
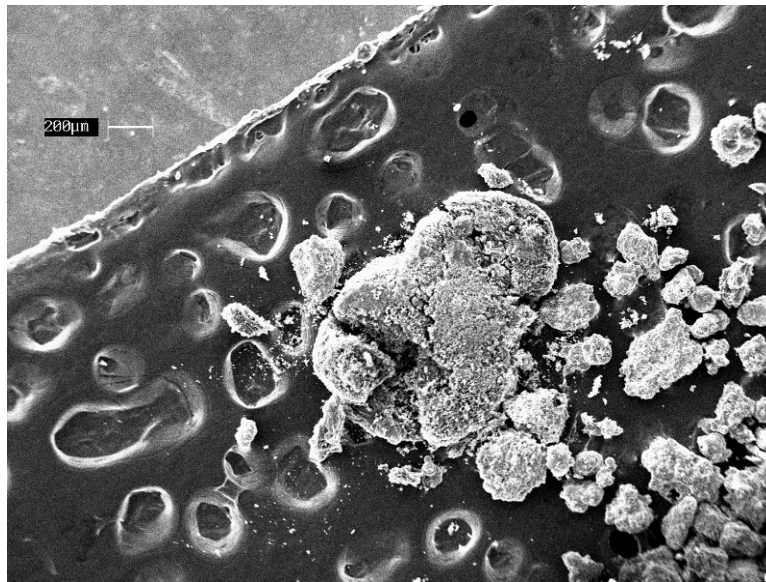


Figure A6, Volume 1. Scanning electron micrograph of a large carbon particle sieved from fly ash (top).

A backscatter image of the same particle shows the denser elements (the metal components of the typical oxides) in lighter tones.

3.2 Iron-rich particles

Other ash constituents besides residual coal fragments may contribute to ash darkness. For example, particles possessing high iron contents have been observed to be dark in color. The iron-rich particles in Figure A7 were extracted from ash by stirring an aqueous ash mixture with a magnetic stir rod for several minutes. After stirring, the particles sticking to the stir rod due to magnetic attraction were removed and dried in an oven then viewed with an optical microscope at 100 times magnification. The particles in Figure A7 are generally spherical in shape and have smooth, shiny surfaces. Elemental analysis, shown in Figure A8, of the surfaces of several magnetic particles suggests that iron is the major constituent; however, the other major minerals

of silica, alumina and calcium oxides are also present. Other researchers have studied the presence and distribution of magnetic fly ash particles (Chaddha and Seehra, 1983).

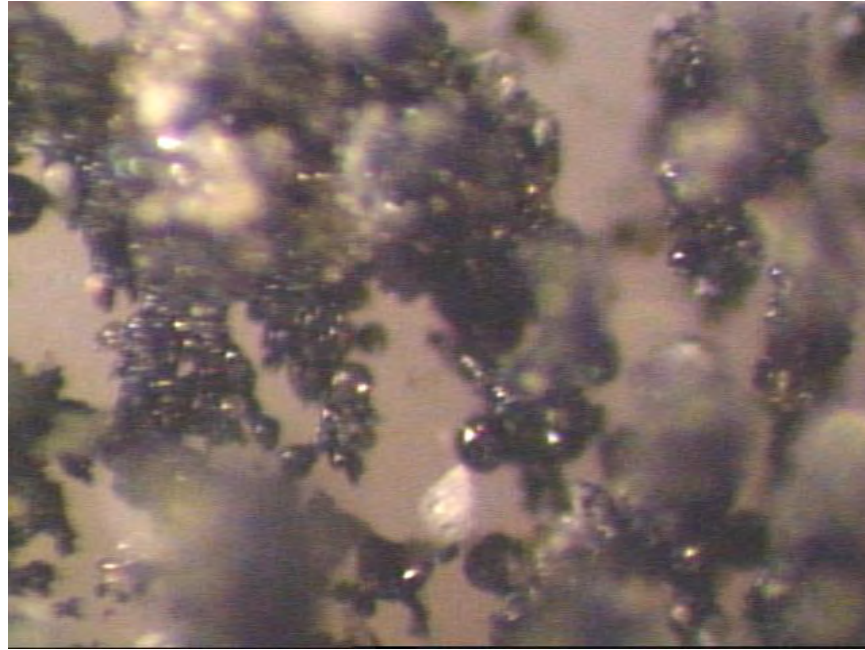


Figure A7, Volume 1. Magnetic ash particles.

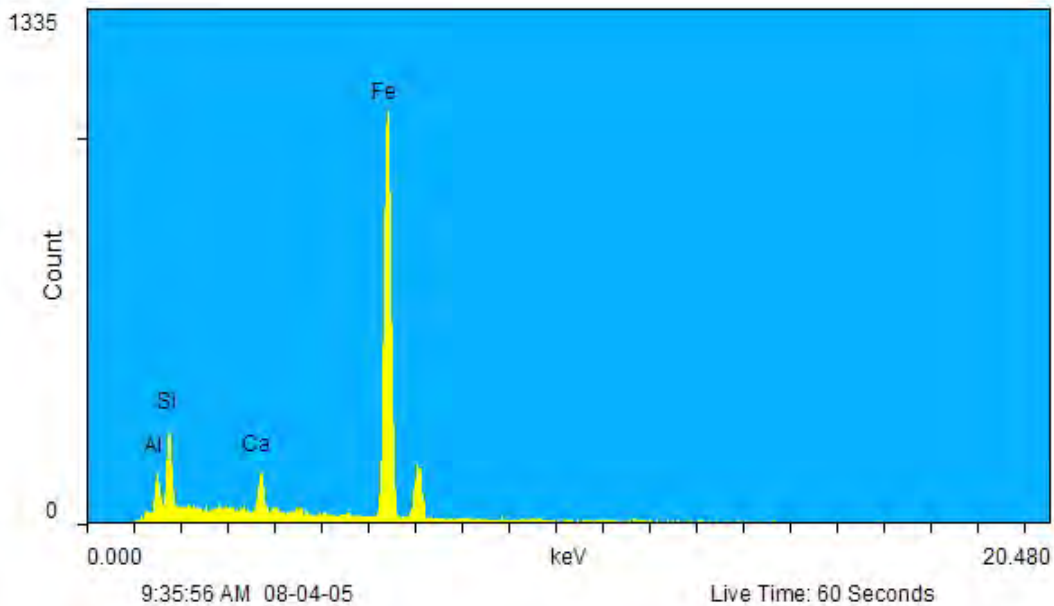


Figure A8, Volume 1. Elemental analysis of magnetic fly ash. Peak height corresponds with concentration within the analysis region.

Typically, pulverized coal fly ash is composed of many different mineral components. Bulk chemical analysis by XRF produces the approximate percentage of the basic metal oxides

present in the ash, but does not indicate which mineral groups are present. As noted earlier, the major inorganic components in fly ash are composed of both crystalline and amorphous minerals. The crystalline mineral content can include quartz (SiO_2), mullite ($3\text{Al}_2\text{O}_3\cdot\text{SiO}_2$), maghemite (Fe_2O_3), periclase (MgO) and other phases. Fly ash amorphous minerals content can consist of various quantities of aluminosilicate, calcium aluminosilicate, calcium aluminate and other glassy phases (Helmuth, 1987; Joshi and Lohtia, 1997). Metal elements detected by the analysis can be constituents of many different phases. Calcium, for example, may be present as calcium hydroxide, calcium sulfate, calcium carbonate or in a calcium-containing glass. While the crystalline phases present can be determined and quantified using X-Ray diffraction, no reliable method for measuring the various amorphous phases exists. Based on this discussion, it should be noted that the oxides present in ash samples are not likely to be present in a pure form or physically separable from the other constituents.

3.3 Image resolution

The resolution of the digital ash images produced by a desktop scanner is too coarse to identify individual particles. The pixels that comprise the image are average color representations of a region of the ash sample. In Figure A9, sixty-four pixels from a scan of an ash sample have been expanded to show the variety of colors present. Thirteen different 24-bit RGB colors are represented in the sixty-four enlarged pixels of Figure A9. The minimum, maximum, and average RGB values of the pixels are shown in Table A2.

It should be noted that the gray value used to describe an ash obtained by the standard analysis procedure is a rough characterization of a complex distribution of particles of many colors and sizes. During color analysis by the RGB Stack Analysis script in the ImageTool, the colors of the individual pixels are averaged, and then the average values are converted to a single average gray value by equation 1. The average gray value of the 64 pixels in Figure A9 is 121.0. (Average RGB and gray values may be decimal numbers; however, the values that describe a specific color will always be whole numbers. Gray 121 is shown at the right of Figure A9 for comparison.)



Figure A9, Volume 1. An enlarged view of 64 pixels (24-bit color) from the analysis region (left) and the average grayscale value (8-bit color) of the pixels (right).

Table A2, Volume 1. Minimum, maximum and average RGB values of the 64 pixels in Figure A9.

	R	G	B
Minimum	131	112	108
Maximum	144	125	121
Average	135.8	116.8	112.8

3.4 Summary

The macroscopic color of ash and the gray value obtained by analysis are indicative of the relative amounts of light and dark materials present. The dark materials are composed of both the organic coal residuals and certain dark mineral components such as the high iron content particles. The amount of organic coal residuals can be highly variable in a single ash source and is dependent not only on coal type but on furnace burner configuration, (See Section 2.3.9.3). The mineral constituents of a given ash sample are dependent primarily upon the parent coal source. Individual ash particles cannot be distinguished in the scanned image. The pixels of the image as well as the 8-bit grayscale value representation of an ash are averaged descriptions of a region of the ash.

4. Correlating ash grayscale value and chemical composition

As described above, ash color as seen by the eye is a composite of many differently colored particles. Ash color as quantified by the color analysis method described in this chapter is an average value of all the pixels that comprise the digital image. As the mineral composition or carbon content of the ash changes, the change is reflected in the overall color of the ash. The following experiments were performed to identify the link between ash grayscale value and ash mineralogical composition.

4.1 Grayscale values of imitation ash samples

Because ash samples produced at different power stations may come from different parent coal sources, the minerals and bulk chemistry that comprise the ash samples likely vary. An experiment was performed to determine how analysis color is influenced by the proportions of the materials in a sample. The experiment was performed by mixing five ingredients, aluminum oxide, calcium hydroxide, powdered charcoal, iron oxide and silica flour in different proportions to create six unique samples. Each of the five ingredients was individually scanned and the color analyzed; the resulting gray values of the analyses are shown at the top of Table A3. The percent compositions and grayscale values of the six combinations are also shown in Table A3. Note that though the basic mineral ingredients chosen for this experiment represent the major mineral constituents of fly ash, the physical compositions of the created samples are not intended to be equivalent to those found in actual ash specimens.

Table A3, Volume 1. Ingredients, compositions and gray values of six samples.

	Aluminum oxide	Calcium hydroxide	Powdered charcoal	Iron oxide	Silica flour	
Gray value	251	233	36	58	190	
	Percent Composition by Mass					Gray value
Sample 1	20.2	9.9	9.9	9.9	50.1	71.3
Sample 2	22.7	12.9	4.8	8.5	51.1	90.0
Sample 3	12.4	14.2	2.6	7.7	63.1	107.7
Sample 4	17.7	3.1	2.5	2.6	74.1	120.0
Sample 5	32.6	7.2	1.4	1.3	57.5	139.0
Sample 6	23.3	14.7	5.8	4.9	51.3	92.0

Multivariable linear regression of the compositions and resulting gray values was performed to determine if a relationship could be described by a linear equation. Multivariable linear regression is used to determine the equation of a line that best fits the data by the least squares method. The equation of the line is:

$$y = m_1x_1 + m_2x_2 + \dots + b \quad \text{eqn. 2}$$

where the dependent y-value (the grayscale value of the samples) is a function of the independent x-values (the mineral percent compositions). The m-values are coefficients corresponding to each x-value, and b is the y-axis intercept. Four of the five ingredients were used in the regression since the fifth ingredient is dependent on the values of the four (the sums of all the composition percentages are equal to 100). The m-coefficients and b value determined by the regression are shown in Table A4. The gray values estimated using the regression coefficients versus the actual analysis values are plotted in Figure A10. The coefficient of determination (R^2) of the regression is 0.96 the adjusted R^2 is 0.82 and standard error of the estimate is 10.2 grayscale values.

Table A4, Volume 1. Regression coefficients.

Aluminum oxide	Calcium hydroxide	Powdered charcoal	Iron oxide	B
M_1	m_2	m_3	m_4	
0.5	-0.9	-5.5	-1.3	185.2

The results of the regression for the limited number of test samples suggest that a strong linear correlation may exist between sample composition and sample grayscale value. The magnitudes of the regression coefficients suggest that the darkly colored ingredients (charcoal gray value is 36 and iron oxide gray value is 58) have the strongest influence on ash color. When only iron oxide and charcoal are included in the regression, R^2 decreases to 0.94, however adjusted R^2 increases to 0.90 and the standard error of the estimate decreases to 7.6.

Based on the results of the experiment, it can be concluded that the colors of the experimental samples are dependent on the combined proportions of the ingredients. This conclusion was applied to the ash samples studied in this research. It was hypothesized that the grayscale values of ash samples could be used as a measurement of the dark colored constituents. The constituents of most interest in the fly ash samples are the organic coal residuals. To measure the influence organic coal residuals on ash color, the contribution of the other minerals ingredients of the ash must be considered.

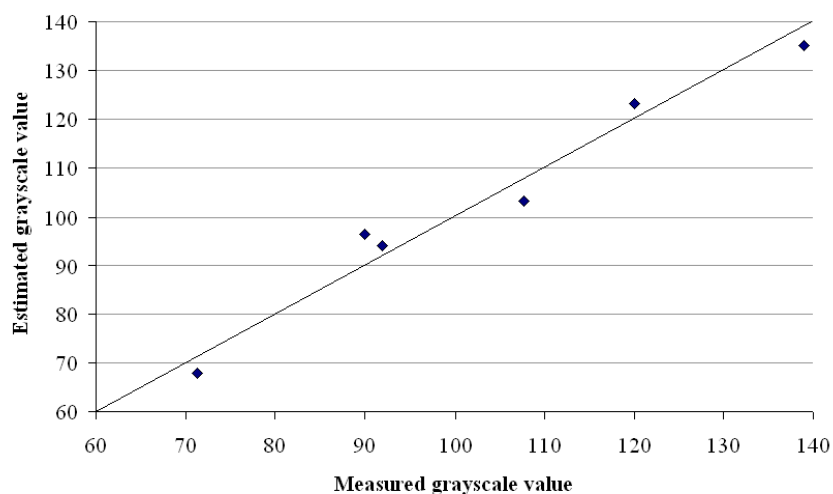


Figure A10, Volume 1. Estimated gray values versus measured gray values of the six experimental samples.

4.2 Correlation between ash color and bulk chemical analysis

A regression analysis similar to the experiment described above was performed on the set of Texas fly ash samples. For the analysis, the dependent y-values (from equation 2) were the average grayscale values of the oven-dried ash samples. The independent x-variables were the major metal oxides percentages present in the ashes (as determined by bulk oxide analyses) and the inorganic carbon contents of the ashes (as determined by total organic carbon analyses). Sixteen ash samples were included in the regression.

The regression was performed by first including all thirteen metal oxides contents determined in the bulk chemistry analysis (Section 3.2.2.1) and organic carbon content (Section 3.2.3.2) in the analysis. Then, the oxides for which the corresponding coefficient could not be reliably claimed as non-zero were removed one by one until a 95% or greater confidence ($\text{Prob} > |t|$ less than 0.05) was achieved for all coefficients. The R^2 and adjusted R^2 of the final regression was 0.98 and 0.96 respectively (actual versus predicted grayscale values are shown in Figure A11). The coefficients, standard error, t ratio and probability of the estimated coefficient existing outside the error ($\text{Prob} > |t|$) are shown in Table A5.

Table A5, Volume 1. Regression coefficients

Term	Estimate	Std Error	t Ratio	Prob > t
Intercept	-3001.6	606.5	-4.95	0.003
Al ₂ O ₃	38.9	6.5	6.02	0.001
SiO ₂	30.5	6.0	5.05	0.002
P ₂ O ₅	-63.4	11.7	-5.43	0.002
SO ₃	49.6	9.6	5.20	0.002
K ₂ O	110.9	29.1	3.81	0.009
CaO	35.9	7.0	5.10	0.002
Fe ₂ O ₃	20.2	4.9	4.14	0.006
BaO	276.8	51.2	5.41	0.002
Org Carbon	-113.8	9.3	-12.23	0.000

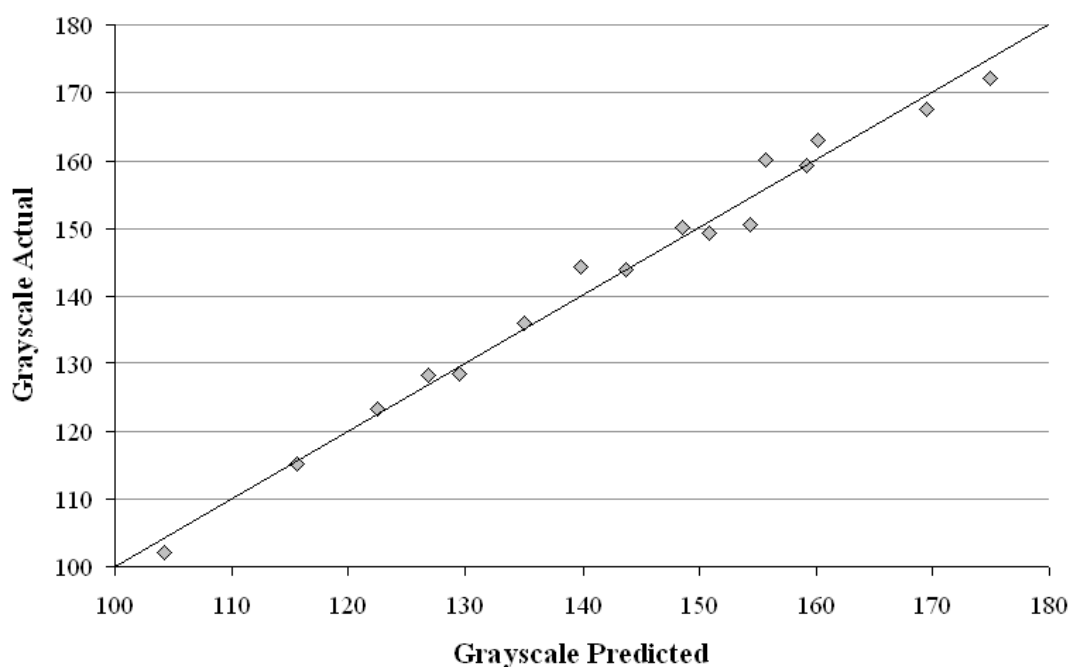


Figure A11, Volume 1. Actual grayscale value versus predicted grayscale value.

The R^2 values suggests a strong correlation between the selected ash components and ash grayscale value, though only a limited number (sixteen) of samples were tested. The carbon and phosphorus pentoxide coefficients both have negative values, suggesting that large contributions of these materials in ash results in decreased grayscale value or darker tones. Unlike the regression analysis performed on the “imitation” ash samples above, the coefficient for iron oxide is not negative. A y-intercept value of -3001.6 is a number determined by the statistical method and suggests the limits of the correlation.

In conclusion, a statistical approach to measuring the influence of ash bulk chemistry on oven-dried ash color suggests that a correlation between the two exists. The correlation between the bulk chemical composition and color is strong even though the ash samples studied were

produced at different power stations using different source coals. Further study on the correlation using a larger ash data set is recommended. The ashes used in this data were produced entirely from the combustion of Texas lignitic coals and/or Wyoming sub-bituminous coals. It is possible that ashes produced from coals obtained from different geographical locations may vary from those used in this study.

5. Determination of carbon content based on ash color

Determination of the quantities of the mineral and organic components that contribute to general ash color based on the grayscale value alone is impossible since, as evidenced by the two previously described experiments linking composition to grayscale value, many independent factors contribute to the ash grayscale value. However, because color is strongly influenced by organic carbon content, color could be used to measure the carbon content of samples under certain conditions. These conditions are 1) ash samples in which the mineral content does not vary greatly from sample to sample or 2) in a single ash sample before and after the removal of the carbon. These conditions are explored below.

5.1 Same ash source, different carbon content

In ash samples in which the mineral components are uniform, changes in ash color from sample to sample can indicate changes in residual carbon content. In the set of Texas ashes, five sample pairs, listed in Table A6, were obtained from five coal-fired power units at different dates of production. Because the samples were collected months apart, it was unlikely that the source coals of the collected sample pairs were identical since coal by nature is a complex, heterogeneous material. Variability in the coal source is reflected by the changes in metal oxides contents shown in Table A6. However, the differences in oxide contents are relatively small and the data presented was the best data available to test this carbon versus color relationship.

The ash samples in each pair differ in grayscale value and organic carbon content as shown by the changes in these values in Table A6. Carbon content alone, however, does not account for the changes in grayscale values. Multivariate correlations suggest that for these samples, grayscale is likely primarily dependent on both iron oxide and carbon content.

Least squares regression of the changes in grayscale values as the dependent variables and the changes in carbon and iron oxide contents as the independent variables produced a strong linear correlation with a coefficient of determination of 0.96 and standard error of the estimate of 5.8 grayscale units.

Table A6, Volume 1. Change in percent metal oxides content, percent carbon content and grayscale value between pairs of ashes collected from the same source.

Source	Change in percent content														Change in grayscale
	Na ₂ O	MgO	Al ₂ O ₃	SiO ₂	P ₂ O ₅	SO ₃	K ₂ O	CaO	TiO ₂	Fe ₂ O ₃	SrO	Mn ₂ O ₃	BaO	carbon	
FR-1 and 2	0.04	-0.45	-1.19	3.65	0.00	0.08	0.10	-3.24	-0.13	1.04	-0.06	-0.03	0.06	0.49	-43.8
FB-1 and 2	-0.17	-0.28	-0.87	-1.44	-0.03	0.02	-0.16	0.07	0.07	3.21	-0.01	0.03	0.03	-0.03	-23.6
CP-1 and 2	-0.12	-0.85	1.39	2.35	0.15	-0.15	0.18	-3.01	0.05	-0.24	-0.07	-0.02	-0.08	-0.12	12.5
FM-1 and 2	-0.17	-0.30	0.49	3.44	0.04	-0.23	0.10	-3.05	-0.01	0.30	-0.13	-0.04	-0.11	-0.06	-7.8
CG-1 and 2	0.00	-0.17	-0.38	-0.81	-0.32	0.12	-0.07	0.81	0.10	0.54	-0.04	0.02	-0.06	-0.02	-0.9

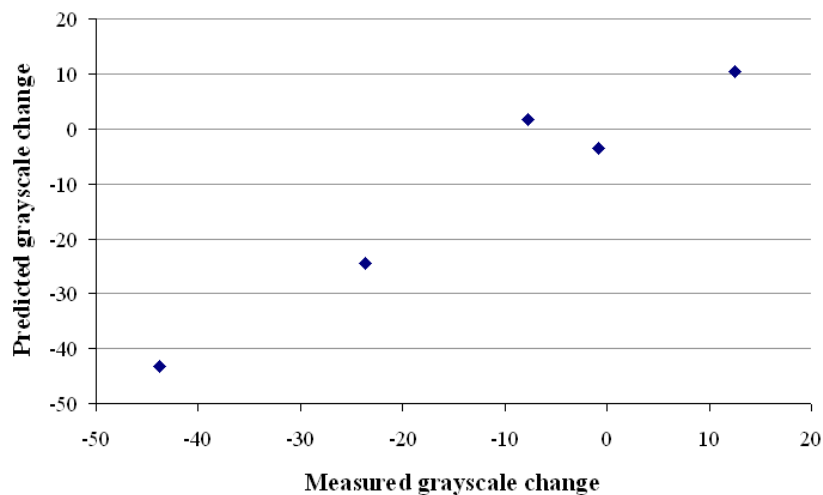


Figure A12, Volume 1. Predicted grayscale change versus measured grayscale change of five ash pairs

While the data presented suggests that a relationship likely exists, more data is necessary to determine whether this method can be used as a measure of carbon content. The validity of this method could be tested by collecting several fly ash samples from a single power station burning a consistent coal type under different operating conditions. Color, bulk chemistry, and total organic carbon analyses could then be performed on the sample set to establish the predicted relationships.

This method of measuring carbon content in ash has potential as a quick method for assessing the ash produced at a single source where the feed coal ash chemical composition and post-combustion chamber mineralogy does not change greatly over time.

5.2 Color change due to organic carbon removal

This method was described in Chapter 6 Part II.

6. Ash color change due to temperature exposure

6.1 Ash lightening

At least two separate phenomena appear to be occurring in the ash samples shown in Chapter 6 Part II Figure A1: first a lightening of the ash in the temperature range of 300 to 500 or 600°C and second, a darkening of the ash at temperatures above 500 to 600°C. In all ash samples shown in Chapter 6 Part II Figures 1 and 2, lightening, if it occurs at all, does not happen until exposure to temperatures greater than approximately 300 to 400°C in air. As described in chapter 6, the lightening of the ash samples is likely primarily explained by the removal of organic coal residuals from the ash. The Class C fly ash samples likely did not experience significant darkening in the 300 to 500°C range because of the very low organic carbon content of the ash samples.

6.2 Ash darkening

From Chapter 6 Part II Figures 1 and 2, it appears that darkening of the ash begins to occur at temperatures greater than approximately 500°C. The changes that cause darkening of the ash samples are not well understood. Possible explanations are changes in oxidation states of certain minerals, such as iron oxide or the creation or decomposition of stable minerals at the higher temperatures. Attempts to replicate the behavior with pulverized iron oxide (99.8% Fe₂O₃) were unsuccessful. Iron oxide would turn from dark red to black when exposed to temperatures above 600°C, as observed immediately after removal from the furnace, but would then return to a lighter color upon cooling. When imitation ash similar in composition to those discussed in Section 8.1 above was exposed to a range of temperatures, the lightening of the sample occurred in the same temperature range as the ash samples; however, no significant darkening of the sample after 500 °C could be reproduced. Limited x-ray diffraction testing did not identify any potential sources of the color change. Many of the oxides present in ash are commonly used as colorants or fluxing agents in ceramic glazes. Interactions among the various minerals have been determined to produce a variety of colors under controlled conditions. The reactions that occur in the furnace that cause ash darkening are likely complex and involve multiple minerals and possible phase changes.

An experiment was performed to identify which oxides might be contributing to ash darkening between 500 and 800°C. For the experiment, ash samples from 12 sources were heated in an air atmosphere furnace at 500°C for 1 hour (the samples were stirred at the midpoint) then

placed into cuvettes, scanned and analyzed according to the standard method. This was repeated for samples from the same 12 sources but at a furnace temperature of 800°C. The difference in grayscale values between 500 and 800°C for the samples was determined. The changes varied from -9 to -40 grayscale units.

Multivariable linear regression was performed using the 500 to 800°C grayscale change values as the dependent variables and the bulk chemistry metal oxide contents as the independent variables similar to the method used in Section 8.2. Organic carbon content of the ash samples was not included in the regression since it was expected that the majority of the organic carbon in the samples was oxidized during the 500°C exposure.

The regression included 12 samples and seven of the thirteen oxides. The regression coefficients and statistics are shown in Table A7. The R^2 was 0.99 and adjusted R^2 was 0.97. The actual grayscale value change versus the predicted change based on the regression coefficients in Table A7 are shown in Figure A13. Note that absolute values for grayscale change were used in the regression even though the grayscale values for all the samples were negative (decreased from 500 to 800°C).

Table A7, Volume 1. Regression coefficient and statistics.

Term	Estimate	Std error	t Ratio	Prob> t	Oxide Content, %	
					Min	Max
Intercept	-17.9	5.8	-3.08	0.037		
MgO	19.6	3.9	4.96	0.008	2.0	6.6
P ₂ O ₅	-26.6	9.3	-2.87	0.045	0.1	1.3
SO ₃	-24.1	4.1	-5.88	0.004	0.2	3.8
Fe ₂ O ₃	-1.6	0.6	-2.43	0.072	3.5	8.5
SrO	-115.4	36.2	-3.19	0.033	0.1	0.5
Mn ₂ O ₃	109.8	34.4	3.19	0.033	0.0	0.2
BaO	122.4	30.2	4.06	0.015	0.1	0.9

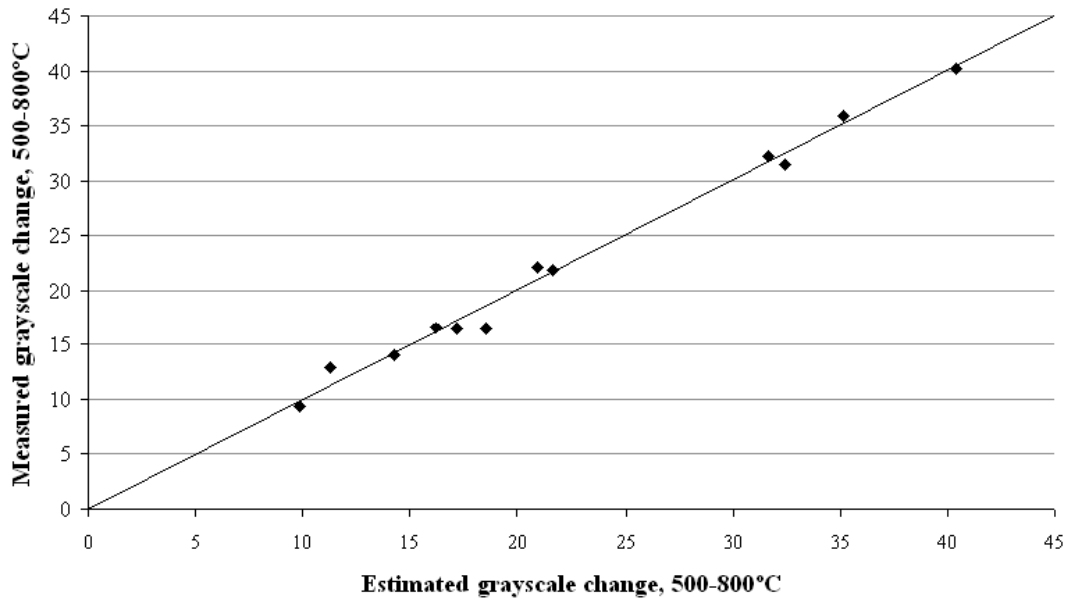


Figure A13, Volume 1. Measured grayscale value change versus predicted grayscale change between 500-800°C.

The regression suggests a strong correlation between the oxides contents and ash darkening. Magnesium oxide and barium oxide appear to have the greatest influence on ash darkening based on the corresponding regression coefficients and oxide contents in the samples tested. Iron oxide content unexpectedly did not appear to be a major factor influencing grayscale value.

This regression does not conclusively identify the minerals involved in ash darkening. Some of the oxides included in the regression may not actually play a role and were included due to chance and/or because of the statistical methods used. Combinations of minerals that include some of those in Table A7 as well as others not included can produce correlations of similar quality. In addition, as discussed previously, the oxide contents do not adequately represent the various amorphous or crystalline minerals that are present in the ash. Once improved techniques for identifying the amorphous materials in the ash are available, clearer identification of the composition-color links can be established.

Future work on in this area could begin with increasing the number of samples in the data set to help highlight the major contributors to ash darkening. Use of a controlled-atmosphere furnace could also be useful in determining if a portion of the reactions occurring in the furnace are oxidation reactions and for more precisely identifying the temperature range in which darkening begins to occur.

A2. References

Gann, R. *Desktop scanners: image quality evaluation*, Hewlett-Packard Company, Prentice Hall PTR, 1999.

UTHSCSA ImageTool product description, <http://ddsdx.uthscsa.edu/dig/itdesc.html>, 1997.

Chaddha, G., Seehra, M.S., "Magnetic components and particle size distribution of coal flyash,"
J. Phys. D: Appl. Phys., 16, pp. 1767-1776, 1983.

Helmuth, R., *Fly Ash in Cement and Concrete*, Portland Cement Association, 1987, Skokie, IL.

Joshi, R.C., Lohtia, R.P., *Fly Ash in Concrete*, OPA, Amsterdam, 1997.

Volume II—Appendix A: Hardened Air-Void Analysis Parameters

A.1 Introduction

This appendix presents a study on the effects of two parameters, threshold value and analysis length, on the results of an automated hardened air-void analysis completed with the Rapid-Air 457 (Concrete Experts International). These are two parameters for which little or no previous guidance exists on how they can affect the results. Therefore some simple tests were performed and this appendix presents the results and gives the justification for the values and methodology used in this report.

A.1.1 *Length of Linear Traverse*

One advantage of utilizing an automated system to analyze the surface of a lapped concrete specimen is that certain parameters can be adjusted to provide a more thorough analysis with very little increase in time; this type of testing would be too costly and time prohibitive to be done regularly with a human analysis. One parameter that is easily adjusted is the length of the traverse in the analysis, as the RapidAir457 has a feature that permits multiple linear traverse lines to be used to simultaneously investigate the viewing area. This is useful as it allows the camera to travel the typical distance of one linear traverse while completing an actual analysis equal to the number of lines chosen multiplied by the length of traverse. For example if the user chooses to run three linear traverse lines simultaneously, then the actual traverse length of the specimen will be equal to three times the length the camera travels over the specimen. Therefore, multiple traverse lengths can be covered in the same amount of time it would take for the camera to complete a single linear traverse. This feature could also be used to lower the time needed to complete a single linear traverse as multiple traverse lines could be utilized while covering a shorter distance. The reduction in distance needed to complete a typical ASTM C 457 traverse length will be proportional to the number of simultaneous traverse lines used.

A.1.2 *Threshold Value*

As described in Volume II: Appendix B and Chapter 13 the surfaces of the polished concrete specimens must be colored black and filled with a white powder once the polishing is complete in order for it to be analyzed with the automated hardened air-void analysis. The operator of the automated analysis system must choose a “threshold value” for the sample. This parameter sets the definition of what is considered black and white by deciding a shade of gray as the point of differentiation between the two in the analysis. Currently, there is no standard method to choose this parameter and it is the responsibility of the user to use his or her judgment to decide which value to use for the specimen. Figure A1 shows several screen shots of the same area of analysis with different threshold values. The raw black and white image is also provided for comparison. As the threshold value is decreased the amount of white is reduced on the screen and hence the amount of apparent air-voids. In the Rapid-Air 457 manual and in the training provided by the equipment supplier, on how to select this number. When asked about this in the training for the system it was suggested that “The user[s] should choose the threshold value that they think best represents the sample” (Jakobsen, 2005). Since this is a possible source of variability in the test it was decided to be investigated further.

A.2 Experimental Methods

A.2.1 Linear Traverse

Five specimens with hardened air contents between 2.6% and 7% and with a nominal aggregate size of 25 mm were compared in the automated hardened air void analysis with traverse lengths and area to be investigated specified in ASTM C 457. Another analysis was completed where the camera started in the same position and covered the same traverse path but three traverse lines were utilized. This allowed a distance three times the amount specified in ASTM C 457 to be covered. Both of these analyses were started in the same location and traversed the specimen in the same path.

A.2.2 Threshold Value

As a part of the computer interface with the Rapid-Air 457, a value is provided that reports to the user the amount of white (estimated air content) that is currently in the analysis window. This value will change as one adjusts the threshold value as discussed previously and shown in Figure A.1. In order to investigate how the threshold value affects the amount of air determined in the viewing window, a test was completed where two different spots on the sample surface were examined under varying threshold values and the resulting percentage of white was recorded.

Next a comparison was made between threshold values of three different users from twelve different locations on the surface of a specimen. These locations were chosen so that they would be at approximately 12 equal spaced locations on the surface of the specimen. Each user chose the threshold value in private and the results were not shared between users. The only instruction provided to the user was to “choose the threshold value that best represents the sample.

Finally, three samples were analyzed with different threshold values to investigate the impact on the results of the automated analysis. The same sample utilized in the survey for the three different users was analyzed utilizing the average threshold values from the survey. All of the samples used the same traverse length and path on each sample and so the threshold value is the only variable being investigated. These specimens were chosen as they had air contents which consistently provided air void parameters that were very close to the common recommended values for air-void parameters in hardened concrete (spacing factor 0.200 mm and specific surface $24 \text{ mm}^2/\text{mm}^3$). Therefore, it seemed important to investigate how these specimens were impacted by changes in threshold value.

A.3 Results and Discussion

A.3.1 Length of Linear Traverse

Table A.1 presents the results of the hardened air-void analysis for traverse lengths as required by linear traverse analysis for ASTM C 457 and for the larger length with the Rapid-Air 457. One significant difference between the results is the number of voids analyzed with the longer traverse length. This would suggest that since a larger number of voids have been inspected then a more representative analysis of the air-void parameters should be provided. For the majority of the comparisons shown in Table A.1 the results are similar. The samples that had the lowest air contents showed very similar results between the typical and extended traverse

length. However, as the air content of the mixtures increased, then there was more of a difference between analysis results. The air content seemed to be the parameter that was most sensitive to the hardened air-void analysis. It would be expected, but not proven herein, that the precision of the longer traverse lengths to the actual air content in the mixture would be better compared to the precision of the shorter traverse lengths.

A.3.2 *Threshold Value*

The values for the percentages white displayed at two different places on a sample's surface are shown in Figure A.2. The results from this examination suggest that the percentage white displayed on the screen versus the threshold value is an S shaped curve. This curve shows a large change in the percentage of white displayed at the extremes of the curve and a linear portion between these two values. This plot suggests that the amount of white detected by the analysis window should change linearly between threshold values chosen away from the extremes of the threshold values.

The individual results and average threshold values are reported in Table A.2 for the three different users. As can be seen from the data the average threshold for users 2 and 3 were essentially the same and the average value for user 1 was 15% less. When interviewed after the test, users 2 and 3 both said that they adjusted the threshold value so that the analysis window best matched the raw data image. User 1 said that he changed the threshold value to best replicate all of the small air voids and did not attempt to make the entire image represent the raw image. These data suggest that when different users have the same opinion about the way something should look then the average results were similar for 12 different observations. However, different opinions of users can lead to different threshold values chosen for a sample.

In Table A.3 the results of three different samples are compared with different threshold values and the different results from the hardened air-void analysis. In the table the percentage change is reported in parenthesis for each one of the air-void parameters but also for the change in the threshold value. All of the threshold values were in the central portion of the characteristic "S" shape shown in Figure A.2. Also, the threshold value in which the other two analyses are compared to those chosen by user 2 using the same methodology used in the survey. The first specimen shown in the table was the same one used in the previous comparison of threshold values for three different users. The low threshold value for the first sample was chosen to match the result of user 1. The high threshold value was chosen to be the same percent difference between the results of the two users. The results suggest that none of the air-void parameters change at a larger percentage rate than the threshold change. Of all the parameters investigated it appears the void frequency is the most affected by the changes in threshold value. This parameter seems to change at a similar percentage as the threshold value. The air content and specific surface seem to change at a percentage rate that is approximately 50% of the change in the threshold value and change in the specific surface seems to be approximately 25% of the change in the threshold value. It should be noted that in all of these mixtures the paste to air ratio was determined to be larger than 4.342 and so the following equation was used to calculate the spacing factor as determined by ASTM C 457:

$$\bar{L} = \frac{3}{\alpha} \left[1.4 \left(1 + \frac{p}{A} \right)^{1/3} - 1 \right] \quad \text{Equation 1}$$

This indicates that the offset of the changes in the specific surface and the paste to air ratio consistently offsets to provide a spacing factor that is approximately 50% of the threshold value change. These results may be different if a different sample preparation technique, paste content, or if a different range of threshold values were chosen.

A.4 Conclusion

This appendix presented the results from an investigation of how the traverse length and the threshold value impacted the results of the Rapid-Air 457 analysis.

It was determined that the longer traverse length should be used as it investigated a large number of air-voids and therefore, should provide a better characterization of the hardened air-void system while having a minimum impact on the amount of time required to complete the analysis for that specimen.

For this study it was decided that the user should choose the threshold value by adjusting the analysis image until it best matches the raw image. Furthermore, in order to better characterize the threshold value for a specimen it was decided to take a threshold reading at 12 equally spaced locations on the surface of the sample, as this would provide a reasonable estimate of a threshold value for the entire specimen. From these 12 measurements the high and low values were removed and then the other ten were averaged. This was done because occasionally a location is analyzed in the paste where the amount of white is either very high or very low. In these locations it was determined that the threshold value chosen to match the analysis image to the raw image was significantly different than the other threshold values chosen. By removing the high and low values the probability for these areas to affect the average value is lowered. For the hardened air-void analysis reported in this paper the threshold values used were between 158 and 174.

Table A.1, Volume 2. Results from a hardened air-void analysis with different traverse lengths.

ASTM C 231 air content (%)	hardened						
	traverse length (mm)	air content (%)	specific surface (mm ² /mm ³)	spacing factor (mm)	void freq. (mm ⁻¹)	avg. chord length (mm)	number of voids
2.8	2413	2.62	23.11	0.261	0.152	0.173	366
	7240	2.66	23.27	0.258	0.155	0.175	1321
3.3	2413	3.07	28.75	0.195	0.225	0.139	577
	7240	3.07	28.40	0.198	0.218	0.141	1576
4.4	2413	4.37	32.16	0.148	0.352	0.124	849
	7240	4.70	31.81	0.145	0.374	0.126	2706
5.2	2413	4.54	29.48	0.158	0.335	0.136	808
	7240	4.80	27.46	0.165	0.330	0.146	2387
7.8	2413	7.12	25.19	0.125	0.449	0.159	1083
	7240	6.71	26.19	0.128	0.439	0.153	3180

Table A.2, Volume 2. Comparison of the threshold value chosen for three different users.

	User		
	1	2	3
	166	163	161
	135	166	150
	107	169	153
	120	166	153
	133	159	163
	197	160	157
	200	166	168
	102	170	170
	117	163	166
	126	153	169
	148	159	159
	122	163	188
Average	139	163	163

Table A.3, Volume 2. A comparison of hardened air-void results with different threshold values.

ASTM C 231 air content (%)	hardened											
	black/white threshold		air content (%)		specific surface (mm ² /mm ³)		spacing factor (mm)		void freq. (mm ⁻¹)		avg. chord length (mm)	
2.8	188	(+15.3)	2.48	(-6.8)	22.10	(-5.0)	0.280	(+8.7)	0.137	(-11.6)	0.181	(+3.4)
	163		2.66		23.27		0.258		0.155		0.175	
	138	(-15.3)	2.89	(+8.6)	24.57	(+5.6)	0.235	(-8.8)	0.178	(+14.8)	0.163	(-6.9)
3.3	175	(+11.5)	2.87	(-6.5)	27.57	(-2.9)	0.210	(+6.2)	0.198	(-9.2)	0.145	(+2.8)
	157		3.07		28.40		0.198		0.218		0.141	
	142	(-9.6)	3.27	(+6.5)	28.78	(+1.3)	0.190	(-4.1)	0.235	(+7.8)	0.139	(-1.4)
4.4	174	(+9.4)	4.32	(-8.1)	30.95	(-2.7)	0.153	(+5.9)	0.326	(-12.8)	0.131	(+4.0)
	159		4.7		31.81		0.145		0.374		0.126	
	142	(-10.7)	5.16	(+9.8)	32.67	(2.7)	0.135	(-6.7)	0.422	(+12.8)	0.122	(-3.2)

These values are not adjusted for the aggregate correction factor in order to best represent actual practice.

Numbers shown in parenthesis are the percent change in the parameter against the median threshold. For example between the first two rows in the table the threshold value was changed by 15.3% (from 163 to 188). This change in threshold value leads to a reduction in the air content by 6.8% (from 2.66% to 2.48%).

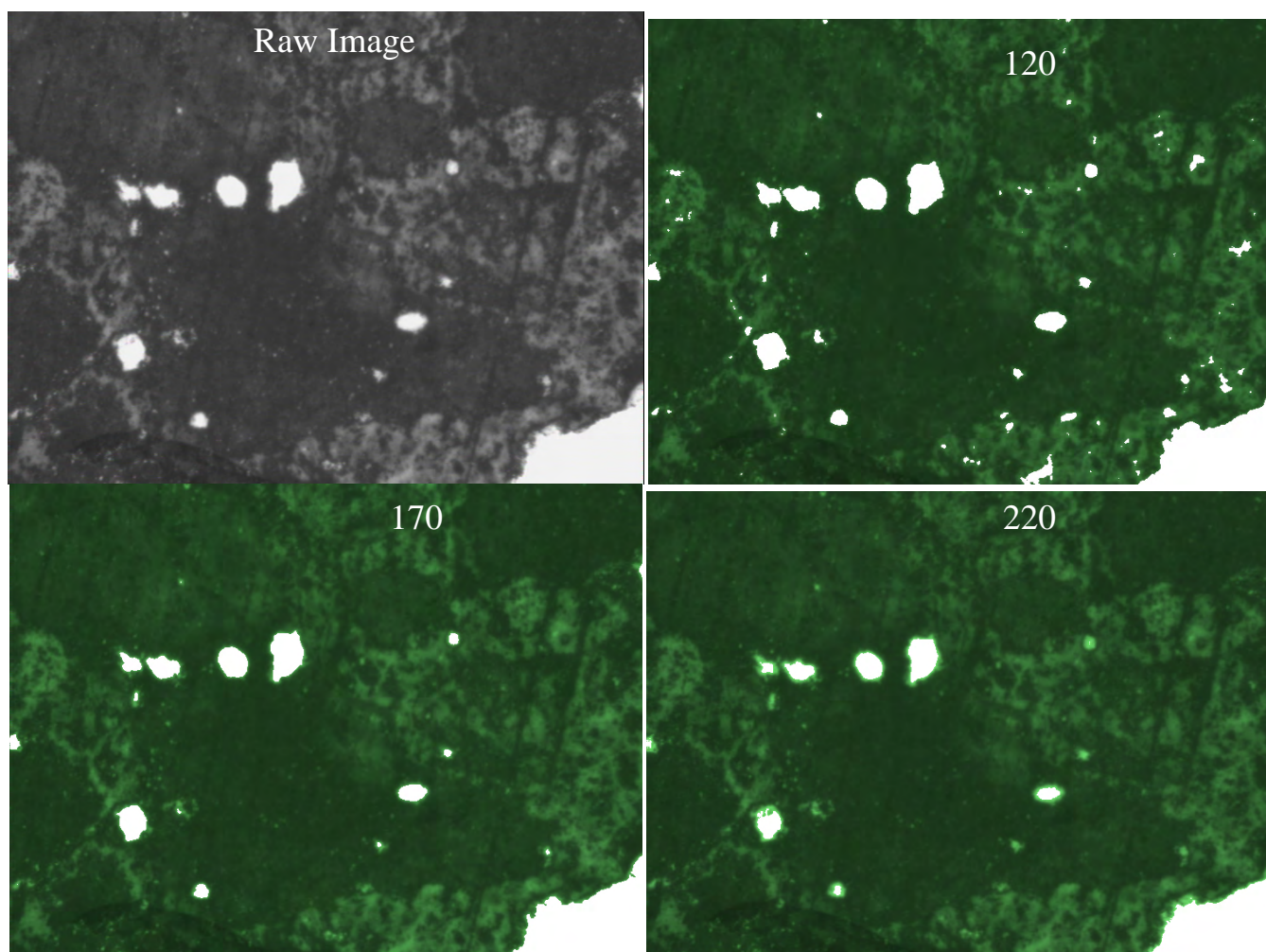


Fig. A.1, Volume 2. A raw image and images with reported threshold values.

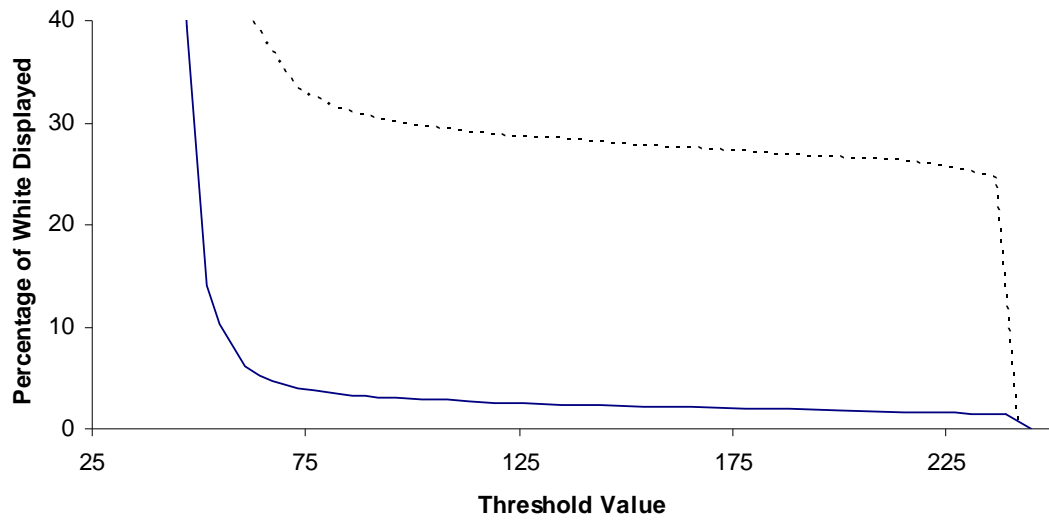


Fig. A.2, Volume 2. Percentage white displayed on the screen as a function of the threshold value chosen for two different locations on the sample surface.

Volume II—Appendix B: Sample Preparation for Hardened Air-Void Analysis

B.1 Introduction

This appendix contains a summary of the sample preparation techniques for the hardened air-void analysis. This appendix was created to give the reader a description of the methods utilized and to also serve as a guide to future researchers that may need to complete a hardened air-void analysis.

B.2 Equipment Needed for Concrete Lapping (ASTM C 457)

Items needed:

- Construction crayon (yellow works best as it does not resemble paste or aggregate)
- Acetone
- Fine grained paint brush (for cleaning specimens)
- Paint brush (for applying lacquer)
- Polishing plates: nickel plated diamond discs with magnetic backing obtained from ASW diamond (www.aswdiamond.com). One should never use the felt discs to polish concrete.
- Lacquer (obtained from Sherwin-Williams Co. The manufacturer is Sheffield Bronze Paint Corporation. The product name is “Clear Lacquer.”)

B.3 Cutting the Sample

Place the wooden jig at the back of the automated Buehler Labpro 24 (lapidary) saw. Ensure that the concrete specimen is pushed snugly against the jig, and then tighten the clamp. After making the first cut, loosen the clamp, reposition the sample against the jig, retighten the clamp, and make the next cut. The jig setup has been designed to provide a pair of cuts that are parallel and leave a reasonable size sample (20 mm) to lap and analyze with the Rapid-Air 457. After cutting the specimen wash the surface to remove any residue left behind from the saw. Pigeon and Pleu (1986) suggest leaving the cut specimens in water for a few days to help harden the surface. This technique was never tried.

B.4 Concrete Lapping

Apply thinned lacquer (20% lacquer/80% acetone) to the surface to strengthen the paste and to help reinforce the voids. Let the specimen sit for a minute or until dry. Be sure that the sample is left to dry in either a fume hood or a very well ventilated area. Use the construction crayon to mark a 10-mm x 10-mm grid on the surface to be analyzed.

Use the 80-grit pad to quickly remove any high spots or non uniform cuts made by the saw. Lap the sample until the crayon is completely removed. Care should be taken to insure that the surface is not preferentially lapped. This is easily checked by placing the long edge of a machinist’s rule on the lapped surface of the specimen with a light behind it. The rule should be

very flat and, if the lapped surface is not flat, one will see light between it and the rule. While some light will always get through this gap, large differences can be seen and the lapping technique adjusted to ensure that the sample surface is made flat. It is imperative that the sample be flat before leaving this grit size.

The time required to lap a specimen is determined by the condition of the lapping plate. New plates take about 30 seconds on this pad, and badly worn plates can take up to 30 minutes. The surface should be marked and lapped until all the crayon has been removed two times. Again, it is very important that the sample is plane before going on to the next step. Wash the sample well with the water hose and a fine grained paint brush. The specimen should be dried with a cloth towel before applying the next coat of lacquer. The surface of the specimen needs to be carefully and continuously protected when it is not being lapped, as small scratches are difficult to remove during later (fine grit) stages of the sample preparation. One simple method to protect the specimens is to keep paper towels covering the surface to be analyzed. Another method is to keep the specimen in a plastic baggy.

Paint the sample again with the thinned lacquer, and when dry, mark again with the construction crayon. Lap the specimen with the 100-grit plate until the crayon is removed. Pay close attention and apply even pressure to the specimen as you lap so that one side is not preferentially polished with respect to another. If the crayon is removed evenly from the surface, it only needs to be lapped one time. If not, color the surface again and lap. Recheck the surface with the machinist's rule to ensure the specimen is still flat. Clean the surface of the prepared specimen with fresh water and the fine bristled paint brush. The specimen should be dried with a cloth towel before treated with the lacquer.

Paint the surface again with the thinned lacquer and let it dry. Now lap the specimen on the 180-grit plate. With 180-grit it is difficult to tell when the surface of the specimen is ready to move onto the next plate. The best method is to hold the specimen up to the light at an angle and look for the light to sheen on the surface of the specimen. One should be able to see the sheen of the coarse and fine aggregates. Also one can run his/her thumb over the boundary between the coarse aggregates and the adjacent paste. The specimen should not go to the next stage until this interface feels somewhat smooth. Once a specimen has been deemed finished then it should again be checked with the rule to make sure it is flat. It is very important that there is only a very small relief between the coarse aggregate and paste, as the next plate will never be able to improve the specimen, if the relief depth is large. Once the amount of lapping time is determined on this plate for a specimen with a given aggregate and w/cm then this can be used as a standard minimum amount of time the specimen is lapped before being checked. Clean the surface of the prepared specimen with fresh water and the fine bristled paint brush. The specimen should be dried with a cloth towel before being treated with the lacquer.

Paint the surface again with the thinned lacquer and let it dry before lapping the specimen on the 260 plate. Again, with this fine grit it is very difficult to tell when the sample receives enough lapping but expect that it will take a significant amount of time to prepare a sample on this plate. One method for checking is to hold the specimen up to the light, and once it is finished, the entire specimen should show a constant gleam from the reflection. Also, one can take the palm of his/her hand, and rub in a circular pattern on the specimen to feel for any relief between the paste and the aggregate. The specimen should again be checked with the rule.

Once this specimen is believed to be finished, it can be taken to a stereomicroscope for viewing. The paste should be inspected at 20x and 50x magnification. In the completed specimen the paste should look very clean. Next, one of the lights should be adjusted to a very low angle,

so that the relief of the surface can be inspected. If shadows are cast by coarse aggregates on the surface of the specimen, then more lapping is needed, as the paste has not been polished adequately. If the sample surface looks to be fairly uniform, one should lightly bounce the light with a finger, while inspecting the interface between the paste and an aggregate particle. If the interface between the aggregate and the paste moves as the light bounces, the sample is not finished yet, since this movement indicates that a low shadow between the aggregate and the paste. If the shadow/interface does not move and the paste looks clean and polished, the sample is finished.

Next the sample is soaked in acetone to remove the thinned lacquer. Gloves should be worn when placing and removing the sample from the acetone. This should be completed in a fume hood or in a well ventilated area.

This sample preparation process was developed to be used with limestone or river gravel aggregates with a strength of 5000 psi and a 0.45 w/cm with air contents from 2%-8%. When samples were investigated that contained air content between 6% and 10% more care had to be taken to insure that the walls of the air voids were not damaged. This can especially be true if several of these voids are close together. If the concrete is weak or of a very high air content then it has been suggested to take the cut specimen and to cover the surface in paraffin wax in an oven. The wax should melt and penetrate into the voids. Now the specimen can be lapped as above without using the thinned lacquer. Once the lapping is finished then the specimen can be put back into the oven while inverted. The wax will again melt and should leave the specimen. This method was never tried in our facility, but was suggested by Jakobsen (2005) of Concrete Experts International, the distributors of the RapidAir.

It was not necessary to lap the specimens in this study to a size below the 260 plate, as polishing of the coarse aggregate occurred and, the marker would no longer stick to the surface, and the reflection from the observation light provided unwanted artifacts in the analysis. However, this should be investigated further for other materials besides the one used in this study.

B.5 Lapping Clean up

Cleaning the equipment after each use is critical and should follow the following steps:

- Use water to clean the lapper, polishing plates (both sides), and make sure the tub is draining.
- Use a rag to dry off the lapper plates and the lapper itself.
- Allow the magnetic polishing plates to air dry.
- Remove the steel plate with an Allen wrench.
- Make sure both sides are clean.
- Wipe down the steel plate with WD40.

Always make sure the drain is working properly in the lapper, as contaminated standing water can cause the bearing to go bad. Lube the bearing in two places every three months with a grease gun. The magnetic polishing plates will last much longer if they are kept clean.

B.6 Rapid-Air 457 Sample Preparation

Now that the sample has been lapped, it is ready to be darkened, so that it can be investigated with the Rapid-Air 457. The surface should be colored with a black ink that will not smear off of the surfaces of the fine or coarse aggregates once it has dried. This is VERY

important as these small aggregates are very difficult to color later in the procedure. It was determined that permanent ROUNDED-TIP Sharpie® markers work best. Although the chisel tips would appear to be much more useful for coloring a large surface, it is the author's experience that the ink in that type will smear. Other brands were not tried. After the surface has been completely covered in one direction then the specimen should be rotated 90° and colored again. The specimen should be left to dry overnight to insure the marker has had adequate time to stain the entire surface. The next step is to cover the sample's surface in barium sulfate. This is a very fine powder that is <1µm and very white. Next a solid rubber stopper should be used to force the barium sulfate into the surface. The force on the stopper should be just the weight of your hand going up and coming down. After the powder has been forced into the surface the majority of the remaining powder should be brushed off with one's hand. The palm of the hand can be used to pass over the surface of the specimen allowing the extra powder to fall to the ground. This method uses the moisture from the surface of the palm to remove the powder from the surface but not from the voids. Once this is completed the sample should be black with white only in the voids. While rubbing the specimen, black marker will get on the user's hands and will sometimes get into the voids. This needs to be corrected, or the specimen will not be analyzed correctly. If some of the voids do become stained with the black then the specimen can be lightly slapped with your hand while being slightly inverted. This action will cause the stained powder on the surface of the voids to be removed while leaving the rest of the void still white. One should wash his/her hands after rubbing each specimen.

Now any voids found inside the aggregate need to be colored. While this is a tedious process, with experience it can be completed fairly quickly. The author has found that it is best to first color in all of the coarse aggregate particles that can be seen with the eye. This can be done in a well-lit room or with the specimen illuminated with the microscope lights. After this color application is completed the specimen should then be investigated under the stereo-microscope, and any small voids should be colored with a fine point permanent marker. Care should be taken to only color in the voids in the aggregates. With time one will quickly be able to distinguish air-entrained voids in the paste from voids in the aggregates. The specimen is now ready to be analyzed.

Volume II—Appendix C: Summary of Test Results for Fly Ash

fly ash number		1	2	3	4	5	6	7	8	9	10	11	12	13
Chemical Tests	Silicon Dioxide (SiO ₂), %	56.18	30.76	36.36	54.75	34.47	52.07	52.04	63.84	49.07	37.16	33.14	35.67	33.28
	Aluminum Oxide (Al ₂ O ₃), %	20.37	17.75	17.44	19.92	20.35	23.65	23.75	18.10	19.72	20.55	18.12	19.56	18.72
	Iron Oxide (Fe ₂ O ₃), %	6.77	5.98	6.08	8.66	5.65	4.55	4.59	4.10	7.87	6.06	6.65	6.47	6.72
	Sum of SiO ₂ , Al ₂ O ₃ , Fe ₂ O ₃ , %	83.32	54.49	59.88	83.33	60.47	80.27	80.38	86.04	76.66	63.77	57.91	61.70	58.72
	Calcium Oxide (CaO), %	9.95	28.98	25.68	9.37	26.50	12.76	12.63	8.12	15.12	24.76	27.49	24.62	27.24
	Magnesium Oxide (MgO), %	2.55	6.55	6.15	2.43	4.70	2.02	2.01	1.91	2.93	4.29	5.45	4.58	5.87
	Sulfur Trioxide (SO ₃), %	0.53	3.64	2.03	0.46	1.71	0.78	0.79	0.22	1.06	1.23	2.71	2.56	1.85
	Sodium Oxide (Na ₂ O), %	0.47	2.15	1.90	0.64	1.76	0.31	0.28	0.47	0.66	1.63	1.91	1.73	1.91
	Potassium Oxide (K ₂ O), %	1.08	0.30	0.46	1.13	0.46	0.80	0.81	1.17	0.95	0.45	0.30	0.48	0.38
	Total Alkalies (as Na ₂ O), %	1.18	2.35	2.20	1.38	2.06	0.84	0.81	1.24	1.29	1.93	2.11	2.05	2.16
Classification (ASTM C 618)	F	C	C	F	C	F	F	F	F	F	C	C	C	C
Physical Tests	mL AEA/100 kg cm for 6% air in	31	44		83	50	138*	147	42	44*	39	36		
	LOI (ASTM C 311)	0.12	0.35			0.11		0.79			0.07			
	Foam Index (mLAEA /g fly ash)	1	1			1		5			1			
	Surface Area (m ² /g)	0.89	0.95					4.02						

* High dosages of WR required for an acceptable slump. This high dosage of WR could cause a change in the AEA demand of the mixture.

fly ash number		14	15	16	17	18	19	20	21	22	23	24	25	26	27
Chemical Tests	Silicon Dioxide (SiO ₂), %	50.98	49.80	47.18	41.32	38.57	33.35	54.59	55.78	31.55	34.62	48.48	51.04	52.56	38.07
	Aluminum Oxide (Al ₂ O ₃), %	18.84	21.63	22.82	19.25	18.84	18.74	20.88	30.59	17.78	21.16	25.01	20.59	19.82	20.75
	Iron Oxide (Fe ₂ O ₃), %	7.87	5.01	4.62	6.48	6.69	6.69	8.56	5.07	6.81	5.69	3.56	8.23	4.72	5.50
	Sum of SiO ₂ , Al ₂ O ₃ , Fe ₂ O ₃ , %	77.69	76.44	74.62	67.05	64.10	58.78	84.03	91.44	56.14	61.47	77.05	79.86	77.10	64.32
	Calcium Oxide (CaO), %	14.39	13.01	14.62	21.58	23.54	27.30	9.02	1.10	30.81	25.35	15.92	12.20	14.35	23.78
	Magnesium Oxide (MgO), %	2.91	3.42	3.51	4.43	4.76	5.83	2.65	0.71	4.20	4.62	2.50	2.99	3.16	4.42
	Sulfur Trioxide (SO ₃), %	0.95	0.46	0.66	1.25	1.43	1.85	0.51	0.14	2.28	1.55	0.72	0.73	0.92	1.11
	Sodium Oxide (Na ₂ O), %	0.57	1.42	1.69	1.43	1.71	1.93	0.56	0.27	1.75	1.74	0.30	0.73	0.73	1.65
	Potassium Oxide (K ₂ O), %	0.94	1.01	0.78	0.78	0.65	0.38	1.19	2.29	0.45	0.47	0.71	1.10	1.11	0.52
	Total Alkalies (as Na ₂ O), %	1.19	2.08	2.20	1.94	2.14	2.18	1.34	1.78	2.05	2.05	0.77	1.45	1.46	1.99
Classification (ASTM C 618)	F	F	F	C	C	C	F	F	C	C	F	F	F	F	C
Physical Tests	mL AEA/100 kg cm for 6% air in	93	49	52			34	49			32	24	48	64	38
	LOI (ASTM C 311)	0.26									1.12	0.63		0.39	0.13
	Foam Index (mLAEA /g fly ash)	3.3									1	1		2.5	1
	Surface Area (m ² /g)											0.96			

Volume III—Appendix A: Fresh Concrete Properties for Phase I Mixtures

Table A.1, Volume 3. Fresh Concrete Properties for Re-tempered Mixtures Containing Air-Entraining Admixture “A”

Mix #	CA Type	AEA	Dosage oz/cwt	WR Dosage oz/cwt	Starting w/c	Ending w/c	Stage	Slump, inches	Air content (pressure method), %	Unit Weight, lb/ft ³	Gravimetric Air Content, %
1	RG	A	0.50	2.50	0.45	0.48	1	3.75	2.1	147.8	1.3
							2	4.13	5.8	142.4	4.9
							3	6.75	6.1	141.2	5.2
2	RG	A	0.25	1.25	0.45	0.48	1	1.50	2.0	148.5	0.9
							2	3.00	4.1	145.2	3.0
							3	6.00	4.5	143.7	3.5
3	RG	A	0.75	1.25	0.45	0.48	1	2.88	1.7	149.1	0.5
							2	3.75	5.9	142.7	4.7
							3	5.13	6.2	141.3	5.1
4	RG	A	1.22	1.25	0.45	0.48	1	3.75	1.9	148.6	0.8
							2	5.50	8.4	138.6	7.4
							3	7.50	9.0	136.7	8.2
5	RG	A	0.30	1.25	0.45	0.48	1	1.75	2.0	148.3	1.0
							2	2.25	4.0	145.6	2.8
							3	4.00	3.7	145.5	2.3
6	RG	A	0.75	1.25	0.45	0.48	1	1.75	2.1	148.0	1.2
							2	3.25	6.9	141.1	5.8
							3	5.25	6.8	140.9	5.4
7	RG	A	1.22	1.25	0.45	0.48	1	1.75	2.1	147.9	1.3
							2	4.00	8.5	138.4	7.6
							3	5.25	9.0	137.0	8.0

Table A.2, Volume 3. Fresh Concrete Properties for Re-tempered Mixtures Containing Air-Entraining Admixture “A”

Mix #	CA Type	AEA	Dosage oz/cwt	WR Dosage oz/cwt	Starting w/c	Ending w/c	Stage	Slump, inches	Air content (pressure method), %	Unit Weight, lb/ft ³	Gravimetric Air Content, %
8	RG	A	0.25	1.25	0.45	0.47	1	2.50	2.2	148.2	1.1
							2	3.25	4.2	145.3	3.0
							3	3.75	4.3	144.9	3.0
9	RG	A	0.75	1.25	0.45	0.47	1	2.38	1.8	149.0	0.6
							2	4.25	6.7	141.7	5.4
							3	4.50	5.7	142.7	4.5
10	RG	A	1.22	1.25	0.45	0.47	1	5.50	2.1	147.8	1.3
							2	5.75	9.4	137.0	8.5
							3	7.00	8.5	138.1	7.5
11	RG	A	0.25	1.25	0.45	0.50	1	3.00	2.0	148.7	0.7
							2	4.00	4.6	145.0	3.2
							3	7.25	5.0	143.4	3.4
12	RG	A	0.75	1.25	0.45	0.50	1	3.50	2.0	148.1	1.1
							2	5.25	6.9	140.9	6.0
							3	8.00	7.4	139.0	6.4
13	RG	A	1.22	1.25	0.45	0.50	1	3.25	2.0	148.2	1.0
							2	4.75	8.9	137.7	8.1
							3	7.75	11.0	133.1	10.3

Table A.3, Volume 3. Fresh Concrete Properties for Re-tempered Mixtures Containing Air-Entraining Admixture “B” & “C”

Mix #	CA Type	AEA	Dosage oz/cwt	WR Dosage oz/cwt	Starting w/c	Ending w/c	Stage	Slump, inches	Air content (pressure method), %	Unit Weight, lb/ft ³	Gravimetric Air Content, %
14	RG	B	0.30	2.50	0.45	0.48	1	3.75	2.0	148.4	0.9
							2	4.75	4.9	144.2	3.8
							3	7.00	5.6	142.3	4.4
15	RG	B	0.30	1.25	0.45	0.48	1	2.00	1.9	148.6	0.8
							2	3.25	3.5	145.8	2.6
							3	6.00	3.2	145.3	2.4
16	RG	B	0.83	1.25	0.45	0.48	1	2.00	1.9	147.1	1.8
							2	4.50	5.7	142.3	5.0
							3	7.00	6.2	141.6	4.9
17	RG	B	1.35	1.25	0.45	0.48	1	2.13	2.0	148.6	0.8
							2	3.75	8.1	139.6	6.8
							3	6.50	8.5	138.4	7.1
18	RG	C	0.20	1.25	0.45	0.48	1	2.50	1.8	148.8	0.7
							2	3.00	3.6	146.5	2.2
							3	5.25	3.8	145.5	2.3
19	RG	C	0.65	1.25	0.45	0.48	1	2.25	1.9	148.7	0.7
							2	3.25	5.7	142.9	4.6
							3	5.75	7.2	139.7	6.2
20	RG	C	1.20	1.25	0.45	0.48	1	3.25	1.9	148.2	1.1
							2	3.75	7.8	139.6	6.8
							3	4.75	10.0	135.9	8.7

Table A.4, Volume 3. Fresh Concrete Properties for Non-Re-tempered Mixtures

Mix #	CA Type	AEA	Dosage oz/cwt	WR Dosage oz/cwt	Starting w/c	Ending w/c	Stage	Slump, inches	% Air Content (pressure method)	Unit Weight, lb/ft ³	% Gravimetric Air Content
21	RG	A	0.50	2.50	0.48	0.48	1	6.75	2.1	146.5	1.6
							2	8.25	9.8	135.5	9.0
							3	7.00	8.5	137.9	7.4
22	RG	A	0.50	2.00	0.48	0.48	1	7.00	1.9	146.6	1.6
							2	7.50	9.7	136.0	8.7
							3	6.50	8.3	139.1	6.6
23	RG	A	0.30		0.48	0.48	1	7.00	1.8	147.1	1.2
							2	7.00	3.9	144.6	2.9
24	RG	A	0.75		0.48	0.48	1	4.25	1.8	148.2	0.5
							2	5.00	6.6	140.7	5.5
25	RG	A	1.22		0.48	0.48	1	3.00	1.8	148.0	0.6
							2	5.00	9.0	138.8	6.8
26	RG	B	0.30		0.48	0.48	1	3.25	1.8	148.1	0.5
							2	2.75	2.9	147.1	1.2
27	RG	B	0.97		0.48	0.48	1	2.75	1.7	148.7	0.1
							2	3.75	6.4	141.6	4.9
28	RG	B	1.49		0.48	0.48	1	2.25	1.7	148.3	0.4
							2	4.25	9.0	137.8	7.5
29	RG	C	0.20		0.48	0.48	1	3.25	1.8	147.8	0.7
							2	4.50	3.2	146.3	1.7

Table A.4 (cont'd): Fresh Concrete Properties for Non-Re-tempered Mixtures

Mix #	CA Type	AEA	Dosage oz/cwt	WR Dosage oz/cwt	Starting w/c	Ending w/c	Stage	Slump, inches	% Air Content (pressure method)	Unit Weight, lb/ft ³	% Gravimetric Air Content
30	RG	C	0.65		0.48	0.48	1	3.75	1.7	147.9	0.7
							2	4.00	5.5	142.8	4.1
31	RG	C	1.20		0.48	0.48	1	4.50	1.7	148.0	0.6
							2	5.00	8.5	137.5	7.6
32	RG	A	0.30		0.50	0.50	1	5.50	1.7	147.8	0.5
							2	5.25	4.0	144.6	2.6
33	RG	A	0.75		0.50	0.50	1	4.00	1.8	147.8	0.4
							2	5.50	7.3	140.4	5.4
34	RG	A	1.22		0.50	0.50	1	5.50	1.6	148.0	0.3
							2	6.75	9.3	136.6	8.0

Volume III—Appendix B: Hardened Concrete Properties for Phase I Mixtures

Table B.1, Volume 3. Compressive Strengths for Re-tempered Mixtures Containing Air-Entraining Admixture “A”

Mix #	CA Type	AEA	Dosage oz/cwt	WR Dosage oz/cwt	Starting w/c	Ending w/c	Stage	7-Day Compressive Strength, psi	28-Day Compressive Strength, psi
1	RG	A	0.50	2.50	0.45	0.48	1		7630
							2		5580
							3		5370
2	RG	A	0.25	1.25	0.45	0.48	1	6510	7940
							2	5090	6700
							3	4360	6410
3	RG	A	0.75	1.25	0.45	0.48	1	6480	7640
							2	4510	5600
							3	4350	5280
4	RG	A	1.22	1.25	0.45	0.48	1	6410	7710
							2	3680	4430
							3	3350	3810
5	RG	A	0.30	1.25	0.45	0.48	1	6020	7880
							2	5550	7030
							3	5320	6550
6	RG	A	0.75	1.25	0.45	0.48	1	6470	8400
							2	4510	5680
							3	4300	5400
7	RG	A	1.22	1.25	0.45	0.48	1	6190	8190
							2	3780	4990
							3	3410	4380

Table B.2, Volume 3. Compressive Strengths for Re-tempered Mixtures Containing Air-Entraining Admixture “A”

Mix #	CA Type	AEA	Dosage oz/cwt	WR Dosage oz/cwt	Starting w/c	Ending w/c	Stage	7-Day Compressive Strength, psi	28-Day Compressive Strength, psi
8	RG	A	0.25	1.25	0.45	0.47	1	6140	8050
							2	5340	6750
							3	5180	6160
9	RG	A	0.75	1.25	0.45	0.47	1	6200	7890
							2	4270	5300
							3	4500	5880
10	RG	A	1.22	1.25	0.45	0.47	1	6550	7900
							2	3430	4200
							3	3500	3700
11	RG	A	0.25	1.25	0.45	0.50	1	5340	7120
							2	5140	6260
							3	4590	5690
12	RG	A	0.75	1.25	0.45	0.50	1	6060	7750
							2	4170	5220
							3	3600	4720
13	RG	A	1.22	1.25	0.45	0.50	1	6380	7760
							2	3490	4240
							3	2810	3590

Table B.3, Volume 3. Compressive Strengths for Re-tempered Mixtures Containing Air-Entraining Admixture B & C

Mix #	CA Type	AEA	Dosage oz/cwt	WR Dosage oz/cwt	Starting w/c	Ending w/c	Stage	7-Day Compressive Strength, psi	28-Day Compressive Strength, psi
14	RG	B	0.30	2.50	0.45	0.48	1	6700	7930
							2	5280	6530
							3	4980	6100
15	RG	B	0.30	1.25	0.45	0.48	1	6190	7530
							2	5640	7370
							3	5300	6740
16	RG	B	0.83	1.25	0.45	0.48	1	6280	7960
							2	4530	5580
							3	4190	5240
17	RG	B	1.35	1.25	0.45	0.48	1	6390	7960
							2	3720	4740
							3	3560	4270
18	RG	C	0.20	1.25	0.45	0.48	1	6550	7880
							2	5950	7300
							3	5420	6570
19	RG	C	0.65	1.25	0.45	0.48	1	6650	8110
							2	4710	5560
							3	3850	4810
20	RG	C	1.20	1.25	0.45	0.48	1	6550	7930
							2	3680	4230
							3	2620	3140

Table B.4, Volume 3. Compressive Strengths for Non-Re-tempered Mixtures

Mix #	CA Type	AEA	Dosage oz/cwt	WR Dosage oz/cwt	Starting w/c	Ending w/c	Stage	7-Day Compressive Strength, psi	28-Day Compressive Strength, psi
21	RG	A	0.50	2.50	0.48	0.48	1	5810	7570
							2	3650	4640
							3	4160	5000
22	RG	A	0.50	2.00	0.48	0.48	1	5820	7510
							2	3310	4320
							3	3840	4560
23	RG	A	0.30		0.48	0.48	1	5800	7100
							2	5080	6380
24	RG	A	0.75		0.48	0.48	1	5980	7470
							2	4280	5220
25	RG	A	1.22		0.48	0.48	1	5860	7300
							2	3600	4370
26	RG	B	0.30		0.48	0.48	1	6180	7660
							2	5560	7120
27	RG	B	0.97		0.48	0.48	1	6030	7400
							2	4210	5480
28	RG	B	1.49		0.48	0.48	1	5900	7150
							2	3470	4240
29	RG	C	0.20		0.48	0.48	1	5810	7520
							2	5520	7060
30	RG	C	0.65		0.48	0.48	1	6080	7560
							2	4020	5610
31	RG	C	1.20		0.48	0.48	1	5680	7330
							2	2970	3830
32	RG	A	0.30		0.50	0.50	1	5700	7520
							2	4830	7400
33	RG	A	0.75		0.50	0.50	1	5760	7500
							2	4090	5180
34	RG	A	1.22		0.50	0.50	1	5250	6970
							2	3020	4120

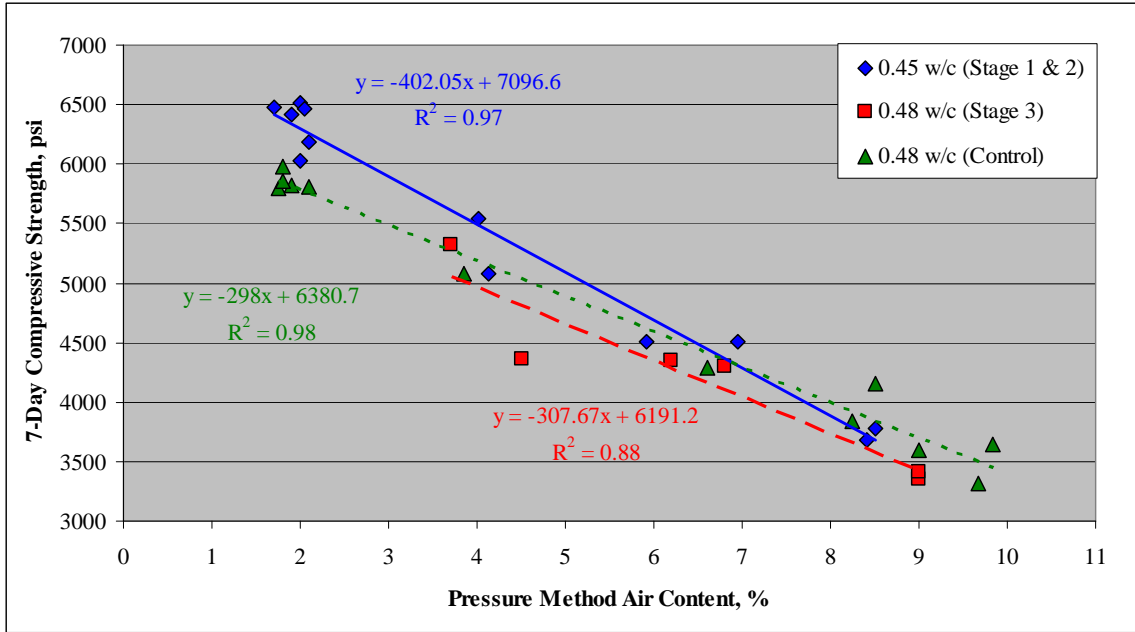


Figure B.1, Volume 3. 7-Day Compressive Strength vs. Air Content (pressure method) for Mixtures Containing AEA "A" and Re-tempered to a 0.48 w/c

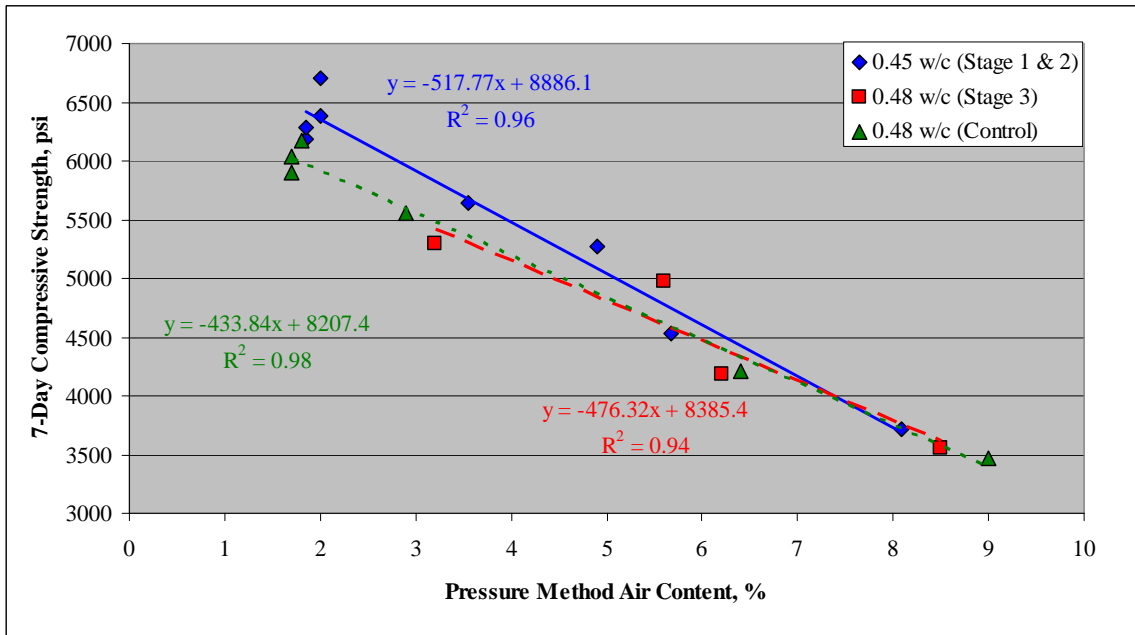


Figure B.2, Volume 3. 7-Day Compressive Strength vs. Air Content (pressure method) for Mixtures Containing AEA "B" and Re-tempered to a 0.48 w/c

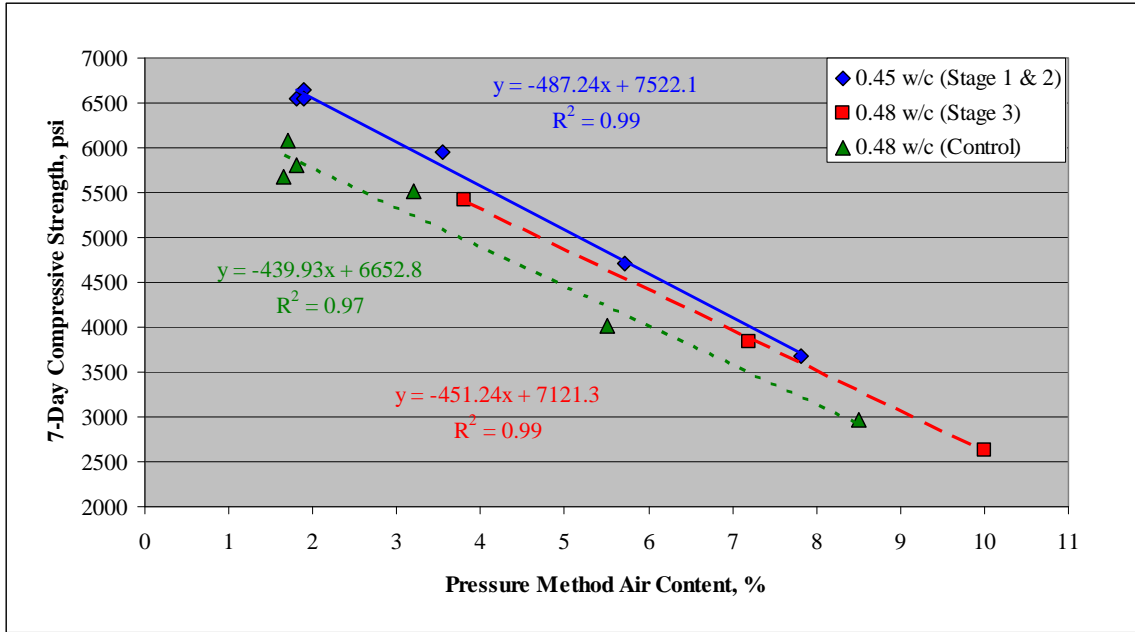


Figure B.3, Volume 3. 7-Day Compressive Strength vs. Air Content (pressure method) for Mixtures Containing AEA "C" and re-tempered to a 0.48 w/c

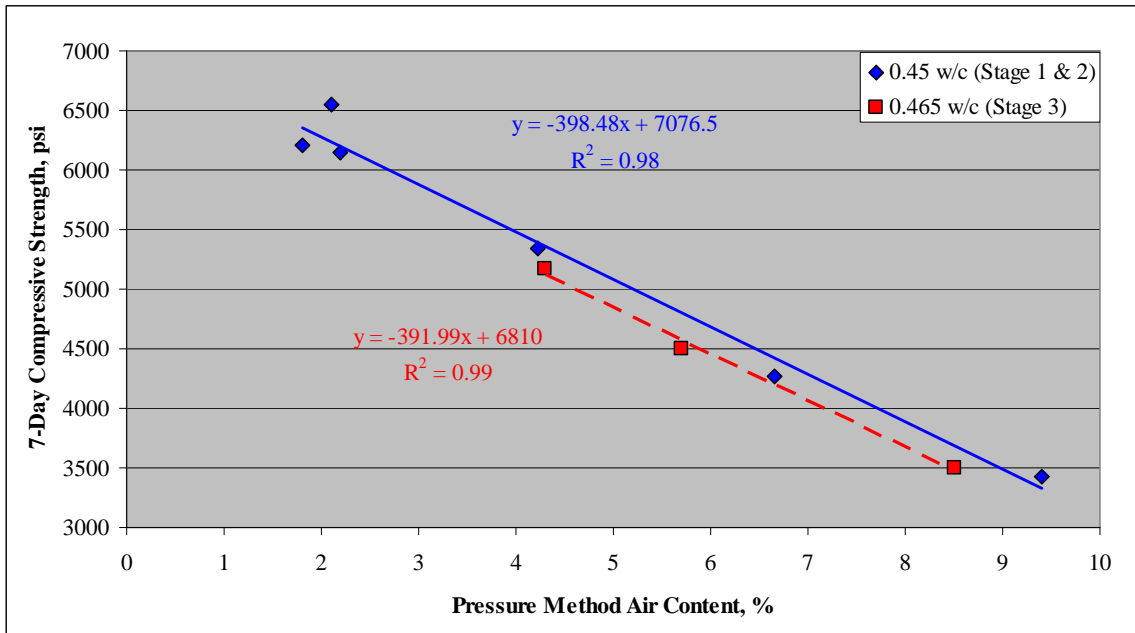


Figure B.4, Volume 3. 7-Day Compressive Strength vs. Air Content (pressure method) for Mixtures Containing AEA "A" and Re-tempered to a 0.47 w/c

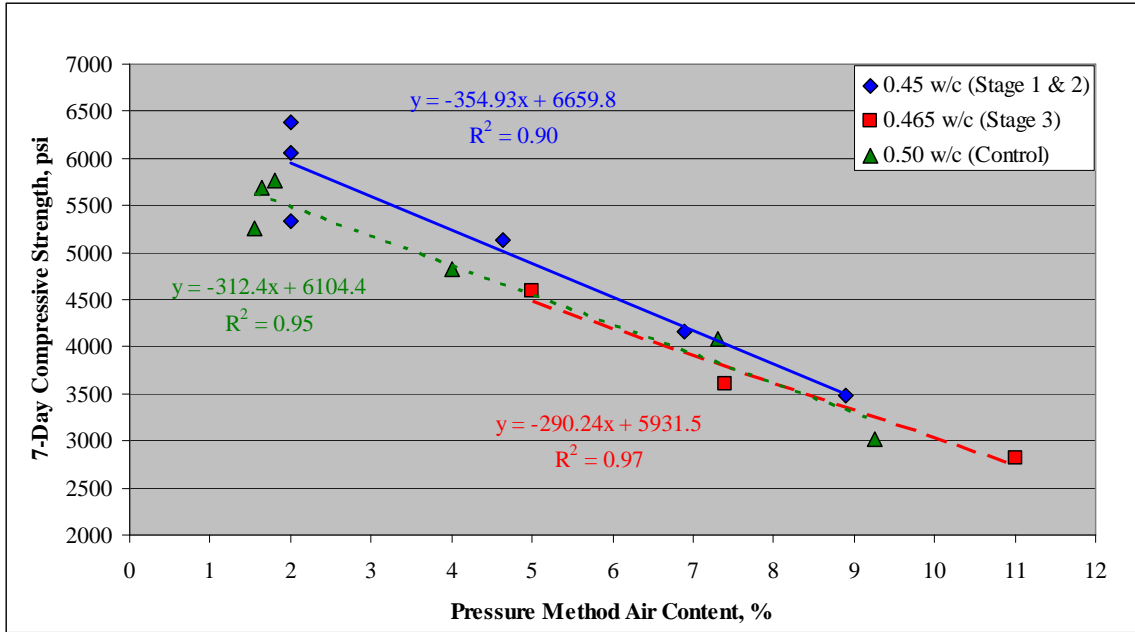


Figure B.5, Volume 3. 7-Day Compressive Strength vs. Air Content (pressure method) for Mixtures Containing AEA "A" and Re-tempered to a 0.50 w/c

Table B.5, Volume 3. Composite Clustering Ratings for Re-tempered Mixtures Containing Air-Entraining Admixture “A”

Mix #	Stage	Rating				Composite Rating	Air content (pressure method), %
		0	1	2	3		
1	2	13	33	3	0	0.80	5.8
	3	6	17	17	0	1.28	6.1
2	2	56	5	0	0	0.08	4.1
	3	42	18	0	0	0.30	4.5
3	2	38	11	0	0	0.22	5.9
	3	11	25	3	0	0.79	6.2
4	2	9	36	13	0	1.07	8.4
	3	1	28	16	0	1.33	9.0
5	2	53	0	0	0	0.00	4.0
	3	42	18	0	0	0.30	3.7
6	2	17	27	2	0	0.67	6.9
	3	13	27	9	0	0.92	6.8
7	2	19	26	4	0	0.69	8.5
	3	0	24	26	2	1.58	9.0
8	2	42	13	0	0	0.24	4.2
	3	47	6	0	0	0.11	4.3
9	2	17	20	2	0	0.62	6.7
	3	9	32	4	0	0.89	5.7
10	2	1	34	8	0	1.16	9.4
	3	0	28	15	0	1.35	8.5
11	2	23	12	0	0	0.34	4.6
	3	24	20	4	0	0.58	5.0
12	2	10	34	2	0	0.83	6.9
	3	0	19	24	0	1.56	7.4
13	2	6	37	3	0	0.93	8.9
	3	0	26	16	0	1.38	11.0

Table B.6, Volume 3. Composite Clustering Ratings for Re-tempered Mixtures Containing Air-Entraining Admixtures “B” and “C”

Mix #	Stage	Rating				Composite Rating	Air content (pressure method), %
		0	1	2	3		
14	2	33	21	3	0	0.47	4.9
	3	14	24	9	0	0.89	5.6
15	2	46	0	0	0	0.00	3.6
	3	39	0	0	0	0.00	3.2
16	2	0	36	6	0	1.14	6.9
	3	9	29	2	0	0.83	6.2
17	2	1	33	15	2	1.35	8.1
	3	0	35	13	0	1.27	8.5
18	2	43	0	0	0	0.00	3.6
	3	35	9	0	0	0.20	3.8
19	2	17	20	0	0	0.54	5.7
	3	10	24	2	0	0.78	7.2
20	2	0	31	14	1	1.35	7.8
	3	0	15	19	4	1.71	10.0

Table B.7, Volume 3. Composite Clustering Ratings for Non- Re-tempered Mixtures

Mix #	Rating				Composite Rating	Air Content (pressure method), %
	0	1	2	3		
21	5	20	21	0	1.35	9.8
22	2	25	22	4	1.53	10.7
23	37	15	1	0	0.32	3.9
24	17	29	7	0	0.81	6.6
25	11	24	13	0	1.04	9.0
26	47	0	0	0	0.00	2.9
27	21	29	1	0	0.61	6.4
28	0	36	7	0	1.16	9.0
29	52	1	0	0	0.02	3.2
30	12	38	5	0	0.87	5.5
31	0	25	15	0	1.38	8.5

Volume III—Appendix C: Fresh Concrete Properties for Phase II Mixtures

Table C.1, Volume 3. Fresh Concrete Properties for Re-tempered Mixtures Containing Air-Entraining Admixtures “A” and “B”

Mix #	CA Type	AEA	Dosage oz/cwt	WR Dosage oz/cwt	Starting w/c	Ending w/c	Stage	Slump, inches	% Air Content (pressure method)	Unit Weight, lb/ft ³	% Gravimetric Air Content
35	LS	A	0.75	1.25	0.45	0.48	1	0.75	2.4	148.1	0.8
							2	1.25	4.9	144.5	3.2
							3	1.75	5.6	142.5	3.9
36	LS	A	1.22	1.25	0.45	0.48	1	1.5	2.3	148.0	0.8
							2	1	6.2	142.7	4.4
							3	2.75	8.5	138.6	6.6
37	LS	B	0.68	1.25	0.45	0.48	1	0.5	2.3	148.6	0.4
							2	1	3.4	146.9	1.6
							3	1.75	4.4	144.4	2.7
38	LS	B	1.00	2.50	0.45	0.48	1	1.5	2.4	147.9	0.9
							2	1.75	5.4	143.7	3.7
							3	3	7.0	140.3	5.5
39	RG	A	0.50	1.25	0.45	0.48	1	1	2.4	147.7	1.4
							2	1.5	4.5	144.0	3.9
							3	3.25	5.0	143.6	3.6
40	RG	A	0.75	1.25	0.45	0.48	1	1	2.2	148.5	0.9
							2	1.75	5.2	144.2	3.7
							3	3.5	5.8	142.4	4.4

Table C.2, Volume 3. Fresh Concrete Properties for Non-Re-tempered Mixtures Containing Air-Entraining Admixtures “A” and “B”

Mix #	CA Type	AEA	Dosage oz/cwt	WR Dosage oz/cwt	Starting w/c	Ending w/c	Stage	Slump, inches	% Air Content (pressure method)	Unit Weight, lb/ft³	% Gravimetric Air Content
41	LS	A	Varied	0	0.48	0.48	1	3.5	2.0	147.3	0.7
							2	4.5	6.6	140.3	5.4
							3	4	7.0	140.1	5.6
42	LS	B	Varied	0	0.48	0.48	1	2.5	2.3	147.4	0.7
							2	2.75	4.6	144.0	3.0
							3	2.75	6.2	141.2	4.8
43	RG	A	Varied	0	0.48	0.48	1	4	2.3	147.1	1.8
							2	5.25	5.9	141.5	5.5
							3	4.75	8.0	138.2	7.2

Volume III—Appendix D: Hardened Concrete Properties for Phase II Mixtures

Table D.1, Volume 3. Hardened Concrete Properties for Re-tempered Mixtures Containing Air-Entraining Admixtures “A” and “B”

Mix #	CA Type	AEA	Dosage oz/cwt	WR Dosage oz/cwt	Starting w/c	Ending w/c	Stage	7-Day Compressive Strength, psi	28-Day Compressive Strength, psi	7-Day Splitting-Tensile Strength, psi	28-Day Splitting-Tensile Strength, psi	7-Day Flexural Strength, psi
35	LS	A	0.75	1.25	0.45	0.48	1	7250	8790	675	880	920
							2	6170	7800	610	760	860
							3	5470	6910	535	665	795
36	LS	A	1.22	1.25	0.45	0.48	1	8140	9420	660	765	985
							2	6010	7480	615	720	850
							3	4270	5290	495	520	705
37	LS	B	0.68	1.25	0.45	0.48	1	7720	8430	770	775	940
							2	6650	7820	690	745	930
							3	6180	7490	610	715	810
38	LS	B	1.00	2.50	0.45	0.48	1	7680	9040	760	835	960
							2	6280	7380	715	675	880
							3	5250	6310	595	650	790
39	RG	A	0.50	1.25	0.45	0.48	1	6360	7940	650	760	785
							2	5120	6720	580	675	760
							3	4750	5590	550	660	715
40	RG	A	0.75	1.25	0.45	0.48	1	6510	7820	710	780	860
							2	5150	6320	620	675	675
							3	5010	5760	595	685	650

**Table D.2, Volume 3. Hardened Concrete Properties for Non-Re-tempered Mixtures Containing Air-Entraining Admixtures
“A” and “B”**

Mix #	CA Type	AEA	Dosage oz/cwt	WR Dosage oz/cwt	Starting w/c	Ending w/c	Stage	7-Day Compressive Strength, psi	28-Day Compressive Strength, psi	7-Day Splitting-Tensile Strength, psi	28-Day Splitting-Tensile Strength, psi	7-Day Flexural Strength, psi
41	LS	A	Varied	0	0.48	0.48	1	6750	6750	535	945	870
							2	4920	4920	535	705	720
							3	4400	4400	510	685	695
42	LS	B	Varied	0	0.48	0.48	1	6950	6950	705	770	835
							2	5920	5920	645	625	810
							3	5280	5280	595	615	765
43	RG	A	Varied	0	0.48	0.48	1	6090	7620	640	780	740
							2	4390	5830	580	660	695
							3	3770	4790	500	560	610

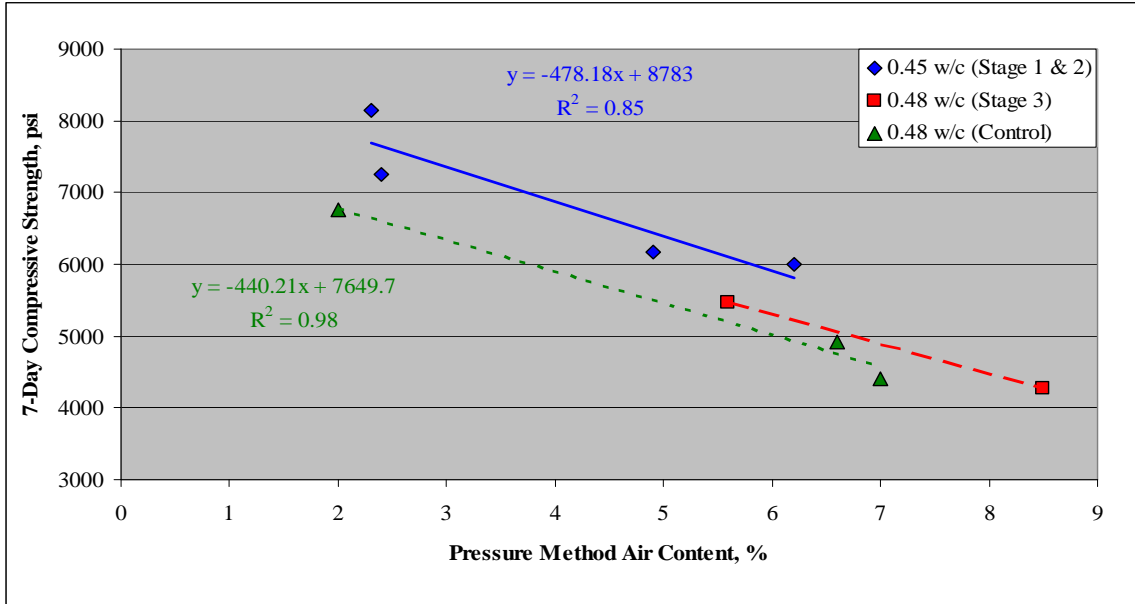


Figure D.1, Volume 3. 7-Day Compressive Strength vs. Air Content (pressure method) for Mixtures Containing AEA "A" and Limestone Coarse Aggregate and Re-tempered to a 0.48 w/c

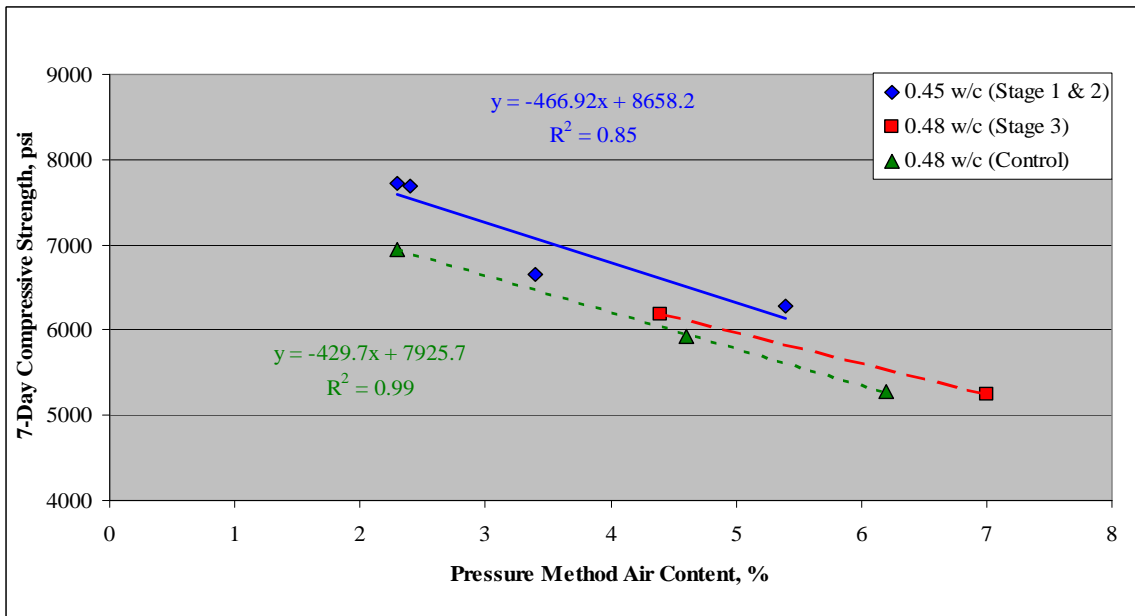


Figure D.2, Volume 3. 7-Day Compressive Strength vs. Air Content (pressure method) for Mixtures Containing AEA "B" and Limestone Coarse Aggregate and Re-tempered to a 0.48 w/c

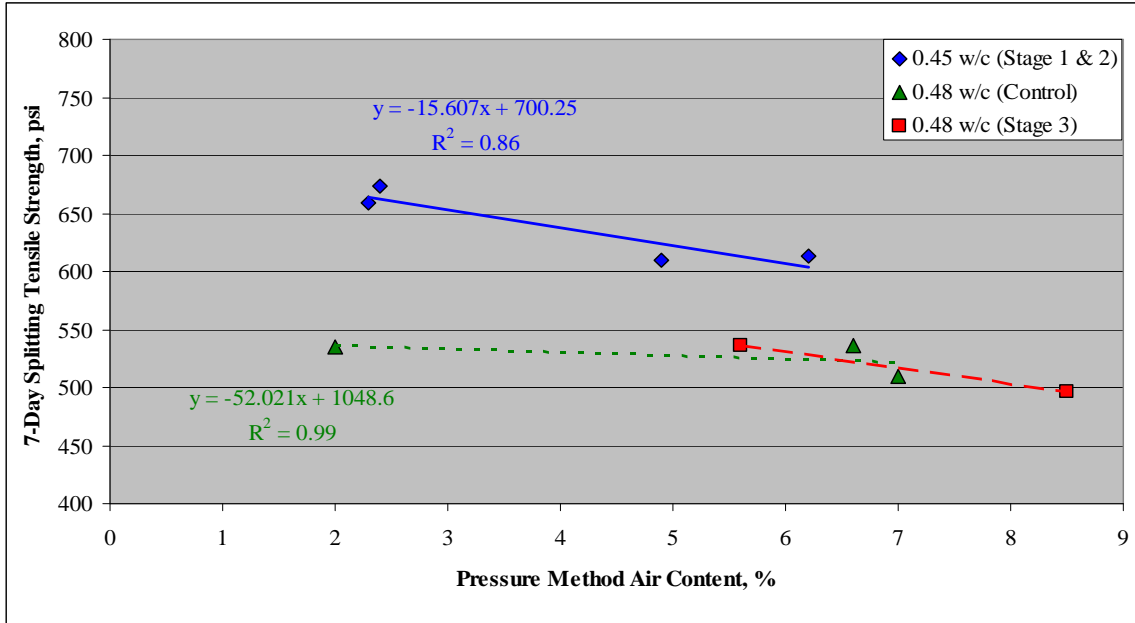


Figure D.3, Volume 3. 7-Day Splitting Tensile Strength vs. Air Content (pressure method) for Mixtures Containing AEA "A" and Limestone Coarse Aggregate and Re-tempered to a 0.48 w/c

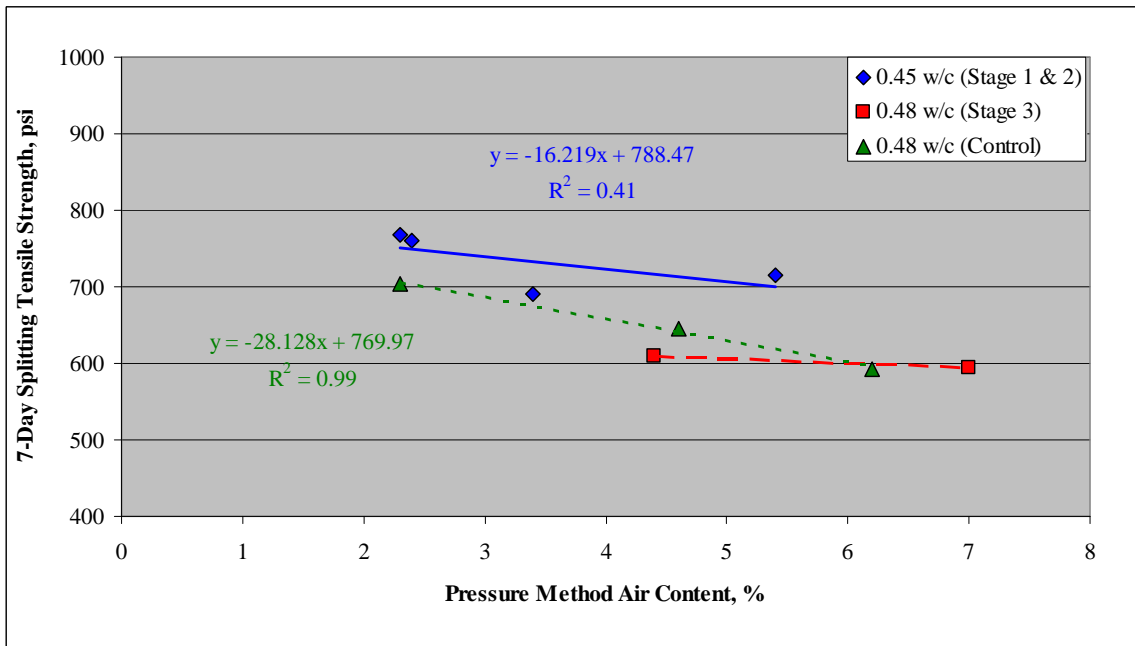


Figure D.4, Volume 3. 7-Day Splitting Tensile Strength vs. Air Content (pressure method) for Mixtures Containing AEA "B" and Limestone Coarse Aggregate and Re-tempered to a 0.48 w/c

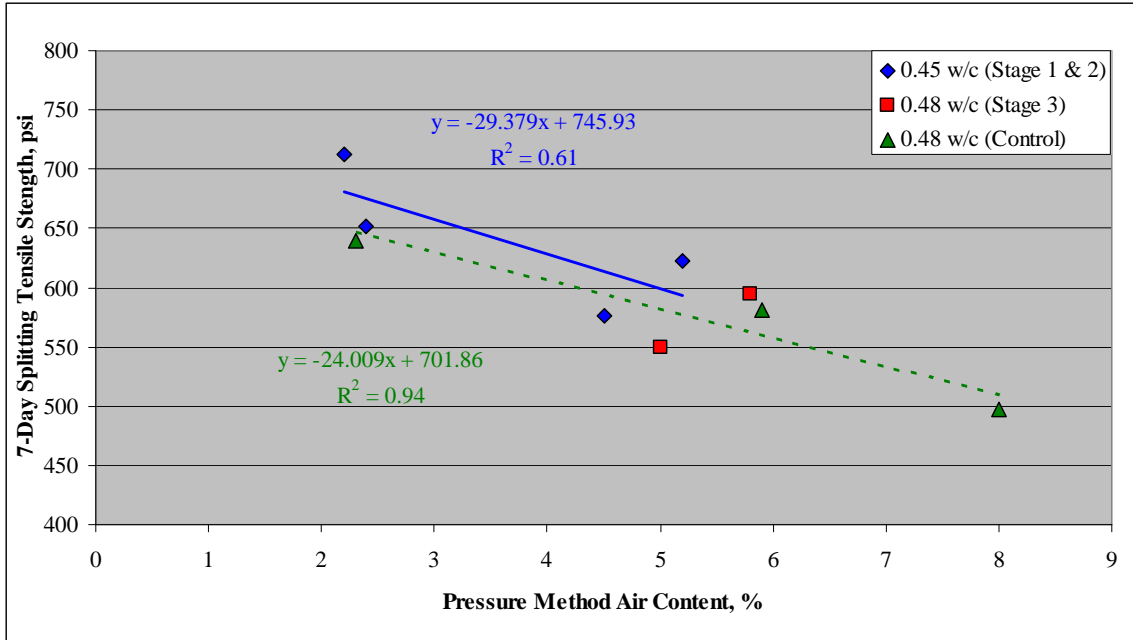


Figure D.5, Volume 3. 7-Day Splitting Tensile Strength vs. Air Content (pressure method) for Mixtures Containing AEA “A” and Siliceous Coarse Aggregate and Re-tempered to a 0.48 w/c

Table D.3, Volume 3. Composite Clustering Ratings for Re-tempered Mixtures

Mix #	Stage	Rating					Composite Rating	Air Content (pressure method), %
		0	1	2	3			
35	2	53	0	0	0	0.00	4.9	
	3	45	0	0	0	0.00	5.6	
36	2	51	0	0	0	0.00	6.2	
	3	20	26	2	0	0.63	8.5	
37	2	46	0	0	0	0.00	3.4	
	3	49	0	0	0	0.00	4.4	
38	2	43	5	0	0	0.10	5.4	
	3	46	2	0	0	0.04	7.0	
39	2	47	13	0	0	0.22	4.5	
	3	10	32	3	0	0.84	5	
40	2	58	0	0	0	0.00	5.2	
	3	9	48	0	0	0.84	5.8	

Table D.4, Volume 3. Composite Clustering Ratings for Non-Re-tempered Mixtures

Mix #	Rating					Air Content (pressure method), %
	0	1	2	3	Composite Rating	
41	45	8	0	0	0.15	6.6
	37	15	0	0	0.29	7.0
42	44	1	0	0	0.02	4.6
	33	14	0	0	0.30	6.2
43	18	33	0	0	0.65	5.9
	0	17	35	0	1.67	8.0

Volume III—Appendix E: Hardened Air Analysis for Phase I and Phase II Mixtures

Table E.1, Volume 3. Hardened Air Void Analysis

Mix #	Stage	Air Content (pressure method), %	ASTM C 457 Air Content, %	Spacing Factor, in.	Specific Surface, in. ⁻¹
2	2	4.1	2.9	0.0072	845
	3	4.5	4.8	0.0057	844
5	2	4.0	3.2	0.0068	847
	3	3.7	3.5	0.0070	807
6	2	6.9	7.7	0.0034	958
	3	6.8	9.0	0.0031	919
11	2	4.6	5.0	0.0044	1080
	3	5.0	6.2	0.0044	960
15	2	3.5	3.5	0.0065	859
	3	3.2	2.4	0.0075	893
16	2	5.7	7.0	0.0035	1046
	3	6.2	6.8	0.0036	1084
35	2	4.9	4.7	0.0045	1076
	3	5.6	5.7	0.0037	1204
36	2	6.2	4.3	0.0050	989
	3	8.5	6.0	0.0037	1149
37	2	3.4	3.7	0.0072	757
	3	4.4	4.4	0.0052	964
38	2	5.4	4.3	0.0047	1070
	3	7.0	4.6	0.0044	1122
39	2	4.5	4.9	0.0062	758
	3	5.0	5.5	0.0049	934
40	2	5.2	4.8	0.0051	943
	3	5.8	6.8	0.0036	1080